lead to up-regulation of IL-6R in T cells are not known, and as hepatocytes do not express the receptors for IL-2 (Tato and Cua, 2008), it is unlikely that IL-2 is a general or the sole regulator of IL-6R expression. In at least one case it was reported that IL-6 can induce the expression of its own IL-6R (Thabard et al., 2001). Whether and how IL-11R expression is regulated has not been studied thus far.

IL-6 and IL-11 signaling: similarities and differences

IL-6 signaling via gp130 and the membrane-bound IL-6R is called classic signaling (Garbers et al., 2012) (Figure 1). In addition to the membrane-bound IL-6R, up to 50 ng/ml soluble forms of the IL-6R (sIL-6R) were found in the serum of man, which can rise up to 170 ng/ml under pathophysiological conditions (Gaillard et al., 1993; Mitsuyama et al., 1995; Montero-Julian, 2001). More than 90% of the sIL-6R is generated by limited proteolysis of the membrane-bound IL-6R by the proteases ADAM10 or ADAM17 and up to 10% of the sIL-6R is generated by translation from a differentially spliced mRNA. In differential splicing, the exon coding for the trans-membrane region of the IL-6R is skipped, resulting in premature termination of the IL-6R open reading frame and a new short C-terminus (Chalaris et al., 2011). Importantly, both forms of the sIL-6R can still bind to IL-6. In contrast to most other soluble receptors, sIL-6R does not act as an antagonist but as an agonist. Consequently, the interaction of the IL-6/sIL-6R complex with gp130 can activate cells, which do not necessarily express the membrane-bound IL-6R and are therefore unresponsive to IL-6 classic signaling. IL-6 signaling via the sIL-6R was called IL-6 trans-signaling (Figure 1) (Rose-John and Heinrich, 1994; Chalaris et al., 2011).

The complex of IL-6 and sIL-6R can stimulate all cells of the body and thereby mimic signals from other cytokines of the IL-6 family, especially IL-11 signaling (Jones et al., 2011). Interestingly, IL-6 trans-signaling is mimicked by the viral orthologue of IL-6 (vIL-6) encoded by the human herpes virus 8 (HHV8), which directly binds to and stimulates gp130 and does not depend on IL-6R (Adam et al., 2009; Suthaus et al., 2012).

IL-11 signaling is mediated by gp130 and the specificity factor IL-11R (Figure 1) (Pflanz et al., 1999), which means that both IL-6 and IL-11 signal via the same gp130 homodimeric signal-transducing receptor complex. In principle, a soluble IL-11R can also form biologically active soluble complexes with IL-11 (Pflanz et al., 1999). A naturally occurring soluble IL-11R has, however, not been described thus far, leaving open the question of if an IL-11 trans-signaling pathway exists *in vivo* (Figure 1).

To date, no functional role in signal transduction was assigned to the α-receptors IL-6R and IL-11R. The early signaling pathways of IL-6 and IL-11 via homodimeric gp130 appear similar or identical and include phosphorylation of the JAKs, STAT1 and 3, and activation of the mitogen-activated protein (MAP) kinase pathway. Only the local cytokine expression and the α-receptor expression pattern decide whether a cell reacts towards IL-6 or IL-11. Detailed comparative analysis of dynamic signal transduction of IL-6 and IL-11 have, however, not been performed to date. Future experiments have to functionally compare IL-6 and IL-11 signal transduction *in vitro* and *in vivo*. This is of particular importance because IL-6 and IL-11 have in part opposing roles *in vivo* and at least some cells are not able to conduct the full spectrum of signal transduction pathways after IL-6/IL-11 activation (see section 'Comparison of IL-6 and IL-11 *in vivo*').

The single nucleotide polymorphism (SNP) rs2228145, located within exon 9 of the IL-6R gene locus, is characterized by a coding mutation resulting in an amino acid exchange from Asp(358)Ala. This SNP is quite common, as up to 20% of people genotyped were homozygous (Galicia et al., 2004). These individuals are characterized by reduced cellular IL-6R level and increased sIL-6R level resulting in reduced responsiveness to classic signaling IL-6 (Ferreira et al., 2013). Furthermore, the increased level of sIL-6R might lead to increased IL-6 trans-signaling (Scheller and Rose-John, 2012). It is currently unknown whether the increased sIL-6R levels are caused by increased shedding of membrane-bound IL-6R or other mechanisms. For the IL-11R, no such dominant SNP is known. Nevertheless, single case reports of individuals with missense mutations within the IL-11R have been described (Nieminen et al., 2011). These amino acid alterations lead to IL-11R variants that are not capable to fulfill IL-11-mediated signal transduction, and the patients suffered from craniosynostosis, delayed tooth eruption, and supernumerary teeth (Nieminen et al., 2011).

Therapeutic intervention of IL-6 and IL-11 signaling

The signaling pathway of IL-6 and IL-11 offers multiple ways of intervention, either through inhibition or enhancement, and nearly all of them have been used either experimentally or therapeutically in the clinic. In this section, we will discuss the possible steps of intervention and

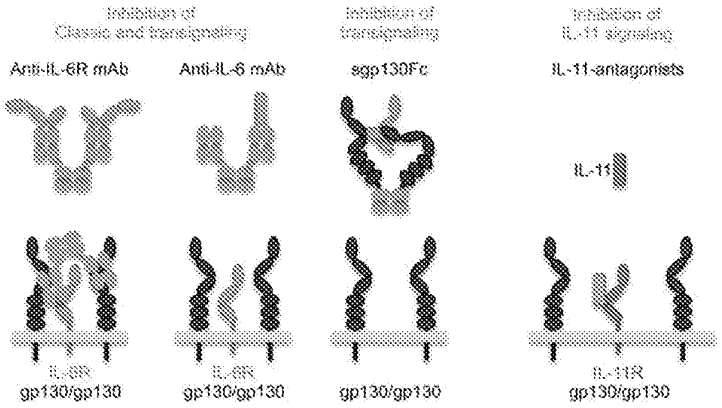

Figure 3 Strategies of therapeutic IL-6/IL-11 blockade.
Antibodies to IL-6 or IL-6R neutralize IL-6/IL-6R complexes and block both, IL-6 classic and trans-signaling and interfere with binding of IL-6 to IL-6R. Anti-IL-6 mAbs might lead to high-level accumulation of IL-6 because of decreased clearance (Lu et al., 1992). IL-6R neutralizing antibodies only lead to moderate elevation of IL-6 levels because of impaired internalization and subsequent degradation of IL-6 (Nishimoto et al., 2008). The sgp130Fc protein specifically blocks IL-6 trans-signaling without affecting classical signaling via the membrane-bound IL-6R, as IL-6 alone has no measurable affinity to sgp130Fc. IL-11 antagonists bind to IL-11R. Typically, these antagonists have not binding site(s) for gp130 and inhibit complex formation of IL-11/IL-11R/gp130.

highlight which compounds actually made their way from the bench to the bedside (Figure 3).

As mentioned previously, soluble forms of the IL-6R can be found in human body fluids, which led to the discrimination of IL-6 classic and trans-signaling. In addition to sIL-6R, soluble forms of gp130 (sgp130) were also found in human serum at 100–200 ng/ml. It was shown that sgp130 acts as natural inhibitor of IL-6 trans-signaling to inactivate circulating IL-6 in IL-6/sIL-6R/sgp130 complexes (Müller-Newen et al., 1998; Jostock et al., 2001). Despite a molar excess of sIL-6R over IL-6, free IL-6 and IL-6 in IL-6/sIL-6R complexes are present, which allows both classic and trans-signaling. Under these conditions, sgp130 was, however, able to trap all free IL-6 molecules in IL-6/sIL-6R/sgp130 complexes, resulting in inhibition of classic signaling by sgp130 (Garbers et al., 2011). IL-6 is known to exhibit pro-inflammatory and regenerative activities (Scheller et al., 2011b). For example, IL-6 deficient mice are more susceptible in an inflammatory bowel disease model as compared to wild-type mice (Grivennikov et al., 2009) but protected in mouse models of rheumatoid arthritis (Nowell et al., 2003, 2009). As sgp130 is not able to directly inhibit IL-6 classic signaling via the membrane-bound IL-6R, recombinant sgp130 was used to distinguish between classic- and trans-signaling *in vivo*. It turned out that IL-6 trans-signaling has mostly pro-inflammatory properties and is the main driving force of IL-6-signaling during chronic inflammation. IL-6 classic signaling has, however, regenerative activities and is needed, for example for induction of the hepatic acute-phase response (Scheller et al., 2011b). This has led to the evaluation of an Fc-fusion protein of sgp130 (sgp130Fc) as a therapeutic principle to neutralize the pro-inflammatory activities of IL-6, which would not compromise other beneficial activities of IL-6 classic signaling (Rose-John et al., 2007; Waetzig and Rose-John, 2012). Importantly, sgp130Fc does not inhibit the signaling of the other IL-6-type cytokines (Scheller et al., 2005), but would interfere with a hypothetical IL-11 trans-signaling pathway. Whether the recently uncovered IL-30/sIL-6R complex, which also can be blocked by sgp130Fc, plays a role *in vivo* is currently unknown (Garbers et al., 2013). A phase I clinical trial with the sgp130Fc protein is planned for 2013.

In addition to sgp130, monoclonal antibodies are used to specifically inhibit IL-6 signaling. The most prominent example is the humanized antibody tocilizumab marketed as Actemra (RoActemra in the EU), which is approved for the treatment of rheumatoid arthritis and systemic juvenile idiopathic arthritis in Europe and the US (Nishimoto et al., 2005; Tanaka et al., 2012). Tocilizumab specifically binds to site 1 of the IL-6R, thereby blocking binding of IL-6 to IL-6R. Besides blocking IL-6-induced signal transduction, tocilizumab also prevented cellular internalization and degradation of IL-6. As a consequence, IL-6R neutralizing antibodies lead to moderate elevation of overall IL-6 levels (Nishimoto et al., 2008). Other IL-6-directed neutralizing antibodies are in clinical development as anti-inflammatory and anticancer therapeutics. It remains to be seen whether these novel

anti-IL-6 mAbs also result in high-level accumulation of IL-6 because of decreased clearance (Lu et al., 1992). In contrast to sgp130, the anti-IL-6R antibody tocilizumab and all other agents block IL-6 classic and trans-signaling (Jones et al., 2011).

Because of the broad pro-inflammatory properties of IL-6, the therapeutic use of the cytokine itself does not seem to be a good choice. However, in a recent paper it was shown that treatment with recombinant IL-6 was protective via classic signaling in a mouse model of epidermolysis bullosa acquisita (EBA), an autoimmune disease induced by autoantibodies against type VII collagen, whereas inhibition of IL-6 trans-signaling by sgp130Fc was not beneficial (Samavedam et al., 2013). This example illustrates that also recombinant IL-6 might be an option to treat certain diseases.

In contrast, recombinant IL-11 is used to accelerate recovery of the hematopoietic system after cancer therapy, especially to treat severe thrombocytopenia associated with chemotherapy, for which it is approved in the USA by the US Food and Drug Administration (FDA) (Du and Williams, 1997; Putoczki and Ernst, 2010). Inhibition of IL-11 signaling is an attractive therapeutic option (for details in IL-11-dependent malignancies see the following section 'Comparison of IL-6 and IL-11 *in vivo*'), but to date no anti-IL-11 or anti-IL-11R inhibitory monoclonal antibodies were described. However, two IL-11 antagonists have been described (Underhill-Day et al., 2003; Lee et al., 2008). In the W147A antagonist, the amino acid 147 is mutated from a tryptophan to an alanine, which destroys the so-called 'site III' of IL-11. This mutant can therefore bind to the IL-11R, but engagement of the gp130 homodimer fails, resulting in efficient blockade of IL-11 signaling (Underhill-Day et al., 2003). However, it is unclear if these two proteins are beneficial in inflammatory diseases that depend upon IL-11, as systematic explorations in animal models are still missing.

All the above-mentioned interventions take place outside of the cell, thereby preventing the binding of the cytokine or cytokine/receptor complex to the signal-transducing β-receptor gp130. Another way to inhibit IL-6/IL-11 signaling is the use of small cell-permeable compounds that block proteins further downstream of the signaling cascade. The most promising candidates to date are inhibitors of the Janus kinases, which are responsible for phosphorylation of gp130 as well as STAT1 and STAT3. The importance of these proteins is further underlined by the fact that numerous patients suffering from myeloproliferative disorders show gain-of-function mutations in the *JAK2* gene. Ruxolitinib, a chemical that blocks both Jak1 and Jak2, is approved for the use against myelofibrosis. Furthermore, it was tested in a phase II study in patients with rheumatoid arthritis (RA) (Williams et al., 2008), showing promising results. Another Jak1/2 inhibitor, baracitinib, is also currently evaluated for the clinical use against RA (O'Shea et al., 2013). Tofacitinib is already approved by the FDA and can be therapeutically used in RA patients, who cannot be properly treated with methotrexate anymore. Tofacitinib blocks Jak1, Jak2 and Jak3 (Jiang et al., 2008; Haan et al., 2011). Efficacy of tofacitinib has been shown in clinical studies against, for example, RA (Fleischmann et al., 2012; van Vollenhoven et al., 2012) or ulcerative colitis (Sandborn et al., 2012).

However, it has to be noted that the blockade of Jak family members by small chemical compounds is rather unselective compared to the specific inhibition of IL-6 or IL-11 mentioned before. Both cytokines (and numerous other cytokines and growth factors) trigger activation of JAKs, and all these beneficial and/or destructive effects are simultaneously gone when the mentioned inhibitors are applied. Therefore, we think that blocking the binding of a single cytokine to its receptor is an alternative therapeutic strategy, which might lead to reduced side effects.

Comparison of IL-6 and IL-11 *in vivo*

In this section, we will directly compare and discuss the current view of the biological function of IL-6 and IL-11 *in vivo* (Figure 4). We will, however, not list all functions of IL-6 but concentrate on main functions of IL-11 and discuss the role of IL-6 in these settings.

Organ	IL-6	IL-11
Heart	Hypertrophy+fibrosis	Regeneration
Lung	TH2 cells ↑	TH2 cells ↓
Colon	Tissue damage + regeneration	Regeneration
Stomach	?	Tumor formation
Bone	Osteoclasts ↑	Osteoblasts ↑

Figure 4 Overview of IL-6 and IL-11 in (patho-)physiology.
The table summarizes the main finding of the opposite functions of IL-6 and IL-11 *in vivo* described in this review.

IL-6 and IL-11 promote opposite functions in heart failure

Heart failure is the leading cause of mortality. The onset of heart failure is caused by cardiovascular diseases, including myocardial infarction, hypertension, viral infections and others. IL-6 type cytokines, in particular CT-1 and LIF, have a wide range of biological functions in the heart, e.g., in cardiomyocytes and in controlling immune reactions of cardiovascular diseases (Fujio et al., 2011).

IL-11R has been shown to be expressed by cardiac myocytes and cardiac fibroblasts (Kimura et al., 2007), thereby making this organ a potential target of IL-11 *in vivo*. Indeed, several studies have underlined a functional role of IL-11 within the heart. Intravenous administration of recombinant IL-11 before coronary artery ligation greatly reduced the infarct size in a murine model of ischemia/reperfusion (I/R) (Kimura et al., 2007). Injection of IL-11 has been shown to reduce cardiac fibrosis, thereby attenuating cardiac dysfunction, in a myocardial infarction model by coronary ligation in mice (Obana et al., 2010). The authors showed that a cardiac-specific knockout of STAT3 resulted in a complete loss of IL-11-beneficial effects, and conversely that this could be mimicked through a cardiac-specific transgenic expression of a constitutively active STAT3 mutant (Obana et al., 2010). They further show that IL-11 mRNA is 60-fold up-regulated one day after myocardial infarction, suggesting an endogenous role of IL-11 in the heart besides its beneficial effects when administered intravenously (Obana et al., 2010). Within the ischemia/reperfusion model, IL-11 prevented not only cardiac damage when administered in advance of the IR, but was still effective when injected at the start of the reperfusion, thereby reducing cardiac injury and preserving cardiac function (Obana et al., 2012). This post-conditioning effect was mediated by activation of STAT3, as mice with a cardiac-specific STAT3 knock-out were not protected in an IL-11-dependent manner against I/R injury (Obana et al., 2012). Also in hindlimb ischemia, a mouse model for peripheral vascular disease, therapeutic administration of recombinant IL-11 has been shown to be beneficial, as it leads to an increase in recovery after femoral artery ligation and enhanced collateral vessel growth (Aitsebaomo et al., 2011).

In humans, increased IL-6 and sIL-6R level were found in acute myocardial infarction (Kanda et al., 2000). Interleukin-6 is produced by hypoxic myocytes and plays an important role in neutrophil-mediated reperfusion injury in the myocardium (Yamauchi-Takihara et al., 1995; Sawa et al., 1998). Transgenic mice overexpressing IL-6 and membrane-bound IL-6R (actin promoter) develop cardiac hypertrophy, whereas either transgenic mice for IL-6 or IL-6R alone did not show detectable myocardial abnormalities (Hirota et al., 1995). In rats, IL-6 trans-signaling leads to myocardial fibrosis, hypertension, and diastolic dysfunction (Meléndez et al., 2010). Moreover, IL-6 neutralization partially reduced cardiac hypertrophy as well as collagen synthesis in rat heart in a STAT3-dependent manner (Mir et al., 2012). In ischemia/reperfusion, infarct size in IL-6 deficient mice was similar to wild-type mice. However, preconditioning reduced infarct size in wild-type but not in IL-6 deficient mice (Dawn et al., 2004).

Treatment with a neutralizing anti-IL-6R antibody, tested in a murine model of myocardial infarction, also did not reduce initial infarct size, but reduced neutrophil and macrophage infiltration, matrix-metalloproteinase 2 activity, and led to an improvement of contractile function, which resulted in improved survival 28 days after surgery (Kobara et al., 2010).

These results suggested that production of IL-6 in the heart and in particular IL-6 trans-signaling may be a pathophysiological response that contributes to hypertrophy and progresses into heart failure. Therefore, inhibition of IL-6 trans-signaling was suggested as a potential therapy for hypertension and cardiac hypertrophy (Coles et al., 2007). The importance of IL-6 in cardiovascular diseases was further supported by a recent study, showing that in murine experimental autoimmune myocarditis IL-6 and IL-6R expression was up-regulated and disease development was prevented by neutralizing anti-IL-6R antibodies and pharmacological inhibition of STAT3 (Camporeale et al., 2013). Specific inhibition of IL-6 trans-signaling by sgp130 was, however, sufficient to effectively block the development of atherosclerosis in mice underlining the pro-inflammatory role of IL-6 trans-signaling (Schuett et al., 2012). The recently described conditional IL-6R deficient mice have not been studied so far in cardiovascular disease models (McFarland-Mancini et al., 2010). As IL-6R can also transmit signals of p28 (cytokine subunit of IL-27) and CNTF (Schuster et al., 2003; Garbers et al., 2013), it would be interesting to see if IL-6 and IL-6R deficient mice have the same phenotype in cardiovascular disease models.

Furthermore, the coding IL-6R rs2228145 SNP leads to reduced production of acute-phase proteins such as C-reactive protein and fibrinogen and a lower risk of coronary heart disease (Collaboration, 2012; Consortium, 2012). This is caused by a reduced level of membrane-bound IL-6R and/or an increased soluble IL-6R level. Mechanistically, the decreased risk of coronary heart disease for homozygous carriers of the rs2228145 SNP

might be caused by reduced IL-6 classic signaling on target cells, such as hepatocytes, monocytes and macrophages and/or an increased buffering of secreted IL-6 by the sIL-6R and sgp130 proteins (Ferreira et al., 2013; Scheller & Rose-John, 2012). Both modes would reduce the overall IL-6 activity.

To date it is not completely understood, why IL-11 and IL-6 have opposing functions in cardiovascular diseases. IL-6 but not IL-11 contributes to the activation and attraction of immune cells, e.g., neutrophils' attraction to the damaged heart. Inhibition of neutrophil invasion after heart damage has been shown to be beneficial (Litt et al., 1989). Unlike IL-11R, IL-6R is not expressed on cardiomyocytes (Meléndez et al., 2010), which might explain different biological outcomes. However, stimulation of cardiomyocytes with IL-6 trans-signaling via the sIL-6R or IL-11 induces STAT3 phosphorylation, but detrimental effects are only observed for IL-6 trans-signaling. There are, however, at least two possible explanations for these phenomenon: firstly, signal transduction might be different in terms of signal kinetics (duration and intensity), even though IL-6 and IL-11 use the same signal transducing gp130 receptors. Secondly, IL-6 trans-signaling unselectively activates all cells within the heart, which may cause the overall negative outcome in comparison to IL-11, which specifically activates only cardiomyocytes and cardiofibroblasts. These issues might be addressed by activation of IL-11 trans-signaling in all heart cells via an IL-11/sIL-11R fusion protein, as IL-6 and IL11 trans-signaling would not be restricted to IL-6R and IL-11R expressing cells, respectively. We would expect that the net result of IL-6/sIL-6R and IL-11/sIL-11R during ischemia/reperfusion injury would be the same. However, this has to be shown in side-by-side experiments. Alternatively, IL-6 might be modified in a way, that it selectively targets only cardiomyocytes/fibroblasts *in vivo*. This might be achieved by an IL-6 variant that uses IL-11R but not IL-6R as an α-receptor. Here, we would expect that this IL-11R-specific IL-6 variant would act like IL-11. However, if these predictions are not true, than the signal kinetics of IL-6 and IL-11 must be different. It is not clear how different signal kinetics are regulated on the molecular level.

Similarities and dissimilarities of IL-6 and IL-11 in asthma

IL-11 mRNA and protein is largely absent from normal lung tissue and primary lung cells and lung cell lines. However, several stimuli have been shown to induce IL-11 expression in these cells (Elias et al., 1994a,b, 1997). Furthermore, IL-11 is present in secretions from patients with viral respiratory infections (Einarsson et al., 1996). Specific overexpression of IL-11 in the lung using the CC10 promoter (Clara cell 10 kDa protein), resulted in airway obstruction, remodeling of the bronchial space through fibrosis of the subephithelium, and lymphocytic inflammation through accumulation of peribronchiolar mononuclear cells (Tang et al., 1996). Interestingly, the phenotype of transgenic mice for IL-6 under the control of the CC10 promoter was very similar to IL-11 transgenic mice (DiCosmo et al., 1994; Doganci et al., 2005b). In mice, 50–60% of the airway cells are Clara cells (Pack et al., 1981), ensuring a local, lung-restricted distribution of IL-6 and IL-11.

This phenotype observed in mice mimicked in several aspects the pathophysiological situation in human asthmatic patients. Furthermore, IL-11 is highly expressed in patients with moderate and severe forms of asthma, but not in mild forms of asthmatic or healthy humans. IL-11 was expressed in eosinophils as well as epithelial cells, and the amount of IL-11 expression correlated with the severity of the disease (Minshall et al., 2000). However, IL-11 was also shown to selectively block pulmonary eosinophilia caused by aeroallergens and the accompanying TH2-type inflammation (Wang et al., 2000).

Increased levels of IL-6 are found in blood (Yokoyama et al., 1995), bronchoalveolar lavage fluid (BALF) (Broide et al., 1992), and lung tissues (Marini et al., 1992) of asthmatic patients. Moreover, increased levels of sIL-6R have been observed in the airways of patients with allergic asthma (Doganci et al., 2005a,b). TH2 cells are critical allergic driver cells. IL-6 trans-signaling via sIL-6R supports expansion of TH2 effector cells and cytokine production in the lung. At the same time, IL-6 classic signaling suppresses the activity of regulatory T cells (Treg) leading to reduced peripheral tolerance (Pasare and Medzhitov, 2003; Doganci et al., 2005a).

Consequently, administration of anti-IL-6R antibodies that block classic and trans-signaling in experimental asthma leads to cell death of lung effector T cells via activation of regulatory T cells (Finotto et al., 2007). Moreover, a combination of extracellular matrix deposition, inflammation, angiogenesis, and airway smooth muscle (ASM) mass results in airway wall thickening during asthma. Because ASM cells did not express membrane-bound IL-6R, IL-6 trans-signaling may contribute to vessel expansion in airway walls of asthmatic subjects (Ammit et al., 2007).

The IL-6R SNP rs2228145 is a potential modifier of lung function in subjects with asthma and might identify subjects at risk for more severe asthma (Hawkins et al., 2012).

Whereas IL-6 promotes expansion of TH2 cells, IL-11 restricts TH2-driven inflammation in allergic lung diseases. A role of IL-11 on the development of regulatory T cells was not investigated so far. Again on the cellular and molecular level, opposing functions of IL-6 and IL-11 are not understood. A recent study showed that depending on the cell type, IL-11 is able to activate STAT1 and STAT3 or solely STAT1 (Onnis et al., 2013), and differential activation of signal transduction pathways might contribute to divergent outcomes of IL-6 and IL-11 signaling. Again, a detailed analysis of cellular IL-6R and IL-11R expression profiles and cell type specific signal transduction analysis in allergic asthma and other diseases is mandatory.

Regenerative and inflammatory potential of IL-6 and IL-11 in the colon

The IL-11R is expressed in human colonic epithelial cells (Kiessling et al., 2004), also making the colon a target for IL-11 *in vivo*. The pathogen *Citrobacter rodentium* induces barrier disruption of the colon and infiltration of immune cells such as macrophages and neutrophils, which makes it a well-established model for infectious colitis (Eckmann, 2006). Application of recombinant IL-11 to *C. rodentium*-caused colitis in TLR2-deficient mice prevented lethality. IL-11 led to activation of STAT3 in and regeneration of intestinal epithelial cells. In line with this, signaling via TLR2 induced IL-11 expression, which in turn helped to maintain the barrier function of the intestinal epithelium (Gibson et al., 2010). The human leucocyte antigen A variant HLA-B27 is associated with a class of inflammatory diseases known as spondyloarthropathies (Brown et al., 1996). Transgenic rats, which overexpress the human β2-microglobulin together with HLA-B27, have been shown to be a good model of inflammatory diseases, including inflammatory bowel disease (Hammer et al., 1990). These rats showed down-regulation of IFNγ, TNFα and IL-1β when treated with recombinant IL-11 and an overall reduced clinical disease severity score compared to control animals (Peterson et al., 1998). First clinical trials with recombinant hIL-11 for the treatment of Crohn's disease have also shown promising results (Sands et al., 1999, 2002).

Levels of IL-6 in sera correlate with disease severity in inflammatory bowel disease (Hosokawa et al., 1999). Mainly lamina propria mononuclear cells and T cells secrete IL-6 and sIL-6R in Crohn's disease patients. In a T cell transfer colitis mouse model, anti-IL-6R monoclonal antibodies prevented the development of signs and symptoms of colitis (Yamamoto et al., 2000) and the humanized anti-IL-6R monoclonal antibody tocilizumab may be a promising drug for Crohn's disease (Ito et al., 2004). IL-6 trans-signaling but not classic signaling caused detrimental anti-apoptosis of T cells and tissue damage. Consequently, blockage of IL-6 trans-signaling with sgp130Fc suppressed T cell responses in experimental colitis and improved the clinical severity score (Atreya et al., 2000). Blockade of IL-6 trans-signaling also prevented the development of spontaneous ileitis in SAMP1/Yit mice via reduction of STAT3 phosphorylation (Mitsuyama et al., 2006). In addition, like IL-11, IL-6 signaling can stimulate survival and proliferation of intestinal epithelial cells. Abrogation of regenerative pathways in the intestine may explain why IL-6 deficient mice displayed a widespread damage of the colonic mucosa in the non-T cell-dependent DSS-colitis model (Grivennikov et al., 2009). It is not clear if epithelial regeneration is induced by classic or trans-signaling, since intestinal epithelial cells largely lack membrane-bound IL-6R.

Increased expression of pro-inflammatory cytokines, including IL-6, were found in colitis-associated cancer (CAC) patients (Mitsuyama et al., 1991). In a murine model of CAC, IL-6 deficient mice had a decreased tumor load suggesting that IL-6 was necessary for tumor development and growth (Grivennikov et al., 2009). Among others, TGF-β signaling is considered to be a tumor-suppressive pathway, and therefore inactivating mutations within the TGF-β signaling play an important role in CAC development. TGF-β is secreted by tumor infiltrating T cells. Expression of a dominant-negative form of the TGF-βRII (dnTGF-βRII) chain in murine T cells resulted in significantly higher IL-6 levels in the colonic tissue, suggesting a negative regulatory circuit between TGF-β and IL-6 production (Becker et al., 2004, 2005). Consequently, TGF-β suppressed colon cancer tumor progression through the inhibition of IL-6 trans-signaling (Becker et al., 2004). When crossed on an IL-6 deficient background, dnTGF-βRII/IL-6 deficient mice showed reduced signs of colitis but autoimmune cholangitis was exaggerated. It was suggested that therapeutic blockade of IL-6 in autoimmune diseases such as colitis might be undertaken with caution in patients who have accompanying liver diseases (Zhang et al., 2010).

Recently, an unexpected role of IL-11 in CAC-associated metastasis has been described (Calon et al., 2012). Secreted TGF-β from the cancer cells stimulates IL-11 secretion from cancer-associated fibroblasts, which in turn activates STAT3 signaling via gp130 in tumor cells. This circuit increases the survival rate of metastatic cells, thereby enhancing metastasis formation (Calon et al., 2012). In line with this, expression of the IL-11R was shown

to correlate with tumor invasion and lymphatic infiltration of human colorectal adenocarcinomas (Yoshizaki et al., 2006).

Taken together, murine colitis models, which are based on the detrimental activity of the acquired immune response, appear to benefit from the blockade of IL-6 signaling. However, in DSS-induced colitis, which is characterized by a massive destabilization of the intestinal barrier and mainly activates the innate immune system, IL-6 contributes to regeneration of the epithelial barrier and has protective functions. It remains to be seen how both functions of IL-6 contribute to human forms of inflammatory bowel disease, e.g., Crohn's disease and ulcerative colitis. The role of IL-11 may be restricted to the maintenance of the intestinal barrier. However, data from IL-11 deficient mice or blockade of IL-11 are still missing. TGF-β appears to block IL-6 but stimulate IL-11 production, suggesting that IL-6 and IL-11 have in part opposing roles in colitis and CAC.

Requirement of IL-11 but not of IL-6 in gastric tumors

Cytokine signaling is tightly regulated by negative feedback loops. Both the phosphatase SHP2 and SOCS3 bind to the phosphorylated tyrosine residue pY759 (human) / pY757 (mouse) of the IL-6 cytokine family signal transducer gp130. Whereas SHP2 is constantly expressed in the cell and gets phosphorylated and therefore dissociates from the receptor after ligand binding (Lu et al., 2001, 2003), SOCS3 is usually absent, but is synthesized after cytokine binding to terminate signaling. Homozygous gp130–757$^{F/F}$ knock-in mice, where this critical tyrosine is replaced by a phenylalanine, develop gastric hyperplasia and tumors within certain regions of the stomach (Tebbutt et al., 2002). The lack of negative signal regulation in gp130–757$^{F/F}$ knock-in mice leads to hyper-activation of STAT1 and STAT3 signaling and was solely dependent on IL-11. gp130–757$^{F/F}$ mice showed a more than 30-fold up-regulation of IL-11 mRNA within the gastric tumors. Interestingly, gp130–757$^{F/F}$ mice crossed onto an IL-6 deficient background showed no reduction in tumor burden, whereas gp130–757$^{F/F}$:IL-11Ra deficient mice developed no gastric tumors and were indistinguishable from wild-type animals (Ernst et al., 2008).

In another study, four different gastric cancer mouse models were compared. In addition to the gp130–757$^{F/F}$ mice, mice with a specific knock-out for the H^+/K^+ adenosine triphosphatase (ATPase)-β subunit (HK$\beta^{-/-}$, develop gross fundic hyperplasia), transgenic mice overexpressing cyclooxygenase-2 and microsomal prostaglandin E (K19-C2mE, develop hyperplastic fundic tumors) as well as these mice crossed on a K19-Wnt-1 background (K19-Wnt1/C2mE, develop dysplastic fundic tumors) were analyzed for IL-11 expression. In all mouse models, IL-11 mRNA was drastically up-regulated within the tumor tissue. The same was found in biopsies from human gastric cancer patients. Gastric tumor size was diminished in gp130–757$^{F/F}$ and HK$\beta^{-/-}$ mice when crossed onto an IL-11R$^{-/-}$ background. Furthermore, the authors show that chronic treatment with IL-11 induces pre-tumorigenic changes in fundus and antrum of wild-type mice (Howlett et al., 2009). These data emphasize an important role of IL-11 in the development and maintenance of gastric tumorigenesis in mice and men.

Recently, it has been shown that STAT3 phosphorylation is significantly increased in biopsies from human patients with *H. pylori*-dependent gastritis (Jackson et al., 2007). This was accompanied by elevated expression of IL-6 and IL-11 in the biopsies, and the authors concluded that the STAT3 activation is driven by IL-11, which causes gastric cancer progression and leads to enhanced cellular proliferation (Jackson et al., 2007). In another analysis of human gastric adenocarcinomas, the expression of IL-11R correlated with vessel infiltration as well as tumor invasion (Nakayama et al., 2007). Taken together, these results clearly show that gastric tumor formation is critically dependent on IL-11.

Even though IL-6 has not been shown to play a role in gastric tumor development, IL-6 expression is found in the human stomach, and elevated in precancerous lesions (Jackson et al., 2007) as well as in gastric adenocarcinoma (Kabir and Daar, 1995; Jackson et al., 2007). sIL-6R had not been analyzed thus far. Moreover, serum IL-6 levels are positively correlated with stage, lymphatic invasion and metastasis (Wu et al., 1996; Tang et al., 2006) and negatively with gastric cancer survival (Tang et al., 2006). Interestingly, IL-6 and IL-11 were increased in gastric mucosa, correlating with staging but only IL-6 and not IL-11 showed a significant correlation with patient's survival time (Necula et al., 2012). The role of IL-6 in *H. pylori*-induced chronic gastritis and other pre-neoplastic lesions in human gastric cancer development was, however, not investigated thus far.

Funtional role of IL-6 and IL-11 in bone homeostasis

Cytokines of the IL-6 family are involved in bone homeostasis and contribute to osteopenia and osteoporosis.

Furthermore, they play a role in bone tumor formation. The human breast cancer cell line MDA-MB-231 is known to form osteolytic bone metastasis in mice, and this activity is increased by TGFβ (Yin et al., 1999). When the gene expression signature that was associated with the osteolytic bone metastatic activity was analyzed, one of the genes whose expression correlates with strong metastatic activity was IL-11 (Kang et al., 2003).

Furthermore, IL-11R was shown to be highly expressed in osteosarcoma cell lines (Lewis et al., 2009). In an orthotopic metastatic mouse model of osteosarcoma, where osteosarcoma cells are injected directly into the tibia, IL-11R expression was localized to the intratibial lesion, whereas it was absent from normal bone. IL-11R was also detectable in metastatic lesions in the lung. In line with this, high IL-11R expression was found in patient samples of primary osteosarcoma and lung metastatic tumors derived from there (Lewis et al., 2009).

Bone metabolism and maintenance critically depends on the balanced activity of osteoblasts and osteoclasts. Transgenic overexpression of IL-11 in mice led to increased osteoblastogenesis, which resulted in the prevention of bone mass loss during aging (Takeuchi et al., 2002). In contrast, transgenic mice overexpressing IL-6 showed in an insulin-like growth factor (IGF-)1 dependent growth defect, mimicking the retarded growth accompanying human chronic inflammatory diseases (De Benedetti et al., 1997). Moreover during pre-puberty, these mice exhibit accelerated bone resorption, reduced bone formation, and defective ossification caused by increased osteoclastogenesis, and reduced osteoblast activity (De Benedetti et al., 2006). Surprisingly, this phenotype vanishes in adulthood (Kitamura et al., 1995; De Benedetti et al., 2006), which suggests that the influence of IL-6 on bone homeostasis depends on the stage of development. Estrogen blocks osteoclast differentiation via interfering with RANKL activity. IL-6 appears to be a crucial factor for osteoclast differentiation, whenever estrogen-induced blockade of osteoclast differentiation is abrogated because IL-6 deficient mice are protected from bone loss caused by estrogen depletion (ovariectomy) (Poli et al., 1994). Under inflammatory conditions of experimental arthritis, IL-6 deficient mice have reduced osteoclastogenesis and osteoclast recruitment to the inflamed joint and reduced joint destruction (Wong et al., 2006). Consequently, blockade of IL-6 signaling has been approved for treatment of RA and also inhibits local bone resorption in RA (Hashimoto et al., 2011), indicating that IL-6 contributes to bone loss and joint erosions in RA. Osteoclasts were identified as the key cell type-mediating erosions in inflammatory arthritis (Walsh et al., 2005). Mechanistically, IL-6 trans-signaling via the sIL-6R promotes RANKL expression/secretion from stromal/osteoblastic cells, which subsequently causes osteoclastogenesis (Palmqvist et al., 2002). RANKL is expressed by synovial fibroblasts (Gravallese et al., 2000), osteoblasts (Kong et al., 1999), and activated T lymphocytes (Kotake et al., 2001), which lack reasonable expression of membrane-bound IL-6R and are therefore unresponsive to classic signaling. T cells lose their IL-6R expression during activation via ectodomain shedding (Briso et al., 2008). Controversely, IL-6 classic signaling via the membrane-bound IL-6R can directly activate osteoclast progenitor cells and inhibit osteoclastogenesis (Yoshitake et al., 2008). The authors speculate that under physiological conditions, which are characterized by low concentrations of sIL-6R, IL-6 classic signaling suppresses bone resorption by inhibiting the differentiation of osteoclast progenitors. Under inflammatory conditions, characterized by increased concentrations of sIL-6R, IL-6 trans-signaling can activate osteoblasts to support bone loss, whereas IL-6 classic signaling still activates osteoblasts to block bone loss (Yoshitake et al., 2008). Depending on the ratio of IL-6 and sIL-6R classic or trans-signaling dominates (Garbers et al., 2011), leading to bone loss (more IL-6 trans-signaling) or bone formation (more IL-6 classic signaling). The situation might be even more complicated, as IL-6R expressing osteoclasts can also respond to IL-6 trans-signaling. However, if the hypothesis is correct, that IL-6 trans-signaling promotes bone loss and IL-6 classic signaling inhibits bone loss, than IL-6 transgenic mice, crossed to sgp130Fc expressing mice, which should still allow IL-6 classic but not IL-6 trans-signaling, should not develop the pre-puberty bone loss phenotype of IL-6 transgenic mice.

Concluding remarks

IL-6 and IL-11 are the only IL-6 type cytokines that signal via a homodimeric gp130 receptor. Therefore, one might expect similar or even identical biological outcomes of IL-6 and IL-11. However, it appears that only limited functional overlap or redundancy exists between IL-6 and IL-11. In contrast, we have illustrated examples of apparently opposing functions of IL-6 and IL-11. This might be explained by the restricted and at least in part different expression patterns of IL-6R and IL-11R (Figure 2). On cells that express both receptors, such as hepatocytes, IL-6 and IL-11 can induce the same biological outcome, e.g., the induction of the acute-phase response (Benigni et al., 1996). It remains to be seen whether the observed

biological differences of IL-6 and IL-11 are simply caused by different IL-6R and IL-11R expression patterns, or if more sophisticated differences exist in signal dynamics and kinetics. Some data might also point to the latter and both cytokines play important roles *in vivo* and have made their way into the clinic. IL-6 is one of the major novel targets for treatment of patients with chronic inflammatory diseases. Therapies with tailor-made monoclonal antibodies specifically targeting IL-6 did, however, not consider the pro- and anti-inflammatory/regenerative properties of IL-6. IL-6 trans-signaling appears to be specifically activated under immunological stress conditions such as chronic inflammation and cancer. Selective inhibition of IL-6 trans-signaling, which leaves intact essential parts of innate immunity, such as the acute-phase response, emerges as an alternative therapeutic strategy. In contrast, application of the cytokine IL-11 is used to accelerate recovery of the hematopoietic system after cancer therapy. However, recent data unravel a role of IL-11 in tumor development and first IL-11 antagonists are currently under development. In the future, major progress has to be made in the understanding of IL-6 and IL-11 biology because both cytokines promise high potential as therapeutic targets in human diseases.

Acknowledgements: This work was funded by grants from the Deutsche Forschungsgemeinschaft, Bonn, Germany (to J.S. – DFG SCHE 907/2) and the Research Commission of the Medical Faculty of the Heinrich-Heine-University (to C.G. and J.S.).

Received May 2, 2013; accepted May 30, 2013; previously published online June 4, 2013

References

Adam, N., Rabe, B., Suthaus, J., Grötzinger, J., Rose-John, S., and Scheller, J. (2009). Unraveling viral interleukin 6 binding to gp130 and activation of STAT-signaling pathways independent of interleukin 6-receptor. J. Virol. *83*, 5117–5126.

Aitsebaomo, J., Srivastava, S., Zhang, H., Jha, S., Wang, Z., Winnik, S., Veleva, A., Pi, X., Lockyer, P., Faber, J., et al. (2011). Recombinant human interleukin-11 treatment enhances collateral vessel growth after femoral artery ligation. Arterioscler. Thromb. Vasc. Biol. *31*, 306–312.

Ammit, A.J., Moir, L.M., Oliver, B.G., Hughes, J.M., Alkhouri, H., Ge, Q., Burgess, J.K., Black, J.L., and Roth, M. (2007). Effect of IL-6 trans-signaling on the pro-remodeling phenotype of airway smooth muscle. Am. J. Physiol. Lung Cell Mol. Physiol. *292*, 199–206.

Atreya, R., Mudter, J., Finotto, S., Müllberg, J., Jostock, T., Wirtz, S., Schütz, M., Bartsch, B., Holtmann, M., Becker, C., et al. (2000). Blockade of interleukin 6 trans signaling suppresses T-cell resistance against apoptosis in chronic intestinal inflammation: evidence in crohn disease and experimental colitis in vivo. Nat. Med. *6*, 583–588.

Bazan, J.F. (1989). A novel family of growth factor receptors: a common binding domain in the growth hormone, prolactin, erythropoietin and IL-6 receptors, and the p75 IL-2 receptor β-chain. Biochem. Biophys. Res. Commun. *164*, 788–795.

Bazan, J.F. (1990). Haemopoietic receptors and helical cytokines. Immunol. Today *11*, 350–354.

Becker, C., Fantini, M.C., Schramm, C., Lehr, H.A., Wirtz, S., Nikolaev, A., Burg, J., Strand, S., Kiesslich, R., Huber, S., et al. (2004). TGF-β suppresses tumor progression in colon cancer by inhibition of IL-6 trans-signaling. Immunity *21*, 491–501.

Becker, C., Fantini, M.C., Wirtz, S., Nikolaev, A., Lehr, H.A., Galle, P.R., Rose-John, S., and Neurath, M.F. (2005). IL-6 signaling promotes tumor growth in colorectal cancer. Cell Cycle *4*, 217–220.

Benigni, F., Fantuzzi, G., Sacco, S., Sironi, M., Pozzi, P., Dinarello, C.A., Sipe, J.D., Poli, V., Cappelletti, M., Paonessa, G., et al. (1996). Six different cytokines that share GP130 as a receptor subunit, induce serum amyloid A and potentiate the induction of interleukin-6 and the activation of the hypothalamus-pituitary-adrenal axis by interleukin-1. Blood *87*, 1851–1854.

Boulanger, M.J., Bankovich, A.J., Kortemme, T., Baker, D., and Garcia, K.C. (2003). Convergent mechanisms for recognition of divergent cytokines by the shared signaling receptor gp130. Mol. Cell *12*, 577–589.

Briso, E.M., Dienz, O., and Rincon, M. (2008). Cutting edge: soluble IL-6R is produced by IL-6R ectodomain shedding in activated CD4 T cells. J. Immunol. *180*, 7102–7106.

Broide, D.H., Lotz, M., Cuomo, A.J., Coburn, D.A., Federman, E.C., and Wasserman, S.I. (1992). Cytokines in symptomatic asthma airways. J. Allergy Clin. Immunol. *89*, 958–967.

Brown, M.A., Pile, K.D., Kennedy, L.G., Calin, A., Darke, C., Bell, J., Wordsworth, B.P., and Cornélis, F. (1996). HLA class I associations of ankylosing spondylitis in the white population in the United Kingdom. Ann. Rheum. Dis. *55*, 268–277.

Calon, A., Espinet, E., Palomo-Ponce, S., Tauriello, D., Iglesias, M., Céspedes, M., Sevillano, M., Nadal, C., Jung, P., Zhang, X., et al. (2012). Dependency of colorectal cancer on a TGF-β-driven program in stromal cells for metastasis initiation. Cancer Cell *22*, 571–584.

Camporeale, A., Marino, F., Papageorgiou, A., Carai, P., Fornero, S., Fletcher, S., Page, B.D., Gunning, P., Forni, M., Chiarle, R., et al. (2013). STAT3 activity is necessary and sufficient for the development of immune-mediated myocarditis in mice and promotes progression to dilated cardiomyopathy. EMBO Mol. Med. *5*, 572–590.

Chalaris, A., Garbers, C., Rabe, B., Rose-John, S., and Scheller, J. (2011). The soluble Interleukin 6 receptor: generation and role in inflammation and cancer. Eur. J. Cell Biol. *90*, 484–494.

Chow, D., He, X., Snow, A.L., Rose-John, S., and Garcia, K.C. (2001). Structure of an extracellular gp130 cytokine receptor signaling complex. Science *291*, 2150–2155.

Coles, B., Fielding, C.A., Rose-John, S., Scheller, J., Jones, S.A., and O'Donnell, V.B. (2007). Classic interleukin-6 receptor signaling and interleukin-6 trans-signaling differentially control angiotensin II-dependent hypertension, cardiac signal transducer and activator of transcription-3 activation, and vascular hypertrophy in vivo. Am. J. Pathol. *171*, 315–325.

Collaboration, I. R. G. C. E. R. F. (2012). Interleukin-6 receptor pathways in coronary heart disease: a collaborative meta-analysis of 82 studies. Lancet *379*, 1205–1213.

Collison, L.W., Delgoffe, G.M., Guy, C.S., Vignali, K.M., Chaturvedi, V., Fairweather, D., Satoskar, A.R., Garcia, K.C., Hunter, C.A., Drake, C.G., et al. (2012). The composition and signaling of the IL-35 receptor are unconventional. Nat. Immunol. *13*, 290–299.

Consortium, T. I.-R. M. R. A. I. R. M. (2012). The interleukin-6 receptor as a target for prevention of coronary heart disease: a mendelian randomisation analysis. Lancet *379*, 1214–1224.

Curtis, D.J., Hilton, D.J., Roberts, B., Murray, L., Nicola, N., and Begley, C.G. (1997). Recombinant soluble interleukin-11 (IL-11) receptor α-chain can act as an IL-11 antagonist. Blood *90*, 4403–4412.

Dawn, B., Xuan, Y.T., Guo, Y., Rezazadeh, A., Stein, A.B., Hunt, G., Wu, W.J., Tan, W., and Bolli, R. (2004). IL-6 plays an obligatory role in late preconditioning via JAK-STAT signaling and upregulation of iNOS and COX-2. Cardiovas. Res. *64*, 61–71.

De Benedetti, F., Alonzi, T., Moretta, A., Lazzaro, D., Costa, P., Poli, V., Martini, A., Ciliberto, G., and Fattori, E. (1997). Interleukin 6 causes growth impairment in transgenic mice through a decrease in insulin-like growth factor-I. A model for stunted growth in children with chronic inflammation. J. Clin. Invest. *99*, 643–650.

De Benedetti, F., Rucci, N., Del Fattore, A., Peruzzi, B., Paro, R., Longo, M., Vivarelli, M., Muratori, F., Berni, S., Ballanti, P., et al. (2006). Impaired skeletal development in interleukin-6-transgenic mice: a model for the impact of chronic inflammation on the growing skeletal system. Arthritis Rheum. *54*, 3551–3563.

DiCosmo, B.F., Geba, G.P., Picarella, D., Elias, J.A., Rankin, J.A., Stripp, B.R., Whitsett, J. A., and Flavell, R.A. (1994). Airway epithelial cell expression of interleukin-6 in transgenic mice. Uncoupling of airway inflammation and bronchial hyperreactivity. J. Clin. Invest. *94*, 2028–2035.

Doganci, A., Eigenbrod, T., Krug, N., De Sanctis, G.T., Hausding, M., Erpenbeck, V.J., Haddad, E.-B., Lehr, H.A., Schmitt, E., Bopp, T., et al. (2005a). The IL-6R alpha chain controls lung $CD4^+CD25^+$ Treg development and function during allergic airway inflammation *in vivo*. J. Clin. Invest. *115*, 313–325.

Doganci, A., Sauer, K., Karwot, R., and Finotto, S. (2005b). Pathological role of IL-6 in the experimental allergic bronchial asthma in mice. Clin. Rev. Allergy Immunol. *28*, 257–270.

Du, X. and Williams, D. (1997). Interleukin-11: review of molecular, cell biology, and clinical use. Blood *89*, 3897–3908.

Eckmann, L. (2006). Animal models of inflammatory bowel disease: lessons from enteric infections. Ann. N. Y. Acad. Sci. *1072*, 28–38.

Einarsson, O., Geba, G., Zhu, Z., Landry, M., and Elias, J. (1996). Interleukin-11: stimulation in vivo and in vitro by respiratory viruses and induction of airways hyperresponsiveness. J. Clin. Invest. *97*, 915–924.

Elias, J., Zheng, T., Einarsson, O., Landry, M., Trow, T., Rebert, N., and Panuska, J. (1994a). Epithelial interleukin-11. Regulation by cytokines, respiratory syncytial virus, and retinoic acid. J. Biol. Chem. *269*, 22261–22268.

Elias, J., Zheng, T., Whiting, N., Trow, T., Merrill, W., Zitnik, R., Ray, P., and Alderman, E. (1994b). IL-1 and transforming growth factor-beta regulation of fibroblast-derived IL-11. J. Immunol. *152*, 2421–2429.

Elias, J., Wu, Y., Zheng, T., and Panettieri, R. (1997). Cytokine- and virus-stimulated airway smooth muscle cells produce IL-11 and other IL-6-type cytokines. Am. J. Physiol. *273*, 648–655.

Ellingsgaard, H., Ehses, J.A., Hammar, E.B., Van Lommel, L., Quintens, R., Martens, G., Kerr-Conte, J., Pattou, F., Berney, T., Pipeleers, D., et al. (2008). Interleukin-6 regulates pancreatic α-cell mass expansion. Proc. Natl. Acad. Sci. USA *105*, 13163–13168.

Ernst, M., Najdovska, M., Grail, D., Lundgren-May, T., Buchert, M., Tye, H., Matthews, V., Armes, J., Bhathal, P., Hughes, N., et al. (2008). STAT3 and STAT1 mediate IL-11-dependent and inflammation-associated gastric tumorigenesis in gp130 receptor mutant mice. J. Clin. Invest. *118*, 1727–1738.

Eulenfeld, R., Dittrich, A., Khouri, C., Muller, P. J., Mutze, B., Wolf, A., and Schaper, F. (2012). Interleukin-6 signalling: more than Jaks and STATs. Eur. J. Cell Biol. *91*, 486–495.

Ferreira, R.C., Freitag, D.F., Cutler, A.J., Howson, J.M.M., Rainbow, D.B., Smyth, D.J., Kaptoge, S., Clarke, P., Boreham, C., Coulson, R.M., et al. (2013). Functional IL6R 358Ala allele impairs classical IL-6 receptor signaling and influences risk of diverse inflammatory diseases. PLos Genetics *9*, e100344.

Finotto, S., Eigenbrod, T., Karwot, R., Boross, I., Doganci, A., Ito, H., Nishimoto, N., Yoshizaki, K., Kishimoto, T., Rose-John, S., et al. (2007). Local blockade of IL-6R signaling induces lung $CD4^+$ T cell apoptosis in a murine model of asthma via regulatory T cells. Int. Immunol. *19*, 685–693.

Fleischmann, R., Kremer, J., Cush, J., Schulze-Koops, H., Connell, C., Bradley, J., Gruben, D., Wallenstein, G., Zwillich, S., Kanik, K., et al. (2012). Placebo-controlled trial of tofacitinib monotherapy in rheumatoid arthritis. N. Engl. J. Med. *367*, 495–507.

Fujio, Y., Maeda, M., Mohri, T., Obana, M., Iwakura, T., Hayama, A., Yamashita, T., Nakayama, H., and Azuma, J. (2011). Glycoprotein 130 cytokine signal as a therapeutic target against cardiovascular diseases. J. Pharmacol. Sci. *117*, 213–222.

Gaillard, J.P., Bataille, R., Brailly, H., Zuber, C., Yasukawa, K., Attal, M., Maruo, N., Taga, T., Kishimoto, T., and Klein, B. (1993). Increased and highly stable levels of functional soluble interleukin-6 receptor in sera of patients with monoclonal gammopathy. Eur. J. Immunol. *23*, 820–824.

Galicia, J., Tai, H., Komatsu, Y., Shimada, Y., Akazawa, K., and Yoshie, H. (2004). Polymorphisms in the IL-6 receptor (IL-6R) gene: strong evidence that serum levels of soluble IL-6R are genetically influenced. Genes Immunity *5*, 513–516.

Garbers, C., Thaiss, W., Jones, G.W., Waetzig, G.H., Lorenzen, I., Guilhot, F., Lissilaa, R., Ferlin, W.G., Grotzinger, J., Jones, S.A., et al. (2011). Inhibition of classic signaling is a novel function of soluble glycoprotein 130 (sgp130), which is controlled by the ratio of interleukin 6 and soluble interleukin 6 receptor. J. Biol. Chem. *286*, 42959–42970.

Garbers, C., Hermanns, H.M., Schaper, F., Müller-Newen, G., Grötzinger, J., Rose-John, S., and Scheller, J. (2012). Plasticity

and cross-talk of interleukin 6-type cytokines. Cytokine Growth Factor Rev. *23*, 85–97.

Garbers, C., Spudy, B., Aparicio-Siegmund, S., Waetzig, G.H., Sommer, J., Hölscher, C., Rose-John, S., Grötzinger, J., Lorenzen, I., and Scheller, J. (2013). An interleukin-6 receptor-dependent molecular switch mediates signal transduction of the IL-27 cytokine subunit p28 (IL-30) via a gp130 protein receptor homodimer. J. Biol. Chem. *288*, 4346–4354.

Gibson, D., Montero, M., Ropeleski, M., Bergstrom, K., Ma, C., Ghosh, S., Merkens, H., Huang, J., Månsson, L., Sham, H., et al. (2010). Interleukin-11 reduces TLR4-induced colitis in TLR2-deficient mice and restores intestinal STAT3 signaling. Gastroenterology *139*, 1277–1288.

Gravallese, E.M., Manning, C., Tsay, A., Naito, A., Pan, C., Amento, E., and Goldring, S.R. (2000). Synovial tissue in rheumatoid arthritis is a source of osteoclast differentiation factor. Arthritis Rheum. *43*, 250–258.

Grivennikov, S., Karin, E., Teric, J., Mucida, D., Yu, G.Y., Vallabhapurapu, S., Scheller, J., Rose-John, S., Cheroutre, H., Eckmann, L., et al. (2009). IL-6 and STAT3 are required for survival of intestinal epithelial cells and development of colitis associated cancer. Cancer Cell *15*, 103–113.

Haan, C., Rolvering, C., Raulf, F., Kapp, M., Drückes, P., Thoma, G., Behrmann, I., and Zerwes, H.G. (2011). Jak1 has a dominant role over Jak3 in signal transduction through γc-containing cytokine receptors. Chem. Biol. *18*, 314–323.

Hammer, R., Maika, S., Richardson, J., Tang, J., and Taurog, J. (1990). Spontaneous inflammatory disease in transgenic rats expressing HLA-B27 and human β2m: an animal model of HLA-B27-associated human disorders. Cell *63*, 1099–1112.

Hashimoto, J., Garnero, P., van der Heijde, D., Miyasaka, N., Yamamoto, K., Kawai, S., Takeuchi, T., Yoshikawa, H., and Nishimoto, N. (2011). Humanized anti-interleukin-6-receptor antibody (tocilizumab) monotherapy is more effective in slowing radiographic progression in patients with rheumatoid arthritis at high baseline risk for structural damage evaluated with levels of biomarkers, radiography, and BMI: data from the SAMURAI study. Mod. Rheumatol. *21*, 10–15.

Hawkins, G.A., Robinson, M.B., Hastie, A.T., Li, X., Li, H., Moore, W.C., Howard, T.D., Busse, W.W., Erzurum, S.C., Wenzel, S.E., et al. (2012). The IL6R variation Asp(358)Ala is a potential modifier of lung function in subjects with asthma. J. Allergy Clin. Immunol. *130*, 510–515.

Heinrich, P., Behrmann, I., Haan, S., Hermanns, H., Müller-Newen, G., and Schaper, F. (2003). Principles of interleukin (IL)-6-type cytokine signalling and its regulation. Biochem. J. *374*, 1–20.

Hirota, H., Yoshida, K., Kishimoto, T., and Taga, T. (1995). Continuous activation of gp130, a signal-transducing receptor component for interleukin 6-related cytokines, causes myocardial hypertrophy in mice. Proc. Natl. Acad. Sci. USA *92*, 4862.

Hosokawa, T., Kusugami, K., Ina, K., Ando, T., Shinoda, M., Imada, A., Ohsuga, M., Sakai, T., Matsuura, T., Ito, K., et al. (1999). Interleukin-6 and soluble interleukin-6 receptor in the colonic mucosa of inflammatory bowel disease. J. Gastroenterol. Hepatol. *14*, 987–996.

Howlett, M., Giraud, A., Lescesen, H., Jackson, C., Kalantzis, A., Van Driel, I., Robb, L., Van der Hoek, M., Ernst, M., Minamoto, T., et al. (2009). The interleukin-6 family cytokine interleukin-11 regulates homeostatic epithelial cell turnover and promotes gastric tumor development. Gastroenterology *136*, 967–977.

Ito, H., Takazoe, M., Fukuda, Y., Hibi, T., Kusugami, K., Andoh, A., Matsumoto, T., Yamamura, T., Azuma, J., Nishimoto, N., et al. (2004). A pilot randomized trial of a human anti-interleukin-6 receptor monoclonal antibody in active Crohn's disease. Gastroenterology *126*, 989–996.

Jackson, C.B., Judd, L.M., Menheniott, T.R., Kronborg, I., Dow, C., Yeomans, N.D., Boussioutas, A., Robb, L., and Giraud, A.S. (2007). Augmented gp130-mediated cytokine signalling accompanies human gastric cancer progression. J. Pathol. *213*, 140–151.

Jiang, J.K., Ghoreschi, K., Deflorian, F., Chen, Z., Perreira, M., Pesu, M., Smith, J., Nguyen, D.T., Liu, E.H., Leister, W., et al. (2008). Examining the chirality, conformation and selective kinase inhibition of 3-((3R,4R)-4-methyl-3-(methyl(7H-pyrrolo[2,3-d] pyrimidin-4-yl)amino)piperidin-1-yl)-3-oxopropanenitrile (CP-690,550). J. Med. Chem. *51*, 8012–8018.

Jones, S.A., Scheller, J., and Rose-John, S. (2011). Therapeutic strategies for the clinical blockade of IL-6/gp130 signaling. J. Clin. Invest. *121*, 3375–3383.

Jostock, T., Mullberg, J., Ozbek, S., Atreya, R., Blinn, G., Voltz, N., Fischer, M., Neurath, M.F., and Rose-John, S. (2001). Soluble gp130 is the natural inhibitor of soluble interleukin-6 receptor transsignaling responses. Eur. J. Biochem. *268*, 160–167.

Kabir, S. and Daar, G.A. (1995). Serum levels of interleukin-1, interleukin-6 and tumour necrosis factor-α in patients with gastric carcinoma. Cancer Lett. *95*, 207–212.

Kanda, T., Inoue, M., Kotajima, N., Fujimaki, S., Hoshino, Y., Kurabayashi, M., Kobayashi, I., and Tamura, J. (2000). Circulating interleukin-6 and interleukin-6 receptors in patients with acute and recent myocardial infarction. Cardiology *93*, 191–196.

Kang, Y., Siegel, P., Shu, W., Drobnjak, M., Kakonen, S., Cordón-Cardo, C., Guise, T., and Massagué, J. (2003). A multigenic program mediating breast cancer metastasis to bone. Cancer Cell *3*, 537–549.

Kiessling, S., Muller-Newen, G., Leeb, S., Hausmann, M., Rath, H., Strater, J., Spottl, T., Schlottmann, K., Grossmann, J., Montero-Julian, F., et al. (2004). Functional expression of the interleukin-11 receptor alpha-chain and evidence of antiapoptotic effects in human colonic epithelial cells. J. Biol. Chem. *279*, 10304–10315.

Kimura, R., Maeda, M., Arita, A., Oshima, Y., Obana, M., Ito, T., Yamamoto, Y., Mohri, T., Kishimoto, T., Kawase, I., et al. (2007). Identification of cardiac myocytes as the target of interleukin 11, a cardioprotective cytokine. Cytokine *38*, 107–115.

Kitamura, H., Kawata, H., Takahashi, F., Higuchi, Y., Furuichi, T., and Ohkawa, H. (1995). Bone marrow neutrophilia and suppressed bone turnover in human interleukin-6 transgenic mice. A cellular relationship among hematopoietic cells, osteoblasts, and osteoclasts mediated by stromal cells in bone marrow. Am. J. Pathol. *147*, 1682–1692.

Kobara, M., Noda, K., Kitamura, M., Okamoto, A., Shiraishi, T., Toba, H., Matsubara, H., and Nakata, T. (2010). Antibody against interleukin-6 receptor attenuates left ventricular remodelling after myocardial infarction in mice. Cardiovas. Res. *87*, 424–430.

Kong, Y.Y., Feige, U., Sarosi, I., Bolon, B., Tafuri, A., Morony, S., Capparelli, C., Li, J., Elliott, R., McCabe, S., et al. (1999).

Activated T cells regulate bone loss and joint destruction in adjuvant arthritis through osteoprotegerin ligand. Nature *402*, 304–309.

Kotake, S., Udagawa, N., Hakoda, M., Mogi, M., Yano, K., Tsuda, E., Takahashi, K., Furuya, T., Ishiyama, S., Kim, K.J., et al. (2001). Activated human T cells directly induce osteoclastogenesis from human monocytes: possible role of T cells in bone destruction in rheumatoid arthritis patients. Arthritis Rheum. *44*, 1003–1012.

Ladenburger, A., Seehase, M., Kramer, B., Thomas, W., Wirbelauer, J., Speer, C., and Kunzmann, S. (2010). Glucocorticoids potentiate IL-6-induced SP-B expression in H441 cells by enhancing the JAK-STAT signaling pathway. American Journal of Physiology. Lung Cell Mol. Physiol. *299*, 84.

Lee, C., Hartl, D., Matsuura, H., Dunlop, F., Scotney, P., Fabri, L., Nash, A., Chen, N.-Y., Tang, C.-Y., Chen, Q., et al. (2008). Endogenous IL-11 signaling is essential in Th2- and IL-13-induced inflammation and mucus production. Am. J. Respir. Cell Mol. Biol. *39*, 739–746.

Lewis, V., Ozawa, M., Deavers, M., Wang, G., Shintani, T., Arap, W., and Pasqualini, R. (2009). The interleukin-11 receptor α as a candidate ligand-directed target in osteosarcoma: consistent data from cell lines, orthotopic models, and human tumor samples. Cancer Res. *69*, 1995–1999.

Liao, W., Lin, J.-X., Wang, L., Li, P., and Leonard, W. (2011). Modulation of cytokine receptors by IL-2 broadly regulates differentiation into helper T cell lineages. Nat. Immunol. *12*, 551–559.

Litt, M.R., Jeremy, R.W., Weisman, H.F., Winkelstein, J.A., and Becker, L.C. (1989). Neutrophil depletion limited to reperfusion reduces myocardial infarct size after 90 minutes of ischemia. Evidence for neutrophil-mediated reperfusion injury. Circulation *80*, 1816–1827.

Lu, Z.Y., Brochier, J., Wijdenes, J., Brailly, H., Bataille, R., and Klein, B. (1992). High amounts of circulating interleukin (IL)-6 in the form of monomeric immune complexes during anti-IL-6 therapy. Towards a new methodology for measuring overall cytokine production in human *in vivo*. Eur. J. Biochem. *22*, 2819–2824.

Lu, W., Gong, D., Bar-Sagi, D., and Cole, P.A. (2001). Site-specific incorporation of a phosphotyrosine mimetic reveals a role for tyrosine phosphorylation of SHP-2 in cell signaling. Mol. Cell *8*, 759–769.

Lu, W., Shen, K., and Cole, P.A. (2003). Chemical dissection of the effects of tyrosine phosphorylation of SHP-2. Biochemistry *42*, 5461–5468.

Lupardus, P.J., Skiniotis, G., Rice, A.J., Thomas, C., Fischer, S., Walz, T., and Garcia, K.C. (2011). Structural snapshots of full-length Jak1, a transmembrane gp130/IL-6/IL-6Rα cytokine receptor complex, and the receptor-Jak1 holocomplex. Structure *19*, 45–55.

Marini, M., Vittori, E., Hollemborg, J., and Mattoli, S. (1992). Expression of the potent inflammatory cytokines, granulocyte-macrophage-colony-stimulating factor and interleukin-6 and interleukin-8, in bronchial epithelial cells of patients with asthma. J. Allergy Clin. Immunol. *89*, 1001–1009.

Matadeen, R., Hon, W.C., Heath, J.K., Jones, E.Y., and Fuller, S. (2007). The dynamics of signal triggering in a gp130-receptor complex. Structure *15*, 441–448.

McFarland-Mancini, M.M., Funk, H.M., Paluch, A.M., Zhou, M., Giridhar, P.V., Mercer, C.A., Kozma, S.C., and Drew, A.F. (2010). Differences in wound healing in mice with deficiency of IL-6 versus IL-6 receptor. J. Immunol. *184*, 7219–7228.

Meléndez, G.C., McLarty, J.L., Levick, S.P., Du, Y., Janicki, J.S., and Brower, G.L. (2010). Interleukin 6 mediates myocardial fibrosis, concentric hypertrophy, and diastolic dysfunction in rats. Hypertension *56*, 225–231.

Minshall, E., Chakir, J., Laviolette, M., Molet, S., Zhu, Z., Olivenstein, R., Elias, J., and Hamid, Q. (2000). IL-11 expression is increased in severe asthma: association with epithelial cells and eosinophils. J. Allergy Clin. Immunol. *105*, 232–238.

Mir, S.A., Chatterjee, A., Mitra, A., Pathak, K., Mahata, S.K., and Sarkar, S. (2012). Inhibition of signal transducer and activator of transcription 3 (STAT3) attenuates interleukin-6 (IL-6)-induced collagen synthesis and resultant hypertrophy in rat heart. J. Biol. Chem. *287*, 2666–2677.

Mitsuyama, K., Sasaki, E., Toyonaga, A., Ikeda, H., Tsuruta, O., Irie, A., Arima, N., Oriishi, T., Harada, K., Fujisaki, K., et al. (1991). Colonic mucosal interleukin-6 in inflammatory bowel disease. Digestion *50*, 104–111.

Mitsuyama, K., Toyonaga, A., Sasaki, E., Ishida, O., Ikeda, H., Tsuruta, O., Harada, K., Tateishi, H., Nishiyama, T., and Tanikawa, K. (1995). Soluble interleukin-6 receptors in inflammatory bowel disease: relation to circulating interleukin-6. Gut *36*, 45–49.

Mitsuyama, K., Matsumoto, S., Rose-John, S., Suzuki, A., Hara, T., Tomiyasu, N., Handa, K., Tsuruta, O., Funabashi, H., Scheller, J., et al. (2006). STAT3 activation via interleukin-6 trans-signaling contributes to ileitis in SAMP1/Yit mice. Gut *55*, 1263–1269.

Mohr, A., Chatain, N., Domoszlai, T., Rinis, N., Sommerauer, M., Vogt, M., and Müller-Newen, G. (2012). Dynamics and non-canonical aspects of JAK/STAT signalling. Eur. J. Cell Biol. *91*, 524–532.

Montero-Julian, F.A. (2001). The soluble IL-6 receptors: serum levels and biological function. Cell. Mol. Biol. *47*, 583–597.

Müller-Newen, G., Küster, A., Hemmann, U., Keul, R., Horsten, U., Martens, A., Graeve, L., Wijdenes, J., and Heinrich, P.C. (1998). Soluble IL-6 receptor potentiates the antagonistic activity of soluble gp130 on IL-6 responses. J. Immunol. *161*, 6347–6355.

Nakayama, T., Yoshizaki, A., Izumida, S., Suehiro, T., Miura, S., Uemura, T., Yakata, Y., Shichijo, K., Yamashita, S., and Sekin, I. (2007). Expression of interleukin-11 (IL-11) and IL-11 receptor α in human gastric carcinoma and IL-11 upregulates the invasive activity of human gastric carcinoma cells. Int. J. Oncol. *30*, 825–833.

Necula, L.G., Chivu-Economescu, M., Stanciulescu, E.L., Bleotu, C., Dima, S.O., Alexiu, I., Dumitru, A., Constantinescu, G., Popescu, I., and Diaconu, C.C. (2012). IL-6 and IL-11 as markers for tumor aggressiveness and prognosis in gastric adenocarcinoma patients without mutations in Gp130 subunits. J. Gastrointestin. Liver Dis. *21*, 23–29.

Nieminen, P., Morgan, N., Fenwick, A., Parmanen, S., Veistinen, L., Mikkola, M., van der Spek, P., Giraud, A., Judd, L., Arte, S., et al. (2011). Inactivation of IL11 signaling causes craniosynostosis, delayed tooth eruption, and supernumerary teeth. Am. J. Hum. Genet. *89*, 67–81.

Nishimoto, N., Kanakura, Y., Aozasa, K., Johkoh, T., Nakamura, M., Nakano, S., Nakano, N., Ikeda, Y., Sasaki, T., Nishioka, K., et al. (2005). Humanized anti-interleukin-6 receptor antibody treatment of multicentric Castleman disease. Blood *106*, 2627–2623.

Nishimoto, N., Terao, K., Mima, T., Nakahara, H., Takagi, N., and Kakehi, T. (2008). Mechanisms and pathologic significances in increase in serum interleukin-6 (IL-6) and soluble IL-6 receptor after administration of an anti-IL-6 receptor antibody, tocilizumab, in patients with rheumatoid arthritis and Castleman disease. Blood *112*, 3959–3964.

Nowell, M.A., Richards, P.J., Horiuchi, S., Yamamoto, N., Rose-John, S., Topley, N., Williams, A.S., and Jones, S.A. (2003). Soluble IL-6 receptor governs IL-6 activity in experimental arthritis: blockade of arthritis severity by soluble glycoprotein 130. J. Immunol. *171*, 3202–3209.

Nowell, M.A., Williams, A.S., Carty, S.A., Scheller, J., Hayes, A.J., Jones, G.W., Richards, P.J., Slinn, S., Ernst, M., Jenkins, B.J., et al. (2009). Therapeutic targeting of IL-6 trans signaling counteracts STAT3 control of experimental inflammatory arthritis. J. Immunol. *182*, 613–622.

Obana, M., Maeda, M., Takeda, K., Hayama, A., Mohri, T., Yamashita, T., Nakaoka, Y., Komuro, I., Takeda, K., Matsumiya, G., et al. (2010). Therapeutic activation of signal transducer and activator of transcription 3 by interleukin-11 ameliorates cardiac fibrosis after myocardial infarction. Circulation *121*, 684–691.

Obana, M., Miyamoto, K., Murasawa, S., Iwakura, T., Hayama, A., Yamashita, T., Shiragaki, M., Kumagai, S., Miyawaki, A., Takewaki, K., et al. (2012). Therapeutic administration of IL-11 exhibits the postconditioning effects against ischemia-reperfusion injury via STAT3 in the heart. Am. J. Physiol.-Heart C. *303*, 77.

Onnis, B., Fer, N., Rapisarda, A., Perez, V.S., and Melillo, G. (2013). Autocrine production of IL-11 mediates tumorigenicity in hypoxic cancer cells. J. Clin. Invest. *123*, 1615–1629.

O'Shea, J., Kontzias, A., Yamaoka, K., Tanaka, Y., and Laurence, A. (2013). Janus kinase inhibitors in autoimmune diseases. Annals Rheum. Dis. *72* (*Suppl 2*), ii111–ii115.

Pack, R.J., Al-Ugaily, L.H., and Morris, G. (1981). The cells of the tracheobronchial epithelium of the mouse: a quantitative light and electron microscope study. J. Anat. *132*, 71–84.

Palmqvist, P., Persson, E., Conaway, H.H., and Lerner, U.H. (2002). IL-6, leukemia inhibitory factor, and oncostatin M stimulate bone resorption and regulate the expression of receptor activator of NF-κB ligand, osteoprotegerin, and receptor activator of NF-κB in mouse calvariae. J. Immunol. *169*, 3353–3362.

Pasare, C. and Medzhitov, R. (2003). Toll pathway-dependent blockade of $CD4^+CD25^+$ T cell-mediated suppression by dendritic cells. Science *299*, 1033–1036.

Peterson, R., Wang, L., Albert, L., Keith, J., and Dorner, A. (1998). Molecular effects of recombinant human interleukin-11 in the HLA-B27 rat model of inflammatory bowel disease. Lab. Invest. *78*, 1503–1512.

Pflanz, S., Tacken, I., Grötzinger, J., Jacques, Y., Minvielle, S., Dahmen, H., Heinrich, P.C., and Muller-Newen, G. (1999). A fusion protein of interleukin-11 and soluble interleukin-11 receptor acts as a superagonist on cells expressing gp130. FEBS Lett. *450*, 117–122.

Poli, V., Balena, R., Fattori, E., Markatos, A., Yamamoto, M., Tanaka, H., Ciliberto, G., Rodan, G. A., and Costantini, F. (1994). Interleukin-6 deficient mice are protected from bone loss caused by estrogen depletion. EMBO J. *13*, 1189–1196.

Putoczki, T. and Ernst, M. (2010). More than a sidekick: the IL-6 family cytokine IL-11 links inflammation to cancer. J. Leukoc. Biol. *88*, 1109–1117.

Rose-John, S. and Heinrich, P.C. (1994). Soluble receptors for cytokines and growth factors: generation and biological function. Biochem. J. *300*, 281–290.

Rose-John, S., Schooltink, H., Lenz, D., Hipp, E., Dufhues, G., Schmitz, H., Schiel, X., Hirano, T., Kishimoto, T., and Heinrich, P. (1990). Studies on the structure and regulation of the human hepatic interleukin-6 receptor. Eur. J. Biochem. *190*, 79–83.

Rose-John, S., Waetzig, G.H., Scheller, J., Grotzinger, J., and Seegert, D. (2007). The IL-6/sIL-6R complex as a novel target for therapeutic approaches. Expert Opin. Ther. Targets *11*, 613–624.

Samavedam, U., Kalies, K., Scheller, J., Sadeghi, H., Gupta, Y., Jonkman, M., Schmidt, E., Westermann, J., Zillikens, D., Rose-John, S., et al. (2013). Recombinant IL-6 treatment protects mice from organ specific autoimmune disease by IL-6 classical signalling-dependent IL-1ra induction. J. Autoimmun. *40*, 74–85.

Sandborn, W., Ghosh, S., Panes, J., Vranic, I., Su, C., Rousell, S., Niezychowski, W., and Study, A.I. (2012). Tofacitinib, an oral Janus kinase inhibitor, in active ulcerative colitis. N. Engl. J. Med. *367*, 616–624.

Sands, B., Bank, S., Sninsky, C., Robinson, M., Katz, S., Singleton, J., Miner, P., Safdi, M., Galandiuk, S., Hanauer, S., et al. (1999). Preliminary evaluation of safety and activity of recombinant human interleukin 11 in patients with active Crohn's disease. Gastroenterology *117*, 58–64.

Sands, B., Winston, B., Salzberg, B., Safdi, M., Barish, C., Wruble, L., Wilkins, R., Shapiro, M., Schwertschlag, U., and group, R.-C. s. S. (2002). Randomized, controlled trial of recombinant human interleukin-11 in patients with active Crohn's disease. Aliment. Pharmacol. Ther. *16*, 399–406.

Sawa, Y., Ichikawa, H., Kagisaki, K., Ohata, T., and Matsuda, H. (1998). Interleukin-6 derived from hypoxic myocytes promotes neutrophil-mediated reperfusion injury in myocardium. J. Thorac. Cardiovasc. Surg. *116*, 511–517.

Scheller, J. and Rose-John, S. (2012). The interleukin 6 pathway and atherosclerosis. Lancet *380*, 338.

Scheller, J., Schuster, B., Holscher, C., Yoshimoto, T., and Rose-John, S. (2005). No inhibition of IL-27 signaling by soluble gp130. Biochem. Biophys. Res. Commun. *326*, 724–728.

Scheller, J., Chalaris, A., Garbers, C., and Rose-John, S. (2011a). ADAM17: a molecular switch controlling inflammatory and regenerative responses. Trends Immunol. *32*, 380–387.

Scheller, J., Chalaris, A., Schmidt-Arras, D., and Rose-John, S. (2011b). The pro- and anti-inflammatory properties of the cytokine interleukin-6. Biochim. Biophys. Acta *1813*, 878–888.

Schuett, H., Oestreich, R., Waetzig, G.H., Annema, W., Luchtefeld, M., Hillmer, A., Bavendiek, U., von Felden, J., Divchev, D., Kempf, T., et al. (2012). Transsignaling of interleukin-6 crucially contributes to atherosclerosis in mice. Arterioscler. Thromb. Vasc. Biol. *32*, 281–290.

Schuster, B., Kovaleva, M., Sun, Y., Regenhard, P., Matthews, V., Grötzinger, J., Rose-John, S., and Kallen, K.J. (2003). Signaling of human ciliary neurotrophic factor (CNTF) revisited. The interleukin-6 receptor can serve as an α-receptor for CTNF. J. Biol. Chem. *278*, 9528–9535.

Snyers, L., De Wit, L., and Content, J. (1990). Glucocorticoid up-regulation of high-affinity interleukin 6 receptors on human epithelial cells. Proc. Natl. Acad. Sci. USA *87*, 2838–2842.

Suthaus, J., Stuhlmann-Laeisz, C., Tompkins, V.S., Rosean, T.R., Klapper, W., Tosato, G., Janz, S., Scheller, J., and Rose-John, S. (2012). HHV8 encoded viral IL-6 collaborates with mouse IL-6 in MCD-like development in mice. Blood *119*, 5173–5181.

Takeuchi, Y., Watanabe, S., Ishii, G., Takeda, S., Nakayama, K., Fukumoto, S., Kaneta, Y., Inoue, D., Matsumoto, T., Harigaya, K., et al. (2002). Interleukin-11 as a stimulatory factor for bone formation prevents bone loss with advancing age in mice. J. Biol. Chem. *277*, 49011–49018.

Tanaka, T., Narazaki, M., and Kishimoto, T. (2012). Therapeutic targeting of the interleukin-6 receptor. Annu. Rev. Pharmacol. Toxicol. *52*, 199–219.

Tang, W., Geba, G., Zheng, T., Ray, P., Homer, R., Kuhn, C., Flavell, R., and Elias, J. (1996). Targeted expression of IL-11 in the murine airway causes lymphocytic inflammation, bronchial remodeling, and airways obstruction. J. Clin. Invest. *98*, 2845–2853.

Tang, L.P., Cho, C.H., Hui, W.M., Huang, C., Chu, K.M., Xia, H.H., Lam, S.K., Rashid, A., Wong, B.C., and Chan, A.O. (2006). An inverse correlation between Interleukin-6 and select gene promoter methylation in patients with gastric cancer. Digestion *74*, 85–90.

Tato, C.M. and Cua, D.J. (2008). SnapShot: Cytokines I. Cell *132*, 324.

Tebbutt, N., Giraud, A., Inglese, M., Jenkins, B., Waring, P., Clay, F., Malki, S., Alderman, B., Grail, D., Hollande, F., et al. (2002). Reciprocal regulation of gastrointestinal homeostasis by SHP2 and STAT-mediated trefoil gene activation in gp130 mutant mice. Nat. Med. *8*, 1089–1097.

Thabard, W., Collette, M., Mellerin, M.P., Puthier, D., Barillé, S., Bataille, R., and Amiot, M. (2001). IL-6 upregulates its own receptor on some human myeloma cell lines. Cytokine *14*, 352–356.

Underhill-Day, N., McGovern, L., Karpovich, N., Mardon, H., Barton, V., and Heath, J. (2003). Functional characterization of W147A: a high-affinity interleukin-11 antagonist. Endocrinology *144*, 3406–3414.

van Vollenhoven, R., Fleischmann, R., Cohen, S., Lee, E., García Meijide, J., Wagner, S., Forejtova, S., Zwillich, S., Gruben, D., Koncz, T., et al. (2012). Tofacitinib or adalimumab versus placebo in rheumatoid arthritis. N. Engl. J. Med. *367*, 508–519.

Waetzig, G.H. and Rose-John, S. (2012). Hitting a complex target: an update on interleukin-6 trans-signalling. Expert Opin. Ther. Targets *16*, 225–236.

Walsh, N.C., Crotti, T.N., Goldring, S.R., and Gravallese, E.M. (2005). Rheumatic diseases: the effects of inflammation on bone. Immunol. Rev. *208*, 228–251.

Wang, J., Homer, R., Hong, L., Cohn, L., Lee, C., Jung, S., and Elias, J. (2000). IL-11 selectively inhibits aeroallergen-induced pulmonary eosinophilia and Th2 cytokine production. J. Immunol. *165*, 2222–2231.

Williams, W., Scherle, P., Shi, J., Newton, R., McKeever, E., Fridman, J., Burn, T., Vaddi, K., Levy, R., and Moreland, L. (2008). A randomized placebo-controlled study of INCB018424, a selective Janus kinase 1 & 2 (JAK1 & 2) inhibitor in rheumatoid arthritis (RA). Arthritis Rheum. *58*, S431.

Wong, P.K., Quinn, J.M., Sims, N.A., van Nieuwenhuijze, A., Campbell, I.K., and Wicks, I.P. (2006). Interleukin-6 modulates production of T lymphocyte-derived cytokines in antigen-induced arthritis and drives inflammation-induced osteoclastogenesis. Arthritis Rheum. *54*, 158–168.

Wu, C.W., Wang, S.R., Chao, M.F., Wu, T.C., Lui, W.Y., P'eng, F.K., and Chi, C.W. (1996). Serum interleukin-6 levels reflect disease status of gastric cancer. Am. J. Gastroenterol. *91*, 1417–1422.

Xu, Y., Kershaw, N.J., Luo, C.S., Soo, P., Pocock, M.J., Czabotar, P.E., Hilton, D.J., Nicola, N.A., Garrett, T.P., and Zhang, J.G. (2010). Crystal structure of the entire ectodomain of gp130: insights into the molecular assembly of the tall cytokine receptor complexes. J. Biol. Chem. *285*, 21214–21218.

Yamamoto, I., Yoshizaki, K., Kishimoto, T., and Ito, H. (2000). IL-6 is required for the development of Th1 cell-mediated murine colitis. J. Immunol. *164*, 4878–4882.

Yamauchi-Takihara, K., Ihara, Y., Ogata, A., Yoshizaki, K., Azuma, J., and Kishimoto, T. (1995). Hypoxic stress induces cardiac myocyte-derived interleukin-6. Circulation *91*, 1520–1524.

Yin, J., Selander, K., Chirgwin, J., Dallas, M., Grubbs, B., Wieser, R., Massagué, J., Mundy, G., and Guise, T. (1999). TGF-β signaling blockade inhibits PTHrP secretion by breast cancer cells and bone metastases development. J. Clin. Invest. *103*, 197–206.

Yokoyama, A., Kohno, N., Fujino, S., Hamada, H., Inoue, Y., Fujioka, S., Ishida, S., and Hiwada, K. (1995). Circulating interleukin-6 levels in patients with bronchial asthma. Am. J. Respir. Crit. Care Med. *151*, 1354–1358.

Yoshitake, F., Itoh, S., Narita, H., Ishihara, K., and Ebisu, S. (2008). Interleukin-6 directly inhibits osteoclast differentiation by suppressing receptor activator of NF-κB signaling pathways. J. Biol. Chem. *283*, 11535–11540.

Yoshizaki, A., Nakayama, T., Yamazumi, K., Yakata, Y., Taba, M., and Sekine, I. (2006). Expression of interleukin (IL)-11 and IL-11 receptor in human colorectal adenocarcinoma: IL-11 up-regulation of the invasive and proliferative activity of human colorectal carcinoma cells. Int. J. Oncol. *29*, 869–876.

Zhang, W., Tsuda, M., Yang, G.X., Tsuneyama, K., Rong, G., Ridgway, W.M., Ansari, A.A., Flavell, R.A., Coppel, R.L., Lian, Z.X., et al. (2010). Deletion of interleukin-6 in mice with the dominant negative form of transforming growth factor beta receptor II improves colitis but exacerbates autoimmune cholangitis. Hepatology *52*, 215–222.

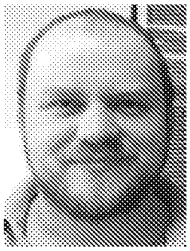

Christoph Garbers received his diploma degree in Pharmacy in 2007 at the University of Kiel, Germany, and his licensure as pharmacist in 2008. He joined the group 'Cytokine and Metalloproteinase Research' at the Institute of Biochemistry of the University of Kiel in 2008 and obtained his Dr. rer. nat. in 2011 for the functional characterization of ADAM proteases in IL-6R shedding. He then moved to the Heinrich-Heine-University Düsseldorf, Germany, and has worked since 2011 at the Institute of Biochemistry and Molecular Biology II as a postdoctoral research associate. His current interests are focused on limited proteolysis of cytokine receptors and signal transduction of IL-6 type cytokines.

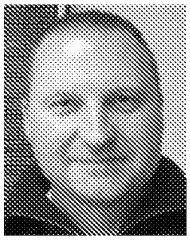

Jürgen Scheller finished his diploma study of Biology in 1997 at the Georg-August University of Göttingen, Germany and obtained his Dr. rer. nat. in 1999 for the role of MPH1 in DNA-repair of *Saccharomyces cerevisiae*. He joined the group 'Phytoantibodies' at the Leibniz-Institut IPK in Gatersleben, Germany in 1999. From 1999 to 2002 he worked on spider silk proteins from transgenic plants. In 2002 he became assistant professor at the Biochemical Institute at Christian-Albrechts-Universität of Kiel, Germany. In 2008 he became W2-Professor for 'Cytokine Signaling' within the Cluster of Excellence 'Inflammation at Interfaces' at Christian-Albrechts-Universität of Kiel, Germany. In 2010 he moved to the Heinrich-Heine-University and became the director of the Institute of Biochemistry and Molecular Biology II as a W3-Professor. His present interests are focused on *in vitro* and *in vivo* studies of IL-6-type cytokines.

Available online at www.sciencedirect.com
ScienceDirect
Current Opinion in Pharmacology

Airway remodeling in asthma

Rabih Halwani[1,3], Saleh Al-Muhsen[1,2,3] and Qutayba Hamid[1,3,4]

Asthmatic airway remodeling is the pathophysiological modifications of the normal airway wall structure which include changes in the composition and organization of its cellular and molecular constituents. These modifications are the major cause of the symptoms associated with decreased pulmonary function. Airway remodeling is partially reversible in mild asthma but mostly irreversible in chronic severe asthma. It is initiated as a repair process in response to airway wall injuries caused by inflammation; however, dysregulation of this process leads to airway remodeling. In this review, we will summarize the most recent findings about the different structural changes in airways of asthmatics as well as mediators involved in this process.

Addresses
[1] Asthma Research Chair, King Saud University, Riyadh, Saudi Arabia
[2] Department of Pediatrics College of Medicine, King Saud University, Riyadh, Saudi Arabia
[3] Prince Naif Center for Immunology Research, King Saud University, Riyadh, Saudi Arabia
[4] Meakins-Christie Laboratories, McGill University, 3626 St. Urbain, Montreal, Quebec, Canada

Corresponding author: Hamid, Qutayba (qutayba.hamid@mcgill.ca)

Current Opinion in Pharmacology 2010, 10:236–245

This review comes from a themed issue on
Respiratory
Edited by Jeffrey Fedan and Giovanni Piedimonte

1471-4892/$ – see front matter

DOI 10.1016/j.coph.2010.06.004

Introduction

Tissues and cells are usually able to adapt themselves to injury and mechanical demands and remodel by changing geometry, structure and properties. Tissue remodeling is the modification of the normal properties of the tissue and involves changes in its composition and structural organization. Remodeling occurs in a wide range of tissues and organs including the skin [1], vessels [2], heart tissue [3], gastrointestinal tract [4,5], airways and lung tissues, and could be observed in almost all tissues susceptible to repeated chronic injury. In this review, we will focus on airway remodeling in asthma.

Asthma, a chronic inflammatory disorder manifest as airway hyperresponsiveness and inflammation, is often characterized by pathological modifications of the bronchial airway structures. These structural changes are termed airway remodeling. Structural changes of the airway include epithelial changes, subepithelial fibrosis, increased airway smooth muscle (ASM) mass, decreased distance between ASM and the epithelium, mucous gland and goblet cell hyperplasia, vascular changes and edema [6–9]. Airway remodeling is believed to start as a repair process in response to airway injuries resulting from sustained inflammation or mechanical stretch. In addition to the role of inflammatory cells in remodeling, structural cells, including ASM cells, epithelial cells and fibroblasts may participate in enhancing inflammation and remodeling through the release of cytokines, chemokines and ECM proteins [10–12].

Tissue remodeling is believed to start at an early age and to develop with asthma progression [13]. Several groups investigating airway remodeling in asthmatic children reported evidence of increased collagen deposition and thickening of the lamina reticularis, increased smooth muscle mass and angiogenesis [14,15•,16]. However there are no long-term studies that examine the natural history of this process in asthma.

Physiological evidence of airway remodeling

It is becoming widely accepted that airway remodeling contributes significantly to lung physiological dysfunction and hence to clinical symptoms [17,18]. A low post-bronchodilator FEV_1/VC ratio as well as reduced airway dispensability was suggested to be due to irreversible airway remodeling [19–21]. In addition, the thickness of the reticular basement membrane has been correlated to airflow obstruction and increased airway hyperresponsiveness [22,23] suggesting a direct correlation between airway remodeling and asthma. Patients with severe asthma develop progressive persistent airflow limitation with longer disease durations providing further evidence that airway remodeling plays a role in the impairment of lung function [24]. Although remodeling is believed to be correlated with airway narrowing, the thickening and stiffness of the inner wall (the layer between the ASM cells and the basement membrane) could protect against excessive airway narrowing by attenuating the ability of the smooth muscles layer to shorten [25].

Pathological changes in airway remodeling

Features of airway remodeling have been described using tissue obtained from fatal asthma and bronchial biopsies from mild, moderate and severe asthmatic patients. Epithelial detachment, subepithelial fibrosis, increased smooth muscle mass, goblet cell hyperplasia and angiogenesis are common features of asthmatic bronchial tissue [26•]. Although it is not uncommon to see bronchial

epithelial detachment in healthy individuals, the level of detachment increases with asthma development. In fact, the rate of apoptosis in bronchial epithelial cells from asthmatic patients has been shown to be significantly higher than that from healthy subjects [27]. This process is mainly driven by TNF-α [28].

Subepithelial fibrosis is another feature of tissue remodeling associated with asthma. In normal subjects, a loose array of collagen fibrils resides beneath the basal membrane. In asthmatics, however, this layer is replaced by a dense network of collagen fibrils [29]. The deposition of ECM protein is driven by the secretion of a number of cytokines and the mechanical stress that is characteristic of asthma [29]. Epithelial fibroblast interaction could also play a major role in this process.

ASM cell proliferation (hyperplasia), increase in ASM cell size (hypertrophy), migration of ASM cells towards the epithelium, and decreased rate of ASM cellular apoptosis could all contribute to the increase in airway smooth muscle mass, a hallmark feature of tissue remodeling. This increase in ASM mass has been reported to correlate with the severity of asthma [30–32].

Goblet cell hypertrophy and hyperplasia are also greatly involved in airway remodeling leading to excessive mucus production. IL-9 and IL-13 may play a role in triggering the induction of mucus hyper-secretion, which eventually leads to airflow obstruction [33,34].

An abnormal increase in the number and size of microvessels within the bronchial tissue of asthmatic patients has also been reported [35]. An imbalance between VEGF and angiopoitin-1 (Ang-1) is believed to be involved in the progress of these abnormalities [36]. In fact, VEGF acts on increasing the permeability of these abnormal blood vessels [37] resulting in vessel dilation and formation of edema, which contributes to airway narrowing. These vessels are also the source of inflammatory cells and of plasma-derived mediators and cytokines [35]. In addition, structural and biochemical changes in airway cartilage, an important determinant of wall stiffness and integrity, contribute to tissue

Figure 1

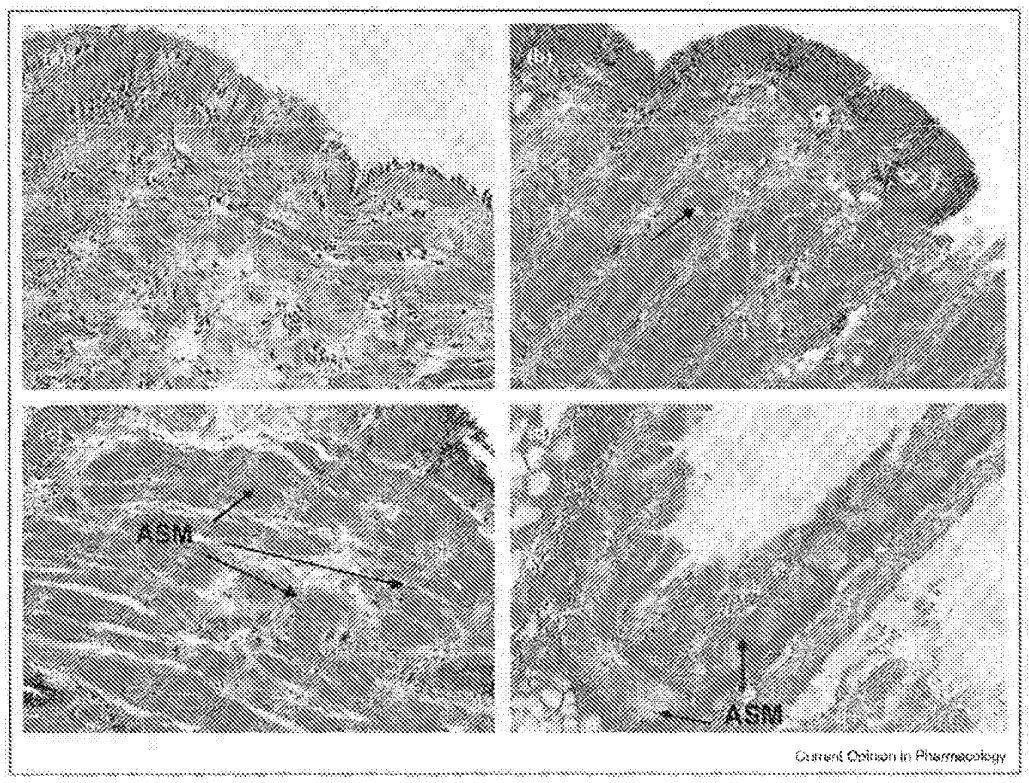

Bronchial tissue remodeling in severe asthma. Endobronchial biopsies stained with hematoxylin and eosin of subjects with severe asthma. (A) Infiltration of inflammatory cells into bronchial tissue with mild subepithelial fibrosis in mild asthma. (B) Extensive subepithelial fibrosis in bronchial biopsy of severe asthmatics. (C) Extensive increase in muscle mass in biopsy of severe asthmatics. (D) Small airways showing severe remodeling process. ASM: airway smooth muscle.

remodeling [38] and may result in increased bronchoconstriction in asthmatic subjects.

Cells contributing to airway remodeling

Many cells have been implicated in the regulation and dysregulation of the tissue injury and repair process. These include inflammatory and structural cells (Figure 1).

T-helper cells

Besides its role in initiating and maintaining airway inflammation in asthma, T-helper cells, particularly Th-2 type cells, play a role in the development of airway remodeling in asthmatics. Studies of airway remodeling in GATA-3 transgenic mice (a model for Th-2 inflammation) showed a significance enhancement of airway remodeling, upon allergen exposure, including subepithelial fibrosis and ASM hyperplasia [39••]. In fact, bronchial biopsies from asthmatic patients with remodeled airways had increased expression level of Th-2 and GATA-3 (favoring Th-2 response) and reduced levels of T-bet (favoring Th1 response) [40]. This suggests an association between high levels of Th-2 cells and tissue remodeling in asthma. Several studies suggested a key role of Th-2 derived cytokines (ex IL-5, IL-13 and IL-4) in tissue remodeling [41•,42]. Although the role of Th-1 cells in airway inflammation in asthma is not clear [43], it has been shown that mice with increased number of Th-1 cells (T-bet transgenic mice) had lower level of remodeling compared to GATA-3 transgenic mice [39••].

Regulatory T (Treg) cells

Treg cells might play an important role in airway remodeling. Natural Tregs (CD4+CD25+) develop in the thymus and may expand in the peripheral blood upon antigen exposure. They suppress neighboring T cells by cell-to-cell contact via membrane-bound molecules [44]. In contrast, Adaptive Tregs (CD4+CD25−) exhibit cytokine-dependent suppressive mechanism via the secretion of IL-10 and TGF-β [45–48]. The role of Tregs in asthma development and progression is not yet clear. However the capacity of natural Tregs, isolated from bronchoalveolar lavage (BAL) of asthmatic patients, to suppress T cell proliferation and Th-2 cytokine production was shown to be impaired [49•]. Further studies are required to unravel the role of Tregs in asthma and their contribution to tissue remodeling.

Th-17

Following antigenic stimulation, naive CD4+ T cells proliferate and differentiate into various effectors subsets such as Th-1 and Th-2 cells and the recently identified subset, Th-17 [50••]. These IL-17 producing cells are implicated in inducing tissue inflammation and autoimmunity [51]. Th-17 cells are characterized by the production of IL-17A and IL-17F and, to a lesser extent, IL-6 and tumor necrosis factor (TNF-α) [50••]. In addition to their pro-inflammatory properties, Th-17 related cytokines have been suggested to play a role in airway remodeling [52•,53••]. They have been shown to induce the production of ECM proteins and regulate smooth muscle function [52•,54]. IL-6 has been shown to be a remodeling-associated cytokine. Its over-expression leads to subendothelial fibrosis, collagen deposition and increased accumulation of α-actin-containing smooth muscle cells [55]. TNF-α is also a powerful proinflammatory cytokine that can induce fibroblast, epithelial cells and ASM cells to produce excessive amounts of ECM proteins [52•].

Eosinophils

The role of eosinophils in airway remodeling is well documented and widely accepted [56–58]. Eosinophil accumulation in the airways is regulated by local production of proinflammatory chemokines such as RANTES and Eotaxin. Several mediators were reported to be produced by eosinophils including the profibrotic cytokine, TGF-β [59]. Our group has shown that 65% of the TGF-β1 mRNA positive cells in bronchial biopsies of severe asthmatics were eosinophils [56]. Eosinophils are suggested to play a crucial role in the pathogenesis of airway remodeling [41•,57]. This has been further supported by knocking out IL-5 (using IL-5 deficient mice) [41•] or by treating asthmatic patients with anti-IL-5 antibodies [57]. IL-5 deficient mice had significantly lower levels of subepithelial fibrosis as well as significant reduction in smooth muscle mass. Treatment of asthmatic patients with anti-IL-5 reduced the level of BAL eosinophils, and tissue remodeling by significantly decreasing ECM protein deposition. More efficient approach used to eliminate eosinophils is via targeting CCR3 chemokine receptor highly expressed on eosinophils. Targeting CCR3 using a low molecular weight antagonist or anti-CCR3 antibodies in an asthma mouse model demonstrated significant reduction in subepithelial fibrosis, goblet cell hyperplasia, collagen deposition and ASM mass [60,61•]. All these studies support the role of eosinophils and associated TGF-β in the development of tissue remodeling. Eosinophils were also shown to be a site for the production of other proinflammatory/remodeling cytokines including IL-6, IL-11 and IL-17 [62–64].

Epithelial cells

Epithelial cell attachment to the basement membrane and other cells have been reported to be loose in asthma. It is believed that injury to the epithelial layer during asthma together with the impaired repair process drives the inflammatory and remodeling responses in the underlying submucosa [65]. In response to pathogens, allergens, pollutants, or cigarette smoke, epithelial cells produce cytokines and chemokines, which can then drive tissue remodeling [66]. In support of the role of airway epithelium in tissue remodeling, it has been shown that blocking the NF-KB-regulated cytokines and chemokines in mice

airway epithelium resulted in a significant decrease in subepithelial fibrosis, airway mucus, airway eosinophils and bronchial CD4+ T cells [67]. In addition, transgenic overexpression of IL-25 (IL-17E) in mice lung epithelium resulted in enhanced mucus production and eosinophil infiltration. Blocking IL-25 also reduced tissue remodeling in mouse model [68].

IL-4 and IL-13 produced by infiltrating T lymphocytes of the asthmatic airways were shown to induce epithelial cells, through the activation of STAT-6, to produce a number of chemokines. These include IL-8 (neutrophil chemoattractant) [69], RANTES and eotaxin involved in inflammatory as well as structural cell chemoattraction and modulation [70]. Furthermore, damaged epithelial cells in asthma release a number of growth factors including epidermal growth factor (EGF), platelet-derived growth factor (PDGF), TGF-β and VEGF all of which contribute to airway remodeling by increasing ASM proliferation, ECM deposition and angiogenesis [71••].

ASM cells

The physiological and pathological contribution of ASM cells is critical to the process of airway tissue remodeling [72,73]. ASM cell hyperplasia and hypertrophy were clearly demonstrated in fatal asthma [74]. Evidence of either hypertrophy, hyperplasia, or both was also reported in mild, moderate, or severe asthma and correlated with the severity of the disease [8]. The increase in ASM mass could also be attributed to the increase in survival rate of ASM cells [75]. We have recently also reported that migration of ASM cells towards the epithelium, upon the stimulation of epithelium-derived chemokines, could be an additional mechanism for increased ASM mass in asthmatic airways [70]. ASM cells are known to proliferate in response to numerous growth factors and mediators that are released in asthmatic airways [76]. Not only ASM cells themselves can remodel (proliferate, increase in size and shape, migrate, etc.) but also they participate in the inflammatory and remodeling process through their release of pro-inflammatory cytokines (e.g. TGF-β), chemokines and ECM proteins [10,77].

Airway ASM cells express cellular adhesion molecules (CAMs), in addition to receptors for cytokines (mainly TNF-α) and chemokines (RANTES, Eotaxin, MIP-1α and IL-8). Many studies have clearly suggested that interactions of ASM cells with inflammatory cells, including eosinophils and T cells, via CAMs can directly contribute to tissue airway remodeling in asthma [78,79]. In addition to CAMs, TNF-α, IL-1β and INF-γ have also been shown to induce the expression of TLRs on ASM cells [80•]. In fact, LPS of gram-negative bacteria was suggested to promote airway hyperresponsiveness via its interaction with TLRs on ASM cells [81]. Activation of TLR receptors, either through infection or contamination with viral/bacterial components, may, therefore, play an important role in ASM activation and tissue remodeling.

Fibroblasts

Fibroblasts form a sheath of large, flat stellate cells in close proximity to the epithelium. These fibroblasts differentiate, in response to various stimuli, into myofibroblasts that secrete ECM proteins as well as proinflammatory mediators. Subepithelial fibrosis occurs due to the increased deposition of ECM proteins, including collagens I, III, V, proteoglycan, tenascin and fibronectin. ECM proteins influence structural cell behavior and its composition determines the elasticity of the airway tissue [82]. Matrix metalloprotinease (MMP-9), which degrades collagen 4, and its inhibitor, tissue inhibitor of matrix metalloproteinase (TIMP-1), are both secreted by fibroblasts to regulate ECM protein deposition. Imbalance between MMP-9 and TIMP-1 results in the accumulation of ECM proteins and hence fibrosis [83].

Goblet cells

The increase in mucus hyper-secretion due to goblet cell proliferation is a common feature of asthmatic airways. Their stimulation by various inflammatory mediators results in an increase in mucus production and secretion, predisposing to occlusion of the airway and thus, impairment of lung function [84]. Several mucous-related genes were reported to be dysregulated in asthma including MUC1, II and V. These genes are induced by a number of cytokines including IL-4, IL-9 and IL-13. Goblet cell hyperplasia and increased secretion of mucus are not a consistent feature of chronic severe asthma and could be identified only in a subgroup of patients.

Mediators associated with airway remodeling

Many studies on airway remodeling in asthma have focused on determining the cytokines, chemokines and growth factors involved in this process. Several mediators of remodeling have been identified including TGF-β, IL-4, IL-9, IL-11, IL-13, IL-17 and VEGF [85].

Profibrotic cytokines

TGF-β is known to modulate different features of airway remodeling. Depending on the pathway activated, TGF-β can induce an apoptotic or anti-apoptotic effect on airway epithelial cells [86]. TGF-β can also promote the differentiation of fibroblast precursors to myofibroblast cells as well as triggering their proliferation [87]. It induces the release of fibroblast growth factor-2 (FGF-2) [88] as well as the connective tissue growth factor (CTGF) [89] which enhances migration of mesenchymal cells and synthesis of ECM proteins [88,89]. TGF-β also induces the expression of the counterbalancing regulators of ECM proteins turnover, MMPs and TIMPs [90]. Moreover, it has been shown to enhance ASM proliferation via the MAPK pathway or by upregulating the integrin receptor α5β1, essential for ASM proliferation

[91]. We have recently shown a role of TGF-β in enhancing ASM cell migration towards the epithelial layer, a mechanism that contributes to tissue remodeling [92]. On the other hand, TGF-β2 was suggested to enhance production of mucin in bronchial epithelial cells [93]. In fact, treatment with antibody to TGF-β reduced the number of mucus-secreting goblet cells in an asthmatic mouse model [94•]. TGF-β was also shown to contribute to microvascular congestion through the enhancement of the production and secretion of several pro-angiogenic factors including VEGF [95]. All these diverse properties of TGF-β support its role in airway remodeling.

IL-11 is considered as a profibrotic cytokine. Overexpression of IL-11 was shown to be associated with subepithelial fibrosis, airway wall thickening, and increased myofibroblasts and smooth muscle cell numbers. IL-11 transgenic mice were shown to have asthma-like symptoms and hyporesponsiveness to methacholine [96]. We have shown that the expression of IL-11 is correlated to asthma severity and to the extent of subepithelial fibrosis and suggested a role of this cytokine in airway remodeling [62].

ADAM33

Another newly explored role of TGF-β is its effect on the asthma susceptibility gene, a disintegrin and metalloprotease 'ADAM33', which has been implicated as an asthma remodeling gene. ADAM33 was the first asthma susceptibility gene to be identified by positional cloning, showing associations with asthma and bronchial hyperresponsiveness (BHR) but not atopy [97••]. Asthma-related single nucleotide polymorphisms (SNPs) in ADAM33 predict reduced lung function in adults as well as young children [98], suggesting that the influence of ADAM33 begins early in life. The functional contribution of ADAM33 to asthma pathogenesis and remodeling is yet to be confirmed. In fact, a soluble form of ADAM33 (sADAM33) has been reported in BAL of subjects with asthma, but not healthy subjects, and levels of sADAM33 were inversely correlated with lung function [99]. This soluble form of ADAM33 was also shown recently to promote angiogenesis, further reinforcing its role in airway remodeling [100]. This has provided the first clue of a disease-related effect of ADAM33 in asthma. In the same study, TGF-β was shown to be involved in the shedding of sADAM33 in a time-dependent and dose-dependent fashion [100].

Other cytokines and chemokines

Increased levels of the pro-angiogenic cytokine VEGF have been very well documented in asthmatic airways and suggested to be responsible for enhanced angiogenesis in airway tissues [101]. It was shown to be elevated in BAL, sputum, and bronchial biopsies of asthmatic patients [101]. Studies with VEGF lung transgenic mice suggested that VEGF induces tissue remodeling and enhances Th-2-mediated sensitization and inflammation in the lungs [102]. Nitric oxide (NO) has also been shown to regulate the remodeling effects of VEGF [103].

Th-2 cytokines, including IL-4, IL-5, IL-9 and IL-13 play important roles in the airway remodeling in asthma. Their role in enhancing eosinophilic inflammation in the airways via recruiting eosinophils to the lungs is very well documented [104]. Th-2 cytokines have been reported to induce mucus gene expression in airway epithelial cells. In fact, overexpression of IL-4, IL-5, IL-9 and IL-13, is associated with increased mucus production, subepithelial fibrosis as well as hypertrophy of the epithelium [105].

Recent reports have uncovered a central role for chemokines, including eotaxin, regulated on activation of normal T-cell expressed and secreted (RANTES), MIP-1α and monocyte chemotactic proteins (MCPs), in the development of airway remodeling. This is mainly achieved via the recruitment and trafficking of inflammatory as well as structural cells to the site of inflammation. The upregulation of CC chemokines during on-going inflammation or following exacerbation of asthma is controlled by a variety of cytokines. Inflammatory cytokines, including IL-1β and TNF-α, can induce the synthesis of various chemokines, such as eotaxin [106] and RANTES [107] from human lung epithelial cells. Using a murine model of airway hyperresponsiveness, Gonzalo *et al.* [108] showed that neutralizing chemokines such as eotaxin, RANTES and MCPs significantly reduced bronchial hyperresponsiveness as well as leukocyte migration. Although epithelial cells constitute the main source of chemokines within the bronchial airways, many evidences suggest that ASM could also be a prominent source of chemokines in these tissues. RANTES, MCP-1 and, CXCL10 were shown to be expressed in ASM bundles of bronchial biopsy specimens in asthmatic subjects [109]. Moreover, ASM cells possess receptors for epithelial-derived CC and CXC chemokine such as CCR3, CCR1, CCR5, CXCL1 and 2 [110,111•,112]. Using these receptors, chemokines drive the migration of those cells towards the epithelium [70]. In addition, we have also observed that chemokines act on enhancing the proliferation as well as survival of ASM cells (unpublished data).

Animal model of airway remodeling

Animal models of asthma have been very helpful in examining the mechanisms of the disease, the activity of a variety of genes and cellular pathways, and in predicting the safety of new drugs before being used in clinical studies [113]. A wide variety of animal models of asthma including mice, rats, guinea pigs, ferrets, dogs, sheep, monkeys and horses have been employed to study the inflammatory processes and alterations in airway functions and tissue remodeling [114,115]. However, the majority of studies of allergic airway diseases are now carried on using mice and rat models. Asthma mouse

model has several limitations including the facts that their lungs are more fully developed at birth and hence environmental influences have different effects. The structure of the mouse lungs is also different from those of humans [116]. Nevertheless, although no mouse model fully mimics the full range of clinical manifestations of asthma, many do reproduce a collection of its features, including tissue remodeling [116–118]. The various components of airway remodeling described in human asthma have been successfully reproduced in mice and rat animal models. Most of the data have been contributed by mice/rat models of allergic sensitization and repeated challenge, transgenic mouse models of cytokine overexpression localized to the lung and, more recently, allergen-driven mouse models using wild-type inbred strains [119,120]. Therefore, asthma animal models should be seen as an important opportunity to generate and test hypotheses in simple, easy to manipulate, controlled systems.

Therapeutic implications of airway remodeling

Corticosteroids are currently the most effective anti-inflammatory therapy of persistent asthma. Their efficacy in controlling airway inflammation in asthma has been well documented [121]; however, its effect on airway remodeling is still debatable. Although some studies suggested a modest effect of corticosteroids on airway remodeling, the majority of literature showed that corticosteroids have little or no effect on tissue remodeling [63,122]. In particular, human studies have failed to show any effect of corticosteroids on TGF-β expression or the deposition of ECM proteins [63].

The effect of leukotriene inhibitors on airway remodeling has also been investigated. CysLT receptor 1 inhibitor has been demonstrated to reverse features of airway remodeling in an asthma mouse model [123]. Moreover, treatment of asthmatic patients with a CysLT receptor 1 antagonist reduced the number of myofibroblasts in the airway [124]. However, further investigations are required to confirm the effect of leukotriene inhibitors on tissue remodeling.

In conclusion, since anti-inflammatory medications have limited impact on airway remodeling [63,122], elucidating the mechanisms involved in remodeling, including the role of structural cells in asthma might open new horizons for more effective therapeutic interventions.

Remodeling is not restricted to airways and asthma

Airways of patients with chronic obstructive pulmonary disease (COPD) share most of airway remodeling features with asthma including loss of epithelial cilia, goblet cell hyperplasia, mucus gland enlargement, smooth muscle hypertrophy [125] and angiogenesis [126]. Tissue fibrosis, which has been implicated in the development of emphysema, is also observed in the small airways of COPD lungs mostly due to imbalance between profibrotic proteases and protective antiproteases [125]. Basement membrane thickening could be observed in COPD patients' large, but not small, airways [125]. Bronchiectasis and cystic fibrosis are other lung diseases that are characterized by extensive remodeling and fibrosis.

Tissue remodeling is observed in all atopic diseases supporting the hypothesis that remodeling is an inflammatory-driven process. Allergen exposure of patients with allergic rhinitis, atopic dermatitis and asthma triggers a very similar profile of inflammation, mediators, and adhesion molecules and ultimately remodeling. Although inflammatory reaction induced by allergens is similar in upper and lower airways, tissue structural modifications slightly differ. For example, subepithelial fibrosis is usually observed in asthma but not in allergic rhinitis [127].

Unmet needs in airway remodeling research

The relationship between inflammation and remodeling is still highly debatable and incompletely understood. The presence of airway inflammation in patients with asthma does not always translate to airway remodeling in many cases; and the correlation between the degree of inflammation and the degree of remodeling is not always positive [8]. The detection of airway remodeling very early in asthma development in pediatric population raises further questions about the association between inflammation and remodeling and suggests a genetic susceptibility that needs to be explored [13]. Furthermore, in a murine model, although airway inflammation can be resolved upon allergen avoidance, remodeling persists, suggesting that ongoing inflammation is not required for the persistence of remodeled airway [128]. It is also important to perform long-term studies to study the natural history of remodeling and to provide strong evidence for the association between remodeling and physiological changes in asthma. Finally, identification of biomarkers for remodeling is essential to study a large number of patients and to clarify the effect of various treatments.

References and recommended reading

Papers of particular interest, published within the annual period of review, have been highlighted as:

- * of special interest
- ** of outstanding interest

1. Jorgensen LN: **Collagen deposition in the subcutaneous tissue during wound healing in humans: a model evaluation.** *APMIS Suppl* 2003:1-56.
2. Rizzoni D, Muiesan ML, Porteri E, De Ciuceis C, Boari GE, Salvetti M, Paini A, Rosei EA: **Vascular remodeling, macro- and microvessels: therapeutic implications.** *Blood Press* 2009, 18:242-246.
3. Minicucci MF, Azevedo PS, Paiva SA, Zornoff LA: **Cardiovascular remodeling induced by passive smoking.** *Inflamm Allergy Drug Targets* 2009, 8:334-339.

4. Lawrance IC, Maxwell L, Doe W: **Inflammation location, but not type, determines the increase in TGF-beta1 and IGF-1 expression and collagen deposition in IBD intestine**. *Inflamm Bowel Dis* 2001, **7**:16-26.

5. Gao Q, Meijer MJ, Kubben FJ, Sier CF, Kruidenier L, van Duijn W, van den Berg M, van Hogezand RA, Lamers CB, Verspaget HW: **Expression of matrix metalloproteinases-2 and -9 in intestinal tissue of patients with inflammatory bowel diseases**. *Dig Liver Dis* 2005, **37**:584-592.

6. Vignola AM, Mirabella F, Costanzo G, Di Giorgi R, Gjomarkaj M, Bellia V, Bonsignore G: **Airway remodeling in asthma**. *Chest* 2003, **123**:417S-422S.

7. Vignola AM, Kips J, Bousquet J: **Tissue remodeling as a feature of persistent asthma**. *J Allergy Clin Immunol* 2000, **105**:1041-1053.

8. Benayoun L, Druilhe A, Dombret MC, Aubier M, Pretolani M: **Airway structural alterations selectively associated with severe asthma**. *Am J Respir Crit Care Med* 2003, **167**:1360-1368.

9. Sumi Y, Hamid Q: **Airway remodeling in asthma**. *Allergol Int* 2007, **56**:341-348.

10. Panettieri RA Jr: **Airway smooth muscle: an immunomodulatory cell**. *J Allergy Clin Immunol* 2002, **110**:S269-274.

11. Hakonarson H, Maskeri N, Carter C, Grunstein MM: **Regulation of TH1- and TH2-type cytokine expression and action in atopic asthmatic sensitized airway smooth muscle**. *J Clin Invest* 1999, **103**:1077-1087.

12. Johnson PR: **Role of human airway smooth muscle in altered extracellular matrix production in asthma**. *Clin Exp Pharmacol Physiol* 2001, **28**:233-236.

13. Saglani S, Payne DN, Zhu J, Wang Z, Nicholson AG, Bush A, Jeffery PK: **Early detection of airway wall remodeling and eosinophilic inflammation in preschool wheezers**. *Am J Respir Crit Care Med* 2007, **176**:858-864.

14. Cokugras H, Akcakaya N, Seckin, Camcioglu Y, Sarimurat N, Aksoy F: **Ultrastructural examination of bronchial biopsy specimens from children with moderate asthma**. *Thorax* 2001, **56**:25-29.

15. * Barbato A, Turato G, Baraldo S, Bazzan E, Calabrese F, Panizzolo C, Zanin ME, Zuin R, Maestrelli P, Fabbri LM *et al.*: **Epithelial damage and angiogenesis in the airways of children with asthma**. *Am J Respir Crit Care Med* 2006, **174**:975-981.
This article was among the first to show that epithelial damage and basement membrane thickening, which are pathologic features characteristic of adult asthma, were present even in childhood asthma (children age 2–15) indicating that these pathologic changes occur early in the natural history of asthma.

16. Fedorov IA, Wilson SJ, Davies DE, Holgate ST: **Epithelial stress and structural remodelling in childhood asthma**. *Thorax* 2005, **60**:389-394.

17. McParland BE, Macklem PT, Pare PD: **Airway wall remodeling: friend or foe?** *J Appl Physiol* 2003, **95**:426-434.

18. James AL, Wenzel S: **Clinical relevance of airway remodelling in airway diseases**. *Eur Respir J* 2007, **30**:134-155.

19. Rasmussen F, Taylor DR, Flannery EM, Cowan JO, Greene JM, Herbison GP, Sears MR: **Risk factors for airway remodeling in asthma manifested by a low postbronchodilator FEV1/vital capacity ratio: a longitudinal population study from childhood to adulthood**. *Am J Respir Crit Care Med* 2002, **165**:1480-1488.

20. Johns DP, Wilson J, Harding R, Walters EH: **Airway distensibility in healthy and asthmatic subjects: effect of lung volume history**. *J Appl Physiol* 2000, **88**:1413-1420.

21. Ward C, Johns DP, Bish R, Pais M, Reid DW, Ingram C, Feltis B, Walters EH: **Reduced airway distensibility, fixed airflow limitation, and airway wall remodeling in asthma**. *Am J Respir Crit Care Med* 2001, **164**:1718-1721.

22. Boulet LP, Laviolette M, Turcotte H, Cartier A, Dugas M, Malo JL, Boutet M: **Bronchial subepithelial fibrosis correlates with airway responsiveness to methacholine**. *Chest* 1997, **112**:45-52.

23. Jeffery PK, Wardlaw AJ, Nelson FC, Collins JV, Kay AB: **Bronchial biopsies in asthma, an ultrastructural, quantitative study and correlation with hyperreactivity**. *Am Rev Respir Dis* 1989, **140**:1745-1753.

24. Bumbacea D, Campbell D, Nguyen L, Carr D, Barnes PJ, Robinson D, Chung KF: **Parameters associated with persistent airflow obstruction in chronic severe asthma**. *Eur Respir J* 2004, **24**:122-128.

25. Lambert RK, Wiggs BR, Kuwano K, Hogg JC, Pare PD: **Functional significance of increased airway smooth muscle in asthma and COPD**. *J Appl Physiol* 1993, **74**:2771-2781.

26. * Kaminska M, Foley S, Maghni K, Storness-Bliss C, Coxson H, Ghezzo H, Lemiere C, Olivenstein R, Ernst P, Hamid Q *et al.*: **Airway remodeling in subjects with severe asthma with or without chronic persistent airflow obstruction**. *J Allergy Clin Immunol* 2009, **124**:e41-44.
This paper was the first to show that contrary to severe asthmatic patients without chronic persistent obstruction (CPO), patients with CPO have different histopathologic and radiologic characteristics with increased airway smooth muscle and ongoing T(H)1 and T(H)2 inflammatory responses.

27. Bucchieri F, Puddicombe SM, Lordan JL, Richter A, Buchanan D, Wilson SJ, Ward J, Zummo G, Howarth PH, Djukanovic R *et al.*: **Asthmatic bronchial epithelium is more susceptible to oxidant-induced apoptosis**. *Am J Respir Cell Mol Biol* 2002, **27**:179-185.

28. Trautmann A, Schmid-Grendelmeier P, Kruger K, Crameri R, Akdis M, Akkaya A, Brocker EB, Blaser K, Akdis CA: **T cells and eosinophils cooperate in the induction of bronchial epithelial cell apoptosis in asthma**. *J Allergy Clin Immunol* 2002, **109**:329-337.

29. Roche WR, Beasley R, Williams JH, Holgate ST: **Subepithelial fibrosis in the bronchi of asthmatics**. *Lancet* 1989, **1**:520-524.

30. Johnson PR, Roth M, Tamm M, Hughes M, Ge Q, King G, Burgess JK, Black JL: **Airway smooth muscle cell proliferation is increased in asthma**. *Am J Respir Crit Care Med* 2001, **164**:474-477.

31. Martin JG, Ramos-Barbon D: **Airway smooth muscle growth from the perspective of animal models**. *Respir Physiol Neurobiol* 2003, **137**:251-261.

32. Madison JM: **Migration of airway smooth muscle cells**. *Am J Respir Cell Mol Biol* 2003, **29**:8-11.

33. Vermeer PD, Harson R, Einwalter LA, Moninger T, Zabner J: **Interleukin-9 induces goblet cell hyperplasia during repair of human airway epithelia**. *Am J Respir Cell Mol Biol* 2003, **28**:286-295.

34. Wills-Karp M, Chiaramonte M: **Interleukin-13 in asthma**. *Curr Opin Pulm Med* 2003, **9**:21-27.

35. McDonald DM: **Angiogenesis and remodeling of airway vasculature in chronic inflammation**. *Am J Respir Crit Care Med* 2001, **164**:S39-45.

36. Makinde T, Murphy RF, Agrawal DK: **Immunomodulatory role of vascular endothelial growth factor and angiopoietin-1 in airway remodeling**. *Curr Mol Med* 2006, **6**:831-841.

37. Lal BK, Varma S, Pappas PJ, Hobson RW 2nd, Duran WN: **VEGF increases permeability of the endothelial cell monolayer by activation of PKB/akt, endothelial nitric-oxide synthase, and MAP kinase pathways**. *Microvasc Res* 2001, **62**:252-262.

38. Haraguchi M, Shimura S, Shirato K: **Morphometric analysis of bronchial cartilage in chronic obstructive pulmonary disease and bronchial asthma**. *Am J Respir Crit Care Med* 1999, **159**:1005-1013.

39. ** Kiwamoto T, Ishii Y, Morishima Y, Yoh K, Maeda A, Ishizaki K, Iizuka T, Hegab AE, Matsuno Y, Homma S *et al.*: **Transcription factors T-bet and GATA-3 regulate development of airway remodeling**. *Am J Respir Crit Care Med* 2006, **174**:142-151.
This paper was the first to show that T-bet and GATA-3, the key transcription factors for differentiation toward Th1 and Th2 cells, regulate the development of airway remodeling in asthmatic patients by shifting the balance between Th1/Th2 cytokines.

40. Nakamura Y, Ghaffar O, Olivenstein R, Taha RA, Soussi-Gounni A, Zhang DH, Ray A, Hamid Q: **Gene expression of the GATA-3 transcription factor is increased in atopic asthma.** *J Allergy Clin Immunol* 1999, **103**:215-222.

41. • Cho JY, Miller M, Baek KJ, Han JW, Nayar J, Lee SY, McElwain K, McElwain S, Friedman S, Broide DH: **Inhibition of airway remodeling in IL-5-deficient mice.** *J Clin Invest* 2004, **113**:551-560.
This paper is among the first to determine, *in vivo*, that excluding eosinophil infiltration, using IL-5 knock out, resulted in dramatic decrease in airway remodeling and TGF-b tissue levels; also indicating, indirectly, the importance of eosinophil as a major source of TGF-b in asthmatic tissue.

42. Zhu Z, Homer RJ, Wang Z, Chen Q, Geba GP, Wang J, Zhang Y, Elias JA: **Pulmonary expression of interleukin-13 causes inflammation, mucus hypersecretion, subepithelial fibrosis, physiologic abnormalities, and eotaxin production.** *J Clin Invest* 1999, **103**:779-788.

43. Mazzarella G, Bianco A, Catena E, De Palma R, Abbate GF: **Th1/Th2 lymphocyte polarization in asthma.** *Allergy* 2000, **55(Suppl 61)**:6-9.

44. Jonuleit H, Schmitt E: **The regulatory T cell family: distinct subsets and their interrelations.** *J Immunol* 2003, **171**:6323-6327.

45. van Oosterhout AJ, Bloksma N: **Regulatory T-lymphocytes in asthma.** *Eur Respir J* 2005, **26**:918-932.

46. Larche M: **Regulatory T cells in allergy and asthma.** *Chest* 2007, **132**:1007-1014.

47. Tournoy KG, Hove C, Grooten J, Moerloose K, Brusselle GG, Joos GF: **Animal models of allergen-induced tolerance in asthma: are T-regulatory-1 cells (Tr-1) the solution for T-helper-2 cells (Th-2) in asthma?** *Clin Exp Allergy* 2006, **36**:8-20.

48. Seroogy CM, Gern JE: **The role of T regulatory cells in asthma.** *J Allergy Clin Immunol* 2005, **116**:996-999.

49. • Hartl D, Koller B, Mehlhorn AT, Reinhardt D, Nicolai T, Schendel DJ, Griese M, Krauss-Etschmann S: **Quantitative and functional impairment of pulmonary CD4+CD25hi regulatory T cells in pediatric asthma.** *J Allergy Clin Immunol* 2007, **119**:1258-1266.
This paper was the first to provide evidence that pulmonary CD4(+)CD25(hi) Tregs were impaired in pediatric asthma. Inhaled corticosteroid treatment was associated with increased percentages of CD4(+)CD25(hi) T cells in peripheral blood and BALF.

50. •• Miossec P, Korn T, Kuchroo VK: **Interleukin-17 and type 17 helper T cells.** *N Engl J Med* 2009, **361**:888-898.
One of the best recent reviews on the role of Interleukin-17 and Th17 Cells in Disease.

51. Chang SH, Dong C: **IL-17F: regulation, signaling and function in inflammation.** *Cytokine* 2009, **46**:7-11.

52. • Letuve S, Lajoie-Kadoch S, Audusseau S, Rothenberg ME, Fiset PO, Ludwig MS, Hamid Q: **IL-17E upregulates the expression of proinflammatory cytokines in lung fibroblasts.** *J Allergy Clin Immunol* 2006, **117**:590-596.
This is the first report to provide an insight into the role of IL-17E on airway remodeling. The authors show that IL-17E upregulates the expression of proinflammatory cytokines in lung fibroblasts.

53. •• Molet S, Hamid Q, Davoine F, Nutku E, Taha R, Page N, Olivenstein R, Elias J, Chakir J: **IL-17 is increased in asthmatic airways and induces human bronchial fibroblasts to produce cytokines.** *J Allergy Clin Immunol* 2001, **108**:430-438.
This is the first report to show an increase in IL-17 in asthmatic airways. They also demonstrated for the first time that eosinophils are a potential source of IL-17 within asthmatic airways.

54. Lajoie-Kadoch S, Joubert P, Letuve S, Halayko AJ, Martin JG, Soussi-Gounni A, Hamid Q: **TNF-alpha and IFN-gamma inversely modulate expression of the IL-17E receptor in airway smooth muscle cells.** *Am J Physiol Lung Cell Mol Physiol* 2006, **290**:L1238-1246.

55. Kuhn C 3rd, Homer RJ, Zhu Z, Ward N, Flavell RA, Geba GP, Elias JA: **Airway hyperresponsiveness and airway obstruction in transgenic mice. Morphologic correlates in mice overexpressing interleukin (IL)-11 and IL-6 in the lung.** *Am J Respir Cell Mol Biol* 2000, **22**:289-295.

56. Minshall EM, Leung DY, Martin RJ, Song YL, Cameron L, Ernst P, Hamid Q: **Eosinophil-associated TGF-beta1 mRNA expression and airways fibrosis in bronchial asthma.** *Am J Respir Cell Mol Biol* 1997, **17**:326-333.

57. Flood-Page P, Menzies-Gow A, Phipps S, Ying S, Wangoo A, Ludwig MS, Barnes N, Robinson D, Kay AB: **Anti-IL-5 treatment reduces deposition of ECM proteins in the bronchial subepithelial basement membrane of mild atopic asthmatics.** *J Clin Invest* 2003, **112**:1029-1036.

58. Vignola AM, Chanez P, Chiappara G, Merendino A, Pace E, Rizzo A, la Rocca AM, Bellia V, Bonsignore G, Bousquet J: **Transforming growth factor-beta expression in mucosal biopsies in asthma and chronic bronchitis.** *Am J Respir Crit Care Med* 1997, **156**:591-599.

59. Wong DT, Weller PF, Galli SJ, Elovic A, Rand TH, Gallagher GT, Chiang T, Chou MY, Matossian K, McBride J *et al.*: **Human eosinophils express transforming growth factor alpha.** *J Exp Med* 1990, **172**:673-681.

60. Wegmann M, Goggel R, Sel S, Erb KJ, Kalkbrenner F, Renz H, Garn H: **Effects of a low-molecular-weight CCR-3 antagonist on chronic experimental asthma.** *Am J Respir Cell Mol Biol* 2007, **36**:61-67.

61. • Munitz A, Bachelet I, Levi-Schaffer F: **Reversal of airway inflammation and remodeling in asthma by a bispecific antibody fragment linking CCR3 to CD300a.** *J Allergy Clin Immunol* 2006, **118**:1082-1089.
This paper was the first to show that, in mice model of chronic experimental asthma, cross-linking of CD300a inhibited mast cell and eosinophil activation using a bispecific antibody fragment resulting in significant reduction in lung inflammation, collagen deposition, and smooth-muscle thickening.

62. Minshall E, Chakir J, Laviolette M, Molet S, Zhu Z, Olivenstein R, Elias JA, Hamid Q: **IL-11 expression is increased in severe asthma: association with epithelial cells and eosinophils.** *J Allergy Clin Immunol* 2000, **105**:232-238.

63. Chakir J, Shannon J, Molet S, Fukakusa M, Elias J, Laviolette M, Boulet LP, Hamid Q: **Airway remodeling-associated mediators in moderate to severe asthma: effect of steroids on TGF-beta, IL-11, IL-17, and type I and type III collagen expression.** *J Allergy Clin Immunol* 2003, **111**:1293-1298.

64. Hamid Q, Barkans J, Meng Q, Ying S, Abrams JS, Kay AB, Moqbel R: **Human eosinophils synthesize and secrete interleukin-6, *in vitro*.** *Blood* 1992, **80**:1496-1501.

65. Davies DE: **The role of the epithelium in airway remodeling in asthma.** *Proc Am Thorac Soc* 2009, **6**:678-682.

66. Schleimer RP, Kato A, Kern R, Kuperman D, Avila PC: **Epithelium: at the interface of innate and adaptive immune responses.** *J Allergy Clin Immunol* 2007, **120**:1279-1284.

67. Broide DH, Lawrence T, Doherty T, Cho JY, Miller M, McElwain K, McElwain S, Karin M: **Allergen-induced peribronchial fibrosis and mucus production mediated by IkappaB kinase beta-dependent genes in airway epithelium.** *Proc Natl Acad Sci U S A* 2005, **102**:17723-17728.

68. Angkasekwinai P, Park H, Wang YH, Chang SH, Corry DB, Liu YJ, Zhu Z, Dong C: **Interleukin 25 promotes the initiation of proallergic type 2 responses.** *J Exp Med* 2007, **204**:1509-1517.

69. Mullings RE, Wilson SJ, Puddicombe SM, Lordan JL, Bucchieri F, Djukanovic R, Howarth PH, Harper S, Holgate ST, Davies DE: **Signal transducer and activator of transcription 6 (STAT-6) expression and function in asthmatic bronchial epithelium.** *J Allergy Clin Immunol* 2001, **108**:832-838.

70. Takeda N, Sumi Y, Prefontaine D, Al Abri J, Al Helaly N, Al-Ramli W, Michoud MC, Martin JG, Hamid Q: **Epithelium-derived chemokines induce airway smooth muscle cell migration.** *Clin Exp Allergy* 2009, **39**:1018-1026.

71. •• Holgate ST: **The airway epithelium is central to the pathogenesis of asthma.** *Allergol Int* 2008, **57**:1-10.

This review placed the epithelium at the forefront of asthma pathogenesis and hence suggested that different approaches to treatment can be focused more on protecting vulnerable airways against environmental injury rather than focusing on suppressing airway inflammation or manipulating the immune response.

72. Fernandes DJ, Mitchell RW, Lakser O, Dowell M, Stewart AG, Solway J: **Do inflammatory mediators influence the contribution of airway smooth muscle contraction to airway hyperresponsiveness in asthma?** *J Appl Physiol* 2003, **95**:844-853.

73. Ma X, Cheng Z, Kong H, Wang Y, Unruh H, Stephens NL, Laviolette M: **Changes in biophysical and biochemical properties of single bronchial smooth muscle cells from asthmatic subjects**. *Am J Physiol Lung Cell Mol Physiol* 2002, **283**:L1181-1189.

74. Ebina M, Takahashi T, Chiba T, Motomiya M: **Cellular hypertrophy and hyperplasia of airway smooth muscles underlying bronchial asthma. A 3-D morphometric study**. *Am Rev Respir Dis* 1993, **148**:720-726.

75. Hirst SJ, Martin JG, Bonacci JV, Chan V, Fixman ED, Hamid QA, Herszberg B, Lavoie JP, McVicker CG, Moir LM *et al.*: **Proliferative aspects of airway smooth muscle**. *J Allergy Clin Immunol* 2004, **114**:S2-17.

76. Gosens R, Roscioni SS, Dekkers BG, Pera T, Schmidt M, Schaafsma D, Zaagsma J, Meurs H: **Pharmacology of airway smooth muscle proliferation**. *Eur J Pharmacol* 2008, **585**:385-397.

77. Howarth PH, Knox AJ, Amrani Y, Tliba O, Panettieri RA Jr, Johnson M: **Synthetic responses in airway smooth muscle**. *J Allergy Clin Immunol* 2004, **114**:S32-50.

78. Hughes JM, Arthur CA, Baracho S, Carlin SM, Hawker KM, Johnson PR, Armour CL: **Human eosinophil-airway smooth muscle cell interactions**. *Mediators Inflamm* 2000, **9**:93-99.

79. Lee CW, Lin WN, Lin CC, Luo SF, Wang JS, Pouyssegur J, Yang CM: **Transcriptional regulation of VCAM-1 expression by tumor necrosis factor-alpha in human tracheal smooth muscle cells: involvement of MAPKs, NF-kappaB, p300, and histone acetylation**. *J Cell Physiol* 2006, **207**:174-186.

80. • Sukkar MB, Xie S, Khorasani NM, Kon OM, Stanbridge R, Issa R, Chung KF: **Toll-like receptor 2, 3, and 4 expression and function in human airway smooth muscle**. *J Allergy Clin Immunol* 2006, **118**:641-648.
In this paper, TLR ligands, and their activation was shown to mediate chemokine release in ASMCs. Proinflammatory responses mediated by activation of pathogen-recognition receptors in ASMCs might hence contribute to infectious exacerbations of airway inflammatory conditions, such as asthma.

81. Luo SF, Wang CC, Chiu CT, Chien CS, Hsiao LD, Lin CH, Yang CM: **Lipopolysaccharide enhances bradykinin-induced signal transduction via activation of Ras/Raf/MEK/MAPK in canine tracheal smooth muscle cells**. *Br J Pharmacol* 2000, **130**:1799-1808.

82. Postma DS, Timens W: **Remodeling in asthma and chronic obstructive pulmonary disease**. *Proc Am Thorac Soc* 2006, **3**:434-439.

83. James AJ, Penrose JF, Cazaly AM, Holgate ST, Sampson AP: **Human bronchial fibroblasts express the 5-lipoxygenase pathway**. *Respir Res* 2006, **7**:102.

84. Shale DJ, Ionescu AA: **Mucus hypersecretion: a common symptom, a common mechanism?** *Eur Respir J* 2004, **23**:797-798.

85. Doherty T, Broide D: **Cytokines and growth factors in airway remodeling in asthma**. *Curr Opin Immunol* 2007, **19**:676-680.

86. Undevia NS, Dorscheid DR, Marroquin BA, Gugliotta WL, Tse R, White SR: **Smad and p38-MAPK signaling mediates apoptotic effects of transforming growth factor-beta1 in human airway epithelial cells**. *Am J Physiol Lung Cell Mol Physiol* 2004, **287**:L515-524.

87. Michalik M, Pierzchalska M, Legutko A, Ura M, Ostaszewska A, Soja J, Sanak M: **Asthmatic bronchial fibroblasts demonstrate enhanced potential to differentiate into myofibroblasts in culture**. *Med Sci Monit* 2009, **15**:BR194-201.

88. Khalil N, Xu YD, O'Connor R, Duronio V: **Proliferation of pulmonary interstitial fibroblasts is mediated by transforming growth factor-beta1-induced release of extracellular fibroblast growth factor-2 and phosphorylation of p38 MAPK and JNK**. *J Biol Chem* 2005, **280**:43000-43009.

89. Leivonen SK, Hakkinen L, Liu D, Kahari VM: **Smad3 and extracellular signal-regulated kinase 1/2 coordinately mediate transforming growth factor-beta-induced expression of connective tissue growth factor in human fibroblasts**. *J Invest Dermatol* 2005, **124**:1162-1169.

90. Mattos W, Lim S, Russell R, Jatakanon A, Chung KF, Barnes PJ: **Matrix metalloproteinase-9 expression in asthma: effect of asthma severity, allergen challenge, and inhaled corticosteroids**. *Chest* 2002, **122**:1543-1552.

91. Chen G, Khalil N: **TGF-beta1 increases proliferation of airway smooth muscle cells by phosphorylation of map kinases**. *Respir Res* 2006, **7**:2.

92. Ito I, Fixman ED, Asai K, Yoshida M, Gounni AS, Martin JG, Hamid Q: **Platelet-derived growth factor and transforming growth factor-beta modulate the expression of matrix metalloproteinases and migratory function of human airway smooth muscle cells**. *Clin Exp Allergy* 2009, **39**:1370-1380.

93. Chu HW, Balzar S, Seedorf GJ, Westcott JY, Trudeau JB, Silkoff P, Wenzel SE: **Transforming growth factor-beta2 induces bronchial epithelial mucin expression in asthma**. *Am J Pathol* 2004, **165**:1097-1106.

94. • McMillan SJ, Xanthou G, Lloyd CM: **Manipulation of allergen-induced airway remodeling by treatment with anti-TGF-beta antibody: effect on the Smad signaling pathway**. *J Immunol* 2005, **174**:5774-5780.
This is the first report to suggest that anti-TGF-beta Ab treatment in a mouse model prevents the progression of airway remodeling following allergen challenge even when given in a therapeutic mode. The molecular mechanism behind this effect was shown to involve regulation of active TGF-beta signaling.

95. Kobayashi T, Liu X, Wen FQ, Fang Q, Abe S, Wang XQ, Hashimoto M, Shen L, Kawasaki S, Kim HJ *et al.*: **Smad3 mediates TGF-beta1 induction of VEGF production in lung fibroblasts**. *Biochem Biophys Res Commun* 2005, **327**:393-398.

96. Tang W, Geba GP, Zheng T, Ray P, Homer RJ, Kuhn C 3rd, Flavell RA, Elias JA: **Targeted expression of IL-11 in the murine airway causes lymphocytic inflammation, bronchial remodeling, and airways obstruction**. *J Clin Invest* 1996, **98**:2845-2853.

97. •• Van Eerdewegh P, Little RD, Dupuis J, Del Mastro RG, Falls K, Simon J, Torrey D, Pandit S, McKenny J, Braunschweiger K *et al.*: **Association of the ADAM33 gene with asthma and bronchial hyperresponsiveness**. *Nature* 2002, **418**:426-430.
This paper is a reference paper for the identification and characterization of ADAM33 as a putative asthma susceptibility gene.

98. Simpson A, Maniatis N, Jury F, Cakebread JA, Lowe LA, Holgate ST, Woodcock A, Ollier WE, Collins A, Custovic A *et al.*: **Polymorphisms in a disintegrin and metalloprotease 33 (ADAM33) predict impaired early-life lung function**. *Am J Respir Crit Care Med* 2005, **172**:55-60.

99. Lee JY, Park SW, Chang HK, Kim HY, Rhim T, Lee JH, Jang AS, Koh ES, Park CS: **A disintegrin and metalloproteinase 33 protein in patients with asthma: relevance to airflow limitation**. *Am J Respir Crit Care Med* 2006, **173**:729-735.

100. Puxeddu I, Pang YY, Harvey A, Haitchi HM, Nicholas B, Yoshisue H, Ribatti D, Clough G, Powell RM, Murphy G *et al.*: **The soluble form of a disintegrin and metalloprotease 33 promotes angiogenesis: implications for airway remodeling in asthma**. *J Allergy Clin Immunol* 2008, **121**: 1400-1406, 1406, e1401-1404.

101. Hoshino M, Nakamura Y, Hamid QA: **Gene expression of vascular endothelial growth factor and its receptors and angiogenesis in bronchial asthma**. *J Allergy Clin Immunol* 2001, **107**:1034-1038.

102. Lee CG, Link H, Baluk P, Homer RJ, Chapoval S, Bhandari V, Kang MJ, Cohn L, Kim YK, McDonald DM *et al.*: **Vascular endothelial growth factor (VEGF) induces remodeling and enhances TH2-mediated sensitization and inflammation in the lung**. *Nat Med* 2004, **10**:1095-1103.

103. Bhandari V, Choo-Wing R, Chapoval SP, Lee CG, Tang C, Kim YK, Ma B, Baluk P, Lin MI, McDonald DM *et al.*: **Essential role of nitric oxide in VEGF-induced, asthma-like angiogenic, inflammatory, mucus, and physiologic responses in the lung**. *Proc Natl Acad Sci U S A* 2006, **103**:11021-11026.

104. Wills-Karp M, Karp CL: **Biomedicine. Eosinophils in asthma: remodeling a tangled tale**. *Science* 2004, **305**:1726-1729.

105. McGee HS, Agrawal DK: **TH2 cells in the pathogenesis of airway remodeling: regulatory T cells a plausible panacea for asthma**. *Immunol Res* 2006, **35**:219-232.

106. Lilly CM, Nakamura H, Kesselman H, Nagler-Anderson C, Asano K, Garcia-Zepeda EA, Rothenberg ME, Drazen JM, Luster AD: **Expression of eotaxin by human lung epithelial cells: induction by cytokines and inhibition by glucocorticoids**. *J Clin Invest* 1997, **99**:1767-1773.

107. Stellato C, Beck LA, Gorgone GA, Proud D, Schall TJ, Ono SJ, Lichtenstein LM, Schleimer RP: **Expression of the chemokine RANTES by a human bronchial epithelial cell line. Modulation by cytokines and glucocorticoids**. *J Immunol* 1995, **155**:410-418.

108. Gonzalo JA, Lloyd CM, Wen D, Albar JP, Wells TN, Proudfoot A, Martinez AC, Dorf M, Bjerke T, Coyle AJ *et al.*: **The coordinated action of CC chemokines in the lung orchestrates allergic inflammation and airway hyperresponsiveness**. *J Exp Med* 1998, **188**:157-167.

109. Hardaker EL, Bacon AM, Carlson K, Roshak AK, Foley JJ, Schmidt DB, Buckley PT, Comegys M, Panettieri RA Jr, Sarau HM *et al.*: **Regulation of TNF-alpha- and IFN-gamma-induced CXCL10 expression: participation of the airway smooth muscle in the pulmonary inflammatory response in chronic obstructive pulmonary disease**. *FASEB J* 2004, **18**:191-193.

110. Joubert P, Lajoie-Kadoch S, Labonte I, Gounni AS, Maghni K, Wellemans V, Chakir J, Laviolette M, Hamid Q, Lamkhioued B: **CCR3 expression and function in asthmatic airway smooth muscle cells**. *J Immunol* 2005, **175**:2702-2708.

111. • Joubert P, Lajoie-Kadoch S, Welman M, Dragon S, Letuvee S, Tolloczko B, Halayko AJ, Gounni AS, Maghni K, Hamid Q: **Expression and regulation of CCR1 by airway smooth muscle cells in asthma**. *J Immunol* 2008, **180**:1268-1275.
This paper showed for the first time that ASMC express CCR1 mRNA and protein, both *in vitro* and *in vivo*. CCR1 is hence suggested to be involved in the pathogenesis of asthma, through the activation of ASMC by its ligands.

112. Yahiaoui L, Gvozdic D, Danialou G, Mack M, Petrof BJ: **CC family chemokines directly regulate myoblast responses to skeletal muscle injury**. *J Physiol* 2008, **586**:3991-4004.

113. Karol MH: **Animal models of occupational asthma**. *Eur Respir J* 1994, **7**:555-568.

114. Schneider T, van Velzen D, Moqbel R, Issekutz AC: **Kinetics and quantitation of eosinophil and neutrophil recruitment to allergic lung inflammation in a brown Norway rat model**. *Am J Respir Cell Mol Biol* 1997, **17**:702-712.

115. Ricciardolo FL, Nijkamp F, De Rose V, Folkerts G: **The guinea pig as an animal model for asthma**. *Curr Drug Targets* 2008, **9**:452-465.

116. Shin YS, Takeda K, Gelfand EW: **Understanding asthma using animal models**. *Allergy Asthma Immunol Res* 2009, **1**:10-18.

117. Oberholzer HM, Pretorius E: **Investigating lung remodeling in Modul8-treated BALB/c asthmatic animals**. *Micron* 2009, **40**:775-782.

118. Lederlin M, Ozier A, Montaudon M, Begueret H, Ousova O, Marthan R, Berger P, Laurent F: **Airway remodeling in a mouse asthma model assessed by *in vivo* respiratory-gated micro-computed tomography**. *Eur Radiol* 2010, **20**:128-137.

119. Ramos-Barbon D, Ludwig MS, Martin JG: **Airway remodeling: lessons from animal models**. *Clin Rev Allergy Immunol* 2004, **27**:3-21.

120. Martin JG, Suzuki M, Ramos-Barbon D, Isogai S: **T cell cytokines: animal models**. *Paediatr Respir Rev* 2004, **5(Suppl A)**:S47-S51.

121. Kelly MM, O'Connor TM, Leigh R, Otis J, Gwozd C, Gauvreau GM, Gauldie J, O'Byrne PM: **Effects of budesonide and formoterol on allergen-induced airway responses, inflammation, and airway remodeling in asthma**. *J Allergy Clin Immunol* 2010, **125**: 349–356, e313.

122. Molet SM, Hamid QA, Hamilos DL: **IL-11 and IL-17 expression in nasal polyps: relationship to collagen deposition and suppression by intranasal fluticasone propionate**. *Laryngoscope* 2003, **113**:1803-1812.

123. Henderson WR Jr, Chiang GK, Tien YT, Chi EY: **Reversal of allergen-induced airway remodeling by CysLT1 receptor blockade**. *Am J Respir Crit Care Med* 2006, **173**:718-728.

124. Kelly MM, Chakir J, Vethanayagam D, Boulet LP, Laviolette M, Gauldie J, O'Byrne PM: **Montelukast treatment attenuates the increase in myofibroblasts following low-dose allergen challenge**. *Chest* 2006, **130**:741-753.

125. Aoshiba K, Nagai A: **Differences in airway remodeling between asthma and chronic obstructive pulmonary disease**. *Clin Rev Allergy Immunol* 2004, **27**:35-43.

126. Kranenburg AR, de Boer WI, Alagappan VK, Sterk PJ, Sharma HS: **Enhanced bronchial expression of vascular endothelial growth factor and receptors (Flk-1 and Flt-1) in patients with chronic obstructive pulmonary disease**. *Thorax* 2005, **60**:106-113.

127. Bousquet J, Jacot W, Vignola AM, Bachert C, Van Cauwenberge P: **Allergic rhinitis: a disease remodeling the upper airways?** *J Allergy Clin Immunol* 2004, **113**:43-49.

128. Leigh R, Ellis R, Wattie J, Southam DS, De Hoogh M, Gauldie J, O'Byrne PM, Inman MD: **Dysfunction and remodeling of the mouse airway persist after resolution of acute allergen-induced airway inflammation**. *Am J Respir Cell Mol Biol* 2002, **27**:526-535.

Interleukin-11 Drives Early Lung Inflammation during *Mycobacterium tuberculosis* Infection in Genetically Susceptible Mice

Marina A. Kapina, Galina S. Shepelkova, Vadim G. Avdeenko, Anna N. Guseva, Tatiana K. Kondratieva, Vladimir V. Evstifeev, Alexander S. Apt*

Department of Immunology, Central Institute for Tuberculosis, Moscow, Russia

Abstract

IL-11 is multifunctional cytokine whose physiological role in the lungs during pulmonary tuberculosis (TB) is poorly understood. Here, using *in vivo* administration of specific antibodies against IL-11, we demonstrate for the first time that blocking IL-11 diminishes histopathology and neutrophilic infiltration of the lung tissue in TB-infected genetically susceptible mice. Antibody treatment decreased the pulmonary levels of IL-11 and other key inflammatory cytokines not belonging to the Th1 axis, and down-regulated IL-11 mRNA expression. This suggests the existence of a positive feedback loop at the transcriptional level, which is further supported by up-regulation of IL-11 mRNA expression in the presence of rIL-11 in *in vitro* cultures of lung cells. These findings imply a pathogenic role for IL-11 during the early phase of *Mycobacterium tuberculosis*-triggered disease in a genetically susceptible host.

Citation: Kapina MA, Shepelkova GS, Avdeenko VG, Guseva AN, Kondratieva TK, et al. (2011) Interleukin-11 Drives Early Lung Inflammation during *Mycobacterium tuberculosis* Infection in Genetically Susceptible Mice. PLoS ONE 6(7): e21878. doi:10.1371/journal.pone.0021878

Editor: Patricia T. Bozza, Fundação Oswaldo Cruz, Brazil

Received March 24, 2011; **Accepted** June 11, 2011; **Published** July 15, 2011

Funding: This study was financially supported by the NIH R01 grant AI078864 (to ASA), and the Russian Foundation for Basic Research grants 09-04-91321 (to GSS) and 10-04-00053 (to TKK). The funders had no role in study design, data collection and analysis, decision to publish, or preparation of the manuscript.

Competing Interests: The authors have declared that no competing interests exist.

* E-mail: asapt@aha.ru

Introduction

IL-11 is multifunctional cytokine with hematopoietic, immunomodulatory, and epithelial cell protective activities [1]. It is a member of the IL-6 cytokine family which includes cytokines that share the use of the gp130 molecule in their receptor complexes [2,3]. In several clinical and experimental studies, IL-11 displayed anti-inflammatory activity [4–7], although its over-expression may have a significant pro-inflammatory effect [8]. IL-11 augmented bone marrow recovery and platelet production, down-regulated pro-inflammatory type 1 cytokines, and has been approved for the human use for corresponding indications [1,9,10]. In the lungs, IL-11 was shown to be produced by epithelial cells, fibroblasts, smooth muscle cells and antigen-presenting cells in response to different stimuli, including respiratory viruses [11–14]. Using the ovalbumin-induced asthma model in transgenic and IL-11Rα-disrupted mice, it was demonstrated that IL-11 is involved in regulation of such Th2-type pulmonary responses as eosinophilic inflammation, mucus metaplasia and IL-13 production, without shifting the response towards Th1 inflammation [15–17].

The role of IL-11 during pulmonary tuberculosis (TB) and accompanying lung inflammation is poorly understood. *In vitro* studies from our laboratory demonstrated that the important producers of IL-11 are interstitial lung macrophages, and that the level of mRNA for IL-11 in these cells differs substantially between mouse strains, being higher in TB-susceptible I/St compared to TB-resistant A/Sn mice [18]. More recently, using infected (I/St×A/Sn) F2 hybrids segregating for the level of TB severity, it was demonstrated that the individual levels of IL-11 mRNA in the lung tissue correlated inversely with rapid body weight loss, the phenotype characteristic for *Mycobacterium tuberculosis*-triggered disease [19]. However, there was no direct physiologic evidence that disease progression and immune responses in the lungs could be altered by manipulating IL-11 production *in vivo*. Here, we show that blocking endogenous IL-11 with specific antibodies *in vivo* attenuates the severity of TB in genetically susceptible I/St mice. Moreover, we demonstrate that antibody treatment not only decreases the lung IL-11 content, but also down-regulates its mRNA expression, suggesting the existence of a positive feed-back loop at the transcriptional level, which is supported by *in vitro* experiments.

Results and Discussion

Rapid IL-11 response in the lungs of genetically susceptible mice after TB challenge and therapeutic effect of the anti-IL-11 treatment

Earlier we found that isolated and cultured interstitial lung macrophages from TB-susceptible I/St mice produced significantly more IL-11 than their counterparts from TB-resistant A/Sn mice [18]. Since numerous cell types are capable of producing this cytokine in the lungs [11–14,18], it was useful to evaluate whether or not TB-susceptible and resistant mice differed in the expression of IL-11 *in vivo* at the whole-organ level before and after TB infection. Assessment of mRNA extracted from the whole lungs of mice of the two strains by DNA microarray provided a ~5-fold increase ($2^{\Delta Ct} = 2.3$) in *il11* expression in TB-infected compared to naïve I/St mice, whereas its expression in A/Sn mice did not

change after TB challenge ($2^{\Delta Ct} = 0.7$). To address this issue more precisely, we compared the expression level of the *il11* gene in the lungs before and after TB challenge using qrt-PCR. At the whole-organ level, naïve A/Sn mice produced slightly more IL-11 mRNA compared to naïve I/St mice, which may reflect its production by cells other than lung macrophages and/or the difference between *in vivo* and *in vitro* systems. However, at 2 weeks post challenge, the levels of IL-11 mRNA remained the same in the lungs of A/Sn mice, but increased ~10-fold ($P<0.01$) in I/St mice (Fig. 1), suggesting an altered control of the infection-induced early IL-11 production in genetically susceptible animals. Importantly, the different kinetics of *il11* expression in the two mouse strains can not be explained by a more rapid accumulation of mycobacteria (stimulus) in the lungs of I/St mice, since there is no difference in mycobacterial growth between I/St and A/Sn mice until 3 weeks post challenge ([20], confirmed in this study, data not shown). It is also unlikely that a rapid increase in IL-11 response is due to some specific features of I/St genetic background: a reverse correlation between the level of IL-11 expression in the lungs and severity of early TB was demonstrated in a big segregating population of (I/St×A/Sn) F2 mice with highly diverse individual genetic compositions [19]. These observations prompted us to perform blocking experiments in an attempt to diminish the severity of the TB course in I/St mice.

Groups of I/St mice were infected and treated with either anti-IL-11 antibodies or pre-immune globulin as described in Materials & Methods, and mycobacterial loads in the lungs were compared between groups at day 24 post challenge. As shown in Fig. 2A, significantly fewer CFU were recovered from the lungs of anti-IL-11-treated mice, indicating a beneficial effect of treatment. We also compared the severity of lung pathology between experimental and control groups and found that anti-IL-11-treated animals did not develop necrotizing and/or coalescing TB foci (Fig. 2C), which were readily detected in a proportion of control animals

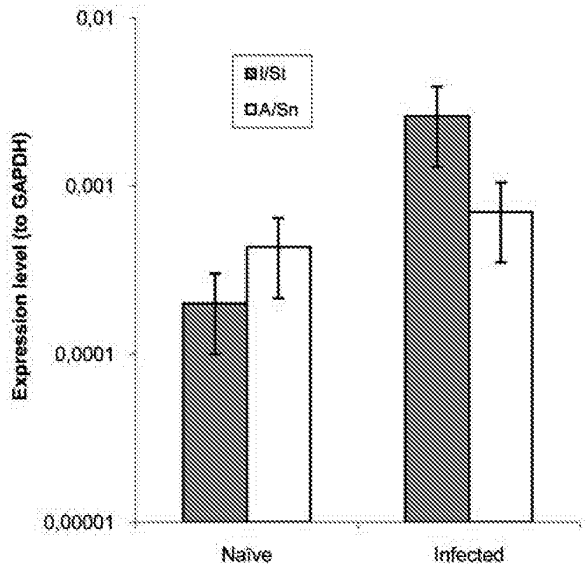

Figure 1. Two weeks after TB challenge the level of IL-11 mRNA increases ~1 log in the lungs of TB-susceptible I/St but does not change in TB-resistant A/Sn mice. Mean ± SEM expression level plotted against that of GABDT in 4 individual mice per group is displayed ($P<0.01$, ANOVA, between naïve and infected I/St mice).
doi:10.1371/journal.pone.0021878.g001

(Fig. 2B). This is an important observation, since both in humans and animals areas of necrosis and surrounding acellular matrix (rim structure) are primary sites for production of large numbers of bacteria [21,22], which provides a good explanation for the difference in CFU counts. A quantitative evaluation of pathology demonstrated that significantly smaller areas of the lung tissue were affected by inflammation in the experimental compared to the control group (Fig. 2D).

Taken together, these results clearly demonstrate a detrimental effect of the early IL-11 hyper-production in response to mycobacteria and suggest its causative role in pathogenesis of *M. tuberculosis*-triggered lung disease in mice.

Cellular infiltration and immune responses in the lungs

To find out how anti-IL-11 treatment alters infection-induced cellular infiltration, we assessed the content of major immune cell types in the lungs of infected mice. As shown in Table 1, the only statistically significant difference between mice that received non-immune rabbit globulin and anti-IL-11 antibodies was a reduced neutrophil content in the latter group. There is ample evidence that neutrophilic inflammation plays a detrimental role in mycobacteria-induced pathology. We and others, using genetic approaches, demonstrated deleterious rather than beneficial effects of these early inflammatory cells in the course of chronic mycobacterial infections [23–26]. The data presented herein add to this line of evidence, demonstrating the role of IL-11 in neutrophilia and providing an explanation for an early appearance of necrotic zones in the lungs of control mice displayed in Fig. 1B. As the granulomata mature, lung-infiltrating neutrophils die rapidly and the sites of their accumulation are replaced by necrotic zones [24].

We also assessed how the blocking of IL-11 influences the production of major cytokines in the lungs of infected mice. Treatment with anti-IL-11 antibodies significantly decreased the level of IL-11 itself, as well as the levels of key pro-inflammatory and immunoregulatory molecules – IL-6, TNF-α and MIP-2. On the other hand, the Th1-shifted immune response was not affected by the antibody administration: the prominent production of IL-12 and IFN-γ and the marginal to un-measurable production of IL-10 and IL-4 (not shown) was equal in antibody-treated and control mice (Fig. 3).

The question about IL-11 involvement in Th1/Th2 modulation remains unresolved. For example, there is evidence in cell culture systems that IL-11 can down-regulate IL-12 and IFN-γ production [27,28], but *in vivo* studies in gene knock-out and transgenic mice demonstrated its capacity to down-regulate Th2 cytokine production [11,17]. It is difficult to judge which activity, if any, might predominate during natural, un-manipulated *in vivo* conditions. The results of our blocking experiments in the mouse model of pulmonary TB clearly demonstrate that IL-11 substantially promotes lung inflammation but does not inhibit the Th1 response. It is quite possible that there is no general physiological pattern of immune response regulation by IL-11, and that it is dependent upon the biological context within which the effects of IL-11 are assessed.

Autocrine regulation of IL-11 production at the transcriptional level

Our data demonstrate that elevated lung IL-11 production starts very early after infection, and that neutralization of IL-11 diminishes both lung pathology and production of key regulatory cytokines. To find out whether a decrease in pulmonary IL-11, IL-6, TNF-α and MIP-2 protein production at day 24 post challenge was due to down-regulation of the expression of the corresponding

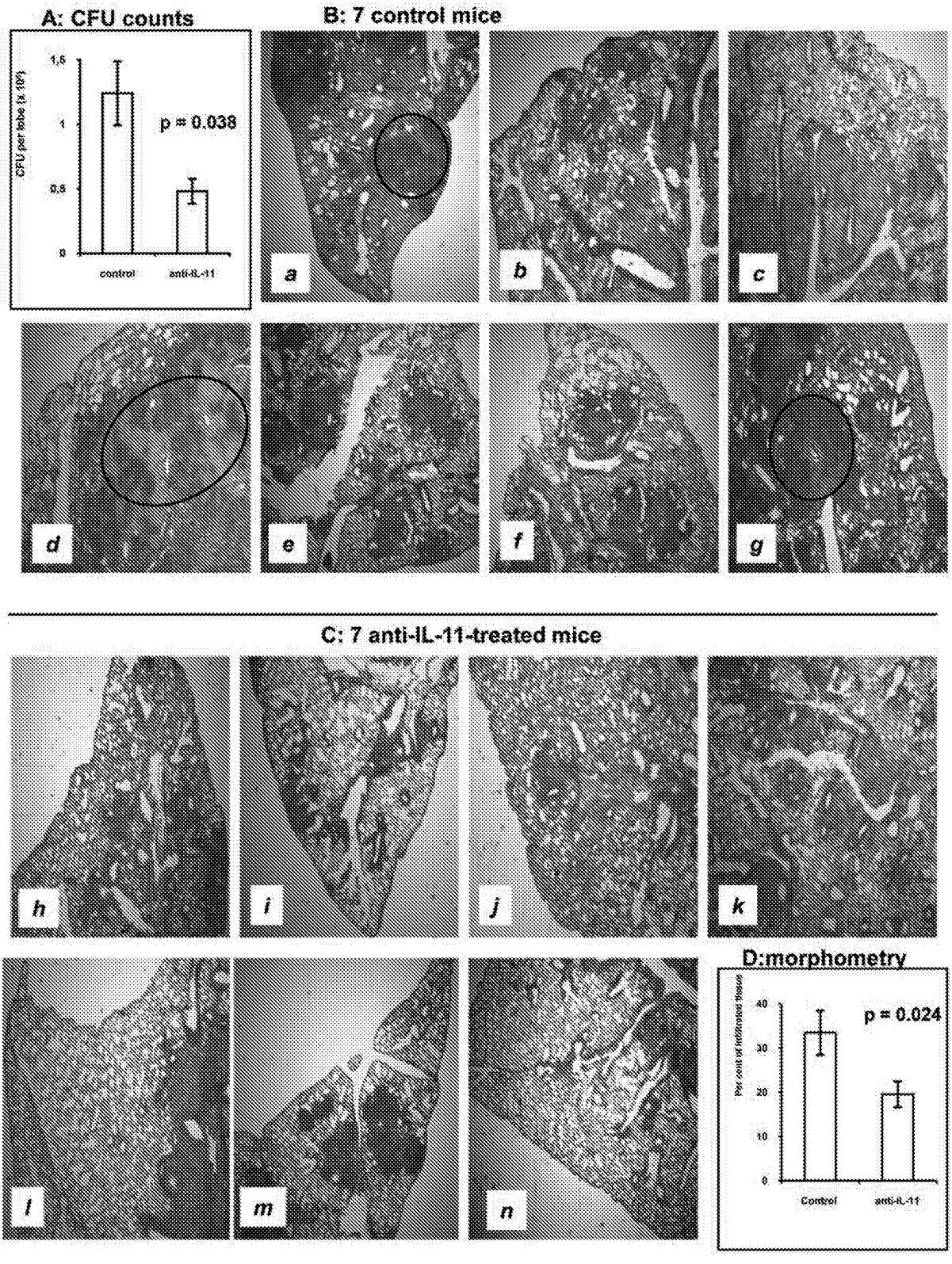

Figure 2. Treatment with anti-IL-11 antibodies significantly attenuates the severity of TB in I/St mice. (A) ~3-fold decrease in lung CFU counts compared to control animals. (B and C) Lung pathology in individual animals. None of anti-IL-11-treated mice developed necrotic TB foci evident in control mice *a, d* and *g* (circled). (D) Statistical evaluation of the proportion of inflamed lung tissue. CFU counts and morphometry were performed in all mice included in 2 independent experiments (total N = 16 and 17 for experimental and control groups, respectively). Histology is displayed for individual mice analyzed in one experiment (N = 7 for each group).
doi:10.1371/journal.pone.0021878.g002

genes, we assessed the levels of *il11*, *il6*, *tnfa* and *mip2* mRNA in the lung tissue of mice treated with either anti-IL-11 antibodies or control globulin. To our surprise, the only factor whose lung mRNA expression significantly decreased in anti-IL-11 treated mice was IL-11 itself (Fig. 4A). This result suggested that IL-11 expression is regulated post-infection in an autocrine manner at the translational level. On the other hand, no significant changes at the mRNA expression level were observed for IL-6, TNF-α and MIP-2, indicating that their decreased production in anti-IL-11-treated mice may well be due to reduced inflammation compared to control animals. To test the existence of a positive feed back loop, we assessed the level of IL-11 mRNA in lung cells cultured in the presence or absence of recombinant murine IL-11. As shown in Fig. 4B, 12-h incubation of lung cells in the presence of 100 ng/ml of rmIL-11 resulted in a significant increase in the *il11* mRNA levels compared to control cells, supporting our hypothesis.

Overall, our findings suggest that IL-11 production is rapidly elevated and self-supported in the lungs of genetically susceptible TB-infected mice. This promotes the development of early inflammation with a substantial contribution by neutrophils which, in turn, biases the response towards necrotic granuloma formation, accompanied by accelerated mycobacterial multiplication and a "cytokine storm" [29], thus, exacerbating pulmonary TB pathology.

Materials and Methods

Animals

Female mice of the I/StSnEgYCit strain (hereafter – I/St) aged 9–10 weeks were used. Compared to several inbred mouse strains, including A/SnEgCit (A/Sn) also used in this study, these mice display an extremely high level of susceptibility to TB, severity of lung pathology and prominent infiltration of *M. tuberculosis*-infected lung tissue with neutrophils, regardless to the dose and route of challenge [23,24,30,31]. Mice were bred under conventional conditions at the Animal Facilities of the Central Institute for Tuberculosis (CIT, Moscow, Russia), in accordance with the guidelines from the Russian Ministry of Health # 755, NIH Office of Laboratory Animal Welfare (OLAW) Assurance #A5502. Water and food were provided *ad libitum*. All experimental procedures were approved by the CIT animal care committee (IACUC protocols #2, 7, 8, 11, 13 approved on September 20, 2009).

Anti-IL-11 antibodies

Two conventional white rabbits were immunized with 0.05 μg of recombinant murine (rm) IL-11 (Sigma, St-Louis, MA) in incomplete Freund's adjuvant (Sigma), thrice, subcutaneously, with a 3-wk interval between injections. Before the first immunization, animals were bled and their serum immunoglobulin was affinity purified and depleted of anti-mycobacterial activity using procedures identical to those described below for immune sera. The mixed globulin preparation obtained from two non-immune rabbits served as the autologous control for *in vivo* administration. One month after the third immunization, animals were bled, and the level of anti-IL-11 antibodies in their mixed sera was assessed by indirect ELISA using rmIL-11 and immune anti-rabbit IgG conjugate (Bio-Rad, Richmond, CA). Serum IgG was isolated using Sepharose CL4B-protein A adsorbent (Pharmacia, Uppsala, Sweden).

Normal rabbit immunoglobulin possesses an intrinsic anti-mycobacterial activity which, after *in vivo* administration, could modulate the course of mycobacterial infection [32]. To avoid interference with their specific anti-IL-11 activity, immune and non-immune preparations were depleted of anti-mycobacterial activity using affinity chromatography. To this end, we prepared an immune adsorbent of *Mycobacterium tuberculosis* H37Rv sonicate bound to BrCN-activated Sepharose CL6B (Pharmacia, Uppsala, Sweden), as described [33], and repeatedly absorbed immunoglobulin preparations until the activity against mycobacterial sonicate assessed by immune blotting was completely lost (data not shown). Reactivity of the control and anti-IL-11 immunoglobulin preparations was assessed in the ELISA format and by immune blotting using rmIL-11 (Fig. 5A, B).

Table 1. Administration of anti-IL-11 antibodies decreases neutrophil influx in the lungs of TB-infected mice*.

Group	Cellular composition[a]											
	Total cell count	$CD4^+$		$CD8^+$		$CD19^+$		$F4/80^+$		$Ly\text{-}6G^+$	
		Per cent	10^6/lobe	Per cent	10^6/lobe	Per cent	10^6/lobe	Per cent	10^6/lobe	Per cent	10^6/lobe
Control Ig	15.1±1.5	40.6±2.4	6.1±0.5	19.6±1.8	3.0±0.2	14.1±1.2	2.2±0.2	8.7±0.6	1.3±0.2	**15.2±2.5**	**2.3±0.3**
Anti-IL-11	12.8±1.3	40.7±2.3	5.2±0.5	19.4±1.2	2.5±0.4	19.9±2.6	2.6±0.3	9.1±0.6	1.2±0.1	**8.4±1.2**	**1.1±0.2**
P	0.278	>0.7		>0.5		0.384		>0.8		**0.024**[b]	

*Middle right lobes were individually isolated from two groups of mice (two independent experiments, exp. 1: N = 7 and 7; exp. 2: N = 9 and 10; total $N = 16_{control}$ and $N = 17_{exp.}$), enzymatically disrupted, and single-cell suspensions analyzed by flow cytometry using FITC- or PE-labeled mAbs to the indicated surface markers. Results are presented as summarized mean ± SD for all animals.

[a]For $F4/80^+$ macrophages and $Ly\text{-}6G^+$ PMN: per cent of the total cell count; for B- and T-lymphocytes: per cent of the population gated for the lymphocyte size. Significant (Student's *t*-test) difference in the neutrophil content between experimental and control groups is highlighted in bold.

[b]The only statistically significant difference between mice that received control rabbit globulin and anti-IL-11 antibodies was a decrease in the lung neutrophil infiltration in the latter group.

doi:10.1371/journal.pone.0021878.t001

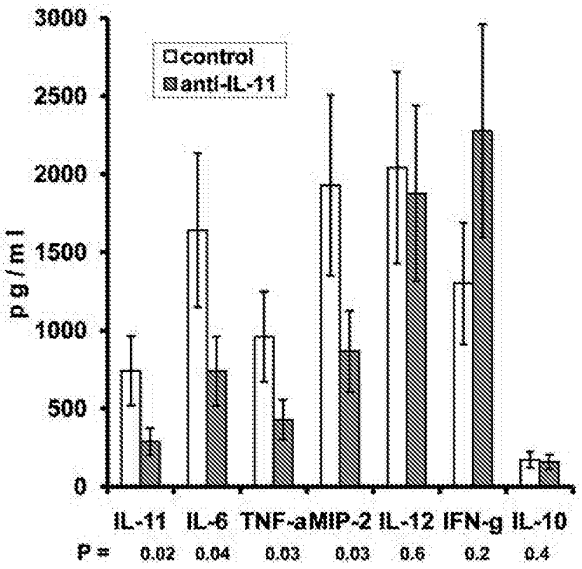

Figure 3. Anti-IL-11 antibody therapy decreases levels of IL-11 and pro-inflammatory factors in the lung tissue without shifting the IL-12 – IFN-γ/IL-10 balance. Cytokine contents in lung homogenates were assessed by ELISA for 4 mice in each group. The results of one of two similar experiments are displayed as mean ± SEM.
doi:10.1371/journal.pone.0021878.g003

Administration of antibodies and infection

At day 0, mice were infected with 10^3 CFU *Mycobacterium tuberculosis* H37Rv (Pasteur) via intra-tracheal route exactly as described previously [31]. At days −1, +2, +14, +17, +20 and +22 mice were injected peritoneally with 50 µg/mouse of either anti-IL-11 (experiment) or pre-immune (control) purified rabbit immunoglobulin preparation. Two independent experiments in groups of 7–10 control and experimental animals each provided almost identical results, which were combined for the statistical analysis of the major phenotypes.

CFU counts

Mice were sacrificed at day 24 post-challenge. Apical right lobes from individual mice (in two experiments total $N = 17_{contr.}$ and $N = 18_{exp.}$) were homogenized in 1 ml of sterile saline, and 0.1 ml of serial 10-fold dilutions of homogenates were plated onto Dubos agar. Colonies were counted after 18–20 days of incubation at 37°C.

Histopathology

Left lungs of individual mice were removed, inflated with 4% formalin in PBS (pH = 7.2) via the bronchus, and fixed in 4% formalin for 24 h. The samples were processed, embedded in paraffin, sectioned and stained with hematoxylin and eosin. Morphometry was performed at the ×37.5 magnification using Axioskop 40 microscope and AxioVision 4.8.1.0 software (Carl Zeiss, Berlin, Germany). The area of inflamed lung parenchyma, excluding vessels and airways, was measured and calculated as a percentage of the area of total lung parenchyma.

Cytokine mRNA quantification

Total RNA from the lower right lung lobes of individual mice was isolated using the commercial SV Total RNA Isolation System, and reverse transcription of mRNA was performed using reagents and protocols from Promega, Madison, WI. To detect the mRNA levels for a number of inflammation-related genes, quantitative real-time RT-PCR (qrt-PCR) with cDNA was performed using the iCycler iQ Multicolor Real-Time PCR Detection System (BioRad, Hercules, CA), and specific primers, TaqMan probes and reagents from Applied Biosystems (Foster City, CA). Gene expression levels in the lung tissue of individual mice were normalized to those of GAPDH. To quantify the results

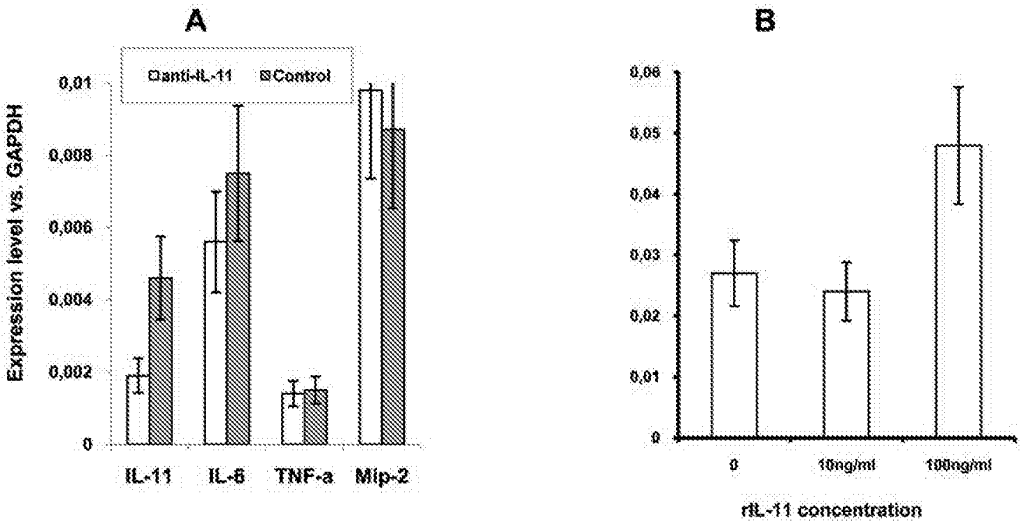

Figure 4. Protein levels of IL-11 affect IL-11 mRNA expression. (A) *In vivo* administration of anti-IL-11 antibodies leads to a selective down-regulation of IL-11 mRNA. The level of expression was quantified in 5 individual mice per group, using qrt-PCR and normalization against the level of GAPDH expression. Results obtained in 1 of 2 similar experiments are expressed as mean ± SEM (for IL-11 expression $P = 0.021$, for other cytokines $P > 0.05$). (B) Introduction of 100 ng/ml rIL-11 in cultures of lung cells up-regulates the expression of IL-11 mRNA. Results of two similar experiments are expressed as mean of 3 wells ± SEM ($P < 0.01$, ANOVA, compared to negative controls and cultures stimulated with 10 ng/ml IL-11).
doi:10.1371/journal.pone.0021878.g004

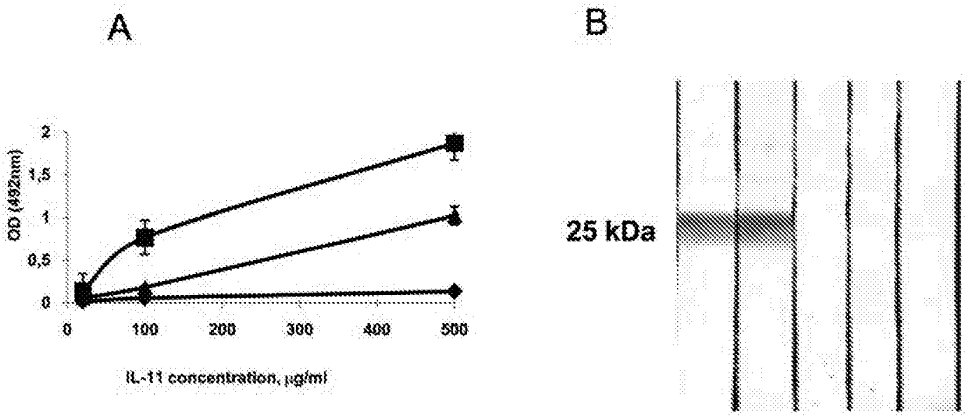

Figure 5. Properties of anti-IL-11 polyclonal antibodies. (A) Reactivity of affinity purified rabbit globulin preparation against mIL-11 assessed in ELISA format. No reactivity was found in pre-immune globulin (diamonds); immunoglobulin from rabbits immunized thrice with rmIL-11 showed very strong reactivity (squares); after exhaustion on mycobacterial sonicate adsorbent, specific anti-IL-11 reactivity dropped but was readily detected (triangles). (B) Immune blotting with rmIL-11 with polyclonal rabbit anti-mIL-11 antibodies (preparation identical to one displayed as triangles in (A). Tracks: 1, 2 – immune rabbits 1 and 2; 3, 4 – pre-immune rabbits 1 and 2; 5 – conjugate-free control.
doi:10.1371/journal.pone.0021878.g005

obtained by real-time PCR, the comparative threshold method was used exactly as described in [34], with the expression of the results as mean fold increase ± SEM for groups of 4 mice each.

To assess the ability of rIL-11 to up-regulate its own mRNA production, lung cell suspensions were prepared as described in [31], and cultured in RPMI-1640 medium containing 5% FCS and standard supplements (all components – HiClone, HiClone, Logan, UT, USA). Lung cells were cultured in 6-well plates (Costar, Badhoevedorp, The Netherlands) at 1.5×10^6 cells/ml in the absence or presence of 10 ng/ml and 100 ng/ml rmIL-11 (ImmunoTools, Friesoythe, Germany) for 12 h before RNA was isolated, reversely transcribed, and *il11* expression was assessed with normalization to that of GAPDH. Two independent experiments, performed with mixtures of RNA from 3 I/St mice each, provided similar results.

Flow cytometry and cytokine ELISA

Middle right lobes were individually isolated, enzymatically disrupted as described in [31], and single-cell suspensions analyzed by flow cytometry using FITC- or PE-labeled mAbs to the indicated surface markers (Table 1). Results are presented as summarized mean ± SEM for all animals.

To measure cytokine contents, the rest of each sample was centrifuged, and the pellets frozen at −70°C until assessed. The thawed samples from 4 mice in each group were diluted in 2 ml of PBS, debris removed by centrifugation at 500 g, and the cytokine content assessed in ELISA format using the ELISA kits for IL-6, IL-10, IL-12, MIP-2, TNF-α and IFN-γ purchased from PharMingen, San-Diego, CA, and for IL-11 purchased from R&D Systems, Minneapolis, MI, according to the manufacturers' instructions.

Statistical Analyses

One-tail analysis of variance (ANOVA) and Student's *t*-test were used as indicated in figure legends and table footnotes. $P<0.05$ was considered statistically significant.

Author Contributions

Conceived and designed the experiments: AA MK GS VE. Performed the experiments: MK GS VA AG TK VE. Analyzed the data: AA GS MK. Contributed reagents/materials/analysis tools: MK GS VA AG TK VE AA. Wrote the paper: AA.

References

1. Du X, Williams DA (1997) Interleukine-11: review of molecular, cell biology, and clinical use. Blood 89: 3897–3908.
2. Taga T, Kishimoto T (1997) GP 130 and the interleukine-6 family of cytokines. Ann Rev Immunol 15: 797–819.
3. Sims NA, Walsh NC (2010) GP 130 cytokines and bone remodeling in health and disease. BMB Reports 43: 513–523.
4. Trepicchio WL, Bozza M, Pedneault G, Dorner AJ (1996) Recombinant human IL-11 attenuates the inflammatory response through down-regulation of proinflammatory cytokine release and nitric oxide production. J Immunol 157: 3627–3634.
5. Peterson RL, Wang L, Albert L, Keuth JC, Jr., Dorner AJ (1998) Molecular effects of recombinant human interleukine-11 in the HLA-B27 rat model of inflammatory bowel disease. Lab Invest 78: 1503–1512.
6. Herrlinger KR, Witthoeft T, Raedler A, Bokemeyer B, Krummenerl T, et al. (2006) Randomized, double-blind, controlled trial of subcutaneous recombinant human interleukin-11 versus prednisolone in active Crohn's disease. Am J Gastroenterol 101: 793–797.
7. Bosani M, Ardizzione S, Porro GB (2009) Biological targeting in the treatment of inflammatory bowel disease. Biologics: Targets & Therapy 3: 77–97.
8. Wang PK, Campbell IK, Robb L, Wicks IP (2005) Endogenous IL-11 is pro-inflammatory in acute methylated bovine serum albumin/IL-1-induced (mBSA/IL-1) arthritis. Cytokine 29: 72–76.
9. Trepicchio WL, Ozawa M, Walters IB, Kikuchi T, Gilleaudeau P, et al. (1999) Interleukin-11 therapy selectively downregulates type I cytokine proinflammatory pathways in psoriasis lesions. J Clin Invest 104: 1527–1537.
10. Feinglass S, Deodhar A (2001) Treatment of lupus-induced thrombocytopenia with recombinant human interleukin-11. Arthritis Rheum 44: 70–75.
11. Zheng T, Nathanson MH, Elias JA (1994) Histamine augments cytokine-stimulated IL-11 production by human lung fibriblasts. J Immunol 153: 4742–4752.
12. Elias JA, Zheng T, Whiting NL, Trow TK, Merrill WW, et al. (1994) IL-1 and TGF-beta regulation of fibroblast-derived IL-11. J Immunol 152: 2421–2429.
13. Einarsson O, Geba GP, Zhu Z, Elias JA (1996) Interleukin-11: stimulation *in vivo* and *in virtro* by respiratory viruses and induction of airways hyper-responsiveness. J Clin Invest 97: 915–924.
14. Bartz H, Buning-Pfaue F, Turkel O, Schauer U (2002) Respiratory virus induces prostaglandin E2, IL-10 and IL-11 generation in antigen-presenting cells. Clin Exp Immunol 129: 438–445.

15. Wang J, Homer RJ, Hong L, Cohn L, Lee CG, et al. (2000) IL-11 selectively inhibits aerallergen-induced pulmonary eosinophilia and Th2 cytokine production. J Immunol 163: 2222–2231.
16. Kuhn III CH, Homer RJ, Zhu Z, Ward N, Flavell RA, et al. (2000) Airway hyperresponsiveness and airway obstruction in transgenic mice. Am J Respir Care Mol Med 22: 289–295.
17. Lee CC, Hartl D, Matsuura H, Dunlop FM, Scotney PD, et al. (2008) Endogenous IL-11 signaling is essential in Th2- and IL-13-induced inflammation and mucus production. Am J Respir Cell Mol Biol 39: 739–746.
18. Orlova MO, Majorov KB, Lyadova IV, Eruslanov EB, M'lan CE, et al. (2006) Constitutive differences in gene expression profiles parallel genetic patterns of susceptibility to tuberculosis in mice. Infect Immun 74: 3668–3672.
19. Lyadova IV, Tsiganov EN, Kapina MA, Shepelkova GS, Sosunov VV, et al. (2010) In mice, tuberculosis progression is associated with intensive inflammatory response and the accumulation of Gr-1 cells in the lungs. PLoS One 4: e10469.
20. Nikonenko BV, Averbakh MM, Lavebratt C, Schurr E, Apt AS (2000) Comparative analysis of mycobacterial infections in susceptible I/St and resistant A/Sn inbred mice. Tuber Lung Dis 80: 15–25.
21. Ulrichs T, Kosmiadi GA, Jorg S, Pradl L, Titukhina M, et al. (2005) Differential organization of the local immune response in patients with active cavitary tuberculosis or with nonprogressive tuberculoma. J Infect Dis 192: 89–97.
22. Lenaerts AJ, Hoff D, Aly S, Ehlers S, Andries K, et al. (2007) Mycobacteria in a guinea pig model of tuberculosis revealed by r207910. Antimicrob Agents Chemother 51: 3338–3345.
23. Eruslanov EB, Lyadova IV, Kondratieva TK, Majorov KB, Scheglov IV, et al. (2005) Neutrophil responses to *Mycobacterium tuberculosis* infection in genetically susceptible and resistant mice. Infect Immun 73: 1744–1753.
24. Kondratieva EV, Logunova N, Majorov KB, Averbakh MM, Apt AS (2010) Host genetics in granuloma formation: human-like lung pathology in mice with reciprocal genetic susceptibility to *M. tuberculosis* and *M. avium*. PLoS One 5: e10515.
25. Keller C, Hoffmann R, Lang R, Brandau S, Hermann C, et al. (2006) Genetically determined susceptibility to tuberculosis in mice causally involves accelerated and enhanced recruitment of granulocytes. Infect Immun 74: 4295–4309.
26. Beisiegel M, Kursar M, Koch M, Loddenkemper C, Kuhlmann S, et al. (2009) Combination of host susceptibility and virulence of *Mycobacterium tuberculosis* determines dual role of nitric oxide in the protection and control of inflammation. J Infect Dis 199: 1222–1232.
27. Bozza M, Bliss JL, Dorner AJ, Trepicchio WL (2001) Interleukine-11 modulates Th1/Th2 cytokine production from activated $CD4^+$ T cells. J Interferon Cytokine Res 21: 21–30.
28. Torroella-Kouri M, Keith JC, Ivanova M, Lopez DM (2003) IL-11-induced reduction of C/EBR transcription factor binding may contribute to the IL-12 down-regulation in tumor-bearung mice. Int J Oncol 22: 439–448.
29. Russell D (2007) Who puts the tubercle in tuberculosis? Nat Rev Microbiol 5: 39–47.
30. Nickonenko BV, Apt AS, Moroz AM, Averbakh MM (1985) Genetic analysis of susceptibility of mice to H37Rv tuberculosis infection: sensitivity *versus* relative resistance. Progr Leuk Biol 3: 291–299.
31. Eruslanov EB, Majorov KB, Orlova MO, Mischenko VV, Kondratieva TK, et al. (2004) Lung cell responses to *M. tuberculosis* in genetically susceptible and resistant mice following intratracheal challenge. Clin Exp Immunol 135: 19–28.
32. Glatman-Freedman A, Casadevall A (1998) Serum therapy for tuberculosis revisited: reapprisal of the role of antibody-mediated immunity against *Mycobacterium tuberculosis*. Clin Microbiol Rev 11: 514–532.
33. Pfeiffer NE, Wylier DE, Schuster SM (1987) Immunoaffinity chromatography utilizing monoclonal antibodies. Factors which influence antigen-binding capacity. J Immunol Meth 97: 1–9.
34. Livak KJ, Schmittgen TD (2001) Analysis of relative gene expression data using real-time quantitative PCR and the 2(−Delta Delta C(T)) method. Methods 25: 402–408.

Fibrosis in heart disease: understanding the role of transforming growth factor-β_1 in cardiomyopathy, valvular disease and arrhythmia

Razi Khan and Richard Sheppard
McGill University, Faculty of Medicine, Montreal, Quebec, Canada

doi:10.1111/j.1365-2567.2006.02336.x
Received 25 July 2005; revised 4 January 2006; accepted 4 January 2006.
Conflict of interest: None
Correspondence: Mr Razi Khan, McGill University, Faculty of Medicine, 3550 Jeanne Mance, Apt. 1811E, Montreal, Quebec, Canada H2X 3P7.
Email: razi.khan@mail.mcgill.ca
Senior author: Dr Richard Sheppard, email: richard.sheppard@mcgill.ca

Summary

The importance of fibrosis in organ pathology and dysfunction appears to be increasingly relevant to a variety of distinct diseases. In particular, a number of different cardiac pathologies seem to be caused by a common fibrotic process. Within the heart, this fibrosis is thought to be partially mediated by transforming growth factor-β_1 (TGF-β_1), a potent stimulator of collagen-producing cardiac fibroblasts. Previously, TGF-β_1 had been implicated solely as a modulator of the myocardial remodelling seen after infarction. However, recent studies indicate that dilated, ischaemic and hypertrophic cardiomyopathies are all associated with raised levels of TGF-β_1. In fact, the pathogenic effects of TGF-β_1 have now been suggested to play a major role in valvular disease and arrhythmia, particularly atrial fibrillation. Thus far, medical therapy targeting TGF-β_1 has shown promise in a multitude of heart diseases. These therapies provide great hope, not only for treatment of symptoms but also for prevention of cardiac pathology as well. As is stated in the introduction, most reviews have focused on the effects of cytokines in remodelling after myocardial infarction. This article attempts to underline the significance of TGF-β_1 not only in the post-ischaemic setting, but also in dilated and hypertrophic cardiomyopathies, valvular diseases and arrhythmias (focusing on atrial fibrillation). It also aims to show that TGF-β_1 is an appropriate target for therapy in a variety of cardiovascular diseases.

Keywords: anti-fibrotic treatment; atrial fibrillation; remodelling; Smad; transforming growth factor-β_1

Introduction

Transforming growth factor-β_1 (TGF-β_1) is a profibrotic cytokine that stimulates the production of extracellular matrix proteins in a number of different organ systems. However, overexpression of TGF-β_1 results in tissue fibrosis and organ dysfunction. TGF-β_1 has been implicated in the development of diabetic nephropathy, ulcerative colitis, hepatic fibrosis and congenital disease.[1–4]

Similarly, in the heart, TGF-β_1 appears to be one of several factors that cause disease by inducing cardiac fibrosis, as evidenced by overexpression and knockout models.[5–8] The increased presence of extracellular matrix proteins within the myocardium results in an alteration of ventricular properties that causes both systolic and diastolic dysfunction.[9] TGF-β_1-associated fibrosis also results in an inhomogeneous milieu for electrical propagation. This environment impedes anisotropic or linear conduction leading to the development of arrhythmia.[10] Similarly, excessive production of extracellular proteins within heart valves results in leaflet thickening and impaired motion with associated valvular dysfunction.[11]

The significant pathology correlated with TGF-β_1 overexpression has led to an increasing amount of research examining treatment for TGF-β_1-induced fibrosis. Thus far, TGF-β_1 inhibition has been shown to reverse the

Abbreviations: ACE, angiotensin-converting enzyme; ATF-2, activated transcription factor-2; CTGF, connective tissue growth factor; MAPKKK, mitogen-activated protein kinase kinase kinase; MMP, matrix metalloproteinases; MT-MMP, membrane type-MMP; TAK1, transforming growth factor-β-activated kinase; TGF-β_1, transforming growth factor-β_1.

fibrotic effects of the cytokine in animal models.[12] In addition, the promise of gene therapy used to promote the expression of TGF-β inhibitors offers hope for preventing fibrosis rather than merely treating it.[13]

Until recently most reviews have focused on the effects of TGF-β_1 in postmyocardial infarction remodelling. However, this study attempts to create a new paradigm emphasizing the significance of TGF-β_1 in a variety of heart diseases.

Examining TGF-β_1 and its physiological role

In mammals, TGF-β is found in three isoforms: TGF-β_1, TGF-β_2 and TGF-β_3. TGF-β_1 is expressed in myofibroblasts, vascular smooth muscle cells, endothelial cells and macrophages.[14] The human TGF-β_1 gene is found on chromosome 19, and can be transcribed and translated to form a 390 amino acid propeptide. This propeptide is cleaved intracellularly, producing two identical 112 amino acid peptide subunits joined together by a disulphide bond.[15] TGF-β_1 is secreted initially as a biologically inactive molecule bound to latent associated peptides.[16] Latent TGF-β_1 is then activated by cell–cell interaction, acidification, and enzymatic cleavage.[15]

TGF-β_1 plays a significant physiological role within the body. In the brain, TGF-β_1 acts synergistically with glial-derived neurotrophic factor in promoting the survival of both peripheral and central nervous system neurons.[17] TGF-β_1 acts primarily as a powerful immunosuppressant, inhibiting lymphocyte proliferation in the presence of interleukin-2, as well as modulating differentiation and apoptosis of T cells.[18,19] Studies have also suggested that TGF-β_1 may be important in the stabilization of atherosclerotic plaques through inhibition of local inflammation.[20,21] Finally, TGF-β_1 is released at wound sites initially stimulating the migration of neutrophils, monocytes and fibroblasts to injury zones. It subsequently enhances expression of extracellular matrix proteins from fibroblasts.[22]

Unfortunately, the overexpression of TGF-β_1 is thought to result in increased extracellular matrix protein synthesis. It is this excess of extracellular matrix proteins that defines fibrosis.

Molecular mechanisms of TGF-β_1 action

Up-regulation of TGF-β_1 via angiotensin II

The link between angiotensin II and TGF-β_1 was first noted in the kidney. Angiotensin II was shown to raise TGF-β_1 levels in the kidney, resulting in the development and progression of nephritic glomerular disease.[23] Similarly, Fukuda established that angiotensin II stimulated the expression of TGF-β_1 in vascular smooth muscle cells and led to cellular proliferation.[24]

Regarding the heart, there have been a number of *in vitro* and *in vivo* studies which have indicated that TGF-β_1 is up-regulated by angiotensin II in myofibroblasts and cardiac fibroblasts.[25,26] Administration of angiotensin II to cardiocytes has been shown to be associated with increased TGF-β_1 expression.[27] Using human atrial myocardial tissue, Kupfahl *et al.* noted that angiotensin II did not directly stimulate collagen expression, but rather caused TGF-β_1 up-regulation, which then altered collagen production.[28] Kim *et al.* found that angiotensin II antagonists inhibited the expression of the TGF-β_1 gene in cardiac and vascular tissue in rats.[29] Similarly, in hypertensive rat models, the use of angiotensin II receptor blockers has been shown to suppress the induction of TGF-β_1 and prevent myocardial fibrosis. Finally, Schultz *et al.* demonstrated that angiotensin II could not induce hypertrophy in mice lacking the TGF-β_1 gene.[8]

In clinical trials, a number of studies have indicated that angiotensin-converting enzyme (ACE) inhibitors and angiotensin II receptor antagonists may decrease production of TGF-β_1.[30,31] In patients with cardiorenal damage and associated increased angiotensin II serum levels, Laviades *et al.* noted elevated serum concentrations of TGF-$\beta_1$and C-terminal propeptide of procollagen type I (a marker of collagen type I synthesis) when compared to controls.[32] Administration of losartan reduced serum levels of TGF-β_1 and C-terminal propeptide of procollagen type I.

The ameliorative effects of ACE inhibitors and angiotensin II receptor blockers on the heart are partially attributable to the inhibition of extracellular protein production. Both animal and clinical studies indicate that these effects are most likely mediated through antagonism of TGF-β_1 and its downstream proteins.

Following the TGF-β_1–Smad pathway

After synthesis and release into the extracellular space, TGF-β_1 binds to a dimerized complex, which is comprised of two serine-threonine kinase receptors known as TGF-β_1 receptor 1 and 2.[33] Ligand-receptor binding eventually leads to phosphorylation of Smad proteins, conserved transcriptional proteins that act as second messengers for the TGF-β_1 superfamily, and the formation of a heteromeric complex that regulates expression of DNA. Smad proteins can be categorized into three groups: receptor-activated Smads (Smad1, Smad2, Smad3, Smad5 and Smad8), co-mediator Smads (Smad4 and Smad10) and inhibitory Smads (Smad6 and Smad7).[34]

In the heart, it has been postulated that the effects of TGF-β_1 are primarily mediated through Smad2 phosphorylation.[35] Once phosphorylated, Smad2 forms a complex with Smad3 and Smad4. This complex then translocates into the nucleus and binds to Smad-binding oligonucleotides present in the regulatory regions of

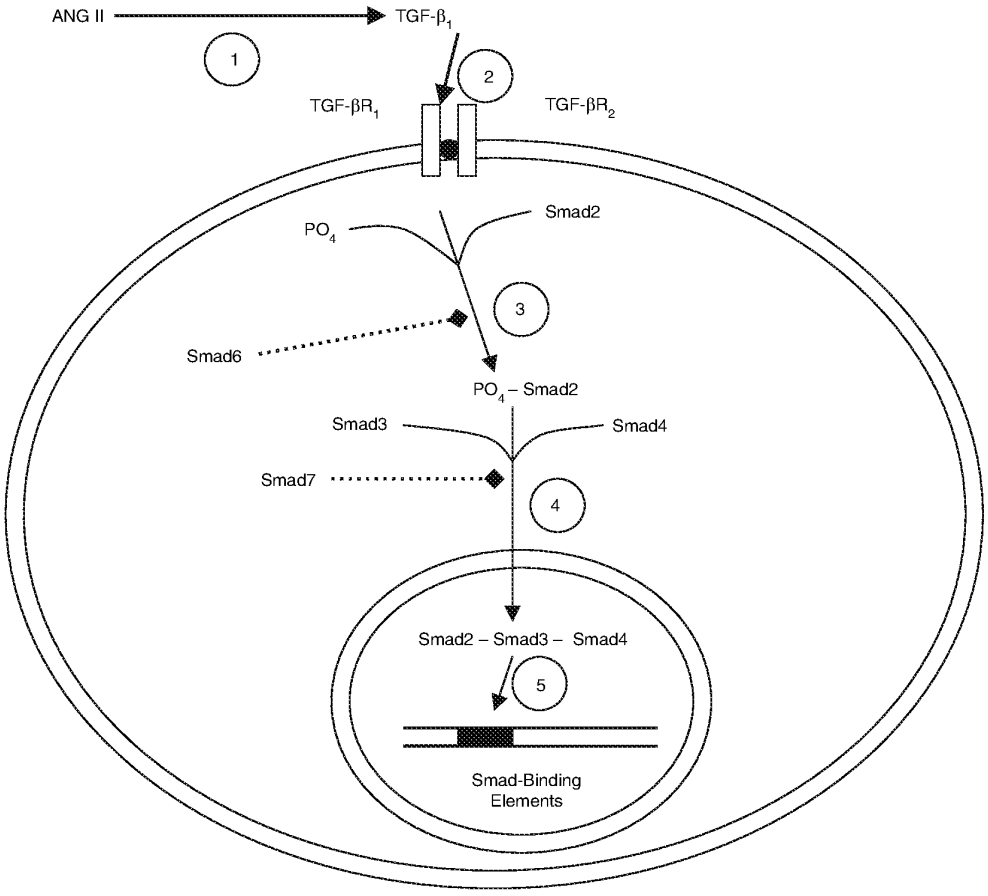

Figure 1. The TGF-β_1–Smad pathway. (1) Initiation of the pathway begins after TGF-β_1 is up-regulated by angiotensin II. (2) Once in the extracellular space, TGF-β_1 binds to a dimerized receptor, consisting of TGF-$\beta_1$receptor 1 (TGF-β_1R1) and TGF-β_1 receptor 2 (TGF-β_1R2), found on the surface of fibroblasts and myofibroblasts. (3) Ligand-receptor binding results in the phosphorylation of Smad2. Smad6, an inhibitory protein in the Smad family, impedes this phosphorylation. (4) Once phosphorylated, Smad2 combines with Smad 3 and Smad 4 to form a Smad complex that translocates across the nuclear membrane. Smad7, another inhibitory Smad protein, interrupts Smad complex formation. (5) Within the nucleus, the Smad complex binds to Smad-binding elements found in the regulatory regions of genes encoding extracellular matrix proteins. This final step promotes the expression of collagen type I and type III in the heart and results in fibrosis.

specific genes, resulting in the alteration of gene expression levels.[36] Smad6 and Smad7 inhibit the action of TGF-β_1 by preventing Smad2 phosphorylation and disrupting Smad complex formation, respectively (Fig. 1).[37]

The TGF-β_1–Smad pathway appears to be involved in the activation of collagen-gene promoter sites, primarily enhancing DNA translation of collagen type I. Evidence from transfected mesangial cell lines indicates that COL1A1 (encoding one component of collagen type I) is a primary site for Smad binding.[38] Verrecchia *et al.* found that the TGF-β_1–Smad pathway in dermal fibroblasts caused the induction of COL1A1, along with COL1A2 (encoding a second component of collagen type I), COL3A1 (encoding a component of collagen type 3), COL6A1 (encoding a component of collagen type VI) and COL6A3 (encoding another component of collagen type VI).[39]

Alternative pathways for TGF-β_1-induced fibrosis

Recently, an alternative pathway for TGF-β_1-induced fibrosis involving TGF-β-activated kinase (TAK1) has been suggested. TAK1, a member of the mitogen-activated protein kinase kinase kinase (MAPKKK) family, is thought to be a significant downstream modulator for the TGF-β_1 superfamily.[40] Zhang *et al.* found that the administration of TGF-β_1 to cardiac fibroblasts resulted in a 200–400% increase in TAK1.[41] The study also noted that constitutive TAK1 activity in transgenic mice led to a 46% increase in cardiac mass, with significant worsening of both systolic and diastolic cardiac functioning. Histological specimens of the myocardium in these mice revealed increased interstitial fibrosis and myocyte hypertrophy.

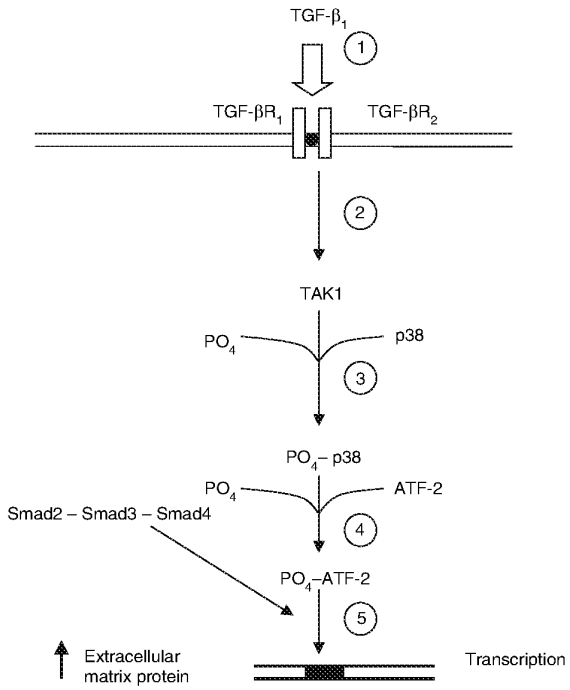

Figure 2. The TGF–TAK1 pathway. (1) Initiation of the pathway begins when TGF- β_1 binds to the dimerized TGF- β_1 receptor 1 (TGF- β_1R1) – TGF- β_1 receptor 2 (TGF- β_1R2) complex. (2) Ligand-receptor binding results in the intracellular activation of TAK1. (3) Activated TAK1 mediates p38 phosphorylation. (4) After being phosphorylated, p38 promotes phosphorylation of ATF-2. (5) The Smad complex then combines with ATF-2 resulting in augmented protein synthesis.

Hanafusa *et al.* also found that TAK1, once activated by TGF-β_1, phosphorylated activated transcription factor-2 (ATF-2), which then combined with the Smad proteins 2, 3 and 4 to form a transcription complex (Fig. 2).[42] Overexpression of non-phosphorylated ATF-2 resulted in inhibition of TGF-β_1 transcriptional activity. The study noted that coexpression of cells with Smad2 and Smad4 along with TAK1 resulted in synergistic activation of promoter sites. Similarly, Sano *et al.* showed that Smad3/Smad4 complex binding to ATF-2 increased the latter's *trans*-activating capacity.[43] Monzen *et al.* have also found that Smad proteins and TAK1 work together in cardiomyocyte differentiation.[44] Although few studies have quantified the importance of the TAK1 pathway on collagen expression and distribution within the heart, overexpression of TAK1 in articular chondrocytes has been shown to increase cellular collagen type II expression more than threefold, approximating the effects of TGF-β_1 stimulation.[45]

TGF-β_1 induction of connective tissue growth factor

TGF-β_1 is thought to up-regulate pro-fibrotic proteins that further stimulate extracellular matrix protein expression. In particular, TGF-β_1 has been shown to increase connective tissue growth factor (CTGF) synthesis within different fibroblast subtypes, including cardiac fibroblasts, most probably by acting on TGF-β_1 response elements localized in CTGF promoter site.[46,47] Chen *et al.* found that rises in myocardial CTGF after infarction paralleled elevations in TGF-β_1 and collagen expression in rats.[48] Furthermore, the use of CTGF antibodies has been shown to partially attenuate TGF-β_1-induced collagen synthesis from fibroblasts.[49]

Interaction between TGF-β_1 and matrix metalloproteinases

Until very recently, the extracellular matrix was considered to be a static network of proteins. However, research now indicates that this network is constantly changing in both structure and composition. Proteolytic enzymes, such as matrix metalloproteinases (MMPs), play an integral role in promoting change and remodelling. Examining left ventricular failure in animal models, Spinale *et al.* showed that MMP expression increased in a time-dependent manner with left ventricular dysfunction and dilatation.[50] Activation of the MMPs led to disruption of the extracellular network surrounding myocytes. Kim *et al.* noted that overexpression of MMP-1 (collagenase) in mice led to compensatory hypertrophy and increased collagen concentration within the myocardium, resulting in eventual ventricular impairment.[51] In addition, targeted deletion of MMP-2 prevented early and late left ventricular remodelling in mouse models.[52]

The roles of TGF-β_1 and MMPs in cardiac remodelling may be intertwined. In fact, both proteins may be part of one complex pathway for fibrosis. It has been noted that levels of both MMP-2 and membrane type-MMP (MT-MMP) are higher in terminally failing hearts, in concordance with when TGF-β_1 expression is also increased.[53] Similarly, Shimizu *et al.* found that TGF-β_1 and MMP-2 concentrations were both elevated in the myocardium of infarcted rats.[54]

Increasing evidence points towards the possibility that TGF-β_1 increases MMP activity within the myocardium. TGF-β_1 appears to up-regulate MMP-2 and membrane-bound MT-MMP in fibroblasts.[55] Briest *et al.* found norepinephrine-induced myocardial TGF-β_1 expression caused elevations in MMP-2 levels.[56] In addition, collagen type I, whose production is regulated by TGF-β_1, has been shown to increase MMP-2 activity.[57]

Stawowy *et al.* noted that TGF-β_1-induced expression of MMP-2 facilitates migration and motility of cardiac fibroblasts.[58] This, in turn, allows for the local production of extracellular proteins and increased fibrosis within the myocardium of the heart associated with cardiac remodelling.

Sources for TGF-β_1 in the myocardium

In the heart, TGF-β_1 is primarily secreted by cardiac fibroblasts. In turn, TGF-β_1 induces the differentiation of cardiac fibroblasts to more active connective tissue cells known as myofibroblasts.[59] Petrov *et al.* found that myofibroblasts can produce up to twice as much collagen as their fibroblast precursors.[60] TGF-β_1 is also involved in raising the production of cellular adhesion molecules, which are thought to increase myofibroblast survival and activity.[61]

Along with fibroblasts, Riemann *et al.* showed that macrophages may be another source of TGF-β_1 production.[62] Macrophages have been shown to colocalize with myofibroblasts in areas of fibrosis within the heart during cardiac hypertrophy.[63] It has been proposed that macrophages may serve as an initial or additional source of TGF-β_1 in the heart.[64] Kagitani *et al.* noted that administration of anti-inflammatory medication to hypertensive rats led to reduced infiltration of macrophages into the myocardium and prevented collagen accumulation when compared to controls.[65]

The TGF-β_1–Smad pathway appears to be an integral component of fibrosis within the heart. However, the pathway and its regulation have yet to be fully elucidated. Furthermore, more research is required to understand cell-signalling overlap between the TGF-β_1–Smad pathway and other extracelullar matrix protein up-regulators, such as osteopontin, to create a global model for pathological fibrosis within the myocardium.

TGF-β_1-induced fibrosis as a cause of cardiomyopathy

Alteration of ventricular properties caused by excess extracellular matrix production

For many years the heart was assumed to be a homogeneous organ, consisting solely of muscle cells. However, current evidence suggests that fibroblasts actually outnumber cardiac myocytes within the heart.[66] These connective tissue cells help to produce an extracellular matrix which allows for fibrosis within the myocardium.

The function of this fibrosis is still not completely known. Yet, more recently, it has come to be understood that networks of elastic tissue within the heart may allow for maintenance of myocardial architecture. Collagen networks are also thought to be involved in the transmission of force generated in muscle tissue.

Unfortunately, excessive deposition of fibrotic tissue in the heart results in cardiac pathology. Most notably, raised levels of collagen within the myocardium cause reduced ventricular compliance. This change can be attributed to the inherent stiffness of collagen type I which, as measured by Young's modulus of elasticity, is $\sim$30-fold greater than that of a cardioctye.[67] Concordantly, Jalil *et al.* noted that passive ventricular stiffness correlated well with collagen volume fraction.[68] Generally, a two- to threefold rise in collagen volume fraction causes notable ventricular stiffening.[69] Increasing chamber stiffness is accompanied by impaired myocyte relengthening during relaxation. Improper myocyte relaxation results in aberrant ventricular filling and is associated with increased filling pressures. Consequential decreases in stroke volume and increases in myocardial demand for oxygen lead to eventual cardiac dysfunction. While examining the role of fibrosis in cardiac pathology, MacKenna *et al.* showed that administration of intra-arteriolar bacterial collagenase into the myocardium of rats resulted in local degradation of collagen, which, in turn, caused increased chamber compliance and reduced diastolic dysfunction.[70]

Systolic dysfunction is also marked by the presence of increased myocardial collagen concentrations. The increased extracellular matrix generally serves as a replacement for necrosed or apoptotic myocytes. Unfortunately, the reduction in muscle tissue associated with this fibrosis results in poor ventricular contraction and reduced cardiac output. In addition, Wu *et al.* have noted that the increase in collagen concentration causes alterations to ventricular geometry, resulting in impaired sarcomere extension.[71] As the force of ventricular contraction is directly related to sarcomere length, the fibrosed heart has a greatly reduced ability to produce adequate pressures for systemic perfusion.

The changes in ventricle size and shape induced by the up-regulation of fibrotic proteins greatly compromise the ability of the heart to function. In fact, studies indicate that fibrosis may contribute greatly to cardiac dysfunction in ischaemic, dilated and hypertrophic cardiomyopathy.

Involvement of TGF-β_1 in ventricular remodelling and the development of ischaemic injury

After infarction, the myocardium undergoes a reparative process where necrotic cardiac tissue is replaced by extracellular matrix proteins, in an effort to protect the integrity of the heart wall. This 'scarred tissue' is dynamic, constantly producing and resorbing collagen. Functionally, the remainder of the heart makes up for the lost muscle tissue by increasing levels of fibrosis and inducing myocyte hypertrophy, allowing for initial compensation of ventricular function. Based on evidence from animal-based and *in vitro* studies, TGF-β_1 is thought to be responsible for this reparative fibrosis. Deten *et al.* showed that TGF-β_1 expression in rats was increased within the first day after infarct.[72] Increased myocardial concentrations of collagen I and collagen III occurred 3 days post-infarction, and coincided with the rise in TGF-β_1 expression. In fact, TGF-β_1 remained elevated for

82 days after infarction and was proposed to be involved in ongoing, rather than just acute, ventricular remodelling. Similarly, Hao *et al.* noted that TGF-β_1, Smad1, Smad2 and Smad3 were all elevated even 8 weeks postinfarction in rats.[73] Wang *et al.* found that levels of Smad7, an inhibitor in the TGF-β_1-Smad pathway, were greatly reduced in rats 2 weeks after myocardial infarction.[74] This reduction was associated with a greater amount of fibrosis. Most importantly, the degree of TGF-β_1 expression in structural remodelling has been shown to correlate with the degree of fibrosis.[75]

Up-regulation of TGF-β_1 receptors also contributes to increased activity of TGF-β_1 signalling. After prolonged ischaemia (4 weeks), TGF-β_1 receptor density has been shown to be raised threefold within the left ventricle and twofold within the right ventricle in rat models.[76] Sites of receptor up-regulation were associated with increased levels of fibrosis.

There is an increasing body of evidence indicating that higher levels of TGF-β_1 are not only produced after an ischaemic myocardial event, but they may also predispose to one as well. Studies, using rabbit models, indicate that TGF-β_1 overexpression in vascular smooth muscle may lead to increased extracellular matrix protein production contributing to artery narrowing.[77,78] Lindner found that injection of soluble TGF-β_1 receptor II, acting as a TGF-β_1 inhibitor, into the carotid arteries of rats resulted in a 65% decrease in intimal lesion formation and an 88% increase in luminal size.[79] Friedl *et al.* noted that intimal hyperplasia in the saphenous vein and internal mammary artery may be attributable to TGF-β_1, as both hyperplastic vein and artery had greater levels of TGF-β_1 expression when compared to patent vessels in patients.[80]

Genetic studies also indicate that TGF-β_1 polymorphisms may predispose individuals to ischaemic heart disease. In their examination of patients with end-stage renal failure, Rao *et al.* discovered that over 52% of patients with TGF-β_1 coding region G→C (915) polymorphisms had associated ischaemic heart disease.[81] Similarly, Yokota *et al.* found that TGF-β_1 T→C (29) polymorphisms were correlated with a greater susceptibility to myocardial infarctions.[82] Not surprisingly, individuals with such polymorphisms exhibit higher levels of serum TGF-β_1.

Single-nucleotide changes in genes encoding downstream proteins in the TGF-β_1–Smad pathway have also been correlated with ischaemic disease. Blom *et al.* have found polymorphisms within the CTGF promoter region that are associated with ischaemic heart disease.[83] These genetic variances caused increased CTGF expression and are thought to result in neointimal proliferation within blood vessels. Both Smad3 and Smad4 proteins within the TGF-β_1 cascade are thought to be the most important regulators of CTGF promoter activity.[84]

TGF-β_1 appears to play a significant role in the pre- and post-infarction environment, although human studies are currently lacking. In both, TGF stimulates extracellular protein production leading to vascular or ventricular dysfunction. Therefore, understanding the regulation, as well as dysregulation, of the TGF-β_1–Smad pathway becomes paramount for prevention of ischaemic heart disease and attenuation of remodelling.

Fibrosis as a pathological process in hypertrophic cardiomyopathy

Hypertrophic cardiomyopathy is characterized by interventricular septum or left ventricular hypertrophy, interstitial fibrosis and arterial wall thickening.[85] The most significant consequence of this hypertrophy is decreased compliance of the ventricles and eventual diastolic dysfunction. Shirani *et al.* found that the collagen network within the hearts of patients with hypertrophic cardiomyopathy was significantly greater than that seen in the hearts of patients without cardiovascular disease.[86] Collagen levels were independent of both structural and clinical disease variables and therefore the increased collagen network size was thought to be the result of a primary pathological process rather than simply serving as a consequence of other factors. In fact, it has been suggested that increased fibrosis, not myocardial hypertrophy, may be the most significant cause of diastolic dysfunction in hypertrophic cardiac disease.[86] Mundhenke *et al.* noted that increased collagen type I within the myocardium was a predictor of both diastolic and systolic dysfunction during exercise in hypertrophic cardiomyopathic patients who underwent transvalvular myectomy.[87]

TGF-β_1 is thought to be an important trigger of fibrosis in the hypertrophied heart. Expression levels of TGF-β_1 in hypertrophic obstructive cardiomyopathy were 2·5 times higher than in non-hypertrophied hearts.[88] Li *et al.* have found that the maximal binding affinity of TGF-β_1 to its receptor was higher in individuals with idiopathic hypertrophic cardiomyopathy.[89] Di Nardo *et al.* noted that early embryonic gene expression, rather than severity of haemodynamic overload, was the trigger for structural changes in the myocardium of hamsters with hereditary hypertrophic cardiomyopathy.[90] In this study, activation and regulation of embryonic gene expression were thought to be caused by TGF-β_1, as a threefold increase in TGF-β_1 gene expression was closely associated with a rise in myocardial early embryonic gene expression.

The involvement of fibrosis in the pathogenesis of hypertrophic cardiomyopathy has altered its perception as a disease consisting solely of myocyte disarray and dysfunction. However, efforts must be made to quantify the role of TGF-β_1 and fibrosis in this disorder. Should myocardial TGF-β_1 levels correlate with heart function

(or dysfunction), these proteins may serve as prognostic markers and obvious targets for disease prevention.

Dilated cardiomyopathy as a consequence of TGF-β_1 overexpression

Dilated cardiomyopathy is characterized by ventricular dilatation of the heart and is associated with very little hypertrophy. In dilated cardiomyopathy, diffuse myocyte damage may arise as a result of known (infections, drugs, etc.) or unknown causes. In this disorder, muscle fibres are replaced by extracellular matrix proteins, resulting in expansion of heart size. Such fibrotic changes are independent of other cardiovascular disease. Brooks *et al.* found that the interstitial levels of collagen were increased in dilated left ventricles that failed to display any pathological signs of ischaemia.[91] Marijianowski *et al.* demonstrated that collagen type I and III, as well as the collagen type I/type III ratio, were all elevated in patients with dilated cardiomyopathy.[92] The presence of increased fibrosis implies a possible role for TGF-β_1 in dilated cardiac pathology.

Sanderson *et al.* noted that the plasma levels of TGF-β_1 were twice as high in patients who had developed idiopathic dilated cardiomyopathy when compared to controls.[93] Levels of TGF-β_1 were also increased in macrophages present within the myocardial tissue of the dilated heart. This becomes increasingly important as Kuhl *et al.* have noted that there are an increased number of macrophages in the heart of individuals with dilated cardiomyopathy.[94]

Thus far, genetic studies have also hinted at the possible involvement of TGF-β_1 in dilated cardiomyopathy. Holweg *et al.* showed that the codon (10) Leu→Pro TGF-β_1 gene polymorphism, which correlates with elevated circulating levels of TGF-β_1, is associated with dilated cardiomyopathy.[95,96] These changes occur within the signal sequence of the TGF-β_1 gene, which is extremely important, as protein synthesis and activity are post-translationally regulated by such sequences.

Alterations in downstream modulators of TGF-β_1 may also predispose to dilated cardiomyopathy. Dixon *et al.* have documented that altered Smad2 and Smad4 expression in rats are associated with increased levels of cardiac fibrosis, elevated collagen turnover and the development of dilated cardiomyopathy.[97] In patients with HIV, up-regulation of TGF-B1 effector molecules such as ATF-2 have also been shown to cause dilated cardiomyopathy.[98]

The importance of fibrosis in dilated cardiomyopathy makes TGF-$\beta_1$1 an apt choice for inducing pathogenesis. If causality between TGF-β_1 overexpression and cardiomyopathy can be proven, the use of antifibrotics such as TGF-β_1 antagonists may provide a means for reversing dilatation of the heart and systolic dysfunction.

Correlation between valvular dysfunction and TGF-β_1 expression

TGF-β_1 appears to play a significant role in valvular pathogenesis. Valves primarily consist of interstitial cells, which secrete typical extracellular matrix proteins such as collagen.[99] These cells are precursors to myofibroblasts, which, as in the myocardium, are known for their ability to produce matrix proteins. The emergence of myofibroblasts in valvular tissue is strongly associated with disease.[100] The presence of these cells has been closely correlated to degenerative lesions and fibrosis of valves.[101] Walker *et al.* noted that TGF-β_1 is extremely important in inducing the differentiation of valvular interstitial cells to myofibroblasts, similar to what is seen in the ventricle.[11]

The local concentration of TGF-β_1 within cardiac valves may also be important because TGF-$\beta_1$appears to directly stimulate extracellular matrix protein expression from valvular interstitial cells even before their differentiation.[102] Surrounding ventricular biopsies of patients with both aortic stenosis and regurgitation showed a 1·5- to 2-fold increase in TGF-β_1 levels as compared with controls.[103] Increased valvular expression of TGF-β_1 has been noted in patients with carcinoid syndrome and it has been correlated with greater collagen deposition, extracellular matrix disorganization and calcification of valves in this population.[104]

The remodelling paradigm created for ischaemic cardiomyopathy may be apt for valvular disease as well. Initial damage to cardiac valves appears to raise local TGF-β_1 expression in a manner similar to that seen in the myocardium after infarction. This overexpression of TGF-β_1, in turn, could result in pathological repair of diseased areas. Inappropriate repair to initial injury may lead to progressive malfunctioning of the valves.

The role of TGF-β_1 in valvular disease is not limited to its overexpression in response to injury. As in ischaemic cardiomyopathy, TGF-β_1 polymorphisms may predispose to valvular disease. Chou *et al.* found that patients with rheumatic heart disease have a lower frequency of TGF-β_1 C→T (509) genotype and a higher frequency of the T→C (869) allele.[105] The inherent raised TGF-β_1 expression associated with the latter polymorphism may allow for increased fibrosis in patients with leaflet infection, creating a link between disease and valvular dysfunction.

In looking at animal models of connective tissue disease, Ng *et al.* found that mice with Marfan syndrome had increased activation of TGF-β_1.[106] This increased activity was associated with raised endothelial cell proliferation and myxomatous changes surrounding the aortic valve. Administration of TGF-β_1 antibodies prevented any such changes from occurring. Although a clear link between Marfan syndrome and TGF-β_1 does not exist, TGF-β_1 is known to play an integral part in the

development of endovascular cushions, the embryonic precursors to cardiac valves. Expression of TGF-β_1 within this tissue is usually limited to the fetal development period. However, persistent expression of TGF-β_1 in this tissue at even a minute level could predispose individuals to valvular disease. This process may occur in Marfan patients because fibrillin, the protein generally deficient in the syndrome, is thought to suppress TGF-β_1 activity.[106]

Although, cardiac surgery is the most common treatment for valvular dysfunction, medical therapy directed at limiting the effects of TGF-β_1 appears to be a viable alternative. Limiting myxomatous changes seen prior to valvular dysfunction will hopefully lessen the need for surgical intervention. This is of particular importance in the elderly where numerous comorbidities often make valvular surgery impossible.

Electrical conduction disturbances associated with TGF-β_1 overexpression

Research involving atrial fibrillation has shown that myocardial fibrosis plays an important role in predisposing to arrhythmia.[107] In fact, the arrhythmogenic activity of the pulmonary veins is partially attributed to the fact that myocardial tissue within these vessels is significantly fibrotic (Fig. 3).[108] Fibrosis is thought to disturb anisotropic conduction and thereby induce slowing of electrical conduction velocities, allowing for the generation of re-entry circuits. In addition, impaired anisotropic conduction leads to chaotic rather than linear electrical propagation which also promotes arrhythmia.[109] Nakajima *et al.* noted that mice with constitutive expression of TGF-β_1 developed selective fibrosis within the atria and not in the ventricles, suggesting that atrial fibroblasts may be particularly sensitive to the actions of TGF-β_1.[6] In a similar study, mice with increased expression of TGF-β_1 were prone to atrial fibrillation development as a result of raised levels of atrial fibrosis.[10] Hanna *et al.* noted that TGF-β_1 levels were increased in the atria after the development of congestive heart failure in dogs.[110] This correlation may help to explain the presence of arrhythmia seen after the onset of ventricular dysfunction. TGF-β_1 polymorphisms are also thought to be involved in inducing congenital heart block as a result of fibrosis, leading to the predisposition of atrial fibrillation.[111,112] The aim of new research should be to determine which TGF-β_1 polymorphisms (if any) enhance the likelihood of atrial fibrillation development. In addition, expression levels of TGF-β_1 in the pulmonary veins must be studied as a possible explanation for the arrhythmogenicity of these vessels.

Figure 3. A histological section of the pulmonary veins at the region of the ostium. Disorganized bundles of the myocardial sleeve extending from the left atrium are surrounded by fibrotic connective tissue. Provided by courtesy of Ivana Kholova, MD.

Regarding treatment, the use of antifibrotics as a preventive measure for atrial fibrillation is intriguing. Using canine models, Shi *et al.* noted that ACE inhibitors prevented the fibrosis that normally arose after heart failure, leading to the reduced development of atrial fibrillation.[113] Similarly, clinical trials show increasing benefits in using ACE and angiotensin II receptor inhibitors for atrial fibrillation in patients with and without underlying cardiopathologies.[114–117] The inhibition of TGF-β_1 may produce similar antiarrhythmic effects.

Treatment directed at TGF-β_1-induced fibrosis

There are a number of strategies that have aimed to reduce fibrosis in cardiovascular pathology. Most recent research has focused on the effectiveness of ACE inhibitors and angiotensin II receptor antagonists in attenuating extracellular matrix production within the heart. However, in a recent clinical trial, Hallberg *et al.* compared the benefits of irbesartan treatment on the ventricular properties of hypertensive groups with two separate TGF-β_1 polymorphisms. Patients with the GG genotype, associated with greater TGF-β_1 expression, were shown to have a greater left ventricular mass index when compared to patients with the GC genotype.[118] This suggests that drugs inhibiting angiotensin may not be able to fully impede the cardiopathological effects of TGF-β_1. It also implies that targeting the TGF-β_1–Smad pathway directly may be more effective in attenuating fibrosis and hypertrophy in the heart.

Thus far, most research has used animal models to examine the effects of TGF-β_1 antagonism. Kuwahara *et al.* were able to induce increased TGF-β_1 expression within the rat heart resulting in progressive myocardial fibrosis and eventual diastolic dysfunction (gauged by immunohistochemistry and echocardiography).[12] Administration of TGF-β_1 monoclonal antibodies to rats, similarly overexpressing TGF-β_1, prevented both fibrosis and diastolic dysfunction. More specifically, these antibodies did not allow for left ventricular hypertrophy and subsequent raised left ventricular end-diastolic pressure, which

normally precedes dysfunction. Koyanagi *et al.* found that TGF-β_1 antagonism blocks the migration of rat monocytes and the production of local myofibroblasts, two cell types that serve as the primary sources for TGF-β_1 production within the myocardium.[119] Tomita *et al.* noted that TGF-β_1 neutralization via polyclonal antibodies resulted in the down-regulation of extracellular matrix gene expression in rats.[5] Tranilast, a novel drug already sold in Japan, serves to inhibit transcription of TGF-β_1.[120] It has been shown to reduce the secretion of TGF-β_1 in fibroblast cell cultures. Much like TGF-β_1 antibodies, tranilast prevents the migration of monocytes to myocardial tissue in hypertensive mice.[65] In addition, it serves to attenuate left ventricular fibrosis in rats with renovascular hypertension.[121] Martin *et al.* have recently shown that tranilast lowers the deposition of cardiac matrix proteins in diabetic rats despite the presence of persistent hyperglycaemia and hypertension.[122] The ongoing PRESTO PCI clinical study is attempting to use an oral regimen of tranilast to reduce restenosis of coronary arteries postintervention.[123]

Regulation of inherent TGF-β_1 inhibitors within the body may also help to prevent fibrosis in the heart. For example, Mujumdar and Tyagi noted that levels of one such physiological inhibitor, decorin, are reduced during the transition of the heart from compensated to decompensated failure in hypertensive rats.[124] In addition, in early myocardial ischaemia, gene expression of decorin is reduced prior to remodelling.[125] Decorin gene transfer to skeletal muscle results in its overexpression. This overexpression is associated with reduced fibrosis levels in many tissues, primarily via a decrease in extracellular matrix protein production through TGF-β_1 inhibition.[126] Another protein, betaglycan, often referred to as TGF-β_1 receptor III, is thought to be a molecule that modulates the binding of TGF-$\beta_1$to TGF-β_1 receptor II in the cardiomyocyte membrane. However, soluble betaglycan, like decorin, has been shown to be a potent physiological inhibitor of TGF-β_1.[127] Administration of betaglycan has been noted to reduce hepatic fibrosis in chronic liver injury.[128] The effects of betaglycan on cardiac fibrosis have not yet been studied.

Recent trends in endocrinology indicate that hormones play a prominent role in the regulation of collagen levels within the heart. Hsu *et al.* report that both ventricular and atrial cells possess receptors for relaxin, a peptide hormone with antifibrotic properties.[129] Du *et al.* noted that relaxin-deficient mice have increased levels of myocardial collagen and develop subsequent ventricular diastolic dysfunction.[130] Dschietzig *et al.* found that plasma concentration and myocardial expression of relaxin was associated with the preservation of cardiac function in patients with heart failure.[131] Samuel *et al.* showed that relaxin, through a currently unknown mechanism, inhibited fibroblast activation and collagen synthesis in cultured cell lines treated with TGF-β_1.[132] Therefore, relaxin holds promise as an important therapeutic tool for patients with heart disease.

Finally, the role of genetics in the development of cardiac remodelling seems to be ever increasing. For this reason, the potential for gene therapy as a means for preventing fibrosis is great. Thus far, very little gene therapy research has focused on the treatment of cardiopathology. However, in a recent animal model study, Okada *et al.* showed that TGF-β_1 receptor II gene therapy begun 3 days after infarction (subacute stage) resulted in the attenuation of remodelling in rats, with marked reduction in cardiac fibrosis and prevention of left ventricular enlargement noted after 4 weeks (chronic stage).[133] Importantly, at this time, left ventricular function and survival were also found to be significantly greater than in non-treated controls. These findings offer great hope for obtaining similar results with TGF-β_1 inhibition in the human heart.

The initial hesitancy to use TGF-$\beta_1$antagonists in the post-infarct state was based on the cardioprotective effects of fibrosis immediately following myocardial necrosis. However, currently, evidence from *in vivo* and animal studies indicates that inhibiting the actions of TGF-β_1 after the acute phase of infarction may prevent or attenuate remodelling and therefore it must be a target for future therapies. These benefits may not be limited to ventricular remodelling, as mechanisms of pathogenesis in the post-infarct state appear to overlap with those seen in arrhythmia and valvular disease.

Potential adverse consequences of TGF-β_1 inhibition

The use of TGF-β_1 antagonists to combat myocardial fibrosis does not come without risks. Knockout model studies have helped to outline the potential dangers of TGF-β_1 inhibition. Most obviously, knockout mice lacking TGF-β_1 are usually unable to survive beyond a few weeks because of aberrant immune regulation, primarily manifested as lethal cardiac and pulmonary inflammation.[134] Deletion of the TGF-β_1 gene is associated with exacerbation of asthma pathology, with notable eisonophil infiltration and mucus secretion.[135–137] Knockout models have also shown the importance of TGF-β_1 in hair follicle, pulmonary and bone development.[138–140]

TGF-β_1 appears to be able to both suppress and stimulate the proliferation of cells, further complicating treatment regimens aimed at TGF-β_1 inhibition. TGF-β_1 is thought to mediate growth arrest by up-regulating cyclin-dependent kinase inhibitors and down-regulating c-*myc* and cell division cycle 25A.[141] Reduced expression or mutational inactivation of the TGF-β_1–Smad pathway is associated with uncontrolled cellular growth, particularly in endothelial cell lines.[142] Studies indicate that TGF-β_1

heterozygous null mice have increased hepatocyte and mammary epithelial cell proliferation potential, as well as decreased levels of apoptosis within the lung and liver.[143] Additionally, loss of TGF-β_1 receptor function has been associated with progression of malignancy and increased tumour growth.[144,145]

Cells whose growth is no longer inhibited by TGF-β_1, but where the TGF-β_1–Smad pathway is still maintained, show increased migration and invasion in response to TGF-β_1 administration.[146] In addition, the increased expression of TGF-β_1 is associated with increased tumour potential. Massagué *et al.* have proposed that TGF-β_1 enhances tumour progression through suppression of the immune system, as well as promotion of angiogenesis.[141]

TGF-β_1 is also thought to cause the proliferation of mesenchymal cells such as fibroblasts, necessary for stroma formation in many organs.[147] Rosenbaum *et al.* noted that administration of TGF-β_1 produces a dose and time-dependent increase in the proliferation of human liver fibroblasts.[148] Although the signalling pathways for these effects are not well known, TGF-β_1 may down-regulate expression of cyclin-dependent kinase inhibitors, facilitating cellular entry into the S-phase of its cycle.[149] Other theories have proposed the TGF-β_1-induced up-regulation of platelet-derived growth factor and fibro blast growth factor are responsible for cellular proliferation.[150–153]

The potential consequences of TGF-β_1 inhibition must be looked at carefully before its clinical use. In particular, the important physiological roles of TGF-β_1 in organ development, immune system regulation and cellular proliferation suggest the possibility of serious side-effects for treatments targeting the actions of TGF-β_1. Further study examining TGF-β_1 inhibition would help to identify patient groups at risk for adverse consequences. In addition, efforts must be made to localize TGF-β_1 inhibition within the heart to prevent systemic side-effects.

Conclusion

Fibrosis appears to be an integral component of most cardiac pathologies. In fibrosis, the excess production of extracellular matrix proteins alters the structure, architecture and shape of the heart. Such changes have marked effects on ventricular contractility, valvular functioning and electrical conduction. In particular, TGF-β_1 has been implicated in the pathogenesis of each of these three facets of cardiac functioning. Although TGF-β_1 is known to promote local collagen production, many details regarding the mechanisms of TGF-β_1-induced fibrosis remain unclear. For example, circulating levels of ACE and angiotensin II are not elevated in valvular disease as they are after infarction. Rather, ACE levels are raised solely within the valvular tissue itself.[154] This may imply that a 'local remodelling' process occurs within the endocardium of valves rather than the diffuse myocardial changes that arise in the post-ischaemic state.

The concept of remodelling can be applied to the atrium as well. Generally, this remodelling refers to changes in ion current flow following persistent atrial fibrillation.[155] However, structural alterations have also been reported with recurrent atrial tachycardias. Patients with chronic atrial fibrillation were shown to have higher levels of myocardial interstitial fibrosis as compared to controls, particularly within the region of the pulmonary veins, which are known to be arrhythmogenic.[156–158] An effort must be made to understand whether TGF-β_1 plays a prominent role within the 'atrial fibrillation begets atrial fibrillation' remodelling paradigm.

As TGF-β_1 appears to be involved in different cardiopathological processes, it is an apt target for future therapy. Thus far, animal studies have shown that inhibiting the actions of TGF-β_1 may attenuate fibrosis in the heart. Also, with increasing evidence indicating that TGF-β_1 gene polymorphism and dysregulation predisposes to heart conditions, drug regimens and gene therapy may act to prevent rather than merely treat disease.

At this time the potential for therapy targeting TGF-β_1 seems unlimited. However, before TGF-β_1 inhibition can be used in a clinical setting, more *in vivo* and animal-based studies are required to understand the potential side-effects of treatment, as well as to provide more than the circumstantial correlation between TGF-β_1 and cardiac fibrosis that exists currently.

Acknowledgement

I would like to thank Sapna Rawal for her patience and support.

References

1 Wolf G. New insights into the pathophysiology of diabetic nephropathy: from haemodynamics to molecular pathology. *Eur J Clin Invest* 2004; **34**:785–96.
2 Vallance BA, Gunawan MI, Hewlett B *et al.* TGF-β1 gene transfer to the mouse colon leads to intestinal fibrosis. *Am J Physiol Gastrointest Liver Physiol* 2005; [Epub ahead of print].
3 Bataller R, Brenner DA. Liver fibrosis. *J Clin Invest* 2005; **115**:209–18.
4 Yang Y, Zhou X, Gao H, Ji SJ, Wang C. The expression of epidermal growth factor and transforming growth factor-beta1 in the stenotic tissue of congenital pelvi-ureteric junction obstruction in children. *J Pediatr Surg* 2003; **38**:1656–60.
5 Tomita H, Egashira K, Ohara Y *et al.* Early induction of transforming growth factor-beta via angiotensin II type 1 receptors contributes to cardiac fibrosis induced by long-term blockade of nitric oxide synthesis in rats. *Hypertension* 1998; **32**:273–9.
6 Nakajima H, Nakajima HO, Salcher O, Dittie AS, Dembowsky K, Jing S, Field LJ. Atrial but not ventricular fibrosis in mice

expressing a mutant transforming growth factor-beta(1) transgene in the heart. *Circ Res* 2000; **86**:571–9.
7 Rosenkranz S, Flesch M, Amann K, Haeuseler C, Kilter H, Seeland U, Schluter KD, Bohm M. Alterations of beta-adrenergic signaling and cardiac hypertrophy in transgenic mice overexpressing TGF-beta(1). *Am J Physiol Heart Circ Physiol* 2002; **283**:H1253–62.
8 Schultz Jel J, Witt SA, Glascock BJ, Nieman ML, Reiser PJ, Nix SL, Kimball TR, Doetschman T. TGF-beta1 mediates the hypertrophic cardiomyocyte growth induced by angiotensin II. *J Clin Invest* 2002; **109**:787–96.
9 Klein G, Schaefer A, Hilfiker-Kleiner D. *et al.* Increased collagen deposition and diastolic dysfunction but preserved myocardial hypertrophy following pressure overload in mice lacking PKCε. *Circ Res* 2005; [Epub ahead of print].
10 Verheule S, Sato T, Everett T 4th *et al.* Increased vulnerability to atrial fibrillation in transgenic mice with selective atrial fibrosis caused by overexpression of TGF-β1. *Circ Res* 2004; **94**:1458–65.
11 Walker GA, Masters KS, Shah DN, Anseth KS, Leinwand LA. Valvular myofibroblast activation by transforming growth factor-beta: implications for pathological extracellular matrix remodeling in heart valve disease. *Circ Res* 2004; **95**: 253–60.
12 Kuwahara F, Kai H, Tokuda K, Kai M, Takeshita A, Egashira K, Imaizumi T. Transforming growth factor-beta function blocking prevents myocardial fibrosis and diastolic dysfunction in pressure-overloaded rats. *Circulation* 2002; **106**:130–5.
13 Isaka Y, Tsujie M, Ando Y, Nakamura H, Kaneda Y, Imai E, Hori M. Transforming growth factor-beta 1 antisense oligodeoxynucleotides block interstitial fibrosis in unilateral ureteral obstruction. *Kidney Int* 2000; **58**:1885–92.
14 Agrotis A, Kalinina N, Bobik A. Transforming growth factor-beta, cell signaling and cardiovascular disorders. *Curr Vasc Pharmacol* 2005; **3**:55–61.
15 Lijnen PJ, Petrov VV, Fagard RH. Induction of cardiac fibrosis by transforming growth factor-beta(1). *Mol Genet Metab* 2000; **71**:418–35.
16 Pedrozo HA, Schwartz Z, Gomez R, *et al.* Growth plate chondrocytes store latent transforming growth factor (TGF)-beta 1 in their matrix through latent TGF-beta 1 binding protein-1. *J Cell Physiol* 1998; **177**:343–54.
17 Krieglstein K, Henheik P, Farkas L, Jaszai J, Galter D, Krohn K, Unsicker K. Glial cell line-derived neurotrophic factor requires transforming growth factor-beta for exerting its full neurotrophic potential on peripheral and CNS neurons. *J Neurosci* 1998; **18**:9822–34.
18 Kehrl JH, Wakefield LM, Roberts AB, Jakowlew S, Alvarez-Mon M, Derynck R, Sporn MB, Fauci AS. Production of transforming growth factor beta by human T lymphocytes and its potential role in the regulation of T cell growth. *J Exp Med* 1986; **163**:1037–50.
19 Luethviksson BR, Gunnlaugsdottir B. Transforming growth factor-beta as a regulator of site-specific T-cell inflammatory response. *Scand J Immunol* 2003; **58**:129–38.
20 Jiang X, Zeng HS, Guo Y, Zhou ZB, Tang BS, Li FK. The expression of matrix metalloproteinases-9, transforming growth factor-beta1 and transforming growth factor-beta receptor I in human atherosclerotic plaque and their relationship with plaque stability. *Chin Med J (Engl)* 2004; **117**:1825–9.
21 Cipollone F, Fazia M, Mincione G *et al.* Increased expression of transforming growth factor-beta1 as a stabilizing factor in human atherosclerotic plaques. *Stroke* 2004; **35**:2253–7.
22 Roberts AB, Sporn MB. The transforming growth factors-β. In: Sporn MB, Roberts AB, eds. *Handbook of Experimental Pharmacology. Peptide Growth Factors and Their Receptors*. New York: Springer-Verlag, 1990: 419–72.
23 Wolf G. Link between angiotensin II and TGF-beta in the kidney. *Miner Electrolyte Metab* 1998; **24**:174–80.
24 Fukuda N. Molecular mechanisms of the exaggerated growth of vascular smooth muscle cells in hypertension. *J Atheroscler Thromb* 1997; **4**:65–72.
25 Lee AA, Dillmann WH, McCulloch AD, Villarreal FJ. Angiotensin II stimulates the autocrine production of transforming growth factor-beta 1 in adult rat cardiac fibroblasts. *J Mol Cell Cardiol* 1995; **27**:2347–57.
26 Campbell SE, Katwa LC. Angiotensin II stimulated expression of transforming growth factor-beta1 in cardiac fibroblasts and myofibroblasts. *J Mol Cell Cardiol* 1997; **29**:1947–58.
27 Kim S, Ohta K, Hamaguchi A, Yukimura T, Miura K, Iwao H. Angiotensin II induces cardiac phenotypic modulation and remodeling *in vivo* in rats. *Hypertension* 1995; **25**:1252–9.
28 Kupfahl C, Pink D, Friedrich K *et al.* Angiotensin II directly increases transforming growth factor beta 1 and osteopontin and indirectly affects collagen mRNA expression in the human heart. *Cardiovasc Res* 2000; **46**:463–75.
29 Kim S, Ohta K, Hamaguchi A *et al.* Angiotensin II type I receptor antagonist inhibits the gene expression of TGF-1 and extracellular matrix in cardiac and vascular tissues of hypertensive rats. *J Pharmacol Exp Ther* 1995; **273**:509–15.
30 el-Agroudy AE, Hassan NA, Foda MA, Ismail AM, el-Sawy EA, Mousa O, Ghoneim MA. Effect of angiotensin II receptor blocker on plasma levels of TGF-beta 1 and interstitial fibrosis in hypertensive kidney transplant patients. *Am J Nephrol* 2003; **23**:300–6.
31 Agarwal R, Siva S, Dunn SR, Sharma K. Add-on angiotensin II receptor blockade lowers urinary transforming growth factor-beta levels. *Am J Kidney Dis* 2002; **39**:486–92.
32 Laviades C, Varo N, Diez J. Transforming growth factor beta in hypertensives with cardiorenal damage. *Hypertension* 2000; **36**:517–22.
33 Rosenkranz S. TGF-beta1 and angiotensin networking in cardiac remodeling. *Cardiovasc Res* 2004; **63**:423–32.
34 Schiller M, Javelaud D, Mauviel A. TGF-beta-induced SMAD signaling and gene regulation. consequences for extracellular matrix remodeling and wound healing. *J Dermatol Sci* 2004; **35**:83–92.
35 Pokharel S, Rasoul S, Roks AJ *et al.* *N*-acetyl-Ser-Asp-Lys-Pro inhibits phosphorylation of Smad2 in cardiac fibroblasts. *Hypertension* 2002; **40**:155–61.
36 Greene RM, Nugent P, Mukhopadhyay P, Warner DR, Pisano MM. Intracellular dynamics of Smad-mediated TGFbeta signaling. *J Cell Physiol* 2003; **197**:261–71.
37 Massague J, Chen YG. Controlling TGF-beta signaling. *Genes Dev* 2000; **14**:627–44.
38 Tsuchida K, Zhu Y, Siva S, Dunn SR, Sharma K. Role of Smad4 on TGF-beta-induced extracellular matrix stimulation in mesangial cells. *Kidney Int* 2003; **63**:2000–9.
39 Verrecchia F, Chu ML, Mauviel A. Identification of novel TGF-beta/Smad gene targets in dermal fibroblasts using a combined

cDNA microarray/promoter transactivation approach. *J Biol Chem* 2001; **276**:17058–62.

40 Yamaguchi K, Shirakabe K, Shibuya H *et al.* Identification of a member of the MAPKKK family as a potential mediator of TGF-beta signal transduction. *Science* 1995; **270**:2008–11.

41 Zhang D, Gaussin V, Taffet GE *et al.* TAK1 is activated in the myocardium after pressure overload and is sufficient to provoke heart failure in transgenic mice. *Nat Med* 2000; **6**:556–63.

42 Hanafusa H, Ninomiya-Tsuji J, Masuyama N, Nishita M, Fujisawa J, Shibuya H, Matsumoto K, Nishida E. Involvement of the p38 mitogen-activated protein kinase pathway in transforming growth factor-beta-induced gene expression. *J Biol Chem* 1999; **274**:27161–7.

43 Sano Y, Harada J, Tashiro S, Gotoh-Mandeville R, Maekawa T, Ishii S. ATF-2 is a common nuclear target of Smad and TAK1 pathways in transforming growth factor-beta signaling. *J Biol Chem* 1999; **274**:8949–57.

44 Monzen K, Shiojima I, Hiroi Y *et al.* Bone morphogenetic proteins induce cardiomyocyte differentiation through the mitogen-activated protein kinase kinase kinase TAK1 and cardiac transcription factors Csx/Nkx-2.5 and GATA-4. *Mol Cell Biol* 1999; **19**:7096–105.

45 Qiao B, Padilla SR, Benya PD. Transforming growth factor (TGF) -beta-activated kinase 1 mimics and mediates TGF-beta-induced stimulation of type II collagen synthesis in chondrocytes independent of Col2a1 transcription and Smad3 signaling. *J Biol Chem* 2005; **280**:17562–71.

46 Moussad EE, Brigstock DR. Connective tissue growth factor: what's in a name? *Mol Genet Metab* 2000; **71**:276–92.

47 Grotendorst GR. Connective tissue growth factor. a mediator of TGF-beta action on fibroblasts. *Cytokine Growth Factor Rev* 1997; **8**:171–9.

48 Chen MM, Lam A, Abraham JA, Schreiner GF, Joly AH. CTGF expression is induced by TGF-beta in cardiac fibroblasts and cardiac myocytes: a potential role in heart fibrosis. *J Mol Cell Cardiol* 2000; **32**:1805–19.

49 Duncan MR, Frazier KS, Abramson S, Williams S, Klapper H, Huang X, Grotendorst GR. Connective tissue growth factor mediates transforming growth factor beta-induced collagen synthesis: down-regulation by cAMP. *FASEB J* 1999; **13**:1774–86.

50 Spinale FG, Coker ML, Thomas CV, Walker JD, Mukherjee R, Hebbar L. Time-dependent changes in matrix metalloproteinase activity and expression during the progression of congestive heart failure. Relation to ventricular and myocyte function. *Circ Res* 1998; **82**:482–95.

51 Kim HE, Dalal SS, Young E, Legato MJ, Weisfeldt ML, D'Armiento J. Disruption of the myocardial extracellular matrix leads to cardiac dysfunction. *J Clin Invest* 2000; **106**:857–66.

52 Hayashidani S, Tsutsui H, Ikeuchi M *et al.* Targeted deletion of MMP-2 attenuates early LV rupture and late remodeling after experimental myocardial infarction. *Am J Physiol Heart Circ Physiol* 2003; **285**:H1229–35.

53 Hein S, Arnon E, Kostin S *et al.* Progression from compensated hypertrophy to failure in the pressure-overloaded human heart: structural deterioration and compensatory mechanisms. *Circulation* 2003; **107**:984–91.

54 Shimizu N, Yoshiyama M, Takeuchi K, Hanatani A, Kim S, Omura T, Iwao H, Yoshikawa J. Doppler echocardiographic assessment and cardiac gene expression analysis of the left ventricle in myocardial infarcted rats. *Jpn Circ J* 1998; **62**:436–42.

55 Overall CM, Wrana JL, Sodek J. Transcriptional and post-transcriptional regulation of 72-kDa gelatinase/type IV collagenase by transforming growth factor-beta 1 in human fibroblasts. Comparisons with collagenase and tissue inhibitor of matrix metalloproteinase gene expression. *J Biol Chem* 1991; **266**:14064–71.

56 Briest W, Homagk L, Rassler B *et al.* Norepinephrine-induced changes in cardiac transforming growth factor-beta isoform expression pattern of female and male rats. *Hypertension* 2004; **44**:410–18.

57 Zigrino P, Drescher C, Mauch C. Collagen-induced proMMP-2 activation by MT1-MMP in human dermal fibroblasts and the possible role of alpha2beta1 integrins. *Eur J Cell Biol* 2001; **80**:68–77.

58 Stawowy P, Margeta C, Kallisch H, Seidah NG, Chretien M, Fleck E, Graf K. Regulation of matrix metalloproteinase MT1-MMP/MMP-2 in cardiac fibroblasts by TGF-beta1 involves furin-convertase. *Cardiovasc Res* 2004; **63**:87–97.

59 Lijnen P, Petrov V. Transforming growth factor-beta 1-induced collagen production in cultures of cardiac fibroblasts is the result of the appearance of myofibroblasts. *Meth Find Exp Clin Pharmacol* 2002; **24**:333–44.

60 Petrov VV, Fagard RH, Lijnen PJ. Stimulation of collagen production by transforming growth factor-beta1 during differentiation of cardiac fibroblasts to myofibroblasts. *Hypertension* 2002; **39**:258–63.

61 Vaughan MB, Howard EW, Tomasek JJ. Transforming growth factor-beta1 promotes the morphological and functional differentiation of the myofibroblast. *Exp Cell Res* 2000; **257**:180–9.

62 Riemann D, Wollert HG, Menschikowski J, Mittenzwei S, Langner J. Immunophenotype of lymphocytes in pericardial fluid from patients with different forms of heart disease. *Int Arch Allergy Immunol* 1994; **104**:48–56.

63 Hinglais N, Heudes D, Nicoletti A, Mandet C, Laurent M, Bariety J, Michel JB. Colocalization of myocardial fibrosis and inflammatory cells in rats. *Lab Invest* 1994; **70**:286–94.

64 Kuwahara F, Kai H, Tokuda K, Takeya M, Takeshita A, Egashira K, Imaizumi T. Hypertensive myocardial fibrosis and diastolic dysfunction. another model of inflammation? *Hypertension* 2004; **43**:739–45.

65 Kagitani S, Ueno H, Hirade S, Takahashi T, Takata M, Inoue H. Tranilast attenuates myocardial fibrosis in association with suppression of monocyte/macrophage infiltration in DOCA/salt hypertensive rats. *J Hypertens* 2004; **22**:1007–15.

66 Nag AC. Study of non-muscle cells of the adult mammalian heart. A fine structural analysis and distribution. *Cytobios* 1980; **28**:41–61.

67 MacKenna DA, Vaplon SM, McCulloch AD. Microstructural model of perimysial collagen fibers for resting myocardial mechanics during ventricular filling. *Am J Physiol* 1997; **273**:H1576–86.

68 Jalil JE, Doering CW, Janicki JS, Pick R, Shroff SG, Weber KT. Fibrillar collagen and myocardial stiffness in the intact hypertrophied rat left ventricle. *Circ Res* 1989; **64**:1041–50.

69 Covell JW. Factors influencing diastolic function: possible role of the extracellular matrix. *Circulation* 1990; **81**:III-115–III-158.

70 MacKenna DA, Omens JH, McCulloch AD, Covell JW. Contribution of collagen matrix to passive left ventricular mechanics in isolated rat hearts. *Am J Physiol* 1994; **266**:H1007–18.

71 Wu Y, Tobias AH, Bell K *et al.* Cellular and molecular mechanisms of systolic and diastolic dysfunction in an avian model of dilated cardiomyopathy. *J Mol Cell Cardiol* 2004; **37**:111–19.

72 Deten A, Holzl A, Leicht M, Barth W, Zimmer HG. Changes in extracellular matrix and in transforming growth factor beta isoforms after coronary artery ligation in rats. *J Mol Cell Cardiol* 2001; **33**:1191–207.

73 Hao J, Ju H, Zhao S, Junaid A, Scammell-La Fleur T, Dixon IM. Elevation of expression of Smads 2, 3 and 4, decorin and TGF-beta in the chronic phase of myocardial infarct scar healing. *J Mol Cell Cardiol* 1999; **31**: 667–78.

74 Wang B, Hao J, Jones SC, Yee MS, Roth JC, Dixon IM. Decreased Smad 7 expression contributes to cardiac fibrosis in the infarcted rat heart. *Am J Physiol Heart Circ Physiol* 2002; **282**:H1685–96.

75 Maekawa Y, Anzai T, Yoshikawa T, Sugano Y, Mahara K, Kohno T, Takahashi T, Ogawa S. Effect of granulocyte-macrophage colony-stimulating factor inducer on left ventricular remodeling after acute myocardial infarction. *J Am Coll Cardiol* 2004; **44**:1510–20.

76 Sun Y, Zhang JQ, Zhang J, Ramires FJ. Angiotensin II, transforming growth factor-beta1 and repair in the infarcted heart. *J Mol Cell Cardiol* 1998; **30**:1559–69.

77 Kanzaki T, Tamura K, Takahashi K *et al. In vivo* effect of TGF-beta 1. Enhanced intimal thickening by administration of TGF-beta 1 in rabbit arteries injured with a balloon catheter. *Arterioscler Thromb Vasc Biol* 1995; **15**:1951–7.

78 Chen X, Ren S, Ma MG, Dharmalingam S, Lu L, Xue M, Ducas J, Shen GX. Hirulog-like peptide reduces restenosis and expression of tissue factor and transforming growth factor-beta in carotid artery of atherosclerotic rabbits. *Atherosclerosis* 2003; **169**:31–40.

79 Lindner V. Vascular repair processes mediated by transforming growth factor-beta. *Z Kardiol* 2001; **90**:17–22.

80 Friedl R, Li J, Schumacher B, Hanke H, Waltenberger J, Hannekum A, Stracke S. Intimal hyperplasia and expression of transforming growth factor-beta1 in saphenous veins and internal mammary arteries before coronary artery surgery. *Ann Thorac Surg* 2004; **78**:1312–18.

81 Rao M, Guo D, Jaber BL, Tighiouart H, Pereira BJ, Balakrishnan VS; HEMO Study Group. Transforming growth factor-beta 1 gene polymorphisms and cardiovascular disease in hemodialysis patients. *Kidney Int* 2004; **66**:419–27.

82 Yokota M, Ichihara S, Lin TL, Nakashima N, Yamada Y. Association of a T29 → C polymorphism of the transforming growth factor-beta1 gene with genetic susceptibility to myocardial infarction in Japanese. *Circulation* 2000; **101**:2783–7.

83 Blom IE, van Dijk AJ, de Weger RA, Tilanus MG, Goldschmeding R. Identification of human ccn2 (connective tissue growth factor) promoter polymorphisms. *Mol Pathol* 2001; **54**:192–6.

84 Holmes A, Abraham DJSaS, Shiwen X, Black CM, Leask A. CTGF and SMADs, maintenance of scleroderma phenotype is independent of SMAD signaling. *J Biol Chem* 2001; **276**:10594–601.

85 Maron BJ, Bonow RO, Cannon RO 3rd, Leon MB, Epstein SE. Hypertrophic cardiomyopathy. Interrelations of clinical manifestations, pathophysiology, and therapy. *N Engl J Med* 1987; **316**:780–9.

86 Shirani J, Pick R, Roberts WC, Maron BJ. Morphology and significance of the left ventricular collagen network in young patients with hypertrophic cardiomyopathy and sudden cardiac death. *J Am Coll Cardiol* 2000; **35**:36–44.

87 Mundhenke M, Schwartzkopff B, Stark P, Schulte HD, Strauer BE. Myocardial collagen type I and impaired left ventricular function under exercise in hypertrophic cardiomyopathy. *Thorac Cardiovasc Surg* 2002; **50**:216–22.

88 Li G, Borger MA, Williams WG, Weisel RD, Mickle DA, Wigle ED, Li RK. Regional overexpression of insulin-like growth factor-I and transforming growth factor-beta1 in the myocardium of patients with hypertrophic obstructive cardiomyopathy. *J Thorac Cardiovasc Surg* 2002; **123**:89–95.

89 Li G, Li RK, Mickle DA *et al.* Elevated insulin-like growth factor-I and transforming growth factor-beta 1 and their receptors in patients with idiopathic hypertrophic obstructive cardiomyopathy. A possible mechanism. *Circulation* 1998; **98**: II144–9.

90 Di Nardo P, Fiaccavento R, Natali A *et al.* Embryonic gene expression in nonoverloaded ventricles of hereditary hypertrophic cardiomyopathic hamsters. *Laboratory Invest* 1997; **77**:489–502.

91 Brooks A, Schinde V, Bateman AC, Gallagher PJ. Interstitial fibrosis in the dilated non-ischaemic myocardium. *Heart* 2003; **89**:1255–6.

92 Marijianowski MM, Teeling P, Mann J, Becker AE. Dilated cardiomyopathy is associated with an increase in the type I/type III collagen ratio: a quantitative assessment. *J Am Coll Cardiol* 1995; **25**:1263–72.

93 Sanderson JE, Lai KB, Shum IO, Wei S, Chow LT. Transforming growth factor-beta (1) expression in dilated cardiomyopathy. *Heart* 2001; **86**:701–8.

94 Kuhl U, Noutsias M, Schultheiss HP. Immunohistochemistry in dilated cardiomyopathy. *Eur Heart J* 1995; **16**:100–6.

95 Holweg CT, Baan CC, Niesters HG, Vantrimpont PJ, Mulder PG, Maat AP, Weimar W, Balk AH. TGF-beta1 gene polymorphisms in patients with end-stage heart failure. *J Heart Lung Transplant* 2001; **20**:979–84.

96 Yamada Y, Miyauchi A, Takagi Y, Tanaka M, Mizuno M, Harada A. Association of a polymorphism of the transforming growth factor-beta1 gene with genetic susceptibility to osteoporosis in postmenopausal Japanese women. *J Bone Miner Res* 1998; **13**:1569–76.

97 Dixon IM, Hao J, Reid NL, Roth JC. Effect of chronic AT (1) receptor blockade on cardiac Smad overexpression in hereditary cardiomyopathic hamsters. *Cardiovasc Res* 2000; **46**:286–97.

98 Kan H, Xie Z, Finkel MS. p38 MAP kinase-mediated negative inotropic effect of HIV gp120 on cardiac myocytes. *Am J Physiol Cell Physiol* 2004; **286**:C1–7.

99 Taylor PM, Batten P, Brand NJ, Thomas PS, Yacoub MH. The cardiac valve interstitial cell. *Int J Biochem Cell Biol* 2003; **35**:113–18.

100 Olsson M, Rosenqvist M, Nilsson J. Expression of HLA-DR antigen and smooth muscle cell differentiation markers by valvular fibroblasts in degenerative aortic stenosis. *J Am Coll Cardiol* 1994; **24**:1664–71.

101 Rabkin E, Aikawa M, Stone JR, Fukumoto Y, Libby P, Schoen FJ. Activated interstitial myofibroblasts express catabolic enzymes and mediate matrix remodeling in myxomatous heart valves. *Circulation* 2001; **104**:2525–32.

102 Jian B, Narula N, Li QY, Mohler ER III, Levy RJ. Progression of aortic valve stenosis: TGF-beta1 is present in calcified aortic

valve cusps and promotes aortic valve interstitial cell calcification via apoptosis. *Ann Thorac Surg* 2003; **75**:457–65.

103 Fielitz J, Hein S, Mitrovic V *et al.* Activation of the cardiac renin-angiotensin system and increased myocardial collagen expression in human aortic valve disease. *J Am Coll Cardiol* 2001; **37**:1443–9.

104 Jian B, Xu J, Connolly J, Savani RC, Narula N, Liang B, Levy RJ. Serotonin mechanisms in heart valve disease I. serotonin-induced up-regulation of transforming growth factor-beta1 via G-protein signal transduction in aortic valve interstitial cells. *Am J Pathol* 2002; **161**:2111–21.

105 Chou HT, Chen CH, Tsai CH, Tsai FJ. Association between transforming growth factor-beta1 gene C-509T and T869C polymorphisms and rheumatic heart disease. *Am Heart J* 2004; **148**:181–6.

106 Ng CM, Cheng A, Myers LA *et al.* TGF-beta-dependent pathogenesis of mitral valve prolapse in a mouse model of Marfan syndrome. *J Clin Invest* 2004; **114**:1586–92.

107 Nattel S, Shiroshita-Takeshita A, Cardin S, Pelletier P. Mechanisms of atrial remodeling and clinical relevance. *Curr Opin Cardiol* 2005; **20**:21–5.

108 Hassink RJ, Aretz HT, Ruskin J, Keane D. Morphology of atrial myocardium in human pulmonary veins: a postmortem analysis in patients with and without atrial fibrillation. *J Am Coll Cardiol* 2003; **42**:1108–14.

109 Spach MS, Dolber PC, Heidlage JF. Interaction of inhomogeneities of repolarization with anisotropic propagation in dog atria. A mechanism for both preventing and initiating reentry. *Circ Res* 1989; **65**:1612–31.

110 Hanna N, Cardin S, Leung TK, Nattel S. Differences in atrial versus ventricular remodeling in dogs with ventricular tachypacing-induced congestive heart failure. *Cardiovasc Res* 2004; **63**:236–44.

111 Clancy RM, Backer CB, Yin X, Kapur RP, Molad Y, Buyon JP. Cytokine polymorphisms and histologic expression in autopsy studies. contribution of TNF-alpha and TGF-beta 1 to the pathogenesis of autoimmune-associated congenital heart block. *J Immunol* 2003; **171**:3253–61.

112 Neuberger HR, Schotten U, Verheule S, Eijsbouts S, Blaauw Y, van Hunnik A, Allessie M. Development of a substrate of atrial fibrillation during chronic atrioventricular block in the goat. *Circulation* 2005; **111**:30–7.

113 Shi Y, Li D, Tardif JC, Nattel S. Enalapril effects on atrial remodeling and atrial fibrillation in experimental congestive heart failure. *Cardiovasc Res* 2002; **54**:456–61.

114 Pedersen OD, Bagger H, Kober L, Torp-Pedersen C. Trandolapril reduces the incidence of atrial fibrillation after acute myocardial infarction in patients with left ventricular dysfunction. *Circulation* 1999; **100**:376–80.

115 L'Allier PL, Ducharme A, Keller PF, Yu H, Guertin MC, Tardif JC. Angiotensin-converting enzyme inhibition in hypertensive patients is associated with a reduction in the occurrence of atrial fibrillation. *J Am Coll Cardiol* 2004; **44**:159–64.

116 Wachtell K, Lehto M, Gerdts E *et al.* Angiotensin II receptor blockade reduces new-onset atrial fibrillation and subsequent stroke compared to atenolol: the Losartan Intervention For End Point Reduction in Hypertension (LIFE) study. *J Am Coll Cardiol* 2005; **45**:712–19.

117 Madrid AH, Bueno MG, Rebollo JM *et al.* Use of irbesartan to maintain sinus rhythm in patients with long-lasting persistent atrial fibrillation: a prospective and randomized study. *Circulation* 2002; **106**:331–6.

118 Hallberg P, Lind L, Billberger K *et al.* Transforming growth factor beta1 genotype and change in left ventricular mass during antihypertensive treatment – results from the Swedish Irbesartan Left Ventricular Hypertrophy Investigation versus Atenolol (SILVHIA). *Clin Cardiol* 2004; **27**:169–73.

119 Koyanagi M, Egashira K, Kubo-Inoue M, Usui M, Kitamoto S, Tomita H, Shimokawa H, Takeshita A. Role of transforming growth factor-beta1 in cardiovascular inflammatory changes induced by chronic inhibition of nitric oxide synthesis. *Hypertension* 2000; **35**:86–90.

120 Ikeda H, Inao M, Fujiwara K. Inhibitory effect of tranilast on activation and transforming growth factor beta 1 expression in cultured rat stellate cells. *Biochem Biophys Res Commun* 1996; **227**:322–7.

121 Hocher B, Godes M, Olivier J *et al.* Inhibition of left ventricular fibrosis by tranilast in rats with renovascular hypertension. *J Hypertens* 2002; **20**:745–51.

122 Martin J, Kelly DJ, Mifsud SA *et al.* Tranilast attenuates cardiac matrix deposition in experimental diabetes: role of transforming growth factor-beta. *Cardiovasc Res* 2005; **65**:694–701.

123 Holmes D, Fitzgerald P, Goldberg S *et al.* The PRESTO (Prevention of restenosis with tranilast and its outcomes) protocol: a double-blind, placebo-controlled trial. *Am Heart J* 2000; **139**:23–31.

124 Mujumdar VS, Tyagi SC. Temporal regulation of extracellular matrix components in transition from compensatory hypertrophy to decompensatory heart failure. *J Hypertens* 1999; **17**:261–70.

125 Simkhovich BZ, Marjoram P, Poizat C, Kedes L, Kloner RA. Age-related changes of cardiac gene expression following myocardial ischemia/reperfusion. *Arch Biochem Biophys* 2003; **420**:268–78.

126 Costacurta A, Priante G, D'Angelo A, Chieco-Bianchi L, Cantaro S. Decorin transfection in human mesangial cells downregulates genes playing a role in the progression of fibrosis. *J Clin Laboratory Anal* 2002; **16**:178–86.

127 Lopez-Casillas F, Payne HM, Andres JL, Massague J. Betaglycan can act as a dual modulator of TGF-beta access to signaling receptors: mapping of ligand binding and GAG attachment sites. *J Cell Biol* 1994; **124**:557–68.

128 Ezquerro IJ, Lasarte JJ, Dotor J *et al.* A synthetic peptide from transforming growth factor beta type III receptor inhibits liver fibrogenesis in rats with carbon tetrachloride liver injury. *Cytokine* 2003; **22**:12–20.

129 Hsu SY, Nakabayashi K, Nishi S, Kumagai J, Kudo M, Sherwood OD, Hsueh AJ. Activation of orphan receptors by the hormone relaxin. *Science* 2002; **295**:671–4.

130 Du XJ, Samuel CS, Gao XM, Zhao L, Parry LJ, Tregear GW. Increased myocardial collagen and ventricular diastolic dysfunction in relaxin deficient mice: a gender-specific phenotype. *Cardiovasc Res* 2003; **57**:395–404.

131 Dschietzig T, Richter C, Bartsch C, Laule M, Armbruster FP, Baumann G, Stangl K. The pregnancy hormone relaxin is a player in human heart failure. *FASEB J* 2001; **15**:2187–95.

132 Samuel CS, Unemori EN, Mookerjee I, Bathgate RA, Layfield SL, Mak J, Tregear GW, Du XJ. Relaxin modulates cardiac fibroblast proliferation, differentiation, and collagen production

and reverses cardiac fibrosis *in vivo*. *Endocrinology* 2004; **145**:4125–33.

133 Okada H, Takemura G, Kosai K *et al.* Postinfarction gene therapy against transforming growth factor-beta signal modulates infarct tissue dynamics and attenuates left ventricular remodeling and heart failure. *Circulation* 2005; **111**:2430–7.

134 Chen W, Wahl SM. TGF-beta: receptors. *Current Directions Autoimmunity* 2002; **5**:62–91.

135 Kulkarni AB, Huh CG, Becker D *et al.* Transforming growth factor beta 1 null mutation in mice causes excessive inflammatory response and early death. *Proc Natl Acad Sci USA* 1993; **90**:770–4.

136 Shull MM, Ormsby I, Kier AB *et al.* Targeted disruption of the mouse transforming growth factor-β 1 gene results in multifocal inflammatory disease. *Nature* 1992; **359**:693–9.

137 Scherf W, Burdach S, Hansen G. Reduced expression of transforming growth factor beta 1 exacerbates pathology in an experimental asthma model. *Eur J Immunol* 2005; **35**:198–206.

138 Foitzik K, Lindner G, Mueller-Roever S *et al.* Control of murine hair follicle regression (catagen) by TGF-beta1 *in vivo*. *FASEB J* 2000; **14**:752–60.

139 Chen H, Sun J, Buckley S, Chen C, Warburton D, Wang XF, Shi W. Abnormal mouse lung alveolarization caused by Smad3 deficiency is a developmental antecedent of centrilobular emphysema. *Am J Physiol Lung Cell Mol Physiol* 2005; **288**:L683–91.

140 Geiser AG, Zeng QQ, Sato M, Helvering LM, Hirano T, Turner CH. Decreased bone mass and bone elasticity in mice lacking the transforming growth factoR-beta1 gene. *Bone* 1998; **23**:87–93.

141 Massague J, Blain SW, Lo RS. TGFbeta signaling in growth control, cancer, and heritable disorders. *Cell* 2000; **103**:295–309.

142 Kim SJ, Im YH, Markowitz SD, Bang YJ. Molecular mechanisms of inactivation of TGF-beta receptors during carcinogenesis. *Cytokine Growth Factor Rev* 2000; **11**:159–68.

143 Tang B, Bottinger EP, Jakowlew SB, Bagnall KM, Mariano J, Anver MR, Letterio JJ, Wakefield LM. Transforming growth factor-beta1 is a new form of tumor suppressor with true haploid insufficiency. *Nat Med* 1998; **4**:802–7.

144 Yin JJ, Selander K, Chirgwin JM *et al.* TGF-beta signaling blockade inhibits PTHrP secretion by breast cancer cells and bone metastases development. *J Clin Invest* 1999; **103**:197–206.

145 Massagué J. TGF-β signal transduction. *Annu Rev Biochem* 1998; **67**:753–91.

146 Cui W, Fowlis DJ, Bryson S, Duffie E, Ireland H, Balmain A, Akhurst RJ. TGFbeta1 inhibits the formation of benign skin tumors, but enhances progression to invasive spindle carcinomas in transgenic mice. *Cell* 1996; **86**:531–42.

147 Wenner CE, Yan S. Biphasic role of TGF-beta1 in signal transduction and crosstalk. *J Cell Physiol* 2003; **196**:42–50.

148 Rosenbaum J, Blazejewski S, Preaux AM, Mallat A, Dhumeaux D, Mavier P. Fibroblast growth factor 2 and transforming growth factor beta 1 interactions in human liver myofibroblasts. *Gastroenterology* 1995; **109**:1986–96.

149 Ravitz MJ, Yan S, Herr KD, Wenner CE. Transforming growth factor beta-induced activation of cyclin E-cdk2 kinase and down-regulation of p27Kip1 in C3H 10T1/2 mouse fibroblasts. *Cancer Res* 1995; **55**:1413–6.

150 Battegay EJ, Raines EW, Seifert RA, Bowen-Pope DF, Ross R. TGF-beta induces bimodal proliferation of connective tissue cells via complex control of an autocrine PDGF loop. *Cell* 1990; **63**:515–24.

151 Win KM, Charlotte F, Mallat A *et al.* Mitogenic effect of transforming growth factor-beta 1 on human Ito cells in culture: evidence for mediation by endogenous platelet-derived growth factor. *Hepatol J* 1993; **18**:137–45.

152 Kay EP, Lee MS, Seong GJ, Lee YG. TGF-beta s stimulate cell proliferation via an autocrine production of FGF-2 in corneal stromal fibroblasts. *Curr Eye Res* 1998; **17**:286–93.

153 Strutz F, Zeisberg M, Renziehausen A, Raschke B, Becker V, van Kooten C, Muller G. TGF-beta 1 induces proliferation in human renal fibroblasts via induction of basic fibroblast growth factor (FGF-2). *Kidney Int* 2001; **59**:579–92.

154 Helske S, Lindstedt KA, Laine M *et al.* Induction of local angiotensin II-producing systems in stenotic aortic valves. *J Am Coll Cardiol* 2004; **44**:1859–66.

155 Wijffels MC, Kirchhof CJ, Dorland R, Power J, Allessie MA. Electrical remodeling due to atrial fibrillation in chronically instrumented conscious goats: roles of neurohumoral changes, ischemia, atrial stretch, and high rate of electrical activation. *Circulation* 1997; **96**:3710–20.

156 Corradi D, Callegari S, Benussi S *et al.* Regional left atrial interstitial remodeling in patients with chronic atrial fibrillation undergoing mitral-valve surgery. *Virchows Arch* 2004; **445**:498–505.

157 Thijssen VL, Ausma J, Liu GS, Allessie MA, van Eys GJ, Borgers M. Structural changes of atrial myocardium during chronic atrial fibrillation. *Cardiovasc Pathol* 2000; **9**:17–28.

158 Tagawa M, Higuchi K, Chinushi M, Washizuka T, Ushiki T, Ishihara N, Aizawa Y. Myocardium extending from the left atrium onto the pulmonary veins: a comparison between subjects with and without atrial fibrillation. *Pacing Clin Electrophysiol* 2001; **24**:1459–63.

ELSEVIER

CYTOKINE

www.elsevier.com/locate/issn/10434666

Cytokine 38 (2007) 107–115

Identification of cardiac myocytes as the target of interleukin 11, a cardioprotective cytokine

Ryusuke Kimura [a,b,1], Makiko Maeda [a,d,1], Atsushi Arita [a], Yuichi Oshima [a,b], Masanori Obana [a], Takashi Ito [a], Yasuhiro Yamamoto [a], Tomomi Mohri [a], Tadamitsu Kishimoto [c], Ichiro Kawase [b], Yasushi Fujio [a,*], Junichi Azuma [a]

[a] *Department of Clinical Pharmacology and Pharmacogenomics, Graduate School of Pharmaceutical Sciences, Osaka University, 1-6 Yamada-oka, Suita City, Osaka 565-0871, Japan*

[b] *Department of Molecular Medicine, Graduate School of Medicine, Osaka University, Japan*

[c] *Laboratory of Immune Response, Graduate School of Frontier Bioscience, Osaka University, Japan*

[d] *School of Pharmacy, Hyogo University of Health Sciences, Japan*

Received 6 February 2007; received in revised form 30 April 2007; accepted 25 May 2007

Abstract

Interleukin (IL)-6 family cytokines, which share glycoprotein 130 (gp130) as a signal-transducing receptor component, play important roles in the maintenance of cardiac homeostasis. IL-11, a member of IL-6 family cytokines, is expressed in cardiac myocytes, though it remains to be elucidated how IL-11 functions in the hearts. In the present study, first, we showed that IL-11 administration reduced the ischemia/reperfusion injury in the hearts. IL-11 receptor α was expressed in cardiomyocytes. IL-11 treatment rapidly activated signal transducer and activator of transcription 3 (STAT3) and extracellular signal-regulated kinase (ERK) 1/2 in cardiac myocytes. IL-11 stimulation resulted in the translocation of phosphorylated STAT3 into nuclei. Immunofluorescence microscopic analyses revealed that IL-11 treatment led to the cell elongation, as is the case with other cardiotrophic members of IL-6 family, such as leukemia inhibitory factor. Finally we showed that IL-11 treatment conferred the resistance to cell death induced by hydrogen peroxide, which was abrogated by adenoviral transfer of dominant negative STAT3, but not by the inhibition of ERK1/2 with U0126. These findings indicate that IL-11 mediates cytoprotective signals in cardiomyocytes, proposing that IL-11 has the potential to exhibit cardioprotection as a novel biological function.

Keywords: Interleukin-11; STAT3; Ischemia/reperfusion; Cardioprotection; Cytokine therapy

1. Introduction

Cardiac homeostasis is maintained by various kinds of neurohumoral factors. Among them, Interleukin-6 (IL-6) family cytokines play critical roles in cardiac functions. IL-6 family cytokines bind their specific α-receptors and glycoprotein 130 (gp130), a common β-receptor subunit, followed by the activation of signaling molecules [1]. Cardiac specific ablation of *gp130* gene results in the heart failure in response to pressure overload [2], suggesting that signals through gp130 transduce the cardioprotective signals in cardiac myocytes. So far, it has been demonstrated that stimulation of gp130 leads to the activation of signal transducer and activator of transcription (STAT) proteins and extracellular signal-regulated kinase (ERK) 1/2 in cardiomyocytes [3]. By using the cardiac specific transgenic mice with the expression of constitutively active STAT3, it was revealed that the activation of STAT3 contributes to cardiac protection and vessel formation [4–6]. Consistently, cardiac specific ablation of *STAT3* gene results in heart failure with impaired capillary growth [7,8]. These findings strongly suggest that activation of gp130/STAT3 system by

* Corresponding author. Fax: +81 6 6879 8253.
E-mail address: fujio@phs.osaka-u.ac.jp (Y. Fujio).
[1] These authors contributed equally to this work.

1043-4666/$ - see front matter © 2007 Elsevier Ltd. All rights reserved.
doi:10.1016/j.cyto.2007.05.011

IL-6 family cytokines could be a promising therapeutic strategy against cardiovascular diseases, though it has not been successfully achieved because of their proinflammatory properties.

Interleukin-11 (IL-11) is a pleiotropic cytokine of IL-6 family [9]. IL-11 functions as a hematopoietic growth factor and immunoregulator [10]. IL-11 exhibits anti-inflammatory effects by regulating immune effector cell function [11]. Importantly, IL-11 increases the platelets in vivo and is clinically administered to the patients with chemotherapy-induced thrombocytopenia [12], indicating that IL-11 activates gp130 system without serious inflammation. Since IL-11 prevents reperfusion injury in intestine [13], it could be proposed that IL-11 functions as a cytoprotective cytokine in non-hematopoietic systems. Recently, IL-11 is reported to be expressed in cardiomyocytes [14], suggesting that IL-11 stimulation could contribute to maintenance of homeostasis in cardiovascular system. Interestingly IL-11 protects microvascular endothelium from injury [15]; however its direct effects on cardiac myocytes remain to be addressed.

In the present study, we examined the biological effects of IL-11 as a cardioprotective cytokine. We demonstrated that IL-11 functioned as a stimulator of STAT3 in cardiac myocytes, mediating cytoprotective signals. Collectively, we propose that IL-11 signaling could be a therapeutic target against cardiovascular diseases.

2. Materials and methods

2.1. Generation of ischemia/reperfusion injury

Recombinant human IL-11 was purchased from Peprotech EC. IL-11 (8 μg/kg) or PBS was intravenously administered in C57Bl/6 mice (10 weeks old, $n = 9$ for vehicle, $n = 8$ for IL-11). Ischemia/reperfusion injury was generated around 15 h after cytokine injection and infarct size was estimated as described previously [6]. Briefly, mice were anesthetized with ketamine (Sankyo Yell Yakuhin, 100 mg/kg) and xylazine (Bayer, 5 mg/kg), and ventilated with 80% oxygen. After left-side thoracotomy, the left coronary artery was ligated with a suture. After 60-min occlusion, the ligature was loosened for 60 min. Ischemia/reperfusion was confirmed by ST-T changes in ECG monitor. Areas at risk were estimated by exclusion of Evans Blue staining. The myocardial infarct areas were detected by staining with 2% triphenyltetrazolium chloride (TTC). Surgical procedures were performed by the researcher who was blinded to the pretreatment.

The care of all animals was in compliance with the Osaka University animal care guideline. The investigation conforms with the *Guide for the Care and Use of Laboratory Animals* published by the US National Institutes of Health (NIH publication No. 85-23, revised 1996).

2.2. Cell culture

Rat neonatal cardiac myocytes were cultured as described previously [16]. Briefly, cardiomyocytes were isolated by collagenase and trypsin digestion from the ventricles of neonatal rats. After preplating the cells on culture dish for 60 min, floating cells were used as cardiomyocytes. More than 95% of total cells were identified as cardiac myocytes that were positively stained with anti-sarcomeric α-actinin antibody (data not shown). Attached cells were cultured for 3 passages and used as fibroblasts. Cells were cultured in serum-free condition for 12 h, followed by the treatment with IL-11. In the experiment concerning gp130 blocking antibody (R&D systems), mouse neonatal cardiac myocytes were prepared according to the same protocol.

The generation of adenovirus vector expressing dominant negative STAT3 (Ad-dnSTAT3) was described previously [17]. U0126, a specific inhibitor for MEK 1/2, was purchased from Cell Signaling.

2.3. RT-PCR analyses

RT-PCR analyses were performed as described previously [16]. Briefly, total RNA was prepared with acid guanidinium thiocyanate–phenol–chloroform method [18]. Total RNA (1 μg) was subjected for first strand cDNA synthesis by using the oligo (dT) first strand primer. The specific primers for IL-11 receptor are as follows; forward: 5′-TCTGGATGCTGGCACCTGGAGCGCCTGGAGC-3′, reverse: 5′-TCAGCTGAAGTTCTCTGGGGTCCTCTGCAGG-3′. The PCR products were size-fractionated by 2% agarose gel electrophoresis.

2.4. Immunoblot analysis

Immunoblot analyses were performed as described previously [19]. Cells were treated with the indicated concentrations of IL-11. After washed with PBS twice, cell lysates were prepared by adding SDS–PAGE sample solution. Proteins were separated by SDS–PAGE and transferred onto the PVDF membrane (Millipore). The membranes were immunoblotted with anti-phospho-STAT3 or anti-phospho-ERK 1/2 (Cell Signaling Technology) antibody diluted 1:200. The membranes were reprobed with anti-STAT3 (Santa Cruz Biotechnology) or anti-ERK 1/2 (Cell Signaling Technology) antibody diluted 1:200. ECL system was used for the detection.

2.5. Immunofluorescent microscopic analyses

Cells were stimulated with IL-11 (20 ng/ml), or LIF (1000 U/ml) for the indicated time and fixed with 3.7% formaldehyde in PBS. Permeabilized with 0.2% Triton X-100, cells were washed with PBS twice and incubated with anti-sarcomeric α-actinin antibody (Sigma) diluted 1:100 and/or anti-phospho-STAT3 antibody (Cell Signaling

Technology) diluted 1:100 as a first antibody. In the case of immunostaining for anti-IL-11 receptor, cells were incubated with anti-IL-11 receptor antibody (Santa Cruz Biotechnology) diluted 1:100 without cell permeabilization, in order to demonstrate the existence of the receptor on cell surface. After washed with PBS three times, cells were incubated with Alexa Fluor 488- or 546-conjugated secondary antibody (Molecular Probe) diluted 1:100. In these procedures, the antibodies were diluted with 10 mg/ml of bovine serum albumin in PBS. After washed with PBS, cells were examined with fluorescent microscopy, Olympus IX70. Non-immune IgG was used as a first antibody, as control.

Morphological changes were analyzed according to the previous study [20]. Sarcomeric α-actinin positive cells ($n = 151$–227) were examined and analyzed by the researcher who was blinded to the assay conditions. Cell surface area and cell length were measured by using Image J (NIH).

2.6. Preparation of nuclear fraction of cardiac myocytes

Nuclear fraction was prepared from cardiac myocytes as described previously [21] with minor modification. Cardiomyocytes (5×10^6 cells per dish) were cultured on 100 mm dish and stimulated with IL-11 (20 ng/ml) for 15 min and washed with ice-cold PBS containing 5 mM orthosodium vanadate twice. Cells were lysed in 500 μl of buffer A (20 mM Hepes (pH 7.6), 20% (v/v) glycerol, 10 mM NaCl, 1.5 mM $MgCl_2$, 0.2 mM EDTA, 1 mM DTT (dithiothreitol), 0.1% (v/v) Nonidet-P40, 5 mM orthosodium vanadate and protease inhibitor mixture) and incubated on ice for 5 min. Cell lysate was centrifuged at 2000*g* for 5 min. The supernatant was used as the cytosolic fraction, while the pellet was resuspended in 500 μl of buffer A and used as the nuclear fraction. The proteins from the equal amount of cytosolic and nuclear fractions were separated on SDS–PAGE and immunoblotted with anti-STAT3 antibody.

2.7. Cell survival analysis

In order to estimate the effects of IL-11 on cell viability/proliferation, MTS (3-(4,5-dimethylthiazol-2-ly)-5-(3-carboxymethoxyphenyl)-2-(4-sulfophenyl)-2H-tetrazorium, inner salt, Promega) metabolizing activities were measured. Cells (1×10^4 cells/well) were cultured in 96-well dishes. Twenty four hours after cultivation, culture medium was changed to the serum free medium containing various concentrations of IL-11. Seventy two hours later, MTS solution was added to the cell culture. MTS metabolizing activity was estimated by measuring the absorbance at 490 nm according to the manufacturer's protocol.

To detect apoptotic cells, annexin V-Alexa Fluor 488 conjugate (Molecular Probes, Inc) was used according to the manufacture's instruction. Briefly, cardiomyocytes cultured on glass cover slips were treated with control vehicle or IL-11 (20 ng/ml) for 3 h, and then incubated with or without 100 μM H_2O_2 for 24 h. After washed with cold phosphate-buffer saline (PBS) and then with annexin-binding buffer (10 mM Hepes, 140 mM NaCl, and 2.5 mM $CaCl_2$, pH 7.4), cells were incubated with annexin V conjugate in the binding buffer for 15 min at room temperature in the dark. After incubation, cells were washed with the binding buffer, fixed with 3.7% formaldehyde in binding buffer for 20 min at room temperature and then double-stained with Hoechst dye. More than 20 fields per assay condition (average, 39–68 cells/field) were selected at random by the researcher who was blinded to the conditions. The frequency of annexin V-positive cells relative to Hoechst-positive nuclei per field was calculated.

2.8. Statistical analysis

Statistical analysis was performed by unpaired *t*-test or ANOVA.

3. Results

3.1. IL-11 reduced ischemia/reperfusion injury in hearts

IL-11 was originally identified as a hematopoietic cytokine [22]. Accumulating evidences have revealed that IL-11 also exhibits pleiotropic effects in non-hematopoietic systems, such as gastrointestinal tracts [23]. Recent studies have demonstrated that administration of IL-11 reduced reperfusion injury in intestine [13]. Based on these findings, in order to address the biological functions of IL-11 in hearts, we examined the effects of IL-11 on ischemia/reperfusion injury in murine hearts (Fig. 1). Intravenous administration of IL-11 reduced the infarct size by 63%, compared with control. There was no difference in area at risk between IL-11-treated and control groups. These findings suggest that cardiac cells are novel targets of IL-11.

3.2. IL-11 activated STAT3 and ERK 1/2 in the cultured cardiac myocytes

To address how IL-11 conferred the resistance to ischemia/reperfusion in the hearts, we examined the effects of IL-11 in vitro. We first confirmed that IL-11receptor α (IL-11Rα) was expressed both in cardiac myocytes and fibroblasts, by RT-PCR (Fig. 2a). Immunofluorescent microscopic analysis was performed to detect IL-11Rα protein (Fig. 2b). Cells were positively stained with anti-IL-11Rα antibody, indicating the expression of the receptor protein. To examine whether IL-11Rα transduces the signals as a functional receptor in cardiomyocytes, cultured cardiac myocytes were stimulated with IL-11 for the indicated time and phosphorylation of STAT3 and ERK 1/2 were analyzed by immunoblotting with anti-phospho-specific antibodies (Fig. 3). STAT3 and ERK 1/2 were activated by the treatment with IL-11, as was the case with LIF, a positive control [3]. The enhancement of STAT3

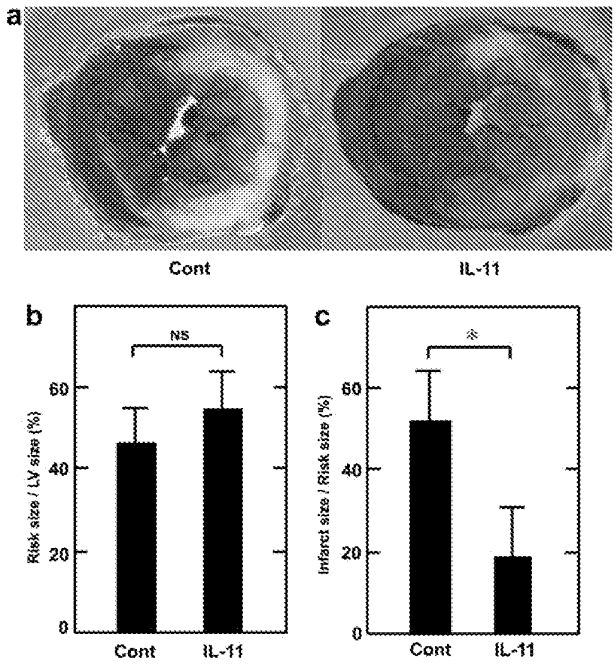

Fig. 1. Pretreatment of IL-11 prevents ischemia/reperfusion injury in hearts. IL-11 (8 μg/kg) or control vehicle (cont) was intravenously injected in C57Bl/6 mice (10 weeks old). Around 15 h later, mice were exposed to 60 min ischemia, followed by 60 min reperfusion. The hearts were stained with Evans Blue and with TTC, as described in Section 2. (a) Representative images are demonstrated. (b and c) Risk area size and infarct size were demonstrated in each condition. Data are shown as means ± SD. $^{*}p < 0.05$ by unpaired t-test. $n = 9$ for control; $n = 8$ for IL-11 treatment.

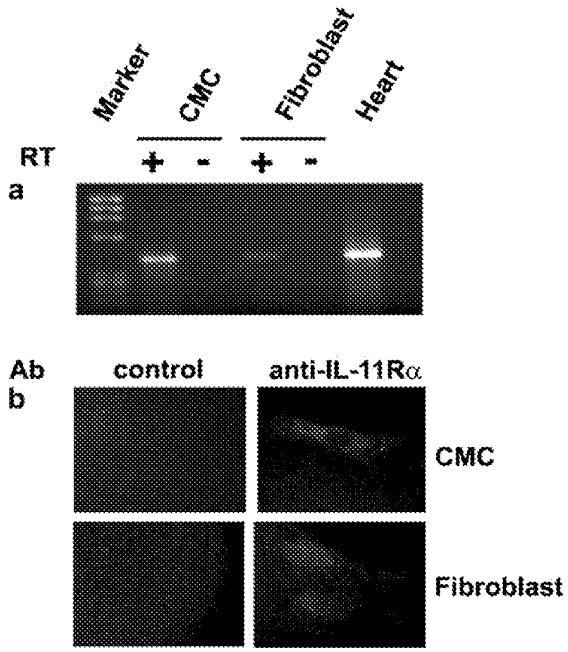

Fig. 2. IL-11 receptor α is expressed in cardiac myocytes. (a) Total RNA was prepared from cultured rat neonatal cardiomyocytes (CMC) and cardiac fibroblasts. The expression of IL-11 receptor α (IL-11Rα) was analyzed by RT-PCR. The DNA fragment of IL-11Rα was amplified from the reverse-transcribed (RT) product (+) by PCR. Total RNAs without RT reaction (−) were used as a negative control. RT product from the whole heart was used as a positive control. The products of $\Phi \times 174$ digested with HaeIII were used as fragment size markers. (b) Cardiac myocytes (CMC) and fibroblasts were stained with anti-IL-11Rα antibody. Non-immune IgG was used as a negative control.

and ERK 1/2 activities was detected within 5 min and their activities were reduced to the basal level 60 min after IL-11 stimulation (Fig. 3a and b). Importantly, STAT3 was submaximally phosphorylated by 20 ng/ml of IL-11 (Fig. 3c), indicating that IL-11 signals can be transduced in cardiac myocytes with the similar kinetics with other cell lineages such as macrophages, reported so far [11]. By using mouse gp130 blocking antibody, we confirmed that gp130 blocking antibody inhibited the IL-11-induced activation of STAT3 and ERK 1/2 in mouse cardiac myocytes (data not shown). Therefore it is suggested that IL-11 utilizes gp130 in its signaling pathway, as is the case with other IL-6 family cytokines [3].

Since IL-11Rα mRNA was also detected in cardiac fibroblasts as well as in cardiac myocytes (Fig. 2), we examined whether IL-11 activated STAT3 and ERK 1/2 in cardiac fibroblasts (Fig. 4). Similar to cardiac myocytes, the treatment with IL-11 resulted in the rapid phosphorylation of STAT3 and ERK 1/2 in cardiac fibroblasts.

In order to briefly estimate the effects of IL-11 on cell viability/proliferation, MTS (3-(4,5-dimethylthiazol-2-ly)-5-(3-carboxymethoxyphenyl)-2-(4-sulfophenyl)-2H-tetrazorium, inner salt) metabolizing activities were measured. Under the serum-depleted conditions, cells were cultured in the presence or absence of IL-11 (20 ng/ml) for 72 h and MTS assay was performed. Treatment with IL-11 resulted in about 2-fold increase in MTS metabolizing activities in cardiac myocytes, while no significant increase was observed in cardiac fibroblasts (data not shown), suggesting the functional relevance of IL-11 as a cardiomyocyte survival factor. Considering the pathophysiological importance of cardiomyocyte survival in the prevention of cardiac dysfunction, further study was focused on the biological effects of IL-11 in cardiac myocytes.

3.3. IL-11 treatment leads to translocation of phosphorylated STAT3 into nuclei

To confirm that cardiac myocytes were direct target of IL-11, we examined the location of phospho-STAT3 in cardiac myocytes by immunofluorescent microscopy (Fig. 5a). Sarcomeric α-actinin was co-stained as a cardiomyocyte marker. In response to IL-11, the intensity of phospho-STAT3 was increased in cardiac myocytes. Importantly, phospho-STAT3 staining was concentrated in the nuclei of sarcomeric α-actinin-positive cells in response to IL-11, indicating the translocation of phospho-STAT3 into nuclei as an evidence for STAT3 activation in cardiac myocytes.

Next we biochemically prepared the cytosolic and nuclear fractions from the cardiac myocyte culture and

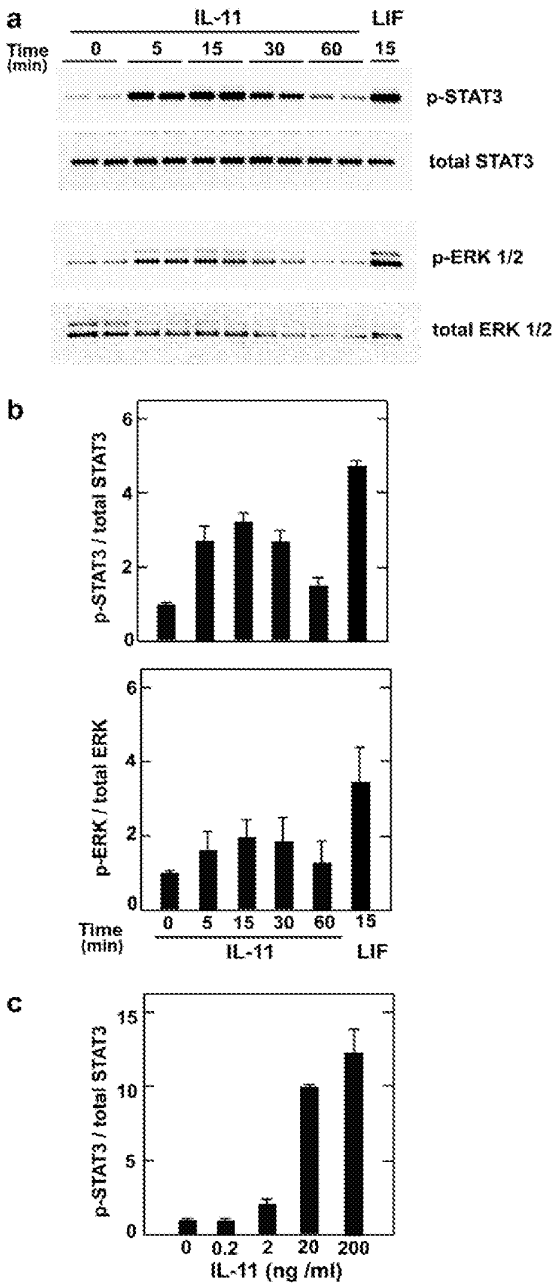

Fig. 3. IL-11 activates STAT3 and ERK 1/2 in cultured cardiomyocytes. (a) Cells were stimulated with IL-11 (20 ng/ml) for the indicated time. Cell lysates were prepared and immunoblotted with anti-phospho-STAT3 or anti-phospho-ERK 1/2 antibody. The membranes were reprobed with anti-STAT3 or anti-ERK 1/2 antibody. LIF (1000 U/ml) was used for the positive control. Four independent experiments were performed, and representative data were shown. (b) Quantitative analyses of the time course of the phosphorylation of STAT3 and ERKs. Data are presented as means ± SE from 4 independent assays. (c) Cells were stimulated with various concentrations of IL-11 for 15 min. Cell lysates were immunoblotted with anti-STAT3 and STAT3 antibodies. Phosphorylation of STAT3 was estimated. Note that IL-11 phosphorylated STAT3 in a dose-dependent manner. Data are presented as means ± SE from 4 independent assays.

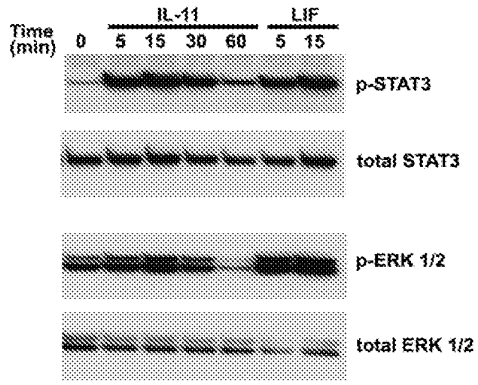

Fig. 4. STAT3 and ERK 1/2 are activated by IL-11 in cardiac fibroblasts. Cardiac fibroblasts were stimulated with IL-11 (20 ng/ml) for the indicated time. LIF (1000 U/ml) was used for the positive control. Cell lysates were prepared and immunoblotted with anti-phospho-STAT3 or anti-phospho-ERK 1/2 antibody. The membrane was reprobed with anti-STAT3 or anti-ERK 1/2 antibody. Three independent assays were performed, and representative data were shown.

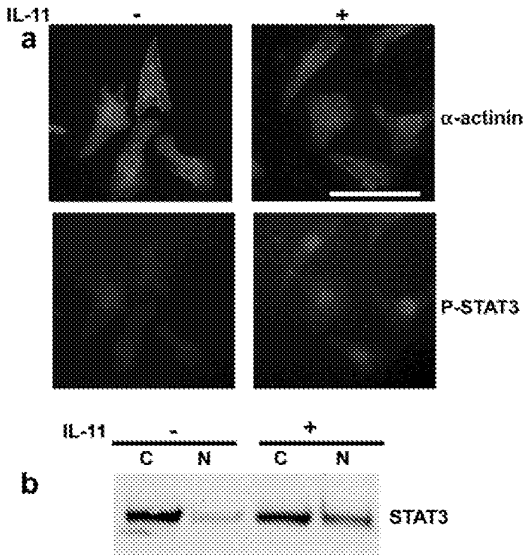

Fig. 5. IL-11 induces the translocation of phosphorylated STAT3 into nuclei in cultured cardiomyocytes. (a) Cultured cardiomyocytes were stimulated with IL-11 (20 ng/ml) for 15 min and stained with anti-sarcomeric α-actinin and anti-phospho-STAT3 antibodies. Bar, 40 μm. Note that the staining of phospho-STAT3 is enhanced and concentrated in nuclei of sarcomeric α-actinin-positive cardiomyocytes in response to IL-11. (b) Cardiac myocytes were stimulated with Il-11 for 15 min. Cytosolic (C) and nuclear (N) fractions were prepared, as described in Section 2. Immunoblot analysis was performed for STAT3 protein. STAT3 band intensity in nuclear fraction was increased by IL-11 stimulation.

analyzed the localization of STAT3 by immunoblotting (Fig. 5b). In the nuclear fraction from IL-11-treated cardiomyocytes, the significant amount of STAT3 protein was detected, while only a low level of the protein was in that from non-treated cells.

3.4. IL-11 induces the increase in cell size with cell elongation in cardiac myocytes

To address the biological effects of IL-11 in cardiac myocytes, first, we examined whether IL-11 induced the morphological changes in cultured cardiomyocytes (Fig. 6). Similar to LIF, a positive control, IL-11 treatment resulted in cardiomyocyte enlargement. We quantitatively analyzed the effects of IL-11 on cardiomyocyte structure according to the previous study [20]. As a result, it was revealed that IL-11 stimulation increased the cell surface area by 22%. Interestingly, IL-11 treatment elongated the cell length in the direction of long axis by 43%, but not short axis, consistent with other signals through gp130 [20,24].

3.5. IL-11 suppressed H_2O_2-induced cell death via STAT3

Reactive oxygen species (ROS) are closely related with the onset and progression of cardiovascular diseases. Especially under the condition of ischemia/reperfusion in the hearts, the rapid accumulation of toxic metabolites such as ROS occurs. Among them, H_2O_2 exhibits serious toxic effects in myocardium. Therefore, we analyzed the effects of IL-11 on apoptotic cell death induced by H_2O_2. Pretreated with IL-11 for 3 h, cardiac myocytes were exposed to H_2O_2 for 24 h and stained with annexin V-conjugated with Alexa Fluor 488 (Fig. 7). H_2O_2-treatment showed about 3-fold increase in the frequency of annexin V-positive cells in the absence of IL-11, compared with control.

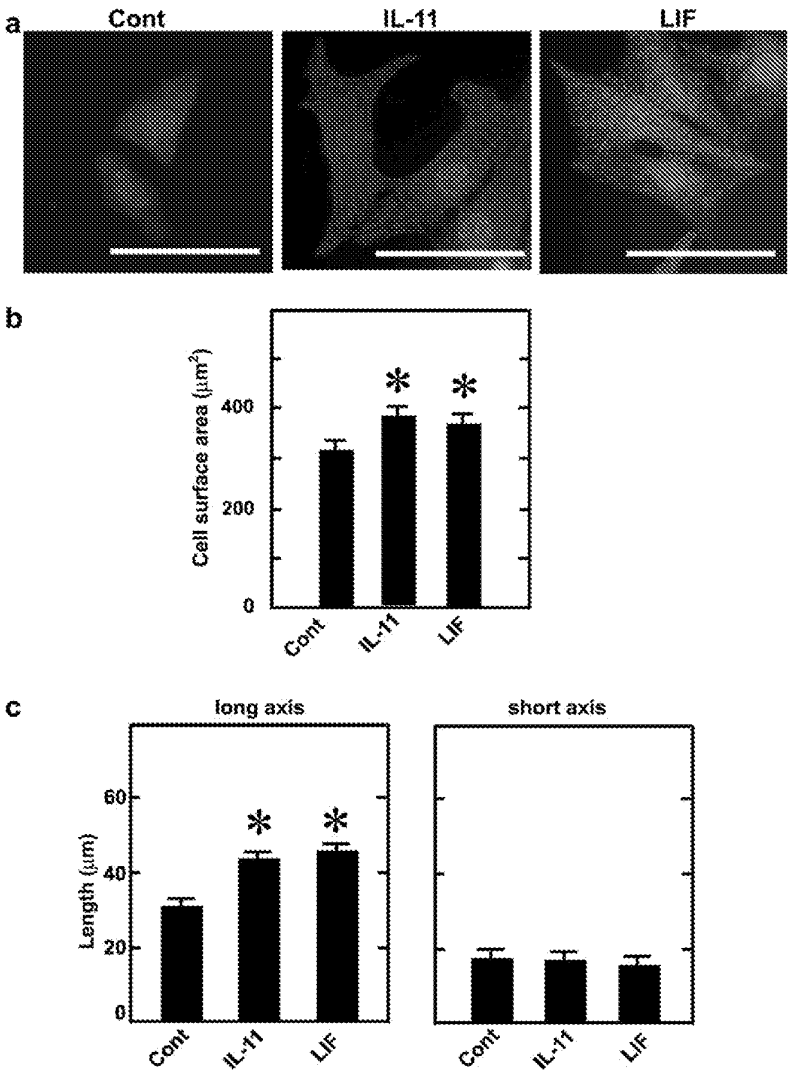

Fig. 6. IL-11 induces the cell elongation in cultured cardiomyocytes. Cultured cardiac myocytes were stimulated with control vehicle (cont), IL-11 (20 ng/ml) or LIF (1000 U/ml) for 24 h. Cells were stained with anti-sarcomeric α-actinin antibody. (a) Representative immunofluorescent microscopic images. Bar, 40 μm. (b) Cell surface areas were measured. Data are shown as means ± SE. (c) Cell length of long axis or short axis was measured. Data are shown as means ± SE. The cell number observed for morphological analysis is as follows; $n = 151$ for control, 187 for IL-11, 227 for LIF. $^*p < 0.05$ versus control. Experiments were repeated three times with similar results.

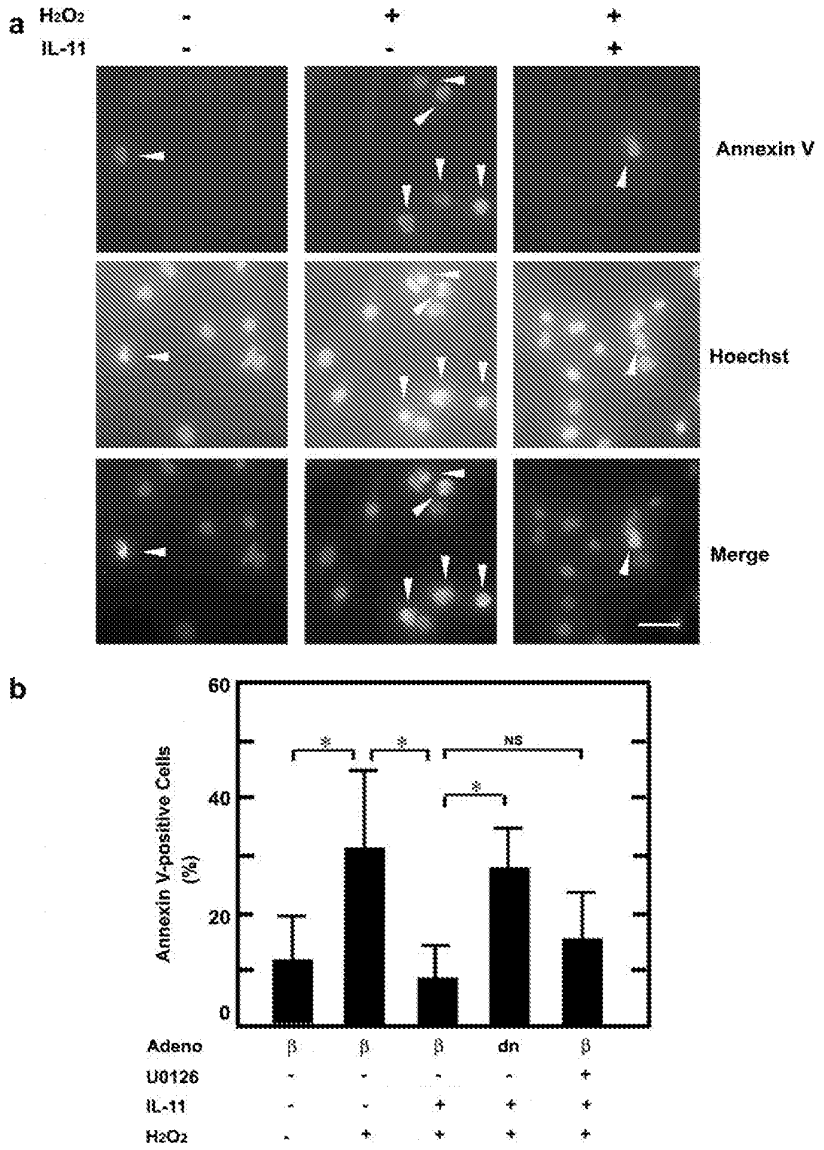

Fig. 7. IL-11 suppressed the apoptotic cell death induced by H_2O_2 through STAT3. (a) IL-11 prevented cardiomyocytes from apoptotic cell death induced by H_2O_2. Cardiomyocytes were pretreated with IL-11 (20 ng/ml) for 3 h and exposed to H_2O_2 for 24 h. Apoptotic cells were detected by staining with annexin V and Hoechst 33342. Representative images were shown. Arrowheads show the annexin V-positive, apoptotic cells. Bar, 40 μm. (b) Quantification of the apoptotic cell death was performed. Cells were transfected with adenovirus vector expressing dnSTAT3 (dn) or β-galactosidase (β), a control vector. Cells were exposed to H_2O_2 with or without pretreatment of IL-11. In order to examine the effects of the inhibition of ERK, cells were preincubated with 10 μM U0126, a MEK 1/2 inhibitor. Data were shown as means ± SD. $^*p < 0.05$ by ANOVA (Fisher's test). NS, not significant.

IL-11 treatment significantly reduced the frequency of annexin V-positive cells, indicating that IL-11 prevented the cell death induced by H_2O_2.

To address the signaling pathways for IL-11-mediated suppression of cell death, we examined effects of the inhibition of STAT3 and ERK 1/2 on H_2O_2-mediated cardiomyocyte death, using dominant negative STAT3 (dnSTAT3) and U0126, a specific inhibitor for MEKs 1/2 that function upstream of ERK 1/2, respectively. IL-11-mediated suppression of cell death was cancelled by the transfection of Ad-dnSTAT3, but not significantly by the treatment of U0126. These data suggest that IL-11 mediates the resistance to cell death induced by H_2O_2 through STAT3.

4. Discussion

In the present study, we demonstrated that IL-11 administration prevented reperfusion injury in hearts. STAT3 and ERKs were rapidly activated by IL-11 in the cultured cardiac myocytes. IL-11 treatment resulted in cardiomyocyte

elongation in vitro. Moreover, IL-11 promoted cell survival against serum depletion in vitro. Interestingly, IL-11 prevented the cell death induced by H_2O_2 through STAT3. This is the first demonstration that IL-11 regulates cardiomyocyte function as a cardioprotective cytokine.

Previously it was reported that IL-11 is expressed in the cardiac myocytes [14]. However, it remains to be elucidated whether IL-11 transduces signals in cardiac myocytes. Here, we demonstrated that IL-11Rα was expressed in the cardiomyocytes and that the stimulation with IL-11 resulted in a rapid activation of STAT3 and ERK 1/2 in cardiac myocytes. Moreover, IL-11 treatment resulted in the rapid translocation of STAT3 into nuclei in cardiac myocytes. These findings indicate that cardiac myocytes are the direct targets of IL-11.

Compared with cardiac myocytes, PCR product for IL-11Rα was detected in low level in the total RNA from cardiac fibroblasts. However, theoretically, it is impossible to compare the expression level of its transcript between cardiac myocytes and cardiac fibroblasts, based on these results, because there might be difference in the content of total RNA per cell, the proportion of mRNA to total RNA and the component of mRNA, between the two cell types. Since IL-11 stimulation resulted in the activation of STAT3 and ERK 1/2 in cardiac fibroblasts, our data demonstrate that functional IL-11 receptor is expressed in cardiac fibroblasts, though its biological significances remain to be elucidated.

IL-11 increased the cell surface area with cell elongation in cardiac myocytes, characteristic of gp130-mediated cardiotrophic effects [20]. However it is unlikely that IL-11 signals play critical roles in cardiac development, because no cardiac abnormality is observed during development either in IL-11R null mice [25,26] or in cardiac specific gp130 null mice [2]. Since cardiac specific ablation of *gp130* gene results in the susceptibility to pressure overload [2], it could be postulated that IL-11 contributes to the resistance to myocardial stresses, in coordination with other cardiotrophic IL-6 family cytokines, such as LIF.

In this context, to address the biological importance of IL-11 in cardiac functions, we examined the effects of IL-11 on cell viability. To induce the cell death, cardiac myocytes were exposed to reactive oxygen species, such as H_2O_2, and the cell death was estimated by staining with annexin V. IL-11 reduced the cell death induced by H_2O_2, through STAT3 pathway. So far, STAT3 pathway has been proposed as the signaling pathways responsible for IL-6 family cytokine-mediated cardioprotection. Constitutive activation of STAT3 reduces the ischemia/reperfusion injury in the hearts [6]. It has been also reported that STAT3 contributes to ischemic preconditioning in the hearts [27,28]. These findings support the functional relevance of STAT3 in IL-11-mediated cardioprotection.

The inhibition of ERK pathway did not significantly affect IL-11-mediated anti-apoptotic effects against H_2O_2 treatment. However, this result does not exclude the possibility that ERK activation is related with IL-11-mediated cardioprotection, because it is proposed that cell elongation by signals through gp130 is mediated by ERK pathway and is closely related with cell viability [29]. IL-11 might differentially utilize STAT3 and/or ERKs as cytoprotective signals, dependent on cytotoxic stimuli.

This study is the first demonstration that IL-11 targets cardiac myocytes and mediates cardioprotective signals. Previous studies have proposed that activation of gp130 or its downstream signal, especially STAT3, by IL-6-family cytokines is a promising strategy against cardiovascular diseases [6,30]. Clinically, IL-11 is utilized for the chemotherapy-induced thrombocytopenia at 25–50 μg/kg. In the preliminary experiments, we examined the phosphorylation status of STAT3 in the hearts after injection of 0, 0.08, 0.8, 8, and 25 μg/kg of IL-11. And we confirmed the sub-maximal activation of STAT3 by the injection of 8 μg/kg of IL-11 (data not shown). Thus we examined the cytoprotective effects of IL-11 injection at 8 μg/kg and demonstrated that this dosage of IL-11 exhibited the cardioprotective effects against ischemia/reperfusion. Considering the clinical availability due to limited adverse effects, our data presented here propose that IL-11 therapy might exert beneficial effects against cardiovascular diseases, because clinical benefits on cardiovascular systems can be achieved at lower dosage than clinical dosage for thrombocytopenia, as described above.

In conclusion, we have demonstrated that IL-11 activated STAT3 and ERK pathways in cardiac myocytes, contributing to cardioprotection. IL-11/IL-11R system might be a promising target to preserve myocardium in cardiovascular diseases.

Acknowledgments

We thank Yasuko Murao for her excellent secretary work. This study was partially supported by a Grant-in-Aid for Scientific Research from Ministry of Education, Science, Sports, and Culture of Japan, by a Grant-in-Aid for Scientific Research from Ministry of Health, Labour and Welfare, by The Pharmacological Research Foundation, Tokyo, and by Takeda Science Foundation.

References

[1] Kishimoto T, Taga T, Akira S. Cytokine signal transduction. Cell 1994;76:253–62.
[2] Hirota H, Chen J, Betz UAK, Rajewsky K, Gu Y, Ross JJ, et al. Loss of a gp130 cardiac muscle cell survival pathway is a critical event in the onset of heart failure during biomechanical stress. Cell 1999;97:189–98.
[3] Kunisada K, Hirota H, Fujio Y, Matsui H, Tani K, Yamauchi-Takihara K, et al. Activation of Jak-STAT and MAP kinases by leukemia inhibitory factor through gp130 in cardiac myocytes. Circulation 1996;94:2626–32.
[4] Funamoto M, Fujio Y, Kunisada K, Negoro S, Tone E, Osugi T, et al. Signal transducer and activator of transcription 3 is required for glycoprotein 130-mediated induction of vascular endothelial growth factor in cardiac myocytes. J Biol Chem 2000;275:10561–6.

[5] Osugi T, Oshima Y, Fujio Y, Funamoto M, Yamashita A, Negoro S, et al. Cardiac-specific activation of signal transducer and activator of transcription 3 promotes vascular formation in the heart. J Biol Chem 2002;277:6676–81.
[6] Oshima Y, Fujio Y, Nakanishi T, Itoh N, Yamamoto Y, Negoro S, et al. STAT3 mediates cardioprotection against ischemia/reperfusion injury through metallothionein induction in the heart. Cardiovasc Res 2005;65:428–35.
[7] Jacoby JJ, Kalinowski A, Liu M-G, Zhang SS-M, Gao Q, Chai G-X, et al. Cardiomyocyte-restricted knockout of STAT3 results in higher sensitivity to inflammation, cardiac fibrosis, and heart failure with advanced age. Proc Natl Acad Sci USA 2003;100:12929–34.
[8] Hilfiker-Kleiner D, Hilfiker A, Fuchs M, Kaminski K, Schaefer A, Schieffer B, et al. Signal transducer and activator of transcription 3 is required for myocardial capillary growth, control of interstitial matrix deposition, and heart protection from ischemic injury. Circ Res 2004;95:187–95.
[9] Trepicchio WL, Dorner AJ. Interleukin-11. A gp130 cytokine. Ann NY Acad Sci 1998;856:12–21.
[10] Opal SM, DePalo VA. Anti-inflammatory cytokines. Chest 2000;117:1162–72.
[11] Trepicchio WL, Wang L, Bozza M, Dorner AJ. IL-11 regulates macrophage effector function through the inhibition of nuclear factor-kB. J Immunol 1997;157:3627–34.
[12] Gordon MS, McCaskill-Stevens WJ, Battiato LA, Loewy J, Loesch D, Breeden E, et al. A phase I trial of recombinant human interleukin-11 (neumega rhIL-11 growth factor) in women with breast cancer receiving chemotherapy. Blood 1996;87:3615–24.
[13] Du X, Liu Q, Yang Z, Orazi A, Rescorla FJ, Grosfeld JL, et al. Protective effects of interleukin-11 in a murine model of ischemic bowel necrosis. Am J Physiol 1997;272:G545–52.
[14] Ancey C, Corbi P, Froger J, Delwail A, Wijdenes J, Gascan H, et al. Secretion of IL-6, Il-11 and LIF by human cardiomyocytes in primary culture. Cytokine 2002;18:199–205.
[15] Kirkiles-Smith NC, Mahboubi K, Plescia J, McNiff JM, Karras J, Schechner JS, et al. IL-11 protects human microvascular endothelium from alloinjury in vivo by induction of survivin expression. J Immunol 2004;172:1391–6.
[16] Fujio Y, Kunisada K, Hirota H, Yamauchi-Takihara K, Kishimoto T. Signals through gp130 upregulate bcl-x gene expression via STAT1-binding cis-element in cardiac myocytes. J Clin Invest 1997;99:2898–905.
[17] Kunisada K, Tone E, Fujio Y, Matsui H, Yamauchi-Takihara K, Kishimoto T. Activation of gp130 transduces hypertrophic signals via STAT3 in cardiac myocytes. Circulation 1998;98:346–52.
[18] Chomczynski P, Sacchi N. Single-step method of RNA extraction by acid guanidinium thiocyanate-phenol-chloroform. Anal Biochem 1987;162:156–9.
[19] Mohri T, Fujio Y, Maeda M, Ito T, Oshima Y, Uozumi Y, et al. Leukemia inhibitory factor induces endothelial differentiation in cardiac stem cells. J Biol Chem 2006;281:6442–7.
[20] Wollert KC, Taga T, Saito M, Narazaki M, Kishimoto T, Glembotski CC, et al. Cardiortrophin-1 activates a distinct form of cardiac muscle cell hypertrophy. Assembly of sarcomeric units in series via gp130/leukemia inhibitory factor receptor-dependent pathways. J Biol Chem 1996;271:9535–45.
[21] Sandri M, Sandri C, Gilbert A, Skurk C, Calabria E, Picard A, et al. Foxo transcription factors induce the atrophy-related ubiquitin ligase atrogin-1 and cause skeletal muscle atrophy. Cell 2004;177:399–412.
[22] Paul SR, Bennett F, Calvetti JA, Kelleher K, Wood CR, O'Hara Jr RM, et al. Molecular cloning of a cDNA encoding interleukin 11, a stromal cell-derived lymphopoietic and hematopoietic cytokine. Proc Natl Acad Sci USA 1990;87:7512–6.
[23] Du X-X, Williams DA. Interleukin-11: review of molecular, cell biology and clinical use. Blood 1997;89:3897–908.
[24] Nakaoka Y, Nishida K, Fujio Y, Izumi M, Terai K, Oshima Y, et al. Activation of gp130 transduces hypertrophic signal through interaction of scaffolding/docking protein Gab1 with tyrosine phosphatase SHP2 in cardiomyocytes. Circ Res 2003;93:221–9.
[25] Robb L, Li R, Hartley L, Nandurkar H, Koentgen F, Begley CG. Infertility in female mice lacking the receptor for interleukin 11 is due to a defective uterine response to implantation. Nat Med 1998;4:303–8.
[26] Bilinski P, Roopenian D, Gossler A. Maternal IL-11Ra is required for normal decidua and fetoplacental development in mice. Genes Dev 1998;12:2234–43.
[27] Xuan Y-T, Guo Y, Han H, Zhu Y, Bolli R. An essential role of the JAK-STAT pathway in ischemic preconditioning. Proc Natl Acad Sci USA 2001;98:9050–5.
[28] Smith RM, Suleman N, Lacerda L, Opie LH, Akira S, Chien KR, et al. Genetic depletion of cardiac myocyte STAT-3 abolishes classical preconditioning. Cardiovasc Res 2004;63:611–6.
[29] Pradervand S, Yasukawa H, Muller OG, Kjekshus H, Nakamura T, Amand TRS, et al. Small proline-rich protein 1A is a gp130 pathway-and stress-inducible cardioprotective protein. EMBO J 2004;23:4517–25.
[30] Zou Y, Takano H, Mizukami M, Akazawa H, Qin Y, Tako H, et al. Leukemia inhibitory factor enhances survival of cardiomyocytes and induces regeneration of myocardium after myocardial infarction. Circulation 2003;108:748–53.

Cysteinyl leukotriene upregulates IL-11 expression in allergic airway disease of mice

Kyung Sun Lee, PhD, So Ri Kim, MD, PhD, Hee Sun Park, MD, PhD, Seoung Ju Park, MD, PhD, Kyung Hoon Min, MD, PhD, Ka Young Lee, MD, Sun Mi Jin, MS, and Yong Chul Lee, MD, PhD *Jeonju, South Korea*

Background: Chronic airway inflammation and airway remodeling are important features of bronchial asthma. IL-11 is one of the important mediators involved in the process of airway inflammation and remodeling. Cysteinyl leukotrienes (cysLTs) play roles in recruitment of inflammatory cells, airway smooth muscle contraction, vascular leakage, increased mucus secretion, decreased mucociliary clearance, and airway fibrosis.
Objective: An aim of the present study was to determine the effect of the cysLTs on the regulation of IL-11 expression.
Methods: We used a C57BL/6 mouse model of allergic airway disease and murine tracheal epithelial cells to examine the effects of cysLTs on the regulation of IL-11 expression.
Results: Our present study with an ovalbumin-induced murine model of allergic airway disease revealed that levels of leukotriene C_4 (LTC_4) in bronchoalveolar lavage fluids were increased and that administration of montelukast or pranlukast reduced the increased levels of LTC_4; the increased expression of IL-11 protein and mRNA in lung tissues; airway inflammation, bronchial hyperresponsiveness; the increased levels of TGF-β_1, IL-4, and IL-13 in bronchoalveolar lavage fluids and lung tissues; and airway fibrosis. In addition, LTC_4 stimulates epithelial cells to produce IL-11. Our results also showed that cysLT type 1 receptor antagonists downregulated the activity of a transcription factor, nuclear factor κB, and BAY 11-7085 substantially reduced the increased levels of IL-11 after ovalbumin inhalation.
Conclusion: These results suggest that cysLTs regulate the IL-11 expression in allergic airway disease.
Clinical implications: These findings provide one of the molecular mechanisms for the effects of cysLTs on airway inflammation and fibrosis in allergic airway diseases. (J Allergy Clin Immunol 2007;119:141-9.)

Key words: *Cysteinyl leukotrienes, IL-11, airway, inflammation, remodeling*

Abbreviations used
BAL: Bronchoalveolar lavage
cysLT: Cysteinyl leukotriene
cysLT1R: Cysteinyl leukotriene type 1 receptor
cysLT2R: Cysteinyl leukotriene type 2 receptor
GAPDH: Glyceraldehyde-3-phosphate dehydrogenase
LT: Leukotriene
NF-κB: Nuclear factor κB
OVA: Ovalbumin
R_L: Airway resistance

Chronic airway inflammation and airway remodeling are important features of bronchial asthma.[1] The airway obstruction observed in asthma is thought to be caused by airway remodeling. The histopathologic features of this process include epithelial changes, subepithelial fibrosis, infiltration of inflammatory cells, hyperplasia and hypertrophy of the bronchial smooth muscle, and mucus hypersecretion. One of the most prominent features of airway remodeling is subepithelial fibrosis, and this characteristic is reportedly a potential marker for disease severity.[2] IL-11 is one of the important mediators involved in the process of airway inflammation and remodeling.[3,4] IL-11 was initially discovered as an IL-6–like plasmacytoma proliferation stimulating activity in supernatants from transformed marrow fibroblasts.[5] Studies have shown that IL-11 acts as a hematopoietic growth factor, stimulates the acute-phase response, augments Ig production, induces the expression of metalloproteinase inhibitors, regulates neural phenotype, regulates bone metabolism, and protects against the combined effects of radiation and chemotherapy.[6-12] Previous studies have also demonstrated that human lung fibroblasts and epithelial cells produce IL-11 in response to cytokines (IL-1 and TGF-β), histamine, and viruses that have been epidemiologically associated with asthma exacerbations.[13-15] In addition, IL-11 has been shown to play an important role in the inflammatory and fibrotic responses in both viral and nonviral human airway disorders.[4]

Leukotrienes (LTs), lipid mediators generated from arachidonic acid by the action of 5-lipoxygenase, play important roles in the pathogenesis of allergic airway inflammation.[16] LTC_4, LTD_4, and LTE_4, known as cysteinyl leukotrienes (cysLTs), are both direct bronchoconstrictors and proinflammatory substances. The cysLTs

From the Department of Internal Medicine, Airway Remodeling Laboratory, Chonbuk National University Medical School, Jeonju.
Supported by a Korean Research Foundation Grant funded by the Korean Government (MOEHRD, Basic Research Promotion Fund; KRF-2005-201-E00014), a grant from the National Research Laboratory Program of the Korean Science and Engineering Foundation, and a grant of the Korea Health 21 R&D Project, Ministry of Health and Welfare (A060169), Republic of Korea.
Disclosure of potential conflict of interest: The authors have declared that they have no conflict of interest.
Received for publication April 3, 2006; revised September 1, 2006; accepted for publication September 1, 2006.
Available online November 2, 2006.
Reprint requests: Yong Chul Lee, MD, PhD, Department of Internal Medicine, Chonbuk National University Medical School, San 2-20, Geumam-dong, Deokjin-gu, Jeonju, 561-180, South Korea. E-mail: leeyc@chonbuk.ac.kr.
0091-6749/$32.00

doi:10.1016/j.jaci.2006.09.001

exhibit a variety of physiologic functions involving recruitment of inflammatory cells, airway smooth muscle contraction, vascular leakage, increase of mucus secretion, decrease of mucociliary clearance, and airway fibrosis.[17-19] However, the mechanisms by which cysLTs induce airway inflammation and remodeling, especially airway fibrosis, are not clearly understood.

In the present study we used a murine model of allergic airway disease and murine tracheal epithelial cells to determine the effect of the cysLTs on the regulation of IL-11 expression.

METHODS

More detailed information about the methods used in this study can be found in the Online Repository at www.jacionline.org.

Animals and experimental protocol

Female C57BL/6 mice, 8 to 10 weeks of age and free of murine-specific pathogens, were obtained from the Korean Research Institute of Chemistry Technology (Daejon, Korea), housed throughout the experiments in a laminar flow cabinet, and maintained on standard laboratory chow *ad libitum*. Mice were sensitized and challenged as previously described,[20] with some modifications.

Administration of montelukast, pranlukast, anti–IL-11 antibody, isotype control mAb, or BAY 11-7085

Montelukast sodium (L-706, 631; 5 mg/kg body weight per day; Merck & Co, Inc, Rahway, NJ) dissolved in 1% methyl cellulose or pranlukast (25 mg/kg body weight per day; Ono Pharmaceutical Co, Ltd, Osaka, Japan) dissolved in distilled water was administered by means of oral gavage 11 times at 24-hour intervals on days 19 to 29, beginning 1 day before the first challenge. Anti–IL-11 antibody or isotype control mAb (8 mg/kg body weight per day; R&D systems, Inc, Minneapolis, Minn) was administered intraperitoneally 2 times to each animal, once on day 23 (1 hour after the last airway challenge) and the second time on day 29 (6 days after the last airway challenge). BAY 11-7085 (20 mg/kg body weight per day; BIOMOL International L.P., Plymouth Meeting, Pa) dissolved in dimethyl sulfoxide and diluted with 0.9% NaCl was administered by means of intraperitoneal injection 2 times to each treated animal, once on day 23 (1 hour before the last airway challenge) and the second time on day 29 (6 days after the last airway challenge, see Fig E1 in the Online Repository at www.jacionline.org).[21,22]

Isolation and primary culture of murine tracheal epithelial cells

Murine tracheal epithelial cells were isolated under sterile conditions, as previously described.[20]

LTC_4 or LTD_4 stimulation and IL-11 production

Cells were seeded in 6-well culture inserts at a density of 1×10^5 cells/mL and grown in culture medium. At confluence, LTC_4 (Sigma-Aldrich, St Louis, Mo) or LTD_4 (BIOMOL International L.P.) was added to the cells at varying concentrations (1-1000 ng/mL).

Western blot analysis

Protein expression levels were analyzed by means of Western blot analysis, as described previously.[20]

Cytosolic or nuclear protein extractions for analysis of nuclear factor κB p65

Cytosolic or nuclear extraction was performed as described previously.[23,24]

RNA isolation and RT-PCR

Levels of mRNA expression were analyzed by means of RT-PCR assay, with total RNA isolated from lung tissues by using a rapid extraction method (TRI-Reagent), as previously described.[25]

Quantitative real-time RT-PCR

Quantitative RT-PCR analysis was performed with the LightCycler FastStart DNA Master SYBR Green I (Roche Diagnostics, Mannheim, Germany).

Densitometric analysis and statistics

All immunoreactive signals were analyzed by means of densitometric scanning (Gel Doc XR; Bio-Rad, Hercules, Calif). Data were expressed as means ± SEM. Statistical comparisons were performed by using 1-way ANOVA, followed by the Scheffe test. Significant differences between 2 groups were determined by using the unpaired Student *t* test. Statistical significance was set at a *P* value of less than .05.

RESULTS

IL-11 protein levels and mRNA expression increased in ovalbumin-sensitized and ovalbumin-challenged mice

Western blot analysis revealed that IL-11 protein levels in lung tissues were increased approximately 4.4-, 5.7-, 6.1-, 7.0-, and 7.1-fold at ½, 1, 3, 5, and 7 days, respectively, after challenge with ovalbumin (OVA) compared with the levels in the control group (Fig 1, *A* and *B*). In contrast, no significant changes in the IL-11 protein level were observed after saline inhalation. Real-time RT-PCR analysis revealed that IL-11 mRNA expression had increased approximately 1.4-, 1.5-, 2.2-, 2.2-, and 2.3-fold at ½, 1, 3, 5, and 7 days, respectively, after OVA inhalation compared with the expression in the control group (Fig 1, *D*). In contrast, no significant changes in the IL-11 mRNA expression were observed after saline inhalation (Fig 1, *C* and *D*).

Effect of montelukast or pranlukast on IL-11 protein levels and mRNA expression in lung tissues of OVA-sensitized and OVA-challenged mice

Western blot analysis revealed that levels of IL-11 protein in lung tissues were increased at 7 days after OVA inhalation compared with levels in control mice (Fig 2, *A* and *B*). The increased IL-11 levels at 7 days after OVA inhalation were decreased by the administration of montelukast or pranlukast. RT-PCR and real-time RT-PCR analyses showed that IL-11 mRNA expression in lung tissues was increased at 7 days after OVA inhalation compared with the expression after saline inhalation (Fig 2, *C* and *D*). The increased IL-11 mRNA expression

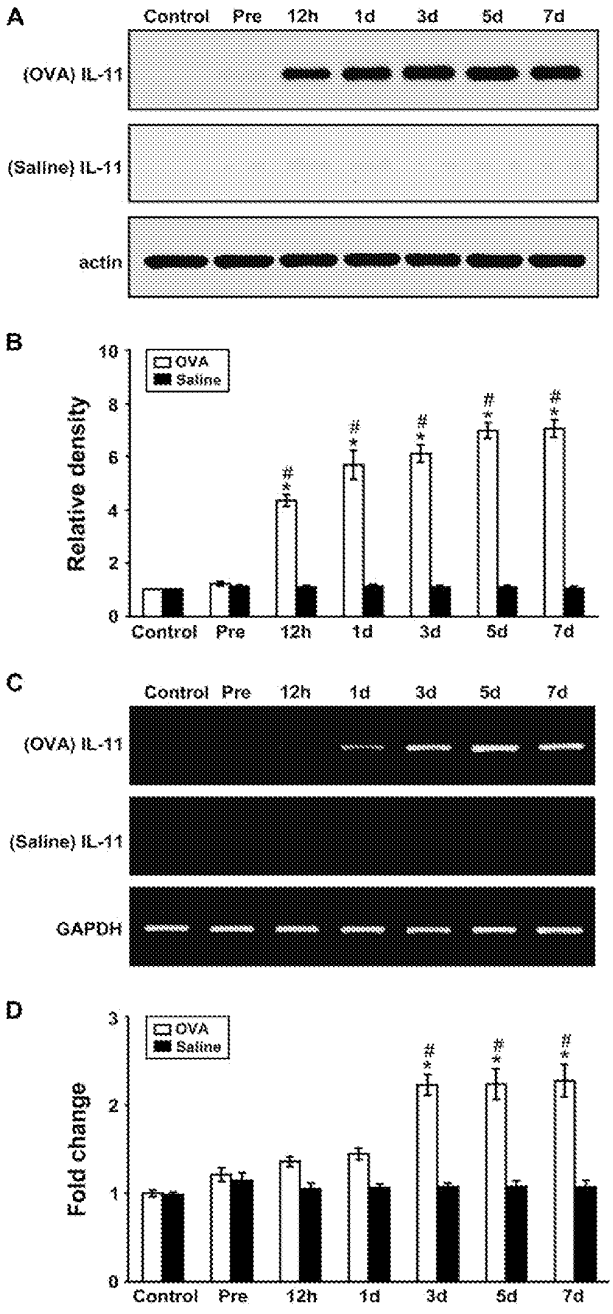

FIG 1. IL-11 protein and mRNA in lung tissues of OVA-sensitized and OVA-challenged mice. Sampling was performed in lung tissues from sensitized mice challenged with OVA or saline. **A**, Western blot analyses of IL-11 protein. **B**, Densitometric analyses are presented as the relative ratio of IL-11 to actin. The relative ratio of IL-11 in the lung tissues of control mice is arbitrarily presented as 1. **C**, Representative RT-PCR analysis of IL-11 mRNA expression. **D**, Quantitative analysis of IL-11 mRNA expression by means of real-time RT-PCR. Data represent means ± SEM from 8 mice per group. Time periods after the last challenge are indicated as ½, 1, 3, 5, and 7 days. *Control*, No treatment; *Pre*, 1 hour before the first challenge. #$P < .05$ versus Pre; *$P < .05$ versus saline inhalation.

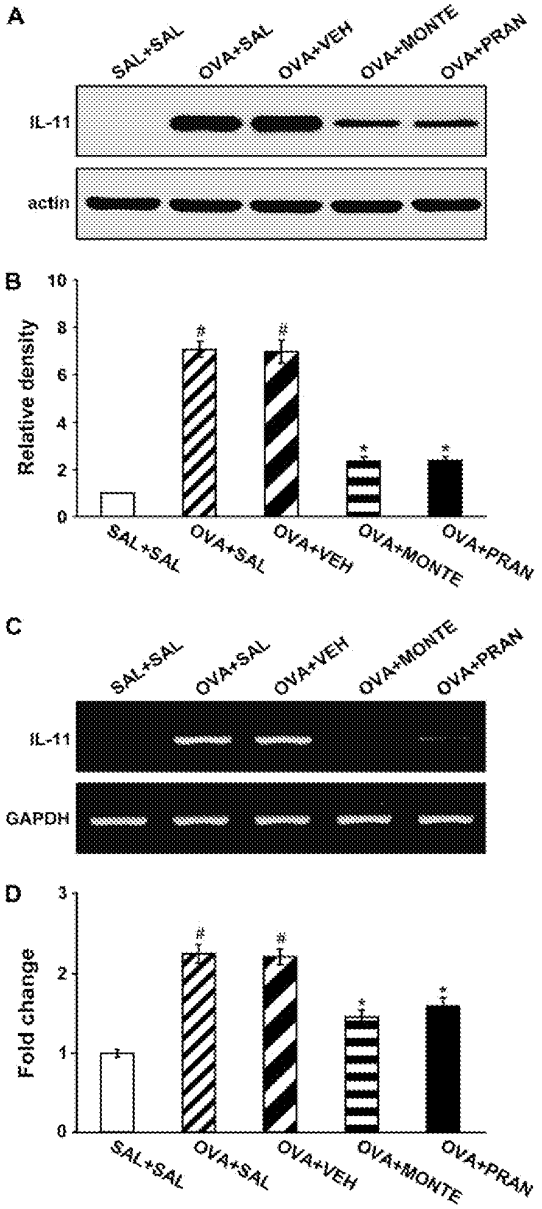

FIG 2. Effect of montelukast or pranlukast on IL-11 protein and mRNA in lung tissues of OVA-sensitized and OVA-challenged mice. **A,** Western blot analysis of IL-11. Sampling was performed at 7 days after the last challenge in saline-challenged mice administered saline *(SAL+SAL),* OVA-challenged mice administered saline *(OVA+SAL),* OVA-challenged mice administered drug vehicle *(OVA+VEH),* OVA-challenged mice administered montelukast *(OVA+MONTE),* and OVA-challenged mice administered pranlukast *(OVA+PRAN).* **B,** Densitometric analyses are presented as the relative ratio of IL-11 to actin. The relative ratio of IL-11 in the lung tissues of saline-inhaled mice administered saline is arbitrarily presented as 1. **C,** Representative RT-PCR analysis of IL-11 mRNA expression. **D,** Quantitative analysis of IL-11 mRNA expression by means of real-time RT-PCR. Data represent means ± SEM from 8 mice per group. #$P < .05$ versus SAL+SAL group; *$P < .05$ versus OVA+SAL group.

was reduced by the administration of montelukast or pranlukast.

Effect of LTC_4 on IL-11 protein and mRNA expression in primary murine tracheal epithelial cells

The effect of LTC_4 on the production of IL-11 from epithelial cells is shown in Fig 3. Western blot analysis revealed that the maximal levels of IL-11 were detected in the presence of LTC_4 (100 ng/mL) at 8 hours of incubation. The release of IL-11 was undetectable at 3 and 5 hours of incubation (data not shown). Epithelial cells were treated with montelukast to suppress the LTC_4-induced IL-11 production. Incubation of montelukast (100 nM) with cells treated with LTC_4 (100 ng/mL) significantly inhibited the production of IL-11 (Fig 3). Montelukast alone had no effect on the IL-11 production of unstimulated cells (data not shown).

RT-PCR analysis was used to detect the mRNA expression of IL-11 in response to stimulation of epithelial cells with LTC_4. At stimulation of epithelial cells with LTC_4, the IL-11 mRNA expression reached a peak at 6 hours (Fig 3, *C*) and faded at 12 hours and 24 hours (data not shown). Real-time PCR was applied to further confirm the increase of IL-11 mRNA expression. At 6 hours of incubation, the expression of IL-11 mRNA was increased approximately 2.1-fold compared with that seen in unstimulated cells (Fig 3, *D*). In addition, montelukast inhibited the gene transcription for IL-11 substantially.

Effect of montelukast or pranlukast on nuclear factor κB p65 protein levels in lung tissues of OVA-sensitized and OVA-challenged mice

Western blot analysis revealed that levels of nuclear factor κB (NF-κB) p65 protein in nuclear protein extracts from lung tissues were increased at 7 days after OVA inhalation compared with levels in control mice (Fig 4). The increased NF-κB p65 levels in nuclear protein extracts were decreased by the administration of montelukast or pranlukast. In contrast, levels of NF-κB p65 protein in cytosolic protein extracts were decreased compared with levels in control mice. The decreased NF-κB p65 levels in cytosolic preparations were increased by the administration of montelukast or pranlukast. These results indicate that montelukast and pranlukast inhibit NF-κB activity by preventing translocation of this transcription factor into the nucleus (Fig 4).

Effect of BAY 11-7085 on IL-11 levels in lung tissues of OVA-sensitized and OVA-challenged mice

Western blot analysis showed that IL-11 protein levels in lung tissues were increased significantly at 7 days after OVA inhalation compared with levels after saline inhalation (Fig 5). The increased IL-11 levels were significantly reduced by the administration of BAY 11-7085.

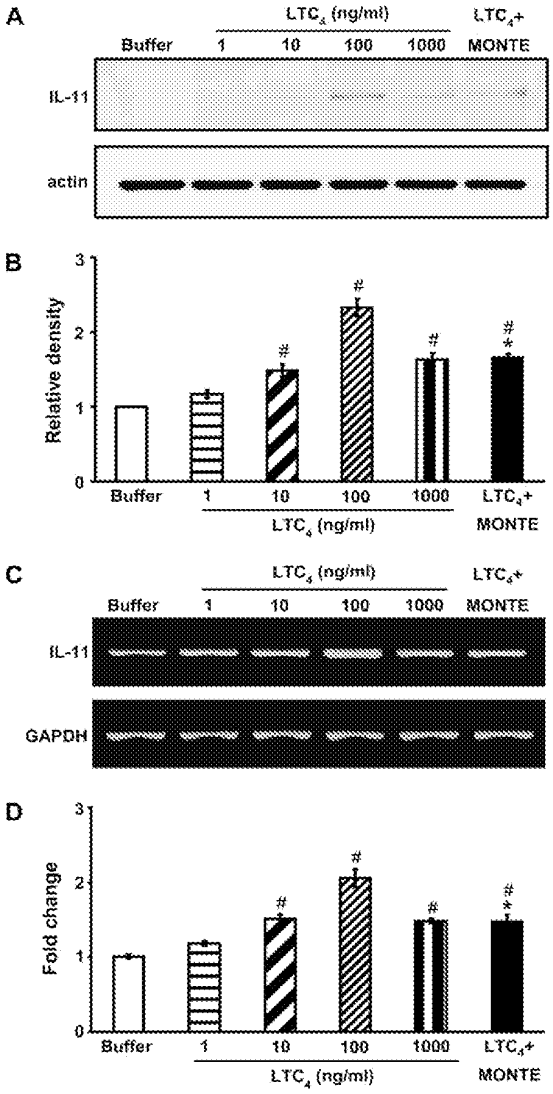

FIG 3. Effect of LTC_4 on IL-11 production by primary tracheal epithelial cells. **A**, Western blot analysis of IL-11. **B**, Densitometric analyses are presented as the relative ratio of IL-11 to actin. The relative ratio of IL-11 in the epithelial cells incubated with buffer alone is arbitrarily presented as 1. **C**, Representative RT-PCR analysis of IL-11 mRNA expression. **D**, Quantitative analysis of IL-11 mRNA expression by means of real-time RT-PCR. Data represent means ± SEM from 6 independent experiments. *MONTE*, Montelukast. #$P < .05$ versus buffer alone; *$P < .05$ versus 100 ng/mL LTC_4.

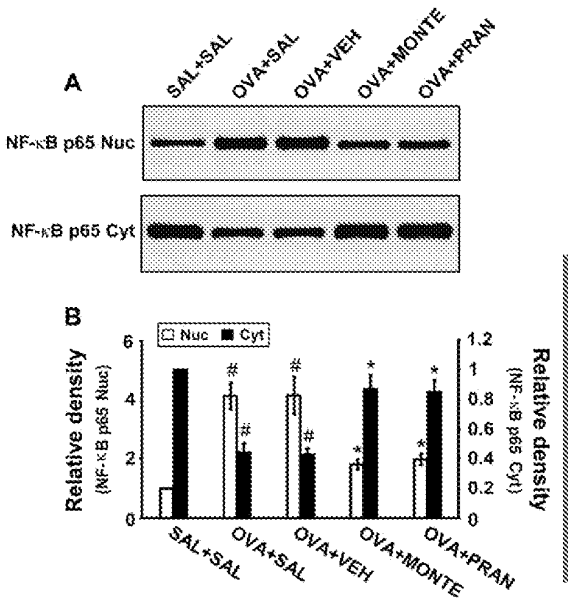

FIG 4. Effect of montelukast or pranlukast on NF-κB p65 protein expression in nuclear and cytosolic protein extracts from lung tissues. **A**, Western blotting of NF-κB p65 in nuclear *(Nuc)* and cytosolic *(Cyt)* protein extracts from lung tissues. **B**, Densitometric analyses are presented as the relative ratio of NF-κB p65 levels in the OVA+SAL, OVA+VEH, OVA+MONTE, or OVA+PRAN groups to those in the SAL+SAL group. The NF-κB p65 level in nuclear protein extracts of the SAL+SAL group is arbitrarily presented as 1. *Bars* represent means ± SEM from 8 mice per group. For definition of groups, see legend for Fig 3. #$P < .05$ versus SAL+SAL group; *$P < .05$ versus OVA+SAL groups.

Effect of montelukast or pranlukast on pathologic changes of OVA-sensitized and OVA-challenged mice

Histologic analyses revealed typical pathologic features of allergic airway disease in the OVA-sensitized and OVA-challenged mice. Numerous inflammatory cells, including eosinophils, infiltrated around the bronchioles; the airway wall was thickened; and mucus and debris had accumulated in the lumen of bronchioles. Mice treated with montelukast or pranlukast showed marked reductions in the thickening of the airway wall, the infiltration of inflammatory cells in the peribronchiolar region, and the amount of debris in the airway lumen. These results indicate that montelukast and pranlukast inhibit antigen-induced inflammation in the lungs, including the influx of eosinophils (see Fig E2 in the Online Repository at www.jacionline.org).

Effect of montelukast, pranlukast, or anti–IL-11 antibody on TGF-β_1 levels in lung tissues and bronchoalveolar lavage fluids of OVA-sensitized and OVA-challenged mice

Western blot analysis showed that TGF-β_1 protein levels in lung tissues were significantly increased at 7 days after OVA inhalation compared with levels in control mice (see Fig E3 in the Online Repository at www.jacionline.org). The increased TGF-β_1 levels were significantly reduced by the administration of montelukast, pranlukast, and anti-IL-11 antibody. Consistent with the results obtained from the Western blot analysis, enzyme immunoassays revealed that levels of TGF-β_1 in bronchoalveolar lavage (BAL) fluids were significantly increased at 7 days after OVA inhalation compared with levels in control mice

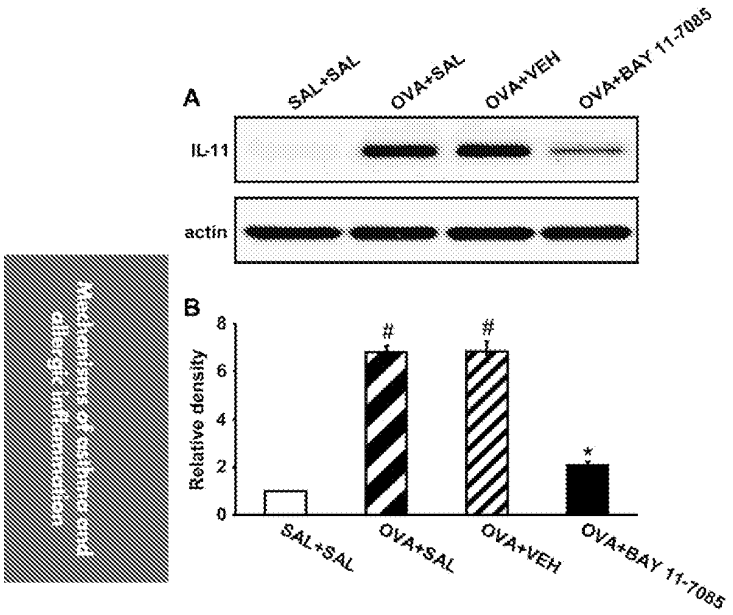

FIG 5. Effects of BAY 11-7085 on IL-11 expression in lung tissues of OVA-sensitized and OVA-challenged mice. **A**, Western blotting of IL-11 in lung tissues. **B**, Densitometric analyses are presented as the relative ratio of IL-11 to actin. The relative ratio of IL-11 in the lung tissues of the SAL+SAL group is arbitrarily presented as 1. *Bars* represent means ± SEM from 8 mice per group. For definition of groups, see legend for Fig 3. #$P < .05$ versus SAL+SAL group; *$P < .05$ versus OVA+SAL group.

(see Fig E3 in the Online Repository). The increased TGF-β_1 levels were significantly reduced by the administration of montelukast, pranlukast, and anti–IL-11 antibody. No significant changes were observed in OVA-sensitized and OVA-challenged mice administered isotype control mAb.

Effect of montelukast, pranlukast, or anti–IL-11 antibody on IL-4 and IL-13 levels in lung tissues and BAL fluids of OVA-sensitized and OVA-challenged mice

Western blot analysis showed that IL-4 and IL-13 protein levels in lung tissues were significantly increased at 72 hours after OVA inhalation compared with levels in control mice (see Fig E4 in the Online Repository at www.jacionline.org). The increased IL-4 and IL-13 levels were significantly reduced by the administration of montelukast, pranlukast, and anti–IL-11 antibody. Consistent with the results obtained from the Western blot analysis, enzyme immunoassays revealed that levels of IL-4 and IL-13 in BAL fluids were significantly increased at 72 hours after OVA inhalation compared with levels in control mice (see Fig E4 in the Online Repository). The increased IL-4 and IL-13 levels were significantly reduced by the administration of montelukast, pranlukast, and anti-IL-11 antibody. No significant changes were observed in OVA-sensitized and OVA-challenged mice administered isotype control mAb.

Effect of montelukast, pranlukast, or anti–IL-11 antibody on peribronchial collagen deposition

OVA-sensitized and OVA-challenged mice had a significant increase in the levels of peribronchial fibrosis compared with levels in control mice, as assessed by means of trichrome staining and determination of total lung collagen content. The administration of montelukast, pranlukast, or anti–IL-11 antibody substantially reduced the increased levels of peribronchial fibrosis after OVA inhalation compared with the levels seen in mice that had no treatment after OVA inhalation (see Fig E5 in the Online Repository at www.jacionline.org).

DISCUSSION

Airway inflammation and fibrosis are prominent features of bronchial asthma and are connected by complex signaling networks. cysLTs and IL-11 are thought to contribute to the pathogenesis of allergic airway disease, but interrelationship between these proteins in airway inflammation and fibrosis has not been clarified. Our present study with an OVA-induced murine model of allergic airway disease has revealed that levels of LTC_4 in BAL fluids were increased (see Fig E6 in Online Repository at www.jacionline.org) and that administration of montelukast or pranlukast reduced the increased levels of LTC_4; the increased expression of IL-11 protein and mRNA in lung tissues; airway inflammation; bronchial hyperresponsiveness (see Fig E7 in Online Repository at www.jacionline.org); the increased levels of TGF-β_1, IL-4, and IL-13 in BAL fluids and lung tissues; and airway fibrosis. In addition, treatment of epithelial cells with LTC_4 stimulated the expression of IL-11 protein and mRNA. Our results have also indicated that cysLT type 1 receptor (cysLT1R) antagonists downregulated the activity of a transcription factor, NF-κB, and that an inhibitor of NF-κB activation, BAY 11-7085, reduced the expression of IL-11 protein. These findings suggest that cysLT1R antagonists inhibit the NF-κB signal transduction pathway by decreasing NF-κB binding activity to the promoter region of the IL-11 gene involved in airway inflammation and remodeling in allergic airway disease.

A pleotropic cytokine, IL-11, is produced by many cell types, including human lung fibroblasts, alveolar and airway epithelial cells, human airway smooth muscle cells, and eosinophils[13,14,26,27] and is classified as a member of the IL-6 family of cytokines based on functional similarities between IL-11 and IL-6 and the shared use of gp130 molecules in their receptor complexes.[28,29] Tang et al[4] have demonstrated that the targeted expression of IL-11 in the mouse airway causes a B and T cell–predominant inflammatory response; airway remodeling with increased type III and I collagen; local accumulation

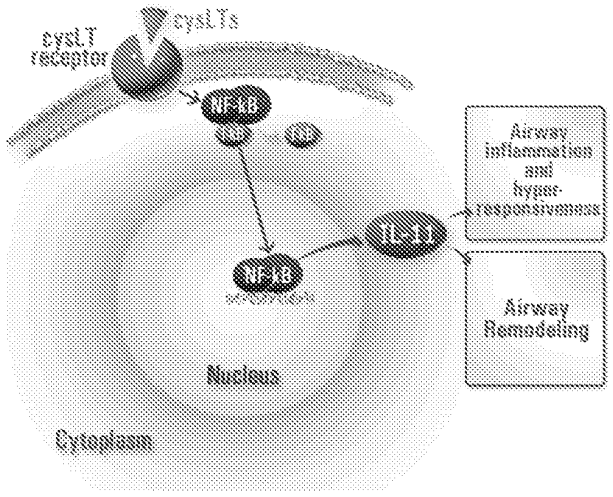

FIG 6. A proposed signaling pathway for cysLT-induced IL-11 expression in allergic airway disease. Our data suggest that cysLT receptor signal is involved in the regulation of IL-11 expression, and the NF-κB pathway could be one of its various regulatory mechanisms. *I-κB*, Inhibitory kappa B.

of fibroblasts, myofibroblasts, and myocytes; and obstructive physiologic dysregulation. They suggest that IL-11 plays an important role in the inflammatory and fibrotic responses in airway disorders. A previous study has shown that IL-11 expression is found to be increased in the airways of patients with asthma compared with in healthy control subjects and seems to correlate with disease severity and a reduced FEV_1.[27] Consistent with these observations, in this study we have found that IL-11 expression was upregulated in OVA-induced allergic airway disease. Interestingly, cysLT1R antagonist blocked LTC_4-stimulated production of IL-11 from epithelial cells, and administration of montelukast or pranlukast reduced the increased IL-11 expression, as well as the increased expression of TGF-β_1, IL-4, and IL-13. In addition, the increased expression of TGF-β_1, IL-4, and IL-13; the increased airway inflammation; and bronchial hyperresponsiveness were decreased substantially by administration of anti-IL-11 antibody. These results suggest that cysLT receptor signaling is associated with the regulation of IL-11 expression and that treatment of the cysLT1R antagonists might improve the features of allergic airway disease through regulation of IL-11 expression.

NF-κB is present in most cell types and is known to play a critical role in immune and inflammatory responses, including asthma.[30-36] As expected, the NF-κB p65 protein level in nuclear protein extracts of lung tissues was substantially increased in the OVA-induced model of allergic airway disease used for the present study. It is known that activation of this transcription factor induces a variety of inflammatory genes that are abnormally expressed in asthma. These genes include cytokines (eg, IL-4, IL-5, IL-9, IL-11, IL-15, and TNF-α), chemokines (eg, RANTES, eotaxin, and monocyte chemotactic protein 3), and adhesion molecules (eg, intracellular adhesion molecule 1 and vascular cell adhesion molecule 1).[37,38] Previous studies have revealed that the signaling pathways related to IL-11 induction are the H7-sensitive serine/threonine kinase and protein kinase C pathway, activator protein 1–mediated pathway, calmodulin-dependent pathway, and mitogen-activated protein kinase–dependent pathway.[7,14,15,39-43] However, the regulatory mechanisms of IL-11 expression are not clear at the present time and are complex and cell/tissue specific. In this study expression of IL-11 was increased significantly after allergen challenge in a murine model of allergic airway disease. Administration of montelukast or pranlukast resulted in significant reduction of NF-κB activity, as well as expression of IL-11. In addition, the increased IL-11 protein levels after OVA inhalation were decreased by administration of an inhibitor of NF-κB activation, BAY 11-7085. Moreover, the administration of BAY 11-7085 decreased the increased IL-11 protein levels in LTC_4-stimulated epithelial cells (data not shown). Therefore these observations suggest that the NF-κB–dependent pathway could be one of the various regulatory mechanisms related with induction of IL-11 expression in allergic airway disease.

There are 2 types of cysLT receptors, cysLT1R and cysLT type 2 receptor (cysLT2R), which were originally defined pharmacologically based on their sensitivity to cysLT1R-specific antagonists. cysLT1R and cysLT2R are only loosely homologous (38% amino acid identity)[44,45] and also share a similar degree of identity (24% to 32%) with the purinergic (P2Y) class of G protein–coupled receptors that mediate cellular responses to extracellular nucleotides.[46] In the present study we have revealed that the expression of both cysLT1R and cysLTR2 in tracheal epithelial cells stimulated with LTC_4 was increased compared with that seen in unstimulated cells (see Fig E8 in

Online Repository at www.jacionline.org). In addition, we have shown that the IL-11 protein levels in epithelial cells were increased significantly after the stimulation of LTD_4, as well as LTC_4, and the increased expression of IL-11 was partially inhibited by montelukast, a cysLT1R antagonist (see Fig E9 in the Online Repository at www.jacionline.org).

Taken together, these findings suggest that cysLT2R, as well as cysLT1R, signaling contributes to the LTC_4- or LTD_4-induced IL-11 expression in allergic airway disease.

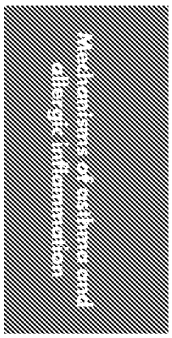

In summary, we have examined the effect of the cysLTs on the regulation of IL-11 expression in a murine model of allergic airway disease and murine tracheal epithelial cells. By using montelukast and pranlukast, specific cysLT1R antagonists, we have shown the important role of cysLTs in OVA-induced airway hyperresponsiveness, inflammation, and fibrosis. Moreover, our results have revealed that LTC_4 stimulated the expression of IL-11 protein and mRNA from epithelial cells, and administration of montelukast and pranlukast reduced IL-11 protein and mRNA expression. On the basis of these observations, we have concluded that cysLT receptor signal is involved in regulation of IL-11 expression (Fig 6). Our findings might also assist a strategy in the treatment of airway fibrosis and inflammation in allergic airway disease.

We thank Professor Mie-Jae Im for critical reading of the manuscript.

REFERENCES

1. Bousquet J, Jeffery PK, Busse WW, Johnson M, Vignola AM. Asthma. From bronchoconstriction to airways inflammation and remodeling. Am J Respir Crit Care Med 2000;161:1720-45.
2. Redington AE, Howarth PH. Airway wall remodelling in asthma. Thorax 1997;52:310-2.
3. Zhu Z, Lee CG, Zheng T, Chupp G, Wang J, Homer RJ, et al. Airway inflammation and remodeling in asthma. Lessons from interleukin 11 and interleukin 13 transgenic mice. Am J Respir Crit Care Med 2001; 164(suppl):S67-70.
4. Tang W, Geba GP, Zheng T, Ray P, Homer RJ, Kuhn C 3rd, et al. Targeted expression of IL-11 in the murine airway causes lymphocytic inflammation, bronchial remodeling, and airways obstruction. J Clin Invest 1996;98:2845-53.
5. Paul SR, Bennett F, Calvetti JA, Kelleher K, Wood CR, O'Hara RM Jr, et al. Molecular cloning of a cDNA encoding interleukin 11, a stromal cell-derived lymphopoietic and hematopoietic cytokine. Proc Natl Acad Sci U S A 1990;87:7512-6.
6. Du XX, Williams DA. Interleukin-11: a multifunctional growth factor derived from the hematopoietic microenvironment. Blood 1994;83: 2023-30.
7. Maier R, Ganu V, Lotz M. Interleukin-11, an inducible cytokine in human articular chondrocytes and synoviocytes, stimulates the production of the tissue inhibitor of metalloproteinases. J Biol Chem 1993; 268:21527-32.
8. Roeb E, Graeve L, Hoffmann R, Decker K, Edwards DR, Heinrich PC. Regulation of tissue inhibitor of metalloproteinases-1 gene expression by cytokines and dexamethasone in rat hepatocyte primary cultures. Hepatology 1993;18:1437-42.
9. Yin TG, Schendel P, Yang YC. Enhancement of in vitro and in vivo antigen-specific antibody responses by interleukin 11. J Exp Med 1992;175:211-6.
10. Fann MJ, Patterson PH. Neuropoietic cytokines and activin A differentially regulate the phenotype of cultured sympathetic neurons. Proc Natl Acad Sci U S A 1994;91:43-7.
11. Girasole G, Passeri G, Jilka RL, Manolagas SC. Interleukin-11: a new cytokine critical for osteoclast development. J Clin Invest 1994;93: 1516-24.
12. Du XX, Doerschuk CM, Orazi A, Williams DA. A bone marrow stromal-derived growth factor, interleukin-11, stimulates recovery of small intestinal mucosal cells after cytoablative therapy. Blood 1994;83:33-7.
13. Elias JA, Zheng T, Einarsson O, Landry M, Trow T, Rebert N, et al. Epithelial interleukin-11. Regulation by cytokines, respiratory syncytial virus, and retinoic acid. J Biol Chem 1994;269:22261-8.
14. Elias JA, Zheng T, Whiting NL, Trow TK, Merrill WW, Zitnik R, et al. IL-1 and transforming growth factor-beta regulation of fibroblast-derived IL-11. J Immunol 1994;152:2421-9.
15. Zheng T, Nathanson MH, Elias JA. Histamine augments cytokine-stimulated IL-11 production by human lung fibroblasts. J Immunol 1994;153:4742-52.
16. Barnes PJ, Chung KF, Page CP. Inflammatory mediators of asthma: an update. Pharmacol Rev 1998;50:515-96.
17. Holgate ST, Peters-Golden M, Panettieri RA, Henderson WR Jr. Roles of cysteinyl leukotrienes in airway inflammation, smooth muscle function, and remodeling. J Allergy Clin Immunol 2003;111(suppl):S18-34; discussion S34-6.
18. Busse WW. Leukotrienes and inflammation. Am J Respir Crit Care Med 1998;157(suppl):S210-3; discussion S247-8.
19. Lee KS, Kim SR, Park HS, Jin GY, Lee YC. Cysteinyl leukotriene receptor antagonist regulates vascular permeability by reducing VEGF expression. J Allergy Clin Immunol 2004;114:1093-9.
20. Kwak YG, Song CH, Yi HK, Hwang PH, Kim JS, Lee KS, et al. Involvement of PTEN in airway hyperresponsiveness and inflammation in bronchial asthma. J Clin Invest 2003;111:1083-92.
21. Pierce JW, Schoenleber R, Jesmok G, Best J, Moore SA, Collins T, et al. Novel inhibitor of cytokine-induced IkappaBalpha phosphorylation and endothelial cell adhesion molecule expression show anti-inflammatory effects in vivo. J Biol Chem 1997;272:21096-103.
22. Yang G, Abate A, George AG, Weng YH, Dennery PA. Maturational differences in lung NF-kappaB activation and their role in tolerance to hypoxia. J Clin Invest 2004;114:669-78.
23. Masmoudi A, Labourdette G, Mersel M, Huang FL, Huang KP, Vincendon G, et al. Protein kinase C located in rat liver nuclei. Partial purification and biochemical and immunochemical characterization. J Biol Chem 1989;264:1172-9.
24. Cobellis G, Vallarino M, Meccariello R, Pierantoni R, Masini MA, Mathieu M, et al. Fos localization in cytosolic and nuclear compartments in neurons of the frog, *Rana esculenta*, brain: an analysis carried out in parallel with GnRH molecular forms. J Neuroendocrinol 1999;11: 725-35.
25. Chomczynski P, Sacchi N. Single-step method of RNA isolation by acid guanidinium thiocyanate-phenol-chloroform extraction. Anal Biochem 1987;162:156-9.
26. Elias JA, Wu Y, Zheng T, Panettieri R. Cytokine- and virus-stimulated airway smooth muscle cells produce IL-11 and other IL-6-type cytokines. Am J Physiol Lung Cell Mol Physiol 1997;273:L648-55.
27. Minshall E, Chakir J, Laviolette M, Molet S, Zhu Z, Olivenstein R, et al. IL-11 expression is increased in severe asthma: association with epithelial cells and eosinophils. J Allergy Clin Immunol 2000;105: 232-8.
28. Neben S, Turner K. The biology of interleukin 11. Stem Cells 1993; 11(suppl 2):156-62.
29. Zhang XG, Gu JJ, Lu ZY, Yasukawa K, Yancopoulos GD, Turner K, et al. Ciliary neurotropic factor, interleukin 11, leukemia inhibitory factor, and oncostatin M are growth factors for human myeloma cell lines using the interleukin 6 signal transducer gp130. J Exp Med 1994;179: 1337-42.
30. Baeuerle PA, Baltimore D. NF-kappa B: ten years after. Cell 1996;87: 13-20.
31. Baldwin AS Jr. The NF-kappa B and I kappa B proteins: new discoveries and insights. Annu Rev Immunol 1996;14:649-83.
32. Barnes PJ, Karin M. Nuclear factor-kappaB: a pivotal transcription factor in chronic inflammatory diseases. N Engl J Med 1997;336:1066-71.
33. Gilmore TD. The Rel/NF-kappaB signal transduction pathway: introduction. Oncogene 1999;18:6842-4.
34. Siebenlist U, Franzoso G, Brown K. Structure, regulation and function of NF-kappa B. Annu Rev Cell Biol 1994;10:405-55.

35. Barnes PJ, Adcock IM. NF-kappa B: a pivotal role in asthma and a new target for therapy. Trends Pharmacol Sci 1997;18:46-50.
36. Kawano T, Matsuse H, Kondo Y, Machida I, Saeki S, Tomari S, et al. Cysteinyl leukotrienes induce nuclear factor kappa b activation and RANTES production in a murine model of asthma. J Allergy Clin Immunol 2003;112:369-74.
37. Komura E, Tonetti C, Penard-Lacronique V, Chagraoui H, Lacout C, Lecouedic JP, et al. Role for the nuclear factor kappaB pathway in transforming growth factor-beta1 production in idiopathic myelofibrosis: possible relationship with FK506 binding protein 51 overexpression. Cancer Res 2005;65:3281-9.
38. Kumar A, Takada Y, Boriek AM, Aggarwal BB. Nuclear factor-kappaB: its role in health and disease. J Mol Med 2004;82:434-48.
39. Yang L, Yang YC. Regulation of interleukin (IL)-11 gene expression in IL-1 induced primate bone marrow stromal cells. J Biol Chem 1994;269: 32732-9.
40. Yang L, Steussy CN, Fuhrer DK, Hamilton J, Yang YC. Interleukin-11 mRNA stabilization in phorbol ester-stimulated primate bone marrow stromal cells. Mol Cell Biol 1996;16:3300-7.
41. Yang L, Yang YC. Heparin inhibits the expression of interleukin-11 and granulocyte-macrophage colony-stimulating factor in primate bone marrow stromal fibroblasts through mRNA destabilization. Blood 1995;86:2526-33.
42. Elias JA, Tang W, Horowitz MC. Cytokine and hormonal stimulation of human osteosarcoma interleukin-11 production. Endocrinology 1995; 136:489-98.
43. Bamba S, Andoh A, Yasui H, Makino J, Kim S, Fujiyama Y. Regulation of IL-11 expression in intestinal myofibroblasts: role of c-Jun AP-1- and MAPK-dependent pathways. Am J Physiol Gastrointest Liver Physiol 2003;285:G529-38.
44. Lynch KR, O'Neill GP, Liu Q, Im DS, Sawyer N, Metters KM, et al. Characterization of the human cysteinyl leukotriene CysLT1 receptor. Nature 1999;399:789-93.
45. Heise CE, O'Dowd BF, Figueroa DJ, Sawyer N, Nguyen T, Im DS, et al. Characterization of the human cysteinyl leukotriene 2 receptor. J Biol Chem 2000;275:30531-6.
46. Di Virgilio F, Chiozzi P, Ferrari D, Falzoni S, Sanz JM, Morelli A, et al. Nucleotide receptors: an emerging family of regulatory molecules in blood cells. Blood 2001;97:587-600.

RESPIRATORY RESEARCH

RESEARCH Open Access

Microarray profiling reveals suppressed interferon stimulated gene program in fibroblasts from scleroderma-associated interstitial lung disease

Gisela E Lindahl[1*†], Carmel JW Stock[1†], Xu Shi-Wen[2], Patricia Leoni[1], Piersante Sestini[3], Sarah L Howat[4], George Bou-Gharios[5], Andrew G Nicholson[6], Christopher P Denton[2], Jan C Grutters[7], Toby M Maher[1], Athol U Wells[1], David J Abraham[2] and Elisabetta A Renzoni[1]

Abstract

Background: Interstitial lung disease is a major cause of morbidity and mortality in systemic sclerosis (SSc), with insufficiently effective treatment options. Progression of pulmonary fibrosis involves expanding populations of fibroblasts, and the accumulation of extracellular matrix proteins. Characterisation of SSc lung fibroblast gene expression profiles underlying the fibrotic cell phenotype could enable a better understanding of the processes leading to the progressive build-up of scar tissue in the lungs. In this study we evaluate the transcriptomes of fibroblasts isolated from SSc lung biopsies at the time of diagnosis, compared with those from control lungs.

Methods: We used Affymetrix oligonucleotide microarrays to compare the gene expression profile of pulmonary fibroblasts cultured from 8 patients with pulmonary fibrosis associated with SSc (SSc-ILD), with those from control lung tissue peripheral to resected cancer (n=10). Fibroblast cultures from 3 patients with idiopathic pulmonary fibrosis (IPF) were included as a further comparison. Genes differentially expressed were identified using two separate analysis programs following a set of pre-determined criteria: only genes significant in both analyses were considered. Microarray expression data was verified by qRT-PCR and/or western blot analysis.

Results: A total of 843 genes were identified as differentially expressed in pulmonary fibroblasts from SSc-ILD and/or IPF compared to control lung, with a large overlap in the expression profiles of both diseases. We observed increased expression of a TGF-β response signature including fibrosis associated genes and myofibroblast markers, with marked heterogeneity across samples. Strongly suppressed expression of interferon stimulated genes, including antiviral, chemokine, and MHC class 1 genes, was uniformly observed in fibrotic fibroblasts. This expression profile includes key regulators and mediators of the interferon response, such as *STAT1*, and *CXCL10*, and was also independent of disease group.

Conclusions: This study identified a strongly suppressed interferon-stimulated gene program in fibroblasts from fibrotic lung. The data suggests that the repressed expression of interferon-stimulated genes may underpin critical aspects of the profibrotic fibroblast phenotype, identifying an area in pulmonary fibrosis that requires further investigation.

Keywords: SSc-ILD, IPF, Pulmonary fibroblasts, Interferon regulated genes

* Correspondence: g.lindahl@imperial.ac.uk
†Equal contributors
[1]Interstitial Lung Disease Unit, Royal Brompton Hospital and National Heart and Lung Institute, Imperial College London, Emmanuel Kaye Building, 1B Manresa Road, London SW3 6LR, UK
Full list of author information is available at the end of the article

Background

Pulmonary fibrosis, characterised by the destruction of lung architecture leading to organ failure, is, together with pulmonary hypertension (PH), the leading cause of death in patients with systemic sclerosis (SSc) [1]. Interstitial lung disease is more common in SSc (SSc-ILD) than in any other connective tissue disease, occurring in > 70% of patients [2], and is most frequently associated with a pattern of non-specific interstitial pneumonia (NSIP) [3]. Despite intense research efforts, the underlying mechanisms of SSc-ILD remain largely unknown [4], and there are currently limited therapeutic options for this serious complication [2].

While a large number of hypothesis-driven studies have identified potential profibrotic mediators [4,5], translation of these into therapeutic targets has so far been largely disappointing [6]. The search for more effective targets in lung fibrosis is now being addressed using hypothesis generating microarray-based strategies [7,8]. The majority of these studies have investigated gene expression in whole lung tissue samples, mostly in the idiopathic setting [5]. Matrix metalloproteinase (MMP) 7 [9], osteopontin [10], Twist1 [11], and MMP19 [12], are among suggested mediators identified using this strategy in idiopathic pulmonary fibrosis (IPF), a disease characterised by a histological pattern of usual interstitial pneumonia (UIP) [13,14]. In SSc, most microarray studies have been performed on skin biopsies and dermal fibroblasts [7]. However, a recent study compared whole lung tissue and fibroblasts isolated, at the time of transplant, from SSc-ILD lungs with a histological pattern of UIP, with those from IPF and idiopathic PH. The investigators reported gene profiles of SSc-ILD/UIP, with either predominant fibrosis or PH, overlapping with profiles of IPF and idiopathic PH, respectively [15].

While the initiating factors for fibrosis development may vary between diseases, the progressive accumulation of scar tissue in the lung is characterised by common themes, including expanding populations of activated fibroblasts, and excessive accumulation of extracellular matrix (ECM) proteins [5]. An important strategy to identify potential therapeutic targets, therefore, is to define fibrotic fibroblast phenotypes so as to delineate underlying key mechanisms for fibrosis progression.

Here we report analysis of the transcriptome of fibroblasts isolated from surgical lung biopsies at the time of diagnosis, from patients with well defined SSc-ILD and the histopathological pattern of NSIP. Although the main aim of this study was to compare SSc-ILD/NSIP fibroblast gene expression profiles with those of control lung fibroblasts, we also included a small number of IPF-derived fibroblast lines, as a separate fibrotic group. Our study confirms, with a robust signature in both diseases, the aberrant expression of previously reported myofibroblast markers and fibrosis mediators, and identifies a number of novel, co-expressed putative disease targets. We also observed the suppression of a large gene program, the interferon stimulated genes (ISGs), reported here for the first time. From the known function of some of these genes [16], it is possible to hypothesise that this suppressed program underlies key fibrotic fibroblast properties, such as hyper-proliferation, and apoptosis resistance. This study therefore identifies a potential new area for investigation and possible intervention in pulmonary fibrosis.

Methods

Patients and primary lung fibroblasts

Primary adult pulmonary fibroblasts were cultured from control tissue samples of unaffected lung from patients undergoing cancer-resection surgery (n=10), and from surgical lung biopsy samples of 11 patients with pulmonary fibrosis (SSc-ILD n=8 and IPF n=3). Independent reviews of the clinical and histopathologic diagnoses were performed and conformed to established criteria [17,18]. All of the SSc-ILD biopsies were characterised by a fibrotic NSIP pattern, and the IPF biopsies by a UIP pattern, based on current consensus criteria for these histological patterns [19]. The control tissue was histologically normal. Median age (range) was 60 (52–78) in controls, 48 (38–69) in SSc-ILD, and 61 (44–67) in IPF. The gender distribution (M/F) was as follows: controls 6/4; SSc-ILD 2/6; IPF 2/1. Four of the SSc-ILD and two of the IPF patients were ex-smokers. Smoking status was not available for all control cases. In SSc-ILD patients, median (range) percent predicted FVC was 72.5% (61–106), median FEV1 was 79% (58–92) and median DLCO was 50% (24–58). In IPF patients, median FVC was 70% (64–75), median FEV1 was 66% (55–79), and median DLCO was 50% (35–53). Patients had not been on corticosteroids or other immunosuppressants prior to surgical biopsy, as the biopsy was performed at the time of diagnosis of the ILD pattern, prior to initiation of treatment. Informed written consent was given by all subjects, and authorisation given by the Royal Brompton Hospital Ethics Committee. Fibroblasts were obtained from the biopsies by explant culture, and cell cultures maintained, as previously described [20,21]. Experiments were performed on fibroblasts at passage 2–5. Only one sample (S1) was used at passage 2. There was no difference in the median passage number between the control (median: 4.5; range: 3–5), SSc-ILD (median: 4; range: 2–5) and IPF (median: 4; range 3–5) groups.

Microarray gene expression and analysis

At confluence, lung fibroblasts were serum-deprived for 42 hours (media changed at 18 hours) in the presence of 0.1% bovine serum albumin (Sigma). Total RNA was harvested (Trizol, Life Technologies), quantified, and the integrity verified by denaturing gel electrophoresis. Samples

with a 28S:18S ratios of approximately 2:1 were accepted for further analysis by the Genomics Laboratory, CSC-MRC, Imperial College London, Hammersmith. RNA samples were prepared for chip hybridisation following manufacturer's guidelines (Affymetrix). Hybridisation of cRNA to Affymetrix human U133Av2 chips, containing approximately 14,500 well characterised human genes, signal amplification, and data collection were performed using an Affymetrix fluidics station and chip reader, according to manufacturer's protocol. Array normalisation, using the invariant set normalisation method, and subsequent calculation of model-based expression values, was performed using DNA-Chip Analyzer (dChip) [22]. A list of differentially expressed genes was generated in dChip using fold change ≥2, difference in means ≥100, and $p<0.05$. Significance analysis of microarrays (SAM) v 4.0 [23] was also used to determine significantly differentially expressed genes with fold change ≥2, difference in means ≥100, delta =1, and a false discovery rate <0.01. Only genes identified as differentially expressed according to both programs were considered as different between groups. Microarray data has been deposited in the Gene Expression Omnibus database [24], accession number GSE40839. Although the main aim of this study was to assess global gene expression profiles in SSc-ILD compared to controls, for completeness we present the comparison between both SSc-ILD and IPF and controls separately in tables. dChip software was used for data visualisation and hierarchical average linkage clustering using Pearson's correlation [22].

Functional category analysis

Functional categories enriched in the differentially expressed genes were identified using the functional annotation and clustering tool of the Database for Annotation, Visualisation, and Integrated Discovery (DAVID) v 6.7 [25,26]. The probability that a Gene Ontology (GO) biological process term [27] is overrepresented was determined by a modified Fisher's exact test, comparing the proportion of genes in the whole genome which are part of that GO term, to the proportion of the differentially expressed genes which are part of the same GO term, and was expressed as an EASE score. Clusters of overrepresented GO terms were then generated based on the similarity of differentially expressed genes assigned to each functional GO term. Clusters were considered significantly overrepresented if they contained a minimum of five GO terms with an EASE score of ≤ 0.01. A summary description of each cluster was generated based on the constitutive GO term names of that cluster which achieved an EASE score <0.05 following Benjamini-Hotchberg correction of multiple comparisons. Only clusters with enrichment scores >3 (minus log transformed geometric mean of the EASE scores of the constitutive terms, equivalent to average EASE score=0.001) were selected. The open access database INTERFEROME [28] was used to identify differentially expressed genes which have been shown experimentally to be regulated by interferons.

qRT-PCR

RNA was extracted using the RNeasy® Mini kit (Qiagen) according to manufacturer's instructions. Samples were quantified and quality assessed using the NanoDrop spectrophotometry system (Thermo Scientific). Complementary DNA (cDNA) was synthesised from 500 ng RNA in a 20 μl reaction using the QuanTitect® reverse transcription kit (Qiagen). Expression levels were measured using a Rotor Gene 6000 (Corbett) in 10 μl reactions containing 2 μl cDNA (five-fold dilution), 1 × SensiMix™ SYBR NO-ROX (Bioline), and 0.5 μM of each forward and reverse primer (Table 1). PCR conditions were: 10 minutes at 95°C, followed by 40 cycles of 10 seconds at 95°C, 15 seconds at 57°C, and 5 seconds at 72°C. All reactions were performed in duplicate and non-template controls were included for each gene. Standard curves were generated for each gene studied using seven two-fold serial dilutions, high standard of 1×10^{7} copies/μl, of primer set amplicons generated from cDNA. Threshold cycle was manually determined at a fixed value of $10^{-0.5}$ and the template quantity calculated using Rotor Gene 6000 Series Software 1.7 (Corbett). Expression levels were normalised to *YWHAZ* and *HPRT1* [29,30].

Western blot analysis

Following pre-incubation for 24 hours in serum-free media (DMEM, 0.1% BSA, penicillin/streptomycin), pulmonary fibroblasts from healthy controls, SSc-ILD, and

Table 1 qRT-PCR primers

Gene	Forward primer	Reverse primer
Normalisation genes		
HPRT1	TGACACTGGCAAAACAATGCA	GGTCCTTTTCACCAGCAAGCT
YWHAZ	ACTTTTGGTACATTGTGGCTTCAA	CCGCCAGGACAAACCAGTAT
Genes of interest		
CXCL10	GAAAGCAGTTAGCAAGGAAAG	ATCCTTGGAAGCACTGCATC
ID1	CCAGAACCGCAAGGTGAG	GGTCCCTGATGTAGTCGATGA
IFITM1	TTCTTGAACTGGTGCTGTCT	ATGAGGATGCCCAGAATCAG
IL11	CCTGTGGGGACATGAACTGT	AGGGTCTGGGGAAACTCG
IRF1	CAGCCCAAGAAAGGTCCTC	TTGAACGGTACAGACAGAGCA
NOX4	CTGCTGACGTTGCATGTTTC	CGGGAGGGTGGGTATCTAA
Serpine 1	GGAAAGGCAACATGACCAG	CAGGTTCTCTAGGGGCTTCC
STAT1	GGATCAGCTGCAGAACTGGT	TTTCTGTTCCAATTCCTCCAA

Shown are the primers, written 5' to 3', used for measuring expression levels by qRT-PCR for validation of the microarray results. All primer pairs except for *YWHAZ*, *IRF1*, and *ID1*, are intron spanning.

IPF (n=3 for each phenotype), were cultured for a further 24 hours in fresh serum-free media. Cells were lysed and western blot analysis was performed using the following primary antibodies: CTGF and STAT1 (Santa Cruz Biotechnology); αSMA (Dako); IFITM1-3, ISG15 and GAPDH (Abcam); IRF-1 (Cell Signaling Technology); horseradish peroxidise conjugated secondary antibodies (Dako and Cell Signaling Technology); and ECL detection (Amersham).

Results

Gene expression profiles of fibrotic lung fibroblasts: approximately two-thirds of differentially expressed genes are down-regulated

Using an Affymetrix platform (U133Av2), we determined basal (serum free) global gene expression levels in fibroblasts prepared from lung tissue of 8 patients with SSc-ILD and 10 control lungs. As a further comparison we also included 3 fibroblast cultures from lung tissue of IPF patients. Unsupervised hierarchical cluster analysis of samples and genes resulted in an overall separation of fibrotic samples from controls (Figure 1). Two of the SSc-ILD samples clustered among the normal controls, demonstrating recognised fibrotic fibroblast sample heterogeneity.

When stringent criteria were applied, as described in the methods section, 478 and 744 probe sets (probes in future), equivalent to 360 and 547 genes, displayed differential expression by at least two-fold in SSc-ILD and IPF fibroblasts, respectively, compared to control fibroblasts. In SSc-ILD fibroblasts, 125 probes (99 genes) showed significantly higher, and 353 probes (261 genes) lower expression levels compared with controls (Additional file 1). In IPF fibroblasts, 239 and 505 probes (181 and 366 genes) had significantly higher and lower expression, respectively, compared with control fibroblasts (Additional file 2). Thus, approximately two thirds of differentially expressed genes were expressed at lower levels in fibroblasts from the two disease groups compared with controls. The sets of underexpressed genes in the disease groups, compared to normal controls, also contained the most significantly differentially expressed genes. Table 2 lists the 20 most significantly differentially expressed, and highest ranking (fold change) genes in SSc-ILD and IPF samples, separately, versus controls. It should be noted here that, while 379 out of a total of 843 probes were differentially expressed in both SSc-ILD and IPF vs. controls, most genes falling outside this overlap were very nearly significant in the other disease group, i.e. followed similar trends without meeting cut-off criteria. When the two disease groups were compared directly, only 8 probes (7 genes) were significantly differentially expressed (Additional file 3). The 843 probes differentially expressed in SSc-ILD and/or IPF, which also include the genes differentially expressed between these two groups, are listed in Additional file 4. Within the pooled fibrotic samples (IPF and SSc-ILD), no significant difference was observed in the 843 probes according to smoking status (SAM analysis, data not shown).

Expression levels of a subset of genes identified by the present microarray analysis were verified by qRT-PCR in the microarray RNA samples demonstrating good correlation between these two techniques (Figure 2). Protein levels for six differentially expressed genes, fibrosis related genes; connective tissue growth factor (CTGF), and alpha-smooth muscle actin (αSMA), and interferon stimulated genes (ISG); signal transducer and activator of transcription 1 (STAT1), IFITM1-3 (all three isoforms are detected by this antibody), ISG15 and IRF-1, were determined by western blot analysis in independent preparations of additional SSc-ILD, IPF, and control fibroblasts (Figure 3).

Functional groups over-represented among differentially expressed genes

As predicted from the similarities between the two disease groups with regards to differentially expressed genes, gene ontology analysis revealed a major overlap in overrepresented functional groups. Enriched functional groups representing six broad categories (GO clusters) were identified among the genes with higher expression in disease fibroblasts compared with normal controls (see Table 3 for a summary of enriched clusters of GO terms, and Additional file 5 for full GO analysis): anatomical structure development, regulation of cell cycle, response to stress and wounding, regulation of apoptosis, cell migration, and smooth muscle contraction. Among underexpressed/downregulated genes, GO clusters included: inflammatory

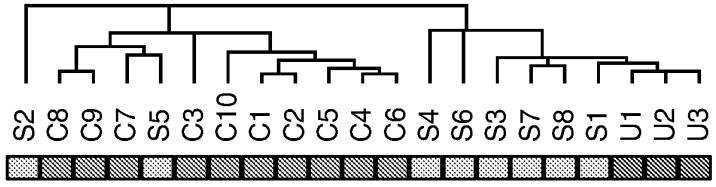

Figure 1 Unsupervised clustering of samples based on full microarray probe set. The sample dendrogram resulting from hierarchical clustering using all 22 K probes, shows clustering of samples by phenotype: control (C, green bar), SSc-ILD (S, orange bar), IPF (U, red bar).

Table 2 Most differentially expressed genes in SSc-ILD and IPF compared to controls

Genes overexpressed in SSc-ILD vs. Control	Probe set ID	Control mean	SSc-ILD mean	Fold change	p value
Inhibitor of DNA binding 1, dominant negative helix-loop-helix protein	208937_s_at	25.5	917.5	36.1	0.00078
Interleukin 11	206924_at	23.6	717.8	30.4	0.015
Inhibitor of DNA binding 3, dominant negative helix-loop-helix protein	207826_s_at	27.7	603.2	21.8	0.00051
Tetraspanin 13	217979_at	37.9	533.9	14.1	0.0033
Elastin	212670_at	43.7	396.9	9.1	0.0021
Xylosyltransferase I	213725_x_at	29.0	255.4	8.8	0.0024
Serpin peptidase inhibitor, clade E, member 1	202628_s_at	329.8	2473.2	7.5	0.0022
Basic helix-loop-helix family, member e40	201170_s_at	44.3	256.1	5.8	0.0014
Connective tissue growth factor	209101_at	467.9	2637.1	5.6	0.00068
Solute carrier family 7, member 5	201195_s_at	56.1	294.2	5.3	0.00022
Tropomyosin 1 (alpha)	206116_s_at	317.5	1619.6	5.1	0.0032
Phosphoribosyl pyrophosphate synthetase 1	208447_s_at	59.0	283.4	4.8	0.0036
Inhibin, beta A	210511_s_at	143.3	688.1	4.8	0.0012
Growth arrest and DNA-damage-inducible, beta	207574_s_at	68.1	306.6	4.5	0.0023
Coiled-coil domain containing 99	221685_s_at	85.1	373.3	4.4	0.0018
Cadherin 2, type 1, N-cadherin (neuronal)	203440_at	105.3	433.0	4.1	0.00095
Desmoplakin	200606_at	80.5	306.1	3.8	0.0016
Insulin-like growth factor binding protein 3	212143_s_at	408.6	1489.1	3.6	0.0068
Microtubule associated monoxygenase, calponin and LIM domain containing 2	212473_s_at	184.7	667.5	3.6	0.0039
Prostaglandin-endoperoxide synthase 1	215813_s_at	102.4	362.0	3.5	0.0083
Genes underexpressed in SSc-ILD vs. Control	**Probe set ID**	**Control mean**	**SSc-ILD mean**	**Fold change**	**p value**
Chemokine (C-X-C motif) ligand 10	204533_at	771.2	19.2	−40.1	0.00034
Chemokine (C-X-C motif) ligand 11	210163_at	179.9	5.0	−36.0	0.0027
Flavin containing monooxygenase 2 (non-functional)	211726_s_at	530.4	15.7	−33.7	0.017
Interferon-induced protein with tetratricopeptide repeats 2	217502_at	707.1	26.1	−27.1	0.0096
Vascular cell adhesion molecule 1	203868_s_at	835.2	32.2	−26.0	0.0049
Bone marrow stromal cell antigen 2	201641_at	315.8	12.5	−25.3	0.0081
Radical S-adenosyl methionine domain containing 2	213797_at	333.8	13.3	−25.1	0.0039
Interferon-induced protein 44-like	204439_at	370.7	15.4	−24.1	0.00033
Interferon-induced protein with tetratricopeptide repeats 1	203153_at	1744.2	82.6	−21.1	0.000039
2',5'-oligoadenylate synthetase 1, 40/46 kDa	205552_s_at	374.6	18.3	−20.5	0.0014
Complement factor B	202357_s_at	837.0	42.6	−19.6	0.0036
Interferon-induced protein with tetratricopeptide repeats 3	204747_at	985.0	61.9	−15.9	0.00031
Chromosome 10 open reading frame 10	209183_s_at	208.8	13.6	−15.3	0.0062
Myxovirus resistance 1, interferon-inducible protein p78 (mouse)	202086_at	1361.9	91.2	−14.9	0.00012
Receptor (chemosensory) transporter protein 4	219684_at	196.4	13.3	−14.8	0.000091
Chemokine (C-C motif) ligand 11	210133_at	529.8	36.2	−14.6	0.0021
Retinoic acid receptor responder (tazarotene induced) 3	204070_at	239.4	17.2	−13.9	0.00024
Alcohol dehydrogenase 1B (class I), beta polypeptide	209613_s_at	268.9	19.8	−13.6	0.011
Secreted and transmembrane 1	213716_s_at	285.0	22.0	−13.0	0.0012
Interferon, alpha-inducible protein 6	204415_at	1196.6	93.7	−12.8	0.00043
Genes overexpressed in IPF vs. Control	**Probe set ID**	**Control mean**	**IPF mean**	**Fold change**	**p value**
Interleukin 11	206924_at	23.6	2374.9	100.6	0.0019
Inhibitor of DNA binding 1, dominant negative helix-loop-helix protein	208937_s_at	25.5	752.8	29.6	0.011

Table 2 Most differentially expressed genes in SSc-ILD and IPF compared to controls *(Continued)*

Tetraspanin 13	217979_at	37.9	1039.1	27.4	0.0052
NADPH oxidase 4	219773_at	12.3	323.6	26.4	0.016
Inhibitor of DNA binding 3, dominant negative helix-loop-helix protein	207826_s_at	27.7	603.4	21.8	0.0025
Phospholamban	204939_s_at	25.7	460.1	17.9	0.035
Elastin	212670_at	43.7	766.9	17.6	0.0026
Xylosyltransferase I	213725_x_at	29.0	443.6	15.3	0.034
Galanin prepropeptide	214240_at	18.4	254.4	13.8	0.014
Cytokine receptor-like factor 1	206315_at	23.4	319.3	13.6	0.0098
Calponin 1, basic, smooth muscle	203951_at	83.0	1048.0	12.6	0.0024
Follistatin-like 3	203592_s_at	32.5	404.8	12.4	0.0048
CTP synthase	202613_at	39.5	454.7	11.5	0.000059
Endothelial cell-specific molecule 1	208394_x_at	10.2	116.8	11.4	0.031
Cadherin 6, type 2, K-cadherin (fetal kidney)	210602_s_at	26.2	298.4	11.4	0.00092
Proenkephalin	213791_at	33.7	366.7	10.9	0.00086
Adhesion molecule with Ig-like domain 2	222108_at	54.7	490.6	9.0	0.025
NUAK family, SNF1-like kinase, 1	204589_at	56.2	489.9	8.7	0.001
Tropomyosin 1 (alpha)	206117_at	30.9	261.7	8.5	0.0069
Inhibin, beta A	210511_s_at	143.3	1198.5	8.4	0.0023
Genes underexpressed in IPF vs. Control	**Probe set ID**	**Control mean**	**IPF mean**	**Fold change**	**p value**
Interferon-induced protein with tetratricopeptide repeats 1	203153_at	1744.2	5.4	−321.4	0.000033
Myxovirus resistance 1, interferon-inducible protein p78 (mouse)	202086_at	1361.9	8.8	−154.1	0.000096
Interferon, alpha-inducible protein 6	204415_at	1196.6	11.8	−101.2	0.00027
Chemokine (C-X-C motif) ligand 10	204533_at	771.2	9.5	−81.3	0.00031
Superoxide dismutase 2, mitochondrial	221477_s_at	2180.4	29.8	−73.2	<0.000001
Myxovirus resistance 2 (mouse)	204994_at	517.3	8.5	−60.6	0.00062
Interferon induced transmembrane protein 1 (9–27)	214022_s_at	3698.0	61.4	−60.3	<0.000001
Interferon-induced protein with tetratricopeptide repeats 3	204747_at	985.0	17.2	−57.2	0.00023
Pentraxin 3, long	206157_at	1415.2	35.2	−40.2	0.000016
Interferon-induced protein 44-like	204439_at	370.7	11.6	−31.9	0.0003
Complement component 3	217767_at	457.9	14.4	−31.8	0.000072
KIAA1199	212942_s_at	799.0	30.8	−26.0	0.00027
Interferon-induced protein 35	209417_s_at	455.6	18.1	−25.1	0.000062
Chemokine (C-X-C motif) ligand 1	204470_at	637.1	26.3	−24.2	<0.000001
Growth arrest-specific 1	204457_s_at	383.2	17.2	−22.3	0.000059
Signal transducer and activator of transcription 1, 91 kDa	209969_s_at	327.3	15.3	−21.4	0.000097
Chemokine (C-C motif) ligand 2	216598_s_at	2676.4	128.3	−20.9	0.00003
Interferon-induced protein 44	214453_s_at	335.0	17.0	−19.7	0.000027
Caspase 1 (interleukin 1, beta, convertase)	211367_s_at	180.6	10.0	−18.1	<0.000001
Tumor necrosis factor, alpha-induced protein 2	202510_s_at	404.2	22.6	−17.9	0.000003

Shown are the top 20 genes, based on fold change, over and under expressed in SSc-ILD and IPF compared to controls. Where more than one probe set corresponding to the same gene were present in the top 20, the probe with the greatest fold change or most significant p-value, is shown.

and immune response, response to biotic stimulus, regulation of apoptosis, regulation of cell migration, regulation of cell proliferation, and regulation of I-κB/NF-κB cascade. By far the most enriched functional groups, compared with control cells, in both SSc-ILD and IPF lung fibroblasts, are genes involved in immune system processes and in microbial/viral defence, which are strongly suppressed in both disease groups. These genes are also among the most significantly differentially expressed genes in this study.

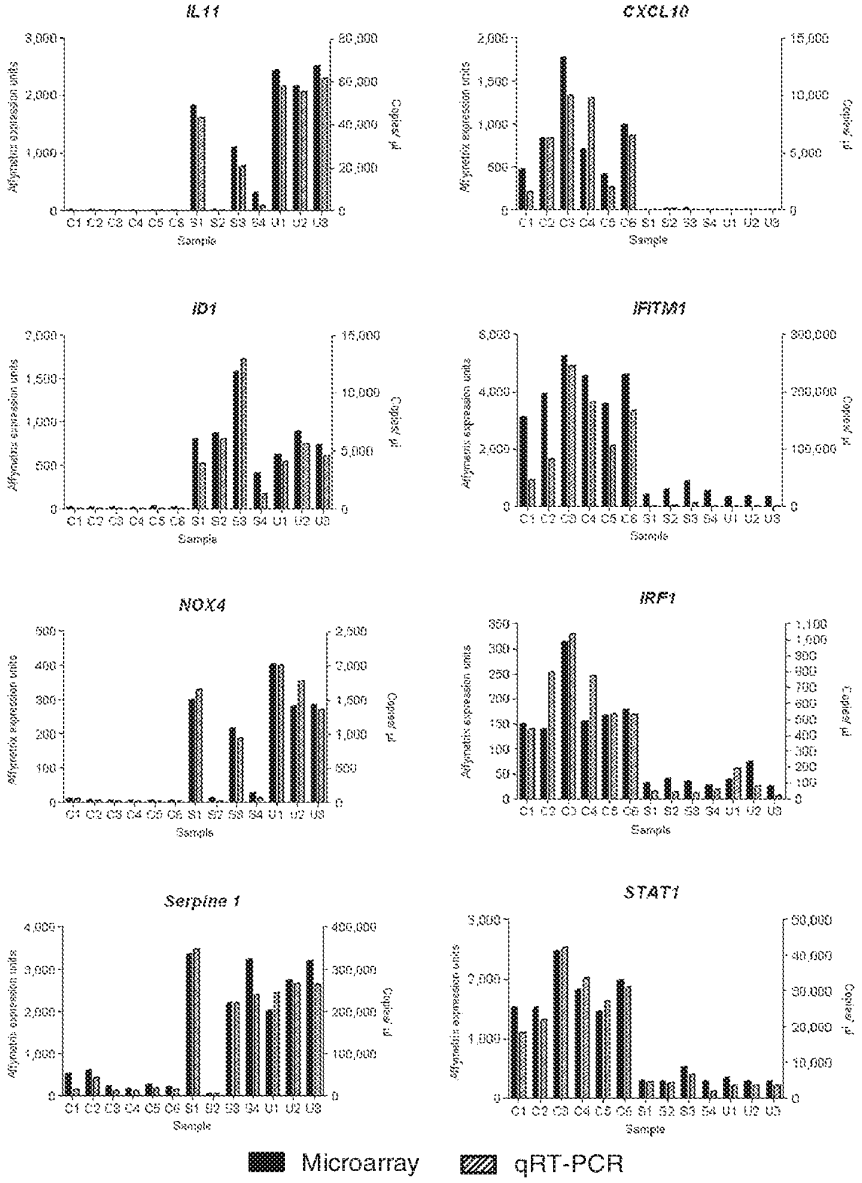

Figure 2 Quantitative RT-PCR confirmation of microarray results. Expression levels of eight genes selected from the microarray data was measured by qRT-PCR in thirteen of the samples used in the microarray. For each sample the microarray data is plotted on the left-hand axis, and the qRT-PCR results plotted on the right-hand axis. qRT-PCR expression levels were normalised to *YWHAZ* and *HPRT1*.

Cluster analysis of differentially expressed genes – ISGs; a major group suppressed in fibrotic lung fibroblasts

To visualise the differential expression across samples and to identify co-expressed genes, average linkage cluster analysis was performed using expression data for the 843 probes sets which displayed differential expression in at least one of the two comparisons: SSc-ILD vs. control, and IPF vs. control (Figure 4A). Within this set are also the eight probes differentially expressed when SSc-ILD and IPF samples were compared directly. Parts of identified gene clusters were selected to illustrate co-expression among upregulated (Figure 4, Panels B-F) and downregulated (Panels H-J) genes, and also to highlight different patterns of sample heterogeneity. Overall, a heterogeneous expression pattern was observed in the upregulated genes, whereas downregulated genes had

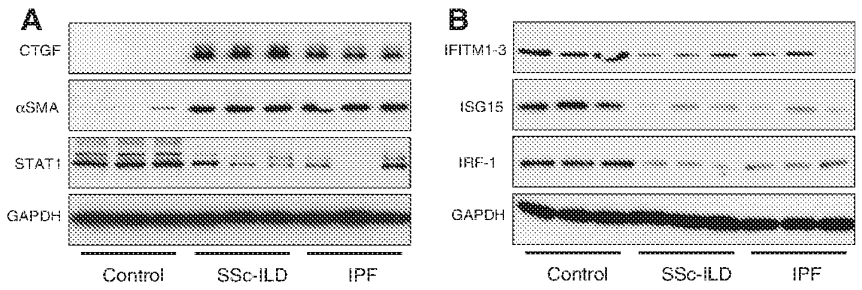

Figure 3 Western blot confirmation of microarray results. Protein expression levels of six significantly differently expressed genes selected from the microarray data were visualised by western blot in fibroblast samples independent to those used in the microarray (n=3 for each group). **A)** Protein expression of fibrosis related genes, CTGF and αSMA; and key regulator of interferon response, STAT1. **B)** Protein expression of interferon stimulated genes (ISG): IFITM1-3, ISG15 and IRF-1.

more uniform expression patterns across samples for the majority of genes in both disease groups. Among upregulated genes, a TGF-β response signature [31,32] including genes encoding for fibrosis mediators and myofibroblast markers, such as *SERPINE1* (*PAI1*), connective tissue growth factor, smoothelin, and transgelin (*SM22*) is prominent (Panel B). Co-expressed with these are strongly upregulated genes: growth arrest and DNA-damage inducible β (*GADD45*), xylosyltransferase 1 (*XYLT1*), N-cadherin, and elastin, with potential roles in the fibrotic disease process. Groups B, C and D all contain genes involved in contraction and migration, however, the degree of heterogeneity between samples differ between these groups: in group B, the majority of fibrotic samples have elevated expression of smoothelin and transgelin compared with controls; in group C, fewer fibrotic samples, 7 out of 11, have enhanced levels of α2 smooth muscle actin (*ACTA2*) expression; and in group D, all three IPF samples, but only 3 out of 8 SSc-ILD samples, have elevated expression of calponin 1 and actin gamma 2 smooth muscle (*ACTG2*). This may indicate different degrees of contractile/migratory phenotypes among these fibrotic cell preparations. Panel E contains *ID1* and *ID3*, which are in the top 20 differentially regulated genes in both disease groups, and are upregulated in most of the fibrotic samples. Group F depicts a cluster of co-expressed cell-cycle associated genes, including cyclins and *TOPO2*, which exhibit heterogeneous expression in both disease groups. Panel G illustrates an area with less clustering, which however includes possible disease specific genes, e.g. Secreted protein, acidic, cysteine-rich (*SPARC*) (IPF, Table 2B) and desmoplakin (SSc-ILD) (Additional file 4). Desmoplakin is among the top 20 most upregulated genes in SSc-ILD with an elevated expression in 7 out of the 8 SSc-ILD fibroblast lines, but with low expression in the three IPF cell preparations and in all controls. Desmoplakin is part of the desmosome complex which forms tight cell-cell contacts [33], and its enhanced expression in SSc-ILD fibroblasts may define a different pathogenesis and cell origin. Panels H-J shows the marked suppressed expression of interferon stimulated genes (ISGs), such as antiviral genes (Group H), chemokine (Group I) and MHC class I genes (Group J). This cluster also includes key regulators of the interferon gene program, *STAT1*, interferon regulatory factor 1 (*IRF1*) and interferon regulatory factor 7 (*IRF7*), as well as chemokine (C-X-C motif) ligand 10 (*CXCL10/IP10*), one of the most strongly suppressed genes in the study, and the most strongly repressed chemokine in both disease groups (Panel H and I).

Comparing the SSc-ILD and IFP fibroblast gene expression profiles with the interferome

Since we observe a clear fibrosis/TGF-β signature together with a strongly suppressed ISG program, and there is a well-documented antagonistic relationship between TGF-β and interferon signalling in the fibrosis literature [34], we next interrogated the Interferome, a database of interferon regulated genes (IRGs) reported in the literature [28]. This database includes 1996 human IRGs, of which 1581 are induced and 415 repressed by interferons. In our study, out of the 99 and 181 overexpressed genes in SSc-ILD and IPF fibroblasts, respectively, 40 (40.4%) and 55 (30.1%) genes were in the Interferome database. Among our underexpressed genes, out of a total of 261 and 366 in SSc-ILD and IPF fibroblasts, respectively, 134 (51.3%) and 173 (74.3%) genes were in the Interferome database. The genes overlapping with IRGs in this database are listed in Additional file 6. The comparison revealed that many of the TGF-β responsive genes upregulated in our microarray data set are indeed genes repressed by IFNs.

Discussion

Previous studies have shown that fibroblasts isolated from SSc-ILD [35] and IPF [5] lungs, while displaying

Table 3 Over-represented functional terms

GO cluster	Description	Enrichment score
Genes overexpressed in SSc-ILD vs. Control		
1	Anatomical structure development	5.50
2	Regulation of cell cycle	4.23
3	Response to stress and wounding	3.33
Genes underexpressed in SSc-ILD vs. Control		
1	Inflammatory response	11.53
2	Regulation of cell proliferation	5.16
3	Regulation of biological process	5.12
4	Inflammatory response/chemotaxis	4.81
5	Regulation of cell migration	4.33
6	Response to external stimulus	4.19
7	Regulation of apoptosis	3.78
8	Inflammatory and immune response	3.77
9	Response to biotic stimulus/ion homeostasis	3.69
10	Regulation of I-κB kinase/NF-κB cascade	3.37
Genes overexpressed in IPF vs. Control		
1	Anatomical structure development/ neurogenesis	4.94
2	Regulation of apoptosis	3.95
3	Cell migration/neurogenesis	3.81
4	Regulation of cell motion	3.45
5	Response to wounding/tissue development	3.17
6	Smooth muscle contraction/Blood circulation	3.03
Genes underexpressed in IPF vs. Control		
1	Immune response	12.65
2	Response to virus, bacteria and LPS	8.66
3	Positive regulation of biological process and cell death	5.29
4	Negative regulation of biological process and cell death	4.91
5	Regulation of immune system and developmental process	4.08
6	Inflammatory response/chemotaxis	3.98
7	Regulation of cell migration and adhesion	3.87
8	Inflammatory and humoral immune response	3.63
9	Anatomical structure development	3.39
10	Response to stimulus and I-κB kinase/NF-κB cascade	3.19
11	Response to extracellular stimulus and oxidative stress	3.18

Using the DAVID functional annotation tool, genes over and under expressed in SSc-ILD and IPF compared to controls were clustered according to Gene Ontology (GO) biological process terms. Shown are the summary descriptions and enrichment scores of the sets of enriched GO terms within each GO cluster with an enrichment score >3.

substantial heterogeneity, are generally more proliferative, migratory, resistant to apoptosis, and ECM producing, than control lung fibroblasts [36]. A greater proportion display elevated αSMA expression, also enhancing their contractility. These features are all consistent with the fibroblast accumulation and scar tissue formation observed in fibrotic lung. The so called myofibroblast phenotype is maintained over several passages in culture [37], suggesting an underlying epigenetic regulation, whether established and maintained in local cells within the chronic disease setting, or supporting the phenotype of a specialised infiltrating wound healing cell type [38]. Regardless of cell origin, this feature enables *in vitro* studies of mechanisms underlying the fibrotic fibroblast phenotype.

In this study we observed a high number of differentially expressed genes between SSc-ILD and/or IPF derived fibroblasts, compared with controls. There was a large overlap between expression profiles of SSc-ILD and IPF fibroblasts, suggesting several common pathways at this stage of the two diseases. Indeed, a direct comparison demonstrated only seven genes with significantly different expression between the two disease groups. Caution should be applied, however, when interpreting data from this direct comparison since only three IPF samples were included here. It is possible that more genes with differential expression between the two disease groups would be identified with a larger numbers of IPF fibroblasts samples. Such studies would also be required to verify the sporadic observations made in this study, such as the elevated expression levels of desmoplakin in SSc-ILD, but not in IPF fibroblasts. Therefore, we stress that the main objective of the study presented here was to gain an overview of potential SSc-ILD target genes, and the study was not designed to detect differences between different fibrotic entities.

Among significantly upregulated genes in both SSc-ILD and IPF/UIP fibroblasts, we identify a recognised fibrosis signature, including smooth muscle actin (*ACTA2*), *CTGF*, and *PAI1* (*SERPINE1*), along with genes more recently associated with lung fibrogenesis, including *ID1*, *ID3*, *IL11*, and *NOX4*. Inhibitor of DNA binding 1 and 3 (*ID1* and *ID3*), are target genes of bone morphogenetic proteins, and control cell differentiation by dominant negative inhibition of helix-loop-helix transcription factors [39]. Chambers et al. described upregulation of *ID1* in lung fibroblasts in response to TGF-β, and linkage to the smooth muscle phenotypic switch [31]. Increased *ID1* and *ID3* gene expression was also observed in lung tissue and fibroblasts from patients with SSc-ILD by Hsu and colleagues, [15]. The ID proteins are overexpressed in many cancers, controlling cell growth and apoptosis, and have been suggested as a therapeutic target [39,40]. In fibroproliferative stages of fibrosis, high *ID1/ID3* expression could maintain fibroblasts in a dedifferentiated, hyperproliferative, and

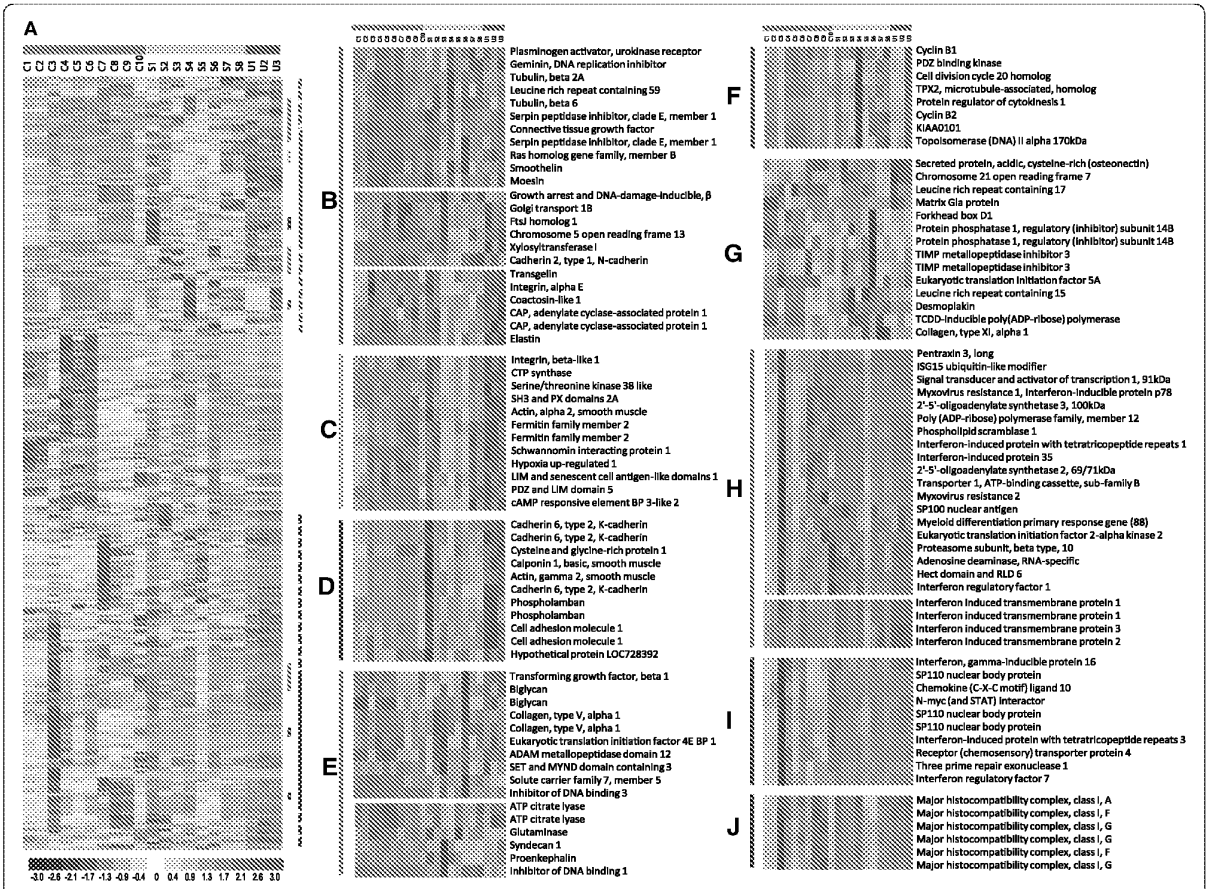

Figure 4 Gene expression profiles of control, SSc-ILD, and IPF pulmonary fibroblasts. A) Supervised hierarchical clustering of probes. The gene set used comprised the 843 probes with a fold change ≥2, difference in means ≥100, and $p<0.05$ (dChip) and FDR<0.01 (SAM), in both the SSc-ILD or IPF samples, compared to controls, which includes also 8 probes differentially expressed between SSc-ILD and IPF samples when compared directly. Each column corresponds to an individual sample (C= control, S=SSc-ILD, U=IPF), and each row corresponds to an individual probe. The coloured bars to the right of the heatmap identify the location of the insets displayed in **B-J**. Panels **B-J** were selected to highlight sample heterogeneity and/or genes co-expressed with high scoring differentially expressed genes.

apoptosis resistant state. Another significantly upregulated gene, though somewhat variably in SSc-ILD fibroblasts, is *NOX4*, encoding a member of the NADPH oxidase (NOX) proteins which generate superoxide by electron transfer to oxygen [41]. Through its involvement in TGF-β-induced fibroblast differentiation into myofibroblasts, two recent studies have suggested a role for NOX4 in IPF, where it is found to be overexpressed [41]. Specific NOX4 inhibitors are now being developed as possible antifibrotic agents [42]. Another potential novel target gene, *GADD45B*, highly induced and coexpressed with the fibrosis related genes in this study, is a pro-survival factor associated with stress-resistant tumours [43], and has been found to be upregulated in SSc skin biopsies [44].

The most striking of our observations is the strongly and uniformly repressed ISG profile in fibrotic fibroblasts. Among these are genes coding for: antiviral protein myxovirus (influenza virus) resistance 1 (*MX1*), interferon gamma inducible protein p16 (*IFI16*), 2',5'-oligoadenylate synthetase 1 (*OAS1*), the chemokines chemokine (C-X-C motif) ligand 10 (*CXCL10/IP10*) and chemokine (C-C motif) ligand 11 (*CCL11*), and antigen presenting MHC I molecules. Key transcriptional regulators of this program, including *IRF1*, *IRF7*, and *STAT1* are also suppressed. To our knowledge, the reduction in expression of a large set of immune response/interferon related genes has not previously been described in either SSc-ILD or IPF derived fibroblasts, or other fibrotic lung diseases. Global gene expression was recently evaluated in scleroderma whole skin biopsies and matched dermal fibroblasts. While 26 genes were differentially expressed in both scleroderma whole skin and fibroblasts compared to controls, nine were found to be discordant [45]. Interestingly, the majority of the discordant genes were

upregulated in skin biopsies but downregulated in fibroblasts, including the ISG genes we identify as repressed in lung fibroblasts, such as *MX1*, *IFI16*, intercellular adhesion molecule 1 (*ICAM1*), and *OAS1*. While the authors argue that the discordant genes are an indication of a scarce representativeness of skin fibroblast gene expression *in vivo* [45], in light of our data, it is likely that they were in fact observing the same phenomenon reported in the current study. As these are mainly interferon regulated genes, the discordance between fibroblasts and whole tissue gene expression could be explained by the known increase of immune cell populations in SSc skin, likely to be overexpressing immunoregulatory genes. The upregulation of *MX1*, *IRF7* and *STAT1* in PBMC from SSc patients would support this notion [46,47]. The downregulation of the ISG program both in SSc-ILD and in IPF fibroblasts suggests that this phenomenon relates to a local fibroblast specific, rather than systemic, profibrotic process, perhaps underpinned by a general susceptibility for tissue fibrosis, common to both diseases.

Additional support for our finding of an aberrantly regulated ISG program in fibrotic lung fibroblasts, comes from work on two of the signature genes from this group, *CXCL10* (*IP10*) and *STAT1*. IP10 levels were found to be downregulated in IPF lung fibroblasts by Keane et al. [48]. More recently, Coward et al. have shown, again in IPF fibroblasts, that epigenetic dysregulation involving both histone deacetylation and hypermethylation is responsible for targeted repression of *IP10* [49]. By contrast, Hsu et al. did not report a significant difference in expression in isolated lung fibroblasts [15], a difference which may relate to experimental design, as discussed below. Further support of a role of suppressed ISGs in pulmonary fibrosis comes from two animal models. Mice deficient in *IP10* [50], and in *STAT1* [51], displayed enhanced susceptibility to pulmonary fibrosis. Based on these studies, the suppressed ISG program indentified in fibroblasts isolated from SSc-ILD and IPF lung, as presented here, would support enhanced lung fibrosis progression through promoting fibroblast proliferation, migration, and apoptosis resistance. Interestingly, IFN-γ treatment in IPF has failed to show a benefit [52], and there was a suggestion of worse pulmonary outcomes in a study investigating treatment of SSc patients with IFN-α compared with placebo [53], with the latter providing indirect support for IFN-related mechanisms involved in organ-specific SSc complications. There could be several possible explanations for these disappointing results, including unexpected adverse effects through circulating cell populations. Activation of pathways downstream of systemically administered interferons is likely to have different direct and indirect effects depending on the cell type and tissue location. The findings shown here add important information to this complexity, and need to be investigated in future detailed mechanistic cell and animal studies.

The signatures observed in our study are remarkably strong, both in terms of fold difference and statistical significance. One possible reason for this is that lung tissue samples were obtained from biopsies at the time of diagnosis, when the disease may be at a relatively early or active wound healing stage, and when perhaps fibroblast proliferation (accumulation) and elastin synthesis, rather than contraction and collagen remodelling, dominate. This is in contrast to the study by Hsu et al., in which gene expression profiles were investigated in SSc lung tissue and fibroblasts from transplant, and therefore possible end-stage, material, also noted by the authors as a potential limitation [15]. Another possibility relates to differences in *in vitro* culture condition as we employed serum free media before harvest, similarly to others, including Coward et al. [49], as opposed to in low serum (0.5%) as applied by e.g. Hsu et al. [15]. Serum withdrawal, a form of cellular stress, may evoke the clear differential expression profiles observed in our study. Whereas in the fibrotic fibroblasts an anti-apoptotic survival gene program is maintained, which may be a result of the suppressed ISGs, this gene program may not be subject to repression in the normal fibroblasts.

While an accepted source of control tissue in studies of ILD [10,12], the use of control fibroblasts from cancer resected specimens, rather than from healthy control subjects (not available for this study), represents a potential limitation. Although obtained from areas of lung with normal histological appearance, differential gene expression in fibroblasts derived from lungs in which cancer has developed cannot be excluded. However, significant gene expression differences were observed in lung cancer associated fibroblasts compared to matched fibroblasts from areas of normal lung from the same patient, suggesting that the cancer associated phenotype of lung fibroblasts is regionally limited to the cancer stroma [54]. A further possible source of bias in gene expression is smoking history. Smoking has been shown to be associated with interstitial fibrotic changes [55], and is itself likely to cause changes in the expression of certain genes. We observed no significant differences among differentially expressed genes according to smoking status in the pooled fibrotic samples, suggesting that the observed changes were related to the fibrotic lung disease itself rather than to smoking. However, as subgroup numbers were small, and it was not possible to separately analyse the two fibrotic lung diseases, further studies are needed to carefully assess the contribution of smoking to gene expression changes in the context of fibrotic lung disease.

While the general hypothesis, that a repressed interferon stimulated gene program at least in part underpins

the fibrotic fibroblast phenotype, will be tested in future studies, it is interesting to note the same phenomenon in several other clinical settings where hyperplasia and apoptosis resistance are key features; certain viruses, including high-risk human papillomaviruses (HPV), have evolved a mechanism to down-regulate ISGs in host cells as an immunoevasive strategy [56], and persistent HPV infection may lead to cervical cancer development; breast cancer metastasis is promoted by *IRF7* silencing [57]; fibroblasts from patients with Li-Fraumeni syndrome become spontaneously immortalised through the downregulation of interferon pathway genes [58]. Conversely, *IRF1* expression reverts the phenotype of oncogenically transformed fibroblasts [59], and IRF-1 enhancing drugs with tumour suppressing properties are currently being developed [60]. Many similar examples in the literature lead to questions about whether fibrosis is a pre-cancerous state [61]. The repressed, or aberrantly regulated, fibroblast specific interferon response network may therefore be a common necessary determinant allowing lung fibrosis progression to occur.

In summary, in this study comparing gene expression profiles of fibroblasts explanted from fibrotic lung tissue (SSc-ILD and IPF), with control fibroblasts from areas of normal lung, we observe: an overall elevated expression of previously reported fibrosis associated genes, with marked heterogeneity across samples; differentially regulated myofibroblast markers which correlate with the expression heterogeneity between samples; and a strongly suppressed interferon stimulated gene program, uniformly present across fibrotic samples. This suppressed gene program displays both the greatest significance and largest fold differences in expression in our data set. Similarly to functional findings in parallel fields, particularly cancer, this group of genes, and the suppression of their expression, could explain essential aspects of the profibrotic fibroblast phenotype. This hypothesis will need to be tested by future studies, with particular focus on epigenetic silencing as a potential underlying mechanism.

Additional files

Additional file 1: Genes differentially expressed in SSc-ILD. Word file, .txt extension. This data set contains all of the genes up- or down-regulated in SSc-ILD fibroblasts compared to control fibroblasts. Included are p-values from dChip analysis and q-values from SAM analysis.

Additional file 2: Genes differentially expressed in IPF. Word file, .txt extension. This data set contains all of the genes up- or down- regulated in IPF fibroblasts compared to control fibroblasts. Included are p-values from dChip analysis and q-values from SAM analysis.

Additional file 3: Genes differentially expressed between IPF and SSc-ILD. Word file, .txt extension. This data set contains all of the genes up- or down- regulated in IPF fibroblasts compared to SSc-ILD fibroblasts. Included are p-values from dChip analysis and q-values from SAM analysis.

Additional file 4: Summary of differentially expressed genes in SSc-ILD and IPF. Word file, .txt extension. This data set contains all of the genes up- or down- regulated in fibroblasts from at least one disease group compared to control fibroblasts. Included are p-values from dChip analysis and q-values from SAM analysis.

Additional file 5: Functional annotation clustering analysis. Excel file, .xlsx extension. Using the DAVID functional annotation tool, genes over and under expressed in SSc-ILD and IPF compared to controls were clustered according to Gene Ontology biological process terms. Shown are the enriched terms within each annotation cluster with an EASE score threshold of ≤ 0.01, and an initial group membership of 5.

Additional file 6: Differentially expressed genes present in Interferome. Excel file, .xlsx extension. The data set contains all of the genes differentially expressed genes in SSc-ILD and IPF fibroblasts compared to control fibroblasts which have been shown experimentally to be regulated by interferons listed in the INTERFEROME database.

Abbreviations

DAVID: Database for annotation, visualisation, and integrated discovery; ECM: Extracellular matrix; GO: Gene ontology; IPF: Idiopathic pulmonary fibrosis; IRG: Interferon regulated genes; ISG: Interferon stimulated gene; NSIP: Nonspecific interstitial pneumonia; PH: Pulmonary hypertension; SAM: Significance analysis of microarrays; SSc: Systemic sclerosis; SSc-ILD: Interstitial lung disease in SSc; UIP: Usual interstitial pneumonia.

Competing interests

The authors declare that they have no competing interests.

Authors' contributions

GEL CJWS contributed to design, data generation, and data analysis of the study, and wrote and prepared the manuscript. XS performed all explant cell preparations, cell culture experiments and western blot analyses. PS contributed to data analysis and interpretation, and critical review of the manuscript. PL SLH contributed to the verification of the microarray data and valuable discussions. GG participated in the microarray work. AGN contributed human lung tissue samples and expert histopathological typing. CPD and JCG contributed patient material and information. DJA, CPD AUW TMM contributed to design and critical supervision of the study. EAR designed the study, performed experimental work and wrote the manuscript. All authors contributed to critical revision of the manuscript. All authors read and approved the final manuscript.

Acknowledgements

This work was supported by the Royal Brompton & Harefield Clinical Research Fund (RBHCRF), the Raynaud's and Scleroderma Association (RSA), the Scleroderma Society, and by the Arthritis Research Council (now AR UK). EAR was funded by a project grant from RSA. CS and PL were funded by a program grant from RSA. The study was also supported by the Respiratory Biomedical Research Unit at Royal Brompton & Harefield NHS Foundation Trust. We would like to thank the Microarray Centre, Genomics Laboratory (CSC, MRC, Imperial College London and Hammersmith Hospital) for support with the microarray analysis.

Author details

[1]Interstitial Lung Disease Unit, Royal Brompton Hospital and National Heart and Lung Institute, Imperial College London, Emmanuel Kaye Building, 1B Manresa Road, London SW3 6LR, UK. [2]Centre for Rheumatology and Connective Tissue Diseases, Royal Free Campus, University College London Medical School, London NW3 2PF, UK. [3]Respiratory Medicine Department, Ospedale "Le Scotte", University of Siena, Siena, Italy. [4]Institute of Pharmaceutical Science, King's College London, Franklin-Wilkins Building, 150 Stamford Street, London SE1 9NH, UK. [5]Kennedy Institute of Rheumatology, University of Oxford, 65 Aspenlea Road, London W6 8HL, UK. [6]Histopathology Department, Royal Brompton Hospital and National Heart and Lung Institute, Imperial College London, Emmanuel Kaye Building, 1B Manresa Road, London SW3 6LR, UK. [7]Center of Interstitial Lung Diseases, St. Antonius Hospital Nieuwegein, and Division of Heart and Lungs, University Medical Centre Utrecht, Utrecht, NL, Netherlands.

Received: 8 December 2012 Accepted: 25 July 2013
Published: 2 August 2013

References

1. Steen VD, Medsger TA: **Changes in causes of death in systemic sclerosis, 1972–2002.** *Ann Rheum Dis* 2007, **66**:940–944.
2. Tan A, Denton CP, Mikhailidis DP, Seifalian AM: **Recent advances in the diagnosis and treatment of interstitial lung disease in systemic sclerosis (scleroderma): a review.** *Clin Exp Rheumatol* 2011, **29**:S66–S74.
3. Bouros D, Wells AU, Nicholson AG, Colby TV, Polychronopoulos V, Pantelidis P, Haslam PL, Vassilakis DA, Black CM, du Bois RM: **Histopathologic subsets of fibrosing alveolitis in patients with systemic sclerosis and their relationship to outcome.** *Am J Respir Crit Care Med* 2002, **165**:1581–1586.
4. du Bois RM: **Mechanisms of scleroderma-induced lung disease.** *Proc Am Thorac Soc* 2007, **4**:434–438.
5. Scotton CJ, Chambers RC: **Molecular targets in pulmonary fibrosis: the myofibroblast in focus.** *Chest* 2007, **132**:1311–1321.
6. Datta A, Scotton CJ, Chambers RC: **Novel therapeutic approaches for pulmonary fibrosis.** *Br J Pharmacol* 2011, **163**:141–172.
7. Sargent JL, Whitfield ML: **Capturing the heterogeneity in systemic sclerosis with genome-wide expression profiling.** *Expert Rev Clin Immunol* 2011, **7**:463–473.
8. Kaminski N, Rosas IO: **Gene expression profiling as a window into idiopathic pulmonary fibrosis pathogenesis: can we identify the right target genes?** *Proc Am Thorac Soc* 2006, **3**:339–344.
9. Zuo F, Kaminski N, Eugui E, Allard J, Yakhini Z, Ben-Dor A, Lollini L, Morris D, Kim Y, DeLustro B, Sheppard D, Pardo A, Selman M, Heller RA: **Gene expression analysis reveals matrilysin as a key regulator of pulmonary fibrosis in mice and humans.** *Proc Natl Acad Sci U S A* 2002, **99**:6292–6297.
10. Pardo A, Gibson K, Cisneros J, Richards TJ, Yang Y, Becerril C, Yousem S, Herrera I, Ruiz V, Selman M, Kaminski N: **Up-regulation and profibrotic role of osteopontin in human idiopathic pulmonary fibrosis.** *PLoS Med* 2005, **2**:e251.
11. Bridges RS, Kass D, Loh K, Glackin C, Borczuk AC, Greenberg S: **Gene expression profiling of pulmonary fibrosis identifies Twist1 as an antiapoptotic molecular "rectifier" of growth factor signaling.** *Am J Pathol* 2009, **175**:2351–2361.
12. Yu G, Kovkarova-Naumovski E, Jara P, Parwani A, Kass D, Ruiz V, Lopez-Otin C, Rosas IO, Gibson KF, Cabrera S, Ramirez R, Yousem SA, Richards TJ, Chensny LJ, Selman M, Kaminski N, Pardo A: **MMP19 is a key regulator of lung fibrosis in mice and humans.** *Am J Respir Crit Care Med* 2012, **186**:752–762.
13. Maher TM, Wells AU, Laurent GJ: **Idiopathic pulmonary fibrosis: multiple causes and multiple mechanisms?** *Eur Respir J* 2007, **30**:835–839.
14. Lynch JP III, Saggar R, Weigt SS, Zisman DA, White ES: **Usual interstitial pneumonia.** *Semin Respir Crit Care Med* 2006, **27**:634–651.
15. Hsu E, Shi H, Jordan RM, Lyons-Weiler J, Pilewski JM, Feghali-Bostwick CA: **Lung tissues in patients with systemic sclerosis have gene expression patterns unique to pulmonary fibrosis and pulmonary hypertension.** *Arthritis Rheum* 2011, **63**:783–794.
16. Saha B, Jyothi PS, Chandrasekar B, Nandi D: **Gene modulation and immunoregulatory roles of interferon gamma.** *Cytokine* 2010, **50**:1–14.
17. Subcommittee for scleroderma criteria of the American Rheumatism Association Diagnostic and Therapeutic Criteria Committee: **Preliminary criteria for the classification of systemic sclerosis (scleroderma).** *Arthritis Rheum* 1980, **23**:581–590.
18. American Thoracic Society: **Idiopathic pulmonary fibrosis: diagnosis and treatment. International consensus statement. American Thoracic Society (ATS), and the European Respiratory Society (ERS).** *Am J Respir Crit Care Med* 2000, **161**:646–664.
19. American Thoracic Society/European Respiratory Society International Multidisciplinary Consensus Classification of the Idiopathic Interstitial Pneumonias: **This joint statement of the American Thoracic Society (ATS), and the European Respiratory Society (ERS) was adopted by the ATS board of directors, June 2001 and by the ERS Executive Committee, June 2001.** *Am J Respir Crit Care Med* 2002, **165**:277–304.
20. Abraham DJ, Shiwen X, Black CM, Sa S, Xu Y, Leask A: **Tumor necrosis factor alpha suppresses the induction of connective tissue growth factor by transforming growth factor-beta in normal and scleroderma fibroblasts.** *J Biol Chem* 2000, **275**:15220–15225.
21. Shi-wen X, Pennington D, Holmes A, Leask A, Bradham D, Beauchamp JR, Fonseca C, du Bois RM, Martin GR, Black CM, Abraham DJ: **Autocrine overexpression of CTGF maintains fibrosis: RDA analysis of fibrosis genes in systemic sclerosis.** *Exp Cell Res* 2000, **259**:213–224.
22. Li C, Wong WH: **Model-based analysis of oligonucleotide arrays: expression index computation and outlier detection.** *Proc Natl Acad Sci U S A* 2001, **98**:31–36.
23. Tusher VG, Tibshirani R, Chu G: **Significance analysis of microarrays applied to the ionizing radiation response.** *Proc Natl Acad Sci U S A* 2001, **98**:5116–5121.
24. NCBI: *GEO Gene Expression Omnibus.* [http://www.ncbi.nlm.nih.gov/geo/]
25. Huang dW, Sherman BT, Lempicki RA: **Systematic and integrative analysis of large gene lists using DAVID bioinformatics resources.** *Nat Protoc* 2009, **4**:44–57.
26. Huang dW, Sherman BT, Lempicki RA: **Bioinformatics enrichment tools: paths toward the comprehensive functional analysis of large gene lists.** *Nucleic Acids Res* 2009, **37**:1–13.
27. Ashburner M, Ball CA, Blake JA, Botstein D, Butler H, Cherry JM, Davis AP, Dolinski K, Dwight SS, Eppig JT, Harris MA, Hill DP, Issel-Tarver L, Kasarskis A, Lewis S, Matese JC, Richardson JE, Ringwald M, Rubin GM, Sherlock G: **Gene ontology: tool for the unification of biology. The Gene Ontology Consortium.** *Nat Genet* 2000, **25**:25–29.
28. Samarajiwa SA, Forster S, Auchettl K, Hertzog PJ: **INTERFEROME: the database of interferon regulated genes.** *Nucleic Acids Res* 2009, **37**:D852–D857.
29. Vandesompele J, De PK, Pattyn F, Poppe B, Van RN, De PA, Speleman F: **Accurate normalization of real-time quantitative RT-PCR data by geometric averaging of multiple internal control genes.** *Genome Biol* 2002, **3**:RESEARCH0034.
30. Stock CJ, Leoni P, Shi-wen X, Abraham DJ, Nicholson AG, Wells AU, Renzoni EA, Lindahl GE: **Identification of stable housekeeping genes for real-time PCR in human pulmonary fibroblasts [abstract].** *Eur Respir J* 2011, **38**(Suppl. 55):3805.
31. Chambers RC, Leoni P, Kaminski N, Laurent GJ, Heller RA: **Global expression profiling of fibroblast responses to transforming growth factor-beta1 reveals the induction of inhibitor of differentiation-1 and provides evidence of smooth muscle cell phenotypic switching.** *Am J Pathol* 2003, **162**:533–546.
32. Renzoni EA, Abraham DJ, Howat S, Shi-wen X, Sestini P, Bou-Gharios G, Wells AU, Veeraraghavan S, Nicholson AG, Denton CP, Leask A, Pearson JD, Black CM, Welsh KI, du Bois RM: **Gene expression profiling reveals novel TGFbeta targets in adult lung fibroblasts.** *Respir Res* 2004, **5**:24.
33. Pieperhoff S, Barth M, Rickelt S, Franke WW: **Desmosomal molecules in and out of adhering junctions: normal and diseased States of epidermal, cardiac and mesenchymally derived cells.** *Dermatol Res Pract* 2010, **2010**:139167.
34. Leask A, Abraham DJ: **TGF-beta signaling and the fibrotic response.** *FASEB J* 2004, **18**:816–827.
35. Shi-wen X, Kennedy L, Renzoni EA, Bou-Gharios G, du Bois RM, Black CM, Denton CP, Abraham DJ, Leask A: **Endothelin is a downstream mediator of profibrotic responses to transforming growth factor beta in human lung fibroblasts.** *Arthritis Rheum* 2007, **56**:4189–4194.
36. Hinz B, Phan SH, Thannickal VJ, Prunotto M, Desmouliere A, Varga J, De WO, Mareel M, Gabbiani G: **Recent developments in myofibroblast biology: paradigms for connective tissue remodeling.** *Am J Pathol* 2012, **180**:1340–1355.
37. Balestrini JL, Chaudhry S, Sarrazy V, Koehler A, Hinz B: **The mechanical memory of lung myofibroblasts.** *Integr Biol (Camb)* 2012, **4**:410–421.
38. Phan SH: **Genesis of the myofibroblast in lung injury and fibrosis.** *Proc Am Thorac Soc* 2012, **9**:148–152.
39. Perk J, Iavarone A, Benezra R: **Id family of helix-loop-helix proteins in cancer.** *Nat Rev Cancer* 2005, **5**:603–614.
40. Mern DS, Hasskarl J, Burwinkel B: **Inhibition of Id proteins by a peptide aptamer induces cell-cycle arrest and apoptosis in ovarian cancer cells.** *Br J Cancer* 2010, **103**:1237–1244.
41. Crestani B, Besnard V, Boczkowski J: **Signalling pathways from NADPH oxidase-4 to idiopathic pulmonary fibrosis.** *Int J Biochem Cell Biol* 2011, **43**:1086–1089.
42. Laleu B, Gaggini F, Orchard M, Fioraso-Cartier L, Cagnon L, Houngninou-Molango S, Gradia A, Duboux G, Merlot C, Heitz F, Szyndralewiez C, Page P: **First in class, potent, and orally bioavailable NADPH oxidase isoform 4 (Nox4) inhibitors for the treatment of idiopathic pulmonary fibrosis.** *J Med Chem* 2010, **53**:7715–7730.

43. Engelmann A, Speidel D, Bomkamm GW, Deppert W, Stocking C: **Gadd45 beta is a pro-survival factor associated with stress-resistant tumors.** *Oncogene* 2008, **27**:1429–1438.
44. Whitfield ML, Finlay DR, Murray JI, Troyanskaya OG, Chi JT, Pergamenschikov A, McCalmont TH, Brown PO, Botstein D, Connolly MK: **Systemic and cell type-specific gene expression patterns in scleroderma skin.** *Proc Natl Acad Sci U S A* 2003, **100**:12319–12324.
45. Gardner H, Shearstone JR, Bandaru R, Crowell T, Lynes M, Trojanowska M, Pannu J, Smith E, Jablonska S, Blaszczyk M, Tan FK, Mayes MD: **Gene profiling of scleroderma skin reveals robust signatures of disease that are imperfectly reflected in the transcript profiles of explanted fibroblasts.** *Arthritis Rheum* 2006, **54**:1961–1973.
46. Tan FK, Zhou X, Mayes MD, Gourh P, Guo X, Marcum C, Jin L, Arnett FC Jr: **Signatures of differentially regulated interferon gene expression and vasculotrophism in the peripheral blood cells of systemic sclerosis patients.** *Rheumatology (Oxford)* 2006, **45**:694–702.
47. York MR, Nagai T, Mangini AJ, Lemaire R, van Seventer JM, Lafyatis R: **A macrophage marker, Siglec-1, is increased on circulating monocytes in patients with systemic sclerosis and induced by type I interferons and toll-like receptor agonists.** *Arthritis Rheum* 2007, **56**:1010–1020.
48. Keane MP, Arenberg DA, Lynch JP III, Whyte RI, Iannettoni MD, Burdick MD, Wilke CA, Morris SB, Glass MC, DiGiovine B, Kunkel SL, Strieter RM: **The CXC chemokines, IL-8 and IP-10, regulate angiogenic activity in idiopathic pulmonary fibrosis.** *J Immunol* 1997, **159**:1437–1443.
49. Coward WR, Watts K, Feghali-Bostwick CA, Jenkins G, Pang L: **Repression of IP-10 by interactions between histone deacetylation and hypermethylation in idiopathic pulmonary fibrosis.** *Mol Cell Biol* 2010, **30**:2874–2886.
50. Tager AM, Kradin RL, LaCamera P, Bercury SD, Campanella GS, Leary CP, Polosukhin V, Zhao LH, Sakamoto H, Blackwell TS, Luster AD: **Inhibition of pulmonary fibrosis by the chemokine IP-10/CXCL10.** *Am J Respir Cell Mol Biol* 2004, **31**:395–404.
51. Walters DM, Antao-Menezes A, Ingram JL, Rice AB, Nyska A, Tani Y, Kleeberger SR, Bonner JC: **Susceptibility of signal transducer and activator of transcription-1-deficient mice to pulmonary fibrogenesis.** *Am J Pathol* 2005, **167**:1221–1229.
52. Spagnolo P, Del GC, Luppi F, Cerri S, Balduzzi S, Walters EH, D'Amico R, Richeldi L: **Non-steroid agents for idiopathic pulmonary fibrosis.** *Cochrane Database Syst Rev* 2010, **9**:CD003134.
53. Black CM, Silman AJ, Herrick AI, Denton CP, Wilson H, Newman J, Pompon L, Shi-wen X: **Interferon-alpha does not improve outcome at one year in patients with diffuse cutaneous scleroderma: results of a randomized, double-blind, placebo-controlled trial.** *Arthritis Rheum* 1999, **42**:299–305.
54. Navab R, Strumpf D, Bandarchi B, Zhu CQ, Pintilie M, Ramnarine VR, Ibrahimov E, Radulovich N, Leung L, Barczyk M, Panchal D, To C, Yun JJ, Der S, Shepherd FA, Jurisica I, Tsao MS: **Prognostic gene-expression signature of carcinoma-associated fibroblasts in non-small cell lung cancer.** *Proc Natl Acad Sci U S A* 2011, **108**:7160–7165.
55. Katzenstein AL, Mukhopadhyay S, Zanardi C, Dexter E: **Clinically occult interstitial fibrosis in smokers: classification and significance of a surprisingly common finding in lobectomy specimens.** *Hum Pathol* 2010, **41**:316–325.
56. Reiser J, Hurst J, Voges M, Krauss P, Munch P, Iftner T, Stubenrauch F: **High-risk human papillomaviruses repress constitutive kappa interferon transcription via E6 to prevent pathogen recognition receptor and antiviral-gene expression.** *J Virol* 2011, **85**:11372–11380.
57. Bidwell BN, Slaney CY, Withana NP, Forster S, Cao Y, Loi S, Andrews D, Mikeska T, Mangan NE, Samarajiwa SA, de Weerd NA, Gould J, Argani P, Moller A, Smyth MJ, Anderson RL, Hertzog PJ, Parker BS: **Silencing of Irf7 pathways in breast cancer cells promotes bone metastasis through immune escape.** *Nat Med* 2012, **18**:1224–1231.
58. Kulaeva OI, Draghici S, Tang L, Kraniak JM, Land SJ, Tainsky MA: **Epigenetic silencing of multiple interferon pathway genes after cellular immortalization.** *Oncogene* 2003, **22**:4118–4127.
59. Kroger A, Dallugge A, Kirchhoff S, Hauser H: **IRF-1 reverts the transformed phenotype of oncogenically transformed cells in vitro and in vivo.** *Oncogene* 2003, **22**:1045–1056.
60. Gao J, Wang Y, Xing Q, Yan J, Senthil M, Akmal Y, Kowolik CM, Kang J, Lu DM, Zhao M, Lin Z, Cheng CH, Yip ML, Yim JH: **Identification of a natural compound by cell-based screening that enhances interferon regulatory factor-1 activity and causes tumor suppression.** *Mol Cancer Ther* 2011, **10**:1774–1783.
61. Vancheri C: **Idiopathic pulmonary fibrosis: an altered fibroblast proliferation linked to cancer biology.** *Proc Am Thorac Soc* 2012, **9**:153–157.

doi:10.1186/1465-9921-14-80
Cite this article as: Lindahl *et al.*: Microarray profiling reveals suppressed interferon stimulated gene program in fibroblasts from scleroderma-associated interstitial lung disease. *Respiratory Research* 2013 **14**:80.

Article

Cell Reports

Proteolytic Cleavage Governs Interleukin-11 Trans-signaling

Graphical Abstract

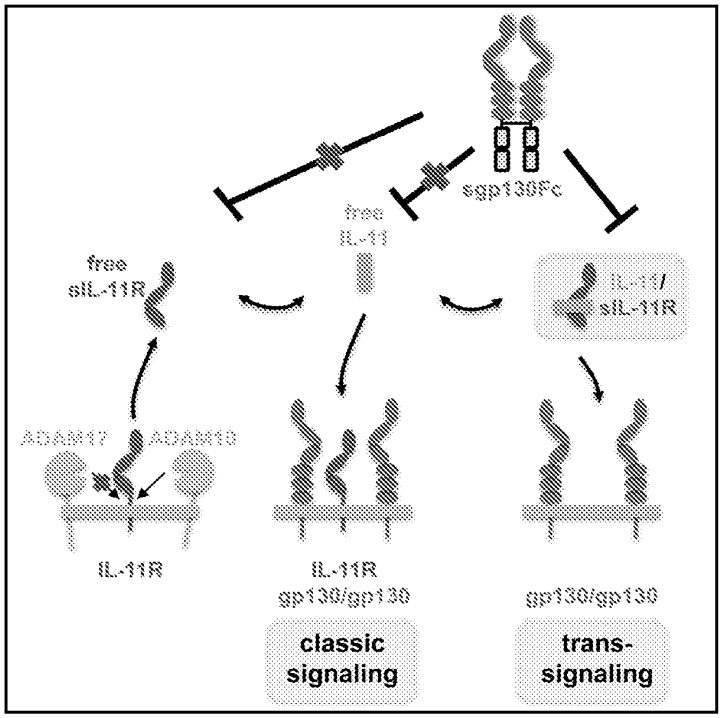

Authors

Juliane Lokau, Rebecca Nitz, Maria Agthe, ..., Stefan Rose-John, Jürgen Scheller, Christoph Garbers

Correspondence

jscheller@uni-duesseldorf.de (J.S.), cgarbers@biochem.uni-kiel.de (C.G.)

In Brief

Lokau et al. show that the IL-11R can be cleaved from cells by the metalloprotease ADAM10, but not by its close relative ADAM17. The soluble IL-11R ectodomain is able to perform trans-signaling, which can be specifically inhibited by the anti-inflammatory therapeutic compound sgp130Fc.

Highlights

- The IL-11R is a substrate for ADAM10, but not ADAM17
- A juxtamembrane region determines the substrate specificity of ADAM17
- The soluble IL-11R binds IL-11 and initiates IL-11 trans-signaling
- IL-11 trans-signaling can be blocked by the anti-inflammatory therapeutic sgp130Fc

Lokau et al., 2016, Cell Reports *14*, 1761–1773
February 23, 2016
http://dx.doi.org/10.1016/j.celrep.2016.01.053

CellPress

Cell Reports
Article

Proteolytic Cleavage Governs Interleukin-11 Trans-signaling

Juliane Lokau,[1] Rebecca Nitz,[2] Maria Agthe,[3] Niloufar Monhasery,[2] Samadhi Aparicio-Siegmund,[3] Neele Schumacher,[3] Janina Wolf,[1] Katja Möller-Hackbarth,[1] Georg H. Waetzig,[4] Joachim Grötzinger,[1] Gerhard Müller-Newen,[3] Stefan Rose-John,[1] Jürgen Scheller,[2,*] and Christoph Garbers[1,*]
[1]Institute of Biochemistry, Kiel University, 24098 Kiel, Germany
[2]Medical Faculty, Institute of Biochemistry and Molecular Biology II, Heinrich-Heine-University, 40225 Düsseldorf, Germany
[3]Institute of Biochemistry and Molecular Biology, RWTH Aachen, 52074 Aachen, Germany
[4]CONARIS Research Institute AG, 24118 Kiel, Germany
*Correspondence: jscheller@uni-duesseldorf.de (J.S.), cgarbers@biochem.uni-kiel.de (C.G.)
http://dx.doi.org/10.1016/j.celrep.2016.01.053

SUMMARY

Interleukin (IL)-11 has been shown to be a crucial factor for intestinal tumorigenesis, lung carcinomas, and asthma. IL-11 is thought to exclusively mediate its biological functions through cell-type-specific expression of the membrane-bound IL-11 receptor (IL-11R). Here, we show that the metalloprotease ADAM10, but not ADAM17, can release the IL-11R ectodomain. Chimeric proteins of the IL-11R and the IL-6 receptor (IL-6R) revealed that a small juxtamembrane portion is responsible for this substrate specificity of ADAM17. Furthermore, we show that the serine proteases neutrophil elastase and proteinase 3 can also cleave the IL-11R. The resulting soluble IL-11R (sIL-11R) is biologically active and binds IL-11 to activate cells. This IL-11 trans-signaling pathway can be inhibited specifically by the anti-inflammatory therapeutic compound sgp130Fc. In conclusion, proteolysis of the IL-11R represents a molecular switch that controls the IL-11 trans-signaling pathway and widens the number of cells that can be activated by IL-11.

INTRODUCTION

Cytokines of the interleukin (IL)-6 family are critically involved in health and disease, fulfilling pro- as well as anti-inflammatory functions (Garbers and Scheller, 2013; Scheller et al., 2014). IL-11, one of its members, can be secreted upon stimulation by a variety of cells, including epithelial cells of the lung and the gastrointestinal tract, or fibroblasts of skin and lung (Putoczki and Ernst, 2015). Upon secretion, IL-11 binds to a membrane-bound IL-11R, which is expressed in a cell-type-specific manner and has been detected in many organs, e.g., bone, heart, lung, spleen, gastrointestinal tract, and uterus (Davidson et al., 1997; Garbers and Scheller, 2013; Putoczki and Ernst, 2015). After formation of the IL-11/IL-11 receptor (IL-11R) complex, signaling is initiated through recruitment of two molecules of the common β-receptor gp130, which leads to the activation of the Janus kinase/signal transducer and activator of transcription (Jak/STAT) pathway and the mitogen-activated protein kinase (MAPK) cascade.

Overshooting activities of IL-11 have been shown to be critically involved in the development of epithelial cancers (Nakayama et al., 2007), especially in gastrointestinal tumorigenesis in mice and humans (Ernst et al., 2008; Ernst and Putoczki, 2014; Howlett et al., 2009; Putoczki et al., 2013). Genetic depletion of the IL-11R or treatment with an inhibitory IL-11 mutein was sufficient to prevent IL-11-dependent tumor formation (Ernst et al., 2008; Putoczki et al., 2013). Furthermore, IL-11 has a profound role in the lung (Garbers and Scheller, 2013). Transgenic expression of IL-11 under a lung-specific promoter led to lung fibrosis and airway obstruction (Tang et al., 1996), mimicking the pathology found in human asthma patients, where IL-11 expression correlates with disease severity (Minshall et al., 2000).

Besides IL-11, IL-6 is the only other cytokine of the family that signals via a gp130 homodimer. Signaling can be initiated through membrane-bound IL-6 receptor (IL-6R) (classic signaling), which is mainly found on hepatocytes and several leukocyte subsets, and soluble forms of the IL-6R (trans-signaling). IL-6 binds to the soluble and the membrane-bound IL-6R with similar affinity, and both complexes activate cells via gp130 homodimerization (Jostock et al., 2001; Taga et al., 1989). Due to the ubiquitous expression of gp130, IL-6 trans-signaling can activate virtually all cells of the body, and this mainly accounts for the pro-inflammatory properties of the cytokine (Rose-John, 2012). Consequently, the specific inhibition of IL-6 trans-signaling via a dimerized variant of soluble gp130 (sgp130Fc) has been shown to be sufficient to block IL-6-driven inflammatory diseases (Jones et al., 2011). Selective blockade of IL-6 trans-signaling might be even superior compared to global IL-6 inhibition, and an optimized sgp130Fc variant is currently in clinical development.

Soluble forms of the IL-6R are found in human serum at high concentrations of about 30–70 ng/ml and are either generated by alternative splicing of the IL-6R mRNA (~10%) or by limited proteolysis of membrane-bound protein precursors (~90%), also known as ectodomain shedding (Chalaris et al., 2011). Major proteases of the IL-6R are the two metalloproteases ADAM10

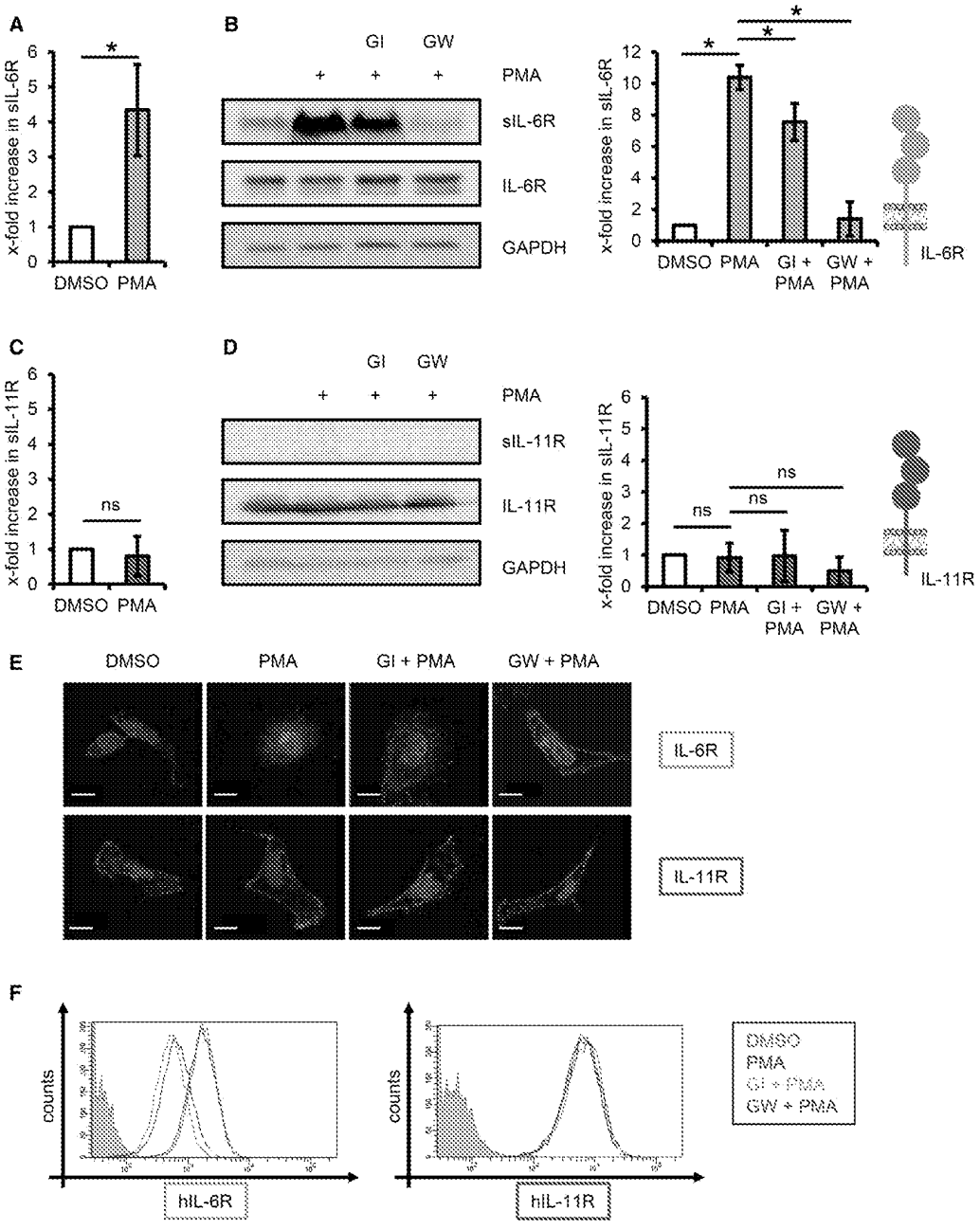

Figure 1. The IL-11R Is No Substrate for ADAM17

(A) HEK293 cells were transiently transfected with a plasmid encoding the human IL-6R and treated with 100 nM PMA for 2 hr. Soluble receptors in the cell-culture supernatant were analyzed by ELISA. The amount of soluble receptor without stimulation was set to 1, and the increase after PMA stimulation was calculated accordingly (n = 3, mean ± SD). *$p < 0.05$.

(B) The experiment was performed as described in (A), but the cells were pre-treated for 30 min with the metalloprotease inhibitors GI and GW where indicated. Soluble IL-6R was precipitated from cell-culture supernatant and visualized by western blot. Cells were lysed, and IL-6R expression was also determined via western blot. GAPDH served as loading control. Western blots from three independent experiments were quantified (mean ± SD). *$p < 0.05$.

(C and D) HEK293 cells were transiently transfected with a plasmid encoding the human IL-11R, and experiments were performed as described for (A) and (B). Error bars indicate mean ± SD. ns, not significant.

(legend continued on next page)

and ADAM17, which release the IL-6R ectodomain from cells (Baran et al., 2013; Garbers et al., 2011a; Matthews et al., 2003). However, the neutrophil-derived serine protease cathepsin G (CG) is also capable of cleaving the IL-6R (Sarik et al., 1999). Despite the detection of an mRNA that encodes a soluble IL-11R (sIL-11R) (Robb et al., 1996), no natural soluble forms of the IL-11R have been described. In vitro experiments with recombinant proteins have shown, however, that IL-11, in combination with sIL-11R, is an agonistic cytokine that induces signaling in cells that do not respond to IL-11 alone (Dams-Kozlowska et al., 2012; Kurth et al., 1999; Pflanz et al., 1999).

In this report, we show that the IL-11R is a substrate for ADAM10, but cannot be cleaved by the related protease ADAM17, and we identify structural traits for this substrate specificity. The cleaved sIL-11R binds IL-11 and induces cellular proliferation via gp130 in a STAT3-dependent manner, which can be completely and specifically blocked by the IL-6 trans-signaling inhibitor sgp130Fc. Finally, we identify the neutrophil serine proteases neutrophil elastase (NE) and proteinase 3 (PR3) as additional sheddases of the IL-11R. In conclusion, we describe a protease regulation of the IL-11 trans-signaling pathway that widens the spectrum of cells that can be activated by IL-11.

RESULTS

The IL-11R Is Not a Substrate for the Metalloprotease ADAM17

It is well established that IL-6 can signal through membrane-bound as well as soluble forms of the IL-6R and that these two modes of signaling possess striking differences with regard to pathophysiology (Scheller et al., 2011b). Surprisingly, no natural soluble forms of the IL-11 receptor α have been described to date; thus, IL-11 is thought to act solely via its membrane-bound IL-11R. To elucidate whether an sIL-11R could be generated, we investigated the proteolysis of the membrane-bound IL-11R by members of the ADAM family of proteases. We focused on ADAM17, which is the major protease of the IL-6R. To compare the proteolyses of IL-6R to that of IL-11R, we first expressed IL-6R in HEK293 cells and stimulated them with the phorbolester phorbol 12-myristate 13-acetate (PMA), the strongest known activator of ADAM17. We detected a significant 4.3- ± 1.3-fold increase in sIL-6R generation after PMA stimulation, using an IL-6R-specific ELISA (Figure 1A), which was confirmed by western blotting of precipitated receptor from the cell supernatant (Figure 1B). Pre-incubation with the ADAM10-specific inhibitor GI254023X (GI) did not block IL-6R proteolysis, but the combined ADAM10/17-specific inhibitor GW280264X (GW) was able to completely abolish PMA-induced shedding, thus confirming ADAM17 as the PMA-induced protease of the IL-6R (Figure 1B) (Garbers et al., 2011a; Müllberg et al., 1993). In contrast, HEK293 cells transfected with an IL-11R expression plasmid showed no significant increase in sIL-11R after PMA stimulation for 2 hr (0.8- ± 0.6-fold; Figure 1C). In line with this, we could not precipitate sIL-11R from cell-culture supernatant (Figure 1D). We detected some sIL-11R after longer stimulation with PMA for up to 24 hr (Figure S1A). However, the amounts were negligible compared to sIL-6R generation (Figures S1B and S1C). We verified our observations by overexpression of both receptors in HeLa cells. IL-6R and the IL-11R were localized at the plasma membrane (Figure 1E). The IL-6R was lost from the cell surface upon PMA stimulation, which could be prevented by pre-incubation with GW but not with GI. In contrast, stimulation of ADAM17 by PMA did not alter the IL-11R levels at the plasma membrane, which confirms that the IL-11R is usually not a substrate for ADAM17 (Figure 1E). As a final proof, we investigated limited proteolysis after PMA stimulation on cells expressing both cytokine receptors endogenously. The human monocytic cell line THP-1 expresses IL-6R and IL-11R (Jones et al., 1998; Karjalainen et al., 2015), and only the IL-6R was lost from the cell surface upon stimulation with PMA, which was, again, sensitive toward GW-mediated inhibition of ADAM17 (Figure 1F). In conclusion, we provide evidence that the IL-11R is not a substrate for the metalloprotease ADAM17.

The Stalk Regions of IL-6R and IL-11R Determine Susceptibility toward Cleavage by ADAM17

To determine which regions are responsible for the difference in the proteolytic processing observed between IL-6R and IL-11R, we constructed four chimeric receptors based on the IL-6R (Figure 2A). We replaced the transmembrane region (termed IL-6R-TM), the intracellular region (IL-6R-ICD), the stalk region (IL-6R-S), or just the ten juxtamembrane amino acid residues Val-356 to Pro-365 (IL-6R-10AS) with their IL-11R counterparts. When transfected in HEK293 cells, both IL-6R-TM and IL-6R-ICD were shed after stimulation with PMA, as analyzed by ELISA and western blot (Figures 2B–2E), indicating that neither the transmembrane nor the intracellular regions of the IL-6R and the IL-11R were important for ADAM17 to discriminate between substrate and non-substrate. This is in line with previous studies showing that the intracellular domain of the IL-6R is dispensable for PMA-mediated shedding (Garbers et al., 2011a; Müllberg et al., 1993). In contrast, IL-6R-S was resistant toward proteolysis by ADAM17 (1.2- ± 0.2-fold increase; Figure 2F), which suggests that a motif within the stalk region of the IL-11R prevents ADAM17-mediated proteolysis and that this can be transferred to the IL-6R. Because the cleavage site of ADAM17 within the IL-6R stalk is known (Müllberg et al., 1994), we swapped only ten amino acid residues from the IL-6R, which included its cleavage site Asp-358/Gln-359, with their IL-11R counterpart (IL-6R-10AS). As shown in Figure 2G, stimulation of IL-6R-10AS-transfected HEK293 cells with PMA resulted in an 1.1- ± 0.1-fold increase, demonstrating that this mutation was sufficient to efficiently prevent proteolysis by ADAM17. These data

(E) HeLa cells were transiently transfected with either IL-6R or IL-11R. Cells were grown on coverslips for 48 hr, stimulated as indicated, and were fixed and stained. Cytokine receptors are stained in red, and the nucleus is stained in blue (DAPI). Scale bars, 10 μm.
(F) THP-1 cells were stimulated with 100 nM PMA with or without pretreatment with the protease inhibitors GI or GW, and cytokine receptor levels at the cell surface were analyzed via flow cytometry.
See also Figure S1.

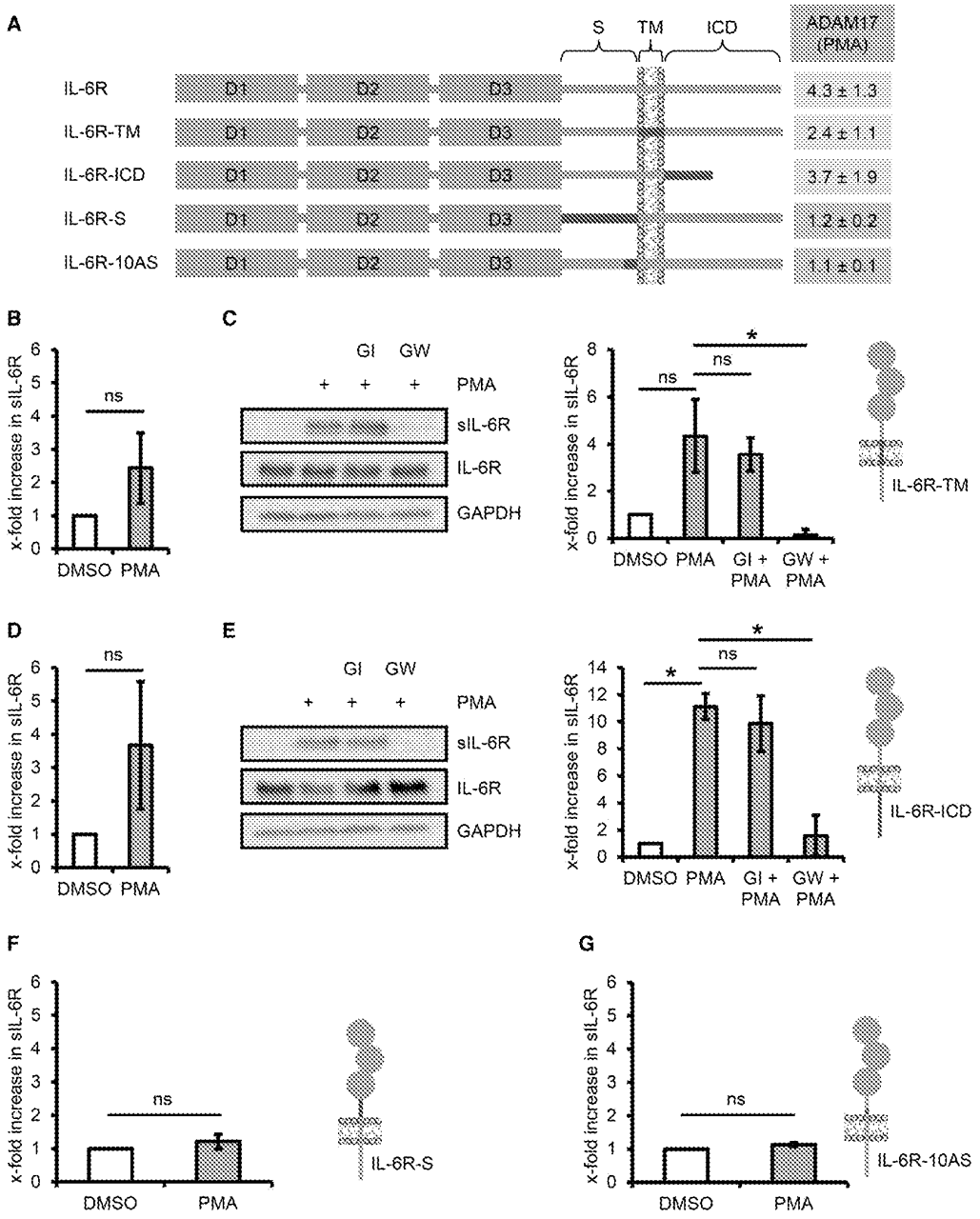

Figure 2. The Stalk Region of the IL-6R Determines Its Cleavage Specificity

(A) Schematic overview of the IL-6R and chimeric variants thereof. IL-6R and IL-11R share the same overall topology, consisting of an immunoglobulin (Ig)-like domain (D1), two fibronectin type III domains (D2 and D3), a stalk (S) region, a transmembrane (TM) region, and an intracellular domain (ICD). The IL-6R is depicted in orange, whereas regions originating from the IL-11R are shown in blue. The values shown besides the chimeras are the x-fold increase after PMA stimulation (mean ± SD, n = 3). To calculate this, the amount of constitutively shed IL-6R or chimera was measured by ELISA and arbitrarily set to 1. The increase after stimulation with PMA was calculated accordingly. Chimeras with at least a 2-fold increase in soluble receptor formation were defined as good substrates for ADAM17 (colored in green), whereas chimeras with values below this were considered weak substrates (colored in red).

(B–G) HEK293 cells were transiently transfected with plasmids encoding IL-6R-TM (B and C), IL-6R-ICD (D and E), IL-6R-S (F), or IL-6R-10AS (G), and the amount of shedding upon PMA stimulation was analyzed by ELISA and western blot, as described in the legend for Figure 1 (mean ± SD). *$p < 0.05$; ns, not significant.

show that replacement of the ADAM17 cleavage site by the corresponding amino acid residues of a non-substrate is sufficient to render the IL-6R unresponsive toward proteolysis by ADAM17.

In light of these results, we sought to analyze whether we could generate an IL-11R mutant that is a substrate for ADAM17. To this end, we first transferred the transmembrane region from the IL-6R to the IL-11R (termed IL-11R-TM; Figure 3A) and analyzed proteolysis in transfected HEK293 cells. Although we observed a 1.9- ± 0.3-fold increase in sIL-11R when we analyzed the supernatant of cells stimulated with PMA (Figure S2A), we could not detect sIL-11R via western blotting after precipitation (Figure S2B). Furthermore, exchange of the intracellular region (IL-11R-ICD) did not result in increased susceptibility toward cleavage by ADAM17 (Figures S2C and S2D). This strongly argues against a role for these two regions, with regard to the substrate specificity of ADAM17, and confirms our results obtained with IL-6R-TM and IL-6R-ICD (Figures 2B–2E).

In contrast, combined transfer of the stalk, the transmembrane, and the intracellular region (IL-11R-S/T/I) or of the stalk region alone (IL-11R-S) resulted in significant cleavage of the IL-11R after PMA stimulation, which was reduced to background levels by treatment with the combined ADAM10/17 inhibitor GW, but not the ADAM10-specific inhibitor GI (Figures 3B and 3C). Strikingly, transfer of ten amino acid residues (Asp-361 to Ala-370, IL-11R-10AS) was sufficient to convert the IL-11R into a substrate for ADAM17 (Figures 3D and 3E). These results indicate that the cleavage site within the stalk region is the critical determinant that distinguishes between substrate and non-substrate. Importantly, this cleavage specificity could be swapped between IL-6R and IL-11R through the exchange of only ten amino acid residues.

The IL-11R Is Cleaved by ADAM10

The human IL-6R is a substrate not only for ADAM17 but also for its close homolog ADAM10 (Garbers et al., 2011a; Matthews et al., 2003). Cellular influx of calcium, mediated by the ionophore ionomycin, is a strong activator of ADAM10-mediated IL-6R shedding (Garbers et al., 2011a; Jones et al., 1998). Therefore, we sought to investigate whether the IL-11R might also be a substrate for ADAM10. First, we verified ADAM10-mediated shedding of the IL-6R after stimulation with ionomycin. HEK293 cells transiently transfected with IL-6R showed ADAM10-mediated proteolysis of the IL-6R, which could be blocked completely by both GI and GW (Figure 4A). Interestingly, we could detect sIL-11R in the supernatant of ionomycin-stimulated HEK293 cells that were transiently transfected with IL-11R (Figure 4B). Generation of the soluble IL-11R ectodomain was significantly diminished when the cells were pre-incubated with GI or GW, strongly arguing for ADAM10 as the responsible protease (Figure 4B).

In order to not solely rely on pharmacological inhibitors, we made use of murine embryonic fibroblasts (MEFs) deficient for either ADAM10 ($A10^{-/-}$), ADAM17 ($A17^{-/-}$), or both ($A10^{-/-}/A17^{-/-}$). As a control, we first stimulated wild-type MEFs transiently transfected with IL-11R with ionomycin and detected sIL-11R generation (Figure 4C). Proteolysis of the IL-11R and subsequent sIL-11R detection in the cell supernatant was significantly diminished in $A10^{-/-}$ MEFs, which was accompanied by elevated amounts of full-length uncleaved IL-11R in the cell lysate (Figure 4C). Stimulation of $A17^{-/-}$ MEFs with ionomycin revealed unaltered sIL-11R generation indistinguishable from wild-type MEFs (Figure 4C). In contrast, we could barely detect sIL-11R in the supernatant of stimulated $A10^{-/-}/A17^{-/-}$ MEFs. Moreover, full-length IL-11R expression in the cell lysate was greatly increased, resembling the findings in the $A10^{-/-}$ MEFs and further strengthening the finding that ADAM10 is the dominant sheddase of the IL-11R. In line with this, stimulation with ionomycin led to the loss of cell-surface expression of both IL-6R and IL-11R in transfected HeLa cells, which could be prevented by both GI and GW (Figure 4D). Furthermore, activation of ADAM10 led to proteolysis of endogenous IL-6R and IL-11R in THP-1 cells (Figure 4E). Taken together, our data identify ADAM10 as a potent sheddase of the IL-11R.

Arg-355 Is Important for ADAM10-Mediated Cleavage of the IL-11R

In order to identify the cleavage site within the IL-11R that is used by ADAM10, we generated three mutants of the IL-11R that contained successive deletions of ten amino acid residues each in the juxtamembrane part of the stalk region (Figure 5A). Removal of the ten amino acid residues Val-363 to Leu-372 (IL-11RΔV363_L372) directly adjacent to the plasma membrane did not influence ionomycin-induced proteolysis of the IL-11R compared to the wild-type (Figure 5B). We observed significantly reduced IL-11R shedding when we deleted the next ten amino acid residues His-353 to Ser-362 (IL-11RΔH353_S362), but we found unaltered proteolysis when the adjacent ten amino acid residues Pro-343 to Pro-352 (IL-11RΔP343_P352) were deleted, suggesting that the ADAM10 cleavage site is located between His-353 and Ser-362 (Figure 5B). Profiling of ADAM10 cleavage sites has revealed a strong preference for arginine residues within the cleavage site, which is not the case for ADAM17 (Tucher et al., 2014). Indeed, when we mutated Arg-355 to a glutamic acid (IL-11R_R355E), which is disfavored in ADAM10 cleavage sites (Tucher et al., 2014), we observed significantly reduced proteolysis of the IL-11R of just 30.9% ± 11.7%, compared to wild-type IL-11R (Figures 5C and 5D; Figure S3B), despite comparable cell-surface expression (Figure S3A). These results suggest that Arg-355 is critical for proteolysis of the IL-11R by ADAM10.

IL-11 Trans-signaling Is Specifically Blocked by sgp130Fc

It has been shown previously that a fusion protein of IL-11 and the IL-11R ectodomain acts as an agonistic cytokine on gp130-expressing cells (Dams-Kozlowska et al., 2012; Kurth et al., 1999; Pflanz et al., 1999). We recapitulated this with recombinant IL-11 and sIL-11R, which were able to stimulate the proliferation of Ba/F3-gp130 cells in a concentration-dependent manner (Figure 6A). Importantly, this mode of IL-11 trans-signaling could be completely and selectively blocked by sgp130Fc (Figure 6B), a designer protein developed previously to block IL-6 trans-signaling through binding and, thus, neutralization of the agonistic IL-6/sIL-6R complex (Garbers et al., 2011b; Jones et al., 2011; Jostock et al., 2001). IL-11-driven

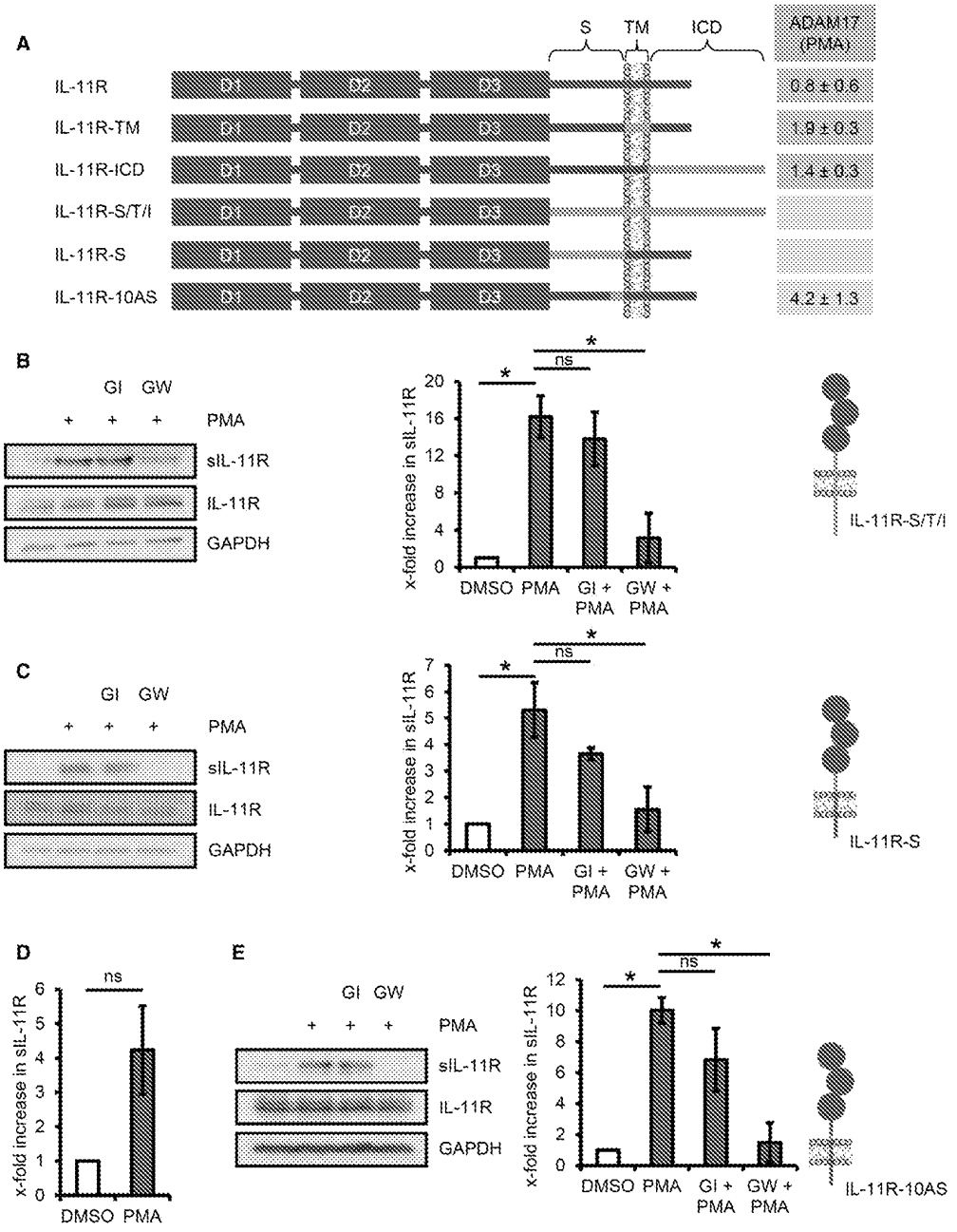

Figure 3. Susceptibility toward Cleavage by ADAM17 Can Be Transferred from the IL-6R to the IL-11R

(A) Schematic overview of the IL-11R and chimeric variants thereof. IL-6R and IL-11R share the same overall topology, consisting of an immunoglobulin (Ig)-like domain (D1), two fibronectin type III domains (D2 and D3), a stalk (S) region, a transmembrane (TM) region, and an intracellular domain (ICD). The IL-11R is depicted in blue, whereas regions originating from the IL-6R are shown in orange. The values shown beside the chimeras are the x-fold increase after PMA stimulation (mean ± SD, n = 3). To calculate this, the amount of constitutively shed IL-11R or chimera was measured by ELISA and arbitrarily set to 1. The increase after stimulation with PMA was calculated accordingly. Chimeras with at least a 2-fold increase in soluble receptor formation were defined as good substrates for ADAM17 (colored in green), whereas chimeras with values below this were considered weak substrates (colored in red). IL-11R-S/T/I and IL-11R-S could not be detected via ELISA.

(B–E) HEK293 cells were transiently transfected with plasmids encoding IL-11R-S/T/I (B), IL-11R-S (C), or IL-11R-10AS (D and E), and the amount of shedding upon PMA stimulation was analyzed by ELISA and western blot as described in the legend to Figure 1 (mean ± SD; n = 3). *$p < 0.05$.

See also Figure S2.

proliferation of Ba/F3-gp130-IL-11R cells was not blocked by sgp130Fc (Figures S4A and S4B). To test whether sIL-11R produced by ectodomain shedding was also able to signal in combination with IL-11, we used a supernatant of HEK293 cells that were transiently transfected with IL-11R cDNA. The supernatant of ionomycin-stimulated cells induced significantly enhanced proliferation of Ba/F3-gp130 cells when IL-11 was added, but not without the cytokine (Figure 6C). Inhibition of ADAM10 with GI or GW prior to ionomycin stimulation not only prevented IL-11R shedding (Figure 4B) but also resulted in significantly less proliferation in this assay (Figure 6C), demonstrating that the released IL-11R ectodomain is, indeed, biologically active. Addition of sgp130Fc to supernatant containing sIL-11R and IL-11, representing protease-controlled, natural IL-11 trans-signaling, blocked the proliferation of Ba/F3-gp130 cells significantly in a dose-dependent manner (Figure 6D) and prevented the phosphorylation of STAT3 (Figure 6E).

Taken together, our data show that IL-11, in complex with the proteolytically generated sIL-11R, is a biologically active composite cytokine, which can induce signaling and proliferation in a gp130-dependent manner.

Neutrophil-Derived Serine Proteases Cleave IL-6R and IL-11R

Besides cleavage by ADAM10 and ADAM17, the IL-6R can also be shed by the neutrophil-derived serine protease CG, but not by NE or PR3 (Bank et al., 1999). To verify this finding, we incubated HepG2 cells with increasing amounts of the three proteases and measured the release of the endogenous IL-6R into the supernatant via ELISA. Indeed, only CG was able to generate sIL-6R in a dose-dependent manner (Figure 7A). To investigate a possible role for these proteases in sIL-11R generation, we stained human primary CD66b+ polymorphonuclear leukocytes (PMNs) and found a high expression of IL-11R on these cells (Figure 7B; Figure S5), indicating that secreted neutrophil proteases could, indeed, target the IL-11R in vivo. We further transiently transfected HEK293 cells with a cDNA encoding the IL-11R and added different amounts of purified proteases to the cells. As shown in Figure 7C, high concentrations of NE (1,000 ng/ml; Figure 7C, NE section at left, white arrowhead) were, indeed, able to shed the IL-11R. In contrast, we did not detect a significant increase in sIL-11R generation when we incubated the cells with CG (Figure 7C, CG section in the middle). PR3 was, however, also able to shed the IL-11R, even at rather low concentrations of 250 ng/ml (Figure 7C, PR3 section at right, white arrowhead). Interestingly, the molecular weight of the sIL-11R derived from cleavage by NE and PR3 appeared to be lower compared to the sIL-11R generated by ADAM10-mediated constitutive cleavage (Figure 7C, black arrowhead), suggesting different cleavage sites. Supernatant from IL-11R- or IL-6R-transfected cells induced proliferation of Ba/F3-gp130 when combined with the appropriate cytokine, confirming that the constitutively released receptors by ADAM10 are biologically active (Figures 7D and 7E). However, also both NE-shed sIL-11R and CG-shed sIL-6R were biologically active, as they significantly enhanced proliferation (Figures 7D and 7E). These data show that neutrophil serine proteases are principally able to cleave both IL-6R and IL-11R, albeit with different specificity toward these two substrates.

In order to investigate a possible IL-11 trans-signaling in vivo, we collected serum from 21 healthy volunteers and analyzed cytokine and cytokine receptor levels via ELISA. IL-6 and IL-11 levels were in the low picogram range, as expected (Figures 7F and 7G), and sIL-6R levels were between 40 and 80 ng/ml (Figure 7H), as shown before (Garbers et al., 2014). Interestingly, we detected sIL-11R in 9 out of 21 serum samples in a range between 20 pg/ml and 4 ng/ml (Figure 7I). These data show that sIL-11R exists in human blood, and they open up the possibility that IL-11 trans-signaling occurs in vivo.

DISCUSSION

Limited proteolysis of membrane-bound protein precursors, also known as ectodomain shedding, is an important post-translational modification that is, in contrast to methylation or phosphorylation, completely irreversible (Khokha et al., 2013; Murphy et al., 2008). Shedding results in loss of cell-surface expression of the protease substrates, and the newly generated soluble ectodomains can fulfill own distinct biological functions, acting either as agonists or antagonists. Recent data show that 10% of all proteins on the plasma membrane of platelets can be shed by proteases (Fong et al., 2011), and it is likely that this is also true for other cell types. Among the plethora of 566 predicted proteolytic enzymes in the human genome, the two metalloproteases ADAM10 and ADAM17 have emerged as important proteases in vivo, with non-redundant functions. ADAM10 is the main secretase for the Notch pathway, and ADAM17 cleaves tumor necrosis factor (TNF)α, as well as several ligands of the epidermal growth factor receptor. Until now, more than 100 substrates are known that are to be cleaved solely by ADAM10, ADAM17, or both (Scheller et al., 2011a). Genetic depletion of either of these proteases in mice results in embryonic lethality (Hartmann et al., 2002; Peschon et al., 1998).

It is well established that IL-6 can signal via membrane-bound and soluble forms of the IL-6R, and the latter one is predominantly generated via limited proteolysis (Chalaris et al., 2011; Garbers et al., 2015; Scheller et al., 2014). Soluble IL-6R is found in human serum at high concentrations of about 30–70 ng/ml. In the present study, we show also that the receptor of its closest family relative, IL-11, can undergo ectodomain shedding. Whereas the IL-6R can be shed by ADAM10 and ADAM17, our experiments with heterologous and endogenously expressed IL-11R revealed that only ADAM10 is capable of cleaving the IL-11R.

With the help of chimeric receptors, in which we exchanged different parts between IL-6R and IL-11R, we could show that transfer of the stalk region was sufficient to reverse this cleavage specificity. Moreover, transfer of ten amino acid residues, which contain the IL-6R cleavage site, were sufficient to generate an IL-11R that could be cleaved by ADAM17, and the corresponding IL-6R mutant containing the respective part of the IL-11R was resistant toward induced proteolysis by ADAM17. Thus, it appears that only the absence of an ADAM17 cleavage site within the IL-11R stalk prevents effective proteolysis of the IL-11R and that no further structural or regulatory elements would be required. We have previously shown that the so-called CANDIS region of ADAM17 binds to the region between Glu-317 and

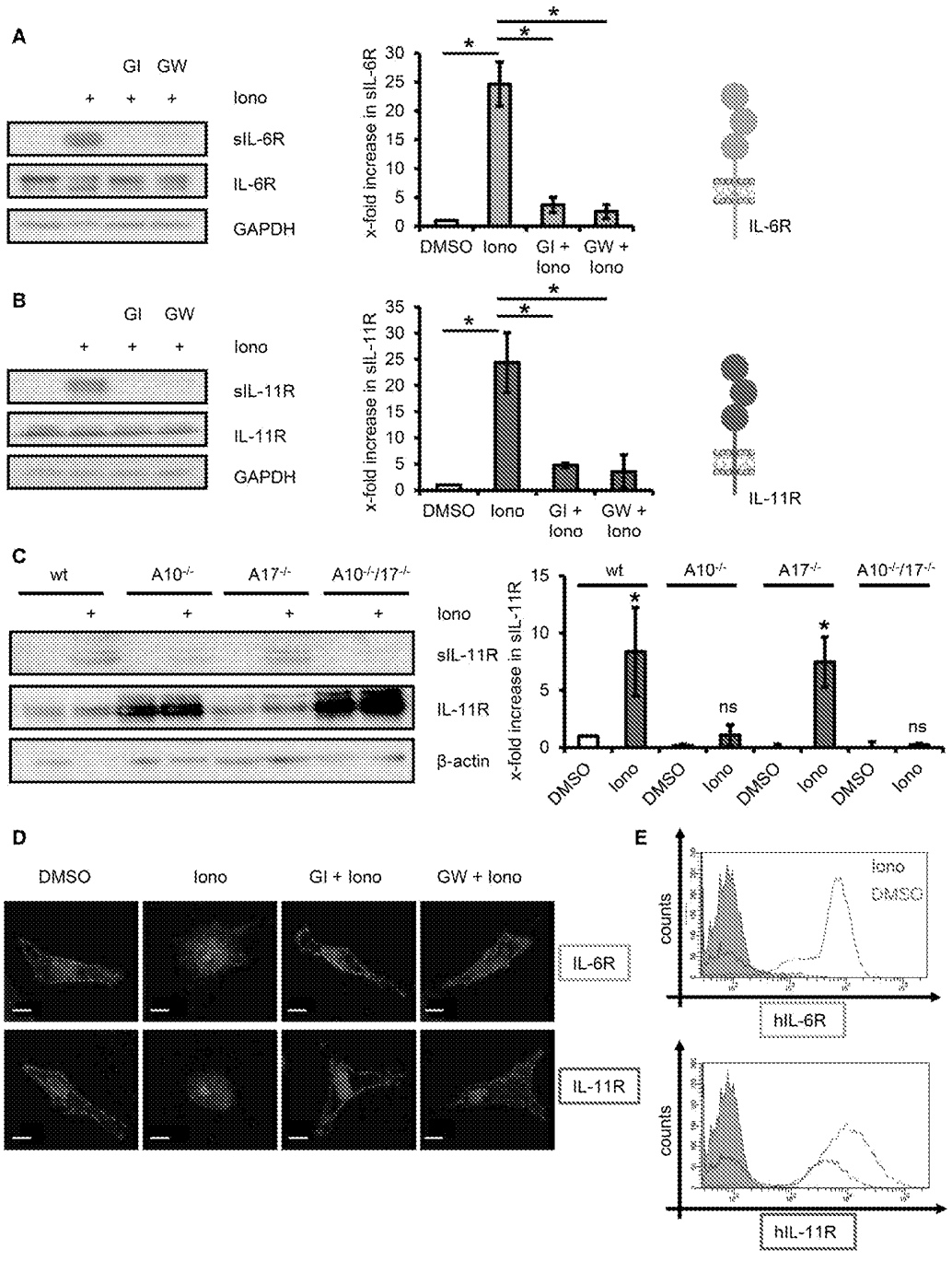

Figure 4. ADAM10 Cleaves the IL-11R

(A and B) HEK293 cells were transiently transfected with plasmids encoding the human IL-6R (A) or the human IL-11R (B) and stimulated with 1 μM ionomycin (Iono) for 1 hr, with or without pre-incubation with the ADAM inhibitors GI or GW. Soluble receptors were precipitated from cell-culture supernatant and visualized by western blot. Cells were lysed, and the lysates were also analyzed by western blot. GAPDH served as loading control. Western blots from three independent experiments were quantified (mean ± SD). *$p < 0.05$.

(legend continued on next page)

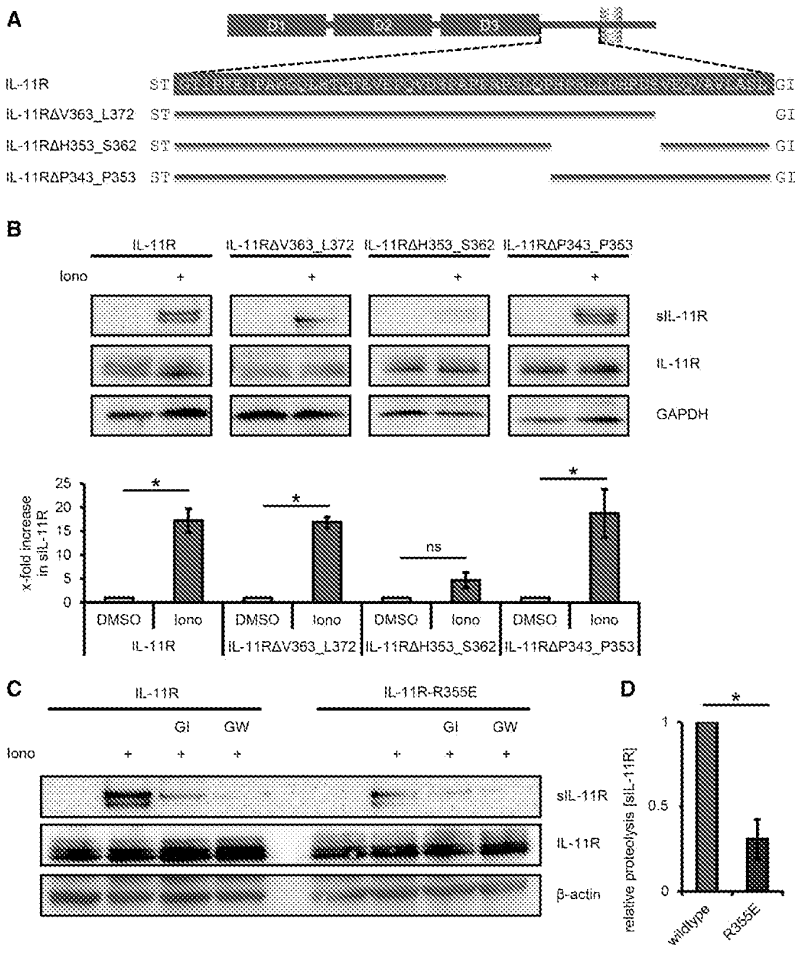

Figure 5. Arginine-355 Is Required for ADAM10-Mediated Shedding of the IL-11R

(A) Schematic overview of the IL-11R and deletion variants thereof. The amino acid sequence from Ser-316 to Ile-374 is shown, with the sequence of the stalk region highlighted in blue. The range of each deletion is shown in front of the schematic drawing.

(B) HEK293 cells were transiently transfected with plasmids encoding the human IL-11R or deletion variants thereof and stimulated with ionomycin (Iono) for 1 hr where indicated. Soluble receptors were precipitated from cell-culture supernatant and visualized by western blot. Cells were lysed, and the lysates were also analyzed by western blot. GAPDH served as loading control. Western blots from three independent experiments were quantified (mean ± SD). *$p < 0.05$; ns, not significant.

(C) HEK293 cells were transiently transfected with IL-11R or the R355E mutant, and ectodomain shedding was analyzed. Experiments were performed as described for (B), but cells were preincubated with the protease inhibitors GI or GW where indicated. One representative western blot is shown.

(D) Relative proteolysis of (C) (mean ± SD). *$p < 0.05$.

See also Figure S3.

Gln-332 within the IL-6R stalk and that deletion of these amino acid residues significantly, albeit not completely, reduces IL-6R shedding (Düsterhöft et al., 2014). Binding of CANDIS to the IL-11R appears not to be essential for IL-11R proteolysis, although it is tempting to speculate that transfer of the CANDIS-binding region, in addition to the cleavage site, into IL-11R might enhance ADAM17-mediated proteolysis.

Cleavage by ADAM10 results in the release of the IL-11R ectodomain. Although it is known that ADAM proteases cleave extracellularly in the juxtamembrane part of their substrates, the establishment of consensus cleavage sites for ADAM proteases has been difficult (Caescu et al., 2009). Our deletion variant IL-11RΔH353_S362 shows strongly reduced shedding by ADAM10, suggesting that ADAM10 cleaves within this region. Recent data obtained with proteome-derived peptide libraries revealed a preference of ADAM10 for arginine residues at the P1 and/or P1′ position of the cleavage site (Tucher et al., 2014). Indeed, mutation of Arg-355 to a glutamic acid residue was sufficient to significantly reduce proteolysis of the IL-11R to 30.9% ± 11.7% compared to the wild-type, strengthening the notion that cleavage by ADAM10 occurs at this site. The cleavage site of ADAM10 within the IL-6R has not been determined yet (Baran et al., 2013).

Similar to ADAM17 and ADAM10, neutrophil-derived serine proteases show differential cleavage specificity for IL-6R and IL-11R. The IL-6R can be shed by CG (Bank et al., 1999). In contrast, this protease is not able to cleave the IL-11R. However, we demonstrated that NE and PR3, which do not cleave the IL-6R, are able to generate sIL-11R.

Signaling of IL-6 via the sIL-6R is believed to account for the pro-inflammatory functions of the cytokine, and specific inhibition of this trans-signaling pathway has been shown to be beneficial in various animal models of human inflammatory diseases (Waetzig and Rose-John, 2012). sgp130 is the natural inhibitor of IL-6 trans-signaling (Jostock et al., 2001), and an Fc-dimerized

(C) MEFs from wild-type (wt) animals and from mice deficient in ADAM10, ADAM17, or both proteases were transiently transfected with IL-11R. Cells were stimulated, and shedding was analyzed by western blots as described for (A) and (B). Western blots from three independent experiments were quantified (mean ± SD). *$p < 0.05$; ns, not significant.

(D) ADAM10-mediated proteolysis of IL-6R and IL-11R in HeLa cells was analyzed as described in the legend to Figure 1. Scale bars, 10 μm.

(E) THP-1 cells were stimulated with 1 μM ionomycin, and the amount of cytokine receptor at the cell surface was analyzed by flow cytometry.

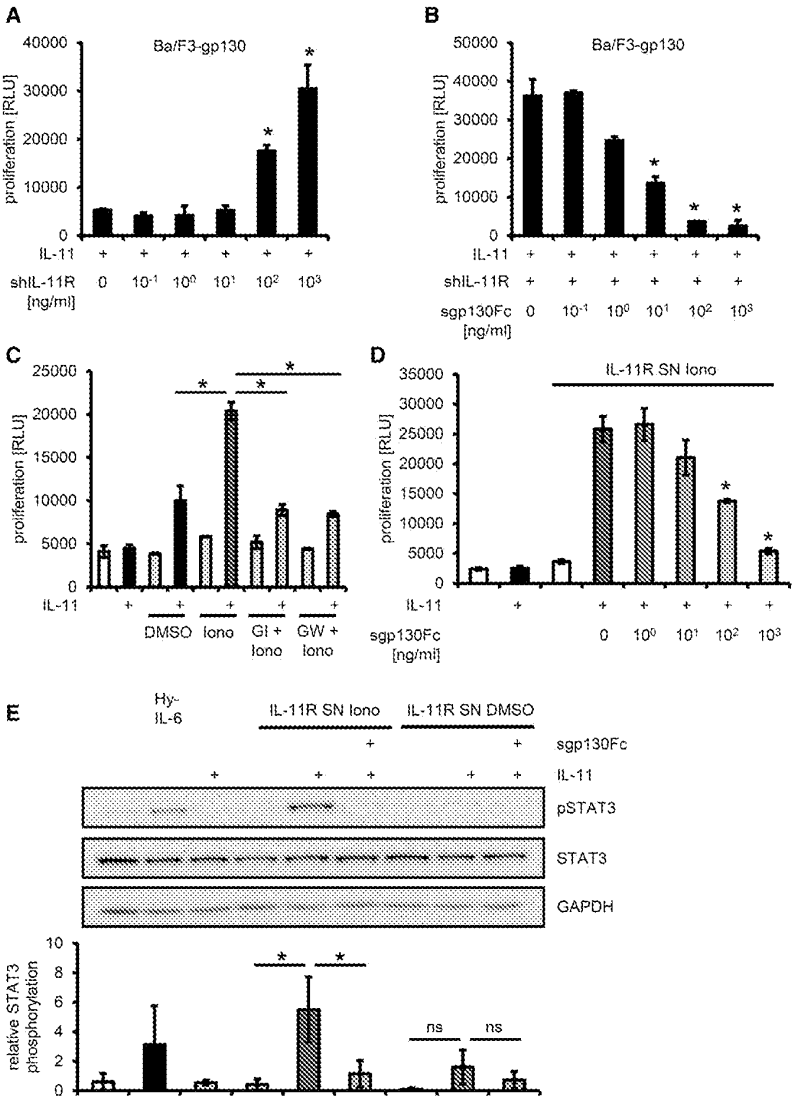

Figure 6. Trans-signaling via the sIL-11R is Blocked by sgp130Fc

(A) Ba/F3-gp130 cells were incubated with 10 ng/ml recombinant IL-11 and increasing amounts of recombinant sIL-11R for 48 hr. Significant increased proliferation, compared to no addition of sIL-11R, is indicated. Error bars indicate mean ± SD. *$p < 0.05$; $n = 3$. RLU, relative light units.

(B) Ba/F3-gp130 cells were incubated with 10 ng/ml recombinant IL-11, 1 μg/ml recombinant sIL-11R, and increasing amounts of sgp130Fc. Significant reduced proliferation, compared to no addition of sgp130Fc, is indicated. Error bars indicate mean ± SD. *$p < 0.05$; $n = 3$.

(C) HEK293 cells were transfected with IL-11R and stimulated with ionomycin with or without pre-incubation with GI or GW as indicated. The supernatant was collected, and Ba/F3-gp130 cells were incubated with the conditioned-cell supernatant (IL-11R SN) in the presence or absence of IL-11 for 48 hr. Error bars indicate mean ± SD. *$p < 0.05$; $n = 3$.

(D) Conditioned cell supernatant from IL-11R expressing HEK293 cells stimulated with ionomycin (IL-11R SN Iono) was produced as described for (C), and Ba/F3-gp130 cells were incubated with this medium in the presence of IL-11 and increasing amounts of sgp130Fc for 48 hr. Significant reduced proliferation, compared to no addition of sgp130Fc, is indicated. Error bars indicate mean ± SD. *$p < 0.05$; $n = 3$.

(E) Ba/F3-gp130 cells were serum starved for 2 hr and then stimulated with conditioned medium from IL-11R-expressing HEK293 cells in the presence or absence of IL-11 and sgp130Fc. Ba/F3-gp130 cells were lysed, and STAT3 phosphorylation was analyzed by western blot. Western blots from three independent experiments were quantified (mean ± SD). *$p < 0.05$; ns, not significant.

See also Figure S4.

version of sgp130 is currently in clinical development (Jones et al., 2011; Waetzig and Rose-John, 2012). Therefore, we speculated that IL-11 trans-signaling via the sIL-11R would also be blocked by sgp130Fc. Indeed, sgp130Fc inhibited cellular proliferation induced by IL-11 trans-signaling and STAT3 activation in a dose-dependent manner. Thus, the beneficial effects of sgp130Fc seen in vivo might not solely depend upon inhibition of IL-6 trans-signaling but could, at least in part, be due to blockade of IL-11 trans-signaling.

In conclusion, we show that the IL-11R can undergo ectodomain shedding by ADAM10 and the serine proteases NE and PR3 and that the sIL-11R, in combination with IL-11, is able to induce trans-signaling via gp130. Using human serum samples from healthy volunteers, we show that sIL-11R exists in human serum. sIL-6R levels are known to be elevated during inflammatory diseases (Garbers et al., 2015), and it appears likely that sIL-11R levels—and, thus, IL-11 trans-signaling—could be enhanced during disease. Our data suggest that, if disease conditions driven by IL-11 trans-signaling were defined, such conditions could well be treated by the IL-6 trans-signaling inhibitor sgp130Fc or its derivatives (Figure S6).

EXPERIMENTAL PROCEDURES

Cells and Reagents

Cells, cytokines, and other reagents have been described previously (Baran et al., 2013; Chalaris et al., 2007; Garbers et al., 2014; Nitz et al., 2016). Details are provided in the Supplemental Experimental Procedures.

Construction of IL-6R/IL-11R Chimeric Receptors and IL-11R Deletion Variants

Chimeras of IL-6R and IL-11R have been described elsewhere (Düsterhöft et al., 2014; Nitz et al., 2015). Stalk deletion variants of the IL-11R were constructed using standard splicing by overlapping extension PCR.

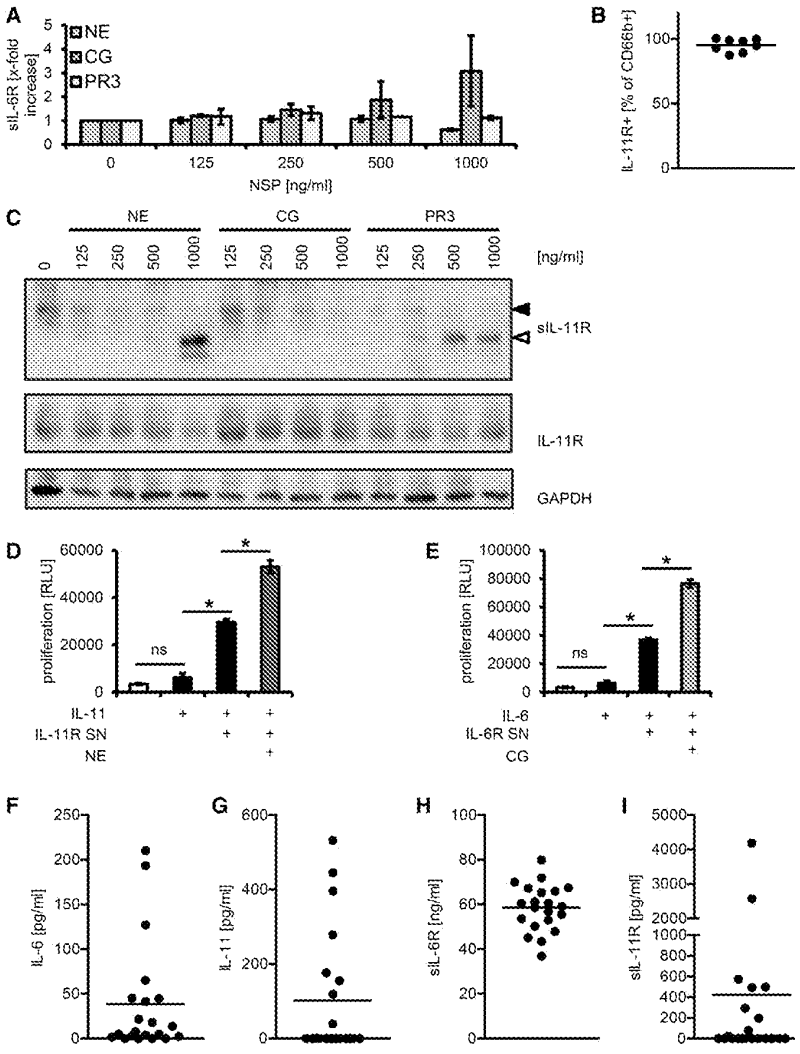

Figure 7. Cleavage of IL-6R and IL-11R by Neutrophil-Derived Serine Proteases

(A) HepG2 cells were incubated for 2 hr with the indicated concentrations of purified neutrophil-derived serine proteases (NE, CG, and PR3) under serum-free conditions. Levels of the sIL-6R in cell-culture supernatants were determined by ELISA. Error bars indicate mean ± SD.

(B) IL-11R expression on CD66b+ human primary neutrophils from eight healthy volunteers was analyzed via flow cytometry. The mean is indicated by a horizontal line.

(C) HEK293 cells were transiently transfected with a construct coding for the IL-11R. 48 hr post-transfection, cells were incubated for 2 hr with the indicated concentrations of purified neutrophil-derived serine proteases under serum-free conditions. Soluble IL-11R from cell-culture supernatants was precipitated with TCA and analyzed by western blot. Additionally, cells were lysed, and IL-11R levels in whole-cell lysates were analyzed by western blot. GAPDH served as loading control.

(D and E) HEK293 cells were transfected with IL-11R or IL-6R and incubated with recombinant NE or CG or left untreated. The supernatants were collected, and Ba/F3-gp130 cells were incubated with the conditioned cell supernatant (IL-11R SN or IL-6R SN) in the presence or absence of IL-11 or IL-6 for 48 hr where indicated. One of two performed experiments with similar outcome is shown (mean ± SD). *$p < 0.05$; ns, not significant.

(F–I) Serum samples from 21 healthy volunteers were analyzed for IL-6, IL-11, sIL-6R, and sIL-11R. Means are indicated by a horizontal line.

See also Figures S5 and S8.

Ba/F3-gp130 Proliferation Assays

Proliferation of Ba/F3-gp130 cells was assessed using the Cell Titer Blue Viability Assay (Promega) as described previously (Baran et al., 2013).

Protease Cleavage Assays

Analysis of cytokine receptor proteolysis has been described in detail elsewhere (Baran et al., 2013; Garbers et al., 2011a).

Neutrophil-Derived Serine Protease Cleavage Assay

HEK293 cells were prepared as described for the ADAM Protease Shedding Assay and stimulated with different concentrations of purified serine proteases for 2 hr in serum-free media. Subsequently, supernatants and cells were harvested and separately analyzed by western blotting. HepG2 cells were seeded in six-well plates. On the following day, cells were stimulated with different concentrations of purified serine proteases for 2 hr in serum-free media. Supernatants were harvested and analyzed by ELISA.

Precipitation of Soluble Receptors

1 ml supernatant of stimulated HEK293 cells was harvested and centrifuged at 1,200 × *g* to remove cells and subsequently at 18,000 × *g* to remove cellular debris. Cleared supernatants were transferred into new tubes, mixed with an equal volume of 20% trichloracetic acid (TCA), and incubated on ice for 30 min. Protein precipitates were collected by centrifugation at 18,000 × *g*, the supernatants were discarded, and the pellets were washed with 350 µl ice-cold acetone. After a second centrifugation at 18,000 × *g*, the acetone was removed and the pellets were allowed to dry. Afterward, the precipitated proteins were boiled in Laemmli buffer and analyzed by western blot.

Western Blot Analysis

Detection of proteins via western blotting was performed as described previously (Baran et al., 2013; Garbers et al., 2014). Quantification of western blots was performed with Image Studio Lite 5.2 (LI-COR Biosciences).

ELISA

An ELISA for the detection of the human IL-6R has been described previously (Chalaris et al., 2007; Garbers et al., 2011a). An ELISA to detect sIL-11R was performed as described previously (Blanc et al., 2009). The IL-6 ELISA was from ImmunoTools, and the IL-11 ELISA was from R&D Systems.

Human Serum and Human PMNs

Ethics approval for this study was obtained from the institutional review boards of the Heinrich-Heine-University (study #3949) and the review board of the medical faculty of Kiel University (study #D 487/13). All participants gave written informed consent. Peripheral blood from healthy volunteers was collected by venipuncture.

Flow Cytometry Analysis

1 × 10^6 THP-1 cells were stimulated with 100 nM PMA or 1 μM ionomycin, washed with fluorescence-activated cell sorting (FACS) buffer (0.5% BSA in PBS), and stained with 1:100 diluted antibodies for 30 min on ice. After two washing steps, cells were incubated with allophycocyanin (APC)-conjugated secondary antibodies for 30 min on ice. The cells were washed twice and resuspended in 500 μl FACS buffer, and cell-surface expression was then analyzed by flow cytometry. To analyze IL-11R on primary cells, heparinized whole human blood was blocked with TruStain FcX (BioLegend), and the IL-11R expression on PMNs was analyzed via staining with the anti-hIL-11R Ab N-20 and the anti-human CD66b Ab (clone G10F5, BioLegend). Red blood cells were removed, and the cells were fixed with RBC Lysis/Fixation Solution (BioLegend).

Confocal Microscopy

Confocal microscopy of transiently transfected HeLa cells was performed as described previously (Garbers et al., 2014).

Statistical Analysis

Statistics were calculated using GraphPad Prism (GraphPad Software). Data were analyzed by Student's t test, and differences were indicated with asterisks ($p < 0.05$). A one-sample t test was used to test for differences to normalized data (e.g., comparison to a value of 1.0). For multiple comparisons, p values were corrected via the Bonferroni correction.

SUPPLEMENTAL INFORMATION

Supplemental Information includes Supplemental Experimental Procedures and six figures and can be found with this article online at http://dx.doi.org/10.1016/j.celrep.2016.01.053.

AUTHOR CONTRIBUTIONS

C.G. designed the experiments and wrote the manuscript. J.S. and S.R.-J. designed experiments. J.L., R.N., M.A., N.M., S.A.-S., N.S., J.W., K.M.-H., and C.G. performed the experiments. G.M.-N. characterized anti-IL-11R antibodies. G.H.W. expressed and purified sgp130Fc and revised the manuscript. J.G. defined domain borders of IL-6R/IL-11R and helped to create the respective chimeras. All authors approved the final version of the manuscript.

CONFLICTS OF INTEREST

S.R.-J. is an inventor of patents owned by CONARIS Research Institute, which develops the sgp130Fc protein together with Ferring Pharmaceuticals, and he has stock ownership in CONARIS. G.H.W. is employed by the CONARIS Research Institute AG.

ACKNOWLEDGMENTS

We thank Annett Lickert and Alyn Gerneth for excellent technical assistance. Protease-deficient MEFs were provided by Paul Saftig (Institute of Biochemistry, Kiel University). Anti-human IL-11R antibodies were provided by Felix A. Montero-Julian (Beckham-Coulter). This work was supported by the Deutsche Forschungsgemeinschaft (DFG) grant GA 2048/1-1 and SFB877 projects A10 (C.G.), A1 (S.R.-J.), and A6 (J.G.); SCHE907/3-1 (J.S.); the Forschungskommission of the Medical Faculty of the HHU Düsseldorf (C.G. and J.S.); and the Cluster of Excellence "Inflammation at Interfaces." J.W. is supported by a grant from Ferring Pharmaceuticals A/S (Copenhagen).

Received: September 29, 2015
Revised: December 22, 2015
Accepted: January 14, 2016
Published: February 11, 2016

REFERENCES

Bank, U., Reinhold, D., Schneemilch, C., Kunz, D., Synowitz, H.J., and Ansorge, S. (1999). Selective proteolytic cleavage of IL-2 receptor and IL-6 receptor ligand binding chains by neutrophil-derived serine proteases at foci of inflammation. J. Interferon Cytokine Res. *19*, 1277–1287.

Baran, P., Nitz, R., Grötzinger, J., Scheller, J., and Garbers, C. (2013). Minimal interleukin 6 (IL-6) receptor stalk composition for IL-6 receptor shedding and IL-6 classic signaling. J. Biol. Chem. *288*, 14756–14768.

Blanc, C., Vusio, P., Schleinkofer, K., Boisteau, O., Pflanz, S., Minvielle, S., Grötzinger, J., Müller-Newen, G., Heinrich, P.C., Jacques, Y., and Montero-Julian, F.A. (2000). Monoclonal antibodies against the human interleukin-11 receptor alpha-chain (IL-11Ralpha) and their use in studies of human mononuclear cells. J. Immunol. Methods *241*, 43–59.

Caescu, C.I., Jeschke, G.R., and Turk, B.E. (2009). Active-site determinants of substrate recognition by the metalloproteinases TACE and ADAM10. Biochem. J. *424*, 79–88.

Chalaris, A., Rabe, B., Paliga, K., Lange, H., Laskay, T., Fielding, C.A., Jones, S.A., Rose-John, S., and Scheller, J. (2007). Apoptosis is a natural stimulus of IL6R shedding and contributes to the proinflammatory trans-signaling function of neutrophils. Blood *110*, 1748–1755.

Chalaris, A., Garbers, C., Rabe, B., Rose-John, S., and Scheller, J. (2011). The soluble Interleukin 6 receptor: generation and role in inflammation and cancer. Eur. J. Cell Biol. *90*, 484–494.

Dams-Kozlowska, H., Gryska, K., Kwiatkowska-Borowczyk, E., Izycki, D., Rose-John, S., and Mackiewicz, A. (2012). A designer hyper interleukin 11 (H11) is a biologically active cytokine. BMC Biotechnol. *12*, 6.

Davidson, A.J., Freeman, S.A., Crosier, K.E., Wood, C.R., and Crosier, P.S. (1997). Expression of murine interleukin 11 and its receptor alpha-chain in adult and embryonic tissues. Stem Cells *15*, 119–124.

Düsterhöft, S., Höbel, K., Oldefest, M., Lokau, J., Waetzig, G.H., Chalaris, A., Garbers, C., Scheller, J., Rose-John, S., Lorenzen, I., and Grötzinger, J. (2014). A disintegrin and metalloprotease 17 dynamic interaction sequences, the sweet tooth for the human interleukin 6 receptor. J. Biol. Chem. *289*, 16336–16348.

Ernst, M., and Putoczki, T.L. (2014). Molecular pathways: IL11 as a tumor-promoting cytokine-translational implications for cancers. Clin. Cancer Res. *20*, 5579–5588.

Ernst, M., Najdovska, M., Grail, D., Lundgren-May, T., Buchert, M., Tye, H., Matthews, V.B., Armes, J., Bhathal, P.S., Hughes, N.R., et al. (2008). STAT3 and STAT1 mediate IL-11-dependent and inflammation-associated gastric tumorigenesis in gp130 receptor mutant mice. J. Clin. Invest. *118*, 1727–1738.

Fong, K.P., Barry, C., Tran, A.N., Traxler, E.A., Wannemacher, K.M., Tang, H.-Y., Speicher, K.D., Blair, I.A., Speicher, D.W., Grosser, T., and Brass, L.F. (2011). Deciphering the human platelet sheddome. Blood *117*, e15–e26.

Garbers, C., and Scheller, J. (2013). Interleukin-6 and interleukin-11: same same but different. Biol. Chem. *394*, 1145–1161.

Garbers, C., Jänner, N., Chalaris, A., Moss, M.L., Floss, D.M., Meyer, D., Koch-Nolte, F., Rose-John, S., and Scheller, J. (2011a). Species specificity of ADAM10 and ADAM17 proteins in interleukin-6 (IL-6) trans-signaling and novel role of ADAM10 in inducible IL-6 receptor shedding. J. Biol. Chem. *286*, 14804–14811.

Garbers, C., Thaiss, W., Jones, G.W., Waetzig, G.H., Lorenzen, I., Guilhot, F., Lissilaa, R., Ferlin, W.G., Grötzinger, J., Jones, S.A., et al. (2011b). Inhibition of classic signaling is a novel function of soluble glycoprotein 130 (sgp130), which is controlled by the ratio of interleukin 6 and soluble interleukin 6 receptor. J. Biol. Chem. *286*, 42959–42970.

Garbers, C., Monhasery, N., Aparicio-Siegmund, S., Lokau, J., Baran, P., Nowell, M.A., Jones, S.A., Rose-John, S., and Scheller, J. (2014). The interleukin-6 receptor Asp358Ala single nucleotide polymorphism rs2228145 confers increased proteolytic conversion rates by ADAM proteases. Biochim. Biophys. Acta *1842*, 1485–1494.

Garbers, C., Aparicio-Siegmund, S., and Rose-John, S. (2015). The IL-6/gp130/STAT3 signaling axis: recent advances towards specific inhibition. Curr. Opin. Immunol. *34*, 75–82.

Hartmann, D., de Strooper, B., Serneels, L., Craessaerts, K., Herreman, A., Annaert, W., Umans, L., Lübke, T., Lena Illert, A., von Figura, K., and Saftig, P. (2002). The disintegrin/metalloprotease ADAM 10 is essential for Notch

signalling but not for alpha-secretase activity in fibroblasts. Hum. Mol. Genet. *11*, 2615–2624.

Howlett, M., Giraud, A.S., Lescesen, H., Jackson, C.B., Kalantzis, A., Van Driel, I.R., Robb, L., Van der Hoek, M., Ernst, M., Minamoto, T., et al. (2009). The interleukin-6 family cytokine interleukin-11 regulates homeostatic epithelial cell turnover and promotes gastric tumor development. Gastroenterology *136*, 957–977.

Jones, S.A., Horiuchi, S., Novick, D., Yamamoto, N., and Fuller, G.M. (1998). Shedding of the soluble IL-6 receptor is triggered by Ca2+ mobilization, while basal release is predominantly the product of differential mRNA splicing in THP-1 cells. Eur. J. Immunol. *28*, 3514–3522.

Jones, S.A., Scheller, J., and Rose-John, S. (2011). Therapeutic strategies for the clinical blockade of IL-6/gp130 signaling. J. Clin. Invest. *121*, 3375–3383.

Jostock, T., Müllberg, J., Özbek, S., Atreya, R., Blinn, G., Voltz, N., Fischer, M., Neurath, M.F., and Rose-John, S. (2001). Soluble gp130 is the natural inhibitor of soluble IL-6R transsignaling responses. Eur. J. Biochem. *268*, 160–167.

Karjalainen, K., Jaalouk, D.E., Bueso-Ramos, C., Bover, L., Sun, Y., Kuniyasu, A., Driessen, W.H., Cardó-Vila, M., Rietz, C., Zurita, A.J., et al. (2015). Targeting interleukin-11 receptor in leukemia and lymphoma: A functional ligand-directed study and hematopathology analysis of patient-derived specimens. Clin. Cancer Res. *21*, 3041–3051.

Khokha, R., Murthy, A., and Weiss, A. (2013). Metalloproteinases and their natural inhibitors in inflammation and immunity. Nat. Rev. Immunol. *13*, 649–665.

Kurn, I., Horsten, U., Pfanz, S., Dahmen, H., Küster, A., Grötzinger, J., Heinrich, P.C., and Müller-Newen, G. (1999). Activation of the signal transducer glycoprotein 130 by both IL-6 and IL-11 requires two distinct binding epitopes. J. Immunol. *162*, 1480–1487.

Matthews, V., Schuster, B., Schütze, S., Bussmeyer, I., Ludwig, A., Hundhausen, C., Sadowski, T., Saftig, P., Hartmann, D., Kallen, K.J., and Rose-John, S. (2003). Cellular cholesterol depletion triggers shedding of the human interleukin-6 receptor by ADAM10 and ADAM17 (TACE). J. Biol. Chem. *278*, 38829–38839.

Minshall, E., Chakir, J., Laviolette, M., Molet, S., Zhu, Z., Olivenstein, R., Elias, J.A., and Hamid, Q. (2000). IL-11 expression is increased in severe asthma: association with epithelial cells and eosinophils. J. Allergy Clin. Immunol. *105*, 232–238.

Müllberg, J., Schooltink, H., Stoyan, T., Günther, M., Graeve, L., Buse, G., Mackiewicz, A., Heinrich, P.C., and Rose-John, S. (1993). The soluble interleukin-6 receptor is generated by shedding. Eur. J. Immunol. *23*, 473–480.

Müllberg, J., Oberthür, W., Lottspeich, F., Mehl, E., Dittrich, E., Graeve, L., Heinrich, P.C., and Rose-John, S. (1994). The soluble human IL-6 receptor. Mutational characterization of the proteolytic cleavage site. J. Immunol. *152*, 4958–4968.

Murphy, G., Murthy, A., and Khokha, R. (2008). Clipping, shedding and RIPping keep immunity on cue. Trends Immunol. *29*, 75–82.

Nakayama, T., Yoshizaki, A., Izumida, S., Sueshiro, T., Miura, S., Uemura, T., Yakata, Y., Shichijo, K., Yamashita, S., and Sekin, I. (2007). Expression of interleukin-11 (IL-11) and IL-11 receptor alpha in human gastric carcinoma and IL-11 upregulates the invasive activity of human gastric carcinoma cells. Int. J. Oncol. *30*, 825–833.

Nitz, R., Lokau, J., Aparicio-Siegmund, S., Scheller, J., and Garbers, C. (2015). Modular organization of interleukin-6 and interleukin-11 α-receptors. Biochimie *119*, 175–182.

Peschon, J.J., Slack, J.L., Reddy, P., Stocking, K.L., Sunnarborg, S.W., Lee, D.C., Russell, W.E., Castner, B.J., Johnson, R.S., Fitzner, J.N., et al. (1998). An essential role for ectodomain shedding in mammalian development. Science *282*, 1281–1284.

Pflanz, S., Tacken, I., Grötzinger, J., Jacques, Y., Minvielle, S., Dahmen, H., Heinrich, P.C., and Müller-Newen, G. (1999). A fusion protein of interleukin-11 and soluble interleukin-11 receptor acts as a superagonist on cells expressing gp130. FEBS Lett. *460*, 117–122.

Putoczki, T.L., and Ernst, M. (2015). IL-11 signaling as a therapeutic target for cancer. Immunotherapy *7*, 441–453.

Putoczki, T.L., Thiem, S., Loving, A., Busuttil, R.A., Wilson, N.J., Ziegler, P.K., Nguyen, P.M., Preaudet, A., Farid, R., Edwards, K.M., et al. (2013). Interleukin-11 is the dominant IL-6 family cytokine during gastrointestinal tumorigenesis and can be targeted therapeutically. Cancer Cell *24*, 257–271.

Robb, L., Hilton, D.J., Wilson, T.A., and Begley, C.G. (1996). Structural analysis of the gene encoding the murine interleukin-11 receptor alpha-chain and a related locus. J. Biol. Chem. *271*, 13754–13761.

Rose-John, S. (2012). IL-6 trans-signaling via the soluble IL-6 receptor: importance for the pro-inflammatory activities of IL-6. Int. J. Biol. Sci. *8*, 1237–1247.

Scheller, J., Chalaris, A., Garbers, C., and Rose-John, S. (2011a). ADAM17: a molecular switch to control inflammation and tissue regeneration. Trends Immunol. *32*, 380–387.

Scheller, J., Chalaris, A., Schmidt-Arras, D., and Rose-John, S. (2011b). The pro- and anti-inflammatory properties of the cytokine interleukin-6. Biochim. Biophys. Acta *1813*, 878–888.

Scheller, J., Garbers, C., and Rose-John, S. (2014). Interleukin-6: from basic biology to selective blockade of pro-inflammatory activities. Semin. Immunol. *26*, 2–12.

Taga, T., Hibi, M., Hirata, Y., Yamasaki, K., Yasukawa, K., Matsuda, T., Hirano, T., and Kishimoto, T. (1989). Interleukin-6 triggers the association of its receptor with a possible signal transducer, gp130. Cell *58*, 573–581.

Yang, W., Geba, G.P., Zheng, T., Ray, P., Homer, R.J., Kuhn, C., 3rd, Flavell, R.A., and Elias, J.A. (1996). Targeted expression of IL-11 in the murine airway causes lymphocytic inflammation, bronchial remodeling, and airways obstruction. J. Clin. Invest. *98*, 2845–2853.

Tucher, J., Linke, D., Koudelka, T., Cassidy, L., Tredup, C., Wichert, R., Pietrzik, C., Becker-Pauly, C., and Tholey, A. (2014). LC-MS based cleavage site profiling of the proteases ADAM10 and ADAM17 using proteome-derived peptide libraries. J. Proteome Res. *13*, 2205–2214.

Waetzig, G.H., and Rose-John, S. (2012). Hitting a complex target: an update on interleukin-6 trans-signalling. Expert Opin. Ther. Targets *16*, 225–236.

Receptors & Clinical Investigation 2016; 3: e1190. doi: 10.14800/rci.1190; © 2016 by Juliane Lokau, *et al.*
http://www.smartscitech.com/index.php/rci

RESEARCH HIGHLIGHT

Signal transduction of interleukin-11 and interleukin-6 α-receptors

Juliane Lokau, Christoph Garbers

Institute of Biochemistry, Kiel University, Kiel, 24118, Germany

Correspondence: Christoph Garbers
E-mail: cgarbers@biochem.uni-kiel.de
Received: January 09, 2016
Published online: February 29, 2016

The cytokines Interleukin (IL)-11 and IL-6 are important mediators that regulate differentiation and proliferation of immune cells. Both cytokines bind to unique non-signaling α-receptors (IL-11R and IL-6R, respectively), and the resulting cytokine/cytokine receptor complexes recruit a homodimer of the signal-transducing β-receptor glycoprotein (gp)130. Gp130 is expressed ubiquitously, whereas both α-receptors show a cell- and tissue-specific expression pattern, thus determining cellular responsiveness towards IL-6 and/or IL-11. Formation of the signaling complexes activates intracellular signaling cascades, most prominently the Janus kinase (Jak)/Signal Transducer and Activator of Transcription (STAT) pathway. In a recent paper published in Biochimie, we analyzed the signaling capacity of eight chimeric receptors consisting of different domains of IL-11R and IL-6R. Our results showed that the intracellular region, the transmembrane region or the stalk region can be swapped between the two receptors, as they are not essential to discriminate between the two cytokines. Selectivity of the two receptors is exclusively warranted by the cytokine binding module (CBM), which resides within the domains D1 to D3. These results underline a modular organization of IL-11R and IL-6R and a comparable signal transduction of both cytokines.

Keywords: Interleukin-11; Interleukin-6; IL-6R; IL-11R; gp130; Jak/STAT

To cite this article: Juliane Lokau, *et al.* Signal transduction of interleukin-11 and interleukin-6 α-receptors. Receptor Clin Invest 2016; 3: e1190. doi: 10.14800/rci.1190.

The cytokines Interleukin (IL)-11 and IL-6 fulfill pleiotropic activities in health and disease and control several physiological conditions [1-3]. They exhibit a four-helical-bundle fold, which is arranged in an up-up-down-down topology (Figure 1A). In healthy individuals, both proteins are only detected in small amounts of 1-10 pg/ml [4, 5]. However, under inflammatory conditions, IL-6 serum levels can rise dramatically and reach several µg/ml [5]. Specific inhibition of IL-6 has been shown to be beneficial in a plethora of inflammatory diseases, and the neutralizing antibody tocilizumab which blocks binding of IL-6 to its receptor is approved for the treatment of Castleman's disease, systemic juvenile idiopathic arthritis, polyarticular juvenile idiopathic arthritis and rheumatoid arthritis [6-9]. Recent evidence suggests that also the specific blockade of IL-11 signaling might be beneficial, e.g. for the treatment of gastric and colon cancer [10, 11].

To activate target cells, IL-11 and IL-6 bind initially to non-signaling α-receptors (IL-11R and IL-6R, respectively). The formation of IL-11/IL-11R and IL-6/IL-6R complexes activates intracellular downstream signaling pathways like

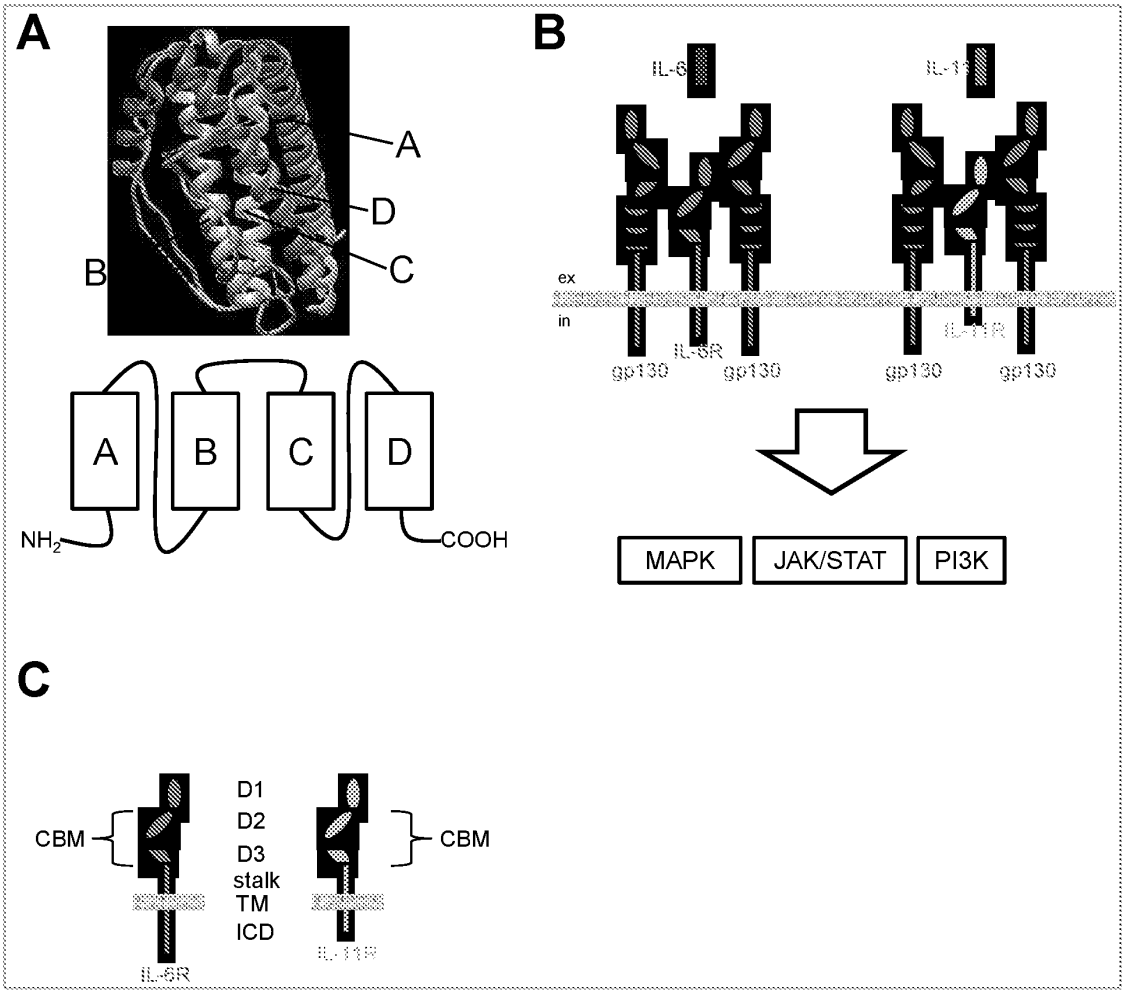

Figure 1. Signal transduction of IL-6 and IL-11. (A) Overlay of the crystal structures of IL-6 (pdb accession code 1alu [37], shown in purple) and IL-11 (pdb accession code 4mhl [38], shown in orange). The image was created using UCSF Chimera 1.10.1 [39]. The four helices A, B, C and D are indicated. The schematic drawing below shows the up-up-down-down topology of both cytokines. **(B)** Signal-transducing complexes of IL-6 (IL-6R/gp130/gp130) and IL-11 (IL-11R/gp130/gp130), which activate Mitogen-Activated Protein Kinase (MAPK), Janus kinase/Signal Transducer and Activator of Transcription (Jak/STAT) and Phosphoinositide 3-kinase (PI3K) signaling cascades. **(C)** Schematic drawing of IL-6R and IL-11R. The extracellular part consists of the three domains D1 to D3, and D2/D3 constitutes the cytokine-binding module (CBM). These are followed by a so-called stalk region, the transmembrane (TM) and the intracellular domain (ICD).

the Janus kinase/Signal Transducer and Activator of Transcription (Jak/STAT) cascade through engagement of a homodimer of the signal-transducing β-receptor glycoprotein 130 (gp130) [12] (Figure 1B). Although Jak1, Jak2 and Tyk2 are phosphorylated after activation of gp130 *in vitro*, experiments with cells derived from Jak1$^{-/-}$ mice have shown unequivocally that Jak1 is the dominant kinase activated by all members of the IL-6 cytokine family, the loss of which cannot be compensated by other kinases [13, 14]. Furthermore, the phosphatidyl-inositol-3-kinase (PI3K)-cascade and the mitogen activated protein kinase (MAPK)-cascade are activated [12] (Figure 1B). Gp130 is ubiquitously expressed, and specificity is thus achieved through cell- and tissue-specific expression of the α-receptors. The IL-11R can be found e.g. on cardiac myocytes and endothelial and epithelial cells of the colon, whereas the IL-6R is expressed e.g. on T cells, monocytes, neutrophils and megakaryocytes. Hepatocytes, B cells, macrophages and osteoclasts have been shown to express both receptors, which makes them a target of both cytokines (reviewed in [3]).

The IL-6R was cloned in 1988 [15] and the IL-11R in 1994 [16]. Both are type-I transmembrane proteins which consist of an extracellular part, a transmembrane region and an intracellular region (Figure 1C). Due to alternative mRNA splicing, a second membrane-bound IL-11R isoform exists in

humans that lacks the intracellular region [17], whereas alternative splicing of the IL-6R mRNA gives rise to a soluble form of the IL-6R [18]. Furthermore, a second IL-11R gene exists in mice, which is only expressed in lymph nodes, testis, and in the thymus [19]. The extracellular part of both receptors is composed of an Ig-like D1 domain, which is followed by the fibronectin-type-III domains D2 and D3 that comprise the cytokine-binding module (CBM), and a so-called stalk region (Figure 1C). We could show previously that an important function of the stalk region is to act as a brace in order to position the CBM of the IL-6R [20]. Although the conformation of gp130 is somewhat flexible [21-24], the CBM has to be kept in a certain distance from the plasma membrane [20]. A minimal length of approximately 83.6 Å of the stalk region, which corresponds to 22 amino acid residues, is required for efficient IL-6 signaling via the membrane-bound receptor, because IL-6R deletion variants containing a shorter stalk region were not biologically active, although they were correctly folded and transported to the cell surface [20]. Similar studies concerning the signaling properties of the IL-11R have not been conducted yet.

In our recent study [25], we analyzed the roles of the different parts of the IL-11R and IL-6R with respect to signal transduction. First, we examined whether a cross reactivity between IL-11 and IL-6 exists using genetically engineered Ba/F3 cell lines. Ba/F3 cells are murine pre-B cells that grow in strict dependence of IL-3, but can be rendered responsive to other cytokines via stable expression of the desired cytokine receptors. Using Ba/F3-gp130-IL-11R cells, we found that IL-6 could neither induce phosphorylation of STAT3 nor cell proliferation, indicating that IL-6 is not a high affinity ligand for the IL-11R. Vice versa, IL-11 could not activate Ba/F3-gp130-IL-6R cells. Taken together, we detected no cross-reactivity between IL-6 and IL-11.

Additionally, we created eight different chimeras of both receptors, where we left the three extracellular domains intact and exchanged either stalk, transmembrane, intracellular region, or all three parts between the two receptors and analyzed their responses to IL-6 and IL-11. We found that exchange of the stalk region between IL-11R and IL-6R did not alter their response towards the cytokines. Swapping the transmembrane or the intracellular part also did not affect signaling. Consequently, exchanging all three regions and keeping only D1-D3 intact still resulted in normal biological activity of the IL-11R or IL-6R, respectively. Notably, the origin of D1-D3 determined by which cytokine the chimeric receptors could be activated, while the other regions showed no influence. Thus, our results show a similar modular organization of IL-11R and IL-6R, which allows transfer of different regions between these receptors without interfering with their signaling capacity.

The intracellular region of the IL-6R contains 82 amino acid residues, the intracellular region of the IL-11R is remarkably shorter and contains only 32 amino acid residues. These regions do not participate in the signal transduction of both cytokines, because IL-11R and IL-6R mutants without their intracellular regions were fully biologically active [26, 27]. This finding is further corroborated by the fact that soluble forms of the IL-6R (sIL-6R) exist which are able to bind IL-6 with similar affinity as the membrane-bound IL-6R [18]. The resulting IL-6/sIL-6R complexes are able to activate cells via gp130 homodimerization irrespective of the presence of membrane-bound IL-6R, a fact that dramatically expands the number of cells which can be activated by IL-6 via so-called trans-signaling [28]. The sIL-6R originates to a minor extent from alternative mRNA splicing (~10 %), whereas the majority is believed to originate from proteolytic cleavage of the membrane-bound IL-6R (~ 90%) [18]. Among several proteases that are able to cleave the IL-6R, the metalloproteases ADAM10 and ADAM17 appear to be the most important enzymes involved in this process [18, 29-31]. Soluble forms of the IL-11R (sIL-11R) have not been described to date, although transcripts potentially encoding sIL-11R have been found [32]. However, experiments with recombinant proteins clearly showed that sIL-11R can bind IL-11, and the sIL-11R/IL-11 complex has agonistic properties that stimulated cell proliferation via gp130 [33-35]. Conflicting data exist whether sIL-11R can also act as an IL-11 antagonist on cells that express membrane-bound IL-11R [33, 36].

In conclusion, although signaling of IL-6 and IL-11 appears to be similar in several aspects, subtle differences in their biochemical properties might explain the different biological functions of these two cytokines *in vivo*.

Conflicting interests

The authors have declared that no conflict of interests exists.

Acknowledgments

Work described in this paper was funded by a grant from the Deutsche Forschungsgemeinschaft, Bonn, Germany (SFB877 project A10).

Author contributions

JL and CG wrote and approved the final manuscript.

References

1. Scheller J, Garbers C, Rose-John S. Interleukin-6: From basic biology to selective blockade of pro-inflammatory activities.

Semin Immunol 2014; 26:2-12.

2. Wolf J, Rose-John S, Garbers C. Interleukin-6 and its receptors: a highly regulated and dynamic system. Cytokine 2014; 70:11-20.
3. Garbers C, Scheller J. Interleukin-6 and interleukin-11: same same but different. Biol Chem 2013; 394:1145-1161.
4. Schwertschlag US, Trepicchio WL, Dykstra KH, Keith JC, Turner KJ, Dorner AJ. Hematopoietic, immunomodulatory and epithelial effects of interleukin-11. Leukemia 1999; 13:1307-1315.
5. Scheller J, Chalaris A, Schmidt-Arras D, Rose-John S. The pro- and anti-inflammatory properties of the cytokine interleukin-6. Biochim Biophys Acta 2011; 1813:878-888.
6. Garbers C, Aparicio-Siegmund S, Rose-John S. The IL-6/gp130/STAT3 signaling axis: recent advances towards specific inhibition. Curr Opin Immunol 2015; 34:75-82.
7. Tanaka T, Kishimoto T. The Biology and Medical Implications of Interleukin-6. Cancer Immunol Res 2014; 2:288-294.
8. Tanaka T, Narazaki M, Kishimoto T. Therapeutic targeting of the interleukin-6 receptor. Annu Rev Pharmacol Toxicol 2012; 52:199-219.
9. Tanaka T, Narazaki M, Ogata A, Kishimoto T. A new era for the treatment of inflammatory autoimmune diseases by interleukin-6 blockade strategy. Semin Immunol 2014; 26:88-96.
10. Putoczki T, Thiem S, Loving A, Busuttil R, Wilson N, Ziegler P, *et al.* Interleukin-11 Is the Dominant IL-6 Family Cytokine during Gastrointestinal Tumorigenesis and Can Be Targeted Therapeutically. Cancer Cell 2013; 24:257-271.
11. Putoczki TL, Ernst M. IL-11 signaling as a therapeutic target for cancer. Immunotherapy 2015; 7:441-453.
12. Garbers C, Hermanns H, Schaper F, Müller-Newen G, Grötzinger J, Rose-John S, *et al.* Plasticity and cross-talk of Interleukin 6-type cytokines. Cytokine Growth Factor Rev 2012; 23:85-97.
13. Rodig SJ, Meraz MA, White MJ, Lampe PA, Riley JK, Arthur CD, *et al.* Disruption of the Jak1 Gene Demonstrates Obligatory and Nonredundant Roles of the Jaks in Cytokine-Induced Biologic Responses. Cell 1998; 93:373-383.
14. Aparicio-Siegmund S, Sommer J, Monhasery N, Schwanbeck R, Keil E, Finkenstädt D, *et al.* Inhibition of protein kinase II (CK2) prevents induced signal transducer and activator of transcription (STAT) 1/3 and constitutive STAT3 activation. Oncotarget 2014; 5:2131-2148.
15. Yamasaki K, Taga T, Hirata Y, Yawata H, Kawanishi Y, Seed B, *et al.* Cloning and expression of the human interleukin-6 (BSF-2/IFN beta 2) receptor. Science 1988; 241:825-828.
16. Hilton DJ, Hilton AA, Raicevic A, Rakar S, Harrison-Smith M, Gough NM, *et al.* Cloning of a murine IL-11 receptor alpha-chain; requirement for gp130 for high affinity binding and signal transduction. EMBO J 1994; 13:4765-4775.
17. Chérel M, Sorel M, Apiou F, Lebeau B, Dubois S, Jacques Y, *et al.* The human interleukin-11 receptor alpha gene (IL11RA): genomic organization and chromosome mapping. Genomics 1996; 32:49-53.
18. Chalaris A, Garbers C, Rabe B, Rose-John S, Scheller J. The soluble Interleukin 6 receptor: generation and role in inflammation and cancer. Eur J Cell Biol 2011; 90:484-494.
19. Robb L, Hilton DJ, Brook-Carter PT, Begley CG. Identification of a second murine interleukin-11 receptor alpha-chain gene (IL11Ra2) with a restricted pattern of expression. Genomics 1997; 40:387-394.
20. Baran P, Nitz R, Grötzinger J, Scheller J, Garbers C. Minimal interleukin (IL-)6 receptor stalk composition for IL-6R shedding and IL-6 classic signaling. J Biol Chem 2013; 288:14756-14768.
21. Xu Y, Kershaw N, Luo C, Soo P, Pocock M, Czabotar P, *et al.* Crystal structure of the entire ectodomain of gp130: insights into the molecular assembly of the tall cytokine receptor complexes. J Biol Chem 2010; 285:21214-21218.
22. Hermanns HM, Müller-Newen G, Heinrich PC, Haan S. Bow to your partner for signaling. Nat Struct Mol Biol 2005; 12:476-478.
23. Lupardus P, Skiniotis G, Rice A, Thomas C, Fischer S, Walz T, *et al.* Structural snapshots of full-length Jak1, a transmembrane gp130/IL-6/IL-6Rα cytokine receptor complex, and the receptor-Jak1 holocomplex. Structure 2011; 19:45-55.
24. Skiniotis G, Boulanger MJ, Garcia KC, Walz T. Signaling conformations of the tall cytokine receptor gp130 when in complex with IL-6 and IL-6 receptor. Nat Struct Mol Biol 2005; 12:545-551.
25. Nitz R, Lokau J, Aparicio-Siegmund S, Scheller J, Garbers C. Modular organization of Interleukin-6 and Interleukin-11 α-receptors. Biochimie 2015; 119:175-182.
26. Taga T, Hibi M, Hirata Y, Yamasaki K, Yasukawa K, Matsuda T, *et al.* Interleukin-6 triggers the association of its receptor with a possible signal transducer, gp130. Cell 1989; 58:573-581.
27. Lebeau B, Montero Julian FA, Wijdenes J, Müller-Newen G, Dahmen H, Chérel M, *et al.* Reconstitution of two isoforms of the human interleukin-11 receptor and comparison of their functional properties. FEBS letters 1997; 407:141-147.
28. Rose-John S. IL-6 trans-signaling via the soluble IL-6 receptor: importance for the pro-inflammatory activities of IL-6. Int J Biol Sci 2012; 8:1237-1247.
29. Chalaris A, Gewiese J, Paliga K, Fleig L, Schneede A, Krieger K, *et al.* ADAM17-mediated shedding of the IL6R induces cleavage of the membrane stub by gamma-secretase. Biochim Biophys Acta 2010; 1803:234-245.
30. Garbers C, Jänner N, Chalaris A, Moss ML, Floss DM, Meyer D, *et al.* Species specificity of ADAM10 and ADAM17 proteins in interleukin-6 (IL-6) trans-signaling and novel role of ADAM10 in inducible IL-6 receptor shedding. J Biol Chem 2011; 286:14804-14811.
31. Scheller J, Chalaris A, Garbers C, Rose-John S. ADAM17: a molecular switch to control inflammation and tissue regeneration. Trends Immunol 2011; 32:380-387.
32. Robb L, Hilton DJ, Willson TA, Begley CG. Structural analysis of the gene encoding the murine interleukin-11 receptor alpha-chain and a related locus. J Biol Chem 1996; 271:13754-13761.
33. Karow J, Hudson KR, Hall MA, Vernallis AB, Taylor JA, Gossler A, *et al.* Mediation of interleukin-11-dependent biological responses by a soluble form of the interleukin-11 receptor. Biochem J 1996; 318 (Pt 2):489-495.
34. Baumann H, Wang Y, Morella KK, Lai CF, Dams H, Hilton DJ, *et al.* Complex of the soluble IL-11 receptor and IL-11 acts as IL-6-type cytokine in hepatic and nonhepatic cells. J Immunol 1996; 157:284-290.

35. Pflanz S, Tacken I, Grötzinger J, Jacques Y, Minvielle S, Dahmen H, *et al*. A fusion protein of interleukin-11 and soluble interleukin-11 receptor acts as a superagonist on cells expressing gp130. FEBS Lett 1999; 450:117-122.

36. Curtis DJ, Hilton DJ, Roberts B, Murray L, Nicola N, Begley CG. Recombinant soluble interleukin-11 (IL-11) receptor alpha-chain can act as an IL-11 antagonist. Blood 1997; 90:4403-4412.

37. Somers W, Stahl M, Seehra JS. 1.9 A crystal structure of interleukin 6: implications for a novel mode of receptor dimerization and signaling. EMBO J 1997; 16:989-997.

38. Putoczki TL, Dobson RCJ, Griffin MDW. The structure of human interleukin-11 reveals receptor-binding site features and structural differences from interleukin-6. Acta Crystallogr D Biol Crystallogr 2014; 70:2277-2285.

39. Pettersen EF, Goddard TD, Huang CC, Couch GS, Greenblatt DM, Meng EC, *et al*. UCSF Chimera--a visualization system for exploratory research and analysis. J Comp Chem 2004; 25:1605-1612.

Am J Physiol Heart Circ Physiol 303: H569–H577, 2012.
First published June 15, 2012; doi:10.1152/ajpheart.00060.2012.

Therapeutic administration of IL-11 exhibits the postconditioning effects against ischemia-reperfusion injury via STAT3 in the heart

Masanori Obana,[1] Kaori Miyamoto,[1] Shiho Murasawa,[1] Tomohiko Iwakura,[1] Akiko Hayama,[1] Tomomi Yamashita,[1] Momoko Shiragaki,[1] Shohei Kumagai,[1] Akimitsu Miyawaki,[1] Kana Takewaki,[1] Goro Matsumiya,[2] Makiko Maeda,[3] Minoru Yoshiyama,[4] Hiroyuki Nakayama,[1] and Yasushi Fujio[1]

[1]*Laboratory of Clinical Science and Biomedicine, Graduate School of Pharmaceutical Sciences, Osaka University, Osaka, Japan;* [2]*Department of Cardiovascular Surgery, Graduate School of Medicine, Chiba University, Chiba, Japan;* [3]*Department of Clinical Pharmacogenomics, School of Pharmacy, Hyogo University of Health Sciences;* [4]*Department of Internal Medicine and Cardiology, Graduate School of Medicine, Osaka City University, Osaka, Japan*

Submitted 26 January 2012; accepted in final form 31 May 2012

Obana M, Miyamoto K, Murasawa S, Iwakura T, Hayama A, Yamashita T, Shiragaki M, Kumagai S, Miyawaki A, Takewaki K, Matsumiya G, Maeda M, Yoshiyama M, Nakayama H, Fujio Y. Therapeutic administration of IL-11 exhibits the postconditioning effects against ischemia-reperfusion injury via STAT3 in the heart. *Am J Physiol Heart Circ Physiol* 303: H569–H577, 2012. First published June 15, 2012; doi:10.1152/ajpheart.00060.2012.—Activation of cardiac STAT3 by IL-6 cytokine family contributes to cardioprotection. Previously, we demonstrated that IL-11, an IL-6 cytokine family, has the therapeutic potential to prevent adverse cardiac remodeling after myocardial infarction; however, it remains to be elucidated whether IL-11 exhibits postconditioning effects. To address the possibility that IL-11 treatment improves clinical outcome of recanalization therapy against acute myocardial infarction, we examined its postconditioning effects on ischemia/reperfusion (I/R) injury. C57BL/6 mice were exposed to ischemia (30 min) and reperfusion (24 h), and IL-11 was intravenously administered at the start of reperfusion. I/R injury mediated the activation of STAT3, which was enhanced by IL-11 administration. IL-11 treatment reduced I/R injury, analyzed by triphenyl tetrazolium chloride staining [PBS, 46.7 ± 14.4%; IL-11 (20 μg/kg), 28.6 ± 7.5% in the ratio of infarct to risk area]. Moreover, echocardiographic and hemodynamic analyses clarified that IL-11 treatment preserved cardiac function after I/R. Terminal deoxynucleotide transferase-mediated dUTP nick-end labeling staining revealed that IL-11 reduced the frequency of apoptotic cardiomyocytes after I/R. Interestingly, IL-11 reduced superoxide production assessed by in situ dihydroethidium fluorescence analysis, accompanied by the increased expression of metallothionein 1 and 2, reactive oxygen species (ROS) scavengers. Importantly, with the use of cardiac-specific STAT3 conditional knockout (STAT3 CKO) mice, it was revealed that cardiac-specific ablation of STAT3 abrogated IL-11-mediated attenuation of I/R injury. Finally, IL-11 failed to suppress the ROS production after I/R in STAT3 CKO mice. IL-11 administration exhibits the postconditioning effects through cardiac STAT3 activation, suggesting that IL-11 has the clinical therapeutic potential to prevent I/R injury in heart.

cardiovascular diseases; cytokine; signal transduction

ISCHEMIA-REPERFUSION (I/R) is one of the major causes of myocardial injury in the clinical setting, especially in the therapeutic process of acute myocardial infarction. Although various kinds of preventive therapies from I/R injury have been proposed so far, clinical trials revealed that they are insufficient. Therefore, it is urgent to develop the therapeutic strategy on a novel concept to prevent myocardial damage after I/R. Accumulating evidence has shown that cardiac homeostasis is maintained by a wide range of neurohumoral factors and cytokines, suggesting that these factors could be therapeutic targets for cardioprotection.

IL-6 family cytokines contribute to cardioprotection by activating various kinds of signaling molecules. In their cytokine signaling pathways, activation of glycoprotein 130/STAT3 axis plays important roles in cytoprotection and angiogenesis (6, 21, 22). Thus the activation of STAT3 by IL-6 family cytokines is considered a potential therapeutic strategy for cardiovascular diseases (5). Experimentally, leukemia inhibitory factor shows the antifibrotic effect after myocardial infarction (29); however, this cytokine has not been considered clinically appropriate because of its proinflammatory properties (7). To establish a novel therapeutic strategy against cardiovascular disease, we focused on IL-11, a member of IL-6 family cytokines, because its proinflammatory activity is limited and because IL-11 exhibits anti-inflammatory activity in some cases (3, 23).

IL-11 exhibits multipotential functions (4). Because IL-11 has the thrombopoietic activity, recombinant human IL-11 is clinically used for thrombocytopenia (9). In addition, IL-11 also shows nonhematopoietic functions. Previously, we reported that IL-11 protects cardiomyocytes from H_2O_2-induced cell death through STAT3 activation and has a late preconditioning effect against I/R injury (16). Recently, we also demonstrated that the therapeutic treatment of IL-11 reduces adverse cardiac remodeling after myocardial infarction in murine model, concomitant with anti-apoptosis and angiogenesis (20). Furthermore, cardiac-specific ablation of STAT3 abrogated IL-11-mediated attenuation of adverse cardiac remodeling, suggesting that cardiac activation of STAT3 mediates antifibrotic effects.

In this study, to address the possibility of clinical application of IL-11 treatment in the therapeutic process of acute myocardial infarction as a cardioprotective strategy, we investigated its postconditioning effects on I/R injury. In addition, we examined whether IL-11 utilizes the cardiac STAT3 signaling pathway in its postconditioning effects.

MATERIALS AND METHODS

Animal care. The care of all animals was approved by the Animal Care and Use Committee of Graduate School of Pharmaceutical Sciences, Osaka University. The investigation conforms to the *Guide for the Care and Use of Laboratory Animals* published by the

Address for reprint requests and other correspondence: Y. Fujio, 1-6 Yamadaoka, Suita City, 565-0871, Osaka, Japan (e-mail: fujio@phs.osaka-u.ac.jp).

National Institutes of Health (NIH publication No. 85-23, revised 1996).

All mice for the experiments were euthanized by inhalation of isoflurane in a euthanasia chamber. Death of the animals was confirmed by monitoring the absence of breath after removal of the carcass from the euthanasia chamber. A total of 172 mice were used in this study.

I/R model and IL-11 treatment. Murine I/R was generated as described previously, with minor modifications (15, 21). Briefly, C57BL/6 mice (8- to 12 wk old; Japan SLC) were anesthetized and ventilated with 80% oxygen containing 1.5% isoflurane (Merck). After left-side thoracotomy, 7-0 silk suture was tied around the left coronary artery with a slipknot. Infarction was confirmed by discoloration of the ventricle and ST-T changes in electrocardiogram monitor. The chest and the skin were closed with 5-0 silk sutures. The mice were revived for a 30-min ischemic period, after which the knot was released and the heart was allowed to reperfuse for 24 h. By this experimental protocol, the mortality was minimized to less than 10%. Twenty four hours after reperfusion, the mice were euthanized and the slipknot was retied. PBS containing 1.5% Evans blue was injected into the left ventricle, and the hearts were removed. Isolated hearts were sectioned, and viable myocardium was stained with 2% triphenyl tetrazolium chloride (Sigma), as described previously (21). The amounts of myocardial area not at risk, area at risk (AAR), and infarcted area were quantified with Scion Image (Scion). In the IL-11 group, basically, 20 μg/kg of recombinant human IL-11 (Peprotech) was intravenously administered at the start of reperfusion (various concentrations in 200 μl of PBS/25 g of body wt), whereas the control group received the same volume of PBS over the same period. In the study concerning the dose-dependent effects of IL-11 on myocardial injury, various concentrations (3, 8, 20, 50 μg/kg) of IL-11 were used. There was no difference in mortality between groups.

Immunoblot analysis. Immunoblot analyses were performed as described previously (18). Briefly, heart homogenates were prepared in buffer containing 150 mM NaCl, 10 mM Tris·HCl (pH 7.5), 1 mM EDTA, 1% Triton X-100, 1% deoxycholic acid, 1% protease inhibitor cocktail, 1 mM dithiothreitol, 1 mM sodium orthovanadate, and 1 mM NaF. Proteins were separated by SDS-PAGE and transferred onto the polyvinylidene difluoride membrane (Millipore). The membrane was immunoblotted with anti-phospho-STAT3 (p-STAT3; Cell Signaling Technology) or anti-STAT3 (Santa Cruz Biotechnology) antibody. The membrane was reprobed with anti-STAT3 or anti-GAPDH (Santa Cruz Biotechnology) antibody to show the equal amount loading. Electrochemiluminescence system was used for the detection.

Echocardiographic analysis. Mice were exposed to I/R injury and IL-11 (20 μg/kg) or PBS, as a control, was administered at start of reperfusion. Twenty four hours after reperfusion, two-dimensional and motionmode (M-mode) transthoracic echocardiography was performed using an iE33 model equipped with a 15-MHz transducer (Philips Electronics, Andover, MA). Echocardiographic measurements were taken on M-mode. The investigator was blinded to the identity of the mice for analysis. Sham indicates the mice underwent thoracotomy without I/R.

Hemodynamic analysis. Hemodynamics was analyzed according to previous report with minor modification (20). Briefly, 24 h after reperfusion, mice were anesthetized (50 mg/kg pentobarbital) and heparinized (50 units) via intraperitoneal injection. The hearts were rapidly excised and placed in ice-cold modified Tyrode's solution containing (in mM) 140 NaCl, 5.4 KCl, 1.8 $CaCl_2$, 0.45 $MgCl_2$, 0.33 NaH_2PO_4, 5.5 glucose, and 5 HEPES (pH 7.4). The aorta was cannulated and retrogradely perfused at a constant pressure of 100 mmH_2O with Tyrode's solution bubbled with 80% oxygen at 37°C. Thus the experiments were performed at 37°C by immersing the heart in Tyrode's solution in a water-jacketed chamber. The hearts were paced at 420 beats/min. The fluid-filled balloon was inserted into the left ventricle to monitor cardiac function. The balloon was attached to a pressure transducer, which was coupled to a 4S PowerLab (AD Instruments). Left ventricular developed pressure and maximal and minimal change in pressure over time were measured.

Terminal deoxynucleotide transferase-mediated dUTP nick-end labeling staining. Twenty four hours after reperfusion, the frozen sections (5 μm thick) were prepared from the portion in the middle of the infarct zone. Apoptotic cell death was detected by terminal deoxynucleotide transferase-mediated dUTP nick-end labeling (TUNEL) staining with in situ apoptosis detection kit (TaKaRa). The sections were costained with anti-sarcomeric α-actinin (Sigma) antibody to identify the cardiomyocytes. Nuclei were simultaneously stained with Hoechst 33258. For quantitative analyses, apoptotic myocytes were counted in number by the researcher who was blinded to the assay conditions.

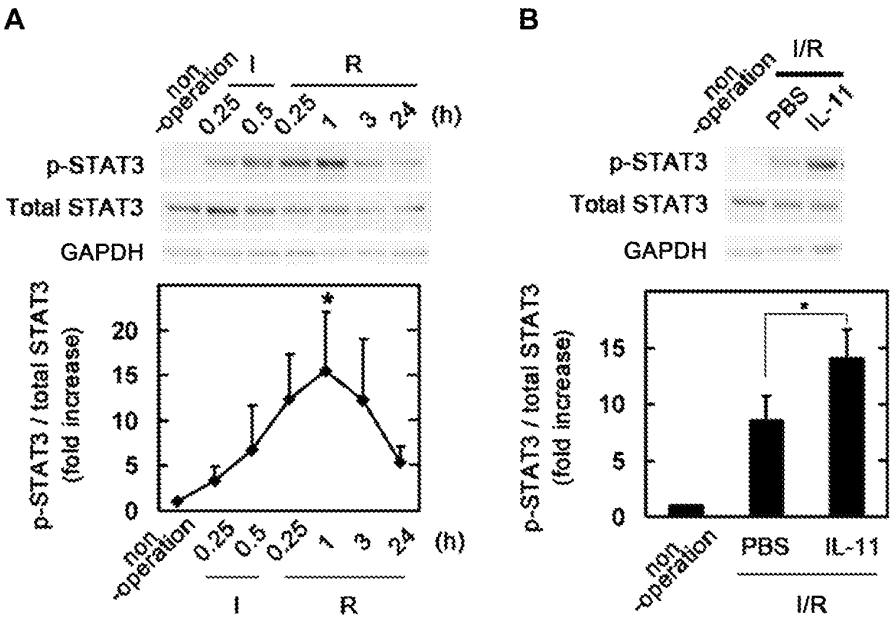

Fig. 1. IL-11 treatment enhanced STAT3 activation in ischemia/reperfusion (I/R) hearts. *A*: mice were exposed to I/R. At indicated time points, mice were euthanized and the lysates from hearts were immunoblotted with anti-phospho-specific STAT3 (p-STAT3) antibody. The blots were reprobed with anti-STAT3 antibody or GAPDH antibody. Representative data (*top*) and quantitative analyses of the p-STAT3 (*bottom*) are shown. Data are shown as means ± SD (n = 3 mice for each condition). *$P < 0.05$ vs. nonoperation, by 1-way ANOVA followed by Bonferroni test. *B*: mice were exposed to I/R. IL-11 (20 μg/kg) or PBS, as a control, was administered intravenously at start of reperfusion. Fifteen minutes after treatment, mice were euthanized and the lysates from hearts were immunoblotted with anti-p-STAT3 antibody. Blots were reprobed with anti-STAT3 antibody or GAPDH antibody. Representative data (*top*) and quantitative analyses of the p-STAT3 (*bottom*) are shown. Data are shown as means ± SD (n = 4 mice for each condition). *$P < 0.05$ vs. nonoperation, by 1-way ANOVA followed by Bonferroni test.

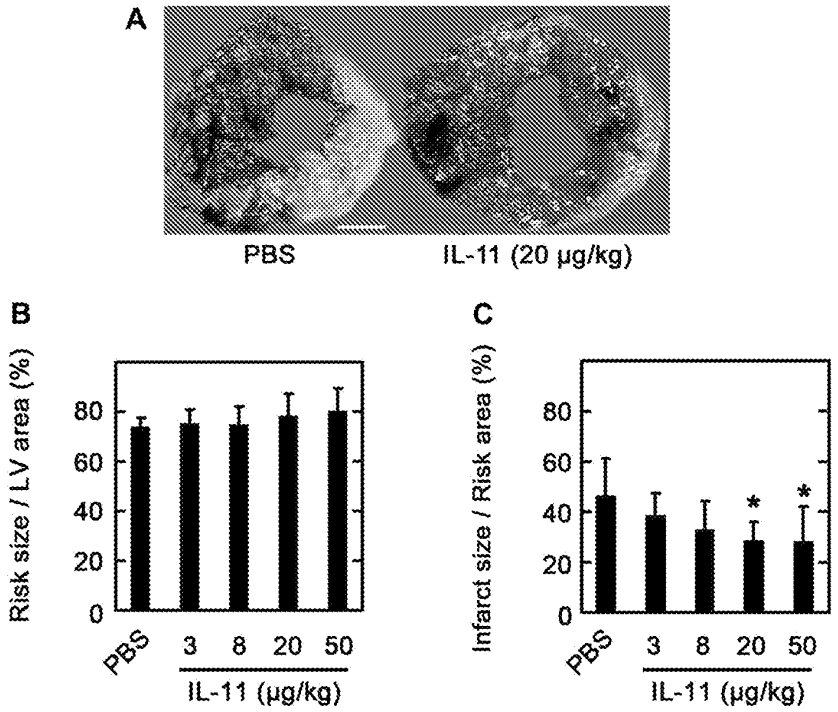

Fig. 2. Single administration of IL-11 at the time of reperfusion attenuated I/R injury. C57BL/6 mice were exposed to 30 min ischemia, followed by 24 h reperfusion. IL-11 or PBS, as a control, was administered intravenously at start of reperfusion. Areas at risk were estimated by exclusion of Evans blue. The myocardial infarct areas were detected by staining with 2% triphenyl tetrazolium chloride (TTC). Representative images are shown (*A*). Scale bar, 1 mm. *B* and *C*: risk area size and infarct size were quantitatively estimated. Data are shown as means ± SD (n = 9 mice for PBS; n = 6 mice for 3 μg/kg of IL-11; n = 7 mice for 8 μg/kg of IL-11; n = 9 mice for 20 μg/kg of IL-11; n = 6 mice for 50 μg/kg of IL-11). *P < 0.05 vs. PBS, by 1-way ANOVA followed by Bonferroni test. LV, left ventricular.

Dihydroethidium fluorescence analysis. Dihydroethidium (DHE) fluorescence analysis was performed to examine the generation of superoxide. The frozen sections (5 μm thick) were prepared and stained with 10 μM DHE in Krebs/HEPES buffer composed of (in mmol/l) 99.01 NaCl, 4.69 KCl, 1.87 $CaCl_2$, 1.20 $MgSO_4$, 1.03 K_2HPO_4, 25.0 $NaHCO_3$, 20.0 Na-HEPES, and 11.1 glucose (pH 7.4) at 37°C for 30 min in a dark. The intensities of fluorescence were quantitatively analyzed with Adobe Photoshop Elements 2.0 (Adobe Systems) by the researcher who was blinded to the assay conditions.

Real-time RT-PCR. Real time RT-PCR was performed according to the manufacturer's protocol. Total RNA was prepared from hearts at 3 h after reperfusion. Total RNA (1 μg) was subjected to first-strand cDNA synthesis with oligo (dT) primer. The mRNA expression was quantified by real-time RT-PCR using the Applied Biosystems StepOne Real-Time PCR systems (Applied Biosystems) with SYBR green system (Applied Biosystems). As an internal control, the expression of GAPDH mRNA was estimated with SYBR green system. The primers used in this study are as follows: metallothionein (MT) 1, forward: CGT AGC TCC AGC TTC ACC AGA TCT C, reverse: TGG TGG CAG CGC TGT TCG T; MT-2, forward: GCT TTT GCG CTC GAC CCA ATA CTC TC, reverse: GGA GCA GCA GCT TTT CTT GCA GGA AG; cyclooxygenase (COX)-2, forward: ACT GCC CAA CTC CCA TGG GT, reverse: AGT CCA CTC CAT GGC CCA GT; MnSOD, forward: AGG AGA GCA GCG GTC GTG TAA ACC T, reverse: CGG TGG CGT TGA GGT TGT TCA CGT A; Cu/ZnSOD, forward: AGA GCC TGA CAG GTG CAG AGA ACC, reverse: ACT TTG GCA TGC GTG TCG CC; redox factor-1, forward: AGA GAC CAA GAA GAG TAA GGG G, reverse: TGC TTC TTC CTT TAC CCA ATC C; peroxiredoxin 5, forward: TCA AGG TGG GAG ATG CCA TTC, reverse: AAC CTT GCC TTC TGC CTG GT; peroxiredoxin 6, forward: AGA TTC ATG GGG CAT TCT CTT TTC C, reverse: TAA GCA TTG ATG TCC TTG CTC CAG; isocitrate dehydrogenase, forward: AAG GAG AAG CTC ATC CTG CC, reverse: TCA GCT TGA ACT CTT CCA CAC G; glutathione reductase, forward: TGA TCA GGC ATG ATA AGG TAC TGA G, reverse: CAT CCG TCT GAA TGC CCA CT; glutathione peroxidase 4, forward: AGG CAG GAG CCA GGA AGT A, reverse: TGA TGG CAT TTC CCA GCA TGC; 5-oxoprolinase, forward: TTC CAG GGC CAG CTA AAG AAT G, reverse: TCT GTG GAT GTG CCT CCC ATG T; nuclear factor-like 1, forward: TGC ACA GTT CCC AGC TGA C, reverse: CTT CCA TAG CCT GCA TTT CCA T;

Table 1. *Effects of IL-11 on cardiac function at 24 h after reperfusion*

Parameter/Group	Sham	I/R + PBS	I/R + IL-11
Ejection fraction, %	79.3 ± 2.5	52.2 ± 5.7$	62.9 ± 10.1#*
Fractional shortening, %	40.8 ± 1.9	21.9 ± 3.1$	28.6 ± 6.2#*
Diastolic interventricular septal thickness, cm	0.085 ± 0.001	0.085 ± 0.012	0.093 ± 0.005
LV, cm			
Diastolic internal diameter	0.391 ± 0.033	0.360 ± 0.036	0.378 ± 0.009
Diastolic posterior wall thickness	0.069 ± 0.003	0.080 ± 0.012	0.077 ± 0.011
Systolic internal diameter	0.232 ± 0.026	0.282 ± 0.035	0.270 ± 0.028
Heart rate-LV, beats/min	494 ± 21	490 ± 52	486 ± 45

Values are means ± SD; n = 3 mice for sham, n = 6 mice for ischemia-reperfusion (I/R) + PBS, and n = 6 mice for I/R + IL-11. Mice were subjected to 30 min of ischemia followed by 24 h reperfusion. IL-11 (20 μg/kg) or PBS, as a control, was intravenously administered at the time of reperfusion. $$P$ < 0.01; #P < 0.05 vs. Sham; *P < 0.05 vs. I/R + PBS, by unpaired t-test. LV, left ventricular.

Table 2. *Effects of IL-11 on hemodynamics at 24 h after reperfusion*

Parameter/Group	Sham	I/R + PBS	I/R + IL-11
LV developed pressure, mmHg	79.5 ± 9.9	55.6 ± 11.0$	69.3 ± 6.7*
+dP/d*t* (mmHg/s)	2347.8 ± 443.2	1532.4 ± 296.1$	2009.0 ± 321.2*
−dP/d*t* (mmHg/s)	−2178.3 ± 387.3	−1395.0 ± 326.1$	−1776.7 ± 132.2$*

Values are means ± SD; $n = 4$ mice for sham, $n = 5$ mice for I/R + PBS, and $n = 6$ mice for I/R + IL-11. Mice were subjected to 30 min of ischemia followed by 24 h reperfusion. IL-11 (20 μg/kg) or PBS, as a control, was intravenously administered at the time of reperfusion. $\$P < 0.05$ vs. Sham; $*P < 0.05$ vs. I/R + PBS, by unpaired *t*-test. ±dP/d*t*, maximal and minimal change in pressure over time.

GAPDH, forward: GCC GGT GCT GAG TAT GTC GT, reverse: CCC TTT TGG CTC CAC CCT T.

Cell culture and reagents. Cardiomyocytes were cultured as described previously (16). Briefly, cardiac ventricles of 1-day-old Wistar rats were minced and cells were isolated with 0.1% trypsin (Difco Laboratories) and 0.1% collagenase type IV (Sigma). To eliminate the nonmyocyte population, isolated cells were plated and incubated for 1 h at 37°C. Nonattached cells were collected as cardiomyocytes and cultured in DMEM/Ham's F-12 (DMEM/F-12) containing 5% neonatal calf serum. More than 90% cells were identified as cardiomyocytes, assessed by immunostaining with anti-sarcomeric specific α-actinin antibody.

STAT3 Stealth RNAi, MT Stealth RNAi, and control Stealth RNAi were purchased from Invitrogen. Cardiomyocytes were transfected with these small interfering RNA (siRNA) using Lipofectamine RNAi MAX (Invitrogen) in DMEM/F-12 containing 5% neonatal calf serum. Cardiomyocytes were cultured in serum-free DMEM/F-12 containing IL-11 and/or H_2O_2 at the indicated concentrations. Apoptotic cells were detected by Annexin V staining, as described in a previous report (16).

Conditional ablation of STAT3 gene in cardiomyocytes of adult murine hearts. Cardiac STAT3 conditional knockout mice were generated as described previously with minor modifications (20). In brief, the cardiac-specific transgenic mice overexpressing Cre recombinase fusion protein to the mutated estrogen receptor domains (MerCreMer) under the control of α-myosin heavy chain (α-MHC) promoter were crossed with STAT3 flox mice ($STAT3^{flox/flox}$) to produce α-MHC-MerCreMer/$STAT3^{flox/flox}$ mice. To activate Cre-recombinase activity, α-MHC-MerCreMer/$STAT3^{flox/flox}$ or α-MHC-MerCreMer/$STAT3^{wild/wild}$ mice, as control mice, were intraperitoneally injected with 8 mg/kg of tamoxifen (Sigma) dissolved in corn oil (Sigma) once a day for 14 consecutive days. After tamoxifen treatment, the mutant mice underwent I/R as described above.

Statistical analysis. Data were presented as means ± SD. The comparison between two groups was performed using an unpaired *t*-test. One-way ANOVA with Bonferroni test was used for comparisons of multiple groups. Differences were considered statistically significant when the calculated *P* value was less than 0.05.

RESULTS

IL-11 treatment enhanced STAT3 activity in I/R hearts. Because it is known that STAT3 is activated during I/R, we first confirmed that STAT3 is endogenously activated in hearts at various time points after I/R in our system (Fig. 1*A*). Immunoblot analyses with anti-p-STAT3 antibody revealed that STAT3 phosphorylation was slightly induced at a 30-min ischemia period. It is important that STAT3 was dramatically activated at 1 h after reperfusion. These data indicated that STAT3 signals are endogenously activated during I/R.

Next, we examined whether IL-11 administration further enhanced STAT3 activity during I/R (Fig. 1*B*). Mice were exposed to I/R injury with intravenous injection of IL-11 at a dose of 20 μg/kg or PBS at start of reperfusion. We analyzed the activation of STAT3 at 15 min after reperfusion by immunoblot analysis, based on the previous findings that the intravenous administration of IL-11 activated STAT3 with its peak at 15 min in nonoperated hearts (20). Fifteen minutes after reperfusion, I/R stimuli induced STAT3 activation, which was enhanced by IL-11 treatment, relative to control.

The therapeutic treatment of IL-11 exhibits the postconditioning effects against I/R injury. Because STAT3 activity was reinforced by IL-11 injection at start of reperfusion in I/R

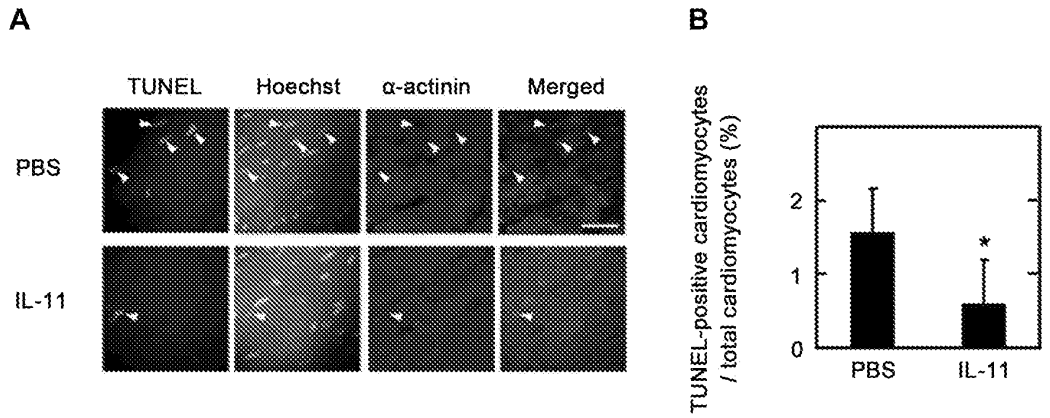

Fig. 3. IL-11 treatment suppressed cardiomyocytes apoptosis after I/R. *A*: frequency of apoptotic cardiomyocytes was estimated by terminal deoxynucleotide transferase-mediated dUTP nick-end labeling (TUNEL) staining 24 h after myocardial infarction. The sections were costained with antisarcomeric α-actinin antibody and Hoechst 33258 dye. The images shown are representative of 75 to 120 images obtained from 5 to 6 mice (15 to 20 fields from each mouse). Arrowheads show TUNEL-positive, apoptotic cardiomyocytes. Scale bar, 50 μm. *B*: quantification of the apoptotic cardiomyocytes is shown. Data are shown as means ± SD [$n = 5$ mice for PBS; $n = 6$ mice for IL-11 (20 μg/kg)]. $*P < 0.05$ by unpaired *t*-test.

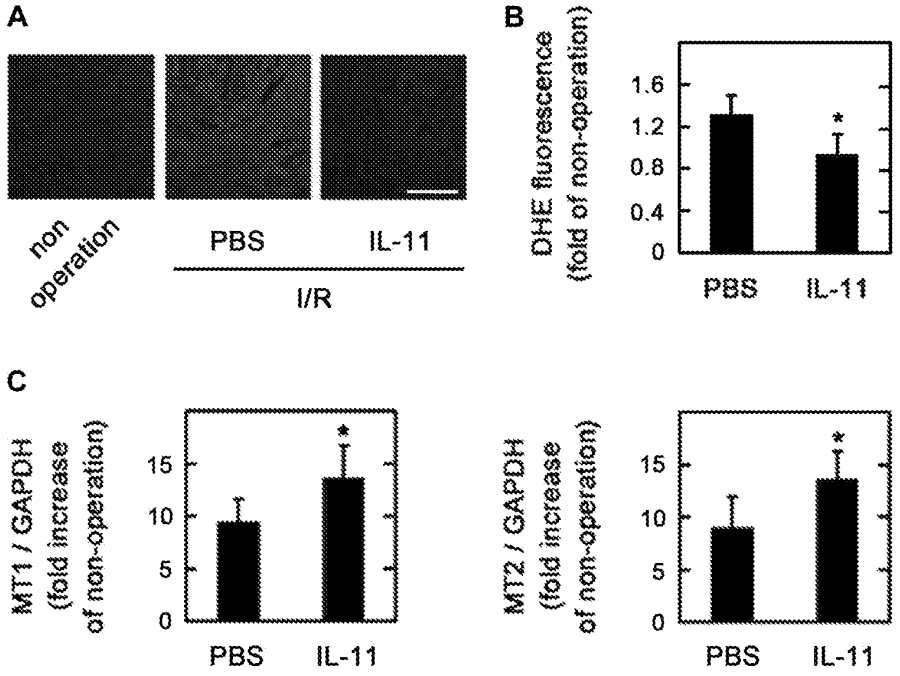

Fig. 4. IL-11 treatment attenuated reactive oxygen species (ROS) production after I/R. Twenty four hours after reperfusion, the heart sections were stained with dihydroethidium (DHE). *A*: representative fluorescent images are shown. Scale bar, 100 μm. *B*: fluorescence intensity at risk area was estimated. Data are shown as means ± SD [n = 4 mice for PBS; n = 5 mice for IL-11 (20 μg/kg)]. *P < 0.05 by unpaired t-test. *C*: three hours after reperfusion, total RNA was prepared from I/R hearts and real time RT-PCR was performed for metallothionein (MT) 1 and 2. The expression of MT1 and MT2 were normalized with that of GAPDH. Data are shown as means ± SD [n = 6 mice for PBS; n = 7 mice for IL-11 (20 μg/kg)]. *P < 0.05 by unpaired t-test.

model, we examined the postconditioning effects of IL-11 on I/R injury (Fig. 2). Mice were subjected to 30 min of left coronary artery ligation followed by 24 h reperfusion. IL-11 or PBS, as a control, was administered intravenously at start of reperfusion. Although there was no significant difference in AAR between IL-11 treatment and control group, the infarct size relative to AAR was decreased by single treatment of IL-11 in a dose-dependent manner (Fig. 2*C*). Treatment of IL-11 at 20 and 50 μg/kg significantly reduced the infarct size by 38.8 and 39.2%, respectively (PBS, 46.7 ± 14.4%; 20 μg/kg of IL-11, 28.6 ± 7.5%; 50 μg/kg of IL-11, 28.4 ± 13.7%). Because it is confirmed that IL-11 treatment at a dose of 20 μg/kg achieved the maximal effect, further studies were performed with the use of IL-11 at a dose of 20 μg/kg. Next, we investigated the cardiac function after I/R by echocardiographic and hemodynamic analysis. Echocardiographic analysis revealed that ejection fraction and fraction shortening were dramatically reduced 24 h after reperfusion (Table 1). Furthermore, hemodynamic analysis elucidated that left ventricular developed pressure and maximal and minimal change in pressure over time were reduced by I/R (Table 2). It is intriguing, however, that IL-11 treatment at a dose of 20 μg/kg significantly preserved cardiac function.

We also examined the effects of the timing of IL-11 treatment on cardioprotection. Mice were exposed to I/R injury, and IL-11 was treated at 3 h after reperfusion. As a result, IL-11 was less effective in cardioprotection when administered at 3 h than immediately after reperfusion (data not shown). Therefore, the therapeutic window of IL-11 is likely to be the early time point after myocardial infarction.

These findings suggest that the administration of IL-11 at reperfusion has the therapeutic potential to prevent I/R injury.

Table 3. *The expressions of cytoprotective genes*

Gene	Non–I/R + IL-11	I/R + PBS	I/R + IL-11
Metallothionein 1	6.73 ± 1.57*	9.48 ± 2.15*	13.61 ± 3.04*#
Metallothionein 2	4.07 ± 0.82*	9.04 ± 2.97*	13.58 ± 2.63*#
Cyclooxygenase-2	0.41 ± 0.20	16.85 ± 10.61*	17.86 ± 8.23*
MnSOD	1.09 ± 0.08	1.12 ± 0.15	1.09 ± 0.17
Cu/ZnSOD	1.09 ± 0.12	0.95 ± 0.08	1.09 ± 0.22
Redox factor-1	2.77 ± 3.07	3.76 ± 5.86	1.73 ± 0.24*
Peroxiredoxin 5	1.02 ± 0.12	1.12 ± 0.21	1.09 ± 0.23
Peroxiredoxin 6	1.06 ± 0.11	1.10 ± 0.20	1.15 ± 0.29
Isocitrate dehydrogenase	1.08 ± 0.04	1.18 ± 0.17	1.15 ± 0.29
Glutathione reductase	0.68 ± 0.29	1.12 ± 0.67	1.48 ± 0.81
Glutathione peroxidase 4	1.03 ± 0.12	1.11 ± 0.19	1.12 ± 0.28
5-Oxoprolinase	1.52 ± 0.45	1.11 ± 0.39	1.18 ± 0.31
Nuclear factor-like 1	1.28 ± 0.04	1.20 ± 0.14	1.29 ± 0.24

Values (fold change of control mice) are means ± SD; n = 3–7 mice. Three hours after treatment of IL-11 at 20 μg/kg or PBS, total RNA was prepared from I/R or nonoperation hearts and real time RT-PCR was performed for the cytoprotective genes. The expression of cytoprotective genes was normalized with that of GAPDH. *P < 0.05 vs. control mice; #P < 0.05 vs. I/R + PBS, by unpaired t-test.

IL-11 treatment suppressed apoptotic cell death and reactive oxygen species generation in I/R hearts. To address the mechanisms of the postconditioning effects of IL-11, we examined whether IL-11 treatment prevented apoptotic cell death by I/R injury (Fig. 3). TUNEL staining revealed that TUNEL-positive cardiomyocytes were detected mainly at the risk area 24 h after reperfusion. It is important that IL-11 treatment significantly reduced the frequency of apoptotic cardiomyocytes compared with the PBS group.

Reactive oxygen species (ROS) is one of the most important inducers of apoptotic and necrotic cell death after I/R. To assess the mechanism of IL-11-mediated suppression of cell death, we focused on the effect of IL-11 on ROS production (Fig. 4*A*). DHE fluorescence staining demonstrated that ROS was induced by I/R at risk area. It is interesting that IL-11 treatment suppressed ROS production relative to PBS group. To clarify the molecular mechanism of the ROS-scavenging effects of IL-11, the expression of ROS-related cytoprotective genes downstream of STAT3 (19, 21, 24, 27) was measured by real time RT-PCR (Table 3). Among them, MT1, MT2, and COX-2 mRNA were upregulated at 3 h after I/R. It is important that IL-11 treatment enhanced the I/R-induced upregulation of *MT1* and *MT2* gene transcripts at 3 h after reperfusion (Fig. 4*B*), whereas the expression of COX-2 mRNA was not reinforced by IL-11 under I/R condition.

We examined whether IL-11 induced MT expression through STAT3 activation in vitro and in vivo (Fig. 5). In the in vitro model, neonatal rat cardiomyocytes were prepared and transfected with control siRNA or with STAT3 siRNA. Twenty four hours later, cells were stimulated with IL-11 (20 ng/ml) for 3 h. Real-time PCR analyses revealed that the stimulation with IL-11 resulted in the increased expressions of MT1 and MT2, which was cancelled by the knockdown of STAT3. In the in vivo model, *STAT3* gene was ablated in a cardiomyocyte-specific manner, using cardiomyocyte-specific tamoxifen-inducible Cre recombinase transgenic mice (α-

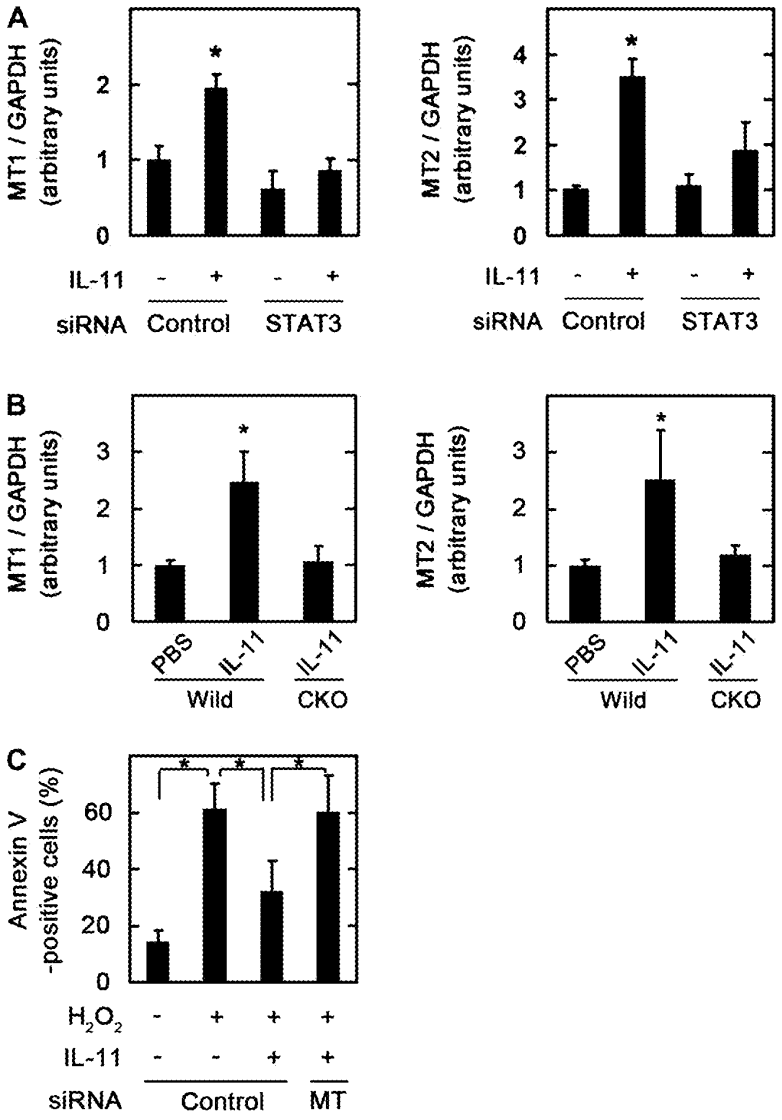

Fig. 5. IL-11 induces MT1 and MT2 through STAT3, contributing to cytoprotection. Neonatal rat cardiomyocytes were transfected with control small interfering RNA (siRNA; control) or with STAT3 siRNA (STAT3). *A*: twenty four hours later, cells were stimulated with IL-11 (20 ng/ml) for 3 h. Total RNA was prepared, and real-time PCR was performed for MT1 (*left*) and MT2 (*right*). The expressions of MT 1 and MT2 were normalized with that of GAPDH. Data are shown as means ± SD ($n = 4$). *$P < 0.05$ vs. control-IL-11 (−), by ANOVA. *B*: α-MHC MerCreMer/STAT3$^{flox/flox}$ mice (CKO) or wild-type (Wild) mice were intraperitoneally administered with tamoxifen for the depletion of *STAT3* gene as described in MATERIALS AND METHODS. After tamoxifen treatment, IL-11 (20 μg/kg) or PBS was intravenously injected. Three hours after injection, total RNA was prepared from hearts and real time RT-PCR was performed for MT1 (*left*) and MT2 (*right*). The expressions of MT1 and MT2 were normalized with that of GAPDH. Data are shown as means ± SD ($n = 4$ mice for each group). *$P < 0.05$ by ANOVA. *C*: neonatal rat cardiomyocytes were transfected with control siRNA or with MT1 and MT2 siRNA. Twenty four hours later, cells were stimulated with IL-11 (200 ng/ml) for 6 h, followed by exposure to H_2O_2 (1 mM) for 24 h. Apoptotic cells were detected by Annexin V staining. Data are shown as means ± SD ($n = 6$). *$P < 0.05$ vs. control-IL-11 ± H_2O_2, by ANOVA.

MHC-MerCreMer mice) on the genetic background of $STAT3^{flox/flox}$. α-MHC-MerCreMer mice on $STAT3^{wild/wild}$ were used as a control. To induce Cre-mediated recombination, mice were treated with tamoxifen as described in MATERIALS AND METHODS. After tamoxifen treatment, the level of STAT3 protein expression decreased (data not shown). Cardiac-specific conditional STAT3-deficient (STAT3 CKO) mice and control (Wild) mice were administered with IL-11. Three hours after IL-11 administration, MT1 and MT2 mRNA expressions were measured by real-time PCR. Although IL-11 increased MT1 and MT2 mRNA in Wild mice, the upregulation of MT1 and MT2 mRNA by IL-11 was abrogated in STAT3 CKO mice.

To address the importance of MT1 and MT2 in IL-11-mediated cardioprotection, cardiomyocytes were transfected with control siRNA or with MT1 and 2 siRNA. Twenty four hours later, cells were incubated with IL-11 (200 ng/ml) for 6 h, followed by exposure to H_2O_2 (1 mM) for 24 h. Apoptotic cells were detected by Annexin V staining. Although H_2O_2 evoked apoptosis in control siRNA-transfected cardiomyocytes, IL-11 suppressed H_2O_2-induced apoptosis, as reported previously (16). It is important that IL-11-mediated attenuation of H_2O_2-induced apoptosis was reduced in MT siRNA-transfected cardiomyocytes. These data indicated that IL-11 prevented ROS-induced cardiomyocyte death, at least partially through STAT3/MT axis.

Activation of cardiac STAT3 is indispensable for IL-11-mediated attenuation of I/R injury. To assess the importance of cardiac STAT3 in IL-11-mediated prevention against I/R injury, we prepared STAT3 CKO mice and control (Wild) mice. Consistent with the previous reports (12, 14, 20), there was no significant difference in cardiac function between CKO mice and control mice, analyzed by echocardiography (data not shown). STAT3 CKO mice and control mice were exposed to I/R and administered with or without IL-11 at the start of reperfusion (Fig. 6, *A* and *B*). STAT3 CKO and control mice showed the similar size of AAR. It is important that the treatment of IL-11 (20 μg/kg) reduced infarct size in wild-type mice; however, IL-11-mediated attenuation of I/R injury was abrogated in STAT3 CKO mice (Wild-PBS, 36.3 ± 10.3%; Wild-IL-11, 24.8 ± 5.2%; CKO-PBS, 44.9 ± 6.3%; CKO-IL-11, 52.3 ± 15.3%).

Finally, because IL-11 postconditioning effects were closely associated with ROS scavenging, we examined ROS generation in STAT3 CKO mice (Fig. 6*C*). It is interesting that IL-11 failed to suppress ROS production in STAT3 CKO mice, indicating that STAT3 activation is essential for ROS scavenging. These findings indicate that cardiac activation of STAT3 is a critical step for the postconditioning effects of IL-11.

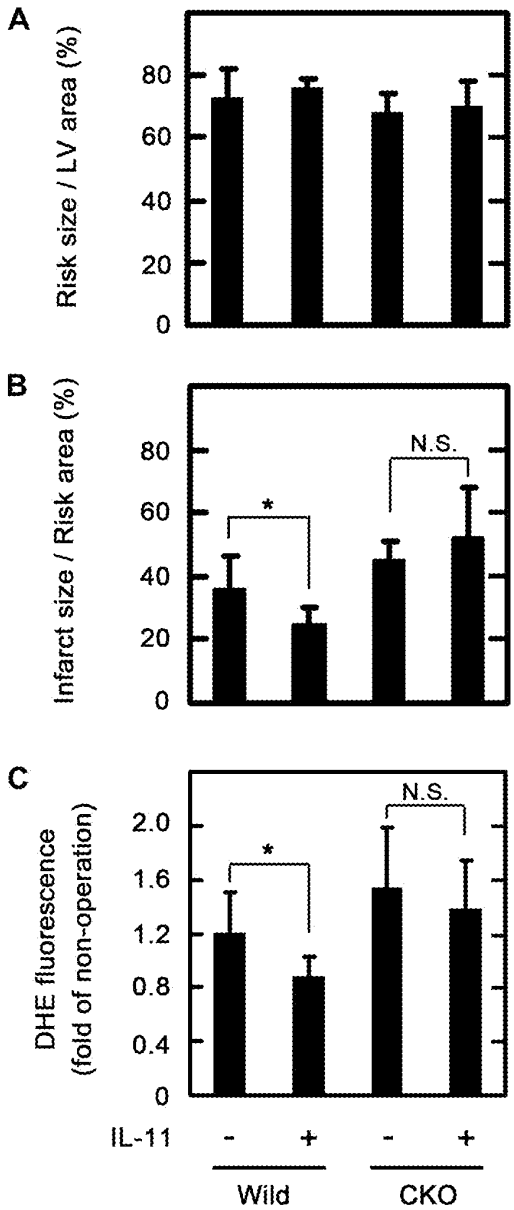

Fig. 6. IL-11-mediated postconditioning against I/R injury was abrogated in STAT3 CKO mice. α-Myosin heavy chain (α-MHC) MerCreMer/$STAT3^{flox/flox}$ (CKO) mice or α-MHC MerCreMer $STAT3^{wild/wild}$ (Wild) mice, as control mice, were intraperitoneally administered with 8 mg/kg of tamoxifen once a day for 14 consecutive days. After tamoxifen treatment, STAT3 CKO mice and wild-type mice were subjected to 30 min ischemia, followed by 24 h reperfusion. IL-11 (20 μg/kg) was administrated intravenously at start of reperfusion. *A* and *B*: areas at risk were estimated by exclusion of Evans blue. The myocardial infarct areas were detected by staining with 2% TTC. Risk area size and infarct size were quantitatively estimated. Data are shown as means ± SD (n = 7 mice for Wild-PBS; n = 5 mice for Wild-IL-11; n = 8 mice for CKO-PBS; n = 6 mice for CKO-IL-11). *P < 0.05 by unpaired t-test. *C*: twenty four hours after reperfusion, the heart sections were stained with DHE. The fluorescence intensity at risk area was estimated. Data are shown as means ± SD (n = 4 mice for Wild-PBS; n = 6 mice for Wild-IL-11; n = 6 mice for CKO-IL-11). *P < 0.05 by unpaired t-test; NS, not significant.

DISCUSSION

In the present study, we examined the postconditioning effects of therapeutic treatment of IL-11 on I/R injury. IL-11 administration enhanced the I/R-induced activation of STAT3 in hearts. Single treatment of IL-11 at the start of reperfusion was sufficient to attenuate I/R injury in mice. IL-11 prevented apoptotic cell death and ROS generation, accompanied by the increase of MT1 and 2 mRNA expressions. It is important that IL-11-mediated cardioprotection against I/R injury was abolished in cardiac-specific conditional STAT3-deficient mice.

Furthermore, IL-11 treatment failed to suppress ROS generation in response to I/R in STAT3 CKO mice. These findings suggest that IL-11 treatment exhibits postconditioning effects through STAT3 pathway in I/R.

IL-11 treatment exhibits cardioprotective effects by distinct mechanisms from the cytokine therapies proposed so far. Recently, much attention has been paid to the cardioprotective effects of granulocyte colony stimulating factor (G-CSF). The administration of G-CSF preserves myocardium in the myocardial infarction model (11) as well as the I/R model (26). In G-CSF signaling, JAK2/STAT3 pathway has been proposed to be important in antifibrotic effects after myocardial infarction during subacute and chronic phase, whereas the Akt/NOS pathway contributes to the beneficial effect of G-CSF in I/R hearts during the acute phase (25). In contrast, IL-11 protects myocardium through STAT3 both in acute and chronic phase. IL-11 attenuated adverse cardiac remodeling after myocardial infarction via cardiac STAT3 pathway (20). And, herein, we revealed that IL-11-mediated suppression of I/R injury was exerted by cardiac STAT3 activation in acute phase. We have also confirmed that IL-11 does not activate Akt signal in murine hearts and neonatal rat cardiomyocytes (data not shown). Thus IL-11 therapy against I/R injury is based on a novel concept, mainly utilizing STAT3 signal.

In the present study, cardiac STAT3 activation is a critical event for IL-11-mediated postconditioning effects in I/R injury. Consistent with our results, previous studies have demonstrated that STAT3 is indispensable for ischemic postconditioning that was induced by repeated exposure to ischemic stress (1). Ischemic postconditioning is complicated and requires at least three signaling pathways, including STAT3, Akt, and TNF-α (8, 17). Indeed, the deficiency in any one of these three signaling pathways abrogates ischemic postconditioning effects; however, it has not been addressed whether the activation of one of these signals could confer the resistance to I/R under the postconditioning situation. Here, as a novel pharmacological approach, we have proposed that the activation of glycoprotein 130/STAT3 pathway simply by IL-11 administration is therapeutically sufficient for postconditioning effects.

It is important that IL-11-mediated suppression of ROS generation was abrogated in STAT3 CKO mice, suggesting that STAT3 utilizes ROS scavenging systems in its cardioprotection. It is interesting that I/R led to the increase of MT1 and 2 expressions, which were enhanced by IL-11. Combined with the previous study that MT1 and 2 are key molecules in cardiac STAT3-mediated attenuation of I/R injury (21), we consider that IL-11 prevented I/R injury at least partially through elevation of MT expression; however, we cannot exclude the possibility that other functions may be involved in STAT3-mediated cardioprotection. For example, recent studies demonstrated that STAT3 exerts protective functions, independently of its transcriptional activation (10). STAT3 contributes to cardioprotection by stimulation of respiration and inhibition of mitochondrial permeability transition pore opening in mitochondria (2). Further investigation might be needed to fully reveal the comprehensive mechanisms of postconditioning effects by IL-11/cardiac STAT3 axis.

In our experiments, IL-11 was intravenously administered to mice immediately after reperfusion to protect against cardiac injury. To utilize IL-11 in clinical situation, it might be informative to determine the therapeutic window of the IL-11 postconditioning. According to previous reports regarding G-CSF, its beneficial effects were exerted when its treatment was started early after myocardial infarction in animal models (11) and clinical trials (13, 28). Because IL-11 directly transduces cardioprotective signals in cardiomyocytes exposed to I/R stress, as is the case with G-CSF, the maximal effects of IL-11 would be achieved by its administration at the early time point of myocardial infarction.

In conclusion, IL-11 exhibits the postconditioning effects against I/R via cardiac STAT3 pathway. Our results propose the IL-11/STAT3 axis is a promising therapeutic target against ischemic heart diseases.

ACKNOWLEDGMENTS

We thank Wakako Okamoto for excellent secretary work.

GRANTS

This study was supported by Grant-in-Aid for Scientific Research (B) from Japan Society for the Promotion of Science, by the Osaka Foundation for Promotion of Clinical Immunology, and by Grant-in-Aid from Knowledge Cluster Initiative (2nd Stage) of the Ministry of Education, Culture, Sports, Science and Technology of Japan.

DISCLOSURES

No conflicts of interest, financial or otherwise, are declared by the author(s).

AUTHOR CONTRIBUTIONS

Author contributions: M.O., G.M., M.M., M.Y., H.N., and Y.F. conception and design of research; M.O., K.M., S.M., T.I., T.Y., S.K., A.M., K.T., and H.N. performed experiments; M.O., A.H., M.S., H.N., and Y.F. analyzed data; M.O. and Y.F. interpreted results of experiments; M.O., K.M., and Y.F. prepared figures; M.O. and Y.F. drafted manuscript; M.O. and Y.F. approved final version of manuscript; H.N. and Y.F. edited and revised manuscript.

REFERENCES

1. **Boengler K, Buechert A, Heinen Y, Roeskes C, Hilfiker-Kleiner D, Heusch G, Schulz R.** Cardioprotection by ischemic postconditioning is lost in aged and STAT3-deficient mice. *Circ Res* 102: 131–135, 2008.
2. **Boengler K, Hilfiker-Kleiner D, Heusch G, Schulz R.** Inhibition of permeability transition pore opening by mitochondrial STAT3 and its role in myocardial ischemia/reperfusion. *Basic Res Cardiol* 105: 771–785, 2010.
3. **Du X, Liu Q, Yang Z, Orazi A, Rescorla FJ, Grosfeld JL, Williams DA.** Protective effects of interleukin-11 in a murine model of ischemic bowel necrosis. *Am J Physiol Gastrointest Liver Physiol* 272: G545–G552, 1997.
4. **Du X, Williams DA.** Interleukin-11: review of molecular, cell biology, and clinical use. *Blood* 89: 3897–3908, 1997.
5. **Fischer P,.** and Hilfiker-Kleiner D. *Survival pathways in hypertrophy and heart failure: the gp130-STAT axis Basic Res Cardiol* 102: 393–411, 2007.
6. **Funamoto M, Fujio Y, Kunisada K, Negoro S, Tone E, Osugi T, Hirota H, Izumi M, Yoshizaki K, Walsh K, Kishimoto T,.** and Yamauchi-Takihara K. *Signal transducer and activator of transcription 3 is required for glycoprotein 130-mediated induction of vascular endothelial growth factor in cardiac myocytes J Biol Chem* 275: 10561–10566, 2000.
7. **Gadient RA, Patterson PH.** Leukemia inhibitory factor, Interleukin 6, and other cytokines using the GP130 transducing receptor: roles in inflammation and injury. *Stem Cells* 17: 127–137, 1999.
8. **Goodman MD, Koch SE, Fuller-Bicer GA, Butler KL.** Regulating RISK: a role for JAK-STAT signaling in postconditioning? *Am J Physiol Heart Circ Physiol* 295: H1649–H1656, 2008.
9. **Gordon MS, McCaskill-Stevens WJ, Battiato LA, Loewy J, Loesch D, Breeden E, Hoffman R, Beach KJ, Kuca B, Kaye J, Sledge GW Jr.** A phase 1 trial of recombinant human interleukin-11 (neumega rhIL-11 growth factor) in women with breast cancer receiving chemotherapy. *Blood* 87: 3615–3624, 1996.

10. **Haghikia A, Stapel B, Hoch M,.** and Hilfiker-Kleiner D. *STAT3 and cardiac remodeling Heart Fail Rev* 16: 35–47, 2010.
11. **Harada M, Qin Y, Takano H, Minamino T, Zou Y, Toko H, Ohtsuka M, Matsuura K, Sano M, Nishi J, Iwanaga K, Akazawa H, Kunieda T, Zhu W, Hasegawa H, Kunisada K, Nagai T, Nakaya H, Yamauchi-Takihara K, Komuro I.** G-CSF prevents cardiac remodeling after myocardial infarction by activating the Jak-Stat pathway in cardiomyocytes. *Nat Med* 11: 305–311, 2005.
12. **Hilfiker-Kleiner D, Hilfiker A, Fuchs M, Kaminski K, Schaefer A, Schieffer B, Hillmer A, Schmiedl A, Ding Z, Podewski E, Podewski E, Poli V, Schneider MD, Schulz R, Park JK, Wollert KC, Drexler H.** Signal transducer and activator of transcription 3 is required for myocardial capillary growth, control of interstitial matrix deposition, and heart protection from ischemic injury. *Circ Res* 95: 187–195, 2004.
13. **Ince H, Petzsch M, Kleine HD, Schmidt H, Rehders T, Korber T, Schumichen C, Freund M, Nienaber CA.** Preservation *from left ventricular remodeling by front-integrated revascularization and stem cell liberation in evolving acute myocardial infarction by use of granulocyte-colony-stimulating factor (FIRSTLINE-AMI) Circulation* 112: 3097–3106, 2005.
14. **Jacoby JJ, Kalinowski A, Liu MG, Zhang SS, Gao Q, Chai GX, Ji L, Iwamoto Y, Li E, Schneider M, Russell KS, Fu XY.** Cardiomyocyte-restricted knockout of STAT3 results in higher sensitivity to inflammation, cardiac fibrosis, and heart failure with advanced age. *Proc Natl Acad Sci USA* 100: 12929–12934, 2003.
15. **Kaiser RA, Bueno OF, Lips DJ, Doevendans PA, Jones F, Kimball TF, Molkentin JD.** Targeted inhibition of p38 mitogen-activated protein kinase antagonizes cardiac injury and cell death following ischemia-reperfusion in vivo. *J Biol Chem* 279: 15524–15530, 2004.
16. **Kimura R, Maeda M, Arita A, Oshima Y, Obana M, Ito T, Yamamoto Y, Mohri T, Kishimoto T, Kawase I, Fujio Y, Azuma J.** Identification of cardiac myocytes as the target of interleukin 11, a cardioprotective cytokine. *Cytokine* 38: 107–115, 2007.
17. **Lacerda L, Somers S, Opie LH, Lecour S.** Ischaemic postconditioning protects against reperfusion injury via the SAFE pathway. *Cardiovasc Res* 84: 201–208, 2009.
18. **Mohri T, Fujio Y, Maeda M, Ito T, Iwakura T, Oshima Y, Uozumi Y, Segawa M, Yamamoto H, Kishimoto T, Azuma J.** Leukemia inhibitory factor induces endothelial differentiation in cardiac stem cells. *J Biol Chem* 281: 6442–6447, 2006.
19. **Negoro S, Kunisada K, Fujio Y, Funamoto M, Darville MI, Eizirik DL, Osugi T, Izumi M, Oshima Y, Nakaoka Y, Hirota H, Kishimoto T,.** and Yamauchi-Takihara K. *Activation of signal transducer and activator of transcription 3 protects cardiomyocytes from hypoxia/reoxygenation-induced oxidative stress through the upregulation of manganese superoxide dismutase Circulation* 104: 979–981, 2001.
20. **Obana M, Maeda M, Takeda K, Hayama A, Mohri T, Yamashita T, Nakaoka Y, Komuro I, Matsumiya G, Azuma J, Fujio Y.** Therapeutic activation of signal transducer and activator of transcription 3 by interleukin-11 ameliorates cardiac fibrosis after myocardial infarction. *Circulation* 121: 684–691, 2010.
21. **Oshima Y, Fujio Y, Nakanishi T, Itoh N, Yamamoto Y, Negoro S, Tanaka K, Kishimoto T, Kawase I, Azuma J.** STAT3 mediates cardioprotection against ischemia/reperfusion injury through metallothionein induction in the heart. *Cardiovasc Res* 65: 428–435, 2005.
22. **Osugi T, Oshima Y, Fujio Y, Funamoto M, Yamashita A, Negoro S, Kunisada K, Izumi M, Nakaoka Y, Hirota H, Okabe M, Yamauchi-Takihara K, Kawase I, Kishimoto T.** Cardiac-specific activation of signal transducer and activator of transcription 3 promotes vascular formation in the heart. *J Biol Chem* 277: 6676–6681, 2002.
23. **Sands BE, Winston BD, Salzberg B, Safdi M, Barish C, Wruble L, Wilkins R, Shapiro M, Schwertschlag US.** Randomized, controlled trial of recombinant human interleukin-11 in patients with active Crohn's disease. *Aliment Pharmacol Ther* 16: 399–406, 2002.
24. **Sarafian TA, Montes C, Imura T, Qi J, Coppola G, Geschwind DH, Sofroniew MV.** Disruption of astrocyte STAT3 signaling decreases mitochondrial function and increases oxidative stress in vitro. *PLoS One* 5: e9532, 2010.
25. **Takano H, Ueda K, Hasegawa H, Komuro I.** G-CSF therapy for acute myocardial infarction. *Trends Pharmacol Sci* 28: 512–517, 2007.
26. **Ueda K, Takano H, Hasegawa H, Niitsuma Y, Qin Y, Ohtsuka M, Komuro I.** Granulocyte colony stimulating factor directly inhibits myocardial ischemia-reperfusion injury through Akt-endothelial NO synthase pathway. *Arterioscler Thromb Vasc Biol* 26: e108–e113, 2006.
27. **Xuan YT, Guo Y, Zhu Y, Han H, Langenbach R, Dawn B, Bolli R.** Mechanism of cyclooxygenase-2 upregulation in late preconditioning. *J Mol Cell Cardiol* 35: 525–537, 2003.
28. **Zohlnhofer D, Ott I, Mehilli J, Schomig K, Michalk F, Ibrahim T, Meisetschlager G, von Wedel J, Bollwein H, Seyfarth M, Dirschinger J, Schmitt C, Schwaiger M, Kastrati A, Schomig A.** Stem cell mobilization by granulocyte colony-stimulating factor in patients with acute myocardial infarction: a randomized controlled trial. *Jama* 295: 1003–1010, 2006.
29. **Zou Y, Takano H, Mizukami M, Akazawa H, Qin Y, Toko H, Sakamoto M, Minamino T, Nagai T, Komuro I.** Leukemia inhibitory factor enhances survival of cardiomyocytes and induces regeneration of myocardium after myocardial infarction. *Circulation* 108: 748–753, 2003.

ELSEVIER

Journal of Immunological Methods 190 (1996) 21–27

JOURNAL OF IMMUNOLOGICAL METHODS

Anti-gp130 transducer monoclonal antibodies specifically inhibiting ciliary neurotrophic factor, interleukin-6, interleukin-11, leukemia inhibitory factor or oncostatin M

Zong-Jiang Gu [a,b,c], John Wijdenes [d], Xue-Guang Zhang [a,b,c], Marie-Martine Hallet [e], Claude Clement [d], Bernard Klein [a,b,*]

[a] *Institute for Molecular Genetics, CNRS, 1919 Route de Mende, 34033 Montpellier, France*
[b] *Unité de Therapie Cellulaire, Hôpital St. Eloi, 2 Av. Bertin Sans, 34000 Montpellier, France*
[c] *Immunology Research Unit, Suzhou Medical College, Suzhou 215007, People's Republic of China*
[d] *Diaclone, 1 Bd Flemming, 25 Besançon, France*
[e] *INSERM U211, Institut de Biologie, 9 quai Moncousu, 44035 Nantes, France*

Received 17 July 1995; revised 25 August 1995; accepted 5 October 1995

Abstract

Five cytokines activate the gp130 IL-6 transducer: ciliary neurotrophic factor, interleukin-6, interleukin-11, leukemia inhibitory factor and oncostatin M. Human plasmacytoma cell lines, completely dependent on the addition of one of these five cytokines for their growth, were used to obtain anti-gp130 monoclonal antibodies specifically inhibiting one of these five cytokines without affecting the biological activity of the others. These antibodies should improve our understanding of the interaction of gp130 transducer using cytokines with gp130 transducer and facilitate the design of new cytokine inhibitors.

Keywords: Ciliary neurotrophic factor; gp130; Leukemia inhibitory factor; IL-6; IL-11; Monoclonal antibody; Receptor; Oncostatin M

1. Introduction

Five identified human cytokines use the gp130 IL-6 transducer (gp130) (Kishimoto et al., 1994). Numerous studies in humans and mice have shown that abnormal production and/or response to one of these cytokines (mainly IL-6) is associated with various tumoral, autoimmune or inflammatory diseases (Bauer and Hermann, 1991; Hirano et al., 1990; Van Snick, 1990). Briefly, these cytokines may induce fever, cachexia, bone resorption or production of acute-phase proteins. They are also tumoral growth factors in various cancers (Bauer and Hermann, 1991; Hirano et al., 1990; Van Snick, 1990). These deleterious effects have led several groups to develop inhibitors of IL-6 activity.

The construction and production of mutated IL-6

* Corresponding author. At: Institute for Molecular Genetics, CNRS, 1919 Route de Mende, 34033 Montpellier, France.

SSDI 0022-1759(95)00232-4

has improved our understanding of the interaction of this cytokine with its receptors, i.e. IL-6 receptor (IL-6R) and gp130. Whereas IL-6 binds IL-6R through one motif, gp130 is bound through two distinct motifs separately identified by two groups (De Hon et al., 1994; Savino et al., 1994). IL-6R itself also binds gp130 (Yawata et al., 1993). These different interactions of IL-6, IL-6R and gp130 result in the formation of a high-affinity hexameric complex (Ward et al., 1994), dimerization of gp130 transducer and activation of signal transduction (Murakami et al., 1993; Kishimoto et al., 1994). This mechanism, recently described for IL-6, probably also applies to other cytokines using the gp130 transducer.

The recent cloning of murine interleukin-11 (IL-11) receptor has revealed that IL-11 first binds to IL-11R and that the complex formed by IL-11 and IL-11R then binds to the gp130 IL-6 transducer in a manner similar to that of IL-6 and IL-6R (Hilton et al., 1994). Leukemia inhibitory factor (LIF) first binds to LIF receptor, and the LIF/LIFR complex then associates with gp130 IL-6 transducer (Gearing et al., 1992). Oncostatin M (OM) first binds to gp130, and this complex then binds LIFR (Gearing et al., 1992). Finally, ciliary neurotrophic factor (CNTF) binds to an alpha chain receptor termed CNTF receptor (CNTFR) before the CNTF/CNTFR complex binds a gp130/LIFR heterodimer (Ip et al., 1993). For these last three cytokines, signal transduction is induced by the heterodimerization of gp130 and LIFR, which are both associated with JAK kinases and further phosphorylated (Kishimoto et al., 1994). For IL-6 and IL-11, signal transduction is activated by homodimerization of gp130 and further activation of associated kinases (Kishimoto et al., 1994; Hilton et al., 1994).

It is important to develop tools to study the interaction of the various gp130 transducer dependent cytokines with their specific receptors and with gp130. Human plasmacytoma cell lines have recently been obtained which depend on the addition of one of the five gp130 activating cytokines for their growth (Zhang et al., 1994b). This paper reports the production of anti-gp130 monoclonal antibodies which inhibit the biological activity of a particular gp130 cytokine without affecting that of other gp130 transducer dependent cytokines.

2. Materials and methods

2.1. Human myeloma cell lines (HMCL)

XG-4 and XG-6 HMCL were obtained by culturing freshly explanted malignant plasma cells from patients with terminal disease using a combination of IL-6 and GM-CSF (Zhang et al., 1994a). XG-4-CNTF and XG-6-IL-11 HMCL were obtained by subcloning XG-4 and XG-6 HMCL with CNTF or IL-11. These HMCL have a plasma cell phenotype and the same immunoglobulin gene rearrangements as the patients' tumor cells. They were free of mycoplasma contamination and were routinely cultured in RPMI 1640 supplemented with 5% fetal calf serum and 1 ng/ml of recombinant CNTF (XG-4-CNTF) or 10 ng/ml of IL-11 (XG-6-IL-11).

2.2. HMCL proliferation assay

To investigate their responsiveness to various cytokines, XG cells were washed once with culture medium, incubated for 5 h at 37°C in culture medium alone and washed again twice. Cells were then cultured at various densities in 96-well flat-bottomed microplates for 5 days with either culture medium alone or graded concentrations of various cytokines. Anti-gp130 mAbs were added at the beginning of the cultures. Mouse purified IgG1 or IgG2a mAb was used as a control antibody. Tritiated thymidine (0.5 mCi; 25 Ci/mM, CEA, Saclay, France) was added for the last 8 h of culture, and tritiated thymidine incorporation was determined as reported elsewhere (Bataille et al., 1989).

2.3. Cloning of human gp130 cDNA

Total cellular RNA was isolated from XG-7 myeloma cells by lysis with guanidium isothiocyanate and centrifugation on a cesium chloride gradient. Oligonucleotides containing predetermined restriction sites were prepared in order to amplify (PCR technique) and clone human gp130 within two fragments and obtain the entire coding sequence. P1 (5′-GCTCGAGCGCAAGATGTTGACGTTGC) and P2 (5′-GGTGCGATGCACGGTACCATCTTC)

oligonucleotides were designed in order to amplify a 1447 bp fragment containing the 5′ coding region cut just after a unique *Kpn*I restriction site. P3 (5′-GAAGATGGTACCGTGCATCGCACC) and P4 (5′-GTCTAGAACTACTAGTCCTTCACTG) oligonucleotides were used to amplify a 1354 bp sequence beginning just before a PvuII site and containing the 3′ coding region. Two reverse transcription (RT) reactions were performed with 1 μg of total RNA and 50 pM of kinased P2 or P4 primers. The RT products were then amplified by PCR using kinased P1-P2 primers or P3-P4 primers. After 30 PCR cycles (94°C, 60″; 50°C, 45″; 72°C, 60″), PCR products of the expected size were purified with a Gene Clean kit (Stratagene, La Jolla, CA, USA) and cloned into the SK^+ plasmid opened with *Sma*I (Stratagene). After the sequence of the cloned gp130 fragments was checked, full cDNA coding for human gp130 was reconstituted in the pKCR6 expression vector (Matrisian et al., 1986), to which part of the polylinker of the pKCSR α plasmid was added in *Kpn*I. The pKCSR α plasmid is derived from the pKCR3 vector (Breathnach and Harris, 1983) and contains an SR α promotor (Takebe et al., 1988). To reconstitute full gp130 cDNA, the 5′ gp130 fragment was excised from SK^+ plasmid using *Xho*I and *Kpn*I enzymes, and the 3′ fragment using *Kpn*I and *Xba*I enzymes. The two fragments were then introduced into the pKCR6 vector opened with *Xho*I and *Xba*I.

2.4. Construction of a cDNA coding for a soluble form of gp130

A cDNA coding for a human gp130 without transmembrane or cytoplasmic regions was prepared in order to introduce a stop codon just after amino acid 620. Accordingly, PCR amplification of the full gp130 cDNA was performed using P3 and P5 (5′-GTCTAGATAAGGCTTCAATTTCTCCTTGAGC) primers, and the PCR fragments were cloned into the SK^+ vector opened with *Sma*I. The cloned fragment was then excised with *Kpn*I-*Xba*I and its sequence checked. It was then integrated into the pKCR6 vector opened with *Xho*I-*Xba*I, together with the *Xho*I-*Kpn*I fragment corresponding to the 5′ coding sequence of gp130.

2.5. Transfectants expressing membrane gp130 or producing soluble gp130

BAF-BO3 murine pre-B cells lacking membrane gp130 (Hibi et al., 1990) were transfected with the pKCR6 plasmid containing full gp130 cDNA by electroporation (200 Ω, 25 μF, 1.5 kV) using a gene pulser transfection apparatus (Bio-Rad, Richmond, CA, USA). The expression of membrane gp130 was checked with X7 anti-gp130 mAb. BAF-BO3 cells stably transfected with human gp130 gene were termed BAF130 cells.

pKCR6 plasmid containing soluble gp130 cDNA was introduced by electroporation (200 Ω, 25 μF, 1.5 kV) into CHO cells deficient for dihydrofolate reductase (DUKX-B11 clone) using a gene pulser transfection apparatus (Bio-Rad, Richmond, CA, USA). Cells positive for dihydrofolate reductase were selected for 3 weeks in RPMI1640 culture medium containing 8% FCS and 2 mM L-glutamine but without nucleosides (Kaufman, 1987).

2.6. Purification of soluble gp130

The concentration of soluble gp130 (sgp130) in culture supernatant of transfected CHO, assayed with an ELISA purchased from R&D Systems (Minneapolis, MN, USA), was 2 μg/ml. This culture supernatant was diluted twice with Tris-HCl 0.1 M, pH 7, and run on a 2 ml Sepharose 4B column (Pharmacia, Uppsala, Sweden) coupled with X7 anti-gp130 MAb according to the manufacturer's recommendations. The column was washed twice with 20 ml of Tris-HCl 0.1 M, pH 7, and bound sgp130 was recovered with 2 ml of acetate buffer (50 mM, pH 4.5). The eluate was dialyzed against Tris-HCl and run second-fold on the anti-gp130 column. Five hundred μg of sgp130 were then purified and used for the immunization of mice.

2.7. Immunization of mice and production of monoclonal antibodies to gp130

Mice were immunized with 20 μg of sgp130 in complete Freund's adjuvant. 3 weeks later, mice were reimmunized with 20 μg of sgp130 in incomplete Freund's adjuvant. After 4 weeks, mice were

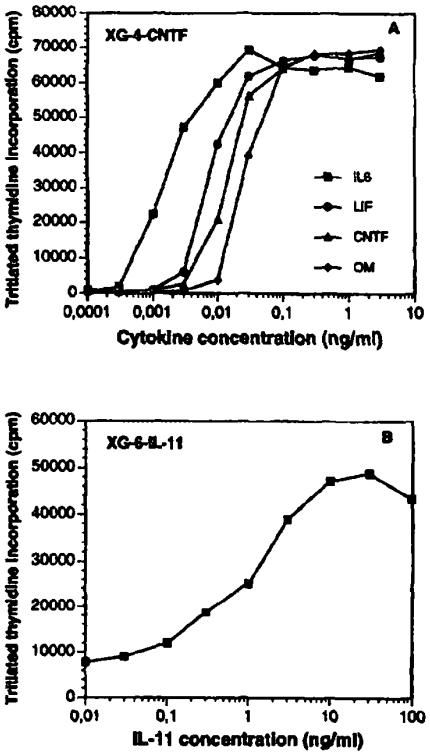

Fig. 1. Proliferation response of XG-4-CNTF and XG-6-IL-11 myeloma cells to various gp130 transducer dependent cytokines. 10^4 cells were cultured for 5 days in 150 ml of culture medium in the presence of various cytokine concentrations. Results are the mean tritiated thymidine incorporations determined in six separate wells after 5 days of culture.

boosted with 10 μg of sgp130. For assays of antibodies to human gp130, plates (Maxisorp, Nunc, Denmark) were coated overnight with 1 μg/ml of goat anti-mouse purified antibodies (Immunotech, Marseille, France) in Tris-HCl (0.1 M, pH 8.9) and then saturated with phosphate-buffered saline and 3% bovine serum albumin (PBS-BSA). 100 μl/well of diluted (1/1000) plasma of immunized mice were incubated overnight at 4°C, washed twice with PBS-BSA and incubated with radioiodinated sgp130. Soluble gp130 was radiolabeled using the chloramine-T methodology as recommended (Harlow and Lane, 1988).

Hybridomas were prepared according to the previously described methodology (Wijdenes et al., 1991). Hybridomas producing antibodies that labelled BAF cells transfected with gp130 cDNA were cloned twice and anti-gp130 antibodies were purified using protein G Sepharose columns. Monoclonal antibodies were biotinylated according to Harlow and Lane (1988). Anti-gp130 antibodies were classified into different clusters each of which recognized a different epitope. With this procedure, one purified anti-gp130 MAb was coated on plates (Maxisorp plate) overnight, and the plates were then washed and saturated with PBS-BSA before being incubated with 100 ng/well of sgp130 for 2 h, washed twice with PBS-BSA and incubated with 1 μg/well of a second biotinylated anti-gp130 MAb for 2 h. The plates were then washed twice, and bound biotinylated antibody was assayed with avidin bound to peroxidase.

3. Reagents

Purified IL-6 was provided by D. Stinchcomb (Synergen, Boulder, CO, USA), OM by M. Shoyab (Bristol Myers Squibb, Seattle, WA, USA), CNTF by Dr. Yancopoulos (Regeneron, Tarrytown, NY, USA) and IL-11 by Dr. Turner (Genetics Institute, Boston, MA, USA). Recombinant LIF was purchased from R&D Systems (Minneapolis, MN, USA). Anti-gp130 X7 MAb was kindly provided by Dr. Yasukawa (Tosoh, Tokyo, Japan).

4. Results

4.1. Production of anti-gp130 mAbs

The mAbs were characterized as anti-gp130 antibody because of their ability to bind BAF-B03 cells transfected with the gp130 gene but not to wild BAF-B03 cells. These mAbs also bound to radiolabeled purified soluble gp130. 15 mAbs were obtained and on the basis of a sandwich ELISA these antibodies were classified into five groups: B-K5, B-P4, B-P8, B-R3 or B-T2 clusters.

4.2. Inhibitory capacity of anti-gp130 mAbs

The results obtained are presented in Figs. 1 and 2. The proliferative response of XG-4-CNTF cells to

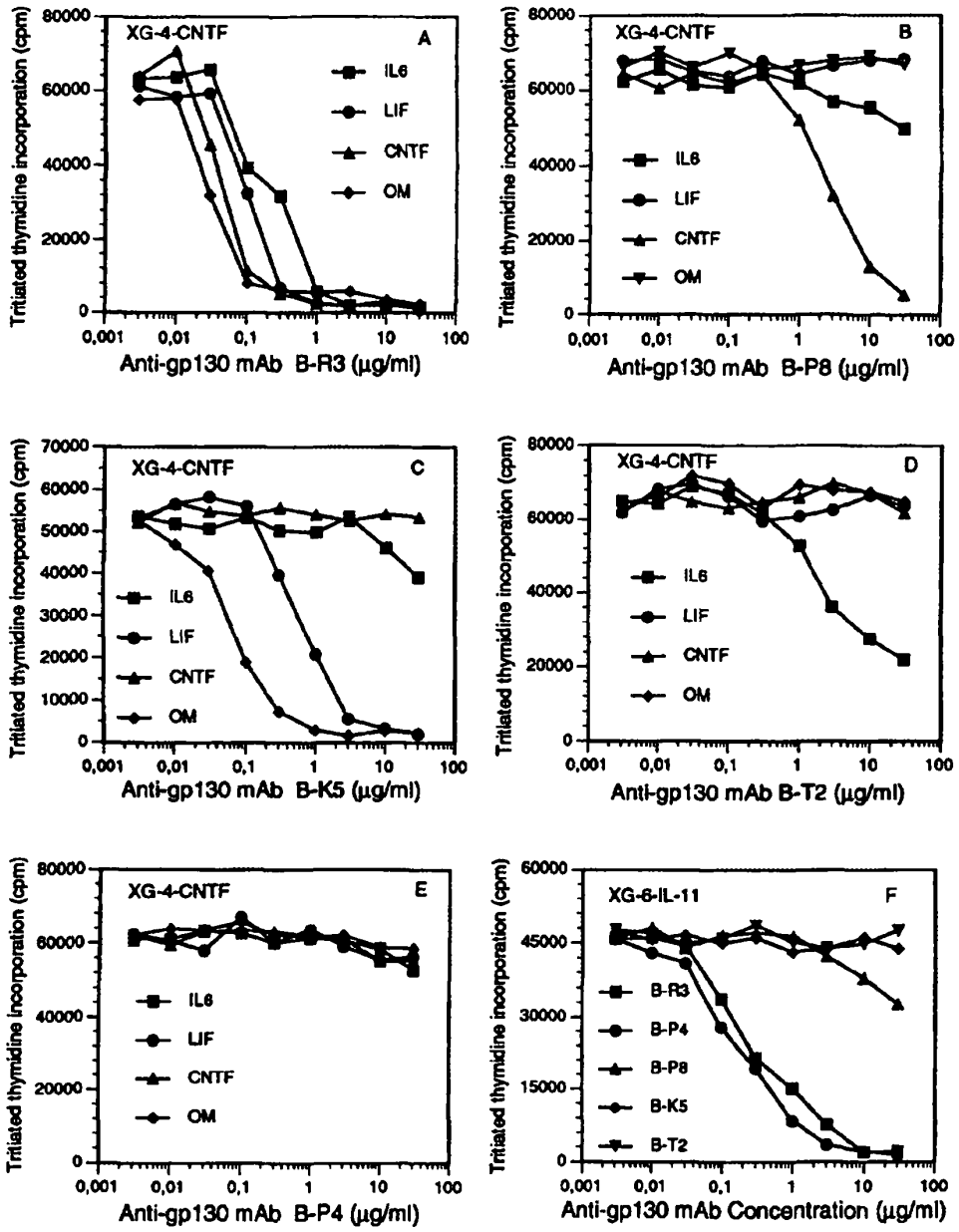

Fig. 2. Inhibitory capacity of anti-gp130 monoclonal antibodies. 10^4 XG-4-CNTF cells were cultured in 150 ml of culture medium for 5 days with either 20 pg/ml of IL-6, or 100 pg/ml of LIF, or 200 pg/ml of CNTF, or 300 pg/ml of OM. 10^4 XG-6-IL-11 cells were cultured for 5 days with 10 ng/ml of IL-11. Graded concentrations of the various anti-gp130 mAbs were added at the beginning of culture. Results are the mean tritiated thymidine incorporations determined in six separate wells at the end of culture.

various gp130 transducer dependent cytokines is depicted in Fig. 1A. Without the addition of exogenous cytokines, XG-4-CNTF cells died within 5 days. Maximal proliferation was obtained with 20 pg/ml of IL-6, 100 pg/ml of LIF, 200 pg/ml of CNTF and 300 pg/ml of OM. As XG-4-CNTF cells responded poorly to IL-11, we used the XG-6-IL-11 cell line in order to assay the capacity of the different anti-gp130 mAbs to neutralize IL-11. Maximal proliferation of XG-6-IL-11 was obtained with 10 ng/ml of IL-11 (Fig. 1B). These concentrations were used in subsequent experiments to investigate the inhibitory capacity of the different antibodies. As depicted in Fig. 2A and Fig. 2F, the B-R3 mAb completely inhibited the activity of the five gp130 transducer dependent cytokines. However, it was ten-fold more efficient when inhibiting OM and CNTF activities. The B-P8 mAb significantly inhibited CNTF activity alone (Fig. 2B and Fig. 2F). The B-K5 mAb inhibited both OM and LIF activities without affecting the other three cytokines (Fig. 2C and Fig. 2F). The B-T2 mAb inhibited only IL-6 activity (Fig. 2D and Fig. 2F) and B-P4 mAb only inhibited IL-11 activity (Fig. 2E and Fig. 2F).

5. Discussion

Our results show for the first time that different epitopes on the gp130 transducer are involved in the biological activity of the different gp130 transducer dependent cytokines. This demonstration was facilitated by the availability of XG-4-CNTF and XG-6-11 plasmacytoma cell lines whose growth is completely dependent on the addition of one of the cytokines using the gp130 transducer. These antibodies should prove very useful for the screening of gp130 mutants in order to identify these different epitopes and for illuminating the mechanisms of interaction of gp130 with the different gp130 transducer dependent cytokines or their α chain receptors.

These antibodies should also be very useful in inhibiting the biological activities of the five cytokines in vivo, especially of IL-6 which is involved in many diseases (Bauer and Hermann, 1991; Hirano et al., 1990). However, as shown by our group, the overall production of IL-6 in vivo is considerable and thus quite difficult to block with only one inhibitor (Lu et al., 1992; Klein and Brailly, 1995). The possibility of specifically inhibiting the gp130 epitope involved in IL-6 activity (the B-T2 epitope) without affecting the other gp130 transducer dependent cytokines should improve the efficiency of antibodies to IL-6 that block the binding of IL-6 to the IL-6 receptor (Wijdenes et al., 1991). This is particularly relevant since knockout mouse technology has demonstrated the viability of inactivation of the IL-6 gene (Kopf et al., 1994), whereas inactivation of the gp130 gene leads to early death of embryos (Yoshida et al., 1993).

Acknowledgements

This work was supported by grants from INSERM (no. 920608), ARC and LFNC (Paris, France).

References

Bataille, R., Jourdan, M., Zhang, X.G. and Klein, B. (1989) Serum levels of interleukin-6, a potent myeloma cell growth factor, as a reflect of disease severity in plasma cell dyscrasias. J. Clin. Invest. 84, 2008.

Bauer, J. and Hermann, F. (1991) Interleukin-6 in clinical medicine. Ann. Hematol. 62, 203.

Breathnach, R. and Harris, B.A. (1983) Plasmids for cloning and expression of full length double-stranded cDNAs under control of the SV40 early or late gene promotor. Nucleic Acids Res. 11, 7119.

De Hon, F.D., Ehlers, M., Rose John, S., Ebeling, S.B., Bos, H.K., Aarden, L.A. and Brakenhoff, J.P. (1994) Development of an interleukin (IL) 6 receptor antagonist that inhibits IL-6-dependent growth of human myeloma cells. J. Exp. Med. 180, 2395.

Gearing, D.P., Comeau, M.R., Friend, D.J., Gimpel, S.D., Thut, C.J., McGourty, J., Brasher, K.K., King, J.A., Gillis, S., Mosley, B., Ziegler, S.F. and Cosman, D. (1992) The IL-6 signal transducer gp130 : an oncostatin M receptor and affinity converter for the LIF receptor. Science 255, 1434.

Harlow, E. and Lane, D. (1988) Antibodies. A Laboratory Manual. Cold Spring Harbor Laboratory, New York.

Hibi, M., Murakami, M., Saito, M., Hirano, T., Taga, T. and Kishimoto, T. (1990) Molecular cloning and expression of an IL-6 signal transducer, gp130. Cell 63, 1149.

Hilton, D.J., Hilton, A.A., Raicevic, A., Rakar, S., Harrison-Smith, M., Gough, N.M., Begley, C.G., Metcalf, D., Nicola, N.A. and Willson, T.A. (1994) Cloning of a murine IL-11 receptor α-chain; requirement for gp130 for high affinity binding and signal transduction. EMBO J. 13, 4765.

Hirano, T., Akira, S., Taga, T. and Kishimoto, T. (1990) Biologi-

cal and clinical aspects of interleukin 6. Immunol. Today 11, 443.

Ip, N.Y., McClain, J., Barrezueta, N.X., Aldrich, T.H., Pan, L., Li, Y., Wiegand, S.J., Friedman, B., Davis, S. and Yancopoulos, G.D. (1993) The alpha component of the CNTF receptor is required for signaling and defines potential CNTF targets in the adult and during development. Neuron 10, 89.

Kaufman, R.J. (1987) High level production of proteins in mammalian cells. In: J.K. Setlow (Ed.), Genetic Engineering: Principles and Methods. Plenum, New York, p. 155.

Kishimoto, T., Taga, T. and Akira, S. (1994) Cytokine signal transduction. Cell 76, 253.

Klein, B. and Brailly, H. (1995) Cytokine-binding proteins stimulating antagonists. Immunol. Today 16, 216.

Kopf, M., Baumann, H., Freer, G., Freudenberg, M., Lamers, M., Kishimoto, T., Zinkernagel, R., Bluethmann, H. and Köhler, G. (1994) Impaired immune and acute-phase responses in interleukin-6-deficient mice. Nature 368, 339.

Lu, Z.Y., Brochier, J., Wijdenes, J., Brailly, H., Bataille, R. and Klein, B. (1992) High amounts of circulating interleukin (IL)-6 in the form of monomeric immune complexes during anti-IL-6 therapy. Towards a new methodology for measuring overall cytokine production in human in vivo. Eur. J. Immunol. 22, 2819.

Matrisian, L.N., Bowden, G.T., Kried, P., Fürstenberger, G., Briand, J.P., Leroy, P. and Breathnach, R. (1986) The mRNA coding for the secreted protease transin is expressed more abundantly in malignant than in benign tumors. Proc. Natl. Acad. Sci. USA 83, 9413.

Murakami, M., Hibi, M., Nakagawa, N., Nakagawa, T., Yasukawa, K., Yamanishi, K., Taga, T. and Kishimoto, T. (1993) IL-6-induced homodimerization of gp130 and associated activation of a tyrosine kinase. Science 260, 1808.

Savino, R., Ciapponi, L., Lahm, A., Demartis, A., Cabibbo, A., Toniatti, C., Delmastro, P., Altamura, S. and Ciliberto, G. (1994) Rational design of a receptor super-antagonist of human interleukin-6. EMBO J. 13, 5863.

Takebe, Y., Seiki, M., Fujisawa, J.I., Hoy, P., Yokota, K., Arai, K.I., Yoshida, M. and Arai, N. (1988) SRa promotor: an efficient and versatile mammalian cDNA expression system composed tof the simian virus 40 early promotor and the R-U5 segment of human T-cell leukemia virus type I long terminal repeat. Mol. Cell Biol. 8, 466.

Van Snick, J. (1990) Interleukin-6. an overview. Annu. Rev. Immunol. 8, 253.

Ward, L.D., Howlett, G.J., Discolo, G., Yasukawa, K., Hammacher, A., Moritz, R.L. and Simpson, R.J. (1994) High affinity interleukin-6 receptor is a hexameric complex consisting of two molecules each of interleukin-6, interleukin-6 receptor, and gp-130. J Biol. Chem. 269, 23286.

Wijdenes, J., Clement, C., Klein, B., Morel-Fourrier, B., Vita, N., Ferrara, P. and Peters, A. (1991) Human recombinant dimeric IL-6 binds to its receptor as detected by anti-IL-6 monoclonal antibodies. Mol. Immunol. 28, 1183.

Yawata, H., Yasukawa, K., Natsuka, S., Marakami, M., Yamasaki, K., Hibi, M., Taga, T. and Kishimoto, T. (1993) Structure-function analysis of human IL-6 receptor: dissociation of amino acid residues required for IL-6-binding and for IL-6 signal transduction through gp130. EMBO J. 12, 1705.

Yoshida, K., Saito, M., Suematsu, S., Yoshida, N., Kumanogoh, A., Taga, T. and Kishimoto, T. (1993) Disruption of the gene for shared cytokine signal transducer, gp130. Tissue Antigen 42, 339.

Zhang, X.G., Gaillard, J.P., Robillard, N., Lu, Z.Y., Gu, Z.J., Jourdan, M., Boiron, J.M., Bataille, R. and Klein, B. (1994a) Reproducible obtaining of human myeloma cell lines as a model for tumor stem cell study in human multiple myeloma. Blood 83, 3654.

Zhang, X.G., Gu, Z.J., Lu, Z.Y., Yasukawa, K., Yancopoulos, G.D., Turner, K., Shoyab, M., Taga, T., Kishimoto, T., Bataille, R. and Klein, B. (1994b) Ciliary neurotropic factor, interleukin 11, leukemia inbitory factor, and oncostatin M are growth factors for human myeloma cell lines using the interleukin 6 signal trasnducer gp130. J. Exp. Med. 179, 1337.

Critical Role of Interleukin-11 in Isoflurane-mediated Protection against Ischemic Acute Kidney Injury in Mice

Ahrom Ham, Ph.D.,* Mihwa Kim, Pharm.D.,† Joo Yun Kim, Ph.D.,* Kevin M. Brown, B.S.,† James Yeh, B.S.,‡ Vivette D. D'Agati, M.D.,§ H. Thomas Lee, M.D.‖

ABSTRACT

Background: Isoflurane releases renal tubular transforming growth factor-β1 (TGF-β1) and protects against ischemic acute kidney injury. Recent studies suggest that TGF-β1 can induce a cytoprotective cytokine interleukin (IL)-11. In this study, the authors tested the hypothesis that isoflurane protects against ischemic acute kidney injury by direct induction of renal tubular IL-11 synthesis.

Methods: Human kidney proximal tubule cells were treated with 1.25–2.5% isoflurane or carrier gas (room air + 5% carbon dioxide) for 0–16 h. The authors also anesthetized C57BL/6 mice with 1.2% isoflurane or with equianesthetic dose of pentobarbital for 4 h. In addition, the authors subjected IL-11 receptor (IL-11R) wild-type, IL-11R–deficient, or IL-11 neutralized mice to 30-min renal ischemia followed by reperfusion under 4 h of anesthesia with pentobarbital or isoflurane (1.2%).

Results: Isoflurane increased IL-11 synthesis in human (approximately 300–500% increase, N = 6) and mouse (23 ± 4 [mean ± SD] fold over carrier gas group, N = 4) proximal tubule cells that were attenuated by a TGF-β1–neutralizing antibody. Mice anesthetized with isoflurane showed significantly increased kidney IL-11 messenger RNA (13.8 ± 2 fold over carrier gas group, N = 4) and protein (31 ± 9 *vs.* 18 ± 2 pg/mg protein or approximately 80% increase, N = 4) expression compared with pentobarbital-anesthetized mice, and this increase was also attenuated by a TGF-β1–neutralizing antibody. Furthermore, isoflurane-mediated renal protection in IL-11R wild-type mice was absent in IL-11R–deficient mice or in IL-11R wild-type mice treated with IL-11–neutralizing antibody (N = 4–6).

Conclusion: In this study, the authors suggest that isoflurane induces renal tubular IL-11 *via* TGF-β1 signaling to protect against ischemic acute kidney injury.

What We Already Know about This Topic

- Halogenated anesthetics protects against acute kidney injury by production of renal tubular transforming growth factor-β1

What This Article Tells Us That Is New

- Isoflurane increased interleukin-11 synthesis in human and mouse proximal tubular cells via transforming growth factor-β1 signaling to protect against ischemic acute kidney injury

ACUTE kidney injury (AKI) remains a major perioperative complication and results in extremely high mortality and morbidity costing more than 10 billion dollars per year in the United States.[1,2] Furthermore, AKI is frequently associated with other life-threatening complications including remote multiorgan injury and sepsis.[2–5] Renal ischemia–reperfusion (I/R) injury or ischemic AKI is a frequent complication for patients subjected to major cardiac, hepatobiliary, or transplant surgery.[3,6] Unfortunately, there is no effective clinically proven therapy for ischemic AKI. Furthermore, patients who survive initial renal injury frequently suffer from long-term chronic kidney disease.

Volatile halogenated anesthetics are one of the most widely used drugs during the perioperative period.[7] Our previous studies demonstrated that clinically used volatile halogenated anesthetics including isoflurane at clinically relevant concentrations (approximately 1–2 minimum alveolar concentration) protect against ischemic AKI by attenuating renal tubular necrosis and by retarding renal tubular inflammation with reduction in influx of proinflammatory leukocytes.[8,9] We also demonstrated that volatile halogenated anesthetics produce direct antiinflammatory and antinecrotic effects in cultured human kidney proximal tubule (HK-2) cells.[10,11] Subsequently, we discovered that volatile halogenated anesthetics protect against renal tubular necrosis and inflammation by direct renal tubular production of transforming growth factor-β1 (TGF-β1).[11–13] However, the downstream signaling

* Postdoctoral Research Scientist, † Research Associate, ‡ Research Student, ‖ Professor, Department of Anesthesiology, § Professor, Department of Pathology, College of Physicians and Surgeons of Columbia University, New York, New York.

Received from the Department of Anesthesiology, Columbia University, New York, New York. Submitted for publication April 30, 2013. Accepted for publication August 8, 2013. This work was supported in part by the Department of Anesthesiology, Columbia University, New York, New York, and R01 DK-058547 and R01 GM-067081 (to Dr. Lee) from the National Institutes of Health, Bethesda, Maryland. The authors declare no competing interests.

Address correspondence to Dr. Lee: Department of Anesthesiology, Anesthesiology Research Laboratories, Columbia University, P&S Box 46 (PH-5), 630 West 168th Street, New York, New York 10032–3784. th128@columbia.edu. Information on purchasing reprints may be found at www.anesthesiology.org or on the masthead page at the beginning of this issue. ANESTHESIOLOGY's articles are made freely accessible to all readers, for personal use only, 6 months from the cover date of the issue.

 Anesthesiology 2013; 119:1389-401

mechanisms of volatile halogenated anesthetic-mediated renal protection generated by TGF-β1 remain incompletely understood. Moreover, isoflurane therapy for critically ill patients may be limited by its anesthetic and cardiovascular effects. One way to mitigate this is to use the distal signaling molecules synthesized with isoflurane treatment devoid of systemic hemodynamic and anesthetic effects.

Interleukin (IL)-11 is a 20 kDa member of the IL-6-type cytokine family. IL-11 promotes megakaryocyte maturation and is already clinically approved to increase platelet counts in patients receiving chemotherapy.[14] In addition to its hematopoietic effects, IL-11 protects against intestinal, cardiomyocyte, and endothelial cell death.[15] We recently showed that recombinant human IL-11 treatment before or after renal ischemia attenuated ischemic AKI in mice.[16] Specifically, IL-11 administration significantly attenuated necrosis, inflammation, and apoptosis after ischemic AKI closely mimicking the renal protective effects of volatile halogenated anesthetics. This IL-11–mediated protection against ischemic AKI requires the downstream induction of another cytoprotective protein sphingosine kinase-1. Interestingly, we also showed that isoflurane-mediated protection against ischemic AKI also requires induction of sphingosine kinase-1.[17] Finally, previous studies suggest that TGF-β1 induces IL-11 in lung epithelial cells and fibroblasts.[18,19] Therefore, in this study, we tested the hypothesis that isoflurane induces TGF-β1–mediated renal proximal tubular IL-11 synthesis. We also tested whether IL-11 plays a critical role in isoflurane-mediated renal protection.

Materials and Methods

Human and Mouse Proximal Tubule Cell Culture and Exposure to Isoflurane

Immortalized human renal proximal tubule (HK-2) cells (American Type Culture Collection, Manassas, VA) were grown and passaged with 50:50 mixture of Dulbecco Modified Eagle Media/F12 with 10% fetal bovine serum (Invitrogen, Carlsbad, CA) and antibiotics (100 U/ml penicillin G, 100 μg/ml streptomycin, and 0.25 μg/ml amphotericin B; Invitrogen) at 37°C in a 100% humidified atmosphere of 5% carbon dioxide–95% air. This cell line has been characterized extensively and retains the phenotypic and functional characteristics of proximal tubule cells in culture.[20] We also cultured mouse kidney proximal tubule cells. Mouse kidneys were removed, minced, and digested in collagenase A (1 mg/ml; Sigma, St. Louis, MO) at 37°C for 45 min with occasional agitation. The cellular digest was filtered through a nylon mesh, centrifuged at 600*g* for 10 min, and washed twice. Mouse kidney proximal tubules were isolated according to the method by Vinay *et al.*[21] with the use of Percoll density gradient separation. Cells were used in the experiments described below when confluent after 24-h serum deprivation.

HK-2 cells or mouse proximal tubules in culture were placed in an air tight, 37°C, humidified modular incubator chamber (Billups-Rothenberg, Inc., Del Mar, CA) with inflow and outflow ports. The inlet port was connected to a vaporizer (Datex-Ohmeda, GE Healthcare, Oklahoma City, OK) to deliver isoflurane (Abbott Laboratories, North Chicago, IL) mixed with 95% air and 5% carbon dioxide (carrier gas) at 10 l/min. The outlet port was connected to a Datex-Ohmeda 5250 RGM gas analyzer that measured isoflurane concentrations. Exposure to isoflurane (1.25–2.5%) lasted 0–16 h. Control cells were exposed to carrier gas in an identical modular incubator chamber. To block the effects of TGF-β1 generated by isoflurane, some HK-2 cells were pretreated with neutralizing TGF-β1 antibody (10 μg/ml; R&D Systems, Minneapolis, MN) 30 min before isoflurane treatment, respectively. We also used nonneutralizing control isotype antibody to test the specificity of the neutralizing TGF-β1 antibody (BD Biosciences, San Jose, CA).

Reverse Transcription Polymerase Chain Reaction for IL-11

By using reverse transcription polymerase chain reaction, we measured messenger RNAs (mRNAs)-encoding human (HK-2 cells) or mouse IL-11 as described.[22] Amplification of the human IL-11 complementary DNA was performed using the following primers: forward primer, 5′-CTG AAG ACT CGG CTG TGA CC-3′ and reverse primer, 5′-CAG GGC AGA AGT CTG TGG AC-3′ at an annealing temperature of 66°C resulting in a 300 base pair product. Amplification of the mouse IL-11 complementary DNA was performed using the following primers: forward primer, 5′-AAC TGT GTT TGT CGC CTG GT-3′ and reverse primer, 5′-AAG CTG CAA AGA TCC CAA TG-3′ at an annealing temperature of 68°C resulting in a 267 base pair product. Glyceraldehyde-3-phosphate dehydrogenase complementary DNA amplification was performed to control for lane loading: forward primer, 5′-ACC ACA GTC CAT GCC ATC AC-3′ and reverse primer, 5′-CAC CAC CCT GTT GCT GTA GCC-3′ at an annealing temperature of 65°C resulting in a 450 base pair product.

IL-11 Enzyme-linked Immunosorbent Assay

HK-2 cell supernatant or mouse kidney cortex lysate IL-11 protein expression was measured using human- or mouse-specific sandwich IL-11 enzyme-linked immunosorbent assay kit (R&D Systems), respectively.

Mouse Anesthesia and Induction of Renal I/R Injury

After approval from the Columbia University Institutional Animal Care and Use Committee (New York, New York), we used adult male IL-11 receptor–deficient (IL-11R knockout) mice or wild-type (WT) litter mates (IL-11R WT) on a C57BL/6 background (B6.129S1-Il11ra1^{tm1Wtbi}/J; Jackson Labs, Bar Harbor, ME). Mice were initially anesthetized with intraperitoneal pentobarbital (Henry Schein Veterinary Co., Indianapolis, IN; 50 mg/kg body weight, or to effect) and subjected to right nephrectomy and 30 min of left renal ischemia or to sham-operation (laparotomy, right nephrectomy without renal ischemia).[8,9] After closure of the abdomen in two layers, the mice were then exposed to an additional 4 h of equipotent doses of either pentobarbital or

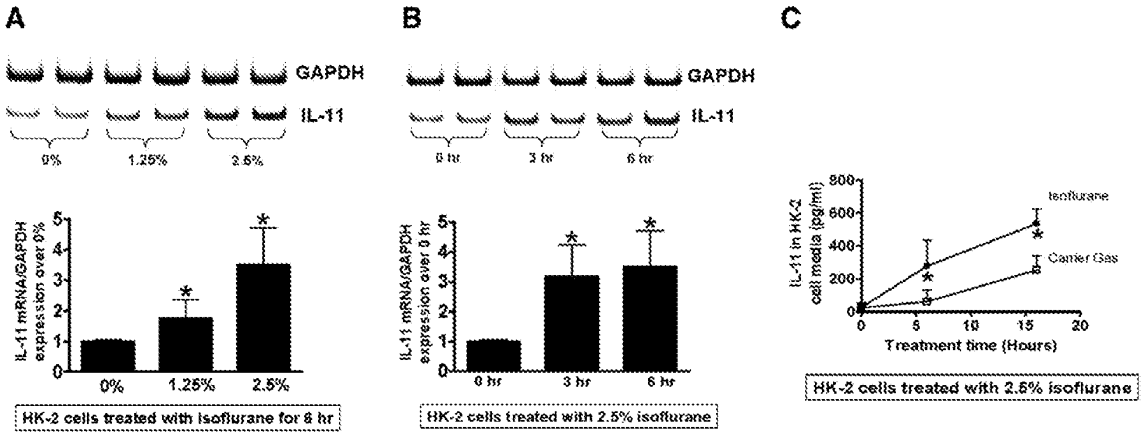

Fig. 1. Isoflurane induces interleukin (IL)-11 messenger RNA (mRNA) and protein synthesis in human kidney proximal tubule (HK-2) cells. (*A* and *B*) IL-11 mRNA measured by reverse transcription polymerase chain reaction in HK-2 cells treated with 0–2.5% isoflurane for 6 h (*A*; N = 6) or 2.5% isoflurane for 0–6 h (*B*, N = 6). Glyceraldehyde-3-phosphate dehydrogenase (GAPDH) mRNA expression was quantified to normalize lane loading. Data are presented as means ± SD. **P* < 0.05 *versus* IL-11 mRNA measured after 0% isoflurane treatment (*A*) or at 0 h (*B*). (*C*) Isoflurane increases IL-11 protein (pg/ml) in cell culture media from HK-2 cells (N = 6). HK-2 cells were treated with 2.5% isoflurane or with carrier gas for 6 or 16 h. **P* < 0.05 *versus* carrier gas–treated group.

1.2% isoflurane as described previously.[33] The mice were placed on a heating pad under a warming light to maintain body temperature approximately 36°–38°C. To neutralize IL-11 *in vivo*, some IL-11R WT mice were injected intravenously with 1 mg/kg monoclonal anti-IL-11 (MAB418; R&D Systems) 20 min before reperfusion of ischemic kidney or sham-operation. We collected kidney (cortex and corticomedullary junction) and plasma 6–24 h after I/R injury to examine the severity of renal

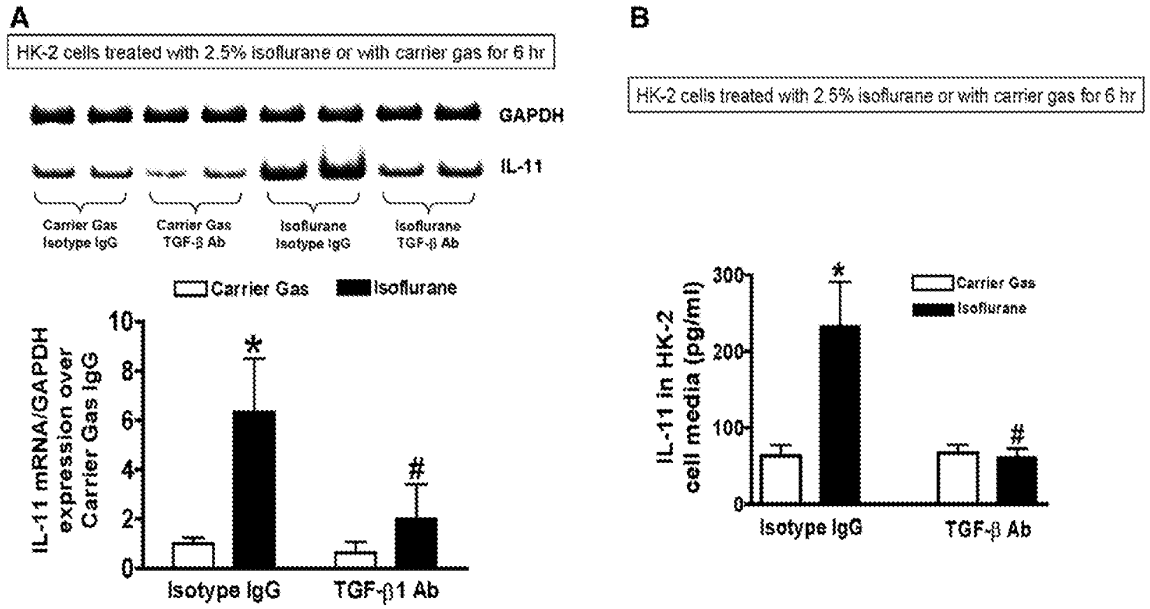

Fig. 2. Isoflurane induces interleukin (IL)-11 in human kidney proximal tubule (HK-2) cells *via* transforming growth factor-β1 (TGF-β1). (*A*) IL-11 messenger RNA (mRNA) (detected by reverse transcription polymerase chain reaction) expression in HK-2 cells treated with 2.5% isoflurane for 6 h (N = 6). Representative images (*top*) and band intensity quantifications (*bottom*) expressed as fold increases in IL-11 expression over carrier gas plus immunoglobulin G (IgG) isotype antibody–treated controls. (*B*) IL-11 protein (detected with enzyme-linked immunosorbent assay) expression in HK-2 cells treated with 2.5% isoflurane for 6 h (N = 6). * *P* < 0.05 *versus* carrier gas group treated with IgG isotype antibody. # *P* < 0.05 *versus* isoflurane group treated with IgG isotype antibody. *Error bars* represent 1 SD. TGF-β1 antibody (10 μg/ml) prevents isoflurane-mediated induction of IL-11 mRNA and protein expression in human proximal tubule cells.

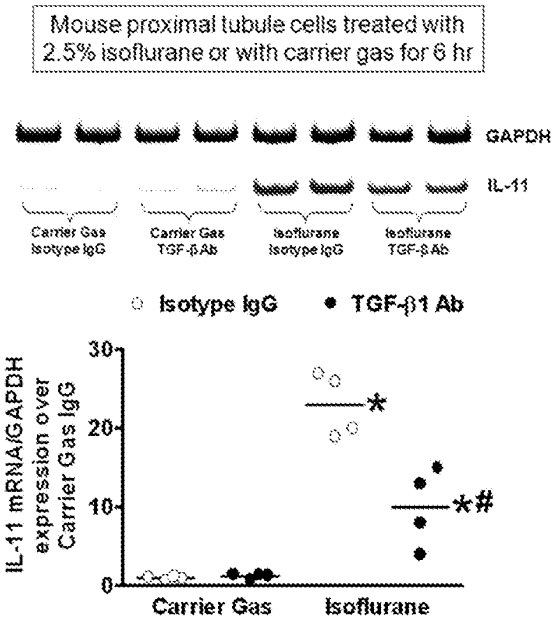

Fig. 3. Isoflurane induces interleukin (IL)-11 messenger RNA (mRNA) expression in primary culture of mouse proximal tubule cells *via* transforming growth factor-β1 (TGF-β1). IL-11 mRNA (detected by reverse transcription polymerase chain reaction) expression in primary culture of mouse proximal tubule cells treated with 2.5% isoflurane for 6 h (N = 4). Representative images (*top*) and band intensity quantifications (*bottom*) expressed as fold increases in IL-11 expression over carrier gas and immunoglobulin G (IgG) isotype antibody–treated controls. Glyceraldehyde-3-phosphate dehydrogenase (GAPDH) mRNA expression was also quantified to normalize lane loading. * $P < 0.05$ *versus* carrier gas group treated with IgG isotype antibody. # $P < 0.05$ *versus* isoflurane group treated with IgG isotype antibody. *Lines* represent means of scatter plots. TGF-β1 antibody (10 μg/ml) prevents isoflurane-mediated induction of IL-11 mRNA and protein expression in mouse proximal tubule cells.

dysfunction (plasma creatinine, renal histology, apoptosis, and neutrophil infiltration) and IL-11 mRNA and protein detection. Plasma creatinine was measured as described with an enzymatic creatinine reagent kit according to the manufacturer's instructions (Thermo Fisher Scientific, Waltham, MA).[24] Unlike the Jaffe method, this method of creatinine measurement largely eliminates the interferences from mouse plasma chromagens.

Some IL-11R WT mice were anesthetized with pentobarbital or with 1.2% isoflurane without being subjected to renal I/R injury. To test the critical role of TGF-β1 signaling in isoflurane-mediated IL-11 induction *in vivo*, some IL-11 WT mice were injected intravenously with 5 mg/kg monoclonal anti-TGF-β1 (MAB240; R&D Systems) or control isotype antibody 30 min before anesthesia with isoflurane or pentobarbital.

Histological Detection of Kidney Necrosis, Apoptosis, and Neutrophil Infiltration

Morphological assessment of kidney hematoxylin and eosin stain staining was performed by renal pathologist (Dr. D'Agati) who was unaware of the treatment that each animal had received. An established grading scale of necrotic injury (0–4, renal injury score) to the proximal tubules was used for the histopathological assessment of I/R-induced damage as outlined by Jablonski *et al.*[25] and as described previously in our studies.[26,27] We detected kidney apoptosis with terminal deoxynucleotidyl transferase 2′-deoxyuridine-5′-triphosphate nick end-labeling staining as described elsewhere[28] using a commercially available *in situ* cell death detection kit (Roche, Indianapolis, IN) according to the instructions provided by the manufacturer. Apoptotic terminal deoxynucleotidyl transferase 2′-deoxyuridine-5′-triphosphate nick end-labeling–positive cells were quantified in five to seven randomly chosen ×100 microscope image fields in the corticomedullary junction, and results were expressed as apoptotic cells counted per ×100 field. Immunohistochemistry for neutrophils was performed as described previously[29] with a rat anti-mouse Ly6B monoclonal antibody against polymorphonuclear leukocytes (clone 7/4; AbD Serotec, Raleigh, NC). A primary antibody that recognized IgG_{2a} (MCA1212; AbD Serotec) was used as a negative isotype control in all experiments. Neutrophils infiltrating the kidney were quantified in five to seven randomly chosen ×200 microscope image fields in the corticomedullary junction, and results were expressed as neutrophils counted per ×200 field.

IL-11 Immunohistochemistry

Immunohistochemistry detected mouse kidney IL-11 protein expression and localization 4 h after anesthesia with pentobarbital or 1.2% isoflurane with rat anti-IL-11 antibody (MAB418; 1:50 dilution; R&D Systems) and biotin-conjugated anti-rat IgG (1:100 dilution; Vector Laboratories, Burlingame, CA). Normal rat IgG2a (Vector Laboratories) was used at the same concentration as the primary antibody as a negative isotype control. Kidney IL-11 immunohistochemistry was quantified as described by Matkowskyj *et al.*[30] with some modifications. Integrated image densities of five to seven randomly selected renal tubule areas from each slide were averaged, and background measured from isotype control slides was subtracted. Renal tubular IL-11 intensity was expressed as fold increase over pentobarbital-anesthetized mice.

Statistical Analysis

The data were analyzed with two-tailed Student *t* test when comparing means between two groups or one-way or two-way ANOVA plus Tukey *post hoc* multiple comparison test when comparing multiple groups. The ordinal values of the renal injury scores were analyzed by the Mann–Whitney nonparametric test. We used Graphad InStat and Graphad

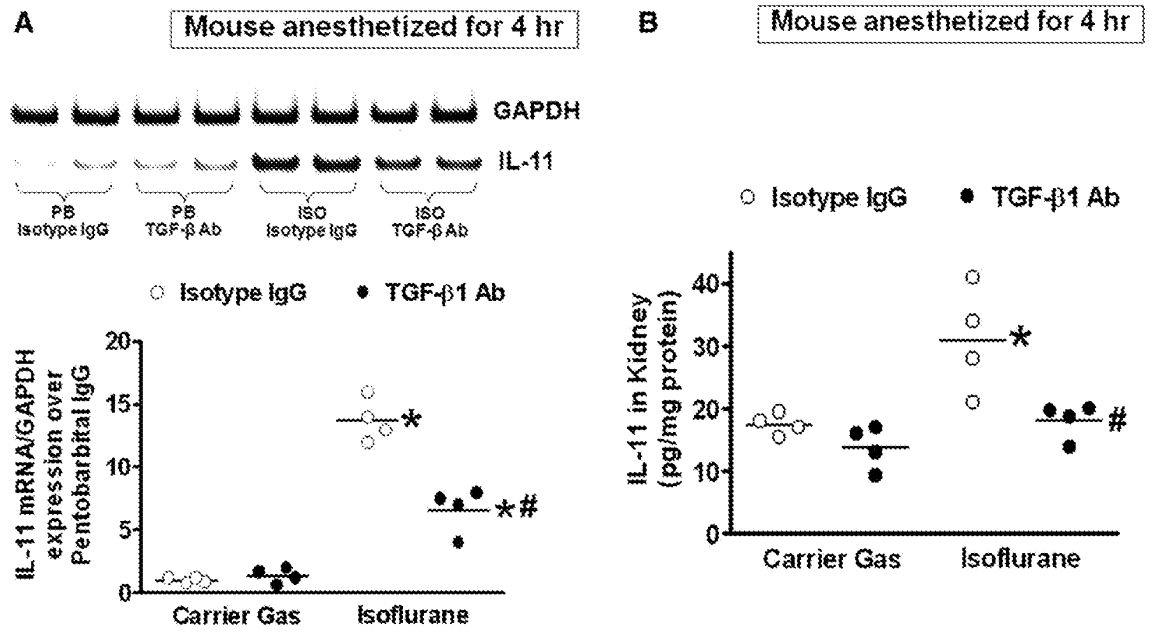

Fig. 4. Isoflurane increases interleukin (IL)-11 messenger RNA (mRNA) and protein synthesis in mouse kidney *via* transforming growth factor-β1 (TGF-β1) signaling. Naïve IL-11 wild-type (WT) mice were exposed to pentobarbital or 1.2% isoflurane for 4 h. (*A*) Representative bands for IL-11 mRNA (detected by reverse transcription polymerase chain reaction) expression in mouse kidney (N = 4). Glyceraldehyde-3-phosphate dehydrogenase (GAPDH) served as an internal loading control. (*B*) Kidney lysate IL-11 protein (detected by enzyme-linked immunosorbent assay) in IL-11 naïve WT mice exposed to pentobarbital or 1.2% isoflurane for 4 h (N = 4). To neutralize TGF-β1 *in vivo*, some IL-11 WT mice were injected with 5 mg/kg monoclonal anti-TGF-β1 (MAB240) antibody intravenous injection. TGF-β1 neutralization prevented the induction of IL-11 after anesthesia with isoflurane. * $P < 0.05$ *versus* pentobarbital-anesthetized mice treated with immunoglobulin G (IgG) isotype antibody. # $P < 0.05$ *versus* isoflurane-anesthetized mice treated with IgG isotype antibody. *Lines* represent means of scatter plots. Anesthesia with isoflurane significantly increased kidney IL-11 mRNA and protein expression in mice. ISO = isoflurane; PB = pentobarbital.

Prism for statistical analyses (GraphPad Software, Inc., La Jolla, CA). In all cases, a probability statistic *P* value less than 0.05 was taken to indicate significance. All data are expressed throughout the text as means ± SD.

Results

Isoflurane Induces IL-11 in Human and Mouse Proximal Tubule Cells via TGF-β1 Signaling

Figure 1A shows a concentration-dependent (0–2.5%) induction of IL-11 mRNA in HK-2 cells after isoflurane treatment (N = 6). Figure 1B shows that 2.5% isoflurane significantly increased IL-11 mRNA after 3- or 6-h treatment. Isoflurane treatment (2.5%) in HK-2 cells for 6–16 h also induced IL-11 protein (released into cell culture media; fig. 1C) in HK-2 cells compared with carrier gas–treated cells (N = 6).

HK-2 cells pretreated with control isotype antibody (mouse IgG) demonstrated a significant induction of IL-11 mRNA (fig. 2A) and protein (fig. 2B) expression (N = 6) after isoflurane exposure (2.5% for 6 h). We determined that TGF-β1–neutralizing antibody (10 μg/ml) significantly attenuated the up-regulation of IL-11 mRNA as well as protein expression after isoflurane treatment.

Figure 3 shows that primary cultures of mouse kidney proximal tubule cells pretreated with control isotype mouse IgG had significant IL-11 mRNA induction after 6-h treatment with 2.5% isoflurane (N = 4). TGF-β1 neutralization significantly attenuated the up-regulation of IL-11 mRNA in isoflurane-treated mouse proximal tubule cells. Therefore, our studies show that isoflurane-induced TGF-β1 directly promotes the synthesis of IL-11 in both immortalized and primary cultures of renal proximal tubule cells.

Isoflurane-mediated Induction of Kidney IL-11 in Vivo via TGFβ1 Signaling

Figure 4 shows that anesthesia with isoflurane (1.2% for 4 h) significantly induced IL-11 mRNA (fig. 4A) and protein expression (fig. 4B) measured in mouse kidneys compared with mice anesthetized with pentobarbital for 4 h (N = 4). We also determined that TGF-β1–neutralizing antibody (5 mg/kg monoclonal anti-TGF-β1, MAB240) prevented the induction of kidney IL-11 mRNA and protein expression after anesthesia with isoflurane in mice (fig. 4; N = 4).

Figure 5A shows diffuse renal tubular IL-11 staining in mice anesthetized with pentobarbital and increased IL-11 staining in the kidneys of mice anesthetized with 1.2%

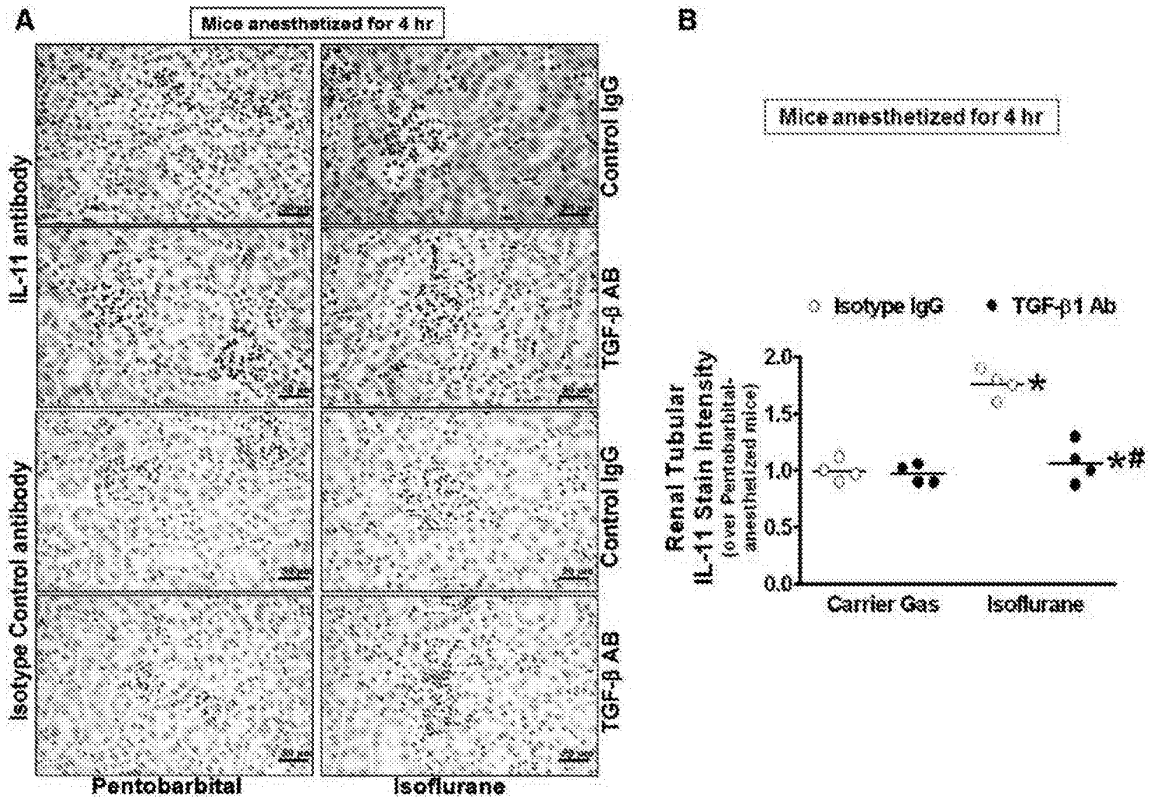

Fig. 5. Isoflurane increases interleukin (IL)-11 immunoreactivity in mouse kidney *via* transforming growth factor-β1 (TGF-β1). (*A*) IL-11 immunohistochemistry (×400 shown, N = 4) in kidneys from IL-11 receptor wild-type (IL-11R WT) mice anesthetized with pentobarbital or with 1.2% isoflurane for 4 h. IL-11 staining was darker in kidneys of mice anesthetized with isoflurane. TGF-β1–neutralizing antibody attenuated isoflurane-mediated increase in IL-11 immunoreactivity. Finally, IL-11 staining was not visible in kidneys from mice stained with negative isotype control antibodies (representative of four experiments). (*B*) Quantifications of renal tubular IL-11 staining in mice anesthetized with pentobarbital or with 1.2% isoflurane for 4 h. Kidney IL-11 immunoreactivity significantly increased in mice anesthetized with isoflurane and attenuated with TGF-β1–neutralizing antibody. # $P <$ 0.05 *versus* isoflurane-anesthetized mice treated with immunoglobulin G (IgG) isotype antibody. * $P < 0.05$ *versus* pentobarbital-anesthetized mice treated with IgG isotype antibody. *Lines* represent means of scatter plots.

isoflurane for 4 h (representative of four experiments, ×100 and ×400 images shown). Quantification of immunohistochemical staining confirmed significant increase in IL-11 immunoreactivity in mice anesthetized with isoflurane (fig. 5B; N = 4). This increase in IL-11 immunoreactivity during anesthesia with isoflurane was again attenuated by treating mice with TGF-β1–neutralizing antibody before anesthesia with isoflurane. Therefore, from these experiments, we concluded that isoflurane induces IL-11 and synthesis *in vivo via* TGF-β1 signaling. IL-11 staining was not visible in the kidneys stained with negative isotype control antibody.

Critical Role of IL-11 in Isoflurane-mediated Protection against Ischemic AKI In Vivo

IL-11R WT mice anesthetized with pentobarbital or with 1.2% isoflurane for 4 h had similar plasma creatinine values after sham-operation (fig. 6). Similarly, IL-11R WT mice pretreated with IL-11–neutralizing antibody or IL-11R knockout mice had similar plasma creatinine values after sham-operation during anesthesia with pentobarbital. Plasma creatinine significantly increased in IL-11R WT mice subjected to 30 min of renal ischemia and 2-h reperfusion compared with sham-operated mice (fig. 6; N = 6). However, IL-11R WT mice anesthetized with 1.2% isoflurane for 4 h after renal ischemia (isoflurane postconditioning) had significantly decreased plasma creatinine 24 h after injury compared with mice anesthetized with pentobarbital after renal ischemia. Supporting a critical role of IL-11 in isoflurane-mediated protection against ischemic AKI, IL-11R knockout or IL-11R WT mice pretreated with IL-11–neutralizing antibody before renal ischemia were not protected against ischemic AKI during anesthesia with isoflurane after renal I/R (fig. 6). IL-11R knockout mice and IL-11R WT mice pretreated with IL-11–neutralizing antibody had

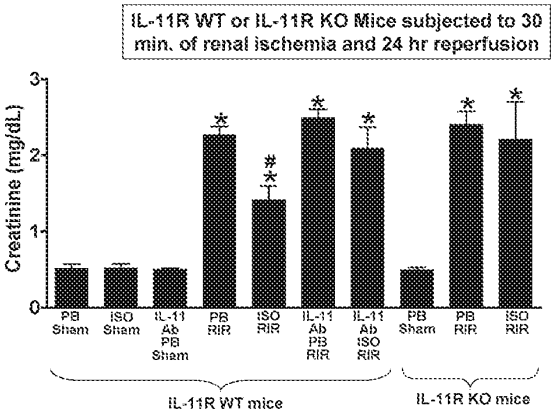

Fig. 6. Interleukin (IL)-11 is critical for isoflurane-mediated renal protection against ischemic acute kidney injury. Plasma creatinine levels from IL-11 wild-type (WT) or IL-11–deficient (knockout [KO]) mice subjected to 30-min renal ischemia and 24-h reperfusion (N = 4–6 per group). After renal ischemia reperfusion (RIR), mice were further anesthetized with 1.2% isoflurane or with equianesthetic dose of pentobarbital. Some IL-11 receptor (IL-11R) WT mice were pretreated with an IL-11–neutralizing antibody (1 mg/kg, intravenous injection) 20 min before reperfusion or sham-operation. Isoflurane postconditioning significantly reduced plasma creatinine after RIR injury in IL-11R WT mice. However, IL-11R deficiency or IL-11–neutralizing antibody prevented the renal protective effects of isoflurane postconditioning. * $P < 0.05$ *versus* respective sham-operated mice. # $P < 0.05$ *versus* pentobarbital-anesthetized mice subjected to RIR. Data are from six mice per group and represented as mean ± SD. ISO = isoflurane; PB = pentobarbital.

similar degree of renal injury after I/R during anesthesia with pentobarbital. Collectively, these studies suggest that IL-11 induction by isoflurane is required to trigger *in vivo* renal protection.

Figure 7A demonstrates severe necrotic renal injury in IL-11R WT mice subjected to renal I/R during anesthesia with pentobarbital. Compared with sham-operated mice (not shown), the kidneys of mice subjected to renal I/R showed significant tubular necrosis, cast formation, and congestion. In contrast, consistent with the plasma creatinine data, anesthesia with isoflurane reduced renal tubular necrosis 24 h after I/R injury (fig. 7A). Supporting a critical role of IL-11 in isoflurane-mediated renal protection against I/R, isoflurane failed to reduce renal tubular necrosis in IL-11R WT mice pretreated with a neutralizing IL-11 antibody or in IL-11R knockout mice. The Jablonski scale[25] renal injury score was used to grade renal tubular necrosis 24 h after renal I/R (fig. 7B). Thirty minutes of renal ischemia and 24 h of reperfusion resulted in severe acute tubular necrosis in IL-11R WT mice anesthetized with pentobarbital after renal I/R injury. Consistent with the renal histology data, isoflurane significantly reduced the renal injury score in IL-11R WT mice but not in IL-11R knockout mice or in IL-11R WT mice pretreated with IL-11–neutralizing antibody.

IL-11 Is Critical for Isoflurane-mediated Reduction in Kidney Neutrophil Infiltration and Apoptosis

Figure 8A shows representative images (from four to six experiments) of neutrophil immunohistochemistry in kidneys (magnification ×200) of mice subjected to 30 min of renal ischemia and 24-h reperfusion. In sham-operated mice, we were unable to detect any neutrophils in the kidney (data not shown). There was heavy neutrophil infiltration (dark brown) in the kidneys of pentobarbital-anesthetized IL-11R WT mice subjected to renal I/R. In contrast, IL-11R WT mice anesthetized with isoflurane for 4 h after renal ischemia had significantly reduced neutrophil infiltration in the kidney 24 h after I/R (fig. 8B). Again, isoflurane failed to reduce kidney neutrophil infiltration in IL-11R WT mice treated with IL-11–neutralizing antibody and in IL-11R knockout mice.

Terminal deoxynucleotidyl transferase 2′-deoxyuridine-5′-triphosphate nick end-labeling staining (from four to five experiments) detected apoptotic renal cells in the kidneys of mice subjected to renal I/R resulting in severe proximal tubule cell apoptosis (fig. 9A, ×100). Renal ischemia and 24 h of reperfusion resulted in significant apoptosis in the kidneys of pentobarbital-anesthetized IL-11R WT mice. However, IL-11R WT mice anesthetized with isoflurane for 4 h after renal ischemia had significantly reduced number of apoptotic terminal deoxynucleotidyl transferase 2′-deoxyuridine-5′-triphosphate nick end-labeling–positive cells in the kidney 24 h after I/R (fig. 9B). Again, isoflurane failed to reduce renal tubular apoptosis in IL-11R WT mice treated with IL-11–neutralizing antibody and in IL-11R knockout mice.

Discussion

We have shown in this study that isoflurane increases renal tubular IL-11 mRNA and protein synthesis *via* TGF-β1–dependent signaling *in vivo* as well as *in vitro*. TGF-β1 is a powerful antiinflammatory cytokine that regulates multiple cellular processes including immune modulation, cellular differentiation and proliferation, and oncogenesis.[31,32] We previously demonstrated that volatile halogenated anesthetics including isoflurane cause translocation of phosphatidylserine from the inner leaflet to the outer leaflet of the plasma membrane (membrane externalization) resulting in the release of antiinflammatory TGF-β1.[11,12] Furthermore, volatile halogenated anesthetics-mediated reduction in renal tubular necrosis and inflammation was dependent on the release of renal tubular TGF-β1. Finally, volatile halogenated anesthetic-mediated renal protection was abolished in mice deficient in TGF-β1 or WT mice treated with neutralizing TGF-β1 antibody.[33]

We also recently demonstrated that exogenous human recombinant IL-11 attenuated ischemic AKI in mice and reduced necrosis and apoptosis in human kidney (HK-2) proximal tubule cells.[16] In mice, recombinant IL-11 treatment attenuated renal tubular necrosis and apoptosis as

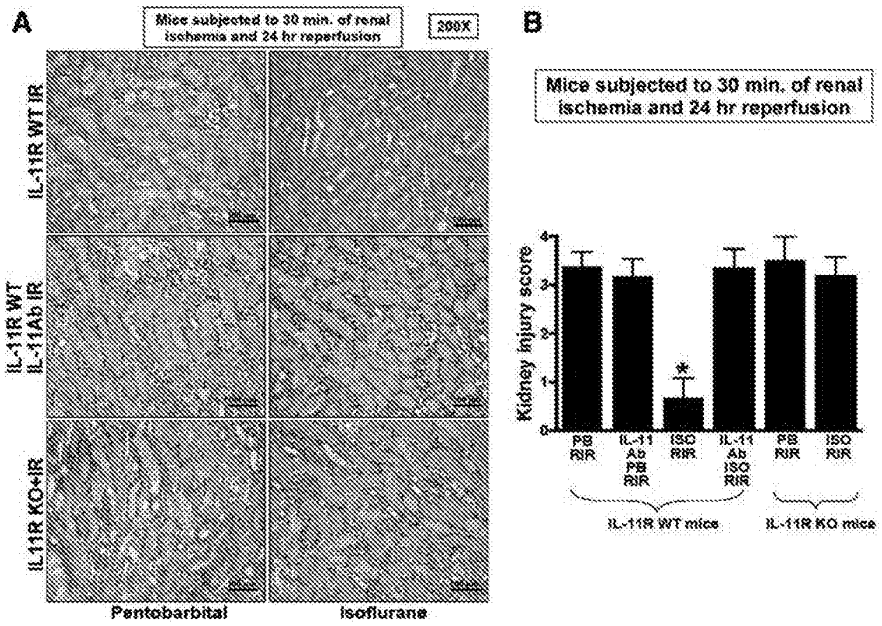

Fig. 7. Interleukin (IL)-11 is critical for isoflurane-mediated reduction in renal tubular necrosis after ischemia and reperfusion (IR). (*A*) Representative photomicrographs of five to six experiments for hematoxylin and eosin staining (magnification ×200) of kidneys of IL-11 receptor wild-type (IL-11R WT) mice, IL-11 receptor–deficient (IL-11R knockout [KO]) mice, and IL-11R WT mice pretreated with IL-11–neutralizing antibody and subjected to 30-min renal ischemia and 24-h reperfusion (I/R). *Scale bars* in all panels of *A* are 100 μm. (*B*) Summary of Jablonski scale renal injury scores (N = 4, graded from hematoxylin and eosin staining, scale 0–4) for mice subjected to renal I/R. * $P < 0.05$ *versus* pentobarbital-anesthetized IL-11R WT mice subjected to renal I/R. *Error bars* represent 1 SD. IL-11R WT mice anesthetized with pentobarbital after renal ischemia showed severe renal tubular necrosis. Isoflurane postconditioning significantly attenuated renal tubular necrosis and renal injury scores after renal IR. IL-11R deficiency (IL-11R KO) or IL-11 neutralization prevented renal protection with isoflurane postconditioning in mice.

well as the influx of proinflammatory neutrophils after renal I/R. We further demonstrated in this study that isoflurane-mediated protection against renal tubular necrosis (Jablonski score), inflammation (neutrophil infiltration), and apoptosis (terminal deoxynucleotidyl transferase 2′-deoxyuridine-5′-triphosphate nick end-labeling staining) is directly mediated by the induction of IL-11 as isoflurane failed to reduce these critical indices of renal injury in IL-11R–deficient mice or mice treated with IL-11–neutralized antibody. Taken together, as blockade or genetic deletion of either TGF-β1 or IL-11 abolished renal protective effects of isoflurane, our current and previous studies suggest that isoflurane induces nonredundant proximal (TGF-β1) and distal (IL-11) cytoprotective signaling molecules to protect against ischemic AKI.

The most exciting aspect of isoflurane-mediated induction of IL-11 leading to renal protection is that recombinant IL-11 (Oprelvekin; Wyeth Pharmaceuticals, Philadelphia, PA) is already clinically approved to treat chemotherapy-induced thrombocytopenia. IL-11 is a member of the IL-6-type cytokine family isolated from bone marrow–derived stromal cells.[34] IL-11 receptor activation potently regulates hematopoiesis by promoting megakaryocyte maturation.[35] However, in addition to its effects on platelets, recent studies show a cytoprotective role of IL-11 as exogenous IL-11 administration attenuates cell death in several cell types and organs.[16,36–38] In the heart, intestine, and endothelial cells, IL-11 directly reduces necrotic as well as apoptotic cell death *via* mitogen-activated protein kinase and the Janus kinase/signal transducers and activators of transcription signaling.[15] In addition to its antiapoptotic and antinecrotic properties, IL-11 receptor activation attenuates lipopolysaccharide-induced systemic inflammation in mice, toxic nephritis, and leukocyte-mediated liver injury.[39–42] Therefore, we propose that isoflurane-mediated induction of IL-11 and renal tubular IL-11 receptor activation produce powerful protection against ischemic AKI by targeting all three pathways of cell death: necrosis, apoptosis, and inflammation. Furthermore, as IL-11 as well as IL-11 receptors are expressed in many tissues and cell types,[15] it remains to be determined whether isoflurane can induce IL-11 in nonrenal cells (*e.g.*, hepatocytes, intestinal epithelial cells, and endothelial cells) and confer protection in these organs against AKI-induced remote organ injury.

The signal transduction mechanisms of IL-11–induced cytoprotection have been investigated in other cell types. IL-11 ligand and receptor complex interacts with a common receptor subunit, glycoprotein 130 (gp130), leading to gp130-associated kinase-mediated tyrosine phosphorylation.[43] In cardiac myocytes, IL-11 reduces injury and fibrosis by the Janus kinase/signal transducers and activators of

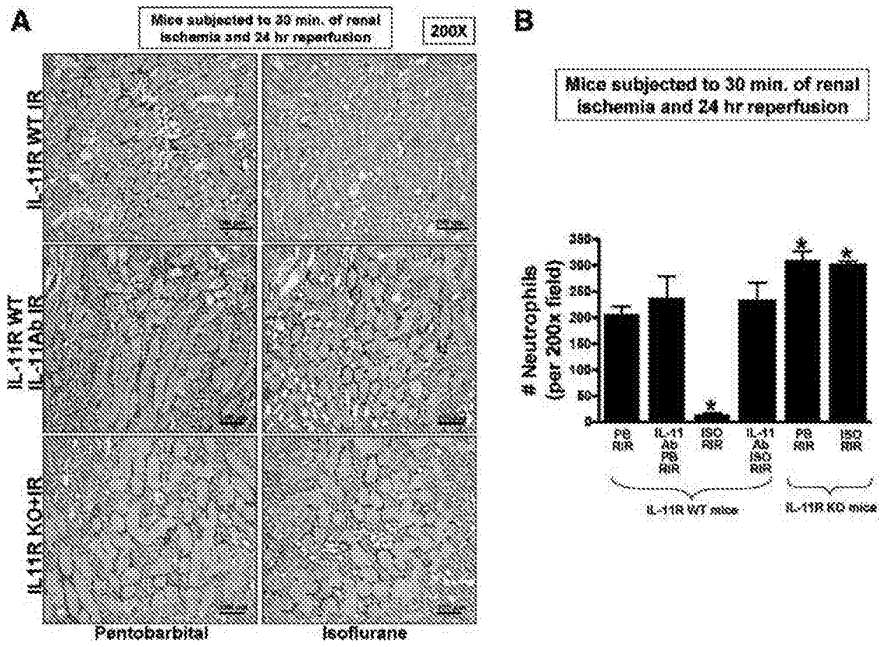

Fig. 8. Interleukin (IL)-11 is critical for isoflurane postconditioning–mediated reduction in renal neutrophil infiltration after ischemia and reperfusion. (*A*) Representative photomicrographs of four to six experiments for immunohistochemistry (*brown staining*) for neutrophil infiltration (×200) from kidneys IL-11 receptor wild-type (IL-11R WT) mice, IL-11 receptor–deficient (IL-11R knockout [KO]) mice, and IL-11R WT mice pretreated with IL-11–neutralizing antibody and subjected to 30-min renal ischemia and 24-h reperfusion. *Scale bars* in all panels of *A* are 100 μm. (*B*) Quantifications of infiltrated neutrophils per ×200 field in the kidneys of mice after renal ischemia reperfusion (RIR). * $P < 0.05$ *versus* vehicle-treated pentobarbital-anesthetized mice subjected to RIR. *Error bars* represent 1 SD. IL-11R WT mice anesthetized with pentobarbital after renal ischemia showed heavy neutrophil infiltration. Isoflurane postconditioning significantly attenuated renal tubular neutrophil infiltration after RIR. IL-11 deficiency (IL-11R KO) or IL-11 neutralization attenuated these reductions in renal neutrophil infiltration with isoflurane postconditioning in mice.

transcription 3 activation.[38,43,44] In vascular endothelial and intestinal epithelial cells, IL-11 protects against oxidant-induced necrosis and apoptosis *via* mechanisms involving extracellular signal-regulated kinase, mitogen-activated protein kinase, protein kinase B, and/or induction of heat shock protein 25.[37,45,46]

Isolfurane-induced IL-11 generation may also produce antiinflammatory effects after renal I/R *via* modulating the nuclear factor-κB activity. Indeed, nuclear factor-κB is one of the most important proinflammatory transcription factors.[47] IL-11 has been shown to attenuate transcription factor NF-kB in several cell lines and in mouse models of kidney inflammation.[40,48,49] Furthermore, IL-11 treatment *in vivo* decreases glomerular nuclear factor-κB activity and reduces renal injury in experimental glomerulonephritis.[50]

We previously showed that IL-11 produces renal protection by direct induction of sphingosine kinase-1 *via* nuclear translocation of hypoxia-inducible factor-1α.[16] Sphingosine kinase-1 produces sphingosine 1-phosphate—a well-known antiinflammatory immune modulator.[51] Based on our previous[9,52] and current experimental data, we propose that isoflurane may directly induce several antiinflammatory signaling molecules (*e.g.*, IL-11, sphingosine 1-phosphate) to protect against hyperinflammatory response after ischemic AKI. Interestingly, several of the IL-11–mediated cytoprotective signal transduction proteins (*e.g.*, extracellular signal-regulated kinase, mitogen-activated protein kinase, protein kinase B, sphingosine kinase) are also activated with volatile halogenated anesthetics as we demonstrated previously.[12,13,17]

We have shown here that isoflurane postconditioning produces potent renal protection against ischemic AKI *via* IL-11–mediated reduction in kidney tubule necrosis, apoptosis, and renal inflammation. We propose that after renal I/R injury, necrotic tubules cells release proinflammatory cytokines (*e.g.*, monocyte chemotactic protein-1 release) that can further aggravate inflammation by stimulating resident kidney macrophages and dendritic cells.[4] These cells in turn release additional proinflammatory cytokines (*e.g.*, macrophage inflammatory protein 2α, keratinocyte-derived cytokine) to promote cytotoxic T-lymphocyte, neutrophil, and macrophage infiltration into the kidney interstitial space. Infiltrating proinflammatory leukocytes release additional cytotoxic proinflammatory and proapoptotic cytokines (*e.g.*, tumor necrosis factor-α) which will exacerbate renal tubular cell necrosis as well as apoptosis. Figure 10 summarizes the potential mechanisms of isoflurane-mediated renal protection involving renal tubular IL-11 synthesis *via* TGF-β1 signaling.

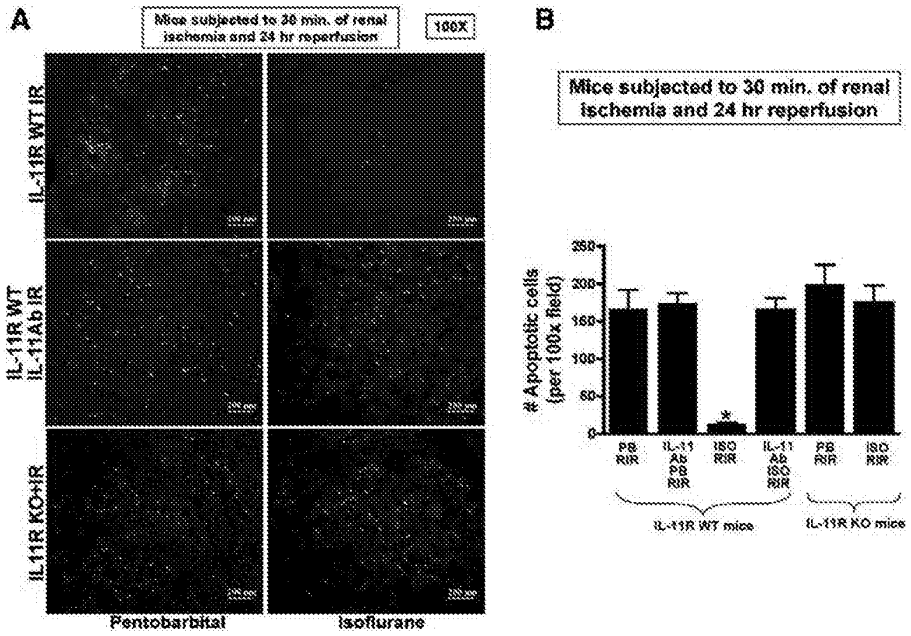

Fig. 9. Interleukin (IL)-11 is critical for isoflurane postconditioning–mediated reduction in renal tubular apoptosis after ischemia and reperfusion. (*A*) Representative photomicrographs of four to six experiments for terminal deoxynucleotidyl transferase dUTP nick end-labeling staining (representing apoptotic nuclei, magnification ×100) from kidneys IL-11 receptor wild-type (IL-11R WT) mice, IL-11 receptor–deficient (IL-11R knockout [KO]) mice, and IL-11R WT mice pretreated with IL-11–neutralizing antibody and subjected to 30-min renal ischemia and 24-h reperfusion. *Scale bars* in all panels of *A* are 200 μm. (*B*) Quantifications of apoptotic cells per ×100 field in the kidneys of mice after renal ischemia reperfusion (R/R). * $P < 0.05$ *versus* vehicle-treated pentobarbital-anesthetized mice subjected to R/R. *Error bars* represent 1 SD. IL-11R WT mice anesthetized with pentobarbital after renal ischemia showed numerous terminal deoxynucleotidyl transferase dUTP nick end-labeling–positive cells. Isoflurane postconditioning significantly attenuated renal tubular apoptosis after R/R. IL-11 deficiency (IL-11R KO) or IL-11 neutralization attenuated these reductions in renal tubular apoptosis with isoflurane postconditioning in mice.

We believe that potential for clinical use of recombinant IL-11 therapy would be far superior to therapy against ischemic AKI with recombinant TGF-β1. Active form of TGF-β1 has a very short plasma half-life (2–3 min) as nonlatent TGF-β1 gets rapidly taken up by the liver, kidneys, lungs, and spleen and degraded.[53] This is in contrast to the more prolonged half-life of recombinant IL-11 (approximately 7 h).[34] Furthermore, prolonged exposure to TGF-β1 may promote kidney fibrosis.[54] Therefore, prolonged TGF-β1 therapy may transiently reduce inflammation and necrosis but may cause increased renal tubular fibrosis that may paradoxically prolong renal dysfunction after I/R. Unlike TGF-β1, prolonged and high-dose IL-11 therapy does not induce tissue fibrosis.

We recently showed that isoflurane *via* TGF-β1 induces ecto-5′-nucleotidase (CD73) to generate cytoprotective adenosine in renal proximal tubule cells.[55] CD73 induction and CD73-mediated adenosine generation were critical for isoflurane-mediated renal protection against ischemic AKI. However, the downstream target of isoflurane-mediated adenosine generation as well as the specific adenosine receptor subtype(s) responsible for renal protection against ischemic AKI remains unclear. We hypothesize that isoflurane-mediated induction of CD73 activity and adenosine generation directly stimulates renal tubular IL-11 synthesis to protect against ischemic AKI. Consistent with this hypothesis, we recently also showed that a specific A_1 adenosine receptor agonist 2-chloro cyclopentyladenosine also induces IL-11 in proximal tubule cells.[56] It remains to be tested in future studies whether isoflurane-mediated adenosine generation results in the activation of renal tubular A_1 adenosine receprors to protect against renal ischemia and reperfusion injury.

There are several limitations to our study. Our results may not completely translate to clinical setting as differences in pathophysiology between human and mouse ischemic AKI exist. Furthermore, our studies focused on renal tubular synthesis of IL-11 and protection whereas clinical AKI results in both impairment of glomerular filtration and renal tubular dysfunction. In addition, our *in vitro* studies have limitation as HK-2 cells used in this study are immortalized and primary culture of proximal tubule cells may undergo rapid phenotypic changes *ex vivo*. Finally, complete isoflurane concentration–response curves were not generated in most of our experiments.

In summary, we demonstrated that a widely used volatile halogenated anesthetic isoflurane protects against renal

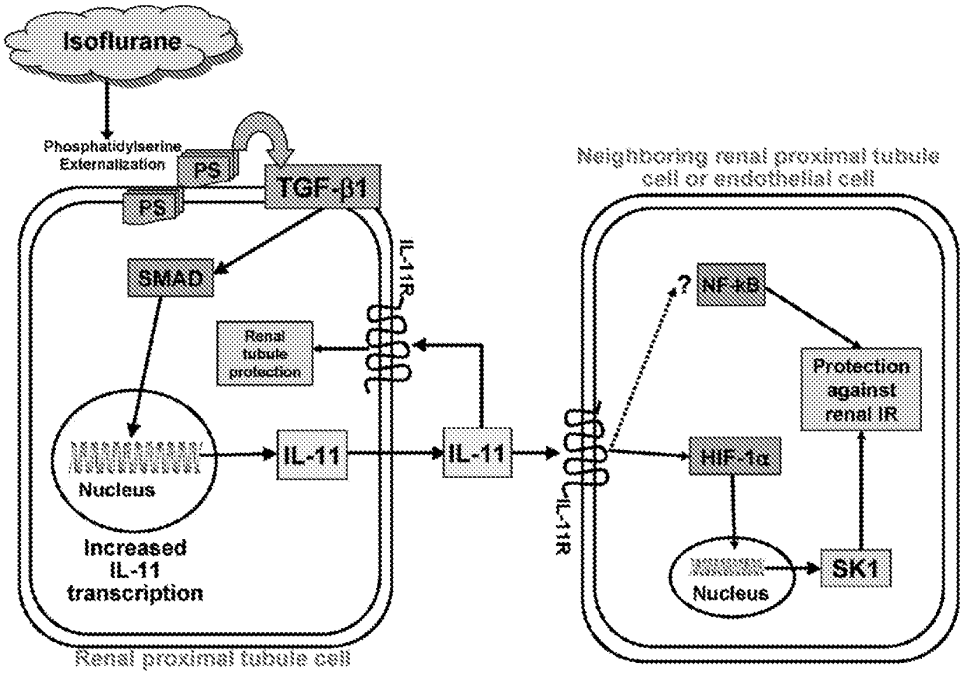

Fig. 10. Proposed summary of cellular mechanisms of renal protection with postischemic isoflurane treatment. Collectively, our data suggest that anesthesia with isoflurane increases interleukin (IL)-11 messenger RNA and protein synthesis *via* transforming growth factor-β1 (TGF-β1) signaling. We propose that IL-11 synthesized subsequently activates interleukin-11 receptor (IL-11R) in neighboring renal tubules or endothelial cells to induce cytoprotective signaling. Because previous studies have shown that IL-11 reduces the activity of a well-known proinflammatory transcription factor NF-kB,[49,50] it is highly possible that IL-11 generated with isoflurane treatment may also attenuate NF-kB activity to protect against renal inflammation and injury after acute kidney injury. SMADs are intracellular proteins that transduce extracellular signals from TGF-β1 to the nucleus to initiate downstream gene transcription. Hypothetical pathways (*e.g.*, NF-kB inhibition) leading to cytoprotection are shown in *dashed lines*. We previously showed that IL-11 produces renal protection by direct induction of sphingosine kinase-1 *via* nuclear translocation of hypoxia-inducible factor (HIF)-1α.[14] IR = ischemia reperfusion; NF-kB = nuclear factor κ-light-chain-enhancer of activated B cells; PS = phosphatidylserine; SMAD = SMA (from *Caenorhabditis elegans* protein sma for small body size) and MAD (from Drosophila protein mothers against decapentaplegic) related family of transduction proteins.

tubular necrosis and inflammation after renal I/R by inducing cytoprotective IL-11 generation.

The authors appreciate the surgical, analytical, and technical assistance provided by Sang Won Park, Ph.D. (Assistant Professor of Pharmacology, Gyeongnam National University, Jin Ju, South Korea).

References

1. Chertow GM, Burdick E, Honour M, Bonventre JV, Bates DW: Acute kidney injury, mortality, length of stay, and costs in hospitalized patients. J Am Soc Nephrol 2005; 16:3365–70
2. Yap SC, Lee HT: Acute kidney injury and extrarenal organ dysfunction: New concepts and experimental evidence. Anesthesiology 2012; 116:1139–48
3. Elapavaluru S, Kellum JA: Why do patients die of acute kidney injury? Acta Clin Belg Suppl 2007; 326–31
4. Okusa MD: The changing pattern of acute kidney injury: From one to multiple organ failure. Contrib Nephrol 2010; 165:153–8
5. Faubel S: Acute kidney injury and multiple organ dysfunction syndrome. Minerva Urol Nefrol 2009; 61:171–88
6. Legrand M, Payen D: Case scenario. Hemodynamic management of postoperative acute kidney injury. Anesthesiology 2013; 118:1446–54
7. Cullen KA, Hall MJ, Golosinskiy A: Ambulatory surgery in the United States, 2006. Natl Health Stat Report 2009; 1–25
8. Lee HT, Ota-Setlik A, Fu Y, Nasr SH, Emala CW: Differential protective effects of volatile anesthetics against renal ischemia-reperfusion injury *in vivo*. Anesthesiology 2004; 101:1313–24
9. Lee HT, Kim M, Kim M, Kim N, Billings FT IV, D'Agati VD, Emala CW Sr: Isoflurane protects against renal ischemia and reperfusion injury and modulates leukocyte infiltration in mice. Am J Physiol Renal Physiol 2007; 293: F713–22
10. Lee HT, Kim M, Jan M, Emala CW: Anti-inflammatory and antinecrotic effects of the volatile anesthetic sevoflurane in kidney proximal tubule cells. Am J Physiol Renal Physiol 2006; 291:F67–78
11. Lee HT, Kim M, Song JH, Chen SW, Gubitosa G, Emala CW: Sevoflurane-mediated TGF-beta1 signaling in renal proximal tubule cells. Am J Physiol Renal Physiol 2008; 294:F371–8
12. Lee HT, Kim M, Kim J, Kim N, Emala CW: TGF-beta1 release by volatile anesthetics mediates protection against renal proximal tubule cell necrosis. Am J Nephrol 2007; 27:416–24

13. Song JH, Kim M, Park SW, Chen SW, Pitson SM, Lee HT: Isoflurane *via* TGF-beta1 release increases caveolae formation and organizes sphingosine kinase signaling in renal proximal tubules. Am J Physiol Renal Physiol 2010; 298:F1041–50
14. Goldman SC, Bracho F, Davenport V, Slack R, Areman E, Shen V, Lenarsky C, Weinthal J, Hughes R, Cairo MS: Feasibility study of IL-11 and granulocyte colony-stimulating factor after myelosuppressive chemotherapy to mobilize peripheral blood stem cells from heavily pretreated patients. J Pediatr Hematol Oncol 2001; 23:300–5
15. Du X, Williams DA: Interleukin-11: Review of molecular, cell biology, and clinical use. Blood 1997; 89:3897–908
16. Lee HT, Park SW, Kim M, Ham A, Anderson LJ, Brown KM, D'Agati VD, Cox GN: Interleukin-11 protects against renal ischemia and reperfusion injury. Am J Physiol Renal Physiol 2012; 303:F1216–24
17. Kim M, Kim M, Kim N, D'Agati VD, Emala CW Sr, Lee HT: Isoflurane mediates protection from renal ischemia-reperfusion injury *via* sphingosine kinase and sphingosine-1-phosphate-dependent pathways. Am J Physiol Renal Physiol 2007; 293:F1827–35
18. Wang J, Zhu Z, Nolfo B, Elias JA: Dexamethasone regulation of lung epithelial cell and fibroblast interleukin-11 production. Am J Physiol 1999; 276(1 Pt 1):L175–85
19. Tang W, Yang L, Yang YC, Leng SX, Elias JA: Transforming growth factor-beta stimulates interleukin-11 transcription *via* complex activating protein-1-dependent pathways. J Biol Chem 1998; 273:5506–13
20. Ryan MJ, Johnson G, Kirk J, Fuerstenberg SM, Zager RA, Torok-Storb B: HK-2: An immortalized proximal tubule epithelial cell line from normal adult human kidney. Kidney Int 1994; 45:48–57
21. Vinay P, Gougoux A, Lemieux G: Isolation of a pure suspension of rat proximal tubules. Am J Physiol 1981; 241:F403–11
22. Kim M, Kim M, Park SW, Pitson SM, Lee HT: Isoflurane protects human kidney proximal tubule cells against necrosis *via* sphingosine kinase and sphingosine-1-phosphate generation. Am J Nephrol 2010; 31:353–62
23. Redel A, Stumpner J, Tischer-Zeitz T, Lange M, Smul TM, Lotz C, Roewer N, Kehl F: Comparison of isoflurane-, sevoflurane-, and desflurane-induced pre- and postconditioning against myocardial infarction in mice *in vivo*. Exp Biol Med (Maywood) 2009; 234:1186–91
24. Siot C: Plasma creatinine determination. A new and specific Jaffe reaction method. Scand J Clin Lab Invest 1965; 17:381–7
25. Jablonski P, Howden BO, Rae DA, Birrell CS, Marshall VC, Tange J: An experimental model for assessment of renal recovery from warm ischemia. Transplantation 1983; 35:198–204
26. Lee HT, Gallos G, Nasr SH, Emala CW: A1 adenosine receptor activation inhibits inflammation, necrosis, and apoptosis after renal ischemia-reperfusion injury in mice. J Am Soc Nephrol 2004; 15:102–11
27. Lee HT, Xu H, Nasr SH, Schnermann J, Emala CW: A1 adenosine receptor knockout mice exhibit increased renal injury following ischemia and reperfusion. Am J Physiol Renal Physiol 2004; 286:F298–306
28. Park SW, Kim M, Chen SW, Brown KM, D'Agati VD, Lee HT: Sphinganine-1-phosphate protects kidney and liver after hepatic ischemia and reperfusion in mice through S1P1 receptor activation. Lab Invest 2010; 90:1209–24
29. Chen SW, Kim M, Kim M, Song JH, Park SW, Wells D, Brown K, Belleroche Jd, D'Agati VD, Lee HT: Mice that overexpress human heat shock protein 27 have increased renal injury following ischemia reperfusion. Kidney Int 2009; 75:499–510
30. Matkowskyj KA, Schonfeld D, Benya RV: Quantitative immunohistochemistry by measuring cumulative signal strength using commercially available software photoshop and matlab. J Histochem Cytochem 2000; 48:303–12
31. Wang XJ, Han G, Owens P, Siddiqui Y, Li AG: Role of TGF beta-mediated inflammation in cutaneous wound healing. J Investig Dermatol Symp Proc 2006; 11:112–7
32. Huynh ML, Fadok VA, Henson PM: Phosphatidylserine-dependent ingestion of apoptotic cells promotes TGF-beta1 secretion and the resolution of inflammation. J Clin Invest 2002; 109:41–50
33. Lee HT, Chen SW, Doetschman TC, Deng C, D'Agati VD, Kim M: Sevoflurane protects against renal ischemia and reperfusion injury in mice *via* the transforming growth factor-beta1 pathway. Am J Physiol Renal Physiol 2008; 295:F128–36
34. Kaye JA: The clinical development of recombinant human interleukin 11 (NEUMEGA rhIL-11 growth factor). Stem Cells 1996; 14(suppl 1):256–60
35. Reynolds CH: Clinical efficacy of rhIL-11. Oncology (Williston Park) 2000; 14(9 suppl 8):32–40
36. Kuenzler KA, Pearson PY, Schwartz MZ: IL-11 pretreatment reduces cell death after intestinal ischemia-reperfusion. J Surg Res 2002; 108:268–72
37. Waxman AB, Mahboubi K, Knickelbein RG, Mantell LL, Manzo N, Pober JS, Elias JA: Interleukin-11 and interleukin-6 protect cultured human endothelial cells from H2O2-induced cell death. Am J Respir Cell Mol Biol 2003; 29:513–22
38. Kimura R, Maeda M, Arita A, Oshima Y, Obana M, Ito T, Yamamoto Y, Mohri T, Kishimoto T, Kawase I, Fujio Y, Azuma J: Identification of cardiac myocytes as the target of interleukin 11, a cardioprotective cytokine. Cytokine 2007; 38:107–15
39. Bozza M, Bliss JL, Maylor R, Erickson J, Donnelly L, Bouchard P, Dorner AJ, Trepicchio WL: Interleukin-11 reduces T-cell-dependent experimental liver injury in mice. Hepatology 1999; 30:1441–7
40. Trepicchio WL, Bozza M, Pedneault G, Dorner AJ: Recombinant human IL-11 attenuates the inflammatory response through down-regulation of proinflammatory cytokine release and nitric oxide production. J Immunol 1996; 157:3627–34
41. Sheridan BC, Dinarello CA, Meldrum DR, Fullerton DA, Selzman CH, McIntyre RC Jr: Interleukin-11 attenuates pulmonary inflammation and vasomotor dysfunction in endotoxin-induced lung injury. Am J Physiol 1999; 277(5 Pt 1):1861–7
42. Lai PC, Cook HT, Smith J, Keith JC Jr, Pusey CD, Tam FW: Interleukin-11 attenuates nephrotoxic nephritis in Wistar Kyoto rats. J Am Soc Nephrol 2001; 12:2310–20
43. Fujio Y, Maeda M, Mohri T, Obana M, Iwakura T, Hayama A, Yamashita T, Nakayama H, Azuma J: Glycoprotein 130 cytokine signal as a therapeutic target against cardiovascular diseases. J Pharmacol Sci 2011; 117:213–22
44. Obana M, Maeda M, Takeda K, Hayama A, Mohri T, Yamashita T, Nakaoka Y, Komuro I, Takeda K, Matsumiya G, Azuma J, Fujio Y: Therapeutic activation of signal transducer and activator of transcription 3 by interleukin-11 ameliorates cardiac fibrosis after myocardial infarction. Circulation 2010; 121:684–91
45. Ropeleski MJ, Tang J, Walsh-Reitz MM, Musch MW, Chang EB: Interleukin-11-induced heat shock protein 25 confers intestinal epithelial-specific cytoprotection from oxidant stress. Gastroenterology 2003; 124:1358–68
46. Naugler KM, Baer KA, Ropeleski MJ: Interleukin-11 antagonizes Fas ligand-mediated apoptosis in IEC-18 intestinal epithelial crypt cells: Role of MEK and Akt-dependent signaling. Am J Physiol Gastrointest Liver Physiol 2008; 294:G728–37
47. Barnes PJ, Karin M: Nuclear factor-kappaB: A pivotal transcription factor in chronic inflammatory diseases. N Engl J Med 1997; 336:1066–71
48. Bamba S, Andoh A, Yasui H, Makino J, Kim S, Fujiyama Y: Regulation of IL-11 expression in intestinal myofibroblasts:

Role of c-Jun AP-1- and MAPK-dependent pathways. Am J Physiol Gastrointest Liver Physiol 2003; 285:G529–38

49. Trepicchio WL, Wang L, Bozza M, Dorner AJ: IL-11 regulates macrophage effector function through the inhibition of nuclear factor-kappaB. J Immunol 1997; 159:5661–70
50. Stangou M, Bhangal G, Lai PC, Smith J, Keith JC Jr, Boyle JJ, Pusey CD, Cook T, Tam FW: Effect of IL-11 on glomerular expression of TGF-beta and extracellular matrix in nephrotoxic nephritis in Wistar Kyoto rats. J Nephrol 2011; 24:106–11
51. Jo SK, Bajwa A, Awad AS, Lynch KR, Okusa MD: Sphingosine-1-phosphate receptors: Biology and therapeutic potential in kidney disease. Kidney Int 2008; 73:1220–30
52. Kim M, Park SW, Kim M, D'Agati VD, Lee HT: Isoflurane activates intestinal sphingosine kinase to protect against renal ischemia-reperfusion-induced liver and intestine injury. Anesthesiology 2011; 114:363–73
53. Wakefield LM, Winokur TS, Hollands RS, Christopherson K, Levinson AD, Sporn MB: Recombinant latent transforming growth factor beta 1 has a longer plasma half-life in rats than active transforming growth factor beta 1, and a different tissue distribution. J Clin Invest 1990; 86:1976–84
54. Roberts AB, Tian F, Byfield SD, Stuelten C, Ooshima A, Saika S, Flanders KC: Smad3 is key to TGF-beta-mediated epithelial-to-mesenchymal transition, fibrosis, tumor suppression and metastasis. Cytokine Growth Factor Rev 2006; 17:19–27
55. Kim M, Ham A, Kim JY, Brown KM, D'Agati VD, Lee HT: The volatile anesthetic isoflurane induces ecto-5'-nucleotidase (CD73) to protect against renal ischemia and reperfusion injury. Kidney Int 2013; 84:90–103
56. Kim JY, Kim M, Ham A, Brown KM, Greene RW, D'Agati VD, Lee HT: IL-11 is required for A1 adenosine receptor-mediated protection against ischemic AKI. J Am Soc Nephrol 2013; [Epub ahead of print]

Endogenous IL-11 Signaling Is Essential in Th2- and IL-13–Induced Inflammation and Mucus Production

Chun Geun Lee[1], Dominik Hartl[1], Hiroshi Matsuura[1], Felicity M. Dunlop[2], Pierre D. Scotney[2], Louis J. Fabri[2], Andrew D. Nash[2], Ning-Yuan Chen[1], Chu-Yan Tang[1], Qingsheng Chen[1], Robert J. Homer[3], Manuel Baca[2], and Jack A. Elias[1]

[1]Section of Pulmonary and Critical Care Medicine, Yale University School of Medicine, New Haven, Connecticut; [2]CSL Limited A.C.N., Parkville, Victoria, Australia; and [3]Department of Pathology, Yale University School of Medicine, and Pathology and Laboratory Medicine Service, VA-CT Health Care System, West Haven, Connecticut

IL-11 and IL-11 receptor (R)α are induced by Th2 cytokines. However, the role(s) of endogenous IL-11 in antigen-induced Th2 inflammation has not been fully defined. We hypothesized that IL-11, signaling via IL-11Rα, plays an important role in aeroallergen-induced Th2 inflammation and mucus metaplasia. To test this hypothesis, we compared the responses induced by the aeroallergen ovalbumin (OVA) in wild-type (WT) and IL-11Rα–null mutant mice. We also generated and defined the effects of an antagonistic IL-11 mutein on pulmonary Th2 responses. Increased levels of IgE, eosinophilic tissue and bronchoalveolar lavage (BAL) inflammation, IL-13 production, and increased mucus production and secretion were noted in OVA-sensitized and -challenged WT mice. These responses were at least partially IL-11 dependent because each was decreased in mice with null mutations of IL-11Rα. Importantly, the administration of the IL-11 mutein to OVA-sensitized mice before aerosol antigen challenge also caused a significant decrease in OVA-induced inflammation, mucus responses, and IL-13 production. Intraperitoneal administration of the mutein to lung-specific IL-13–overexpressing transgenic mice also reduced BAL inflammation and airway mucus elaboration. These studies demonstrate that endogenous IL-11R signaling plays an important role in antigen-induced sensitization, eosinophilic inflammation, and airway mucus production. They also demonstrate that Th2 and IL-13 responses can be regulated by interventions that manipulate IL-11 signaling in the murine lung.

Keywords: IL-11; mutein; airway inflammation; mucus; IL-13

Asthma is a chronic disorder of the airway in which a Th2-dominated inflammatory response and subsequent airway remodeling are felt to play mechanistically important roles (1–4). In keeping with their importance, the cytokines that mediate these responses have been subject to significant investigation. These studies demonstrated that IL-4 plays a key role in Th2 cell differentiation (5). In contrast, IL-13 is now believed to be the major effector of Th2 inflammation and tissue remodeling (4, 6). Studies from our laboratory and others have also defined many of the pathways that are used to induce these alterations. As a result, it is now known that chemokines, matrix metalloproteinases (MMPs), TGF-β, and chitinases contribute to the pathogenesis of pulmonary Th2 inflammation and remodeling (4, 7, 8). However, the importance of IL-6–type cytokines in the generation of OVA- or IL-13–induced inflammation or tissue responses has not been fully defined.

CLINICAL RELEVANCE

This study is the first to demonstrate that endogenous IL-11 signaling is critical to Th2 aeroallergen- or IL-13–induced inflammation and airway mucus production.

IL-11 is a multifunctional IL-6–type cytokine that stimulates hematopoiesis, thrombopoiesis, and megakaryocytopoiesis; enhances bone marrow resorption; regulates macrophage differentiation; and confers mucosal protection after chemotherapy and radiation therapy (9–12). Previous studies from our laboratory demonstrated that epithelial cells, fibroblasts, and airway smooth muscle cells produce IL-11 in response to TGF-β_1, IL-1, histamine, eosinophil major basic protein, and specific respiratory viruses (10, 13–18), and that the transgenic overexpression of IL-11 causes asthma-like airway fibrosis, myocyte hyperplasia, and airways hyperresponsiveness on methacholine challenge (19, 20). Our studies also demonstrated that IL-11 can be detected in exaggerated quantities in the nasal secretions of children with viral upper respiratory tract infections (16) and the airways of patients with asthma (21, 22). However, the role of endogenous IL-11 and IL-11 signaling in the pathogenesis of Th2 inflammation has not been adequately defined.

To define the role(s) of endogenous IL-11 in antigen-induced Th2 inflammation, we compared the acute responses induced by the aeroallergen ovalbumin (OVA) in wild-type (WT) and IL-11Rα–null mutant mice. We also generated and evaluated the effects of an antagonistic IL-11 mutein, on OVA-induced Th2 inflammation and IL-13–induced tissue responses. These studies demonstrate that the IL-11 pathway plays an important role in antigen sensitization and the eosinophilic inflammation, mucus metaplasia, and IL-13 elaboration that are characteristic of pulmonary Th2 responses. They also demonstrate that IL-11 signaling contributes to the effector functions of IL-13 in the murine lung.

MATERIALS AND METHODS

Genetically Modified Mice

IL-11Rα $^{-/-}$ mice were provided by Drs. Lorraine Robb and C. Glenn Begley (The Walter and Eliza Hall Institute, Victoria, Australia) (23). These mice were bred for more than 10 generations onto a C57BL/6 genetic background. C57BL/6 WT controls were obtained from the Jackson Labs (Bar Harbor, ME). CC10-rtTA-IL-13 transgenic mice were generated in our laboratory, bred onto a C57BL/6 background, and used in these studies. These mice use the Clara cell 10-kD protein (CC10) promoter and the reverse tetracycline transactivator (rtTA) to target IL-13

(*Received in original form January 28, 2008 and in final form June 10, 2008*)

These studies were funded by NIH Grants HL-56389 (J.A.E.) and HL-084225 (C.G.L.), and by CSL Limited (Australia) (J.A.E.).

Correspondence and requests for reprints should be addressed to Chun Geun Lee, M.D., Ph.D., Section of Pulmonary and Critical Care Medicine, Yale University School of Medicine, 300 Cedar Street (S441 TAC), P.O. Box 208057, New Haven, CT 06520-8057. E-mail: chungeun.lee@yale.edu

This article has an online supplement, which is accessible from this issue's table of contents at www.atsjournals.org

Am J Respir Cell Mol Biol Vol 39. pp 739–746, 2008
Originally Published in Press as DOI: 10.1165/rcmb.2008-0053OC on July 10, 2008
Internet address: www.atsjournals.org

to the lung in a doxycycline-inducible manner. The methods that were used to generate and characterize these mice were described previously (24).

OVA Sensitization and Challenge

OVA sensitization and challenge were accomplished using a modification of the protocols previously described by our laboratory (23). In brief, 6- to 8-wk-old IL-11Rα–null mutant mice and control littermates received injections containing 20 μg of chicken OVA (Sigma, St. Louis, MO) complexed to alum (Resorptar; Indergen, New York, NY), or alum alone. This process was repeated 5 days later. After an additional 7 days, the animals received three aerosol challenges (40 min/d, 3 d) with 1% OVA (wt/vol) in endotoxin-free PBS or PBS alone. The aerosol was generated in an NE-U07 ultrasonic nebulizer (Omron Health Care, Vernon Hills, IL). The mice were killed 24, 48, or 72 hours after aerosol exposure.

Bronchoalveolar Lavage and Lung Inflammation

Lung inflammation was assessed by bronchoalveolar lavage (BAL) as described previously (23). In brief, animals were anesthetized, a median sternotomy was performed, the trachea was dissected free from the underlying soft tissues, and BAL was performed by perfusing the lungs *in situ* with 0.8 ml of PBS and gently aspirating the fluid back. This was repeated twice. The samples were then pooled and centrifuged, and cell numbers and differentials were assessed. The cell-free BAL fluid was stored at −70°C until used.

Histologic Analysis

The lungs were removed *en bloc* as described above, inflated at 25 cm pressure with PBS containing 0.5% low-melting-point agarose gel, fixed in Streck solution (Streck Laboratories, La Vista, NE), embedded in paraffin, sectioned, and stained. Hematoxylin and eosin, and diastase-periodic acid–Schiff (D-PAS) or modified Congo Red stains, were performed in the Research Histology Laboratory of the Department of Pathology at the Yale University School of Medicine. Histologic mucus index was estimated by the D-PAS stains as previously described (25), and tissue infiltration of the eosinophils was evaluated by Congo Red stains.

Fluorescence-Activated Cell Sorter Analysis

Cells from BAL fluids and lungs cell digests were subjected to fluorescence-activated cell sorter (FACS) analysis. BAL was performed as described previously. Whole lung cell suspensions were obtained by a method modified from that of Rice and coworkers (26). In brief, lung tissue was digested using dispase (5 mg/ml; Stem Cell Technologies, Vancouver, BC, Canada), collagenase (0.04%; Sigma-Aldrich, St. Louis, MO), and 100 U/ml DNase I (Sigma-Aldrich). After several centrifugations (10 min, 300–1,000 × *g*) and hemolysis (precooled hemolysis solution containing 11 mM $KHCO_3$, 152 mM NH_4Cl; washing 5 min, 400 × *g* at 4°C), cells were strained through progressively smaller cell strainers (100–20 μm) and nylon gauze and were finally resuspended in FACS buffer (PBS, 2% BSA, 2% FCS) supplemented with 10 U/ml DNase I. Adherent cells were removed and nonadherent cells were then incubated for 30 minutes at room temperature with purified rat anti-mouse CD16/CD32 mAb (1 μg per 10^5 cells; BD Biosciences, San Diego, CA) to prevent nonspecific binding of antibodies to Fc receptors. For intracellular cytokine staining, cells were stimulated with PMA (50 ng/ml)/ionomycin (500 ng/ml) in RPMI 1640 in the presence of Brefeldin A (2 μM; Sigma-Aldrich) for 6 hours before extracellular staining. Afterward, the cells were incubated for 30 minutes at 4°C with specific antibodies for surface marker staining CD4, CD16, CCR3, CD11c, MHCII, CD80, CD86, CD40, CD8, CD54, CD11b, and B220 to characterize specific cell types. For intracellular staining, cells were fixed with 0.5 ml of ice-cold 2% paraformaldehyde, were permeabilized using 0.5% saponin (Sigma-Aldrich), and were stained with anti–IL-4 or the appropriate isotype control to assess nonspecific staining. Cells were analyzed immediately by flow cytometry (FACSCalibur; Becton-Dickinson, Heidelberg, Germany). All antibodies and FACS reagents were from BD Biosciences. Saturating concentrations of the antibodies as determined by titration experiments before the study. Ten thousand cells per sample were analyzed. Isotype controls were subtracted from the respective specific antibody expression, and the results are reported as mean fluorescence intensity (MFI). Calculations were performed with Cell Quest analysis software (Becton-Dickinson). All experiments were performed in triplicate.

Analysis of Mucus and Mucin Gene Expression

To quantitate the levels of Muc5ac, the major airway mucus in the BAL fluids, 0.1 ml of BAL fluid was slot blotted onto nitrocellulose membranes using a Minifold II slot blot apparatus (Schleicher and Schuell, Keene, NH) according to the protocol provided by the manufacturer. After air-drying, the membrane was blocked with 5% skim milk in TTBS (0.1% Tween 20, 20 mM Tris-Cl, 500 mM NaCl) for 2 hours and washed three times with TTBS. The membranes were then incubated overnight at 4°C with a monoclonal antibody against Mucin-5AC (45M1; NeoMarkers, Union City, CA). After washing with TTBS, the membranes were incubated for 1 hour at room temperature with horseradish peroxidase (HRP)-conjugated anti-mouse immunoglobulin (Ig)-G (Pierce, Rockford, IL). Immunoreactive mucins were detected using a chemiluminescent procedure (ECL Plus Western blotting detection system; Amersham Biosciences, Piscataway, NJ) according to instructions from the manufacturer. The relative density was quantitated using an AlphaImager 2000 Image analyzing system (Alpha Innotech, San Leandro, CA). The levels of Muc5ac mRNA were evaluated via real-time RT-PCR using Muc5ac specific primers (25) and a 7500 real-time PCR machine (Applied Biosystems Inc., Foster City, CA).

Generation of IL-11 Specific Antagonist Mutein

To further demonstrate the specific role of IL-11 signaling in our assay system, we generated IL-11 antagonist mutein, which can specifically inhibit the binding of IL-11 to IL-11Rα. The proposed binding sites of the antagonist to inhibit the interaction between IL-11 and IL11-Rα are schematically illustrated in Figure E1A in the online supplement. After screening a number of antagonistic variants from multiple phage libraries, several clones demonstrating the highest affinities were selected through evaluation of binding affinity and dose-dependent kinetics of the antagonist using competition enzyme-linked immunosorbent assay (ELISA) and Ba/F3 cell proliferation assay (Figures E1B–E1D). A clone 1.21 was found to bind with 20-fold higher affinity relative to the established reference of W147A IL-11 (27). After site-specific polyethyleneglycosylation (PEGylation) of this clone to increase its *in vivo* half life, it was produced in a large quantities, shown to be endotoxin free in the Limulus assay, and used to inhibit IL-11 signaling in these studies.

In Vivo Mutein Treatment

To inhibit IL-11 signaling in the OVA aeroallergen model, mice received OVA plus alum as noted above. The mutein (500 μg/mouse/d) was administrated via intraperitoneal injection at the time of the aerosol OVA challenge. In the experiments with the CC10-rtTA-IL-13 transgenic mice, mutein (500 μg/mouse/d) was administered starting 1 day before transgene induction with doxycycline (Dox).

Serum Total IgE and OVA-Specific IgE Measurements

The levels of total and OVA-specific IgE in the serum were measured by ELISA using BD OptEIA kit (BD Biosciences) according to the manufacturer's protocol with modification (28). In brief, 96-well plates were coated with purified anti-mouse IgE mAb (clone R35-72; BD Biosciences) and a purified mouse IgE isotype (27-25; BD Biosciences) was used as a standard. HRP-conjugated anti-mouse IgE (23G3; Southern Biotechnology, Birmingham, AL) (for total IgE) and HRP-labeled anti-biotin (Vector Laboratories, Barlingame, CA) following biotin-labeled OVA (for OVA-specific IgE) (kindly provided by Dr. Lauren Cohn, Pulmonary and Critical Care Medicine, Yale University) were added to the plates as detection enzymes. Pooled sera with known concentrations of IgE (5,000 pg/ml) were also obtained from Dr. Cohn and used as OVA-specific IgE standards. After adding HRP substrate chromogen 3,3′,5,5′-tetramethylbenzidine, the reaction was terminated and detected with an ultraviolet spectrometer.

Cytokine Measurements

The levels of IL-13 and other Th2 cytokines in BAL fluids were evaluated by ELISA using commercial assays (R&D Systems Inc., Minneapolis, MN) as described by the manufacturer.

Statistics

Normally distributed data are expressed as the mean ± SEM and assessed for significance by Student's *t* test or ANOVA as appropriate.

RESULTS

Role of IL-11α in OVA-Induced Inflammation

To address the importance of IL-11 signaling in Th2 inflammation, we compared the OVA-induced tissue and BAL inflammatory responses in WT and IL-11Rα–null mutant (IL-11Rα$^{-/-}$) mice. In the WT mice, OVA sensitization and challenge caused an increase in BAL cellularity and a comparable increase in tissue inflammatory cell accumulation (Figure 1A and data not shown). In both compartments, increases in eosinophils and macrophages were readily appreciated (Figure 1A and data not shown). Comparable levels of BAL and tissue inflammation were not seen in animals that were not sensitized before aeroallergen challenge or that received systemic sensitization and nebulized saline (data not shown). When similar experiments were undertaken in IL-11Rα $^{-/-}$ mice, an impressive decrease in BAL and tissue cellularity was noted (Figure 1 and data not shown). In these experiments, the recovery of eosinophils and macrophages was reduced at all time points (24, 48, and 72 h) after aerosol Ag exposure (Figure 1 and data not shown). The difference between the OVA-induced inflammation in WT and IL-11$^{-/-}$ mice was particularly impressive 48 hours and 72 hours after Ag exposure. At these time points, total cell, eosinophil, and macrophage recoveries were reduced to levels that were comparable to those in control mice that did not receive OVA challenge (Figures 1B and 1C). When viewed in combination, these studies demonstrate that endogenous IL-11 signaling is essential for BAL and tissue inflammation and eosinophila after aeroallergen challenge.

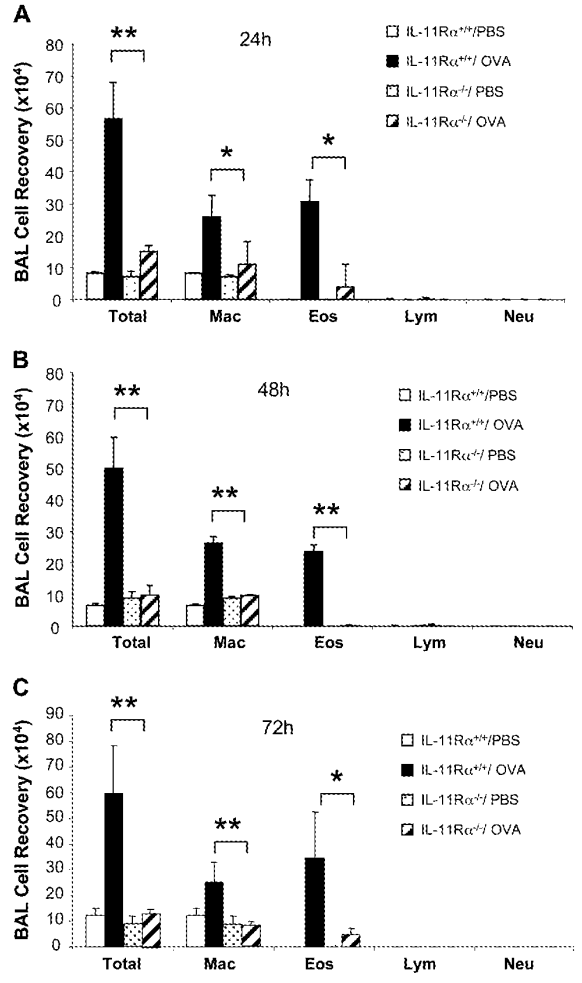

Figure 1. Differential counts of bronchoalveolar lavage (BAL) cells from wild-type (WT) and IL-11Rα–null mutant mice (IL-11Rα$^{-/-}$) after ovalbumin (OVA) sensitization and challenge. BAL was performed at (*A*) 24-hour, (*B*) 48-hour, and (*C*) 72-hour intervals after the last OVA challenge. Values represent the mean ± SEM of a minimum of five animals at each time point. Total, total cell number; Mac, macrophages; Eos, eosinophilis; Lym, lymphocytes; Neu, neutrophils. *$P < 0.05$; **$P < 0.01$.

Role of IL-11α in OVA-Induced Airway Mucus and Mucin Gene Epression

Mucus metaplasia is a characteristic feature of asthma that is also seen at sites of Th2 inflammation in the murine airway. To define the role(s) of IL-11 signaling in this response, we compared the D-PAS staining, levels of Muc5ac mRNA, and levels of Muc5ac in the airways of appropriately sensitized WT and IL-11Rα$^{-/-}$ mice. PAS+ cells were not found or were extremely rare in the airways of WT mice that received a saline aerosol challenge. In contrast, PAS+ cells were readily appreciated after aeroallergen challenge of sensitized WT mice (Figure 2A). The goblet cell hyperplasia in these sensitized and challenged WT mice was also associated with an increase in the levels of Muc5ac in the BAL fluid and the levels of mRNA encoding Muc5ac (Figures 2B and 2C). Each of these responses appeared to involve the IL-11 pathway because, in the absence of IL-11Rα, the frequency of PAS+ cells in the airway was significantly decreased and the levels of BAL Muc5ac and Muc5ac mRNA were impressively decreased (Figure 2).

Role of IL-11α in Aeroallergen Sensitization

Because IL-11 signaling played a critical role in OVA-induced inflammation and mucus metaplasia, studies were next undertaken to determine if it also contributed to antigen sensitization. This was accomplished by comparing the levels of total and antigen-specific IgE in WT and IL-11Rα$^{-/-}$ mice after treatment with OVA plus alum. In these experiments significant increases in the levels of total and antigen-specific IgE were seen in WT mice (Figure 3). In contrast, both of these responses were significantly decreased in mice that were deficient in IL-11Rα$^{-/-}$ (Figure 3). These studies demonstrate that endogenous IL-11 signaling is essential for the optimal aeroallergen-induced sensitization.

Role of IL-11Rα on OVA-Induced Th2 Cytokine Expression

Studies were next undertaken to define the role(s) of IL-11Rα signaling in OVA-induced Th2 cytokine production. IL-4, IL-5, and IL-13 protein and mRNA were not readily detected in the BAL fluids and lung mRNA preparations, respectively, from WT mice that were not challenged with OVA. In contrast, IL-4, IL-5, and IL-13 mRNA and protein were readily detected in the BAL fluids and lungs from WT mice that were sensitized and challenged with OVA (Figure 4 and data not shown). Importantly, in the absence of IL-11Rα, the levels of BAL IL-13 and IL-13 mRNA were significantly decreased (Figure 4 and data not shown). Similar decreases in IL-4 and IL-5 mRNA and protein were also appreciated in sensitized and challenged IL-11Rα–deficient animals (data not shown). These data demonstrate that IL-11Rα plays a critical role in OVA-induced Th2 cytokine induction.

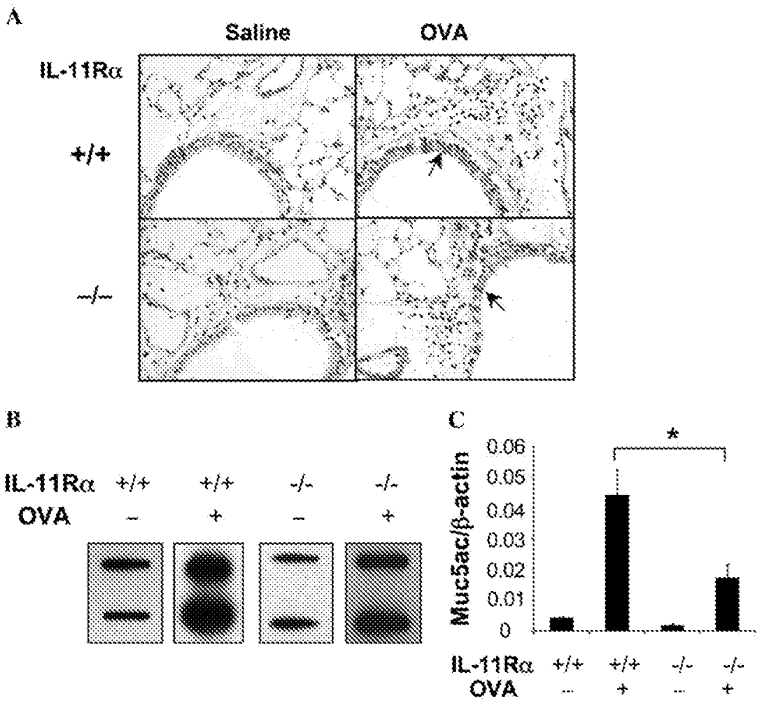

Figure 2. Role of IL-11Rα in the regulation of OVA-induced airway mucus, mucin gene expression. WT (IL-11Rα$^{+/+}$) and IL-11Rα$^{-/-}$ mice were OVA sensitized, challenged, and killed 24 hours after challenge. (*A*) D-PAS stains (×20 original magnification). (*B*) Slot and immunoblotting with Muc5ac antibody. (*C*) Real-time RT-PCR on muc5ac gene. The *solid arrows* in *A* highlight the *pink-stained airway mucus*. *A* and *B* are illustrative of a minimum of three similar experiments. The values in C represent the mean ± SEM of evaluations in a minimum of five animals (*$P < 0.05$).

Effects of Mutein on OVA-Induced Th2 Inflammation

The studies noted above demonstrate that IL-11 signaling plays a critical role in antigen sensitization, Th2 inflammation, mucus metaplasia, and Th2 cytokine elaboration. The alterations that are seen in the absence of IL-11Rα could be entirely due to the defect in sensitization. Alternatively, they could be due to defects in sensitization and defects in Th2 effector responses. To differentiate among these options, we characterized the ability of the IL-11 mutein to alter Th2 responses in OVA-sensitized and -challenged WT mice. This was done by administering the mutein or its polyethylene glycol (PEG) control at the time of OVA aerosol challenge. In these experiments, OVA sensitization and challenge increased total BAL cell recovery by 5- to 6-fold in mice that received the PEG control. In contrast, BAL cell recovery was significantly decreased in mice that received the IL-11 mutein (Figure 5A). In accord with our studies with the IL-11 Rα$^{-/-}$ mice, eosinophil recovery was significantly decreased in the mutein-treated animals (Figure 5A). FACS analysis of the BAL cells further demonstrated that OVA-induced Th2 cell (CD4+IL-4+), dendritic cell (CD11C+ MHCII+), and eosinophil (CCR3+CD16+) numbers were significantly reduced in the mutein treated versus the PEG control–treated animals (Figure 5B). Interestingly, OVA-induced dendritic cell activation (CD86 expression) was also significantly reduced in the mutein-treated mice compared with vehicle-treated mice (Figure 5C).

Effects of Mutein on OVA-Induced IL-13 and Mucin Gene Expression

We next compared the IL-13 production and mucin gene expression in OVA-sensitized WT mice treated with PEG vehicle control or the IL-11 mutein. As noted above, OVA sensitization and challenge increased BAL IL-13 mRNA accumulation, the levels of BAL IL-13, and the levels of Muc5ac mRNA accumulation in the PEG control–treated animals (Figure 6). In all cases, these responses were significantly decreased in mice treated with the IL-11 mutein (Figure 6).

Effects of Mutein on IL-13–Induced Tissue Phenotypes

To gain insight into the mechanism(s) by which the IL-11 mutein could alter OVA-induced Th2 responses, we tested the hypothesis that IL-11 signaling contributes to the pathogenesis of IL-13–induced tissue alterations. This was done by comparing the tissue responses in CC10-rtTA-IL-13 transgenic mice treated with the

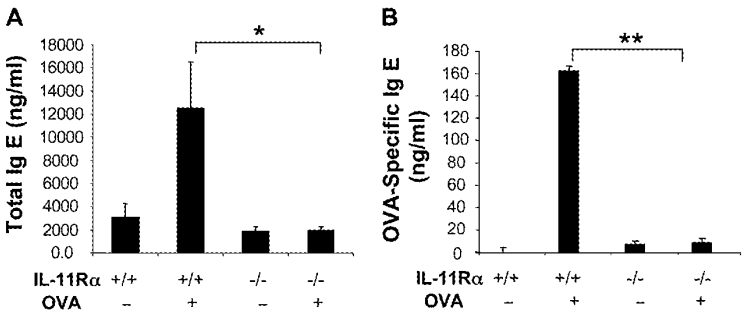

Figure 3. Role of IL-11Rα in the regulation of OVA-induced IgE production. WT (IL-11Rα$^{+/+}$) and IL-11Rα$^{-/-}$ mice were sensitized, challenged, and killed 24 hours after challenge. (*A*) Total and (*B*) OVA-specific IgE levels in sera were evaluated using enzyme-linked immunosorbent assay (ELISA). Values represent the mean ± SEM of minimum of five animals at each time point (*$P < 0.05$; **$P < 0.01$).

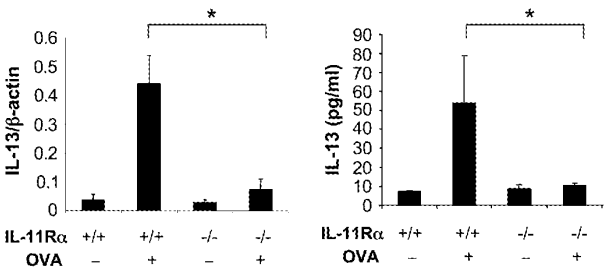

Figure 4. Role of IL-11Rα in the regulation of OVA-induced IL-13. WT (IL-11Rα$^{+/+}$) and IL-11Rα$^{-/-}$ mice were OVA sensitized, challenged, and killed 24 hours after challenge. The expression levels of BAL IL-13 were measured by ELISA. The values represent the mean ± SEM of evaluations in a minimum of five animals (*$P < 0.05$).

PEG vehicle control or the IL-11 mutein. In keeping with our prior studies, transgenic IL-13 caused an eosinophilic inflammatory response, goblet cell hyperplasia, and enhanced mucin gene expression (4) (Figure 7). Importantly, comparisons of transgenic mice treated with the PEG vehicle control and the IL-11 mutein demonstrated that each of these responses was decreased in the mutein-treated animals (Figure 7). These studies demonstrate that IL-11 signaling plays an important role in the pathogenesis of IL-13 effector responses in the murine lung.

DISCUSSION

IL-11 was originally discovered as an IL-6–like molecule that stimulated the proliferation of IL-6–dependent plasmacytoid cells (29). Subsequent studies have focused largely on the effects of exogenously administered rIL-11 and its role as a potential therapeutic agent. These studies demonstrated that IL-11 is an important regulator of platelet accumulation (30, 31) and that it confers cytoprotection, inhibits inflammation, and diminishes cell death (32, 33) at sites of mucosal and tissue injury. As a result of these investigations, rIL-11 has been approved as a therapeutic agent to treat thrombocytopenia (34, 35). It has also received significant attention as an agent that can be a prophylaxis against toxin-induced tissue injury (12, 36) and that can control pathologic inflammatory disorders (9, 37). In contrast, the roles of endogenous IL-11 have not been as extensively investigated. Because IL-11 is known to be overexpressed at sites of Th2 inflammation (22, 38), we used genetically modified mice and developed a soluble mutein that antagonizes IL-11-IL-11Rα binding to characterize the roles of physiologic IL-11R signaling in the pathogenesis of these responses. These studies demonstrate that IL-11 signaling plays a critical role in allergen-induced sensitization, dendritic cell accumulation, and activation and IgE production. They also demonstrated that this IL-11 pathway plays a critical role in the pathogenesis of Th2 inflammation, Th2 cytokine elaboration, and mucus metaplasia. These studies suggest that interventions

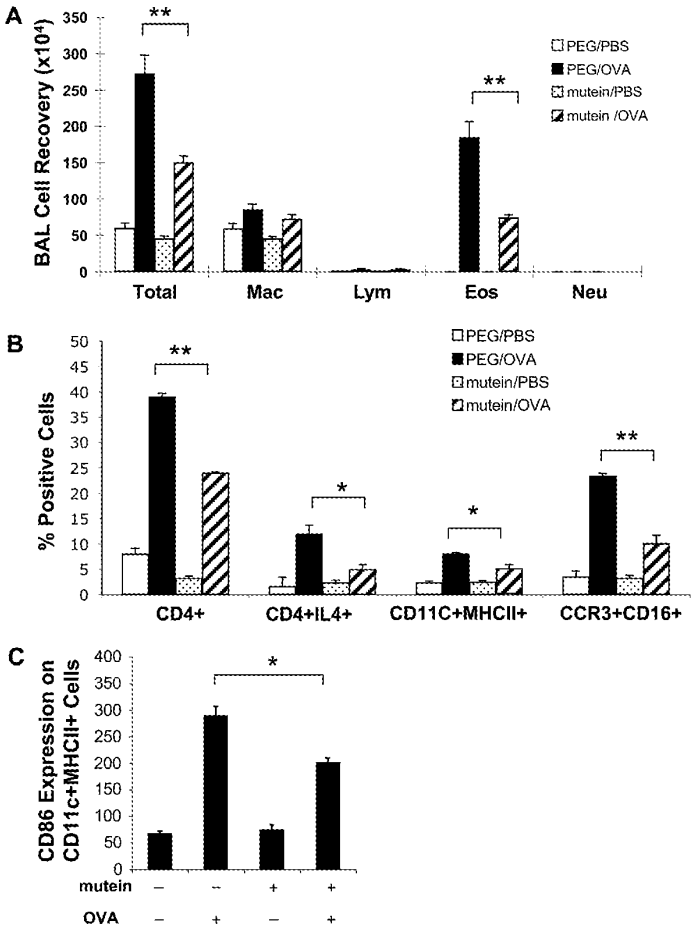

Figure 5. Effect of mutein in the regulation of OVA-induced BAL inflammation. C57 BL/6 mice were OVA sensitized, challenged, and killed 24 hours after challenge. At the time of OVA challenge, mutein (500 μg/mouse/d) or vehicle (PEG) were administrated via intraperitoneal injection. Differential count on BAL cells was illustrated (*A*) and further cellular characterization on BAL cells were performed by FACS analysis (*B* and C). The values represent the mean ± SEM of evaluations in a minimum of five animals (*$P < 0.05$; **$P < 0.01$).

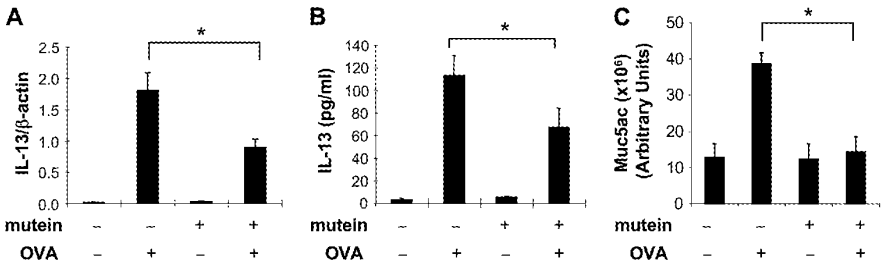

Figure 6. Effect of mutein in the regulation of OVA-induced IL-13 and muc5ac expression. C57 BL/6 mice were OVA sensitized, challenged, and killed 24 hours after challenge. At the time of OVA challenge, mutein (500 μg/mouse/d) or vehicle (PEG) were administrated via intraperitoneal injection. The expression of IL-13 mRNA and protein was evaluated by real-time RT-PCR and ELISA, respectively (*A* and *B*). (*C*) The Muc5ac levels in BAL were quantitated by densitometry after slot and immunoblotting with Muc5ac antibody. The values represent the mean ± SEM of evaluations in a minimum of five animals (*$P < 0.05$).

that control IL-11 signaling can play a useful role in the regulation of disorders characterized by excessive Th2 inflammation and tissue remodeling responses.

Airway inflammation and remodeling are characteristic features of the exaggerated Th2 responses seen in asthma and mechanistically related disorders (3, 39). A number of lines of investigation have demonstrated that IL-11 expression is characteristic of these responses. This includes studies demonstrating that exaggerated levels of IL-11 mRNA can be found in biopsies from individuals with asthma, where they correlate with disease severity and reductions in FEV_1 (21). It also includes murine investigations which demonstrated that IL-11 is induced during antigen-stimulated Th2 responses via a leukotriene-dependent mechanism (38); that IL-11 signaling plays an important role in the pathogenesis of IL-13–induced tissue inflammation, fibrotic, and mucus responses (22); and that the transgenic overexpression of IL-11 induces asthma-like T and B cell–rich inflammation, airway fibrosis, myofibroblast accumulation, and physiologic dysregulation (20). Our present studies add to our understanding of the biology of IL-11 and the role that it plays in Th2 responses by demonstrating, for the first time, that endogenous IL-11 contributes to antigen-induced Th2 sensitization, inflammation, and tissue remodeling and that administration of an IL-11 antagonist can ameliorate these effects. These studies suggest that IL-11 plays a key role in the pathogenic Th2 responses that are seen in diseases like asthma. However, it is important to point out that this may actually be only part of the effector profile of IL-11 in this setting. A number of studies have demonstrated that IL-11 also has potent anti-inflammatory effects, including the ability to inhibit nuclear factor-κB activation (36) and induce the production of the TNF-α antagonist, soluble TNF-α Receptor 1 (40). In keeping with these inhibitory properties, previous studies from our laboratory demonstrated that exogenous IL-11 can also inhibit antigen-induced Th2 inflammation and endothelial VCAM-1 expression (23). When these bodies of investigation are viewed in combination, it is clear that IL-11 has complex, context-specific effects on Th2 inflammation with the endogenous product mediating proinflammatory and remodeling effects, while the exogenous administration of high concentrations of this cytokine activates compensatory pathways that are designed to provide feedback to and control the responses. In many ways, these properties of IL-11 are analogous to findings with transforming growth factor (TGF)-β_1 and IL-6, which have similar bi-directional modulatory effects (41–44) This is an intriguing analogy because IL-6 and IL-11 are closely related members of the IL-6–type cytokine gene family (44), and studies from our laboratory and others have demon-

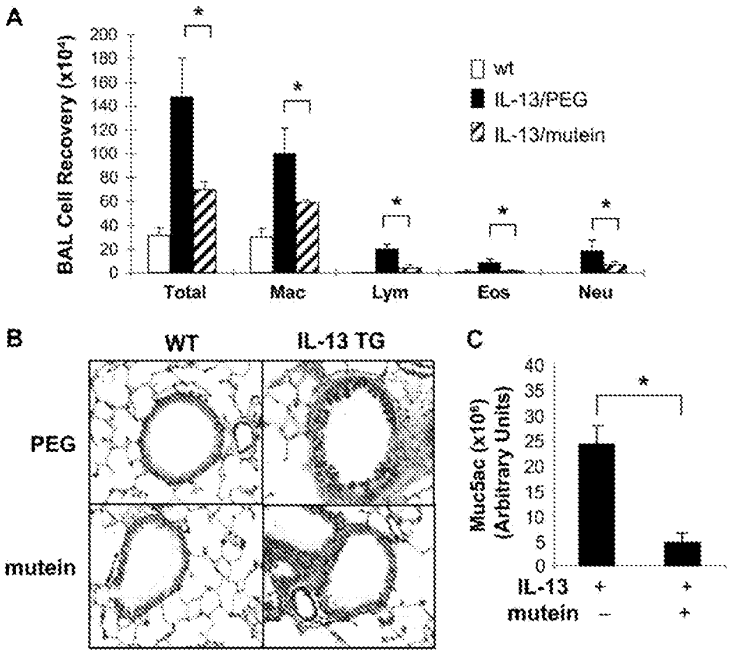

Figure 7. Effect of mutein in the regulation of IL-13–induced BAL inflammation and mucus elaboration. Mutein (500 μg/mouse/d, intraperitoneally) or vehicle (PEG) were daily administrated to the inducible IL-13 transgenic mice (CC10-rtTA-IL-13) from a day before transgene induction by Doxycycline (Dox). After 2 weeks of Dox induction, mice were killed and (*A*) differential count on BAL cells, (*B*) airway mucus evaluation by D-PAS stains (×20 original magnification), and (C) Muc5ac protein expression quantitated by densitometry after slot and immunoblotting with Muc5ac antibody were illustrated. Values in *A* and *C* represent the mean ± SEM of evaluations in a minimum of five animals. *B* is a representative of a minimum of three similar evaluations (*$P < 0.05$).

strated that IL-11 is potently induced by TGF-β_1 in a variety of cells and tissues (10, 17, 45, 46).

Patients with asthma can experience bronchorrhea, and their biopsies are characterized by goblet cell hyperplasia and mucus accumulation (47). This mucus response is nicely modeled in the antigen-sensitized and -challenged murine lung, and has been the topic of significant investigation. These studies have demonstrated that a number of pathways contribute to airway mucus metaplasia, including the elaboration of Th2 cytokines such as IL-13 and the activation of the epidermal growth factor receptor (EGFR) (48–50). Our studies demonstrate that IL-11 signaling also contributes to this important airway response because OVA- and IL-13–induced mucus metaplasia were significantly decreased in IL-11Rα–null mice and mice treated with the IL-11 mutein. This inhibition could be due to the important role that IL-11 signaling plays in the production of IL-13. It is important to point out, however, that direct IL-11–induced regulatory effects cannot be ruled out because the related cytokine IL-6 has been shown to have strong mucus-inducing capacity in primary tracheobronchial epithelial cells (51). Additional investigation will be required to differentiate among these mechanistic options.

IL-13 is a product of a gene on chromosome 5 at q31. Although it was initially felt to be an IL-4–like molecule, it is now known to be a powerful stimulator of eosinophilic inflammation, tissue fibrosis, mucus metaplasia, alveolar remodeling, and airways hyperresponsiveness. It is also known to be dysregulated in, and to potentially contribute to, the pathogenesis of a variety of disorders, including asthma, idiopathic pulmonary fibrosis, scleroderma, viral pneumonia, hepatic fibrosis, nodular sclerosing Hodgkin's disease, and chronic obstructive pulmonary disease (3, 7, 52–56). Previous studies from our laboratory demonstrated that IL-13–induced inflammatory and mucus responses are diminished in IL-11Rα–null mice (22). The present studies add to our understanding of the role of IL-11 in this setting by demonstrating the decreased tissue effects of IL-13 in mice with a normal IL-11 receptor complex by treatment with the IL-11 mutein. This observation demonstrates that interventions which abrogate IL-11-IL-11Rα binding can be used to control the tissue effects of IL-13 in the lung and potentially other organs. However, the mechanism underlying mutein regulation of IL-13–induced inflammation and mucus response still remains to be determined. No significant changes in the STAT (STAT1, STAT3, STAT6) phosphoryaltion or acidic mammalian chitinase (AMCase) expression between the IL-13 transgenic mice with and without mutein treatment were detected in the additional mechanistic studies (N.-Y. Chen and C. G. Lee, unpublished observation). STAT6 is well known to mediate IL-13 signaling, and AMCase plays an critical role in Th2- or IL-13–induced inflammation (8). IL-11 was also known to confer protective effects on epithelial and inflammatory cells via induction of antiapoptotic molecules such as A1(*bfl*1) or survivin (57, 58), and apoptosis is an important mechanism in the resolution of inflammation and maintenance of homeostasis of airway epithelial cells (50, 59). Thus, it is intriguing to speculate that the inhibition of IL-11 signaling by mutein enhances apoptosis of these cells, resulting in fewer inflammatory cells and mucus-producing epithelial cells. To define the exact underlying regulatory mechanism of endogenous IL-11 signaling in allergic inflammation and mucus response, further comprehensive *in vitro* and *in vivo* mechanistic studies are warranted.

In summary, these studies demonstrate that endogenous IL-11 signaling plays an important role in the pathogenesis of Th2 antigen sensitization and the pathogenesis of Th2-induced and IL-13–induced inflammatory and remodeling responses. This establishes the IL-11-IL-11Rα pathway as a worthwhile site for investigations designed to identify therapeutic agents that can be used to treat Th2- and IL-13–mediated disorders.

Conflict of Interest Statement: A.D.N. is an employee of CSL limited. F.M.D. is an employee of CSL limited. P.D.S. is an employee of CSL limited. L.J.F. is an employee of CSL limited. M.B. was an employee of Zenyth Therapeutics Ltd before its acquisition by CSL. None of the other authors has a financial relationship with a commercial entity that has an interest in the subject of this manuscript.

Acknowledgments: The authors thank Kathleen Bertier for excellent secretarial and administrative assistance.

References

1. Bousquet J, Jeffery PK, Busse WW, Johnson M, Vignola AM. Asthma: from bronchoconstriction to airways inflammation and remodeling. *Am J Respir Crit Care Med* 2000;161:1720–1745.
2. Robinson DS, Hamid Q, Ying S, Tsicopoulos A, Barkans J, Bentley AM, Corrigan C, Durham SR, Kay AB. Predominant TH2-like bronchoalveolar T-lymphocyte population in atopic asthma. *N Engl J Med* 1992;326:298–304.
3. Elias JA, Lee CG, Zheng T, Ma B, Homer RJ, Zhu Z. New insights into the pathogenesis of asthma. *J Clin Invest* 2003;111:291–297.
4. Zhu Z, Homer RJ, Wang Z, Chen Q, Geba GP, Wang J, Zhang Y, Elias JA. Pulmonary expression of interleukin-13 causes inflammation, mucus hypersecretion, subepithelial fibrosis, physiologic abnormalities, and eotaxin production. *J Clin Invest* 1999;103:779–788.
5. Steinke JW, Borish L. Th2 cytokines and asthma. Interleukin-4: its role in the pathogenesis of asthma, and targeting it for asthma treatment with interleukin-4 receptor antagonists. *Respir Res* 2001;2:66–70.
6. Wills-Karp M. Interleukin-13 in asthma pathogenesis. *Immunol Rev* 2004;202:175–190.
7. Corry DB, Kheradmand F. Biology and therapeutic potential of the interleukin-4/interleukin-13 signaling pathway in asthma. *Am J Respir Med* 2002;1:185–193.
8. Zhu Z, Zheng T, Homer RJ, Kim YK, Chen NY, Cohn L, Hamid Q, Elias JA. Acidic mammalian chitinase in asthmatic Th2 inflammation and IL-13 pathway activation. *Science* 2004;304:1678–1682.
9. Trepicchio WL, Bozza M, Pedneault G, Dorner AJ. Recombinant human IL-11 attenuates the inflammatory response through down-regulation of proinflammatory cytokine release and nitric oxide production. *J Immunol* 1996;157:3627–3634.
10. Zheng T, Zhu Z, Wang J, Homer RJ, Elias JA. IL-11: insights in asthma from overexpression transgenic modeling. *J Allergy Clin Immunol* 2001;108:489–496.
11. Du XX, Williams DA. Interleukin-11: a multifunctional growth factor derived from the hematopoietic microenvironment. *Blood* 1994;83:2023–2030.
12. Du X, Williams DA. Interleukin-11: review of molecular, cell biology, and clinical use. *Blood* 1997;89:3897–3908.
13. Waxman AB, Einarsson O, Seres T, Knickelbein RG, Warshaw JB, Johnston R, Homer RJ, Elias JA. Targeted lung expression of interleukin-11 enhances murine tolerance of 100% oxygen and diminishes hyperoxia-induced DNA fragmentation. *J Clin Invest* 1998;101:1970–1982.
14. Van der Meeren A, Mouthon MA, Vandamme M, Squiban C, Aigueperse J. Combinations of cytokines promote survival of mice and limit acute radiation damage in concert with amelioration of vascular damage. *Radiat Res* 2004;161:549–559.
15. Orazi A, Du X, Yang Z, Kashai M, Williams DA. Interleukin-11 prevents apoptosis and accelerates recovery of small intestinal mucosa in mice treated with combined chemotherapy and radiation. *Lab Invest* 1996;75:33–42.
16. Einarsson O, Geba GP, Zhu Z, Landry M, Elias JA. Interleukin-11: stimulation *in vivo* and *in vitro* by respiratory viruses and induction of airways hyperresponsiveness. *J Clin Invest* 1996;97:915–924.
17. Elias JA, Zheng T, Whiting NL, Trow TK, Merrill WW, Zitnik R, Ray P, Alderman EM. IL-1 and transforming growth factor-beta regulation of fibroblast-derived IL-11. *J Immunol* 1994;152:2421–2429.
18. Zheng T, Nathanson MH, Elias JA. Histamine augments cytokine-stimulated IL-11 production by human lung fibroblasts. *J Immunol* 1994;153:4742–4752.
19. Ray P, Tang W, Wang P, Homer R, Kuhn C III, Flavell RA, Elias JA. Regulated overexpression of interleukin 11 in the lung: use to dissociate development-dependent and -independent phenotypes. *J Clin Invest* 1997;100:2501–2511.
20. Tang W, Geba GP, Zheng T, Ray P, Homer RJ, Kuhn C III, Flavell RA, Elias JA. Targeted expression of IL-11 in the murine airway causes

lymphocytic inflammation, bronchial remodeling, and airways obstruction. *J Clin Invest* 1996;98:2845–2853.
21. Minshall E, Chakir J, Laviolette M, Molet S, Zhu Z, Olivenstein R, Elias JA, Hamid Q. IL-11 expression is increased in severe asthma: association with epithelial cells and eosinophils. *J Allergy Clin Immunol* 2000; 105:232–238.
22. Chen Q, Rabach L, Noble P, Zheng T, Lee CG, Homer RJ, Elias JA. IL-11 receptor alpha in the pathogenesis of IL-13-induced inflammation and remodeling. *J Immunol* 2005;174:2305–2313.
23. Wang J, Homer RJ, Hong L, Cohn L, Lee CG, Jung S, Elias JA. IL-11 selectively inhibits aeroallergen-induced pulmonary eosinophilia and Th2 cytokine production. *J Immunol* 2000;165:2222–2231.
24. Zheng T, Zhu Z, Wang Z, Homer RJ, Ma B, Riese RJ Jr, Chapman HA Jr, Shapiro SD, Elias JA. Inducible targeting of IL-13 to the adult lung causes matrix metalloproteinase- and cathepsin-dependent emphysema. *J Clin Invest* 2000;106:1081–1093.
25. Lee CG, Homer RJ, Cohn L, Link H, Jung S, Craft JE, Graham BS, Johnson TR, Elias JA. Transgenic overexpression of interleukin (IL)-10 in the lung causes mucus metaplasia, tissue inflammation, and airway remodeling via IL-13-dependent and -independent pathways. *J Biol Chem* 2002;277:35466–35474.
26. Rice WR, Conkright JJ, Na CL, Ikegami M, Shannon JM, Weaver TE. Maintenance of the mouse type II cell phenotype in vitro. *Am J Physiol Lung Cell Mol Physiol* 2002;283:L256–L264.
27. Underhill-Day N, McGovern LA, Karpovich N, Mardon HJ, Barton VA, Heath JK. Functional characterization of W147A: a high-affinity interleukin-11 antagonist. *Endocrinology* 2003;144:3406–3414.
28. Kweon MN, Yamamoto M, Kajiki M, Takahashi I, Kiyono H. Systemically derived large intestinal CD4(+) Th2 cells play a central role in STAT6-mediated allergic diarrhea. *J Clin Invest* 2000;106:199–206.
29. Paul SR, Bennett F, Calvetti JA, Kelleher K, Wood CR, O'Hara RM Jr, Leary AC, Sibley B, Clark SC, Williams DA, *et al.* Molecular cloning of a cDNA encoding interleukin 11, a stromal cell-derived lymphopoietic and hematopoietic cytokine. *Proc Natl Acad Sci USA* 1990;87: 7512–7516.
30. Kaye JA. FDA licensure of NEUMEGA to prevent severe chemotherapy-induced thrombocytopenia. *Stem Cells* 1998;16:207–223.
31. Valent P. Use of interleukin-11 to stimulate platelet production in myelodysplastic syndromes. *Leuk Lymphoma* 2006;47:1999–2001.
32. Uemura T, Nakayama T, Kusaba T, Yakata Y, Yamazumi K, Matsuu-Matsuyama M, Shichijo K, Sekine I. The protective effect of interleukin-11 on the cell death induced by X-ray irradiation in cultured intestinal epithelial cell. *J Radiat Res (Tokyo)* 2007;48:171–177.
33. Kimura R, Maeda M, Arita A, Oshima Y, Obana M, Ito T, Yamamoto Y, Mohri T, Kishimoto T, Kawase I, *et al.* Identification of cardiac myocytes as the target of interleukin 11, a cardioprotective cytokine. *Cytokine* 2007;38:107–115.
34. Ciurea SO, Hoffman R. Cytokines for the treatment of thrombocytopenia. *Semin Hematol* 2007;44:166–182.
35. Bhatia M, Davenport V, Cairo MS. The role of interleukin-11 to prevent chemotherapy-induced thrombocytopenia in patients with solid tumors, lymphoma, acute myeloid leukemia and bone marrow failure syndromes. *Leuk Lymphoma* 2007;48:9–15.
36. Kawakami T, Takahashi T, Shimizu H, Nakahira K, Takeuchi M, Katayama H, Yokoyama M, Morita K, Akagi R, Sassa S. Highly liver-specific heme oxygenase-1 induction by interleukin-11 prevents carbon tetrachloride-induced hepatotoxicity. *Int J Mol Med* 2006;18: 537–546.
37. Opal SM, Keith JC Jr, Jhung J, Palardy JE, Parejo N, Marchese E, Maganti V. Orally administered recombinant human interleukin-11 is protective in experimental neutropenic sepsis. *J Infect Dis* 2003;187: 70–76.
38. Lee KS, Kim SR, Park HS, Park SJ, Min KH, Lee KY, Jin SM, Lee YC. Cysteinyl leukotriene upregulates IL-11 expression in allergic airway disease of mice. *J Allergy Clin Immunol* 2007;119:141–149.
39. Jeffery PK. Comparative morphology of the airways in asthma and chronic obstructive pulmonary disease. *Am J Respir Crit Care Med* 1994;150:S6–S13.
40. Ellis M, Hedstrom U, Frampton C, Alizadeh H, Kristensen J, Shammas FV, al-Ramadi BK. Modulation of the systemic inflammatory response by recombinant human interleukin-11: a prospective randomized placebo controlled clinical study in patients with hematological malignancy. *Clin Immunol* 2006;120:129–137.
41. Lee CG, Cho SJ, Kang MJ, Chapoval SP, Lee PJ, Noble PW, Yehualaeshet T, Lu B, Flavell RA, Milbrandt J, *et al.* Early growth response gene 1-mediated apoptosis is essential for transforming growth factor beta1-induced pulmonary fibrosis. *J Exp Med* 2004;200:377–389.
42. Letterio JJ, Roberts AB. Regulation of immune responses by TGF-beta. *Annu Rev Immunol* 1998;16:137–161.
43. Wahl SM, Swisher J, McCartney-Francis N, Chen W. TGF-beta: the perpetrator of immune suppression by regulatory T cells and suicidal T cells. *J Leukoc Biol* 2004;76:15–24.
44. Heinrich PC, Behrmann I, Haan S, Hermanns HM, Muller-Newen G, Schaper F. Principles of interleukin (IL)-6-type cytokine signalling and its regulation. *Biochem J* 2003;374:1–20.
45. Elias JA, Zheng T, Einarsson O, Landry M, Trow T, Rebert N, Panuska J. Epithelial interleukin-11. Regulation by cytokines, respiratory syncytial virus, and retinoic acid. *J Biol Chem* 1994;269:22261–22268.
46. Elias JA, Wu Y, Zheng T, Panettieri R. Cytokine- and virus-stimulated airway smooth muscle cells produce IL-11 and other IL-6-type cytokines. *Am J Physiol* 1997;273:L648–L655.
47. Rubin BK. The pharmacologic approach to airway clearance: mucoactive agents. *Respir Care* 2002;47:818–822.
48. Rose MC, Voynow JA. Respiratory tract mucin genes and mucin glycoproteins in health and disease. *Physiol Rev* 2006;86:245–278.
49. Voynow JA, Gendler SJ, Rose MC. Regulation of mucin genes in chronic inflammatory airway diseases. *Am J Respir Cell Mol Biol* 2006;34:661–665.
50. Cohn L. Mucus in chronic airway diseases: sorting out the sticky details. *J Clin Invest* 2006;116:306–308.
51. Chen Y, Thai P, Zhao YH, Ho YS, DeSouza MM, Wu R. Stimulation of airway mucin gene expression by interleukin (IL)-17 through IL-6 paracrine/autocrine loop. *J Biol Chem* 2003;278:17036–17043.
52. Belperio JA, Dy M, Burdick MD, Xue YY, Li K, Elias JA, Keane MP. Interaction of IL-13 and C10 in the pathogenesis of bleomycin-induced pulmonary fibrosis. *Am J Respir Cell Mol Biol* 2002;27:419–427.
53. Hancock A, Armstrong L, Gama R, Millar A. Production of interleukin 13 by alveolar macrophages from normal and fibrotic lung. *Am J Respir Cell Mol Biol* 1998;18:60–65.
54. Hasegawa M, Fujimoto M, Kikuchi K, Takehara K. Elevated serum levels of interleukin 4 (IL-4), IL-10, and IL-13 in patients with systemic sclerosis. *J Rheumatol* 1997;24:328–332.
55. van der Pouw Kraan TC, Kucukaycan M, Bakker AM, Baggen JM, van der Zee JS, Dentener MA, Wouters EF, Verweij CL. Chronic obstructive pulmonary disease is associated with the -1055 IL-13 promoter polymorphism. *Genes Immun* 2002;3:436–439.
56. Ohshima K, Akaiwa M, Umeshita R, Suzumiya J, Izuhara K, Kikuchi M. Interleukin-13 and interleukin-13 receptor in Hodgkin's disease: possible autocrine mechanism and involvement in fibrosis. *Histopathology* 2001;38:368–375.
57. He CH, Waxman AB, Lee CG, Link H, Rabach ME, Ma B, Chen Q, Zhu Z, Zhong M, Nakayama K, *et al.* Bcl-2-related protein A1 is an endogenous and cytokine-stimulated mediator of cytoprotection in hyperoxic acute lung injury. *J Clin Invest* 2005;115:1039–1048.
58. Mahboubi K, Li F, Plescia J, Kirkiles-Smith NC, Mesri M, Du Y, Carroll JM, Elias JA, Altieri DC, Pober JS. Interleukin-11 up-regulates survivin expression in endothelial cells through a signal transducer and activator of transcription-3 pathway. *Lab Invest* 2001;81:327–334.
59. Henson PM, Tuder RM. Apoptosis in the lung: induction, clearance and detection. *Am J Physiol Lung Cell Mol Physiol* 2008;294:L601–L611.

Online Data Supplement

Endogenous IL-11 Signaling Is Essential in Th2- and IL-13-Induced Inflammation and Mucus Production

Chun Geun Lee, M.D., Ph.D., Dominik Hartl, M.D., Ph.D., Hiroshi Matsuura, M. Sci. Felicity M. Dunlop, Ph.D., Pierre D. Scotney, Ph.D., Louis J. Fabri, Ph.D., Andrew D. Nash, Ph.D., Ning-Yuan Chen, Ph.D., Chu-Yan Tang, B. Sci., Qingsheng Chen, M.D., Robert J. Homer, M.D., Ph.D., Manuel Baca, Ph.D., Jack A. Elias, M.D.

Online Supplemental Figure E1

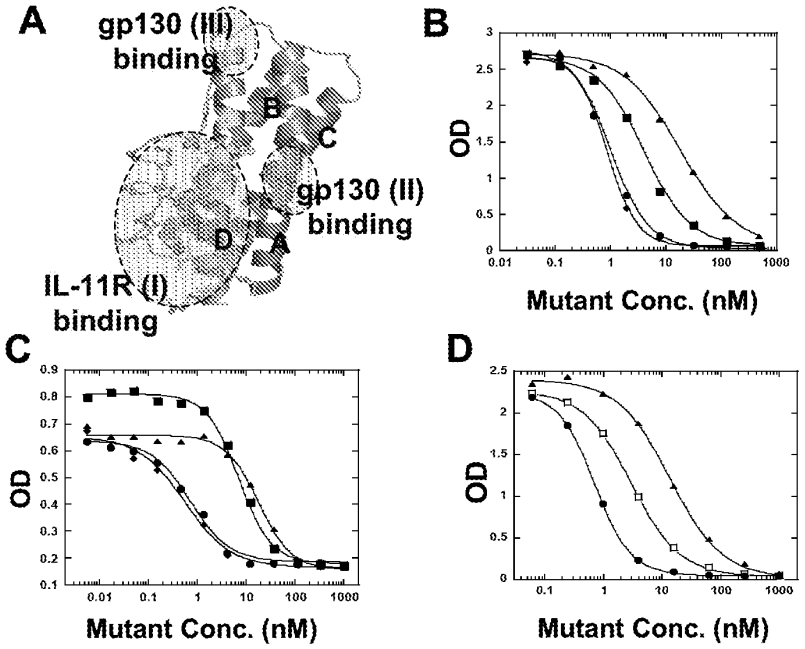

Figure E1. ***A***, a model of IL-11 generated using the Swiss model server by homology modelling on the structure of IL-6 (A). The IL-11 receptor interfaces are shaded and labelled with the gp130 (site II and site III) and IL-11Rα (site I) receptor interfaces. 4 libraries were generated: library 1 (purple) targeting residues 58-62, library 2 (pink) targeting residues 63-67 generated on a clone optimised for residues 58-62, library 3 (green) targeting residues 158, 161, 162, 165, 166 and library 4 (tan) targeting residues 172, 173, 175, 176, 177. Arginine residue R169 (red) was not randomized due to its critical role in IL-11Rα binding. ***B***, Representative clones from libraries 1, 2 and 3 were expressed as soluble protein and tested in a competition ELISA for comparison with unoptimised mIL-11 with only the W147A change (▲, EC_{50} = 18 nM), Clone 1.21-W147A was 20-fold improved (●, 58-62 = PAIDY, EC_{50} = 0.86 nM), Clone 3.5A-W147A (■) was 5-fold improved (155-168 = DGLETTLDF, EC_{50} = 3.6 nM), and Clone 2.4-W147A (♦) was 20-fold improved to similar level of clone 1.21 (58-67 = PAIDYVLNED, EC_{50} = 0.84 nM). ***C***, Representative clones from libraries 1, 2 and 3 were expressed as soluble protein and tested as antagonists in the IL-11 responsive cell line for comparison with unoptimised mIL-11 with only the W147A change (▲, EC_{50} = 19 nM), Clone 1.21-W147A was 22-fold improved (●, 58-62 = PAIDY, EC_{50} = 0.84 nM), Clone 3.5A-W147A (■) was 2-fold improved (155-168 = DGLETTLDF, EC_{50} = 8.2nM), and Clone 2.4-W147A (♦) was 30-fold improved and similar to clone 1.21 (58-67 = PAIDYVLNED, EC_{50} = 0.6 nM). ***D***, The antagonist activity of PEGylated mIL-11-W147A -Clone 1.21 (□, EC_{50} = 3.0 nM) was compared with mIL-11-W147A (▲, EC_{50} = 13 nM) and W147A-Clone 1.21 (●, EC_{50} = 0.71 nM) in the IL-11 responsive cell line.

Rapid publication

IL-11 expression is increased in severe asthma: Association with epithelial cells and eosinophils

Eleanor Minshall, PhD,[a] Jamila Chakir, PhD,[b] Michel Laviolette, MD,[b] Sophie Molet, PhD,[a] Zhou Zhu, MD,[c] Ron Olivenstein, MD,[d] Jack A. Elias, MD,[c] and Qutayba Hamid, MD, PhD[a] *Montreal and Sainte Foy, Quebec, Canada, and New Haven, Connecticut*

Background: IL-11 is a pleiotropic cytokine produced by a variety of stromal cells. Targeted overexpression of this cytokine in mice results in a remodeling of the airways and the development of airway hyperresponsiveness and airway obstruction.

Objectives: Because these alterations mimic important pathologic and physiologic changes in the airways of some asthmatic patients, we investigated the expression of IL-11 messenger RNA (mRNA) within the airways of patients with mild to severe asthma and nonasthmatic control subjects.

Methods: Fiberoptic bronchoscopy to obtain bronchial biopsy specimens was performed on patients with mild (n = 13), moderate (n = 10), and severe (n = 9) asthma and on nonasthmatic control subjects (n = 9).

Results: These patients differed in their extent of airway fibrosis with types I and III collagens being noted in greater quantities in the biopsy specimens from the severe and moderate asthmatics than in those from controls ($P < .05$). IL-11 mRNA expression was observed in the epithelial and subepithelial layers of asthmatic and nonasthmatic control subjects. The number of cells within the epithelium and subepithelium expressing IL-11 mRNA was greater in those with moderate and severe asthma compared with mild asthma and nonasthmatic subjects ($P < .001$). There were also greater numbers of IL-11 mRNA-positive cells within the subepithelium in severe compared with moderate asthma ($P < .001$). Immunostaining for IL-11 within the airway tissues confirmed translation of the mRNA into IL-11–immunoreactive protein in airway epithelial cells. Colocalization of IL-11 mRNA and immunoreactivity with resident inflammatory cells demonstrated that this cytokine was also expressed by major basic protein–positive eosinophils.

Conclusion: These results suggest that IL-11 is involved in the chronic remodeling seen in asthmatic airways and is associated with increasing severity of the disease. (J Allergy Clin Immunol 2000;105:232-8.)

Key words: *Severe asthma, IL-11, airway remodeling, airways inflammation, collagen deposition*

The pathologic features of asthma are associated with airway remodeling as a consequence of hypertrophy/hyperplasia of the airway smooth muscles and of subepithelial fibrosis.[1,2] The latter response is most prominent in the lamina reticularis and results from interstitial collagen, fibronectin, and proteoglycan deposition.[3,4] Although initially described in postmortem studies, these structural alterations can be observed even in mild and newly diagnosed cases of asthma.[3,5] Because any thickening of the airway wall will profoundly increase the maximal degree of airway narrowing caused by airway smooth muscle contraction, it has been proposed that architectural changes similar to those observed in asthmatic patients contribute to the development of chronic airway hyperresponsiveness and the progressive deterioration in lung function over time.[6] To date, many studies have focused on the mechanisms underlying the acute presentations of bronchial asthma. In contrast, the factors responsible for the more chronic structural changes within the airway are poorly defined. Although myofibroblasts are recognized as the cell type responsible for subepithelial collagen deposition in these individuals,[7] the mechanisms contributing to the onset of airway fibrosis in asthma and the role of inflammatory cells, in particular eosinophils and epithelial cells, remains to be established.

IL-11 was originally described as a soluble factor derived from stromal cells, which was capable of stimulating plasmacytoma cell proliferation.[8] It is a member of the IL-6 family of cytokines that share a common receptor β-subunit gp130 molecule.[9] To date, IL-11 has been ascribed a variety of functions including the ability to regulate hematopoiesis, bone metabolism, and epithelial proliferation.[10] Consistent with this pleiotropic nature, IL-11 is produced by various cell types such as stromal cells, fibroblasts, osteoblasts, endothelial cells, and epithelial cells.[8,11-14] Studies from our own laboratories suggest that IL-11 may contribute to the structural airway remodeling and alteration in immune functioning evident

From the [a]Meakins-Christie Laboratories, McGill University, Montreal, [b]Laval Hospital, Sainte Foy, the [c]Montreal Chest Research Institute, Montreal, and the [d]Section of Pulmonary and Critical Care Medicine, Department of Internal Medicine, Yale University School of Medicine, New Haven, Conn.

E.M. and J. C. contributed equally to this work.

Supported by the Medical Research Council of Canada and Astra Pharm, Canada. E. M. is a recipient of a Foulkes Foundation Fellowship. J. M. is the recipient of an FRSQ scholarship.

Received for publication Nov 1, 1999; revised Nov 22, 1999; accepted for publication Nov 22, 1999.

Reprint requests: Qutayba Hamid, MD, PhD, Meakins-Christie Laboratories, McGill University, 3626 St Urbain, Montreal, PQ H2X 2P2, Canada.

0091-6749/2000 $12.00 + 0 **1/1/104572**

Abbreviations used
ICC: Immunocytochemistry
ISH: In situ hybridization
MBP: Major basic protein
mRNA: Messenger RNA
TGF-β: Transforming growth factor-β

in asthmatic subjects. Thus we have demonstrated that IL-11 is produced by human lung fibroblasts and alveolar and airway epithelial cell lines in response to cytokines,[11,14,15] histamine,[16] eosinophil-derived major basic protein (MBP),[17] and respiratory viruses.[15] We have also reported that overexpression of IL-11 within the lungs results in subepithelial fibrosis[18,19] and promotes the accumulation of myocytes and myofibroblasts.[19] Moreover, the functional sequelae of chronic IL-11 expression recapitulate aspects of the abnormal pulmonary physiologic features observed in severe asthma, including the development of airway hyperresponsiveness and baseline airway obstruction.[15,19]

Given these actions of IL-11, we hypothesized that the expression of IL-11 was increased within the airways of asthmatics and that it would be particularly associated with the most severely remodeled individuals. Our aim was therefore to investigate the expression of IL-11 in a range of asthmatic patients with mild to severe disease with use of in situ hybridization (ISH) and to colocalize IL-11 to inflammatory cell types within the airways. These results showed a significantly increased expression of IL-11 messenger RNA (mRNA) within the airways of subjects with severe asthma compared with those with mild asthma and with nonasthmatic control subjects. The IL-11 mRNA expression within the lungs of asthmatic individuals was observed primarily within airway epithelial cells and MBP-positive eosinophils.

METHODS

Subjects studied

To study the expression of IL-11 mRNA in a range of asthmatic subjects, we recruited 32 individuals with mild to severe asthma from the asthma clinic at the Laval Hospital (Sainte Foy) and 9 control subjects from the asthma clinic at the Montreal Chest Hospital (Montreal). Asthmatic severity was defined on the basis of prebronchodilator-measured FEV_1 values, with mildly asthmatic subjects (n = 13) having an FEV_1 value greater than 80% predicted, moderately asthmatic subjects (n = 10) having FEV_1 values between 60% and 80% predicted, and severely asthmatic subjects (n = 9) having FEV_1 values <60% predicted. FEV_1 represented the accepted level of control with therapy. In moderate asthma the mean FEV_1 improved >30% after β_2-agonist administration and further in some subjects with oral prednisone, whereas in severe asthma FEV_1 was less than the historic maximum in some subjects. All patients fulfilled the American Thoracic Society criteria for asthma,[20] had typical clinical symptoms, documented airways reversibility (>15% improvement in FEV_1), and increased airway responsiveness to methacholine (<8 mg/mL) performed only if FEV_1 >70%. On enrollment, the medical history of each patient was taken and a physical examination was performed. None of the subjects had a history of respiratory tract infection within the previous 6 weeks or immunotherapy within the previous 12 months. All subjects were atopic on the basis of positive skin wheals (>3 mm) to one or more of 13 common allergens and were currently nonsmokers (2 and 4 ex-smokers in the moderate and severe asthma groups, respectively).

Seven subjects with severe asthma required the regular use of oral corticosteroids (mean 42 ± 7.7 mg) to maintain acceptable control of symptoms and 2 used inhaled steroids only. In addition, those with severe asthma used inhaled β_2-agonists and theophyline as necessary. Those with moderate asthma had their symptoms controlled by regular use of β_2-agonists and inhaled corticosteroids (mean 1177 ± 225 μg beclomethasone dipropionate equivalent). Three patients also required the regular use of oral corticosteroids. Those with mild asthma used inhaled β_2-agonists only. Nonsmoker nonatopic control subjects volunteered to participate in the study and none had taken corticosteroids in the year preceding the study. Informed consent, approved by the Montreal Chest Research Institute and Laval Hospital Ethics Review Committees, was obtained from all patients before entry into this study.

Fiberoptic bronchoscopy and tissue processing

The technique of fiberoptic bronchoscopy and the methods for processing of bronchial biopsy specimens have been described elsewhere in detail.[21]

Probe preparation

A digoxigenin-labeled complementary RNA probe coding for IL-11 mRNA was prepared from complementary DNA as described previously.[22] In brief, complementary DNA was inserted into PGEM vectors, linearized, and transcribed in vitro in the presence of digoxigenin-11-uridine triphosphate and either SP6 or T7 polymerases. Antisense (complementary to mRNA) and sense probes (identical to mRNA) were prepared.

ISH

Sections of lung tissue were processed for ISH for IL-11 mRNA according to Ying et al.[22] Briefly, after permeabilization with Triton X-100, the tissue sections were then briefly washed in PBS and immersed in a proteinase K solution for 20 minutes at 37°C. The samples were subsequently fixed in 4% paraformaldehyde, washed, and air dried. Hybridization was carried out with use of the hybridization mixture containing the appropriate sense or antisense. Each section was then covered and incubated overnight at 40°C in a humid chamber. Posthybridization, involving a series of high stringency washes of the samples in decreasing concentrations of saline–sodium citrate buffer at 42°C, was then performed. To remove any unbound RNA probes, the samples were washed with ribonuclease solution for 20 minutes at 42°C. The hybridization signal was visualized by incubating the sections for 4 hours with sheep polyclonal antidigoxigenin antibodies (1:1000) conjugated with alkaline phosphatase. Color development was achieved by adding the freshly prepared substrate (X-phosphate-5-bromo-4-chloro-3-indolyl phosphate and nitroblue tetrazolium). Once the reaction was completed, the tissue sections were counterstained with hematoxylin, mounted with a coverslip, and examined under a graduated microscope for positive signals.

Immunocytochemistry

Immunostaining for IL-11 immunoreactivity within the tissues to confirm translation of the IL-11 mRNA was performed with use of the avidin-biotin peroxidase complex method as previously described.[23] Tissue sections (5 μm) from the asthmatic and nonasthmatic subjects were incubated overnight at 4°C with the primary goat antihuman IL-11 antibody (AB-218-NA, R&D Systems, Minneapolis, Minn) or with the primary rabbit antihuman type I or type III collagen antibodies

(Biodesign, Pasadena, Calif). According to the manufacturer's specifications, the IL-11 antibody exhibits no cross-reactivity with other cytokines tested, including IL-6 and leukemia inhibitory factor in direct ELISA. As a control, sections were processed in the absence of the primary antibody with an isotype-matched IgG.

Combined immunocytochemistry and ISH

To ascertain the expression of IL-11 mRNA by eosinophils, we simultaneously applied radiolabeled ISH for IL-11 mRNA with MBP immunoreactivity as previously described in detail elsewhere.[24]

Sequential immunostaining

Double sequential immunostaining for IL-11 immunoreactivity protein and MBP immunoreactivity was performed to localize the protein products of the IL-11 mRNA to eosinophils. The method for sequential immunostaining has been previously published.[25]

Quantification

Slides were coded and positive cells were counted blindly with use of ×100 magnification. Cells with positive signal in the subepithelium were counted and the results were expressed as the mean number of positive cells per square millimeter of submucosa. IL-11 mRNA-positive cells within the epithelium were counted by optical analysis and expressed as a semiquantitative score on the basis of the percentage of the epithelium demonstrating positive signal/total epithelium (0: no staining; 1: less than 12.5%; 2: 12.5%-25%; 3: 25%-37.5%; 4: 37.5%-50%; 5: 50%-62.5%; 6: 62.5%-75%; 7: 75%-87.5%; 8: 87.5%-100%). The within-observer coefficient of variation for repeated measures was less than 5%. The extent of collagen staining in the subepithelium was measured with an image analysis system. The thickness of the collagen layer was taken below the basement membrane and these data are expressed as the mean of 3 measurements.

Statistical analysis

Normality and variance assumptions were tested. The numbers of cells expressing IL-11 mRNA in normal and asthmatic airways were compared with the nonparametric Kruskal-Wallis test. Statistically significant differences between groups were subsequently analyzed with a Mann-Whitney *U* test (Systat version 7.0, SPSS, Chicago, Ill). Correlation coefficients were calculated from Pearson's moment coefficient and were corrected for multiple comparisons by the use of Bonferroni's correction factor. Results were considered statistically significant for P values <.05.

RESULTS

IL-11 expression within the airways

IL-11 mRNA expression was visualized as dark purple staining of individual cells and was seen in the airway submucosa and epithelial cell layer of asthmatic patients and nonasthmatic controls (Fig 1, *A* and *B*, respectively). No positive signals for IL-11 mRNA were observed when the sense probe was used or when the tissue sections were treated with ribonuclease before hybridization of the antisense probe. To confirm transcription of the mRNA for IL-11, the presence of specific immunoreactivity for this cytokine within the tissue sections was confirmed with use of polyclonal antihuman IL-11 antibody. The presence of specific brown staining after the immunocytochemistry (ICC) within the airways of asthmatic patients and nonasthmatic control subjects was indicative of IL-11 immunoreactive protein (Fig 1, *C*). This staining was not observed when the isotype-matched control antibody was used (Fig 1, *D*).

Expression of IL-11 mRNA in mild, moderate, and severe asthma

To further define the potential role of IL-11 in the pathophysiologic mechanisms of asthma, we compared the expression of IL-11 mRNA in nonasthmatic and asthmatic subjects with varying degrees of airway obstruction and fibrosis (Fig 2, *A* and *B*). Within the subepithelial cell layer, the numbers of cells expressing IL-11 mRNA were significantly greater in moderate (10.8 ± 1.5 cells per mm^2 of submucosal tissue) and severe asthma (21.1 ± 2.0 cells per mm^2 of submucosal tissue) compared with mild asthma (2.9 ± 0.7 cells per mm^2 of submucosal tissue) and nonasthmatic control subjects (1.3 ± 0.5 cells per mm^2 of submucosal tissue, $P < .001$). Within the subepithelium, there were also significantly greater numbers of IL-11 mRNA-positive cells in severe asthma compared with moderate asthma ($P < .001$).

In the epithelial cell layer there was an increase in the epithelial score for IL-11 mRNA expression for those with moderate (2.2 ± 0.3) and severe (2.8 ± 0.2) asthma compared with those with mild asthma (0.5 ± 0.2) and the nonasthmatic control subjects (0.2 ± 0.1, $P < .001$). There were no significant differences between the moderate and severe asthmatics in their expression of IL-11 mRNA within the epithelium.

Colocalization of IL-11 mRNA expression

The studies noted above clearly demonstrate that IL-11 is expressed at the mRNA level by cells having eosinophil-like morphologic features within the airway subepithelium. To confirm the identity of these cells, both combined ISH and ICC and double-sequential ICC were used (Fig 1, *E*). In the subepithelium of patients with moderate and severe asthma IL-11 mRNA was mostly colocalized to MBP-positive eosinophils (mean ± SEM, 61% ± 9%, n = 6).

Correlation of IL-11 mRNA expression with an index of lung physiology features

To gain insight into the potential effector functions of IL-11, we compared index values of IL-11 production and airway physiologic features (FEV_1). There were significant inverse correlations between the numbers of cells expressing IL-11 mRNA within the epithelium (Fig 3, *B*, $r^2 = 0.55$) and subepithelium (Fig 3, *A*,, $r^2 = 0.75$) and the FEV_1 values for the group of asthmatic subjects ($P < .05$).

Characterization of extent of remodeling

As noted above, the severity of asthma was initially assessed on the basis of pulmonary function parameters. To see whether this correlated with the extent of airway remodeling or airway fibrosis, the expression of types I and III collagens was assessed in the biopsy specimens from the healthy and asthmatic subjects. The presence of specific collagen immunoreactivity was visualized as brown staining beneath the lamina reticularis after the ICC reaction (Fig 1, *F*). Fig 4 demonstrates the relationship between asthma severity and

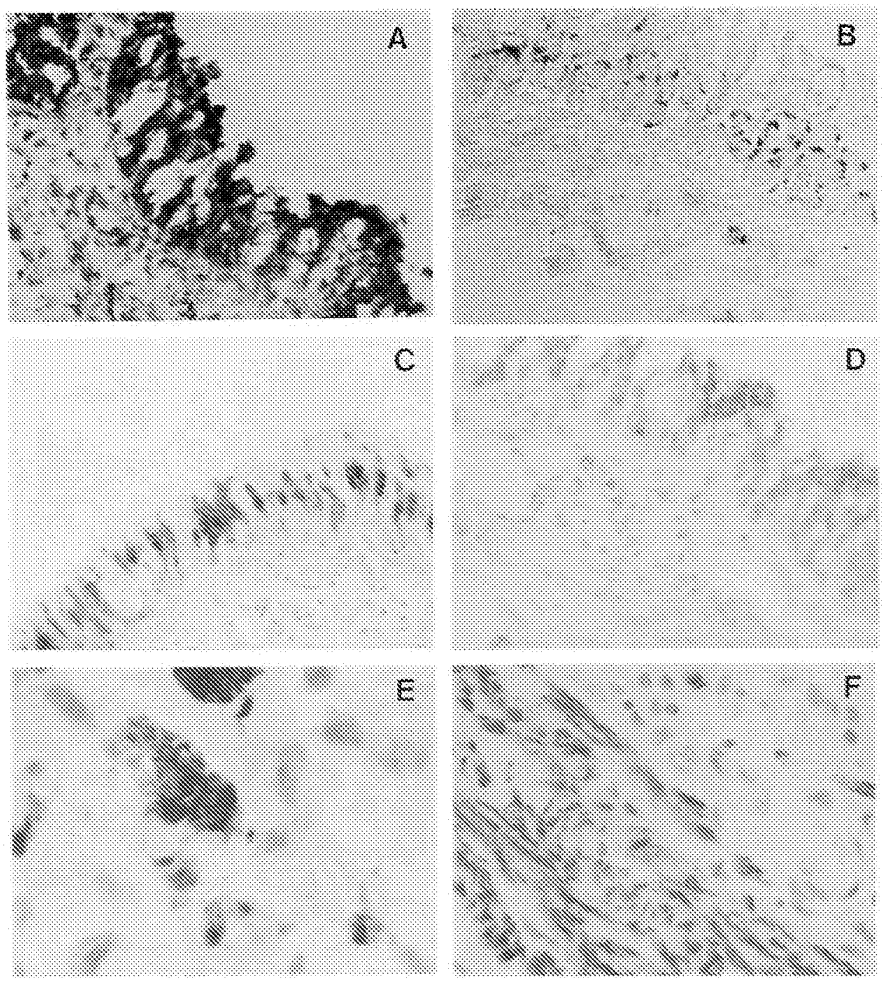

FIG 1. ISH with digoxigenin for IL-11 mRNA in bronchial biopsy specimens from **(A)** patient with severe asthma and **(B)** nonasthmatic control subject. Note presence of dark brown/purple staining indicative of IL-11 mRNA within airways epithelium and associated with individual cells in subepithelium. **C,** Immunostaining for IL-11 in individual with severe asthma. **D,** Primary antibody isotype control for IL-11 immunoreactivity. **E,** Colocalization of IL-11 immunoreactivity and eosinophil specific marker (MBP) in individual with severe asthma. IL-11 immunoreactivity is shown as brown coloration that localizes to MBP-positive cells *(red staining).* **F,** Collagen (type III) immunoreactivity, as determined by avidin-biotin peroxidase method, in individual with severe asthma is shown as brown staining.

collagen immunoreactivity. It shows that for both type I and type III collagen there is increasing expression with the severity of the disorder. There was a significantly greater staining for collagen type III in severe and moderate asthma compared to mild asthma and healthy subjects ($P < .05$). The extent of type I collagen immunoreactivity was also greater in severe asthma compared with the mildly asthmatic and healthy subjects ($P < .05$) and in moderate asthma compared with healthy control subjects ($P < .05$).

Relationships between IL-11 expression and the extent of collagen staining

Correlational analyses were performed between the expression of IL-11 in epithelium, in subepithelium, and the expression of type I and III collagens for all the subjects (nonasthmatics, mild, moderate, and severe asthmatics) included in the study. No significant correlation was found between any of these parameters.

DISCUSSION

Previous studies in mice have demonstrated the capacity of IL-11 to recapitulate many of the features observed in chronic obstructive airway diseases such as severe asthma. To investigate the contribution of this cytokine to the structural alterations evident in a range of asthmatic individuals, we examined the expression of IL-11 mRNA and immunoreactivity and its association with

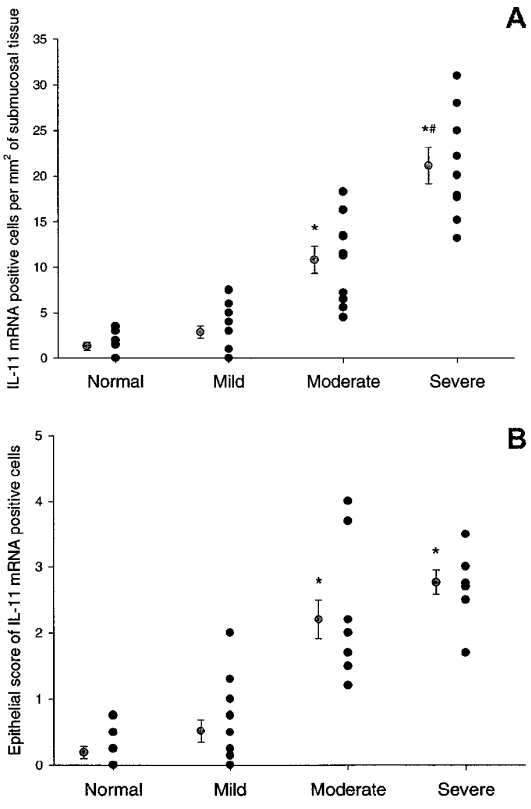

FIG 2. IL-11 mRNA expression within **(A)** subepithelium and **(B)** epithelial cell layer of subjects with mild, moderate, and severe asthma and of nonasthmatic control subjects. There was significant increase in numbers of cells expressing IL-11 mRNA in moderate (n = 10) and severe (n = 9) asthma compared with mild asthma (n = 13) and nonasthmatic control subjects (n = 9, *asterisk*, $P < .001$ compared with controls and mild asthmatics). Within submucosa, patients with severe asthma had significantly increased numbers of IL-11 mRNA-positive cells compared with those with moderate asthma (*pound sign*, $P < .05$).

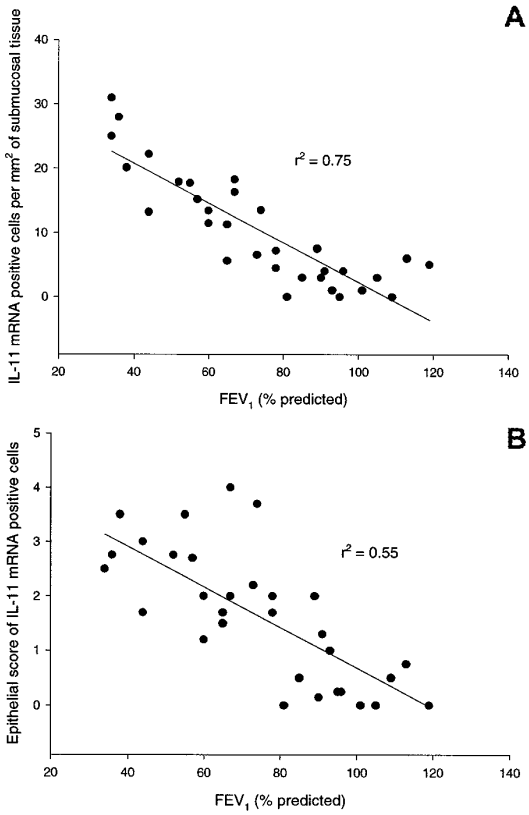

FIG 3. Correlational relationships between percent predicted FEV_1 values and numbers of cells expressing IL-11 mRNA within **(A)** subepithelium and **(B)** epithelial cell layer. There were significant correlations between numbers of IL-11 mRNA-positive cells in both airway epithelium and subepithelial regions and this index of pulmonary function ($P < .05$).

inflammatory cells with use of a combination of ISH and ICC techniques. In addition, we investigated the expression of collagen types I and III within the airways of our asthmatic and healthy individuals. Our results documented the increased numbers of cells expressing IL-11 within the airways of moderate and severe asthmatics and localized the majority of this expression to epithelial cells and to MBP-positive eosinophils. IL-11 expression was directly associated with disease severity but inversely correlated with FEV_1 measurements, suggesting that IL-11 expression is associated with abnormal lung physiologic features. Immunoreactivity for collagen types I and III expression were increased within the airways of our asthmatic subjects, and this was related to the severity of the disorder, as based on FEV_1 values.

IL-11 is a cytokine with potent immunomodulatory properties and the ability to induce substantial remodeling of the airways; however, there was little evidence concerning the importance of IL-11 in human disorders. Therefore the increased numbers of cells expressing IL-11 in moderate and severe asthma is an original finding that suggests that this cytokine may contribute to the sequelae of inflammatory events and structural modifications characterizing these asthmatic individuals. Although prior reports have shown IL-11 immunoreactivity in nasal aspirates from children with viral upper respiratory tract infections, particularly those who exhibited wheezing,[15] our study is the first demonstration that inflammatory and structural cells express striking amounts of IL-11 in vivo in a human disease. It is also the first report showing the expression of IL-11 in normal human epithelial cells in vivo because previous studies have used alveolar and bronchial epithelial cell lines.[14,15]

The mechanisms whereby IL-11 exerts its activity in the airways are complex. IL-11 has previously been shown to have fibrogenic potential in an animal model in eliciting subepithelial fibrosis and the local accumulation of fibroblasts, myofibroblasts, and smooth muscle cells.[18,19] Interestingly, IL-11 enhances the accumulation of collagen type III (and to a lesser extent type I), which

is a profile of expression similar to that observed in the airways of asthmatic subjects.[19] However, in our in vivo study we have not been able to show any correlation between IL-11 expression in bronchial biopsy specimens and types I or III collagens, although tissue fibrosis correlates with the disease severity. These results might be explained by the fact that subepithelial fibrosis and particularly collagen deposition is a progressive phenomenon, so we cannot exclude the fact that a correlation between IL-11 and collagens may be found if bronchial biopsies were done at another stage of the disease. To date, there is a scarcity of literature documenting the mechanisms responsible for the fibrotic response. IL-11 is known, however, to stimulate the production of tissue inhibitor of metalloproteinase-1, which leads to a decrease in collagen degradation.[26] The resultant collagen accumulation may be responsible for the tissue fibrosis observed in our moderately and severely asthmatic subjects, although the presence of alternative mechanisms cannot be ruled out.

In addition to its fibrogenic nature, IL-11 possesses several immunoregulatory functions that are pertinent to the pathophysiologic mechanisms of bronchial asthma, notably its ability to down-regulate IL-12 production by peritoneal and alveolar macrophages[27,28] and to polarize T-cell responses toward T_H2-type cytokine production.[29] Indeed, IL-11 may act to perpetuate the profile of T_H2-type cytokine expression seen within the lungs of asthmatic subjects and further studies addressing this action of IL-11 are warranted. However, IL-11 also has potent anti-inflammatory properties and prevents the nuclear translocation of nuclear factor-κB, inhibiting the induction of genes dependent on this transcription factor.[30] Whether IL-11 exerts predominantly proinflammatory or anti-inflammatory actions within the airways remains to be elucidated.

Regardless of the mechanism of action of IL-11, our data showed this cytokine to be particularly associated with the airways of moderate and severe asthmatics and that both in the epithelium and subepithelium the numbers of cells expressing IL-11 mRNA were inversely correlated to the FEV_1 values of the subjects. This suggests that the release of IL-11 from epithelium and subepithelium tissues may contribute both to the development of airway fibrosis and the subsequent decline in lung function.

Our colocalization data showed the presence of IL-11 mRNA within MBP-positive eosinophils. Previous data from our laboratories have demonstrated the presence of transforming growth factor-β_1 (TGF-β_1) within the asthmatic airways, which also localized to eosinophils.[31] TGF-β_1 is a potent stimulator of IL-11 protein production, mRNA accumulation, and gene transcription in human fibroblasts, alveolar and bronchial epithelial-like cells, and smooth muscle cells.[11,14,16,32] Therefore it is possible that TGF-β_1 also exerts an autocrine-paracrine action and might be a stimulant for eosinophil IL-11 production within asthmatic airways. Regardless of whether such a pathway exists, eosinophil-derived MBP has been previously shown to participate in the production of IL-11 by lung fibroblasts.[17] The finding of IL-11 expression by eosinophils gives further evidence to support the involvement of these cells in the development of structural remodeling of the airways in asthma. In addition, the demonstration that, like TGF-β_1,[31] IL-11 expression correlates to asthma severity has important implications for biology and for disease pathogenesis. This observation raises the possibility that some of the biologic effects attributed to TGF-β_1, especially the fibrogenic response, are in fact mediated by IL-11. Neutralization in vitro or in vivo studies with anti-IL-11 and anti-TGF-β_1 antibodies will need to be performed to determine whether any effects of TGF-β_1 are mediated through the induction of IL-11 and vice versa. Because the expression of both IL-11 and TGF-β_1 seem to be closely associated, it would be of interest to compare them in the same asthmatic specimens to determine whether there is concomitant expression.

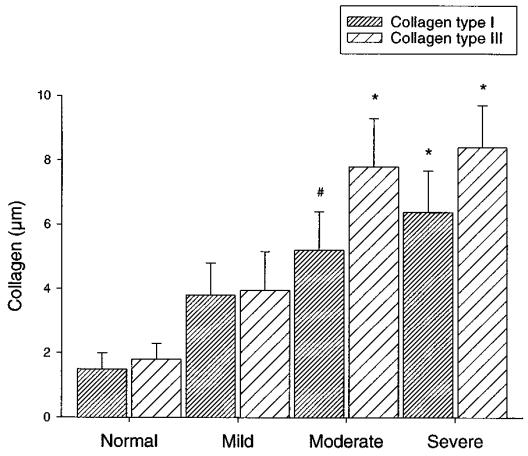

FIG 4. Immunoreactivity for collagens type I and type III in bronchial biopsy specimens from patients with mild, moderate, and severe asthma compared with nonasthmatic control subjects. There was a significant increase in collagen types I and III immunoreactivity in the airways of moderate (n = 10) and severe (n = 9) asthmatics compared with mild asthmatics (n = 13) and nonasthmatic control subjects (n = 9). *Asterisk*, $P < .05$ compared with control subjects and those with mild asthma, except for type I collagen where increase in collagen immunoreactivity in moderate asthma was only significant in comparison to healthy control subjects; *pound sign*, $P < .05$.

In keeping with the close association of IL-11 with IL-6, it is interesting to note that our colocalization of IL-11 to eosinophils is consistent with the production of IL-6 by these cells[24] and the recent intracellular localization of this cytokine to the matrix of the crystalloid granule.[33] IL-6 has also been implicated in the pathogenesis of asthma and is also produced by epithelial cells.[34]

In summary, we have shown increased numbers of cells expressing IL-11 mRNA within the bronchial mucosa and airway epithelial cells of severely asthmatic subjects. Within the subepithelial cell layer this cytokine mRNA was colocalized to MBP-positive eosinophils. The pathophysiologic features of moderate and severe asthma involve the up-regulated expression of IL-11 mRNA, and

therapeutic strategies aimed at regulating the expression of IL-11 may be of use in the treatment of asthma.

The thank Ms Lisa Cameron and Dr Rame Taha for their contributions in the preparation of this manuscript. Special thanks also go to Ms Elsa Schotman for technical assistance.

REFERENCES

1. Dunnill MS. The pathology of asthma, with special reference to changes in the bronchial mucosa. J Clin Pathol 1960;13:27-33.
2. Jeffery PK. Comparative morphology of the airways in asthma and chronic obstructive pulmonary disease. Am J Respir Crit Care Med 1994;150:S6-13.
3. Roche WR, Beasley R, Williams JH, Holgate ST. Subepithelial fibrosis in the bronchi of asthmatics. Lancet 1989;1:520-4.
4. Huang J, Olivenstein R, Taha R, Hamid QA, Ludwig M. Enhanced proteoglycan deposition in the airway wall of atopic asthmatics. Am J Respir Crit Care Med 1999;160:725-9.
5. Jeffery PK, Wardlaw AJ, Nelson FC, Collins JV, Kay AB. Bronchial biopsies in asthma: an ultrastructural, quantitative study and correlation with hyperreactivity. Am Rev Respir Dis 1989;140:1745-53.
6. James AL, Paré PD, Hogg JC. The mechanics of airway narrowing in asthma. Am Rev Respir Dis 1989;139:242-6.
7. Brewster CE, Howarth PH, Djukanovic R, Wilson J, Holgate ST, Roche WR. Myofibroblasts and subepithelial fibrosis in bronchial asthma. Am J Respir Cell Mol Biol 1990;3:507-11.
8. Paul SR, Bennett F, Calvetti JA, Kelleher K, Wood CR, O'Hara RM Jr, et al. Molecular cloning of a cDNA encoding interleukin 11, a stromal cell-derived lymphopoietic and hematopoietic cytokine. Proc Natl Acad Sci U S A 1990;87:7512-6.
9. Zhang XG, Gu JJ, Lu ZY, Yasukawa K, Yancopoulos GD, Turner K, et al. Ciliary neurotropic factor, interleukin 11, leukemia inhibitory factor, and oncostatin M are growth factors for human myeloma cell lines using the interleukin 6 signal transducer gp130. J Exp Med 1994;179:1337-42.
10. Du X, Williams DA. Interleukin-11: review of molecular, cell biology and clinical use. Blood 1997;89:3897-908.
11. Elias JA, Zheng T, Whiting NL, Trow TK, Merrill WW, Zitnik R, et al. IL-1 and transforming growth factor-β regulation of fibroblast-derived IL-11. J Immunol 1994;152:2421-9.
12. Romas E, Udagawa N, Zhou H, Tamura T, Saito M, Taga T, et al. The role of gp130-mediated signals in osteoclast development: regulation of interleukin 11 production by osteoblasts and distribution of its receptor in bone marrow cultures. J Exp Med 1996;183:2581-91.
13. Nilsen EM, Johansen FE, Jahnsen FL, Lundin KE, Scholz T, Brandtzaeg P, et al. Cytokine profiles of cultured microvascular endothelial cells from the human intestine. Gut 1998;42:635-42.
14. Elias JA, Zheng T, Einarsson O, Landry M, Trow T, Rebert N, et al. Epithelial interleukin-11: regulation by cytokines, respiratory syncytial virus, and retinoic acid. J Biol Chem 1994;269:22261-8.
15. Einarsson O, Geba GP, Zhu Z, Landry M, Elias JA. Interleukin-11: stimulation in vivo and in vitro by respiratory viruses and induction of airways hyperresponsiveness. J Clin Invest 1996;97:915-24.
16. Zheng T, Nathanson MH, Elias JA. Histamine augments cytokine-stimulated IL-11 production by human lung fibroblasts. J Immunol 1994;153:4742-52.
17. Rochester CL, Ackerman SJ, Zheng T, Elias JA. Eosinophil-fibroblast interactions: granule major basic protein interacts with IL-1 and transforming growth factor-beta in the stimulation of lung fibroblast IL-6-type cytokine production. J Immunol 1996;156:4449-56.
18. Ray P, Tang W, Wang P, Homer R, Kuhn C III, Flavell RA, et al. Regulated overexpression of interleukin 11 in the lung: use to dissociate development-dependent and -independent phenotypes. J Clin Invest 1997;100:2501-11.
19. Tang W, Geba GP, Zheng T, Ray P, Homer RJ, Kuhn C III, et al. Targeted expression of IL-11 in the murine airway causes lymphocytic inflammation, bronchial remodeling, and airways obstruction. J Clin Invest 1996;98:2845-53.
20. American Thoracic Society. Standards for the diagnosis and care of patients with chronic obstructive pulmonary disease (COPD) and asthma. Am Rev Respir Dis 1987;136:225-44.
21. Azzawi M, Bradley B, Jeffery PK, Frew AJ, Wardlaw AJ, Knowles G K, et al. Identification of activated T lymphocytes and eosinophils in bronchial biopsies in stable atopic asthma. Am Rev Respir Dis 1990;142:1407-13.
22. Ying S, Durham SR, Barkans J, Matsuyama K, Jacobson M, Rak S, et al. T cells are the principal source of interleukin-5 mRNA in allergen-induced rhinitis. Am J Respir Cell Mol Biol 1993;9:356-60.
23. Giaid A, Michel RP, Stewart DJ, Sheppard M, Corrin B, Hamid Q. Expression of endothelin-1 in lungs of patients with cryptogenic fibrosing alveolitis. Lancet 1993;341:1550-4.
24. Hamid Q, Barkans J, Meng Q, Abrams JS, Kay AB, Moqbel R. Human eosinophils synthesize and secrete interleukin-6, in vitro. Blood 1992; 80:1496-501.
25. Moqbel R, Ying S, Barkans J, Newman TM, Kimmitt P, Wakelin M, et al. Identification of messenger RNA for IL-4 in human eosinophils with granule localization and release of the translated product. J Immunol 1995;155:4939-47.
26. Maier R, Ganu V, Lotz M. Interleukin-11, an inducible cytokine in human articular chondrocytes and synoviocytes, stimulates the production of the tissue inhibitor of metalloproteinases. J Biol Chem 1993;268:21527-32.
27. Trepicchio WL, Bozza M, Pedneault G, Dorner AJ. Recombinant human IL-11 attenuates the inflammatory response through down-regulation of proinflammatory cytokine release and nitric oxide production. J Immunol 1996;157:3627-34.
28. Leng SX, Elias JA. Interleukin-11 inhibits macrophage interleukin-12 production. J Immunol 1997;159:2161-8.
29. Bill GR, Cooke KR, Teshima T, Crawford JM, Keith JC Jr, Brinson YS, et al. Interleukin-11 promotes T cell polarization and prevents acute graft-versus-host disease after allogeneic bone marrow transplantation. J Clin Invest 1998;102:115-23.
30. Trepicchio WL, Wang L, Bozza M, Dorner AJ. IL-11 regulates macrophage effector function through the inhibition of nuclear factor-κB. J Immunol 1997;159:5661-70.
31. Minshall EM, Leung DYM, Martin RJ, Song YL, Cameron L, Ernst P, et al. Eosinophil-associated TGF-β_1 mRNA expression and airways fibrosis in bronchial asthma. Am J Respir Cell Mol Biol 1997;17:326-33.
32. Elias JA, Wu Y, Zheng T, Panettieri R. Cytokine- and virus-stimulated airway smooth muscle cells produce IL-11 and other IL-6-type cytokines. Am J Physiol 1997;273:L648-55.
33. Lacy P, Levi-Schaffer F, Mahmudi-Azer S, Bablitz B, Hagen SC, Velazquez J, et al. Intracellular localization of interleukin-6 in eosinophils from atopic asthmatics and effects of interferon gamma. Blood 1998;91:2508-16.
34. Marini M, Vittori E, Hollemborg J, Mattoli S. Expression of the potent inflammatory cytokines, granulocyte-macrophage-colony-stimulating factor and interleukin-6 and interleukin-8, in bronchial epithelial cells of patients with asthma. J Allergy Clin Immunol 1992;89:1001-9.

The Laryngoscope
Lippincott Williams & Wilkins, Inc.

IL-11 and IL-17 Expression in Nasal Polyps: Relationship to Collagen Deposition and Suppression by Intranasal Fluticasone Propionate

Sophie M. Molet, PhD; Qutayba A. Hamid, MD, PhD; Daniel L. Hamilos, MD

Objectives/Hypothesis: **Chronic hyperplastic sinusitis (CHS) with nasal polyps (NP) is characterized by extensive mucosal thickening, goblet cell hyperplasia, and subepithelial fibrosis. These features are described to be part of remodeling in the lower airways. The cytokines interleukin (IL)-11 and IL-17 are believed to play a role in lower airway remodeling, but there has been very little work so far examining these cytokines and their relationship to fibrosis in CHS/NP. The aims of this study were to examine the deposition of collagens types I, III, and V in CHS/NP, evaluate the relationship of collagen deposition to expression of IL-11 and IL-17, and to examine the effect of treatment with intranasal fluticasone on these features.** ***Study Design:*** **Sixteen subjects were included in this double-blind, placebo-controlled study. NP biopsies were obtained at the baseline and after 4 weeks of treatment with intranasal fluticasone propionate (FP, Flonase) or placebo. Normal control middle turbinate biopsies from eight nonallergic subjects without sinusitis were used as a control for cytokine and collagen expression.** ***Methods:*** **Tissues were assessed for deposition of collagen types I, III, and V using immunocytochemistry. The expression of the cytokines IL-11 and IL-17 was examined by immunostaining or in situ hybridization. The pre- to posttreatment results were analyzed using paired t test, and the magnitude of changes were estimated using one-way analysis of variance (ANOVA) statistical test followed by least significance difference post hoc comparisons of means.** ***Results:*** **Compared with normal control nasal turbinate tissues, collagen types I, III, and V were increased in all NP tissues, with a predominance of types III and V. Collagen deposition was most abundant in the submucosal connective tissue and in the basement membrane zone. FP treatment had no significant effect on deposition of any collagen type. Expression of IL-11 and IL-17 was also greatly increased in NP compared with control nasal turbinate tissues. IL-11 expression was observed in both inflammatory cells and the epithelium, whereas IL-17 expression was primarily associated with inflammatory cells. In the pretreatment NP, a correlation was found between the presence of IL-11 and collagen type I ($r = 0.59$, $P = .02$) and also between IL-17 and both $CD4^+$ and $CD8^+$ T lymphocytes ($r = 0.52$, $P = .05$; $r = 0.60$, $P = .02$, respectively). Treatment with FP significantly reduced IL-11 expression in subepithelial inflammatory cells and in the epithelial compartment. In contrast, although IL-17 expression was reduced by FP, this effect did not reach statistical significance.** ***Conclusion:*** **NP manifest an increased expression of collagen types III, V, and I and an increase in profibotic cytokines IL-11 and IL-17. A correlation exists between deposition of collagen type I and expression of IL-11, suggesting a possible role for IL-11 in NP remodeling. Collagen deposition was not reversed by FP treatment, whereas IL-11 expression was suppressed. These results are consistent with a partial insensitivity of NP to FP treatment but also suggest that longer-term treatment or perhaps earlier intervention with FP might reduce proinflammatory cytokine signals and ultimately have a beneficial effect in preventing airway remodeling in NP.** ***Key words:*** **Nasal polyps, fluticasone, IL-11, IL-17, collagen.**
***Laryngoscope*, 113:1803–1812, 2003**

INTRODUCTION

Chronic sinusitis is defined as sinus inflammation persisting for longer than 8 to 12 weeks. In noninfectious chronic sinusitis, patients have mucosal thickening associated with nasal polyposis in approximately 20% of cases. These patients are labeled chronic hyperplastic sinusitis with nasal polyposis (CHS/NP). CHS/NP is one of the most common indications for sinus surgery.[1] Considerable attention has been given to investigating mechanisms governing the inflammatory process in CHS/NP. Immunopathologic features include increased numbers of $CD45^+$

From the Meakins-Christie Laboratories (S.M.M., Q.A.H.), McGill University, Montreal, Quebec, Canada; and Washington University School of Medicine (D.L.H.), St. Louis, MO, U.S.A.

This work was supported in part by a grant from GlaxoSmithKline (Research Triangle Park, NC).

Editor's Note: This Manuscript was accepted for publication May 16, 2003.

Send Correspondence to Dr. Daniel L. Hamilos, Washington University School of Medicine, 660 South Euclid Avenue, Campus Box 8122, St. Louis, Missouri 63110-1093, U.S.A. E-mail: dhamilos@im.wustl.edu

inflammatory cells, MBP^+ or $EG2^+$ eosinophils, $tryptase^+$ mast cells, and $CD4^+$ T cells.[2] Among the numerous cytokines expressed in CHS/NP are granulocyte macrophage-colony stimulating factor (GM-CSF), interleukin (IL)-3, IL-4, IL-5, and interferon (IFN)-γ, with differential expression according to the allergic status of CHS/NP patients.[3] Similar features have been described in asthma, and at least 50% of CHS/NP patients have associated asthma.

Most of our knowledge about inflammation-induced structural changes or remodeling of the airways comes from studies of subjects with asthma.[4] We and others have reported that one feature of this airway remodeling is subepithelial fibrosis, which could be caused by deposition of types III, V, and to a lesser extent, type-I, collagens beneath the basement membrane.[5,6] This fibrosis has demonstrated to contribute to asthma pathology and disease severity.[7–9] During the pathogenesis of lung fibrosis, local over-expression of cytokines or growth factors stimulate resident lung fibroblasts to synthesize increased amounts of extracellular matrix (ECM). Among these mediators, transforming growth factor (TGF)-β has been regarded as a major fibrogenic cytokine[10], and we demonstrated that increased expression of TGF-β in asthmatic airways was directly related to the degree of airway fibrosis.[9] TGF-β1 stimulates epithelial cells, airway smooth muscle cells, and fibroblasts to produce IL-11. In a murine model, over-expression of IL-11 within the lungs leads to subepithelial fibrosis and other structural changes that mimic those seen in severe asthma.[11,12] IL-11 was shown to induce smooth muscle hyperplasia and fibroblast proliferation.[13] We previously demonstrated that IL-11 is expressed in asthma and associated with increasing severity of the disease.[6]

More recently, we put our interest in a newly described cytokine, IL-17,[14] which has been shown to be produced primarily but not exclusively by $CD4^+$ and $CD8^+$ T lymphocytes.[15,16] A major effect of IL-17 was found to be the stimulation of stromal cells to secrete IL-6, IL-8, GM-CSF, prostaglandin E2, and nitric oxide.[16–20] We also found that IL-17 increased the synthesis of IL-6 and IL-11 by bronchial fibroblasts, and we demonstrated that IL-17 is up-regulated in asthma and that eosinophils are one source of its production.[21] These findings suggested that IL-17 might also play an indirect role in airway remodeling in asthma by contributing to the amplification, regulation, or perpetuation of local airway inflammation and profibrotic cytokine production.

Although lower airway remodeling is thought to be the consequence of repeated inflammatory episodes in asthma, little has been shown regarding mediators and mechanisms leading to tissue remodeling in upper airways. Some cytokines, including TGF-α and -β, IL-6, platelet-derived growth factor (PDGF), basic fibroblast growth factor (bFGF), and GM-CSF, have been suggested to be involved in the pathogenesis of NP by way of their connective tissue remodeling actions.[22–28] However, whether inflammation causes changes to matrix structures such as epithelium, basement membrane, and the collagen matrix is not known. CHS/NP is characterized by structural changes reported also in asthma, including basement membrane thickening, atypical gland formation, goblet cell hyperplasia, mononuclear cell infiltration, and subepithelial edema. On the basis of these observations, we speculated that upper airway remodeling in CHS/NP might be pathologically similar to that of asthma.

Allergic inflammation has been demonstrated to be amenable to treatment with topical steroids. Corticosteroids, administered by aerosol or systemically, are known for their efficacy in the treatment of NP disease even though a subset of subjects show progression of NP disease despite topical steroid treatment.[29] Fluticasone propionate (FP) is a highly potent topical intranasal steroid, and we previously demonstrated that a 4-week intranasal FP treatment led to a modest improvement in nasal peak flow rates and a reduction in the number of eosinophils, $CD4^+$ T lymphocytes, and cytokine (IL-4, IL-13) $mRNA^+$ cells.[29] Much less is known about the ability of intranasal FP to prevent or reverse the structural alterations occurring in vivo. Because tissue remodeling plays an important role in CHS/NP disease progression, we wished to examine whether intranasal FP would cause a reduction in collagen deposition or a reduction in the expression of the profibrotic cytokines IL-11 and IL-17 in NP.

METHODS

Study Subjects

This study was approved by the Human Subjects Committee at Washington University School of Medicine. Subjects were recruited through advertisements and physician referral. The 16 subjects (6 female, 10 male with mean age of 47.9 ± 11.1 years) in this study were participants in a previous double-blinded, placebo-controlled study of intranasal FP versus placebo for treatment of nasal polyposis disease.[29] Each subject had symptomatic chronic sinusitis with NP. Systemic and intranasal steroids were withheld for a minimum of 1 month and 2 weeks, respectively, before the initial NP biopsy. Beginning at the screening visit, all intranasal medications were stopped, and none were allowed throughout the study. Subjects were allowed to continue other medications, including oral decongestants, antihistamines, and medications for asthma throughout the study. No new medications were allowed from the time of the screening visit until the end of the study.

The initial NP biopsies were obtained 1 week before initiation of the intranasal study drug. Subjects were instructed to use two 50 μg puffs of FP (n = 8) or two sprays of matching placebo-containing diluent (n = 8) per nostril twice daily for 4 weeks. Subjects were evaluated at weekly intervals during treatment. The clinical responses to intranasal FP were previously reported.[29] Nasal mucosal biopsies obtained from the middle turbinate of eight nonallergic subjects without sinusitis served as the normal control tissues for cytokine and collagen expression, as in previous studies.[2]

NP Biopsies

The nasal passages were decongested with 0.5% Neo-Synephrine and then sprayed with 4% Xylocaine solution to anesthetize the nasal mucosa. Percutaneous 2 to 3mm biopsy specimens from NPs or the middle turbinate mucosae were obtained with 5 mm Thrucut (Smith and Nephew, Memphis, TN) biopsy forceps. Generally, two to four specimens were obtained from both the right and left sides.

Tissue Preparation

A portion of the biopsy specimen was embedded in ornithine carbamoyltransferase (OCT), frozen in 95% ethanol plus dry ice, and then stored at −70°C until processing for immunocytochemistry.

Immunocytochemistry

Cryostat sections (6 μm) were cut from the frozen biopsy specimens, air dried for 1 hour, and fixed in a mixture of equal parts of acetone:methanol, and stained with the following antibodies: anti-IL-17 (1 μg/mL) and anti-IL-11 (20 μg/mL) from R&D Systems (Minneapolis, MN), and antitype I (5 μg/mL), antitype III (5 μg/mL), and antitype V (5 μg/mL) collagens from Medicorp Inc. (Montreal, Canada). The reaction was visualized through the use of the alkaline phosphatase anti-alkaline phosphatase (APAAP) method (IL-11, collagens) or the biotin/streptavidin-alkaline phosphatase complex method (IL-17), as previously described.[21,30] Species and isotype-matched antibodies of irrelevant specificity were used to confirm the specificity of each antibody. The details of immunostaining of NP for inflammatory T cells (CD4, CD8), eosinophils (MBP), macrophages (CD68), and mast cells (tryptase) have been described previously.[29]

To colocalize cytokines with specific inflammatory cells, we used a double immunostaining technique with in situ hybridization for IL-11 and IL-17 and immunostaining for T lymphocytes (CD3), neutrophils (elastase), or eosinophils (MBP) as previously described.[2,3] Results were expressed as the percentage of cytokine-positive cells for IL-11 and IL-17.

Quantification

For immunocytochemistry, sections were counted by a single "blinded" observer in a coded random order by using an Olympus microscope (Tokyo, Japan) with an eyepiece graticule at ×200 or ×400 magnification. The graticule was oriented along the epithelial basement membrane, and cell counts (IL-17, IL-11, and type V collagen) were expressed as mean counts per high-power field. Then results were expressed as number of positive cells per square millimeter of tissue. Regarding type I and type III collagens, a score estimating the staining intensity, extent of collagen deposition, and subepithelial basement membrane thickness was given. Similarly, IL-11 epithelial staining was scored from 1 to 4 depending on intensity.

Statistics

All analyses were done using Statistica 4.3B software package (StatSoft Inc., Tulsa, OK). The pre- to posttreatment results were analyzed using paired t test, and the magnitude of changes in cytokine and collagen expressions and inflammatory markers in the FP versus placebo groups were compared using the one way analysis of variance (ANOVA) statistical test followed by least significance difference post hoc comparisons of means.[31] Correlation studies between cytokine expression and collagen and inflammatory markers were evaluated by linear regression. A P value of .05 was regarded as statistically significant in all comparisons.

RESULTS

Collagen Deposition in Normal Control Nasal Turbinates versus NP

Expression of collagen types I, III, and V was examined in normal control nasal turbinates and untreated NP. As shown on Figure 1 and illustrated in Figure 2, the expression of types III, V, and to a lesser extent, type I collagens was significantly increased in NP compared with control turbinates (P = .002, P = .001, and P = .02 respectively). Significant deposition of type I and III collagens was found beneath the reticular layer of basement membrane and in the submucosa. In contrast with type I and III collagens, type V collagen staining was primarily cell associated.

Effect of FP versus Placebo on Type I, III, and V Collagen Expression in NP

A trend was observed toward increased collagen type I and III expression in subjects receiving placebo treatment; however, neither increase was statistically significant (Fig. 1) (P = .20 and P = .07, respectively). In contrast, the number of type V collagen expressing cells increased significantly in subjects receiving placebo (Fig. 1) (P = .02). FP treatment had no effect on type I or III collagen deposition or on the number of type V collagen expressing cells (Fig. 1) (P = .83, P = .63, and P = .86, respectively).

To further analyze the impact of FP treatment on collagen expression in NP, the magnitude of change in type I and III collagens as well as in the number of type V collagen expressing cells were compared after placebo versus FP treatment. Even when the data were analyzed in this way, FP treatment could not be shown to have any significant effect on expression of collagen types I, III, or type V collagen positive cells in NP. There was a tendency for FP treatment to decrease the number of type V collagen expressing cells, but this effect did not reach statistical significance (P = .06) (Fig. 1).

IL-11 and IL-17 in Normal Control Nasal Turbinates versus NP

The numbers of IL-11 and IL-17 immunoreactive cells (Fig. 2) were increased in NP compared with normal control nasal turbinates (Fig. 3) (P = .001 and P = .002, respectively). IL-11 immunostaining was also seen in the epithelium, and the extent of this staining was significantly increased in NP compared with normal control nasal turbinates (Fig. 4) (P = .001).

Effect of FP versus Placebo on IL-17 and IL-11 Expression in NP

As shown in Figure 3A, the number of IL-11 immunoreactive cells increased in subjects receiving placebo (5 of 7 subjects) but decreased in subjects receiving FP (5 of 8 subjects). By simply comparing the number of IL-11 immunoreactive cells in pre- and posttreatment samples, neither of these results reached statistical significance. Similarly, the IL-11 epithelial score increased in subjects receiving placebo (Fig. 4) (P = .05) but decreased in subjects receiving FP, although the latter decrease did not reach statistical significance.

Figure 3B shows that the number of IL-17 immunoreactive cells increased significantly in subjects receiving placebo in all but one case. In contrast, in subjects receiving FP, the number of IL-17 positive cells decreased (5 of 8 subjects). Again, by simply comparing the number of IL-17 immunoreactive cells in pre- and posttreatment samples, the only significant change was the increase in IL-17 immunoreactive cells in subjects receiving placebo (P = .04).

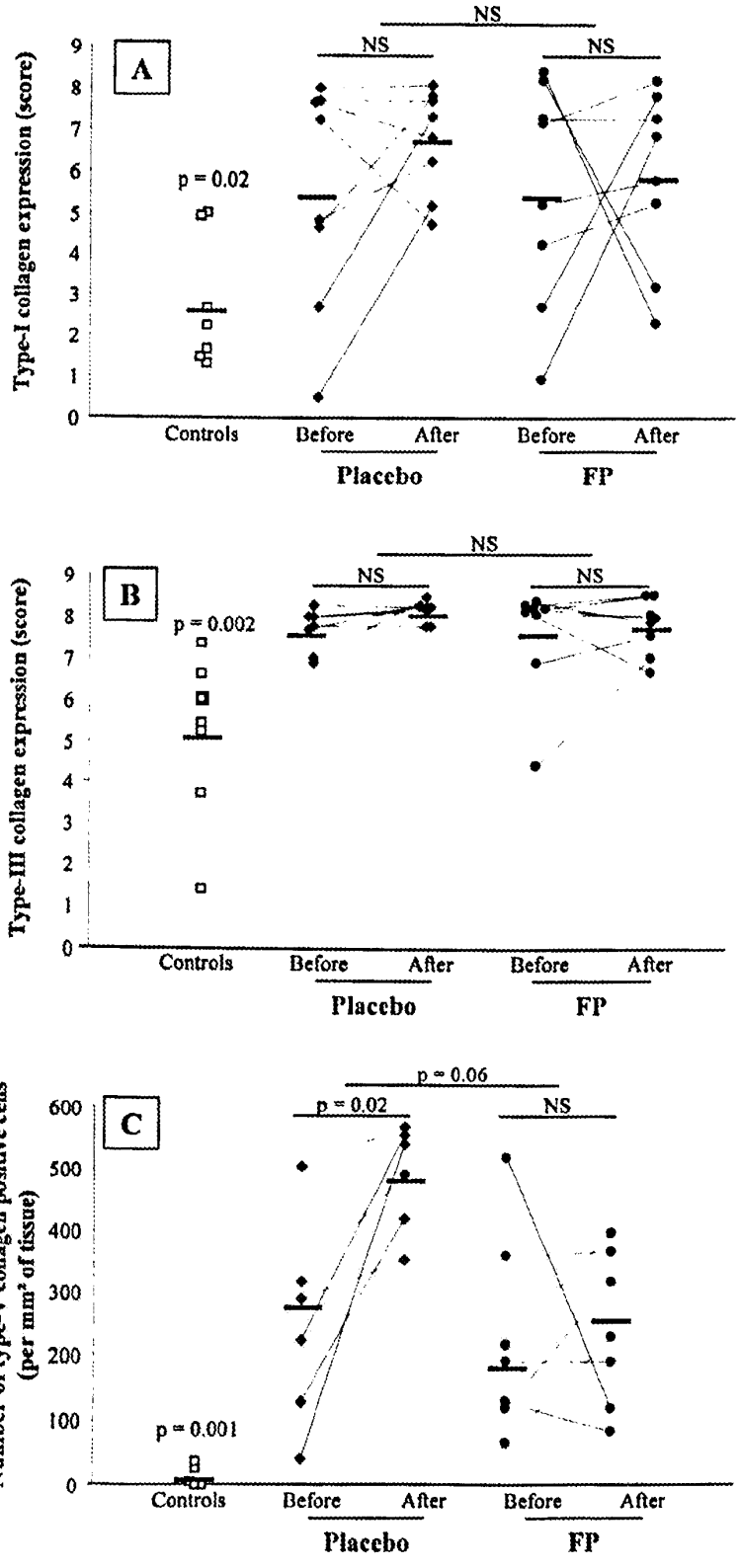

Fig. 1. Expression of type I (A), type III (B), and type V (C) collagens in control nasal turbinates and nasal polyp (NP) tissues before and after intranasal fluticasone propionate (FP) versus placebo treatment for 4 weeks. Type I and III collagen expression was graded by a score (from 1–9) whereby type V collagen expression was expressed as number of immunoreactive cells per square millimeter of nasal polyp tissue. A *P* value of .05 was regarded as statistically significant. The expression of types I, III, V collagen was significantly increased in NP compared with controls.

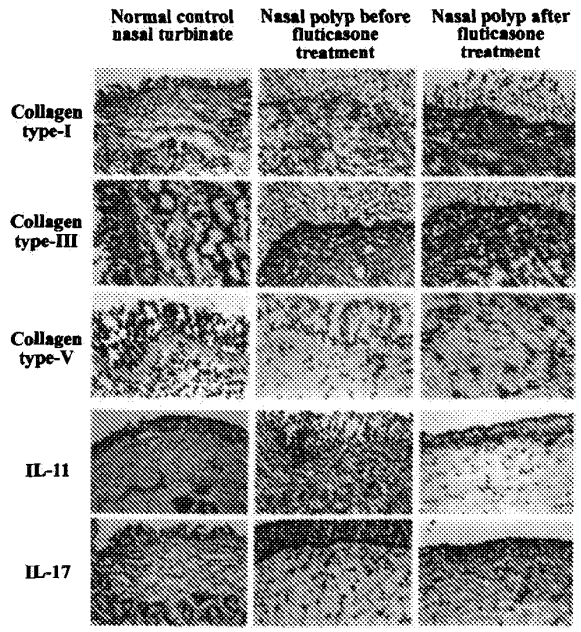

Fig. 2. Collagen type I, III, and V and the cytokines interleukin (IL)-11 and IL-17 in normal control nasal turbinates and nasal polyp tissues. Representative tissue sections and examples of the response of nasal polyp tissue to fluticasone treatment (magnification ×40 except for the panels illustrating IL-11 immunostaining, which are at ×20).

To further analyze the impact of FP treatment on IL-11 and IL-17 expression in NP, the magnitude of change in each cytokine was compared after placebo versus FP treatment. In comparison with placebo treatment, the change in IL-11 after FP treatment (in both inflammatory and epithelial cells) was statistically significant (Figs. 3 and 4) ($P = .05$, respectively) whereas the change in IL-17 did not quite reach statistical significance (Fig. 3) ($P = .07$).

Inflammatory Cells in Normal Control Nasal Turbinates versus NP

The number of inflammatory cells, including MBP^+ eosinophils, $CD4^+$ T lymphocytes, $CD8^+$ T lymphocytes (Fig. 5) ($P = .001$, $P = .05$, and $P = .007$, respectively), and $tryptase^+$ mast cells ($P = .029$) but not $CD68^+$ macrophages ($P = .27$) was increased in NP compared with normal control nasal turbinates.

Effect of FP versus Placebo on Inflammatory Cells in NP

As shown in a previous study,[29] there were no significant changes in the total number of inflammatory cells or the numbers of MBP^+ eosinophils, $CD4^+$ and $CD8^+$ T lymphocytes, $CD68^+$ macrophages, or $tryptase^+$ mast cells after placebo treatment. FP treatment did not reduce the total number of inflammatory cells but caused a significant reduction in the numbers of MBP^+ eosinophils ($P = .02$) and $CD4^+$ T lymphocytes ($P = .03$) (Fig. 5).

Cellular Sources of IL-11 and IL-17

The cellular sources of IL-11 and IL-17 were determined by double immunostaining (see Methods). For IL-11, the predominant cellular sources (not including the epithelium) were eosinophils (37.3 ± 4.7%), neutrophils (31.5 ± 7.3%), and T lymphocytes (7.8 ± 2.5%). Other cell types accounted for 23.4 ± 7.7% of $IL\text{-}11^+$ cells. For IL-17, the predominant cellular sources were T lymphocytes (43.3 ± 9.1%), neutrophils (25.5 ± 5.9%), and eosinophils (17.5 ± 4.6%). Other cell types accounted for 13.7 ± 8.7% of $IL\text{-}17^+$ cells.

Relationships Between Collagen Deposition, Cytokine Expression, and Inflammatory Cells in NP Before Treatment

The relationship between IL-11 and IL-17, collagen deposition, and the inflammatory cells present was examined for the entire group of NP before treatment with either placebo or fluticasone. The number of subepithelial IL-11 immunoreactive cells correlated strongly with the level of epithelial IL-11 expression ($r = 0.935$, $P = .000001$). A correlation was observed between subepithelial IL-11 immunoreactive cells and collagen type I ($r = 0.59$, $P = .021$) but not with collagen type III or type V ($r = 0.40$, $P = .134$; $r = 0.40$, $P = .176$, respectively). No correlation was demonstrated between IL-11 expression and the number of MBP^+ eosinophils or other inflammatory cell types in untreated NP. This was somewhat unexpected because we had previously found that, in the submucosa of asthmatic subjects, the predominant cellular source of IL-11 was eosinophils. By comparison, no correlation was found between IL-17 expression and collagen type I, III, or V. However, IL-17 expression correlated with the presence of $CD4^+$ T lymphocytes ($r = 0.516$, $P = .049$) and also with $CD8^+$ T lymphocytes ($r = 0.601$, $P = .018$) in NP.

DISCUSSION

CHS/NP is an upper airway inflammatory disease in which the structural modifications of epithelium (secretory hyperplasia and squamous metaplasia) and lamina propria mucosa (basement membrane thickening, ECM accumulation, and collagen deposition) are associated with inflammatory cell infiltration. The pathologic processes leading to these structural modifications are complex and poorly understood. Several growth factors have been identified in NP that likely contribute to this process, including TGF-α, TGF-β, bFGF, PDGF, GM-CSF, IL-6.[22–28] Recent studies suggest that additional cytokines, such as IL-11 and IL-17, may also be involved in these modifications at least in the case of asthma. For instance, a recent study from our laboratory found over-expression of IL-11 and IL-17 in asthmatic airways and a relationship between these and collagen deposition.[6,9,21,32] In view of the many similarities in airway remodeling between asthma and nasal polyposis, we undertook to examine whether these same cytokines and collagen types might also be involved in mucosal remodeling in nasal polyposis.

Previous studies in humans and in an animal model of polyp formation suggested that the formation of NPs requires ECM accumulation.[33,34] In this study, we con-

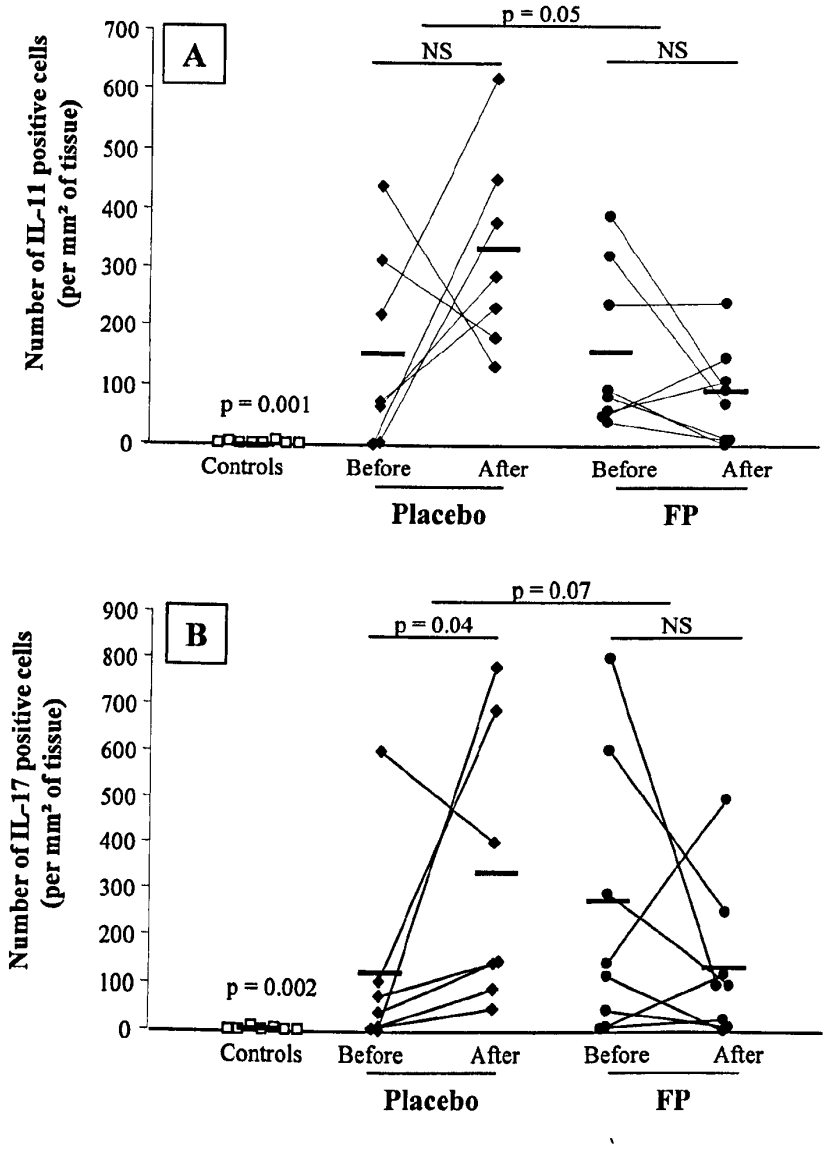

Fig. 3. Number of cells immunoreactive for IL-11 (A) and IL-17 (B) per square millimeter of control nasal turbinates and nasal polyp (NP) tissues before and after intranasal fluticasone propionate (FP) versus placebo treatment for 4 weeks. A *P* value of .05 was regarded as statistically significant. The numbers of interleukin (IL)-11 and IL-17 immunoreactive cells in NP were increased compared with controls.

firmed that collagen components of the ECM, in particular the deposition of collagen types III, V, and I in NP, were indeed increased in NPs in comparison with normal control nasal turbinate tissue. To our knowledge, this is the first study that examines specific collagen types in NP. Interestingly, basement membrane thickening in asthma is largely composed of collagen types III, V, and to a lesser extent, type I.[5] We found that the predominant collagen type in the reticulin layer beneath the basement membrane was type III with a lesser amount of I. In contrast, most of the type V collagen was found to be cell associated. Although we have not directly compared the results in NP with those in the lower airways of asthma, our results at least raise the possibility that the pattern of deposition may be somewhat different in these two conditions.

We found an increased expression of IL-11 in NP compared with a very low level of expression in normal control nasal turbinate tissues. IL-11 expression was increased in submucosal inflammatory cells and also in the epithelium. IL-11 has potent immunomodulatory properties, including the ability to induce substantial remodeling of the airways in animal models.[11,12] The present study is the first to report an increase in the expression of IL-11 in NP. This increased expression was found both in inflammatory cells (e.g., eosinophils, neutrophils, and T lymphocytes) and in the epithelial compartment. In fact, we found a strong correlation between subepithelial and epithelial IL-11 expression. The reason for this is unclear but at least suggests the possibility that an inherited tendency for IL-11 over-expression may be an important feature of

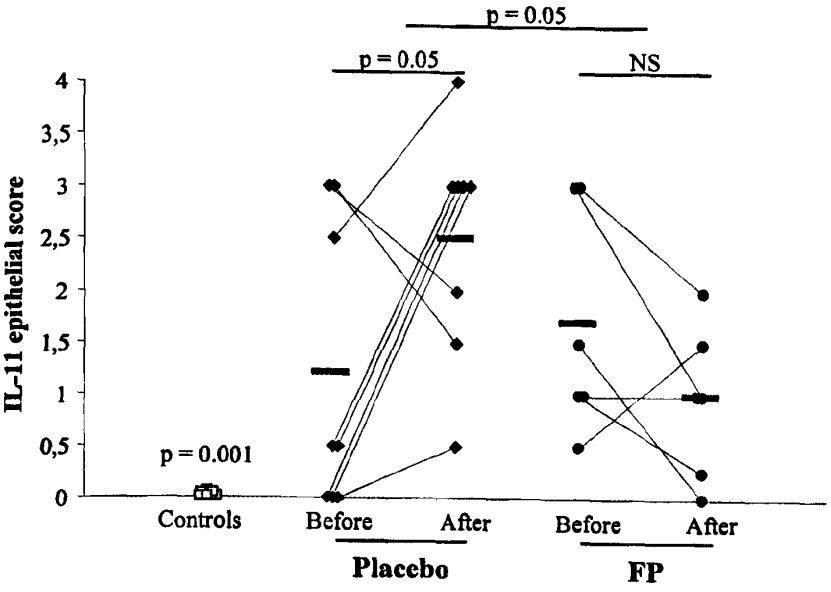

Fig. 4. Interleukin (IL)-11 epithelial score in control nasal turbinates and nasal polyp tissues before and after intranasal fluticasone propionate (FP) versus placebo treatment for 4 weeks. A *P* value of .05 was regarded as statistically significant. In comparison with the change after placebo, the change in IL-11 epithelial score after FP treatment was statistically significant.

NP disease. A correlation was also observed between IL-11 expression and the deposition of collagen type I. Because over-expression of IL-11 in a transgenic mouse model of asthma was associated with an increase in collagen deposition in the lungs,[12] it is possible that the latter correlation reflects an important pathologic relationship. Furthermore, overproduction of IL-11 by NP epithelium could contribute to the localized subepithelial accumulation of collagen (i.e., "basement membrane thickening") that we noted particularly for collagen types III and I and that is characteristic of NP. In a previous study of endobronchial biopsies from subjects with asthma, we found a strong correlation between IL-11 expression and tissue infiltration with MBP^+ eosinophils.[6] The present study did not demonstrate such a correlation in NP. This may reflect a more prominent participation of other inflammatory cell types in IL-11 production in NP. In support of this, we found that 31.5% of the $IL\text{-}11^+$ cells were neutrophils.

A possible role for IL-17 in airway remodeling was only recently suggested.[21] IL-17 is generally regarded as a product of $CD4^+$ and $CD8^+$ T lymphocytes.[15,16] A major effect of IL-17 was found to be the stimulation of stromal cells to secrete IL-6, IL-8, GM-CSF, prostaglandin E2, and nitric oxide.[16–20] IL-17 was also found to increase the synthesis of IL-6 and IL-11 by bronchial fibroblasts. In support of a potential role for IL-17 in airway remodeling, we previously reported that IL-17 is up-regulated in asthma and that eosinophils were a major source of it.[21] By analogy, we reasoned that IL-17 might be up-regulated and contribute to the airway remodeling characteristic of NP. Indeed, in this study, we found increased expression of IL-17 in NP compared with normal control nasal turbinate tissue. Consistent with previous reports, we found that IL-17 expression in NP correlated with the presence of $CD4^+$ and $CD8^+$ T lymphocytes. By colocalization immunostaining, we confirmed that 43.3% of the $IL\text{-}17^+$ inflammatory cells were T lymphocytes. Not surprisingly, other inflammatory cells, including neutrophils and eosinophils, were also found to produce it. IL-17 production was also occasionally seen in the NP epithelium, but the extent of this staining was quite variable among the NP specimens.

Administration of systemically or topically applied corticosteroids (nasal spray or powder) is an established form of treatment in allergic chronic sinusitis and for prevention of recurrences after surgical removal of NP. Topical corticosteroids may also reduce the size of NP without prior surgery. Interestingly, we found that FP treatment for 4 weeks had no significant effect on collagen deposition in NP. This was perhaps the expected outcome, but it is interesting that we observed an increase in collagen deposition in the subjects who received placebo. We acknowledge that the extent of extracellular deposition of collagens in NP tissue is difficult to quantify and could be affected by the expansion of extracellular space such as might occur with extracellular edema. Because FP is known to reduce extracellular edema, this may have partially offset any effect on suppression of collagen deposition. However, this effect would not likely explain why collagen deposition appeared to increase in the subjects receiving placebo. Furthermore, it could be postulated that collagen deposition in the lamina propria might be more difficult to suppress than subepithelial collagen, owing to limited penetration of the FP. However, in a previous study, we found that this same dose and duration of FP treatment had a significant effect to suppress expression of P-selectin on vascular endothelium.[29] This would suggest that the lack of effect of FP on lamina propria collagen deposition was not caused by a lack of FP penetration to this depth. A more precise analysis of collagen synthesis in response to FP treatment would require use

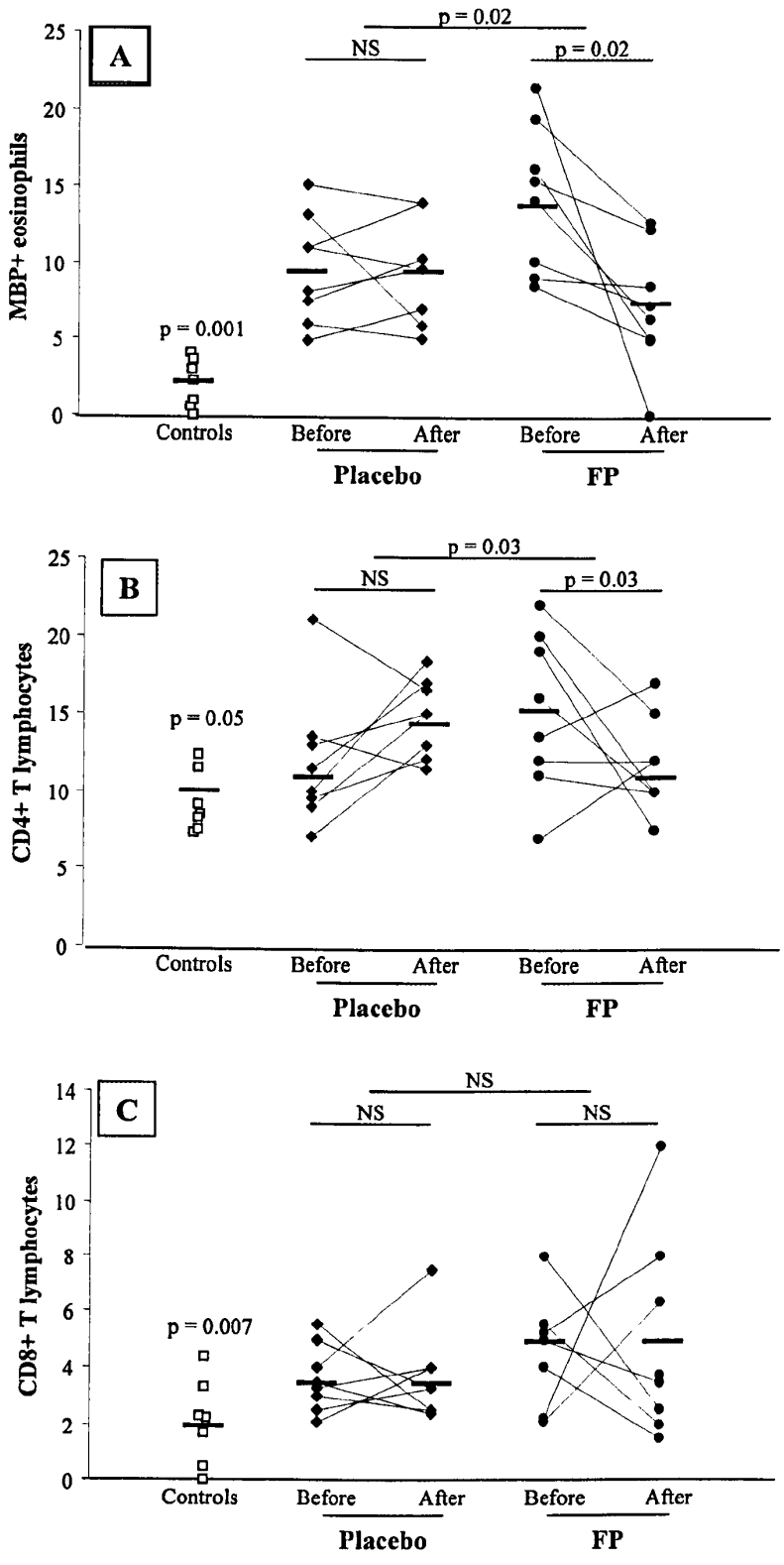

Fig. 5. Number of MBP$^+$ eosinophils, CD4$^+$, and CD8$^+$ T lymphocytes in control nasal turbinates and nasal polyp tissues in response to fluticasone propionate (FP) versus placebo treatment for 4 weeks. A *P* value of .05 was regarded as statistically significant.

of other techniques, such as examination of procollagen mRNA by in situ hybridization or reverse transcriptase polymerase chain reaction (RT-PCR) or measurement of amino-terminal procollagen propeptides of specific collagen types.[35,36] It would also be of interest to study collagen deposition in an earlier state of polyp formation to better understand the relationship between cytokine expression and collagen deposition.

In contrast with its lack of effect on collagen deposition, FP treatment was more effective at suppressing the expression of the profibrotic cytokine IL-11. A similar suppressive effect was observed in terms of IL-11 expression in subepithelial inflammatory cells and in the epithelium. To our knowledge, this is the first demonstration of reduction in IL-11 expression on corticosteroid treatment in allergic disease.

In contrast, the expression of IL-17, albeit reduced, was not significantly affected by FP treatment ($P = .07$). To date, the effect of corticosteroids on IL-17 expression in vivo has not been extensively studied. However, we previously demonstrated that IL-17 expression was significantly reduced in bronchial biopsies from moderate to severe asthmatic subjects after a 2 week course of oral corticosteroid treatment.[32] This suggests that a longer period of treatment with FP might have had a more profound effect on IL-17 expression in NP. Moreover, we and others demonstrated that some of the downstream IL-17-inducible responses were also decreased by corticosteroids, including synthesis of the cytokines IL-6, IL-11, and GM-CSF and of chemokines IL-8 and Gro-α.[17,20,21] We did not find any particularly interesting correlations between IL-17 expression and collagen deposition in NP.

Like most previous studies of airway remodeling in human asthma or NP disease, the results of this study are only descriptive, having focused on only two cytokines potentially involved in the remodeling process. Furthermore, we only looked at correlations between effects on IL-11 and IL-17 and collagen expression. On the basis of in vitro evidence and animal models, it is acknowledged that multiple cytokines and growth factors likely participate in this process. Further insight into the remodeling process will require that we focus attention on specific biochemical events in the complex cascade of events leading to such processes as collagen deposition.

This study was also limited by the relatively small sample size, which limited our ability to detect small changes in cytokine expression, cellular numbers, or collagen deposition. In our previous studies of NP, the variance for immunostaining of inflammatory cells pre and posttreatment with FP, including eosinophils, $CD4^+$ T cells, and $GR\beta^+$ cells, ranged from 32.7% to 40%. Similarly, the variance for IL-4 and IL-5 $mRNA^+$ cells by in situ hybridization was 45%. Given these levels of variance and assuming that we wish to detect a treatment effect with a power of 80% at an alpha level of 0.05, we would need to see more than a 50% change in the inflammatory marker to reach statistical significance in a sample size of eight. The tissues used in this study were used in previous studies, and therefore our sample size was limited by the supply of remaining tissues. Our use of normal control middle turbinate tissue as a comparator with NP tissue is consistent with our previous work.[2,28] The basic premise is that both tissues are lined by pseudostratified columnar respiratory epithelium and that the middle turbinate mucosa is the closest area to sinus mucosa that can be easily biopsied in a subject who is not undergoing sinus surgery. Our studies have consistently found that middle turbinate tissues from nonallergic subjects without sinusitis are uninflamed and show minimal evidence of tissue remodeling.

In summary, our data suggest that IL-11 and IL-17 may contribute, at least partly, to the structural abnormalities such as stromal fibrosis and the basement membrane thickening that characterize NP disease. In addition, the results of this study are consistent with a differential sensitivity of various components of tissue remodeling to the effects of topical FP. This may partially account for the modest improvement in symptoms and gradual reduction in NP size afforded by FP treatment as described in our previous study.[29] The results of this study are also consistent with an important relationship between IL-11 and collagen deposition in NP and further suggest that longer-term treatment or perhaps earlier intervention with FP might reduce proinflammatory cytokine signals and ultimately have a beneficial effect in preventing airway remodeling in NP.

Acknowledgments

The authors thank Ms. Kristy Smith for preparation of the manuscript.

BIBLIOGRAPHY

1. Settipane GA. Epidemiology of nasal polyps. *Allergy Asthma Proc* 1996;17:231–236.
2. Hamilos DL, Leung DY, Wood R, et al. Chronic hyperplastic sinusitis: association of tissue eosinophilia with mRNA expression of granulocyte-macrophage colony-stimulating factor and interleukin-3. *J Allergy Clin Immunol* 1993;92: 39–48.
3. Hamilos DL, Leung DYM, Wood R, et al. Evidence for distinct cytokine expression in allergic versus nonallergic chronic sinusitis. *J Allergy Clin Immunol* 1995;96:537–544.
4. Molet S, Hamid Q. Role of airway remodeling in severe asthma. In: Szefler SJ and Leung DYM, eds. *Severe Asthma: A Multidisciplinary Approach*. New York: Marcel Deckker, 2001:89–124.
5. Roche WR, Beasley R, Williams JH, Holgate ST. Subepithelial fibrosis in the bronchi of asthmatics. *Lancet* 1989;1: 520–523.
6. Minshall E, Chakir J, Laviolette M, et al. IL-11 expression is increased in severe asthma: association with epithelial cells and eosinophils. *J Allergy Clin Immunol* 2000;105: 232–238.
7. Boulet LP, Laviolette M, Turcotte H, et al. Bronchial subepithelial fibrosis correlates with airway responsiveness to methacholine. *Chest* 1997;112:45–52.
8. Chetta A, Foresi A, Del Donno M, et al. Airways remodeling is a distinctive feature of asthma and is related to severity of disease. *Chest* 1997;111:852–857.
9. Minshall EM, Leung DY, Martin RJ, et al. Eosinophil-associated TGF-β1 mRNA expression and airway fibrosis in bronchial asthma. *Am J Respir Cell Mol Biol* 1997;17: 326–333.
10. Border WA, Noble NA. Transforming growth factor β in tissue fibrosis. *N Engl J Med* 1994;331:1286–1292.
11. Ray P, Tang W, Wang P, et al. Regulated overexpression of interleukin-11 in the lung. Use to dissociate development-dependent and -independent phenotypes. *J Clin Invest* 1997;100:2501–2511.

12. Tang W, Geba GP, Zheng T, et al. Targeted expression of IL-11 in the murine airway causes lymphocytic inflammation, bronchial remodeling, and airways obstruction. *J Clin Invest* 1996;98:2845–2853.
13. Elias JA, Wu Y, Zheng T, Panettieri R. Cytokine- and virus-stimulated airway smooth muscle cells produce IL-11 and other IL-6-type cytokines. *Am J Physiol* 1997;273(3 Pt 1):L648–L655.
14. Yao Z, Fanslow WC, Seldin MF, et al. Herpesvirus saimiri encodes a new cytokine, IL-17; which binds to a novel cytokine receptor. *Immunity* 1995;3:811–821.
15. Shin HC, Benbernou N, Fekkar H, et al. Regulation of IL-17, IFN-γ and IL-10 in human $CD8^+$ T cells by cyclic AMP-dependent signal transduction pathway. *Cytokine* 1998;10: 841–850.
16. Fossiez F, Djossou O, Chomarat P, et al. T cell interleukin-17 induces stromal cells to produce proinflammatory and hematopoietic cytokines. *J Exp Med* 1996;183:2593–2603.
17. Laan M, Cui Z-H, Hoshino H, et al. Neutrophil recruitment by human IL-17 via C-X-C chemokine release in the airways. *J Immunol* 1999;162:2347–2352.
18. Attur MG, Patel RN, Abramson SB, Amin AR. Interleukin-17 up-regulation of nitric oxide production in human osteoarthritis cartilage. *Arthritis Rheum* 1997;40:1050–1053.
19. Teunissen MB, Koomen CW, de Waal Malefyt R, et al. Interleukin-17 and interferon-γ synergize in the enhancement of proinflammatory cytokine production by human keratinocytes. *J Invest Dermatol* 1998;111:645–649.
20. Shalom-Barak T, Quach J, Lotz M. Interleukin-17-induced gene expression in articular chondrocytes is associated with activation of mitogen-activated protein kinases and NF-κB. *J Biol Chem* 1998;273:27467–27473.
21. Molet S, Hamid Q, Davoine F, et al. IL-17 is increased in asthmatic airways and induces human bronchial fibroblasts to produce cytokines. *J Allergy Clin Immunol* 2001; 108:430–438.
22. Ohno I, Lea RG, Flanders KC, et al. Eosinophils in chronically inflamed human upper airway tissues express transforming growth factor beta 1 gene (TGF beta 1). *J Clin Invest* 1992;89:1662–1668.
23. Elovic A, Wong DT, Weller PF, et al. Expression of transforming growth factors-alpha and beta 1 messenger RNA and product by eosinophils in nasal polyps. *J Allergy Clin Immunol* 1994;93:864–869.
24. Ghaffar O, Lavigne F, Kamil A, et al. Interleukin-6 expression in chronic sinusitis: colocalization of gene transcripts to eosinophils, macrophages, T lymphocytes, and mast cells. *Otolaryngol Head Neck Surg* 1998;118:504–511.
25. Ohno I, Yamauchi K, Hoshi H, et al. Eosinophils as a potential source of platelet-derived growth factor B-chain (PDGF-B) in nasal polyposis and bronchial asthma. *Am J Respir Cell Mol Biol* 1995;13:639–647.
26. Coste A, Wang QP, Roudot-Thoraval F, et al. Epithelial cell proliferation in nasal polyps could be up-regulated by platelet-derived growth factor. *Laryngoscope* 1996;106: 578–583.
27. Powers MR, Qu Z, LaGesse PC, et al. Expression of basic fibroblast growth factor in nasal polyps. *Ann Otol Rhinol Laryngol* 1998;107:891–897.
28. Hamilos DL, Leung DY, Huston DP, et al. GM-CSF, IL-5 and RANTES immunoreactivity and mRNA expression in chronic hyperplastic sinusitis with nasal polyposis (NP). *Clin Exp Allergy* 1998;28:1145–1152.
29. Hamilos DL, Thawley SE, Kramper MA, et al. Effect of intranasal fluticasone on cellular infiltration, endothelial adhesion molecule expression, and proinflammatory cytokine mRNA in nasal polyp disease. *J Allergy Clin Immunol* 1999;103:79–87.
30. Cordell JL, Falini B, Erber WN, et al. Immunoenzymatic labeling of monoclonal antibodies using immune complexes of alkaline phosphatase and monoclonal anti-alkaline phosphatase (APAAP complexes). *J Histochem Cytochem* 1984;32:219–229.
31. Hajiro T, Nishimura K, Tsukino M, et al. Stages of disease severity and factors that affect the health status of patients with chronic obstructive pulmonary disease. *Respir Med* 2000;94:841–846.
32. Molet S, Chakir J, Laviolette M, et al. Response of remodeling-associated cytokines to steroids in bronchial biopsies of asthmatic patients [abstract]. *Am J Respir Crit Care Med* 2000;161:686.
33. Larsen PL, Tos M, Kuijpers W, Van der Beek JM. The early stages of polyp formation. *Laryngoscope* 1992;102: 670–677.
34. Norlander T, Westrin KM, Fukami M, et al. Experimentally induced polyps in the sinus mucosa: a structural analysis of the initial stages. *Laryngoscope* 1996;106:196–203.
35. Nusgens BV, Humbert P, Rougier A, et al. Topically applied vitamin C enhances the mRNA level of collagens I and III, their processing enzymes and tissue inhibitor of matrix metalloproteinase 1 in the human dermis. *J Invest Dermatol* 2001;116:853–859.
36. Kauh YC, Rouda S, Mondragon G, et al. Major suppression of pro-alpha1(I) type I collagen gene expression in the dermis after keloid excision and immediate intrawound injection of triamcinolone acetonide. *J Am Acad Dermatol* 1997;37: 586–589.

ORIGINAL RESEARCH

Targeting Interleukin-13 with Tralokinumab Attenuates Lung Fibrosis and Epithelial Damage in a Humanized SCID Idiopathic Pulmonary Fibrosis Model

Lynne A. Murray[1], Huilan Zhang[2], Sameer R. Oak[2], Ana Lucia Coelho[2], Athula Herath[1], Kevin R. Flaherty[3], Joyce Lee[4], Matt Bell[1], Darryl A. Knight[5], Fernando J. Martinez[2], Matthew A. Sleeman[1], Erica L. Herzog[6], and Cory M. Hogaboam[2]

[1]MedImmune Ltd, Cambridge, United Kingdom; [2]Department of Pathology, University of Michigan Medical School, Ann Arbor, Michigan; [3]Department of Internal Medicine, Division of Pulmonary and Critical Care Medicine, University of Michigan Health System, Ann Arbor, Michigan; [4]Department of Medicine, University of California, San Francisco School of Medicine, San Francisco, California; [5]Department of Anesthesiology, Pharmacology and Therapeutics, UBC James Hogg Research Centre of the Heart + Lung Institute, University of British Columbia, Vancouver, British Columbia, Canada; and [6]Yale University School of Medicine, New Haven, Connecticut

Abstract

The aberrant fibrotic and repair responses in the lung are major hallmarks of idiopathic pulmonary fibrosis (IPF). Numerous antifibrotic strategies have been used in the clinic with limited success, raising the possibility that an effective therapeutic strategy in this disease must inhibit fibrosis and promote appropriate lung repair mechanisms. IL-13 represents an attractive target in IPF, but its disease association and mechanism of action remains unknown. In the present study, an overexpression of IL-13 and IL-13 pathway markers was associated with IPF, particularly a rapidly progressive form of this disease. Targeting IL-13 in a humanized experimental model of pulmonary fibrosis using tralokinumab (CAT354) was found to therapeutically block aberrant lung remodeling in this model. However, targeting IL-13 was also found to promote lung repair and to restore epithelial integrity. Thus, targeting IL-13 inhibits fibrotic processes and enhances repair processes in the lung.

Keywords: fibroblast; epithelium; fibrosis

Clinical Relevance

Numerous antifibrotic strategies have been used in the clinic with limited success. Here we show that IL-13 is an attractive target for idiopathic pulmonary fibrosis (IPF), being associated with rapidly progressive IPF. Moreover, blocking IL-13 in a humanized mouse model of IPF inhibits lung fibrosis and reduces epithelial apoptosis in the lung.

Idiopathic pulmonary fibrosis (IPF) is characterized by progressive scarring of the lung and ultimate decline in lung function (1, 2). One of the salient features of IPF is excess parenchymal deposition of extracellular matrix (ECM), which promotes the progressive decline in lung function observed in these patients (3). Whereas an increase in ECM components serves to promote wound sterility, restore barrier protection, and maintain the intricate architecture and function of the alveolus, this process is clearly aberrant in IPF, leading to a scarred, ablated alveolar unit unable to facilitate gas exchange (4). The cellular mechanisms leading to IPF are not completely understood, but epithelial damage is commonly observed in the lungs of these patients, and mediators from these cells, such as growth factors and cytokines, directly contribute to an increase in and the persistence of activated fibroblasts and myofibroblasts (5). IPF is highly heterogeneous, with a subset of patients showing rapid progression to death within 1 to 2 years of diagnosis and another subset of patients showing a more slowly

(Received in original form July 29, 2013; accepted in final form November 25, 2013)

This work was supported by National Institutes of Health grants RC2 HL101740 (C.M.H., F.J.M., K.R.F., H.Z., S.R.O., A.L.C., and E.L.H.) and HL109033.

Author Contributions: Conception and design: L.M., M.A.S., C.M.H. Analysis and interpretation: L.M., H.Z., S.R.O., A.L.C., A.H., M.A.S., E.L.H., C.M.H. Substantial acquisition of data: H.Z., S.R.O., A.L.C., K.R.F., J.L., D.A.K., F.J.M., E.L.H. Writing the manuscript: L.M., C.M.H.

Correspondence and requests for reprints should be addressed to Lynne A. Murray, Ph.D., MedImmune Ltd, Granta Park, Cambridge CB21 6GH, UK. E-mail: murrayl@medimmune.com

This article has an online supplement, which is accessible from this issue's table of contents at www.atsjournals.org

Am J Respir Cell Mol Biol Vol 50, Iss 5, pp 985–994, May 2014

Originally Published in Press as DOI: 10.1165/rcmb.2013-0342OC on December 10, 2013
Internet address: www.atsjournals.org

progressive disease course over a 5-year period or longer (6). The clinical heterogeneity likely reflects biological heterogeneity in aberrant lung repair pathways.

Among the more widely implicated cytokines in lung fibrosis is IL-13 (7). This Th2-type cytokine promotes lung fibrosis in a number of experimental settings (8–13), leading to the hypothesis that targeting this key profibrotic mediator alone might prevent or slow the progression of pulmonary fibrosis (7, 14). During chronic lung remodeling, there are numerous immune cell types that can produce IL-13, including T lymphocytes and alternatively activated macrophages, but other putative cellular sources of IL-13, including structural cells, have not been extensively studied. Blocking IL-13 with tralokinumab, a human IL-13–neutralizing immunoglobulin G4 monoclonal antibody, in moderate to severe uncontrolled asthma improved FEV_1 in a recent phase 2 trial (15). Tralokinumab is currently being tested clinically. The same beneficial effect on FEV_1 was reported in patients with uncontrolled asthma in another anti–IL-13 clinical trial (16). In IPF, lung levels of IL-13 are elevated (17–19) and correlate inversely with FVC (19). Both IL-13 receptor subunits (IL-13Rα1 and IL-13Rα2) are highly expressed by IPF fibroblasts (20, 21), thereby enhancing the responsiveness of these cells to IL-13 compared with normal fibroblasts (18). Controversy surrounds the mechanism whereby IL-13 promotes pulmonary fibrosis, with studies showing that it does so in either a transforming growth factor (TGF)-β–dependent (22, 23) or a TGF-β–independent (11, 24) manner. IL-13 signals through its respective receptor subunits via a JAK2-STAT6–dependent (25) and AP1-dependent (23) pathways, but this cytokine can drive lung fibrosis in a STAT6-independent manner (13), and further controversy surrounds the signaling role of IL-13Rα2 in the lung (26). Thus, IL-13 and its receptor subunits contribute to the pathogenesis of pulmonary fibrosis through a poorly defined but targetable mechanism.

In this study, we further explored IL-13–directed mechanisms in pulmonary fibrosis via the use of tralokinumab, an investigational human IgG4 monoclonal antibody that selectively neutralizes human IL-13 (27–29). We observed that the IL-13 pathway was significantly enhanced in biopsy samples from patients who exhibited a rapidly progressing form of IPF compared with patients with IPF with a slower rate of lung function loss (30), and inhibition of human IL-13 with tralokinumab attenuated established pulmonary fibrosis in a humanized SCID mouse model of IPF, notably with a reduction in lung epithelial cell damage. Together these data highlight that targeting IL-13 inhibits the fibrosis and promotes repair processes in the lung.

Materials and Methods

Additional information is provided in the online supplement.

Patient Recruitment

All studies were performed with human institutional care approval at Yale University School of Medicine, The University of Michigan School of Medicine, or UCSF. Patients with a diagnosis of IPF according to the ERS/ATS consensus statement (2) were recruited for involvement in these studies. Additional information is provided in the online supplement.

Humanized SCID Mouse Model of IPF

All studies were approved by the Institutional Animal Care and Use Committee at the University of Michigan Medical School. Female C.B-17-scid-beige (C.B-17SCID/bg) mice received single-cell preparations of IPF and normal fibroblasts (2×10^6 cells/ml) via tail vein injection. In IL-13 neutralization studies, mice were treated with PBS control, CAT251 (IgG4 mAb control, 3 mg/kg), or tralokinumab (anti–IL-13) (MedImmune, Cambridge, UK), a human recombinant IgG4 mAb that specifically binds IL-13 and blocks interactions with IL-13Rα1 and IL-13Rα2, 3 mg/kg, intraperitoneally every other day starting on Day 35. Mice were killed on Day 63 after the human pulmonary fibroblast transfer. Bronchoalveolar lavage (BAL) was taken by flushing the lungs with sterile PBS, and serum was prepared from a post mortem blood draw. Whole lung lobes were dissected for histological and biochemical analysis (*see below*).

Gene and Protein Analyses

The following samples were analyzed: single cell samples or for lung tissue analysis, lung biopsy tissue from patients with IPF/usual interstitial pneumonia, patients with nonspecific interstitial pneumonia (NSIP), the normal margins of lung tumor resections, or lungs from mice and were processed for total RNA was obtained using TRIzol reagent (Invitrogen, Carlsbad, CA) according to the manufacturer's instructions. Gene expression levels were quantitated using real-time RT-PCR (Applied Biosystems, Foster City, CA) or branched-DNA-technology–based QuantiGene Reagent System (Panomics, Freemont, CA) according to the manufacturers' protocols. Transcript levels of genes of interest measured by quantitative RT-PCR were normalized to β-actin mRNA. For protein analysis, cytokine levels were measured by bead-based Luminex analysis or specific ELISA. Serum CC16 levels were measured via CC16 assay (Caltag Medsystems, Buckingham, UK) as per the manufacturer's instructions. BAL caspase 3 activity was measured using CaspaseGlo (Promega, Mannheim, Germany) as per the manufacturer's instructions.

In Vitro Fibroblast and Epithelial Cell Assays

All fibroblast cell lines were propagated via serial passaging, and purity was assessed using morphological and immunohistochemical staining as previously described (46). Fibroblasts were grown and assayed in DMEM media, normal bronchial epithelial cells (NHBECs) were grown, and assays were performed using bronchial epithelial growth media (Cambrex, Lonza, Slough, UK). Fibroblasts or NHBECs were plated into 96-well plates (Costar, Corning, NY) at 1×10^5 cells/well and allowed to adhere for 8 hours. The cells were washed with PBS and cultured overnight in serum-free media containing 1% penicillin and 1% streptomycin at 37°C in 5% CO_2/air. Cells were stimulated with or without recombinant human IL-13 (R&D Systems, Minneapolis, MN). At the designated time points, supernatants were removed, and gene expression levels were quantitated using branched DNA technology (Panomics) as per the manufacturer's instructions. Gene expression fold induction was determined after calibration of IL13Rα2 expression with GAPDH and normalized to corresponding unstimulated cells.

Histologic Analysis

Formalin-fixed and paraffin-embedded lung sections were stained with hematoxylin and

eosin to assess gross morphology or Mallory's trichrome stains to visualize collagen deposition. A modified Ashcroft histopathology scoring scale was used to quantify fibrotic alterations by a reviewer unaware of the treatment groups (32). Briefly, the entire left lung lobe from each animal was scanned and reviewed for fibrotic alterations in the alveolar septa. The alterations varied from none (i.e., normal) to confluent fibrotic masses in at least 50% of the visible lung structure (Grade 5). Five to eight whole lung sections were scanned from each group of mice. Formalin-fixed and paraffin-embedded lung sections were analyzed for immunohistochemical localization of IL-13Rα2. These assessments are described in the online supplement.

Statistics

Normally distributed data were expressed as means ± SEM and assessed for significance by Student's *t* test or ANOVA as appropriate. Data that were not normally distributed were assessed for significance using the Wilcoxon rank sum test or Mann-Whitney U test. Patient demographics were compared using Student's *t* test or Mann-Whitney analysis. Categorical variables were compared using Fisher's exact test. *P* values were determined for multiple comparisons using the Bonferroni correction. Data were clustered using the absolute value of correlation coefficients (distance measure) with hierarchical clustering, thereby identifying the transcripts that were strongly related to each other using the R version 2.13.0 program (47). The "Ward" method, which derives spherical clusters, was used as the agglomeration algorithm for forming clusters. Values of $P \leq 0.05$, $P \leq 0.01$, and $P \leq 0.005$ were considered significant.

Results

Overexpression of IL-13 and Not IL-4 in IPF

IPF is characterized by excess ECM deposition in the lung due in part to an inappropriate IL-13–driven fibrotic process (3). Analysis of biopsied lung tissue from patients with IPF ($n = 8$) and patients with a histologically fibrotic-dominant form of NSIP ($n = 4$) or a histologically cellular-dominant form of NSIP ($n = 3$) indicated that *il-13* gene expression was more highly expressed in IPF lung tissue (Figure 1A) and that *il-4* was most up-regulated in fibrotic NSIP (Figure 1B), in comparison to nonfibrotic control tissue. To further extend this observation, we confirmed the expression of IL-13 at the protein level in lung sections using immunohistochemical approaches. Biopsies from the following histologically verified lung diseases were assembled on a tissue microarray and examined concomitantly for the presence of IL-13 protein: respiratory bronchiolitis interstitial lung disease (Figures 2A and 2C), IPF with acute exacerbation (Figure 2B), normal lung tissue (Figure 2D), fibrotic NSIP (Figure 2E), and IPF (Figure 2F). Under higher magnification (×200), it was apparent that IL-13 was most abundantly expressed in the interstitial areas of the biopsies obtained from patients with IPF who exhibited an acute exacerbation (Figure 2H) or rapid progression of disease in the first year of follow-up after disease diagnosis (Figure 2K). Substantially less IL-13 was detected in normal and stable IPF biopsy samples. Together, these data suggested that IL-13 was expressed in IPF, particularly in severe forms of this disease.

Increased IL-13 Pathway Activation in Patients with IPF Who Rapidly Progress from the Time of Diagnosis

Hierarchical cluster analysis of multiple IL-13–associated and profibrotic mediators in IPF biopsies revealed that there was a statistically significant clustering of many of these mediators; notably, *ccl26*, *ccl2*, and *cc11* were strongly associated with *cecam5*, *gata3*, and *mmp7* (Figure 3A). More importantly, *chi3l1*, *periostin*, *stat6*, *fibronectin*, *il-13rα2*, and *il-4rα* strongly correlated with the clinical parameter "percent predicted FVC" (FVCPPRED), although the relationship between these transcripts and FVCPPRED were either negative (i.e., negative values) or positive (Figure 3A). In another cohort of patients with IPF in which disease progression was known, 11 IL-13–associated transcripts, including *cst2*, *cecam5*, *cpa3*, *cnrip1*, *mfsd2a*, *cdh26*, *gsn*, *dnajc12*, *ptgs1*, *flg*, and *chi3l2*, more abundantly expressed in biopsy samples from patients that exhibited

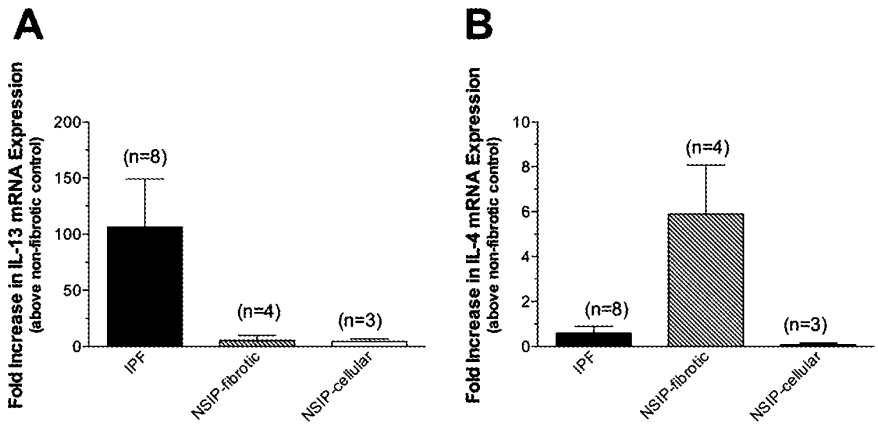

Figure 1. Elevated IL-13 transcript levels in the lungs of patients with idiopathic pulmonary fibrosis (IPF). (*A*, *B*) mRNA expression measured by quantitative RT-PCR in whole lung biopsy tissue from patients with IPF ($n = 8$) and from nonspecific interstitial pneumonia (NSIP)-fibrotic ($n = 4$) and NSIP-cellular ($n = 3$) patients and normalized to normal lung control tissue for *il-13* (*A*) and *il-4* (*B*).

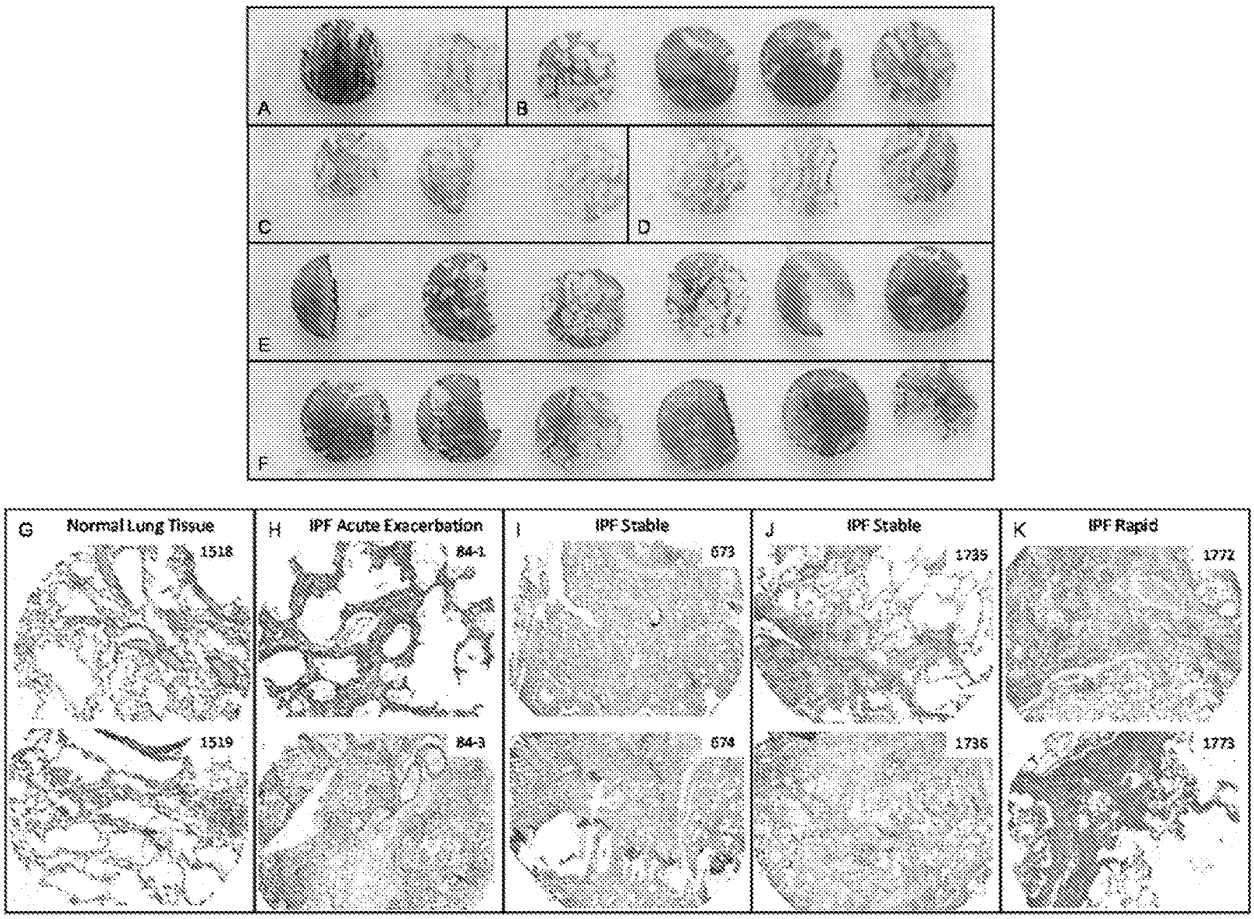

Figure 2. Immunolocalization of IL-13 in interstitial lung diseases. Lung biopsy sections, taken from patients with interstitial lung disease at the time of diagnosis, were stained with anti–IL-13 to visualize the expression of IL-13. Consecutive sections were stained with IgG control (see Figure E1 in the online supplement). Pathologist-identified diseased sections from respiratory bronchiolitis interstitial lung disease (*A*, *C*), patients with IPF who experienced an acute exacerbation within 1 year of diagnosis (*B* and *H*), normal lung tissue (*D* and *G*), fibrotic NSIP (*E*), or IPF (*F*, *I–K*). (*G–K*) Representative histological sections from normal patients and patients with IPF are at ×200 magnification.

a rapidly progressive disease compared with those who exhibited more stable disease (Figure 3B). Analysis of airway epithelial brushing samples indicated that these cells were unlikely to be the source of IL-13 because we did not detect transcripts for this mediator in any of the brushing samples (data not shown), but a subset of epithelial cells from patients with IPF was found to express IL-13–associated targets, including *il-4rα*, *il-13rα1*, *gata3*, and *mmp7* (Figure 3C). In contrast, primary human fibroblasts cultured from patients with IPF, particularly those who showed a rapid course of disease, appeared to be one source of IL-13 in the lung (Figure 3D), whereas normal human lung fibroblasts did not spontaneously release IL-13 (data not shown). Likewise, analysis of plasma from patients with IPF revealed that the IL-13–inducible chemokines CCL2 (Figure 3E) and CCL11 (Figure 3F) were significantly increased in the rapid form of IPF compared with age-matched healthy control subjects or stable patients with IPF. Finally, in this rapid cohort, an inverse correlation between plasma IL-13 levels and event time from diagnosis was observed (Figure 3G). The assessment of the relationship between lung *il-13ra2* and FVC indicated an inverse correlation where patients that had worse lung function had increased *il-13ra2* (Figure 3H). Moreover, lung *il-13ra2* positively correlated with lung *col3a1* expression, suggesting patients with greater matrix and fibrosis having elevated *il-13ra2* expression (Figure 3I). Together, these data confirmed that there is a strong IL-13 signal in IPF whole lung biopsies and plasma, particularly in patients who exhibited a rapidly progressive form of this disease.

IL-13 Directly Up-Regulates IL-13Rα2 in IPF Fibroblasts and Lung Epithelial Cells

To determine the direct effects of IL-13 on IL-13Rα2 expression, IPF fibroblasts or NHBECs were stimulated with IL-13, and *il-13ra2* gene expression and protein expression were assessed (Figure 4). Fibroblasts from patients with IPF were stimulated with increasing concentrations of IL-13 for 24 hours, and elevated *il-13ra2*

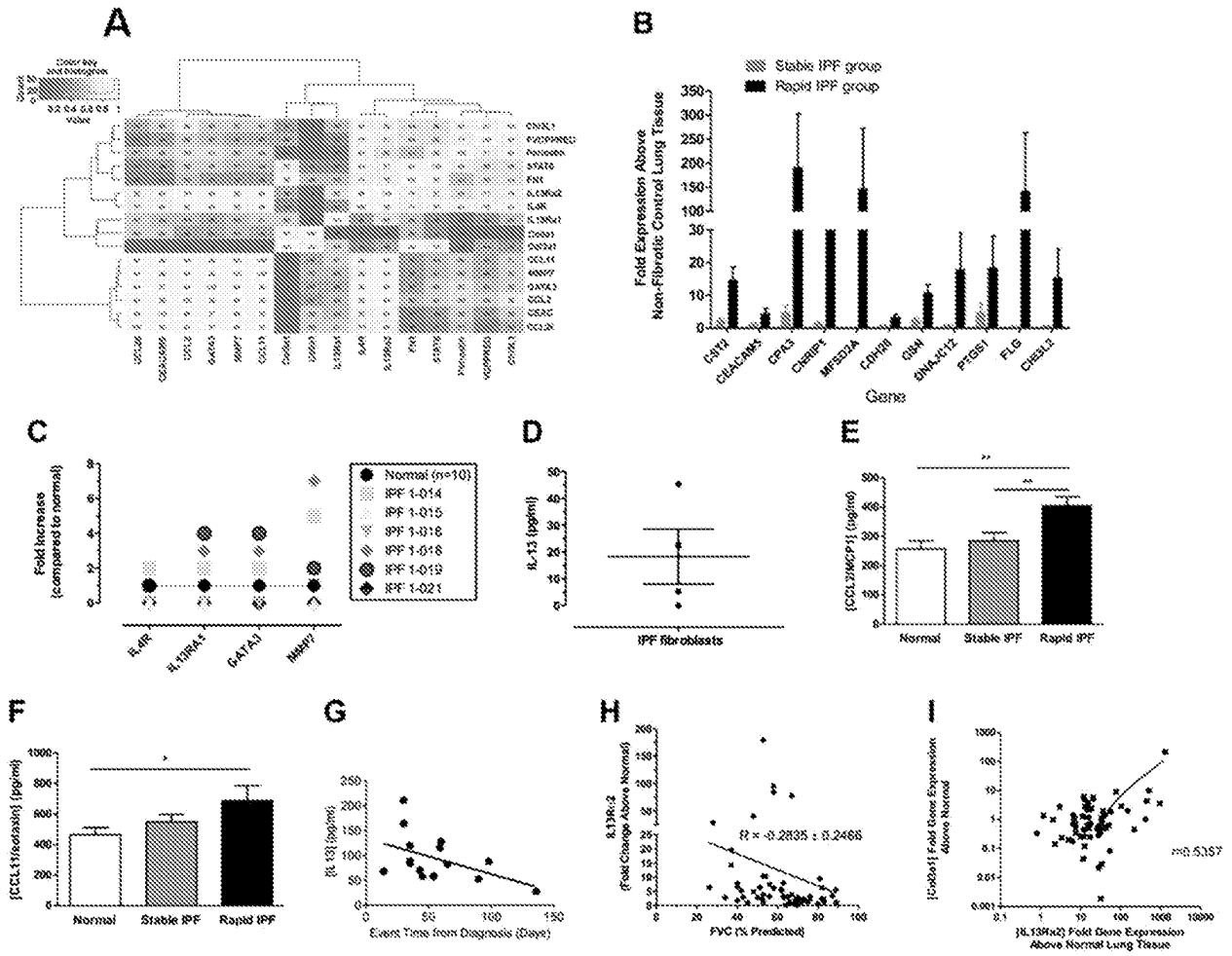

Figure 3. Elevated IL-13 pathway activation in the lungs and circulation, more closely associated with rapidly progressing IPF. (*A*) Correlations in levels of mRNA expression between IL-13 pathway genes and fibrosis markers in IPF lung biopsies ($n = 62$). Lighter colors represent greater correlations between genes. The larger value indicates a stronger the correlation. Negative values represent a negative correlation. (*B*) Increased IL-13 pathway gene expression, as measured by RT-PCR, with rapidly progressing IPF and stabling progressive IPF lung biopsies in comparison to normal healthy lung tissue. (*C*) Increased *il4r*, *il13rα1*, *gata3*, and *mmp7* in epithelial cell brushings from a subset of patients with IPF as measured by RT-PCR. (*D*) Spontaneous release of IL-13 from fibroblasts isolated from the lung biopsies of rapidly progressive patients with IPF. IL-13 was measured using specific ELISA. Data are mean ± SEM from four different patients with IPF. (*E*, *F*) Circulating CCL2/MCP-1 (*E*) and CCL11/eotaxin (*F*) were measured in the plasma of stable ($n = 19$) and rapid ($n = 14$) patients with IPF and healthy age-matched normal control subjects ($n = 20$). (*G*) Correlation of plasma IL-13 levels and the time of the first clinical event postdiagnosis in the rapid IPF patient subgroup. Correlation of lung tissue *il-13rα2* transcript expression and FVC % predicted (*H*) and *collagen 3a1* (*I*) determined by RT-PCR. Each data point represents an individual patient. $^{*}P < 0.05$, $^{**}P < 0.01$, and $^{***}P < 0.005$.

gene expression was detected by branched DNA technology (and presented as fold increase above unstimulated controls) (Figure 4A), which was confirmed and quantitated at the protein level via immunolocalization of IL13Rα2 (Figures 4B–4F). NHBECs were also stimulated with IL-13 for 24 hours, and *il-13ra2* gene induction was quantitated using branched DNA technology (Figure 4G). There were no direct effects of IL-13 on epithelial cell viability or apoptosis observed in the *in vitro* cultures (data not shown).

Immunoneutralization of Human IL-13 with Tralokinumab Therapeutically Inhibits the Pulmonary Fibrotic Response in a Humanized SCID Model

A humanized SCID mouse model in which intravenously injected IPF fibroblasts engraft in the lung and promote aberrant ECM deposition (30) was used to explore the role of human IL-13 in the progression of pulmonary fibrosis. Lung-engrafted fibroblasts also increased mouse *il-13*, *il-13rα1*, and *il-13rα2* transcript levels in a time-dependent manner in SCID mouse whole lung samples (Figures 5A–5C). To determine whether the IL-13 generated by human fibroblasts contributed to the lung remodeling, SCID mice were treated with tralokinumab from Days 35 to 63 after

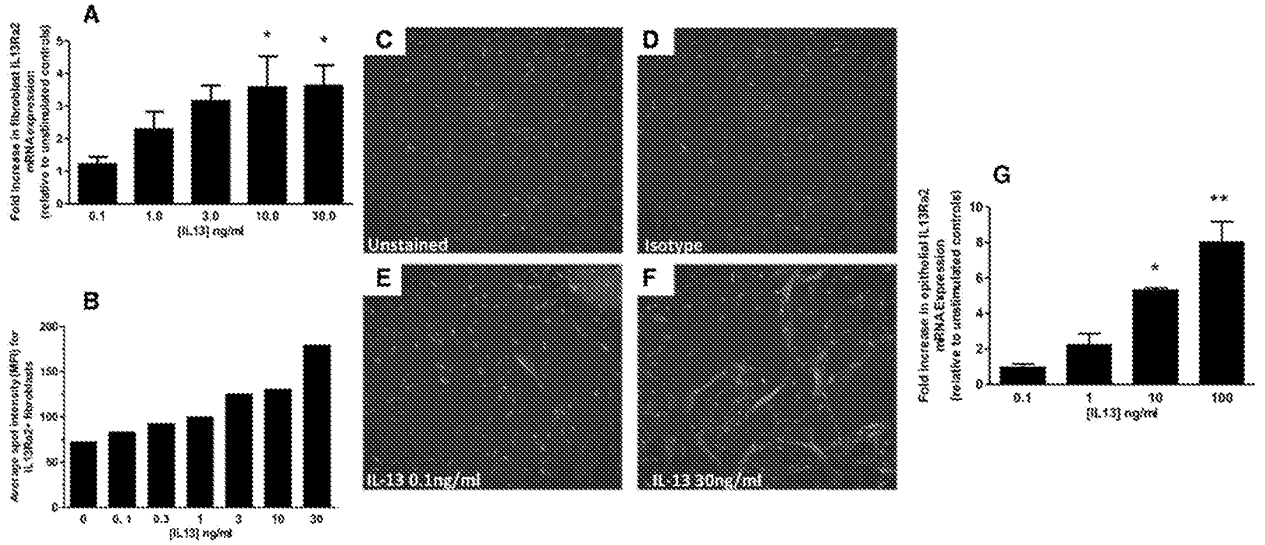

Figure 4. IL-13 stimulation of IPF fibroblasts or epithelial cells results in an up-regulation of IL-13Rα2. (*A–F*) Fibroblasts from patients with IPF were stimulated with increasing concentrations of IL-13 for 24 hours. Supernatants were taken for ELISA analysis, whereas cell monolayers were lysed and assessed for changes in gene expression compared with unstimulated controls using branched DNA technology (Panomics; *A*) or IL-13Rα2 immunolocalized using anti–IL-13Rα2 staining and quantitated (Cellomics; *B–F*). Lung epithelial cells were stimulated with IL-13 for 24 hours, and *il-13ra2* expression was determined using branched DNA technology (*G*). For fibroblast studies, data shown are mean ± SEM from four different donors (gene) and are representative of one individual donor for IL-13Ra2 surface expression (*lower graph, pictures*). Data are mean ± SEM. $^{*}P < 0.05$ and $^{**}P < 0.01$ significance in comparison to unstimulated controls.

the injection of the human fibroblasts from a patient who showed rapidly progressive disease (Figures 5D–5M). Although human IL-13 can signal via murine IL-13 receptors (31), tralokinumab only targets human IL-13 and has no neutralizing capacity on mouse IL-13 (31), indicating that these data are a consequence of inhibiting IPF fibroblast-derived human IL-13. At Day 63 after human fibroblast administration, the immunoneutralization of IL-13 reduced alveolar wall, airway epithelium, and basement membrane thickening, as observed in trichrome-stained lung sections (Figures 5D–5F). Moreover, fibrotic alterations were independently quantified using a modified Ashcroft histopathology scoring scale (32), and tralokinumab-treated mice exhibited significantly decreased fibrosis in comparison to PBS- or isotype control–treated SCID mice at Day 63 after the injection of human fibroblasts (Figure 5G). Tralokinumab also reduced serum CC16 (i.e., a marker of epithelial injury) (Figure 5H) and reduced BAL caspase 3 activity (Figure 5I) in this model. Next, the expression of IL-13Rα2 was determined via immunohistochemical analysis of whole lung samples from SCID mice at Day 63. This analysis demonstrated that there was a marked reduction of the intensity of staining in the airway epithelium of tralokinumab-treated mice when compared with both control groups (Figures 5J–5M). Further examination of lung tissue by quantitative PCR analysis showed that there was no difference in human vimentin across the three SCID groups (Figure 6A), indicating that the beneficial effects induced by blocking IL-13 were not due to an alteration in the total number of fibroblasts in the lung. Moreover, there was no difference in the transcript levels of TGF-β_1 in SCID mice treated with tralokinumab, control IgG, or PBS (Figure 6B). In contrast, tralokinumab treatment enhanced the expression of epithelial-associated genes, including E-cadherin and all of the surfactants, compared with the PBS control-treated SCID mice (Figures 6C–6G). Together, these data demonstrate that human IL-13 promotes lung fibrosis in the humanized SCID model.

Discussion

IL-13 has emerged as a potent mediator of tissue fibrosis in experimental and clinical fibrotic lung disease settings, indicating that it is a key regulator of ECM generation (14, 33). Controversy surrounds the activity of the second α subunit of the IL-13 receptor (whether stimulatory [23] or inhibitory [34]) in mediating cell activation and the TGF-β dependency of this cytokine during the fibrotic process (11, 22, 24, 26). Herein, we confirm published findings (19–21) that most extracellular and intracellular components of the IL-13 pathway show increased expression in lung biopsies from patients with IPF but present the novel finding that the strength of IL-13 signal in lung and blood samples correlates with rapidly progressive IPF. The testing of IL-13 targeting approaches in pulmonary fibrosis has been largely limited to experimental approaches targeting murine IL-13 (7), whereas the data presented herein are among the first to show that targeting fibroblast-derived human IL-13 with a novel human mAb, tralokinumab, attenuated lung fibrosis and the accumulation of ECM in a humanized SCID model of IPF. In this IPF model, the targeting of human IL-13 led to improvements in the expression of transcripts associated with healthy lung epithelium, as indicated by reduced lung

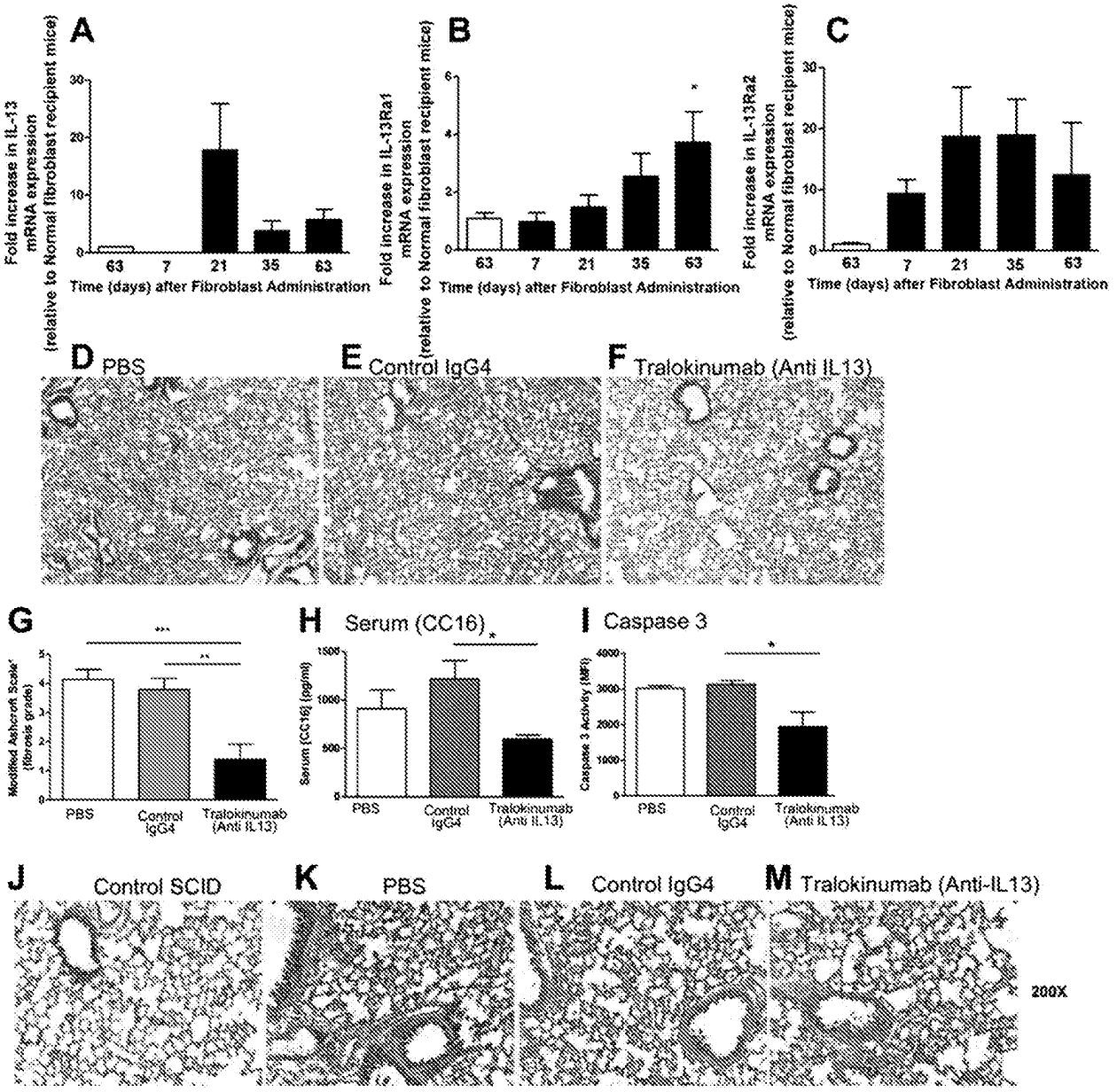

Figure 5. Neutralization of fibroblast-derived IL-13 inhibits lung fibrosis in an established fibroblast-driven disease setting in humanized SCID mice. (*A–C*) Isolated IPF fibroblasts ($n = 5$) or normal lung tissue fibroblasts ($n = 5$) were injected intravenously to SCID mice, and animals were killed at specific subsequent time points. Whole lung mRNA expression was measured by quantitative RT-PCR for *il-13* (*A*), *Il13rα1* (*B*), and *il-13rα2* (*C*) and normalized to lung mRNA expression levels from mice that had received normal lung tissue-derived fibroblasts. (*D–M*) Thirty-five days after IPF fibroblast engraftment, mice were randomized and treated with PBS control, control IgG4, or tralokinumab (anti–IL-13 mAb) every other day until analysis at Day 63. Representative mouse lung sections stained with Masson's trichrome to depict the degree of fibrosis at Day 63 from SCID/IPF mice treated with PBS control (*D*), CAT251 IgG_4 isotype control (*E*), and tralokinumab anti–IL-13 antibody (*F*). Fibrosis was quantitated in all animals using a modified Ashcroft score of histological sections (*G*). Tralokinumab attenuated serum CC16 levels as measured by ELISA (*H*) and BAL caspase 3 activity (*I*). Data are mean ± SEM ($n = 5$). (*J–M*) Representative immunohistochemistry localizing IL-13Rα2 expression in the lungs of control SCID mice that have not received IPF fibroblast (*J*) or SCID/IPF mice treated with PBS control (*K*), isotype control (*L*), or tralokinumab (*M*). Original magnification: *top panels*, ×40; *bottom panels*, ×200. $^*P < 0.05$, $^{**}P < 0.01$, and $^{***}P < 0.005$.

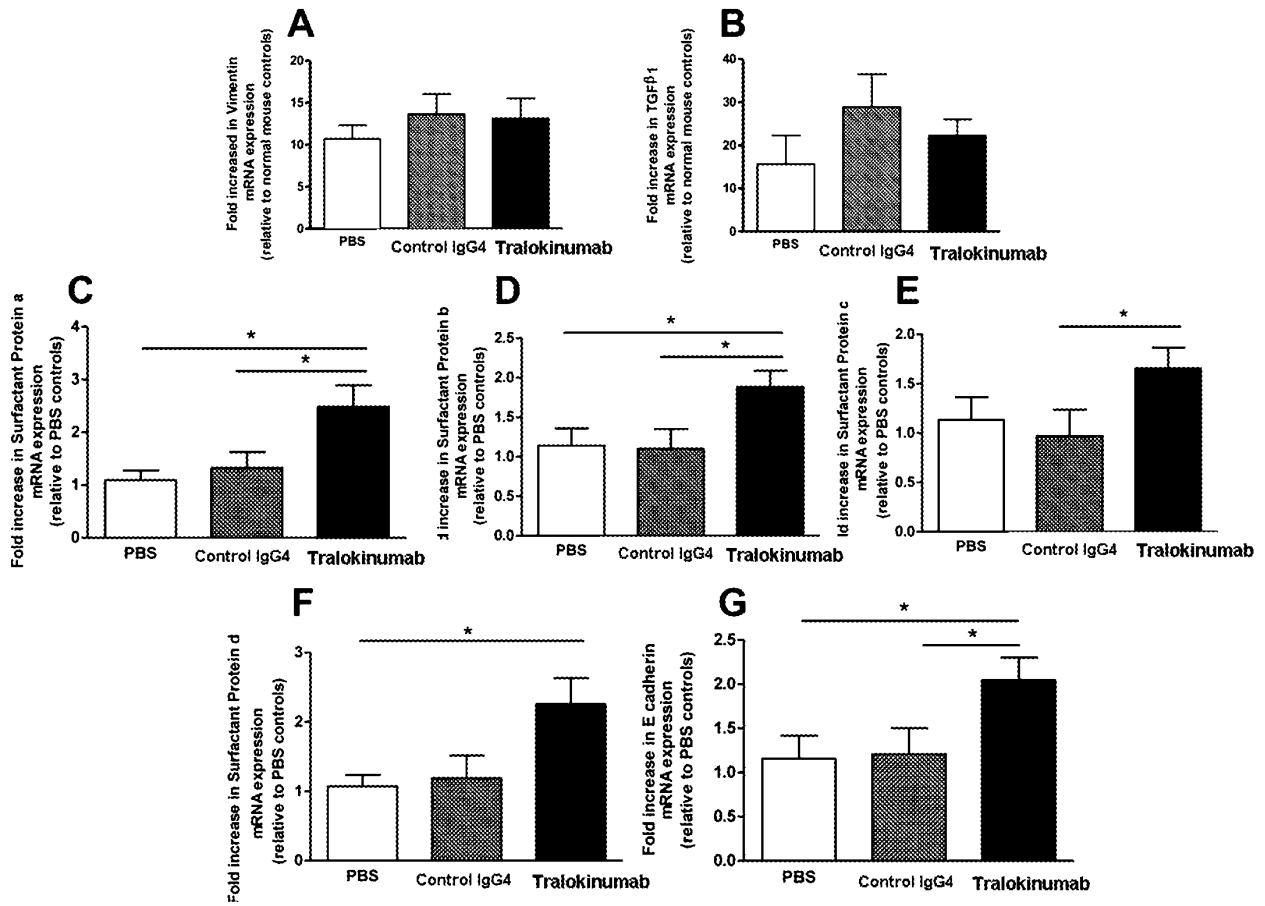

Figure 6. Enhanced epithelial markers in the lungs of SCID/IPF mice treated with tralokinumab. Whole lung mRNA expression from mice treated with isotype control or tralokinumab (anti–IL-13) was measured using quantitative RT-PCR. Levels of vimentin (*A*), TGF-β1 (*B*), surfactant protein a (*C*), surfactant protein b (*D*), surfactant protein c (*E*), surfactant protein d (*F*), and e-cadherin (*G*) were quantitated and normalized to lung mRNA expression levels from SCID/IPF mice that had received PBS control only. Data are mean ± SEM ($n = 5$). *$P < 0.05$.

apoptosis and markers of epithelial injury. Thus, the results from this study demonstrate that IL-13 is elevated in and contributes to IPF, perhaps leading to the rapid progression of this disease due to its inhibitory effects on lung repair mechanisms.

Patients with IPF experience a gradual worsening of symptoms (2, 6) or a rapid disease course punctuated by acute exacerbations (6), which highlights the heterogeneity in the clinical course of this disease (35, 36). When patients exhibit physiologic decline or a clinical event in the first year of follow-up, they are considered to have "rapid progression" (36). Although longitudinal changes in lung physiology (i.e., FVCPPRED) have been extensively studied as a surrogate of lung fibrosis (37), these measurements provide no information about biological pathways that might be driving lung fibrosis in each patient. Recent studies have suggested that the IL-13 pathway might predict progression in IPF. For example, elevated levels of periostin, an IL-13–inducible matricellular protein, have been recently described to be associated with rapidly progressive forms of IPF (38). Experimentally, periostin promotes myofibroblast differentiation and contributes to bleomycin-induced lung fibrosis (39). From the present study, there was a strong inverse correlation between FVCPPRED and many IL-13–induced factors, including *chi3L1*, *stat6*, *fn1*, *il13rα2*, and *il4rα* in IPF. It was also evident that additional IL-13–related factors, including *cst2*, *gsn*, and *cdh26*, were significantly enhanced in biopsy samples from patients who exhibited a rapidly progressing form of IPF compared with those patients with IPF with a slower rate of lung function loss. Specifically, gelsolin (*gsn*) is an actin-regulating protein that has been shown to contribute to cardiac remodeling after experimental myocardial infarction (40), but its role in pulmonary fibrosis requires further investigation. Other IL-13–inducible factors, including profibrotic CCL2 (18) and CCL11 (41), were detected at elevated levels in the circulation of patients with rapidly progressive disease compared with normal lung biopsies or with biopsies from patients who exhibited a more stable course of disease. Although freshly isolated

epithelial cells from patients with IPF did not appear to be a source of IL-13, these cells appeared to be affected by this cytokine on the basis of the increased *stat6* expression status in these cells compared with normal epithelial cells. Surprisingly, a prominent source of IL-13 appeared to be stromal fibroblasts on the basis of our survey of histological lung biopsy samples and cultured primary lung fibroblasts. Thus, IL-13 and several of its induced factors were prominently expressed in IPF, particularly in a subset of these patients who exhibited a rapid progression from the time of diagnosis.

The discovery that human IPF fibroblasts generate IL-13 allowed for an *in vivo* study directed at the role of this cytokine in a humanized SCID model of IPF (30, 42). An antibody-based approach was used in this model using a recombinant human IgG4, tralokinumab, which blocks human IL-13. The administration of tralokinumab at Day 35 after the injection of human IPF fibroblasts and the establishment of fibrosis in the lungs of SCID mice (42) led to a significant reduction in quantifiable histological (i.e., reduced alveolar wall thickening, airway epithelium thickness, and basement membrane thickness), circulating (i.e., serum CC16), and lung-associated (i.e., reduced BAL caspase 3 activity) markers of lung fibrosis compared with PBS- or control IgG4-treated SCID mice that received the same IPF fibroblasts. Taken together, these data indicate that tralokinumab reduced lung fibrosis by inhibiting the profibrotic pathway evoked by IPF fibroblast-derived human IL-13 in a SCID IPF model, leading to improved lung repair. The improved epithelial appearance and reduced apoptosis observed in the tralokinumab-treated humanized SCID mice did not appear to be a direct consequence of IL-13 on the mouse airway epithelium because we observed no proapoptotic effects of IL-13 on the epithelium *in vitro*. However, fibroblasts isolated from fibrotic lung tissue have been shown to promote epithelial cell apoptosis (43), so it is plausible that IL-13 may be acting to modulate the levels of antiapoptotic factors *in vivo*. For example, prostaglandin E_2 has been shown to attenuate epithelial–fibroblast profibrotic responses (44), and dinoprostone protects epithelial cells from apoptosis while promoting fibroblast apoptosis (45). In addition, there may also be a wider role for IL-13 in patients with IPF because fibroblasts are not the only source of IL-13 in IPF, and other cells, including T and B cells, appear to be involved in the pathogenesis of this disease. This is one of the limitations of using a SCID model, in that T and B cells are absent. However, on the basis of our immunolocalization studies in our *in vivo* model, fibroblasts appear to also be a source of this profibrotic cytokine, and blocking IL-13 with tralokinumab had a significant antifibrotic effect in this humanized SCID system. Thus, further assessment of the link between IL-13 and epithelial protective factors, including prostaglandins, in this model is warranted in future studies.

In conclusion, the present study demonstrates that IL-13 contributes to the progression of IPF via its profibrotic and antirepair effects in the lung. The strong correlation between the IL-13 pathway and rapidly progressing IPF is of considerable clinical importance given that predicting rapid progression should allow for timely referral of eligible patients for clinical therapeutic trials or for lung transplantation. ▩

Author disclosures are available with the text of this article at www.atsjournals.org.

Acknowledgments: The authors thank the UCSF ILD program for supplying IPF patient cells, Robin Kunkel for her graphic design assistance, and Kandace Bonner and Rebecca Dunmore for technical assistance.

References

1. Kuhn C III, Boldt J, King TE Jr, Crouch E, Vartio T, McDonald JA. An immunohistochemical study of architectural remodeling and connective tissue synthesis in pulmonary fibrosis. *Am Rev Respir Dis* 1989;140:1693–1703.
2. American Thoracic Society; European Respiratory Society. American Thoracic Society/European Respiratory Society International multidisciplinary consensus classification of the idiopathic interstitial pneumonias. *Am J Respir Crit Care Med* 2002;165:277–304.
3. Gross TJ, Hunninghake GW. Idiopathic pulmonary fibrosis. *N Engl J Med* 2001;345:517–525.
4. Singer AJ, Clark RA. Cutaneous wound healing. *N Engl J Med* 1999;341: 738–746.
5. Scotton CJ, Chambers RC. Molecular targets in pulmonary fibrosis: the myofibroblast in focus. *Chest* 2007;132:1311–1321.
6. Martinez FJ, Safrin S, Weycker D, Starko KM, Bradford WZ, King TE Jr, Flaherty KR, Schwartz DA, Noble PW, Raghu G, *et al.*; IPF Study Group. The clinical course of patients with idiopathic pulmonary fibrosis. *Ann Intern Med* 2005;142:963–967.
7. Wilson MS, Wynn TA. Pulmonary fibrosis: pathogenesis, etiology and regulation. *Mucosal Immunol* 2009;2:103–121.
8. Zhu Z, Homer RJ, Wang Z, Chen Q, Geba GP, Wang J, Zhang Y, Elias JA. Pulmonary expression of interleukin-13 causes inflammation, mucus hypersecretion, subepithelial fibrosis, physiologic abnormalities, and eotaxin production. *J Clin Invest* 1999;103:779–788.
9. Jakubzick C, Kunkel SL, Puri RK, Hogaboam CM. Therapeutic targeting of IL-4- and IL-13-responsive cells in pulmonary fibrosis. *Immunol Res* 2004;30:339–349.
10. Belperio JA, Dy M, Burdick MD, Xue YY, Li K, Elias JA, Keane MP. Interaction of IL-13 and C10 in the pathogenesis of bleomycin-induced pulmonary fibrosis. *Am J Respir Cell Mol Biol* 2002;27: 419–427.
11. Kolodsick JE, Toews GB, Jakubzick C, Hogaboam C, Moore TA, McKenzie A, Wilke CA, Chrisman CJ, Moore BB. Protection from fluorescein isothiocyanate-induced fibrosis in IL-13-deficient, but not IL-4-deficient, mice results from impaired collagen synthesis by fibroblasts. *J Immunol* 2004;172:4068–4076.
12. Keane MP, Gomperts BN, Weigt S, Xue YY, Burdick MD, Nakamura H, Zisman DA, Ardehali A, Saggar R, Lynch JP III, *et al.* IL-13 is pivotal in the fibro-obliterative process of bronchiolitis obliterans syndrome. *J Immunol* 2007;178:511–519.
13. Blease K, Schuh JM, Jakubzick C, Lukacs NW, Kunkel SL, Joshi BH, Puri RK, Kaplan MH, Hogaboam CM. Stat6-deficient mice develop airway hyperresponsiveness and peribronchial fibrosis during chronic fungal asthma. *Am J Pathol* 2002;160:481–490.
14. Kasaian MT, Miller DK. IL-13 as a therapeutic target for respiratory disease. *Biochem Pharmacol* 2008;76:147–155.
15. Piper E, Brightling C, Niven R, Oh C, Faggioni R, Poon K, She D, Kell C, May RD, Geba GP, *et al.* A phase II placebo-controlled study of tralokinumab in moderate-to-severe asthma. *Eur Respir J* 2013;41: 330–338.
16. Corren J, Lemanske RF, Hanania NA, Korenblat PE, Parsey MV, Arron JR, Harris JM, Scheerens H, Wu LC, Su Z, *et al.* Lebrikizumab treatment in adults with asthma. *N Engl J Med* 2011;365: 1088–1098.
17. Hancock A, Armstrong L, Gama R, Millar A. Production of interleukin 13 by alveolar macrophages from normal and fibrotic lung. *Am J Respir Cell Mol Biol* 1998;18:60–65.

18. Murray LA, Argentieri RL, Farrell FX, Bracht M, Sheng H, Whitaker B, Beck H, Tsui P, Cochlin K, Evanoff HL, *et al.* Hyper-responsiveness of IPF/UIP fibroblasts: interplay between TGFbeta1, IL-13 and CCL2. *Int J Biochem Cell Biol* 2008;40:2174–2182.
19. Park SW, Ahn MH, Jang HK, Jang AS, Kim DJ, Koh ES, Park JS, Uh ST, Kim YH, Park JS, *et al.* Interleukin-13 and its receptors in idiopathic interstitial pneumonia: clinical implications for lung function. *J Korean Med Sci* 2009;24:614–620.
20. Jakubzick C, Choi ES, Carpenter KJ, Kunkel SL, Evanoff H, Martinez FJ, Flaherty KR, Toews GB, Colby TV, Travis WD, *et al.* Human pulmonary fibroblasts exhibit altered interleukin-4 and interleukin-13 receptor subunit expression in idiopathic interstitial pneumonia. *Am J Pathol* 2004;164:1989–2001.
21. Jakubzick C, Choi ES, Kunkel SL, Evanoff H, Martinez FJ, Puri RK, Flaherty KR, Toews GB, Colby TV, Kazerooni EA, *et al.* Augmented pulmonary IL-4 and IL-13 receptor subunit expression in idiopathic interstitial pneumonia. *J Clin Pathol* 2004;57:477–486.
22. Lee CG, Homer RJ, Zhu Z, Lanone S, Wang X, Koteliansky V, Shipley JM, Gotwals P, Noble P, Chen Q, *et al.* Interleukin-13 induces tissue fibrosis by selectively stimulating and activating transforming growth factor beta(1). *J Exp Med* 2001;194:809–821.
23. Fichtner-Feigl S, Strober W, Kawakami K, Puri RK, Kitani A. Il-13 signaling through the il-13alpha(2) receptor is involved in induction of tgf-beta(1) production and fibrosis. *Nat Med* 2006;12:99–106.
24. Kaviratne M, Hesse M, Leusink M, Cheever AW, Davies SJ, McKerrow JH, Wakefield LM, Letterio JJ, Wynn TA. IL-13 activates a mechanism of tissue fibrosis that is completely TGF-beta independent. *J Immunol* 2004;173:4020–4029.
25. Nishimura Y, Nitto T, Inoue T, Node K. IL-13 attenuates vascular tube formation via JAK2-STAT6 pathway. *Circ J* 2008;72:469–475.
26. Zheng T, Liu W, Oh SY, Zhu Z, Hu B, Homer RJ, Cohn L, Grusby MJ, Elias JA. IL-13 receptor alpha2 selectively inhibits IL-13-induced responses in the murine lung. *J Immunol* 2008;180:522–529.
27. Blanchard C, Mishra A, Saito-Akei H, Monk P, Anderson I, Rothenberg ME. Inhibition of human interleukin-13-induced respiratory and oesophageal inflammation by anti-human-interleukin-13 antibody (CAT-354). *Clin Exp Allergy* 2005;35:1096–1103.
28. Oh CK, Faggioni R, Jin F, Roskos LK, Wang B, Birrell C, Wilson R, Molfino NA. An open-label, single-dose bioavailability study of the pharmacokinetics of CAT-354 after subcutaneous and intravenous administration in healthy males. *Br J Clin Pharmacol* 2010;69: 645–655.
29. Piper E, Brightling CE, Niven R, Oh CK, Faggioni R, Poon K, She D, Kell C, Geba GP, Molfino NA. A phase II placebo-controlled study of tralokinumab in moderate-to-severe asthma. *Eur Respir J* 2013;41: 330–338.
30. Trujillo G, Meneghin A, Flaherty KR, Sholl LM, Myers JL, Kazerooni EA, Gross BH, Oak SR, Coelho AL, Evanoff H, *et al.* TLR9 differentiates rapidly from slowly progressing forms of idiopathic pulmonary fibrosis. *Sci Transl Med* 2010;2:57ra82.
31. May RD, Monk PD, Cohen ES, Manuel D, Dempsey F, Davis NH, Dodd AJ, Corkill DJ, Woods J, Joberty-Candotti C, *et al.* Preclinical development of CAT-354, an IL-13 neutralizing antibody, for the treatment of severe uncontrolled asthma. *Br J Pharmacol* 2012;166: 177–193.
32. Hubner RH, Gitter W, El Mokhtari NE, Mathiak M, Both M, Bolte H, Freitag-Wolf S, Bewig B. Standardized quantification of pulmonary fibrosis in histological samples. *BioTechniques* 2008;44:507–511, 514–517.
33. Wynn TA. IL-13 effector functions. *Annu Rev Immunol* 2003;21: 425–456.
34. Chiaramonte MG, Mentink-Kane M, Jacobson BA, Cheever AW, Whitters MJ, Goad ME, Wong A, Collins M, Donaldson DD, Grusby MJ, *et al.* Regulation and function of the interleukin 13 receptor alpha 2 during a T helper cell type 2-dominant immune response. *J Exp Med* 2003;197:687–701.
35. Kim DS, Collard HR, King TE Jr. Classification and natural history of the idiopathic interstitial pneumonias. *Proc Am Thorac Soc* 2006;3: 285–292.
36. Kim DS, Park JH, Park BK, Lee JS, Nicholson AG, Colby T. Acute exacerbation of idiopathic pulmonary fibrosis: frequency and clinical features. *Eur Respir J* 2006;27:143–150.
37. Collard HR, King TE Jr, Bartelson BB, Vourlekis JS, Schwarz MI, Brown KK. Changes in clinical and physiologic variables predict survival in idiopathic pulmonary fibrosis. *Am J Respir Crit Care Med* 2003;168: 538–542.
38. Okamoto M, Hoshino T, Kitasato Y, Sakazaki Y, Kawayama T, Fujimoto K, Ohshima K, Shiraishi H, Uchida M, Ono J, *et al.* Periostin, a matrix protein, is a novel biomarker for idiopathic interstitial pneumonias. *Eur Respir J* 2011;37:1119–1127.
39. Uchida M, Shiraishi H, Ohta S, Arima K, Taniguchi K, Suzuki S, Okamoto M, Ahlfeld SK, Ohshima K, Kato S, *et al.* Periostin, a matricellular protein, plays a role in the induction of chemokines in pulmonary fibrosis. *Am J Respir Cell Mol Biol* 2012;46:677–686.
40. Li GH, Shi Y, Chen Y, Sun M, Sader S, Maekawa Y, Arab S, Dawood F, Chen M, De Couto G, *et al.* Gelsolin regulates cardiac remodeling after myocardial infarction through DNase I-mediated apoptosis. *Circ Res* 2009;104:896–904.
41. Puxeddu I, Bader R, Piliponsky AM, Reich R, Levi-Schaffer F, Berkman N. The CC chemokine eotaxin/CCL11 has a selective profibrogenic effect on human lung fibroblasts. *J Allergy Clin Immunol* 2006;117: 103–110.
42. Pierce EM, Carpenter K, Jakubzick C, Kunkel SL, Flaherty KR, Martinez FJ, Hogaboam CM. Therapeutic targeting of CC ligand 21 or CC chemokine receptor 7 abrogates pulmonary fibrosis induced by the adoptive transfer of human pulmonary fibroblasts to immunodeficient mice. *Am J Pathol* 2007;170:1152–1164.
43. Uhal BD, Joshi I, True AL, Mundle S, Raza A, Pardo A, Selman M. Fibroblasts isolated after fibrotic lung injury induce apoptosis of alveolar epithelial cells in vitro. *Am J Physiol* 1995;269:L819–L828.
44. Bozyk PD, Moore BB. Prostaglandin E2 and the pathogenesis of pulmonary fibrosis. *Am J Respir Cell Mol Biol* 2011;45:445–452.
45. Maher TM, Evans IC, Bottoms SE, Mercer PF, Thorley AJ, Nicholson AG, Laurent GJ, Tetley TD, Chambers RC, McAnulty RJ. Diminished prostaglandin E2 contributes to the apoptosis paradox in idiopathic pulmonary fibrosis. *Am J Respir Crit Care Med* 2010;182:73–82.
46. Hogaboam CM, Bone-Larson CL, Lipinski S, Lukacs NW, Chensue SW, Strieter RM, Kunkel SL. Differential monocyte chemoattractant protein-1 and chemokine receptor 2 expression by murine lung fibroblasts derived from Th1- and Th2-type pulmonary granuloma models. *J Immunol* 1999;163:2193–2201.
47. R Core Team. R: a language and environment for statistical computing. Vienna, Austria: R: A Language and Environment for Statistical Computing; 2014 [updated 2014 Feb, accessed 2014 Feb 6]. Available from: http://www.r-project.org/

ONLINE DATA SUPPLEMENT

Targeting IL-13 with tralokinumab attenuates lung fibrosis and epithelial damage in a humanized SCID IPF model

Lynne A. Murray, Huilan Zhang, Sameer R. Oak, Ana Lucia Coelho, Athula Herath, Kevin R. Flaherty, Joyce Lee, Matt Bell, Darryl A. Knight, Fernando J. Martinez, Matthew A. Sleeman, Erica L. Herzog and Cory M. Hogaboam

Supplemental Information

MATERIALS AND METHODS

Patients: All studies were performed with Human Investigations Committee approval at Yale University School of Medicine or University of Michigan School of Medicine. For the plasma and monocyte studies, inclusion criteria were: All patients were greater than 18 years of age who had been diagnosed with IPF/UIP based on the ATS/ERS 2002 guidelines were eligible for enrolment. Exclusion criteria included current or recent use (within 2 months) of immunosuppression or experimental therapy; chronic infection such as HIV, tuberculosis, or hepatitis; known pulmonary hypertension, COPD, or asthma; unstable cardiovascular, renal or neurologic disease; and inability to provide informed consent. Healthy, age-matched controls who self-identified as normal were recruited from the greater New Haven area. Following enrolment and written informed consent, demographic data concerning age, race, sex, and co-morbid conditions were collected on all subjects. In addition, data regarding restrictive ventilatory defect (decreased forced vital capacity, or FVC) and diffusion impairment (decreased diffusion capacity for carbon monoxide, DLCO) and how the diagnosis of IPF/UIP (biopsy or CT scan) was made were obtained from chart abstraction on the patients with IPF/UIP. After one year of follow up, patient charts were reviewed for the following IPF/UIP-relevant outcomes and the time point of occurrence since diagnosis was recorded: Significant (10%) decline in FVC in 6 months following enrolment, new oxygen requirement, hospitalization or treatment for exacerbation of IPF/UIP, and death by any cause.

Immunohistochemical localization of IL13Rα2 in histological tissue sections. Formalin-fixed and paraffin-embedded lung sections were analyzed for immunohistochemical localization of IL13Rα2 as previously described (1). Sections were blocked with normal rabbit serum (Vectorstain ABC-AP kit, Vector Laboratories, Burlingame, CA). Rabbit anti-mouse IL13Rα2 antibody (R&D Systems) and control normal rabbit IgG were diluted in PBS to a final concentration of 5 μg/ml. A secondary rabbit anti-goat biotinylated antibody (Vector Laboratories) was added to each section, then each slide was thoroughly washed and receptor localization was revealed using HRP-Dab Staining Kit (R&D Systems).

FIGURE LEGEND

S1. Corresponding IgG control staining of the lung sections stained for IL-13 in Figure 2.

E1. Jakubzick C, Choi ES, Joshi BH, Keane MP, Kunkel SL, Puri RK, Hogaboam CM. Therapeutic attenuation of pulmonary fibrosis via targeting of il-4- and il-13-responsive cells *J Immunol* 2003;171:2684-2693.

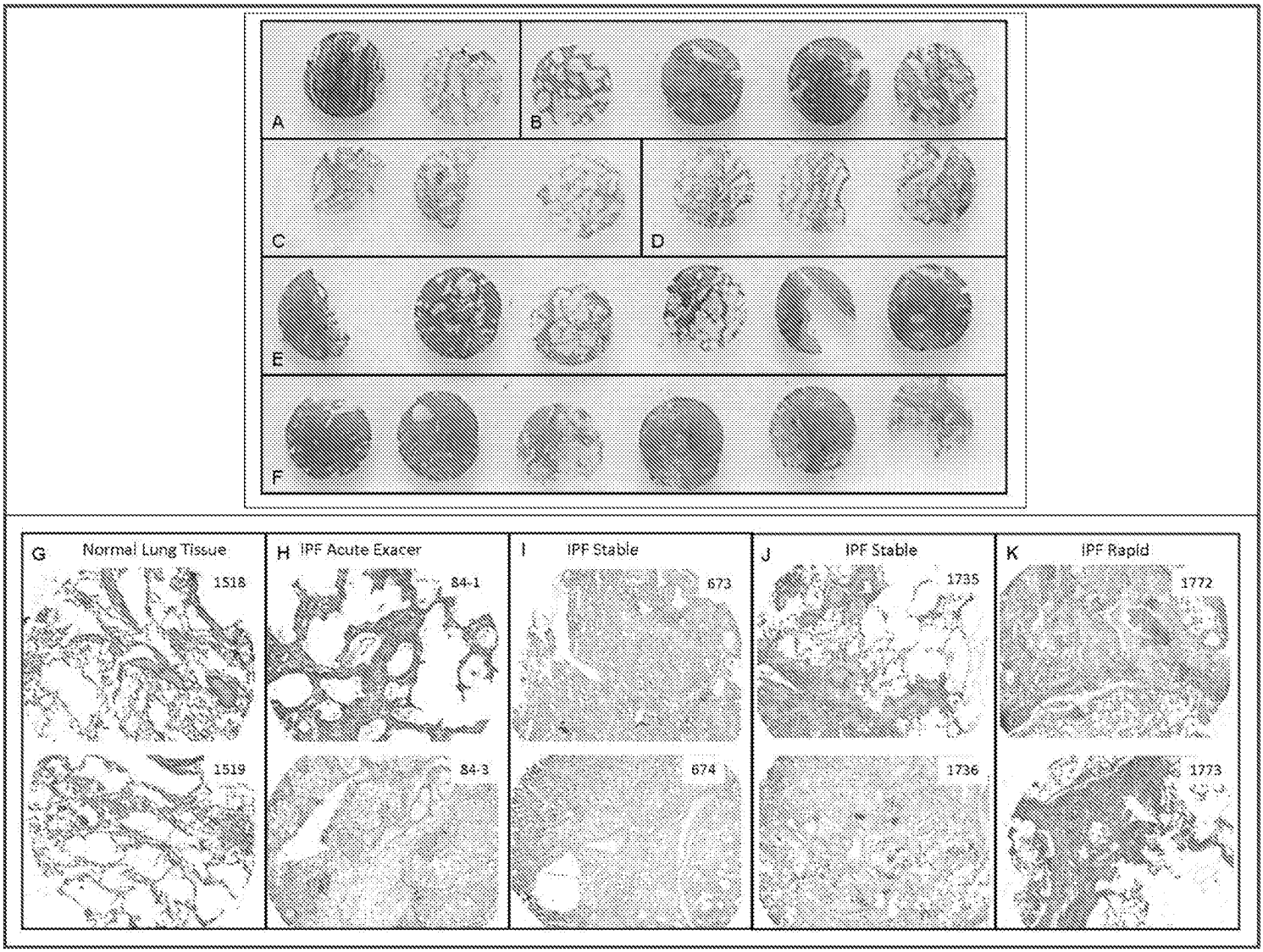
A
B
C
D
E
F
G Normal Lung Tissue
1518
1519
H IPF Acute Exacer
84-1
84-3
I IPF Stable
673
674
J IPF Stable
1735
1736
K IPF Rapid
1772
1773

Therapeutic Activation of Signal Transducer and Activator of Transcription 3 by Interleukin-11 Ameliorates Cardiac Fibrosis After Myocardial Infarction

Masanori Obana, MS; Makiko Maeda, PhD; Koji Takeda, MD; Akiko Hayama, MS; Tomomi Mohri, PhD; Tomomi Yamashita, BS; Yoshikazu Nakaoka, MD, PhD; Issei Komuro, MD, PhD; Kiyoshi Takeda, MD, PhD; Goro Matsumiya, MD, PhD; Junichi Azuma, MD; Yasushi Fujio, MD, PhD

Background—Glycoprotein 130 is the common receptor subunit for the interleukin (IL)-6 cytokine family. Previously, we reported that pretreatment of IL-11, an IL-6 family cytokine, activates the glycoprotein 130 signaling pathway in cardiomyocytes and prevents ischemia/reperfusion injury in vivo; however, its long-term effects on cardiac remodeling after myocardial infarction (MI) remain to be elucidated.

Methods and Results—MI was generated by ligating the left coronary artery in C57BL/6 mice. Real-time reverse transcription polymerase chain reaction analyses showed that IL-11 mRNA was remarkably upregulated in the hearts exposed to MI. Intravenous injection of IL-11 activated signal transducer and activator of transcription 3 (STAT3), a downstream signaling molecule of glycoprotein 130, in cardiomyocytes in vivo, suggesting that cardiac myocytes are target cells of IL-11 in the hearts. Twenty-four hours after coronary ligation, IL-11 was administered intravenously, followed by consecutive administration every 24 hours for 4 days. IL-11 treatment reduced fibrosis area 14 days after MI, attenuating cardiac dysfunction. Consistent with a previous report that STAT3 exhibits antiapoptotic and angiogenic activity in the heart, IL-11 treatment prevented apoptotic cell death of the bordering myocardium adjacent to the infarct zone and increased capillary density at the border zone. Importantly, cardiac-specific ablation of STAT3 abrogated IL-11–mediated attenuation of fibrosis and was associated with left ventricular enlargement. Moreover, with the use of cardiac-specific transgenic mice expressing constitutively active STAT3, cardiac STAT3 activation was shown to be sufficient to prevent adverse cardiac remodeling.

Conclusions—IL-11 attenuated cardiac fibrosis after MI through STAT3. Activation of the IL-11/glycoprotein 130/STAT3 axis may be a novel therapeutic strategy against cardiovascular diseases. **(*Circulation*. 2010;121:684-691.)**

Key Words: interleukins ■ myocardial infarction ■ remodeling ■ signal transduction

After myocardial injury, various kinds of neurohumoral factors and cytokines modulate cardiac remodeling. Among them, leukemia inhibitory factor (LIF) and cardiotrophin-1, which belong to the interleukin (IL)-6 family, play important roles in cardioprotection.[1,2] LIF and cardiotrophin-1 are secreted from cardiomyocytes in response to pathological stress.[3–5] These cytokines bind and activate LIF receptor in cardiomyocytes.[6] Activated LIF receptor makes a dimer with glycoprotein 130 (gp130), followed by activation of signal transducer and activator of transcription 3 (STAT3).[7] STAT3 activation promotes cardiomyocyte survival and vascular formation in the heart.[8–10] Thus, cardiac activation of the gp130/STAT3 system may be a potential therapeutic strategy against cardiovascular diseases; however, therapies targeting gp130 have not been proposed.

Clinical Perspective on p 691

The difficulty in therapeutic activation of gp130 is derived from its receptor system. Gp130 is expressed ubiquitously as the common receptor subunit of IL-6 family cytokines.[11] IL-6 family cytokines bind their specific receptor α subunits, followed by activation of a common gp130 receptor. Pleiotropic effects of IL-6 family cytokines are explained by the differential expression of receptor α subunits. Most members of the IL-6 family, whose receptor α subunits are expressed abundantly in inflammatory cells, would evoke severe in-

Received July 14, 2009; accepted December 4, 2009.

From the Department of Clinical Pharmacology and Pharmacogenomics, Graduate School of Pharmaceutical Sciences, Osaka University, Osaka, Japan (M.O., A.H., T.M., T.Y., J.A., Y.F.); Department of Clinical Pharmacogenomics, School of Pharmacy, Hyogo University of Health Sciences, Hyogo, Japan (M.M., J.A.); and Department of Cardiovascular Surgery (K.T., G.M.), Department of Cardiovascular Medicine (Y.N., I.K.), and Laboratory of Immune Regulation, Department of Microbiology and Immunology (K.T.), Graduate School of Medicine, Osaka University, Osaka, Japan.

The online-only Data Supplement is available with this article at http://circ.ahajournals.org/cgi/content/full/CIRCULATIONAHA.109.893677/DC1.

Correspondence to Yasushi Fujio, MD, PhD, 1-6 Yamada-oka, Suita City, 565-0871, Osaka, Japan. E-mail fujio@phs.osaka-u.ac.jp

Circulation **is available at http://circ.ahajournals.org** **DOI: 10.1161/CIRCULATIONAHA.109.893677**

flammation[12] as a serious adverse event if administered systemically. Therefore, to achieve clinical use of IL-6 family cytokines, the cytokine that induces only a tolerable level of inflammation should be selected.

IL-11 is a hematopoietic IL-6 family cytokine with pleiotropic effects. IL-11 exhibits thrombopoietic activity, and recombinant human IL-11 is used clinically for thrombocytopenia.[13] In contrast to other IL-6 family members, IL-11 exhibits anti-inflammatory activity against chronic inflammatory diseases, such as Crohn disease.[14] Moreover, recombinant human IL-11 protects epithelial cells of the intestine from tissue damage, suggesting its cytoprotective property.[15] Recently, we demonstrated that the IL-11 receptor is expressed in cardiomyocytes and that pretreatment of IL-11 confers resistance to ischemia/reperfusion injury in a murine model as a preconditioning effect.[16] When the limited level of clinical adverse effects of recombinant human IL-11 is considered,[13] IL-11 may be a candidate to be available clinically as cardiac gp130-targeting therapy against heart diseases.

In this study, we investigated the long-term effects of IL-11 treatment after myocardial infarction (MI). In addition, we report that IL-11 treatment prevents adverse cardiac remodeling through the STAT3 pathway.

Methods

Animal Care

The care of all animals was in compliance with the Osaka University animal care guidelines. The investigation conforms to the *Guide for the Care and Use of Laboratory Animals* published by the US National Institutes of Health (National Institutes of Health publication No. 85-23, revised 1996).

Coronary Artery Ligation and IL-11 Treatment

MI was generated by coronary artery ligation according to the previous report[1] with minor modifications. Briefly, C57BL/6 mice (8 to 10 weeks old; Japan SLC) were anesthetized and ventilated with 80% oxygen containing 1.5% isoflurane (Merck). After left-side thoracotomy, the left coronary artery was ligated with 7-0 silk sutures. Infarction was confirmed by discoloration of the ventricle and ST-T changes on ECG. The chest and skin were closed with 5-0 silk sutures. In preliminary experiments, we confirmed that the operation reproducibly generates infarction with the initial area at risk 20% to 25% per left ventricular (LV) area, as analyzed by Evans blue exclusion assays.[16] Sham-operated mice were subjected to similar surgery, except that no ligature was placed. Twenty-four hours after MI operation, mice were randomly assigned to 2 groups: the IL-11 group and control group. In the IL-11 group, recombinant human IL-11 (Peprotech) was administered intravenously for 5 days consecutively; the control group received the same volume of phosphate-buffered saline (PBS) during the same period.

Real-Time Reverse Transcription Polymerase Chain Reaction

Real-time reverse transcription polymerase chain reaction (RT-PCR) was performed according to the manufacturer's protocol. Total RNA was prepared from hearts at various time points after operation. In some experiments, the hearts were cut into 2 pieces: infarct area and remote area. The infarct area is the damaged or fibrotic region with its surrounding border zone, and the remote area is the portion separated from the infarct area by >1 mm.

Total RNA (1 μg) was subjected to first-strand cDNA synthesis with oligo(dT) primer. IL-11 was quantified by real-time RT-PCR with the use of the ABI-PRISM 7700 sequence detection system (Applied Biosystems Inc) with the SYBR green system (Applied Biosystems). As an internal control, the expression of GAPDH mRNA was estimated with the SYBR green system. The primers for IL-11 or GAPDH are as follows: IL-11 forward: 5′-CTGCCC-ACCTTGGCCATGAG-3′; IL-11 reverse: 5′-CCAGGCGAGACA-TCAAGAAAGA-3′; GAPDH forward: 5′-GCCGGTGCTGAGTAT-GTCGT-3′; GAPDH reverse: 5′-CCCTTTTGGCTCCACCCTT-3′.

Immunoblot Analyses

Immunoblot analyses were performed as described previously.[17] Heart homogenates were prepared in buffer containing 150 mmol/L NaCl, 10 mmol/L Tris-HCl (pH 7.5), 1 mmol/L EDTA, 1% Triton X-100, 1% deoxycholic acid, and 1 mmol/L dithiothreitol. Proteins were separated by SDS-PAGE and transferred onto the polyvinylidene difluoride membrane (Millipore). The membrane was immunoblotted with anti-phospho-STAT3 (p-STAT3) (Cell Signaling Technology, Danvers, Mass), anti-Bcl-2 (BD Transduction Laboratories), anti-survivin (Santa Cruz Biotechnology, Inc, Santa Cruz, Calif), or anti-cleaved caspase 3 (Cell Signaling Technology) antibody. The membrane was reprobed with anti-STAT3 (Santa Cruz Biotechnology) or anti-GAPDH (Chemicon, Temecula, Calif) antibody to show equal amount loading.

Histological Estimation of Cardiac Fibrosis

The frozen sections (5-μm thick) were prepared from the portion $\approx$300 μm distal to the ligation point and stained with Masson's trichrome. Photomicrographs were taken, and fibrotic circumference and area were measured with the use of Scion Image (Scion Corporation) by a researcher who was blinded to the treatment. Fibrotic circumference and area were calculated as a percentage of LV circumference and area, respectively. Infarct wall thickness was measured perpendicular to the infarcted wall at 3 separate regions and averaged.

Analysis of Cardiac Function

Fourteen days after MI, mice were anesthetized (50 mg/kg pentobarbital) and heparinized (50 U) via intraperitoneal injection. The hearts were excised rapidly and placed in ice-cold modified Tyrode's solution (140 mmol/L NaCl, 5.4 mmol/L KCl, 1.8 mmol/L $CaCl_2$, 0.45 mmol/L $MgCl_2$, 0.33 mmol/L NaH_2PO_4, 5.5 mmol/L glucose, 5 mmol/L HEPES [pH 7.4]). The aorta was cannulated and retrogradely perfused at a constant pressure of 100 mm Hg with Tyrode's solution bubbled with 80% oxygen at 37°C. The experiments were performed at 37°C by immersing the heart in Tyrode's solution in a water-jacketed chamber. The hearts were paced at 420 bpm. The fluid-filled balloon was inserted into the LV to monitor cardiac function. The balloon was attached to a pressure transducer, which was coupled to a 4S PowerLab (AD Instruments). LV developed pressure and $\pm$dP/dt were measured.

Immunofluorescent Microscopic Analyses

The hearts were harvested 15 minutes after intravenous injection of IL-11, and the frozen sections were prepared. The sections were stained with anti-p-STAT3 and anti-sarcomeric α-actinin (Sigma) antibodies. Alexa Fluor 488–conjugated goat anti-rabbit IgG (Molecular Probes) and Alexa Fluor 546–conjugated goat anti-mouse IgG (Molecular Probes) were used as secondary antibodies. Nuclei were also stained with Hoechst 33258.

Apoptotic cell death was detected by a terminal deoxynucleotide transferase–mediated dUTP nick-end labeling (TUNEL) staining with an in situ Apoptosis Detection Kit (TaKaRa). The section was costained with anti-sarcomeric α-actinin antibody to identify the cardiac myocytes. For quantitative analyses, apoptotic myocytes were counted in number by a researcher who was blinded to the assay conditions.

Immunohistochemical Analyses

The frozen sections were prepared as described above. Capillary density was examined by immunohistochemical staining with the use of the Vectastain ABC kit (Vector Laboratories) with anti-CD31 antibody (BD Biosciences, San Jose, Calif). To estimate capillary

density quantitatively, the number of capillaries was counted by a researcher who was blinded to the assay conditions.

Conditional Ablation of the *STAT3* Gene in Cardiomyocytes of Adult Murine Heart

The transgenic mice in which Cre recombinase fused to the mutated estrogen receptor domains (MerCreMer) were driven by the cardiomyocyte-specific α-myosin heavy chain (α-MHC) promoter, designated as α-MHC-MerCreMer mice, were a gift from Dr Molkentin.[18] We crossed the α-MHC-MerCreMer mice with mice that carried floxed STAT3 alleles ($STAT3^{flox/flox}$)[19] and produced α-MHC-MerCreMer/$STAT3^{flox/flox}$ mutant mice. To induce Cre-mediated recombination, mice were treated with 20 mg/kg tamoxifen (Sigma, St Louis, Mo) by intraperitoneal injection once per day for 5 consecutive days. Five days after the last treatment, the level of STAT3 expression decreased dramatically, and the mutant mice underwent MI as described above.

Cardiac-Specific Transgenic Mice Expressing Constitutively Active STAT3

Generation of cardiac-specific transgenic mice expressing constitutively active STAT3 was described previously.[9]

Statistical Analysis

Data are presented as mean±SD. Comparisons between 2 groups were performed with the use of the unpaired *t* test. One-way ANOVA with the Bonferroni test was used for multiple comparisons. Differences were considered statistically significant when the calculated (2-tailed) *P* value was <0.05.

Results

IL-11 Is a Cardiac Cytokine That Activates STAT3 in Cardiomyocytes In Vivo

We analyzed the expression of IL-11 mRNA in hearts at various time points after MI. Hearts were separated into infarct area and remote area, and the expression of IL-11 mRNA was measured by real-time RT-PCR (Figure 1A). The expression of IL-11 transcript was elevated, with its peak at 1 day after MI, and was gradually reduced at both infarct and remote areas. In the infarct area, the enhanced expression of IL-11 was sustained for 14 days. These data indicate that IL-11 is produced in the heart during cardiac remodeling after MI.

Next, we examined whether intravenous administration of IL-11 stimulates STAT3 in hearts by immunoblot analysis with anti-p-STAT3 antibody (Figure 1B). STAT3 phosphorylation was induced rapidly and reduced to the basal level within 180 minutes after IL-11 injection. IL-11 activated STAT3 in the heart in a dose-dependent manner (Figure I in the online-only Data Supplement).

To confirm that STAT3 activation occurred in cardiomyocytes, we performed immunohistological analyses to detect the nuclear localization of activated p-STAT3 (Figure 1C). Nuclear staining of p-STAT3 was detected in the IL-11–treated hearts but not in untreated hearts. Notably, >90% of nuclei of sarcomeric α-actinin–positive cells were also positively stained with anti-p-STAT3 antibody, indicating that IL-11 treatment results in STAT3 activation in cardiomyocytes in vivo. As is the case with noninfarcted mice, p-STAT3 was localized mainly in cardiomyocyte nuclei of postinfarct hearts, and IL-11 treatment increased the frequency of p-STAT3–positive cardiac myocytes (Figure II in the online-only Data Supplement).

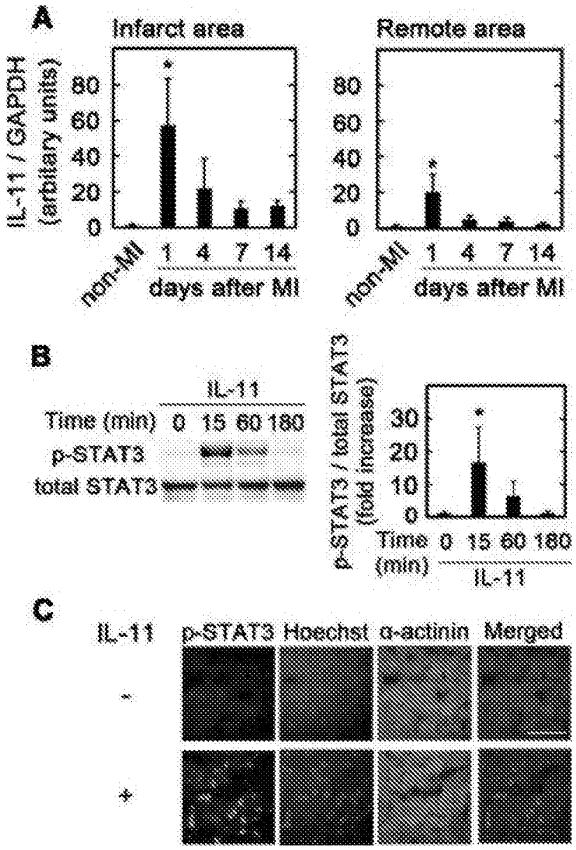

Figure 1. The transcript of IL-11 was elevated after MI, and IL-11 activated STAT3 in cardiomyocytes in murine hearts. A, Expression of IL-11 in infarct area or remote area of postinfarct hearts was analyzed by real-time RT-PCR. Expression of IL-11 was normalized with that of GAPDH. Data are shown as mean±SD (n=4 mice for each condition). *$P<0.05$ vs non-MI (sham) by 1-way ANOVA followed by Bonferroni test. B, IL-11 (8 μg/kg) was administered intravenously in mice for the indicated time. The lysates from hearts were immunoblotted with anti-p-STAT3 antibody. Blots were reprobed with anti-STAT3 antibody. Representative data are shown (left). Quantitative analyses of p-STAT3 are shown (right). Data are shown as mean±SD (n=4 mice for each condition). *$P<0.05$ vs 0 minutes by 1-way ANOVA followed by Bonferroni test. C, Fifteen minutes after injection of IL-11 (8 μg/kg) or PBS, frozen sections were prepared from the hearts. The sections were costained with anti-p-STAT3 and anti-sarcomeric α-actinin antibodies. Hoechst 33258 staining was also performed to identify the nuclei. The images are representative of 20 fields obtained from 4 mice. Bar=50 μm.

IL-11 Administration Attenuates Cardiac Remodeling After MI

To examine the effects of IL-11 on adverse cardiac remodeling, IL-11 was administered to the mice after MI operation, and cardiac fibrosis was histologically estimated at day 14 after MI (Figure 2). Both fibrotic circumference and fibrotic area were reduced by IL-11 in a dose-dependent manner (Figures 2B and C). Treatment of IL-11 at 8 μg/kg achieved a submaximal reduction in fibrotic circumference by 28.9% (PBS, 58.6±9.6%; IL-11, 41.7±10.0%) and fibrotic area by 33.1% (PBS, 39.8±9.3%; IL-11, 26.6±7.4%). Interestingly, IL-11–treated hearts showed an increase in infarct wall thickness compared with PBS-treated hearts (Figure 2D). To

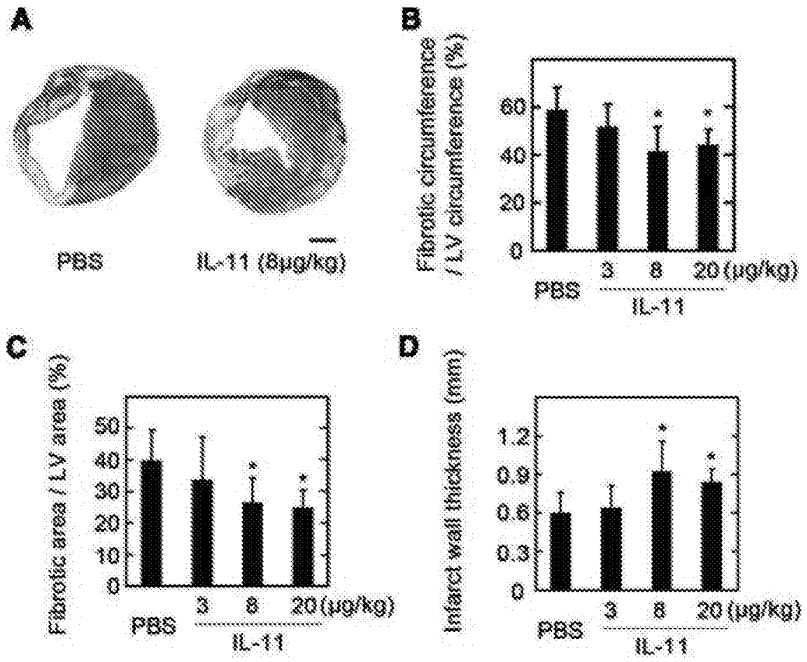

Figure 2. IL-11 attenuated cardiac fibrosis after MI. Heart sections (3 sections from each mouse) were prepared 14 days after MI and stained with Masson's trichrome. A, Images are representative of 24 to 27 obtained from 8 to 9 mice. Bar=1 mm. B to D, Ratio of fibrotic circumference to LV circumference (B), ratio of fibrotic area to LV area (C), and infarct wall thickness (D) were quantitatively estimated. Data are shown as mean±SD (n=8 mice for PBS; n=9 mice for 3 μg/kg; n=9 mice for 8 μg/kg; n=8 mice for 20 μg/kg). *$P<0.05$ vs PBS by 1-way ANOVA followed by Bonferroni test.

examine the effects of IL-11 on LV hypertrophy, we analyzed expression of α-skeletal muscle actin mRNA, a well-known marker of LV hypertrophy (Figure III in the online-only Data Supplement). IL-11 treatment showed a tendency to reduce α-skeletal muscle actin expression, although its reduction was not statistically significant.

To clarify whether IL-11 prevents cardiac dysfunction after MI, we measured LV developed pressure and ±dP/dt by a Langendorff apparatus. As acute myocardial damage, MI rapidly impaired LV developed pressure and ±dP/dt at day 1 (Table I in the online-only Data Supplement) before IL-11 administration was started. Because IL-11 treatment attenuated cardiac fibrosis that occurred during the following 2 weeks, we examined the effects of IL-11 on cardiac function 2 weeks after MI (Table). IL-11 treatment ameliorated chronic cardiac dysfunction in a dose-dependent manner compared with the PBS-treated group. Consistent with the attenuation of fibrosis, treatment of IL-11 at a dose of 8 μg/kg submaximally prevented cardiac dysfunction. Thus, further experiments were performed with the use of IL-11 at a dose of 8 μg/kg.

We also confirmed the inhibitory effects of IL-11 on adverse cardiac remodeling 28 days after MI. IL-11 treatment prevented cardiac fibrosis and preserved cardiac function (Figure IV in the online-only Data Supplement).

Table. Effects of IL-11 on Cardiac Function at Day 14 After MI

		IL-11, μg/kg		
Parameters	PBS	3	8	20
LVDP, mm Hg	32.4±4.4	34.9±6.3	45.3±6.3*	44.3±13.5*
+dP/dt, mm Hg/s	884±113	958±162	1210±148*	1243±324*
−dP/dt, mm Hg/s	−713±93	−737±176	−1022±210*	−1043±326*

Data are mean±SD (n=8 mice for PBS; n=9 mice for 3 μg/kg; n=9 mice for 8 μg/kg; n=8 mice for 20 μg/kg). LVDP indicates LV developed pressure.
*$P<0.05$ vs PBS by 1-way ANOVA followed by Bonferroni test.

To examine whether IL-11 reduces infarct size, infarct size was measured by Evans blue exclusion 2 days after MI. There was no significant difference in infarct size (PBS, 23.0±7.1%; IL-11 [8 μg/kg], 22.0±4.3%; n=4 mice for each group).

IL-11 Treatment Exhibits Antiapoptotic and Proangiogenic Activity in the Heart

Granulocyte colony-stimulating factor (G-CSF) was reported to prevent cardiac remodeling after MI, accompanied by antiapoptotic and proangiogenic effects through STAT3.[20] Because IL-11 activated STAT3 in cardiomyocytes (Figure 1), we examined the effects of IL-11 on cardiomyocyte survival and vascular formation in postinfarct myocardium.

To evaluate the antiapoptotic effects of IL-11, TUNEL staining was performed (Figure 3A). TUNEL-positive cardiomyocytes were detected mainly at the border zone, adjacent to the ischemic area, at both day 2 and day 4 after MI. Importantly, IL-11 treatment significantly reduced the number of apoptotic cardiomyocytes compared with the PBS group. To further confirm the cytoprotective effects, the cleavage of caspase 3 was examined by immunoblot analyses with cleaved caspase 3–specific antibody (Figure 3B). Compared with PBS treatment, IL-11 significantly reduced the band intensity for cleaved caspase 3. To address the antiapoptotic pathways downstream of the IL-11 signal, we examined the expression of cell survival proteins (Figure 3C). Immunoblot analysis revealed that Bcl-2 and survivin proteins, both of which have been characterized as downstream targets of STAT3,[21–23] were increased in the IL-11 group (Bcl-2, 1.9-fold; survivin, 1.5-fold).

Because activation of STAT3 mediated vascular formation during cardiac remodeling,[20,24] capillary density was immu-

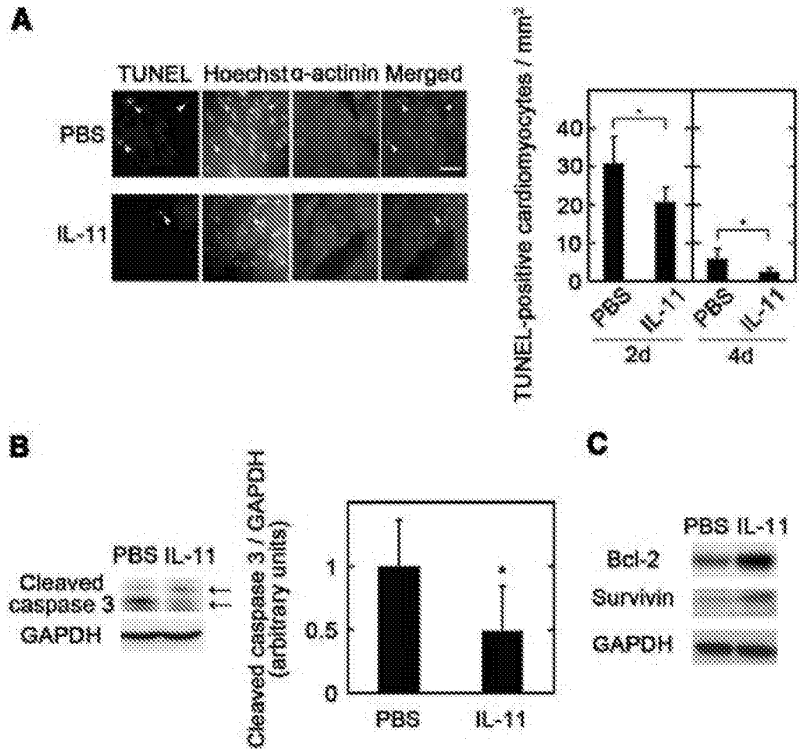

Figure 3. IL-11 treatment suppressed cardiomyocyte apoptosis after MI. A, The frequency of apoptotic cardiomyocytes was estimated by TUNEL staining 2 days and 4 days after MI. The sections were costained with anti-sarcomeric α-actinin antibody and Hoechst 33258 dye. The images are representative of 60 to 100 obtained from 4 to 5 mice (15 to 20 fields from each mouse) (left). Arrowheads show TUNEL-positive, apoptotic cardiomyocytes. Bar=50 μm. Quantification of the apoptotic cardiomyocytes is shown (right). Visual fields (15 to 20) were randomly selected. Data are shown as mean±SD (n=5 mice for PBS [2 days]; n=4 mice for IL-11 [2 days]; n=5mice for PBS [4 days]; n=5 mice for IL-11 [4 days]). *$P<0.05$ vs PBS by unpaired *t* test. B, The lysates from hearts at day 2 after MI were immunoblotted with anti-cleaved caspase 3 and anti-GAPDH antibodies. Arrows indicate the cleaved caspase 3 fragments with molecular weight 17 and 19 kDa (left). Quantitative analysis of cleaved caspase 3 fragments is shown (right). Data are shown as mean±SD (n=6 mice for PBS; n=5 mice for IL-11). *$P<0.05$ vs PBS by unpaired *t* test. C, Representative results of immunoblotting with anti-Bcl-2 and anti-survivin antibodies. Blots were reprobed with anti-GAPDH antibody to show equal amount loading. Experiments were repeated 5 times with similar results.

nohistochemically estimated with anti-CD31 antibody (Figure 4). In the border zone, capillary density was increased by IL-11 in a dose-dependent manner. Because the frequency of apoptosis was higher at day 2 than at day 4 (30.9±7.1 versus 5.7±2.8 TUNEL-positive cardiomyocytes/mm^2, respectively; $P<0.01$), cardiomyocyte loss occurs mainly at days 1 to 3. On the basis of this finding, to clarify the relation between antiapoptosis and angiogenesis mediated by IL-11, we compared the effectiveness between cytokine treatment at days 1 to 3 and that at days 3 to 5 (Table II in the online-only Data Supplement). IL-11 treatment at days 1 to 3 attenuated cardiac fibrosis, whereas that at days 3 to 5 did not. Interestingly, treatment at days 1 to 3 increased capillary density, whereas that at days 3 to 5 did not. Therefore, IL-11–mediated increase in capillary density is likely to be closely associated with improved myocyte viability.

Activation of STAT3 Is Necessary and Sufficient for IL-11–Mediated Prevention of Cardiac Remodeling

To assess the importance of cardiac STAT3 activation in IL-11–mediated attenuation of adverse remodeling, we generated cardiac-specific conditional STAT3-deficient mice (STAT3 CKO mice) by establishing α-MHC-MerCreMer mice on STAT3$^{flox/flox}$ background (Figure 5A). The ablation of the *STAT3* gene did not induce notable histological alterations at day 14 after sham operation. IL-11 treatment ameliorated postinfarct fibrosis in α-MHC-MerCreMer mice on STAT3$^{wild/wild}$ background after MI (Figure V in the online-only Data Supplement), as in the case with nontransgenic mice (Figure 2). Importantly, IL-11–mediated prevention against adverse cardiac remodeling was abrogated in STAT3 CKO mice (Figure 5C and 5D). Interestingly, enlargement of LVs was observed in STAT3 CKO mice compared with wild-type mice exposed to MI without IL-11 treatment (18.02±3.20 mm [n=6] versus 15.08±1.81 mm [n=8]; $P<0.05$), probably because STAT3 is endogenously activated after MI, even without IL-11 treatment (Figures II and VI in the online-only Data Supplement), and contributes to the prevention of adverse cardiac remodeling. Consistently, we also confirmed that IL-11–mediated attenuation of cardiac dysfunction was canceled in STAT3 CKO mice (Figure VII in the online-only Data Supplement). Moreover, the increase in capillary density, which was observed in response to IL-11 in the mice with STAT3$^{wild/wild}$ background, was abrogated by *STAT3* gene ablation (Figure VIII in the online-only Data Supplement). These data indicate that STAT3 is required for IL-11–mediated amelioration of adverse cardiac remodeling after MI.

To reinforce the importance of STAT3 in cardioprotection, transgenic hearts expressing constitutively active STAT3 (caSTAT3) were exposed to MI, and cardiac fibrosis was estimated. In caSTAT3 transgenic hearts, cardiac fibrosis was reduced by 47% compared with nontransgenic littermates (wild-type) (Figure 6). Moreover, similar to IL-11–treated hearts, caSTAT3 transgenic hearts showed an increase in fibrotic wall thickness. Importantly, cardiac dysfunction was ameliorated in caSTAT3 transgenic mice compared with wild-type mice (Figure IX in the online-only Data Supplement). Therefore, activation of STAT3 in cardiomyocytes was sufficient to suppress cardiac remodeling after MI.

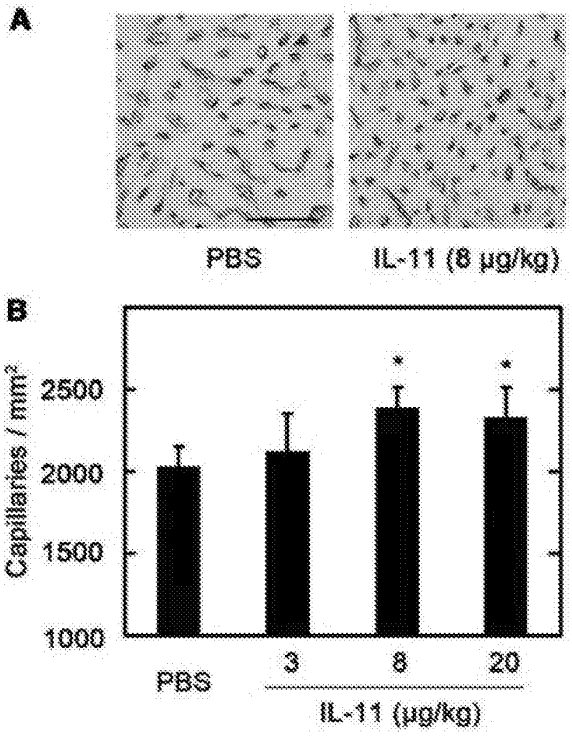

Figure 4. IL-11 increased capillary density in infarcted hearts. Heart sections were prepared 14 days after MI and stained with anti-CD31 antibody. A, The images are representative of 80 to 90 obtained from 8 to 9 mice (10 fields from each mouse). Bar=50 μm. B, CD31-positive capillary density was quantitatively estimated. Ten visual fields were randomly selected. Data are shown as mean±SD (n=8 mice for PBS; n=9 mice for 3 μg/kg; n=9 mice for 8 μg/kg; n=8 mice for 20 μg/kg). *$P<0.05$ vs PBS by 1-way ANOVA followed by Bonferroni test.

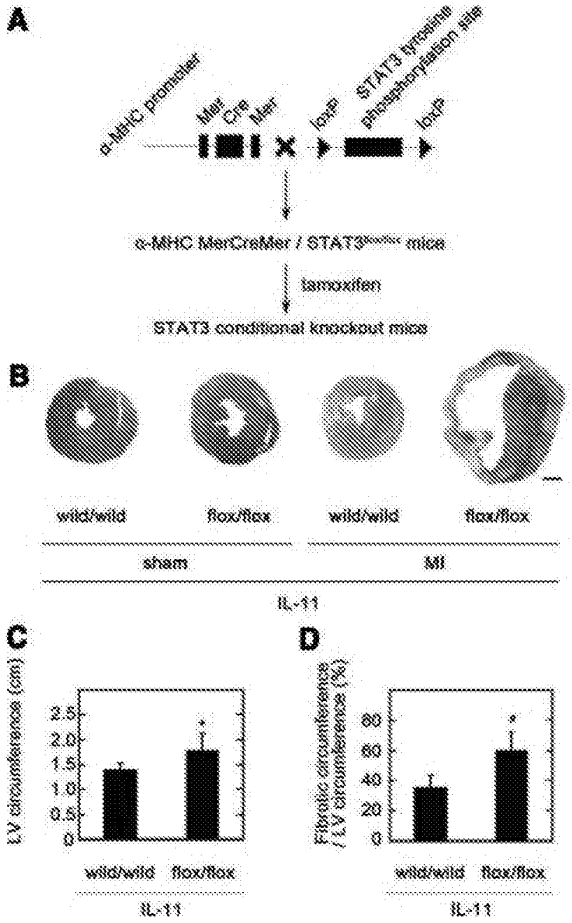

Figure 5. STAT3 was required for IL-11–mediated amelioration of adverse remodeling after MI. A, Generation of STAT3 conditional knockout mice. B, After tamoxifen treatment, sham or MI operation was performed in α-MHC-MerCreMer/STAT3$^{flox/flox}$ (flox/flox; n=5 mice for sham; n=6 mice for MI) or α-MHC-MerCreMer/STAT3$^{wild/wild}$ (wild/wild; n=4 mice for sham; n=6 mice for MI) mice, followed by IL-11 administration. Heart sections (3 sections from each mouse) were prepared 14 days after MI and stained with Masson's trichrome. The images are representative of 12 to 18 obtained from 4 to 6 mice. Bar=1 mm. C, LV circumference was quantitatively estimated. D, Ratio of fibrotic circumference to LV circumference was quantitatively estimated. Data are shown as mean±SD. *$P<0.05$, #$P<0.01$ vs STAT3$^{wild/wild}$ by unpaired t test.

Discussion

In this study, we examined the effects of IL-11 treatment on adverse cardiac remodeling after MI. IL-11 activated STAT3 in cardiomyocytes in vivo. IL-11 ameliorated cardiac fibrosis and attenuated cardiac dysfunction after MI. IL-11 reduced the number of apoptotic myocytes, and IL-11–treated hearts showed an increase in capillary density. Importantly, the preventive effects of IL-11 against adverse remodeling were suppressed in cardiac-specific STAT3-deficient mice. Moreover, cardiac STAT3 activation was sufficient to suppress adverse remodeling. These findings suggest that IL-11 treatment is a promising strategy against adverse cardiac remodeling after MI.

Previously, G-CSF and erythropoietin were reported to exhibit preventive effects against postinfarct fibrosis[20,25,26]; however, a large difference in signaling pathways exists among these cytokines. IL-11 rapidly activates STAT3 in cardiomyocytes at a lower concentration than G-CSF, suggesting that IL-11 is a more potent activator of STAT3. Akt, another cytoprotective signal transducer, is activated by G-CSF and erythropoietin in cardiomyocytes[27–29] and to a lesser extent by IL-11 (data not shown). Moreover, G-CSF confers resistance to ischemia/reperfusion through endothelial Akt activation[30] and IL-11 through cardiomyocyte activation of STAT3.[16] Thus, IL-11 transduces cardioprotective signals via pathways that are distinct from G-CSF or erythropoietin.

IL-11 belongs to the IL-6 cytokine family, which uses gp130 as its common receptor. Interestingly, LIF, a member of the IL-6 cytokine family, has been reported to enhance survival of cardiomyocytes, with mobilization of bone marrow cells to the heart.[1] Similarly, G-CSF stimulates the homing of bone marrow cells to the heart, leading to regeneration of the injured heart.[31] These studies propose that bone marrow cells may contribute to cardiac repair in response to cytokine stimuli. In our experiments, IL-11 failed to show cardioprotective effects in cardiomyocyte-specific STAT3-deficient mice. Therefore, cardiomyocytes are important components in the action of IL-11, and STAT3 activation in cardiomyocytes is a critical factor for IL-11–mediated prevention of adverse cardiac remodeling, although we cannot exclude the possibility that bone marrow cell

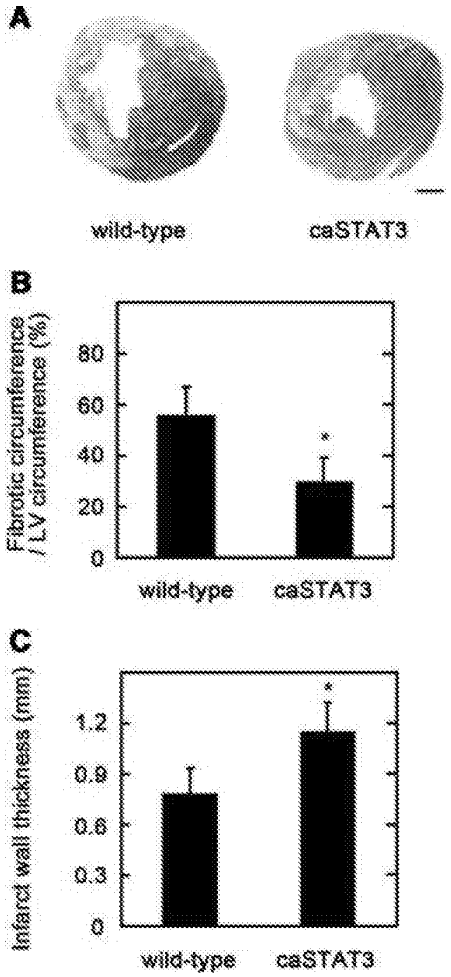

Figure 6. Activation of STAT3 in cardiomyocytes was sufficient to suppress adverse remodeling. Cardiac-specific transgenic mice expressing caSTAT3 or wild-type mice were exposed to MI. At day 14 after MI, heart sections were stained with Masson's trichrome. A, Images are representative of 15 obtained from 5 mice (3 sections from each mouse). Bar=1 mm. B, Ratio of fibrotic circumference to LV circumference was quantitatively estimated. C, Infarct wall thickness was quantitatively estimated. Data are shown as mean±SD (n=5 mice for each group). *$P<0.01$ vs wild-type by unpaired t test.

mobilization is regulated by cardiac STAT3 through some paracrine systems.

Previously, we reported that IL-11 shows cytoprotective effects through STAT3 and prevents ischemia/reperfusion injury in the heart.[16] IL-11 reduced cardiomyocyte apoptosis after MI consistently in this study. In addition to cell-autonomous cytoprotection, we have demonstrated that IL-11 promoted vessel growth in the heart. Importantly, the enhancement of capillary density by IL-11 was not observed in cardiac-specific STAT3-deficient mice. Taken together with previous reports that cardiac activation of STAT3 promotes vascular formation in the heart,[8,10] STAT3 is a critical regulator of the interaction between myocardium and endothelium. Interestingly, IL-11–mediated enhancement of vascular formation was closely associated with improvement of cardiomyocyte viability. Similarly, it was reported recently that cardiac production of angiogenic growth factors was impaired under decompensatory conditions during cardiac remodeling and that angiogenesis was critical to prevent onset of heart failure in response to pathological stress.[32] Collectively, this suggests that IL-11 mediates cardiomyocyte survival and capillary growth in an interdependent manner and that these signals are coordinated by STAT3.

IL-11 exerted preventive effects against adverse cardiac remodeling after MI at almost the same level as G-CSF,[20] whose clinical use was reported to be at least partially beneficial in cardiovascular diseases.[33] Thus, IL-11 treatment may be proposed as a novel cytokine therapy. Although one of the most serious adverse effects of cytokine therapy is inflammation, IL-11 is known to be an anti-inflammatory cytokine.[34] Indeed, IL-11 significantly suppressed expression of proinflammatory cytokines, such as IL-6 and tumor necrosis factor-α, in postinfarct myocardium (Figure X in the online-only Data Supplement), which provides evidence supporting its safety.

In summary, IL-11 transduced cardioprotective signals through STAT3 and suppressed adverse cardiac remodeling after MI. The IL-11/gp130/STAT3 axis may be a novel therapeutic target against cardiovascular diseases.

Acknowledgments

We thank Yasuko Murao for excellent secretarial work.

Sources of Funding

This study was supported by a grant-in-aid for scientific research from the Japan Society for the Promotion of Science, Mitsubishi Pharma Research Foundation, Takeda Science Foundation, Osaka Foundation for Promotion of Clinical Immunology, and a grant-in-aid from Knowledge Cluster Initiative (Second Stage) of the Ministry of Education, Culture, Sports, Science, and Technology of Japan.

Disclosures

None.

References

1. Zou Y, Takano H, Mizukami M, Akazawa H, Qin Y, Toko H, Sakamoto M, Minamino T, Nagai T, Komuro I. Leukemia inhibitory factor enhances survival of cardiomyocytes and induces regeneration of myocardium after myocardial infarction. *Circulation*. 2003;108:748–753.
2. Brar BK, Stephanou A, Liao Z, O'Leary RM, Pennica D, Yellon DM, Latchman DS. Cardiotrophin-1 can protect cardiac myocytes from injury when added both prior to simulated ischaemia and at reoxygenation. *Cardiovasc Res*. 2001;51:265–274.
3. Pan J, Fukuda K, Saito M, Matsuzaki J, Kodama H, Sano M, Takahashi T, Kato T, Ogawa S. Mechanical stretch activates the JAK/STAT pathway in rat cardiomyocytes. *Circ Res*. 1999;84:1127–1136.
4. Hishinuma S, Funamoto M, Fujio Y, Kunisada K, Yamauchi-Takihara K. Hypoxic stress induces cardiotrophin-1 expression in cardiac myocytes. *Biochem Biophys Res Commun*. 1999;264:436–440.
5. Funamoto M, Hishinuma S, Fujio Y, Matsuda Y, Kunisada K, Oh H, Negoro S, Tone E, Kishimoto T, Yamauchi-Takihara K. Isolation and characterization of the murine cardiotrophin-1 gene: expression and norepinephrine-induced transcriptional activation. *J Mol Cell Cardiol*. 2000;32:1275–1284.
6. Pennica D, Shaw KJ, Swanson TA, Moore MW, Shelton DL, Zioncheck KA, Rosenthal A, Taga T, Paoni NF, Wood WI. Cardiotrophin-1: biological activities and binding to the leukemia inhibitory factor receptor/gp130 signaling complex. *J Biol Chem*. 1995;270:10915–10922.
7. Kunisada K, Hirota H, Fujio Y, Matsui H, Tani Y, Yamauchi-Takihara K, Kishimoto T. Activation of JAK-STAT and MAP kinases by leukemia inhibitory factor through gp130 in cardiac myocytes. *Circulation*. 1996;94:2626–2632.

8. Funamoto M, Fujio Y, Kunisada K, Negoro S, Tone E, Osugi T, Hirota H, Izumi M, Yoshizaki K, Walsh K, Kishimoto T, Yamauchi-Takihara K. Signal transducer and activator of transcription 3 is required for glycoprotein 130-mediated induction of vascular endothelial growth factor in cardiac myocytes. *J Biol Chem*. 2000;275:10561–10566.
9. Oshima Y, Fujio Y, Nakanishi T, Itoh N, Yamamoto Y, Negoro S, Tanaka K, Kishimoto T, Kawase I, Azuma J. STAT3 mediates cardioprotection against ischemia/reperfusion injury through metallothionein induction in the heart. *Cardiovasc Res*. 2005;65:428–435.
10. Osugi T, Oshima Y, Fujio Y, Funamoto M, Yamashita A, Negoro S, Kunisada K, Izumi M, Nakaoka Y, Hirota H, Okabe M, Yamauchi-Takihara K, Kawase I, Kishimoto T. Cardiac-specific activation of signal transducer and activator of transcription 3 promotes vascular formation in the heart. *J Biol Chem*. 2002;277:6676–6681.
11. Taga T, Kishimoto T. Gp130 and the interleukin-6 family of cytokines. *Annu Rev Immunol*. 1997;15:797–819.
12. Gadient RA, Patterson PH. Leukemia inhibitory factor, interleukin 6, and other cytokines using the GP130 transducing receptor: roles in inflammation and injury. *Stem Cells*. 1999;17:127–137.
13. Gordon MS, McCaskill-Stevens WJ, Battiato LA, Loewy J, Loesch D, Breeden E, Hoffman R, Beach KJ, Kuca B, Kaye J, Sledge GW Jr. A phase I trial of recombinant human interleukin-11 (neumega rhIL-11 growth factor) in women with breast cancer receiving chemotherapy. *Blood*. 1996;87:3615–3624.
14. Sands BE, Winston BD, Salzberg B, Safdi M, Barish C, Wruble L, Wilkins R, Shapiro M, Schwertschlag US. Randomized, controlled trial of recombinant human interleukin-11 in patients with active Crohn's disease. *Aliment Pharmacol Ther*. 2002;16:399–406.
15. Du X, Liu Q, Yang Z, Orazi A, Rescorla FJ, Grosfeld JL, Williams DA. Protective effects of interleukin-11 in a murine model of ischemic bowel necrosis. *Am J Physiol*. 1997;272:G545–G552.
16. Kimura R, Maeda M, Arita A, Oshima Y, Obana M, Ito T, Yamamoto Y, Mohri T, Kishimoto T, Kawase I, Fujio Y, Azuma J. Identification of cardiac myocytes as the target of interleukin 11, a cardioprotective cytokine. *Cytokine*. 2007;38:107–115.
17. Mohri T, Fujio Y, Maeda M, Ito T, Iwakura T, Oshima Y, Uozumi Y, Segawa M, Yamamoto H, Kishimoto T, Azuma J. Leukemia inhibitory factor induces endothelial differentiation in cardiac stem cells. *J Biol Chem*. 2006;281:6442–6447.
18. Sohal DS, Nghiem M, Crackower MA, Witt SA, Kimball TR, Tymitz KM, Penninger JM, Molkentin JD. Temporally regulated and tissue-specific gene manipulations in the adult and embryonic heart using a tamoxifen-inducible Cre protein. *Circ Res*. 2001;89:20–25.
19. Takeda K, Kaisho T, Yoshida N, Takeda J, Kishimoto T, Akira S. Stat3 activation is responsible for IL-6-dependent T cell proliferation through preventing apoptosis: generation and characterization of T cell-specific Stat3-deficient mice. *J Immunol*. 1998;161:4652–4660.
20. Harada M, Qin Y, Takano H, Minamino T, Zou Y, Toko H, Ohtsuka M, Matsuura K, Sano M, Nishi J, Iwanaga K, Akazawa H, Kunieda T, Zhu W, Hasegawa H, Kunisada K, Nagai T, Nakaya H, Yamauchi-Takihara K, Komuro I. G-CSF prevents cardiac remodeling after myocardial infarction by activating the Jak-Stat pathway in cardiomyocytes. *Nat Med*. 2005;11:305–311.
21. Zushi S, Shinomura Y, Kiyohara T, Miyazaki Y, Kondo S, Sugimachi M, Higashimoto Y, Kanayama S, Matsuzawa Y. STAT3 mediates the survival signal in oncogenic ras-transfected intestinal epithelial cells. *Int J Cancer*. 1998;78:326–330.
22. McGaffin KR, Zou B, McTiernan CF, O'Donnell CP. Leptin attenuates cardiac apoptosis after chronic ischaemic injury. *Cardiovasc Res*. 2009;83:313–324.
23. Jiang H, Yu J, Guo H, Song H, Chen S. Upregulation of survivin by leptin/STAT3 signaling in MCF-7 cells. *Biochem Biophys Res Commun*. 2008;368:1–5.
24. Krishnamurthy P, Rajasingh J, Lambers E, Qin G, Losordo DW, Kishore R. IL-10 inhibits inflammation and attenuates left ventricular remodeling after myocardial infarction via activation of STAT3 and suppression of HuR. *Circ Res*. 2009;104:e9–e18.
25. Ohtsuka M, Takano H, Zou Y, Toko H, Akazawa H, Qin Y, Suzuki M, Hasegawa H, Nakaya H, Komuro I. Cytokine therapy prevents left ventricular remodeling and dysfunction after myocardial infarction through neovascularization. *FASEB J*. 2004;18:851–853.
26. Moon C, Krawczyk M, Ahn D, Ahmet I, Paik D, Lakatta EG, Talan MI. Erythropoietin reduces myocardial infarction and left ventricular functional decline after coronary artery ligation in rats. *Proc Natl Acad Sci U S A*. 2003;100:11612–11617.
27. Iwanaga K, Takano H, Ohtsuka M, Hasegawa H, Zou Y, Qin Y, Odaka K, Hiroshima K, Tadokoro H, Komuro I. Effects of G-CSF on cardiac remodeling after acute myocardial infarction in swine. *Biochem Biophys Res Commun*. 2004;325:1353–1359.
28. Li Y, Takemura G, Okada H, Miyata S, Maruyama R, Li L, Higuchi M, Minatoguchi S, Fujiwara T, Fujiwara H. Reduction of inflammatory cytokine expression and oxidative damage by erythropoietin in chronic heart failure. *Cardiovasc Res*. 2006;71:684–694.
29. Cai Z, Semenza GL. Phosphatidylinositol-3-kinase signaling is required for erythropoietin-mediated acute protection against myocardial ischemia/reperfusion injury. *Circulation*. 2004;109:2050–2053.
30. Ueda K, Takano H, Hasegawa H, Niitsuma Y, Qin Y, Ohtsuka M, Komuro I. Granulocyte colony stimulating factor directly inhibits myocardial ischemia-reperfusion injury through Akt-endothelial NO synthase pathway. *Arterioscler Thromb Vasc Biol*. 2006;26:e108–e113.
31. Orlic D, Kajstura J, Chimenti S, Limana F, Jakoniuk I, Quaini F, Nadal-Ginard B, Bodine DM, Leri A, Anversa P. Mobilized bone marrow cells repair the infarcted heart, improving function and survival. *Proc Natl Acad Sci U S A*. 2001;98:10344–10349.
32. Sano M, Minamino T, Toko H, Miyauchi H, Orimo M, Qin Y, Akazawa H, Tateno K, Kayama Y, Harada M, Shimizu I, Asahara T, Hamada H, Tomita S, Molkentin JD, Zou Y, Komuro I. p53-induced inhibition of Hif-1 causes cardiac dysfunction during pressure overload. *Nature*. 2007;446:444–448.
33. Takano H, Ueda K, Hasegawa H, Komuro I. G-CSF therapy for acute myocardial infarction. *Trends Pharmacol Sci*. 2007;28:512–517.
34. Du X, Williams DA. Interleukin-11: review of molecular, cell biology, and clinical use. *Blood*. 1997;89:3897–3908.

CLINICAL PERSPECTIVE

In ischemic heart diseases, myocardial damage is initially induced by reduction of blood supply and is subsequently expanded by cardiac remodeling, leading to heart failure. A therapeutic strategy to limit myocardial remodeling, such as angiotensin-converting enzyme inhibitors and β-blockers, improves the survival rate; however, the prognosis of heart failure is still not satisfactory. Cardiac remodeling is positively or negatively regulated by a number of neurohumoral factors and cytokines. Here, we examined whether interleukin (IL)-11, a member of the IL-6 family of cytokines, ameliorates postinfarct remodeling, using a model of myocardial infarction by coronary ligation. Treatment with IL-11 reduced fibrosis after myocardial infarction, with attenuation of myocardial dysfunction. IL-11 decreased the frequency of cardiomyocyte death and increased capillary density. IL-11 treatment resulted in STAT3 activation in cardiomyocytes in vivo. Using conditional knockout mice and cardiac-specific transgenic mice, we demonstrated that activation of STAT3 in cardiomyocytes was necessary and sufficient for IL-11–mediated prevention of cardiac adverse remodeling. These findings suggest that IL-11 treatment may be useful as a therapeutic strategy against the onset of heart failure after myocardial infarction. Because human recombinant IL-11, oprelvekin, is clinically used for thrombocytopenia, with a tolerable level of adverse drug effects providing some proof of its safety, our results suggest that IL-11 treatment is a promising novel cytokine therapy for prevention against heart failure.

SUPPLEMENTAL MATERIAL

Supplementary Materials and Methods

Real time RT-PCR

The expression of α-skeletal muscle actin mRNA was quantified by real time RT-PCR using the ABI-PRISM® 7700 sequence detection system with SYBR green system. The primers for α-skeletal muscle actin are as follows;

α-skeletal muscle actin forward: 5'-AGGGCCAGAGTCAGAGCAG -3',

α-skeletal muscle actin reverse: 5'-CCGTTGTCACACACAAGAGC -3'.

The expression of IL-6 or TNF-α mRNA was quantified by real time RT-PCR using the ABI-PRISM® 7700 sequence detection system with TaqMan Assay on Demand Reagents (PE Applied Biosystems Inc.).

Supplementary Figure Legends

Supplementary Figure 1

IL-11 activated STAT3 in murine hearts in a dose-dependent manner.

The various concentrations of IL-11 were intravenously administered to mice. Fifteen minutes after injection, mice were sacrificed. The lysates were prepared from hearts and immunoblotted with anti-phospho-specific STAT3 (p-STAT3) antibody. Blots were reprobed with anti-STAT3 antibody. Experiments were repeated three times with similar results.

Supplementary Figure 2

IL-11 activated STAT3 in the cardiomyocytes at day 1 after MI.

IL-11 (8 μg/kg) or PBS was intravenously administered in mice at day 1 after MI. Fifteen minutes after injection, the hearts were harvested and frozen sections were prepared. The sections were co-stained with anti-phospho-specific STAT3 (p-STAT3) and anti-sarcomeric α-actinin antibodies. Hoechst 33258 staining was also performed to identify the nuclei. The images shown are representative of 15 obtained from 3 mice (5 fields from each mouse). Arrowheads show the p-STAT3-positive nuclei. Bar, 50 μm.

Supplementary Figure 3

The effect of IL-11 on the expression of α-skeletal muscle actin after MI.

Total RNA was prepared from infarct (I) or remote (R) area of hearts after MI and real time RT-PCR was performed for α-skeletal muscle actin. The expression of α-skeletal muscle actin

was normalized with that of GAPDH. Data are shown as mean ± S.D. (n=5 mice for each group).

Supplementary Figure 4

IL-11 attenuated the cardiac remodeling at day 28 after MI.

Mice were exposed to MI operation, followed by the treatment of IL-11 for 5 days. PBS was used as control. Heart sections were prepared 28 days after MI and stained with Masson's Trichrome method to determine fibrosis. The ratio of fibrotic circumference to LV circumference was quantitatively estimated. LVDP and ±dp/dt were measured by a Langendorff apparatus at day 28 after MI. Data are shown as mean ± S.D. (n=4 mice, for PBS; n=7 mice, for IL-11). $^{*}P<0.05$ vs. PBS, by unpaired *t* test.

Supplementary Figure 5

IL-11 treatment reduced the cardiac fibrosis in α-MHC-MerCreMer mice on STAT3$^{wild/wild}$ background after MI.

MI was generated in α-MHC-MerCreMer mice on STAT3$^{wild/wild}$ background, followed by IL-11 treatment for 5 days. Heart sections (3 sections from each mouse) were prepared 14 days after MI and stained with Masson's Trichrome method to determine fibrosis. (A) The images are representative of 18 obtained from 6 mice. Bar, 1 mm. (B) The ratio of fibrotic circumference to LV circumference was quantitatively estimated. Data are shown as mean ± S.D. (n=6 mice for each group). $^{*}P<0.01$ vs. PBS, by unpaired *t* test.

Supplementary Figure 6

Cardiac activation of STAT3 was sustained during cardiac remodeling after MI in mice.

Mice were exposed to MI operation and the hearts were harvested at the indicated time point. The lysates were prepared from hearts and immunoblotted with anti-phospho-specific STAT3 (p-STAT3) antibody. Blots were reprobed with anti-STAT3 antibody.

Supplementary Figure 7

STAT3 was required for IL-11-mediated amelioration of cardiac dysfunction after MI.

After tamoxifen treatment, MI was generated in α-MHC-MerCreMer/STAT3$^{flox/flox}$ (flox/folx, n=4) or α-MHC-MerCreMer/STAT3$^{wild/wild}$ (wild/wild, n=4) mice, followed by the administration of IL-11. At day 14 after MI, LVDP and ±dp/dt were measured by a Langendorff apparatus. Data are shown as mean ± S.D. $^{*}P<0.05$ vs. α-MHC-MerCreMer/STAT3$^{wild/wild}$, by unpaired *t* test.

Supplementary Figure 8

The enhancement of capillary density by IL-11 was not observed in cardiac-specific STAT3-deficient mice.

After tamoxifen treatment, MI was generated in α-MHC-MerCreMer/STAT3$^{flox/flox}$ or α-MHC-MerCreMer/STAT3$^{wild/wild}$ mice, followed by the administration of IL-11. Heart sections were prepared 14 days after MI and stained with anti-CD31 antibody, to detect capillary endothelial cells. The CD31-positive capillary density was quantitatively estimated. Ten visual fields were randomly selected. Data are shown as mean ± S.D. (n=6 mice for each group). $^{*}P<0.01$ vs. STAT3$^{wild/wild}$ without IL-11 treatment. $^{\#}P<0.01$ vs. STAT3$^{flox/flox}$ with IL-11 treatment, by one-way ANOVA followed by Bonferroni test.

Supplementary Figure 9

Activation of STAT3 in cardiomyocytes was sufficient for amelioration of cardiac dysfunction.

Cardiac-specific transgenic mice expressing constitutively active STAT3 (caSTAT3) or wild-type mice were exposed to MI. At day 14 after MI, LVDP and ±dp/dt were measured by a Langendorff apparatus. Data are shown as mean ± S.D. (n=5 mice for each group). $^{*}P<0.05$ vs. wild-type, by unpaired *t* test.

Supplementary Figure 10

IL-11 suppressed the inflammatory reaction in post-infarct myocardium.

Total RNA was prepared from infarct hearts at day 4 after MI or sham operation. The expression level of IL-6 or TNF-α mRNA was measured by real time RT-PCR methods and normalized with that of GAPDH. The cytokine level was expressed as fold induction of that in non-infarct hearts. Data are shown as mean ± S.D. (n=4 mice for each group). $^{*}P<0.05$ vs. sham, $^{\#}P<0.05$ vs. PBS, by one-way ANOVA followed by Bonferroni test.

Supplementary Table 1. Cardiac function at day 1 after MI before IL-11 treatment.

Parameters	Baseline	One day post MI
LVDP(mmHg)	83.0±8.8	53.9±12.6*
+dp/dt (mmHg/s)	2321±390	1485±316*
-dp/dt (mmHg/s)	-2030±353	-1242±290*

Data were shown as mean ± S.D. (n=7 mice, for baseline; n=7 mice, one day post MI).
*P<0.01 vs. Baseline, by unpaired t test.

Supplementary Table 2. The dependency of IL-11 therapy on the treatment timing.

	Fibrotic area / LV area (%)	Capillaries (/mm^2)
PBS	42.6±13.1	2052±118
IL-11		
d1-d3	26.4±8.0*	2304±179*
d3-d5	34.8±9.0	2153±232

Data were shown as mean ± S.D. (n=8 mice, for PBS; n=9 mice, for d1-d3; n=9 mice, for d3-d5). *P<0.05 vs. PBS, by one-way ANOVA followed by Bonferroni test.

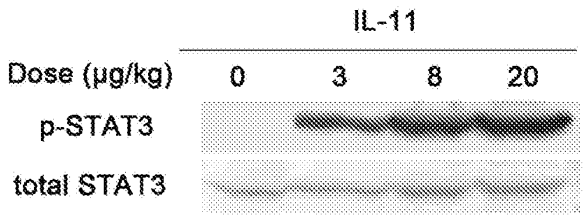

Supplementary Figure 1

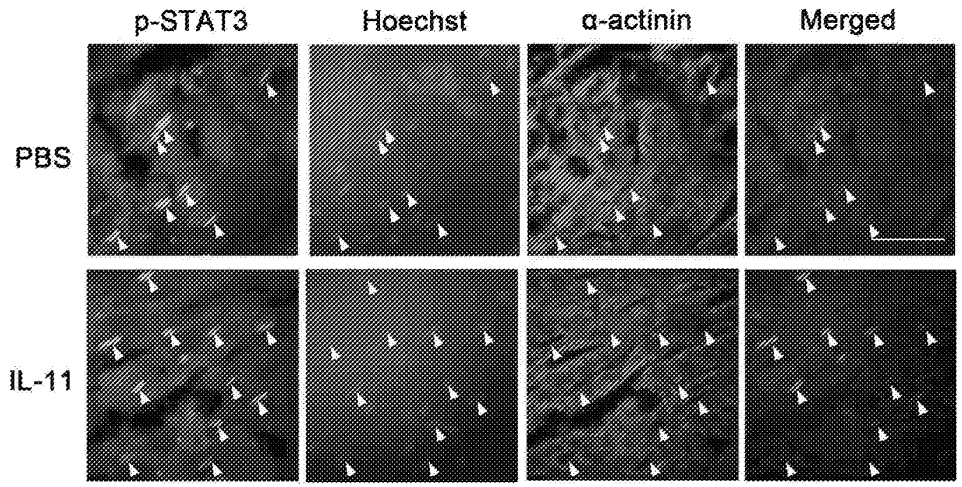

Supplementary Figure 2

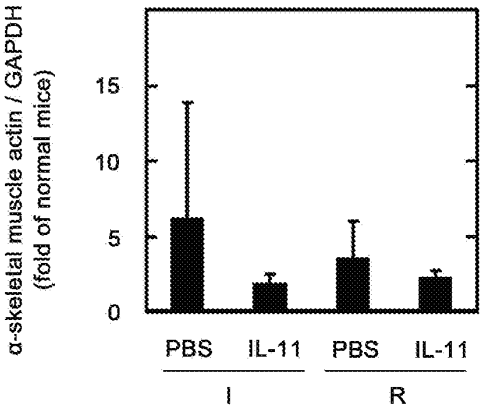

Supplementary Figure 3

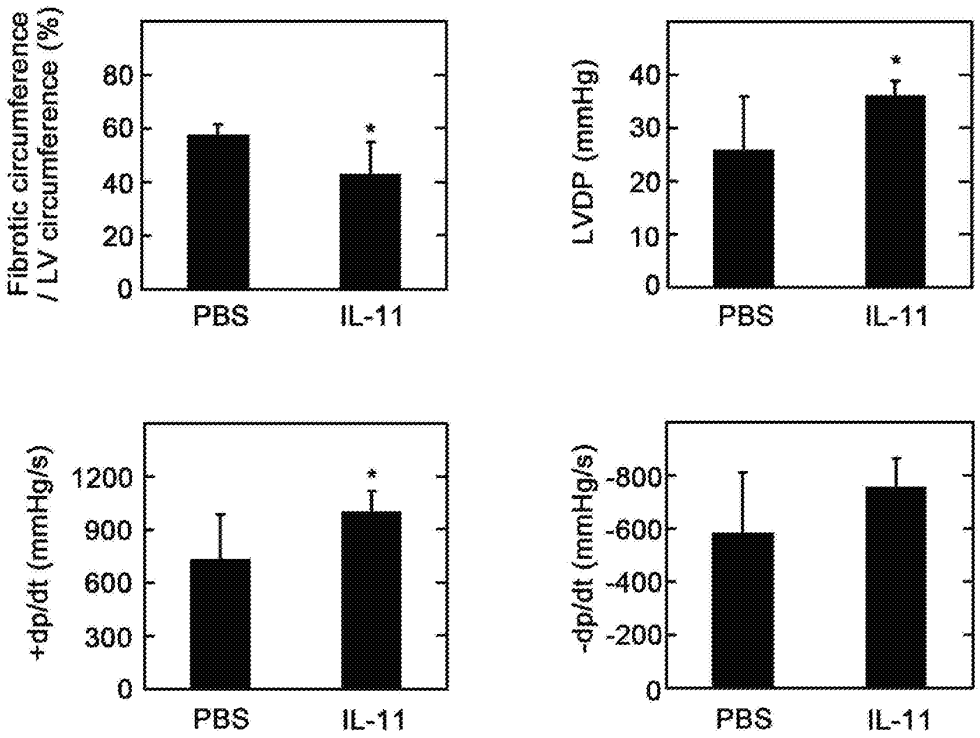

Supplementary Figure 4

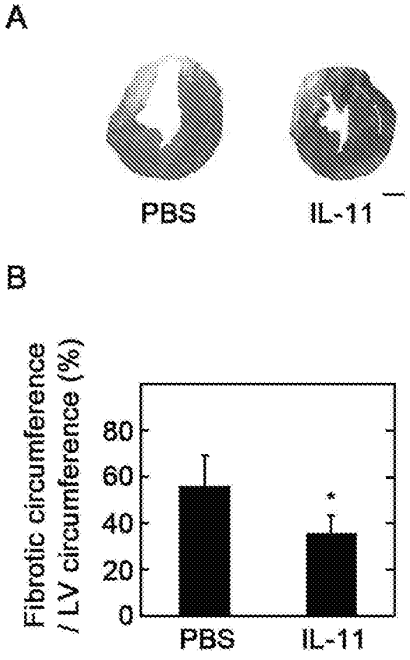

Supplementary Figure 5

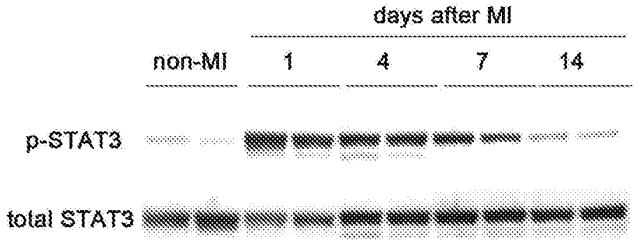

Supplementary Figure 6

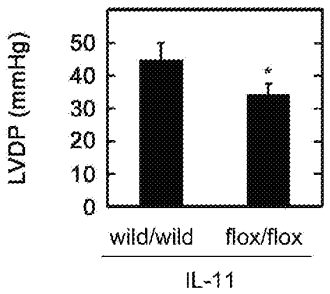

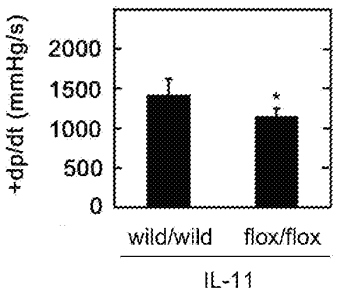

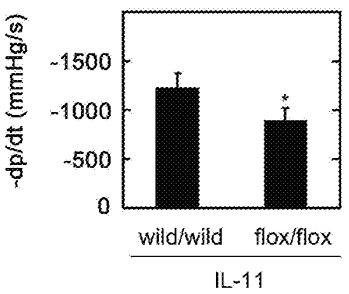

Supplementary Figure 7

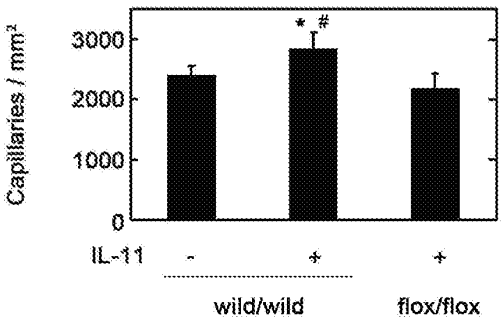

Supplementary Figure 8

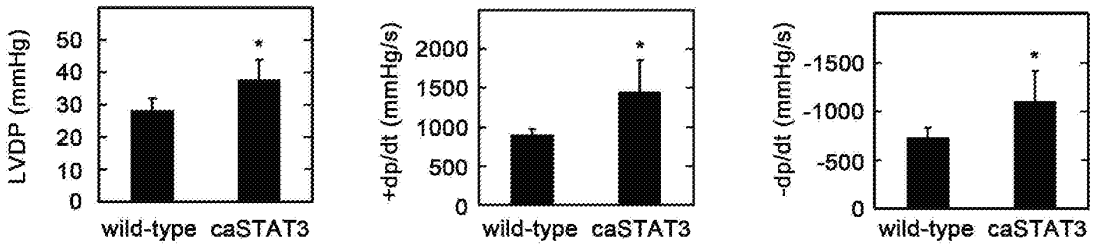

Supplementary Figure 9

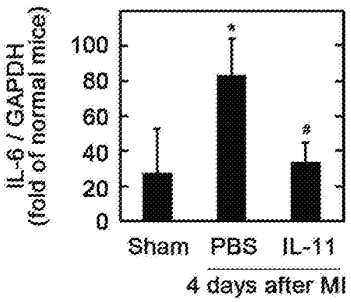

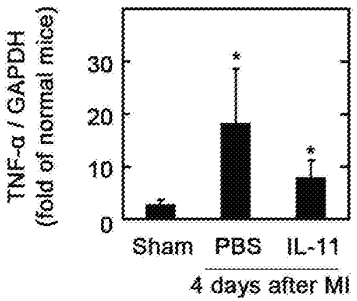

Supplementary Figure 10

Circulation

American Heart Association.

Therapeutic Activation of Signal Transducer and Activator of Transcription 3 by Interleukin-11 Ameliorates Cardiac Fibrosis After Myocardial Infarction

Masanori Obana, Makiko Maeda, Koji Takeda, Akiko Hayama, Tomomi Mohri, Tomomi Yamashita, Yoshikazu Nakaoka, Issei Komuro, Kiyoshi Takeda, Goro Matsumiya, Junichi Azuma and Yasushi Fujio

Circulation. 2010;121:684-691; originally published online January 25, 2010;
doi: 10.1161/CIRCULATIONAHA.109.893677
Circulation is published by the American Heart Association, 7272 Greenville Avenue, Dallas, TX 75231

Print ISSN: 0009-7322. Online ISSN: 1524-4539

Regulated Overexpression of Interleukin 11 in the Lung

Use to Dissociate Development-dependent and -independent Phenotypes

Prabir Ray,* Weiliang Tang,* Ping Wang,* Robert Homer,‡§ Charles Kuhn III,‖ Richard A. Flavell,¶ and Jack A. Elias*

**Yale University School of Medicine, Section of Pulmonary and Critical Care Medicine, Department of Internal Medicine, New Haven, Connecticut 06520-8057; ‡Yale University School of Medicine, Department of Pathology, New Haven, Connecticut 06520-8023; §Connecticut VA Hospital, Pathology and Laboratory Medicine Service, West Haven, Connecticut 06516; ‖Brown University School of Medicine, Memorial Hospital of Rhode Island, Department of Pathology, Pawtucket, Rhode Island 02860; and ¶Yale University School of Medicine, Section of Immunobiology and Howard Hughes Medical Institute, New Haven, Connecticut 06520-8057*

Abstract

Standard overexpression transgenic approaches are limited in their ability to model waxing and waning diseases and frequently superimpose development-dependent and -independent phenotypic manifestations. We used the clara cell 10-kD protein (CC10) promoter and the reverse tetracycline transactivator (rtTA) to create a lung-specific, externally regulatable, overexpression transgenic system and used this system to express human interleukin 11 (IL-11) in respiratory structures. Gene induction could be achieved in utero, in neonates and in adult animals. Moreover, gene expression could be turned off by removal of the inducing stimulus. When gene activation was initiated in utero and continued into adulthood, subepithelial airway fibrosis, peribronchiolar mononuclear nodules, and alveolar enlargement (emphysema) were noted. Induction in the mature lung caused airway remodeling and peribronchiolar nodules, but alveolar enlargement was not appreciated. In contrast, induction in utero and during the first 14 d of life caused alveolar enlargement without airway remodeling or peribronchiolar nodules. Thus, IL-11 overexpression causes abnormalities that are dependent (large alveoli) and independent (airway remodeling, peribronchiolar nodules) of lung growth and development, and the CC10-rtTA system can be used to differentiate among these effector functions. The CC10-rtTA transgenic system can be used to model waxing and waning, childhood and growth and development-related biologic processes with enhanced fidelity. (*J. Clin. Invest.* 1997. 100: 2501–2511.) Key words: emphysema • airway fibrosis • asthma • inducible transgene expression

Introduction

Organ-specific overexpression transgenic modeling uses tissue-specific promoters to drive the expression of the gene(s) of interest. This approach has provided remarkable insights into the biologic effector functions and interactions of a large number of important proteins. However, this approach is not without important limitations. Many occur because the promoters that are used often initiate gene expression in utero and drive gene expression in a largely constitutive fashion thereafter. This confounds phenotypic interpretation by superimposing growth and/or development-related abnormalities on the abnormalities that would otherwise be caused by the gene product in an adult animal. It may also generate phenotypes that are accurate representations of the effects of chronically expressed proteins, but are not representative of the effects of these proteins when they are expressed in an intermittent fashion. Thus, overexpression transgenic approaches have a limited ability to model waxing and waning disease processes and differentiate the effects of genes that are dependent on and independent of organ growth and development.

In an attempt to address the limitations of overexpression transgenic modeling, several investigators have developed transgenic systems in which gene expression can be externally regulated. Early attempts focused on a variety of approaches including the use of steroid-inducible and metallothionein-based (1, 2) promoter systems. More recent approaches have used tet-regulatory systems based on wild-type and mutated tetracycline transactivator fusion proteins (3–5). Subsequent studies have demonstrated that tet-based systems can be externally regulated after direct injection into cardiac tissue (6), transfection into mesangial cells that are subsequently injected into visceral organs (7), and microinjection using standard transgenic technology (8–11). To date, however, these approaches have not been shown to selectively activate transgenes in utero, in neonates, and in adult animals, and have not been demonstrated to differentiate growth and development-dependent and -independent phenotypic abnormalities.

The lung is an outstanding system in which to evaluate the utility of externally regulatable overexpression transgenic systems. It is affected frequently by chronic waxing and waning inflammatory disorders of the airway such as asthma. In addition, early childhood events, such as severe viral infections, are increasingly appreciated to be associated with and potentially involved in the pathogenesis of the asthmatic diathesis (12–14). Overexpression modeling is being used to model asthma (15–17) and other waxing and waning inflammatory respiratory disorders (18, 19). These studies have most frequently used the clara cell 10-kD protein promoter (CC10)[1] and the surfactant apoprotein-C promoter to target genes to the air-

Address correspondence to Jack A. Elias, M.D., Yale University School of Medicine, Section of Pulmonary and Critical Care Medicine, Department of Internal Medicine, 333 Cedar Street, LCI 105, New Haven, CT 06520-8057. Phone: 203-785-4163; FAX: 203-785-3826; E-mail: jack.elias@yale.edu

Received for publication 3 June 1997 and accepted in revised form 29 August 1997.

The Journal of Clinical Investigation
Volume 100, Number 10, November 1997, 2501–2511
http://www.jci.org

1. *Abbreviations used in this paper:* BAL, bronchoalveolar lavage; CC10, clara cell 10-kD protein; CMV, cytomegalovirus; dox, doxycycline; hGH, human growth hormone; pc, postcoitus; rtTA, reverse tetracycline transactivator; tet-O, tetracycline operator.

way and alveolus, respectively. However, these promoters are activated in utero during times of important respiratory morphogenesis (20, 21), setting the stage for targeted transgenes to alter lung development (21). The degree to which development-dependent and -independent abnormalities are being evaluated in these models has not been assessed adequately.

To characterize the merits of externally regulatable overexpression transgenic approaches and to facilitate the modeling of pulmonary disorders, we developed a lung-specific externally regulatable overexpression system and used this system to express human IL-11 for varying periods of time before and after birth. IL-11 was chosen because our previous studies demonstrated that it is produced by lung fibroblasts and epithelial cells in response to cytokines, histamine, eosinophil major basic protein, and respiratory tropic viruses (22–26) and is found in the nasal secretions of children with upper respiratory tract infections (26). The phenotypes of animals with regulated transgene expression were compared with each other and to the phenotype of traditional transgenic animals in which IL-11 was expressed under the influence of the same promoter without this regulatable feature. These studies demonstrate that the pulmonary phenotype of traditional IL-11 overexpression mice is a mixture of development-dependent and -independent manifestations. They also demonstrate that the CC10–reverse tetracycline transactivator (rtTA) system can be used to selectively activate transgenes in utero, in neonates, and in adult animals, and can thus be used to differentiate development-dependent and -independent phenotypes and define crucial temporal windows during development that influence phenotype acquisition.

Methods

Production of transgenic mice

Transgenic mice were generated in which IL-11 was expressed in a lung-specific fashion using genetic constructs that did and did not allow for external regulation of transgene expression. The constructs that were used are illustrated in Fig. 1. Both used the CC10 promoter and took advantage of the fact that the murine respiratory epithelium contains 50–60% clara cells (27).

CC10-rtTA-hIL-11 mice

The externally regulatable transgenic system was based on the generation of animals with two transgenic constructs. The CC10-rtTA construct contained the CC10 promoter, the rtTA, and human growth hormone (hGH) intronic, with its nuclear localization sequence and polyadenylation sequences. The rtTA is a fusion protein made up of a mutated tetracycline repressor and the herpes virus VP-16 transactivator (5). The tet-O-CMV-hIL-11 construct contained a polymeric tetracycline operator (tet-O), minimal cytomegalovirus (CMV) promoter, human IL-11 cDNA, and hGH intronic and polyadenylation signals. In this system the CC10 promoter should direct the expression of rtTA to the lung. In the presence of doxycycline (dox), rtTA is able to bind in trans to the tet-O, and the VP-16 transactivator activates IL-11 gene transcription. In the absence of dox, rtTA binding does not occur and transgene transcription is not activated.

Preparation of the CC10-rtTA construct. A 2.3-kb HindIII fragment containing the rat CC10 promoter was obtained from construct pCC10-CAT (a gift from Dr. J. Whitsett and Dr. B. Stripp, Cincinnati, OH) (28). It was subsequently serially ligated to: (*a*) a 1.0-kb HindIII/BamHI fragment of plasmid 172.1 neo (a gift from Dr. M. Gossen and Dr. H. Bujard, University of Heidelberg, Heidelberg, Germany) (5) containing the rtTA gene; and (*b*) a 2.1-kb BamHI fragment containing the intronic and polyadenylation sequences of the hGH gene from plasmid p1017 (a gift from Roger M. Perlmutter, University of Washington, Seattle, WA). The ligated fragments was then cloned into the Hind III site in plasmid pBluescript II (KS^+) (Stratagene, La Jolla, CA). A 5.4-kb fragment containing the CC10-rtTA-hGH minigene was purified and used for microinjection.

Preparation of the tet-O-CMV-hIL-11 construct. Construct pUHC-13-3 was obtained from Dr. Gossen and Dr. Bujard (5) and a 0.49-kb XhoI/ClaI fragment containing heptamerized tet-O sequences linked to the CMV minimal promoter was isolated. This fragment was then ligated to hGH intronic and polyadenylation sequences and a 0.7-kb human IL-11 cDNA which had been digested previously with SmaI to remove its 3′ untranslated region. The entire DNA fragment was then cloned into the XhoI/BamHI site of pBluescript II (KS^+) (Stratagene). The tet-O-CMV-hIL-11 DNA fragment was then isolated by digestion with BssH2, purified, and used for microinjection.

All constructs were checked for correct orientation of the inserts by restriction enzyme digestion and junction sequences were confirmed by sequencing. Both constructs were purified, linearized, separated by electrophoresis through agarose, and isolated by electroelution into dialysis tubing. The DNA fragments were then purified through Elutip-D columns following the manufacturer's instructions

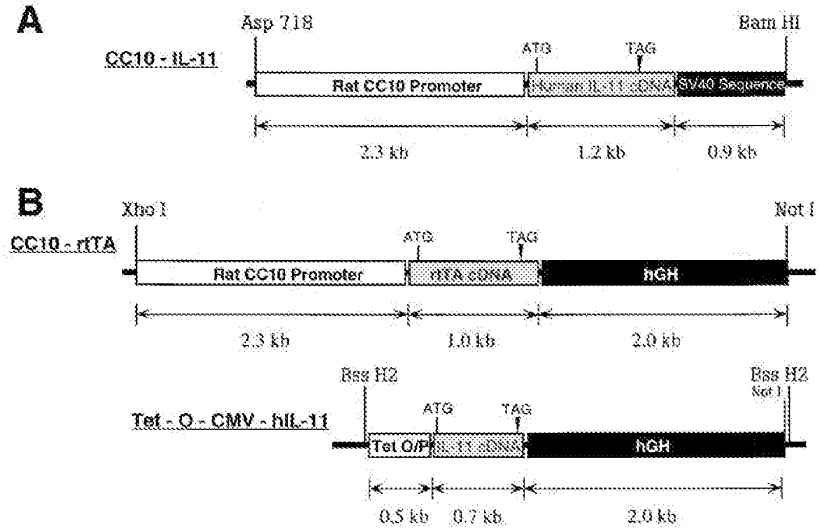

Figure 1. Genetic constructs used in the generation of the IL-11 overexpression transgenic mice. The traditional overexpression system (*A*) used the rat CC10 promoter, IL-11 cDNA, and SV-40 intronic and polyadenylation sequences. The inducible system (*B*) required two genetic constructs. The CC10-rtTA construct used the rat CC10 promoter, rtTA cDNA, and hGH intronic and polyadenylation sequences. The tet-O-CMV-hIL-11 construct used the tet-O, IL-11 cDNA, and hGH intronic and polyadenylation sequences.

(Schleicher & Schuell, Inc., Keene, NH) and dialyzed against injection buffer (0.5 mM Tris-HCl/25 mM EDTA, pH 7.5). Transgenic mice were prepared in [CBA × C57 BL/6] F_2 eggs by mixing and simultaneously injecting the constructs into pronuclei as described previously (16, 17).

CC10-IL-11 mice

These traditional lung-specific IL-11 overexpression mice used a genetic construct containing the CC10 promoter, IL-11 cDNA, and SV-40 intronic and polyadenylation sequences. The generation of these animals has been described previously by this laboratory (16).

Documentation of transgenic status

The presence or absence of the transgenes were initially evaluated using Southern blot analysis and later by PCR.

Southern blotting. Mouse tail biopsy DNA was digested with BamH1 and the resulting fragments were separated by electrophoresis using a 1% agarose gel at 2 V/cm in Tris-borate buffer. The resolved fragments were then transferred to a nylon membrane and hybridization was accomplished using an overnight incubation in a buffer containing 6× SSPE (3 M NaCl, 0.2 M $NaH_2PO_4 \cdot H_2O$, and 0.02 M Na_2EDTA), 0.5% SDS, 50% formamide, 50 μg/ml salmon sperm DNA, and labeled rtTA or IL-11 cDNA probes (5×10^6 cpm/ml of hybridization buffer). The rtTA probe was a 1-kb EcoR1/BamH1 fragment from plasmid 172.1. The IL-11 cDNA probe was a 1.2-kb cDNA fragment. After hybridization, the blots were washed twice for 15 min at room temperature in 6× SSPE/0.2% SDS and then twice for 15 min each at 55°C in 0.2× SSPE/1.0% SDS.

PCR. PCR for rtTA and IL-11 were performed using the following upper and lower primers and incubation conditions. rtTA PCR primers and conditions were: upper primer: 5′-GTCGCTAAAGAAGAAAGGGAAACAC-3′; lower primer: 5′-TTCCAAGGGCATCGGTAAACATCTG-3′; PCR conditions: 1 cycle of 95°C for 5 min, 35 cycles of 95°C for 1 min, 59°C for 1 min, and 72°C for 2 min. IL-11 PCR primers and conditions were: upper primer: 5′-CGACTGGACCGGCTGCTGC-3′; lower primer: 5′-CTAACTAGGGGGAGATAATGGCGGGGGGA-3′; PCR conditions: 30 cycles were performed. Each cycle was heated at 95°C for 1 min, annealed at 63°C for 1 min, and elongated at 70°C for 2 min.

All CC10-rtTA-hIL-11 lineage animals were evaluated for the presence of both transgenes. All CC10-IL-11 lineage animals were evaluated for IL-11 only.

dox water administration

All inducible transgenic mice were maintained on normal water until the point in time when transgene activation was desired. At that time, dox (0.5 mg/ml) was administered using aluminum foil wrapped water bottles to prevent light-induced dox breakdown.

Bronchoalveolar lavage (BAL) and quantification of IL-11 levels

Mice were killed via cervical dislocation, a median sternotomy was performed, blood was obtained via right heart puncture and aspiration, and serum was prepared. The trachea was then isolated via blunt dissection, and small caliber tubing was inserted and secured in the airway. Three successive washes of 0.75 ml of PBS with 0.1% BSA were then instilled and gently aspirated. Each BAL aliquot was centrifuged and the supernatants were harvested and stored individually at −70°C. The levels of IL-11 in the BAL fluid and serum were quantitated immunologically via ELISA. The ELISA was performed as previously described by our laboratory (23, 24) using antibodies 11h3/15.6.1 and 11h3/19.6.1 provided by Dr. Edward Alderman (Genetics Institute, Cambridge, MA).

Northern analysis

Total cellular RNA from a variety of mouse tissues was obtained using guanidine isothiocyanate extraction and formaldehyde-agarose gel electrophoresis as described previously (16). IL-11 gene expression was assessed by probing with ^{32}P-labeled IL-11 cDNA. Equality of sample loading and efficiency of transfer were assessed via ethidium bromide staining.

Histologic evaluation

Animals were killed via cervical dislocation and median sternotomies were performed. The heart and lungs were then removed en bloc and inflated to pressure (25 cm) with neutral buffered 10% formalin, fixed overnight in 10% formalin, embedded in paraffin, and sectioned and stained. Hematoxylin and eosin and Mallory's trichrome stains were performed.

Lung organ cultures

Fetal lung organ cultures were performed using modifications of the techniques of Gross and Wilson (29). The lungs from 14–19-d-old fetuses were isolated and the individual lobes were dissected and cultured separately. Equal fragments (by weight) of pulmonary tissue were placed in 35-mm plastic tissue culture dishes in Waymouth's MB 752/1 medium supplemented with penicillin, streptomycin, and 1% fetal bovine serum. Scratches were made on the culture dishes to ensure the adherence of the explants. They were then incubated in 5% CO_2 at 37°C. For the first 1.5 h they were in stationary cultures and for the remainder of the time they were incubated with gentle rocking. The supernatants surrounding the explants were removed at 24-h intervals and their IL-11 content was assessed by ELISA as described.

Morphometric analysis

Air space size was estimated from the mean chord length of the airspace (30). This measurement is similar to the mean linear intercept, a standard measure of air space size, but has the advantage that it is independent of alveolar septal thickness. Sections were prepared as described above. To obtain images at random for analysis, each glass slide was placed on a printed rectangular grid and a series of dots placed on the cover glass at the intersection of the grid lines, i.e., at ~ 1-mm intervals. Fields as close as possible to each dot were acquired by systemically scanning at 2-mm intervals. Fields containing identifiable artifacts or nonalveolated structures such as bronchovascular bundles or pleura were discarded.

A minimum of 10 fields from each mouse lung was acquired into a Macintosh computer through a framegrabber board. Images were acquired in 8-bit grayscale at a final magnification of 1.5 or 2 pixels per micron. The images were analyzed on a Macintosh computer using the public domain NIH Image program written by Wayne Rasband at the U.S. National Institutes of Health and available at http://rsb.info.nih.gov/nih-image. Images were manually thresholded, then smoothed, and inverted. The image was then subject to sequential logical image match and operations with a horizontal and then vertical grid. At least 200 measurements per field were made in transgene positive animals and 400 measurements per field were made in the transgene negative animals. The length of the lines overlying air space air was averaged as the mean chord length. Standard deviation was calculated using techniques that take animal to animal and field to field variations into account (31, 32). At least four animals were studied at each time point in the presence and absence of dox water. Chord length increases with alveolar enlargement.

Statistical analysis

Values are expressed as means±SEM. Unless otherwise stated, group means were compared by ANOVA with Scheffe's procedure post-hoc analysis using StatView software for the Macintosh.

Results

Generation of transgenic mice. To generate transgenic mice in which IL-11 was overproduced in a lung-specific and externally regulatable fashion, the two necessary genetic constructs

were produced and simultaneously microinjected. From these microinjections, 10 transgenic animals were obtained. One animal had the CC10-rtTA construct only. The other nine contained both of the desired genetic constructs. These founder animals were bred with C57 BL/6 mice and the transgene status of the offspring was similarly analyzed. This analysis demonstrated that both transgenes consistently traveled with one another and passed on to the offspring of the dual transgene positive founder animals in a Mendelian fashion. This suggests that the constructs inserted into the host genome in an identical and/or similar location. Of the dual founder lines, three did not manifest inducible IL-11 production. Two of the others were chosen for detailed analysis based on their low level of basal IL-11 production and significant response to dox water. Since their phenotypes were essentially identical, they are described below in a unified fashion.

Induction of IL-11 expression. To determine if the CC10-rtTA-hIL-11 system was functioning properly, adult (≥ 2 mo of age) dual transgene positive and transgene negative mice were maintained on normal water or water supplemented with dox (0.5 mg/ml) for varying periods of time. Their lungs were then removed, BAL was performed, and the levels of BAL fluid IL-11 were evaluated by ELISA. In accord with the fundamental assumptions of the inducible system, human IL-11 protein was unable to be detected in the BAL fluid of transgene negative mice drinking normal water or dox water, and IL-11 was unable to be detected, or was marginally detected, in the BAL fluid of dual transgene positive mice drinking normal water (Fig. 2 and data not shown). In contrast, human IL-11 protein was readily detected in the BAL fluid of dual transgene positive mice drinking dox water (Fig. 2 *A*). This induction could be appreciated after as little as 24–48 h and appeared to plateau ~ 4–6 d after the addition of dox to the animal's water supply. At all time points, IL-11 was unable to be detected in the serum of these animals (data not shown). In accord with our findings with IL-11 protein, human IL-11 mRNA was unable to be detected in the lungs of transgene negative animals on normal or dox water, and human IL-11 mRNA was barely detected or undetectable in the lungs of dual transgene positive animals drinking normal water (Fig. 2 and data not shown). In contrast, human IL-11 mRNA was readily detected in the lungs of dual transgene positive animals within 24 h of the addition of dox to their water supply (Fig. 2 *B*). These studies demonstrate that, in CC10-rtTA-hIL-11 mice, very modest levels of IL-11 are produced at baseline and that the IL-11 transgene is readily induced by dox water.

Cessation of IL-11 production and gene expression. The rtTA system should allow genes to be turned on and off. Thus studies were undertaken to determine if removal of dox from a dual transgene positive animal's water supply resulted in the

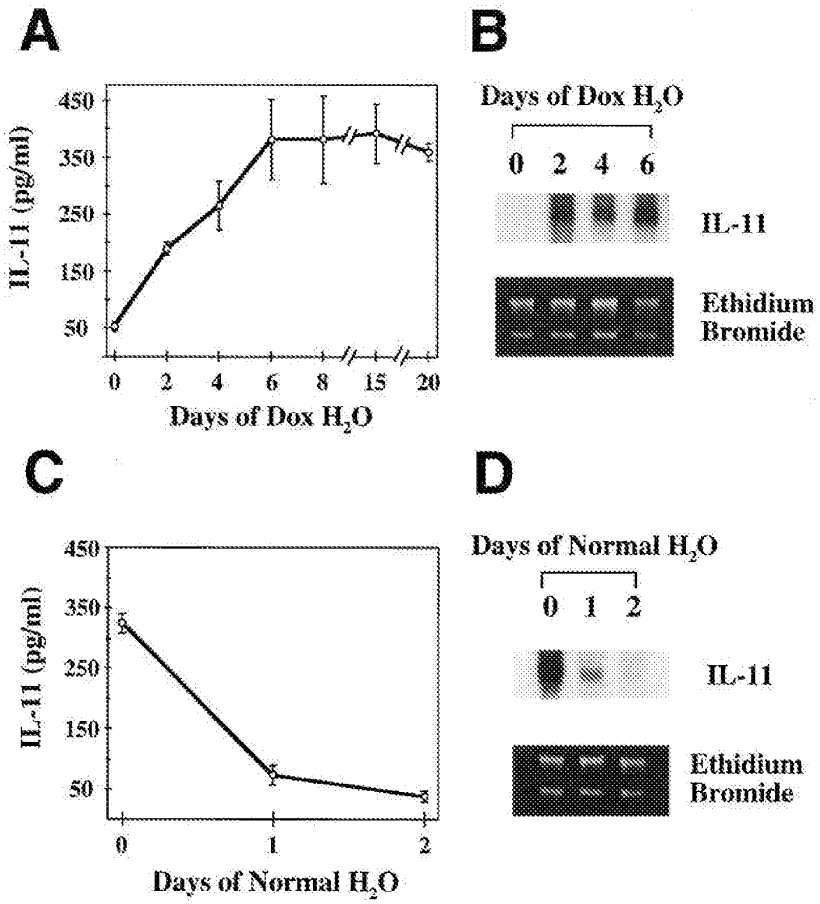

Figure 2. Kinetics of induction and cessation of IL-11 production in CC10-rtTA-hIL-11 mice. In *A* and *B*, dual transgene positive mice were grown to adulthood on normal water and then dox (0.5 mg/ml) was added to their water supply. The levels of BAL IL-11 protein (*A*) and pulmonary IL-11 mRNA (*B*) were assessed at intervals before and after the addition of dox. In *C* and *D*, dual transgene positive mice received dox water for 1 wk and then the dox was removed. The levels of BAL IL-11 protein (*C*) and pulmonary IL-11 mRNA (*D*) were assessed at intervals before and after dox removal. *B* and *D* are representative experiments of $n = 3$. *A* and *C* represent the mean±SEM of triplicate determinations at each time point.

cessation of transgene protein production and gene expression. In these experiments, dual transgene positive adult animals were maintained on dox water for 1 wk and were then placed on normal water. The levels of IL-11 protein and mRNA in their BAL fluid and lungs, respectively, were assessed at intervals thereafter. As shown in Fig. 2, *C* and *D*, IL-11 production in CC10-rtTA-hIL-11 dual transgene positive animals was dox-dependent with IL-11 gene expression and BAL IL-11 protein levels decreasing significantly ($\geq$ 80%) within 24 h of dox removal. In addition, IL-11 gene expression and protein production could be turned on, off, and on in these animals without any overt dampening of the responsiveness of this system (data not shown).

Organ specificity of dox-induced IL-11 expression. This externally regulatable overexpression system is designed to provide lung-specific transgene expression. To determine if the desired respiratory targeting had been accomplished, dual transgenic animals were maintained on dox water for 1 wk and the levels of human IL-11 in their BAL fluid and serum and the levels of human IL-11 mRNA in pulmonary and a variety of other tissues were compared. As noted above, IL-11 protein was readily detected in BAL fluid. However, it was not able to be detected in significant quantities in serum (data not shown). In addition, IL-11 mRNA was readily detected in lung tissue but not in RNA from a variety of other structures including heart, intestine, kidney, liver, muscle, pancreas, skin, spleen, testis, and uterus (Fig. 3 and data not shown). Thus, the CC10-rtTA system successfully targeted IL-11 to the lung.

Activation of the IL-11 transgene in utero and in neonatal animals. A desirable feature of an externally regulatable overexpression transgenic system designed for investigations of organ growth and development is the ability to activate gene expression before birth, just after birth, or in adult animals. The data presented above demonstrate that dox activates IL-11 in adult animals. To determine if dox was able to activate gene expression in utero, dual transgene positive male mice and wild-type female mice were allowed to mate and the resulting gravid female mice were given normal water or dox water. The levels of IL-11 gene expression in the lungs of the resulting pups were assessed at birth. As can be seen in Fig. 4, IL-11 mRNA was unable to be detected in the lungs of transgene negative animals receiving normal water or dox water, and IL-11 gene expression was unable to be detected or was barely detected in the lungs of dual transgene positive animals whose mothers received normal water. In contrast, impressive levels of IL-11 gene expression were detected in the lungs of dual transgene positive pups whose mothers received dox water. This demonstrates that dox is passed through the placenta in quantities that are sufficient to activate gene expression in utero.

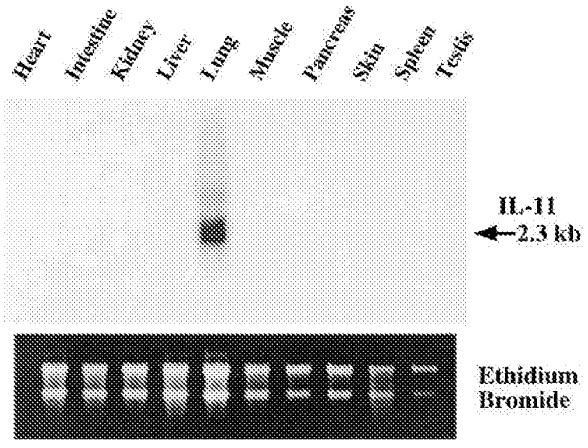

Figure 3. Organ specificity of transgene activation in CC10-rtTA-hIL-11 mice. Dual transgene positive mice were maintained on dox water for 1 wk. The levels of IL-11 gene expression in the noted structures were then assessed by Northern analysis.

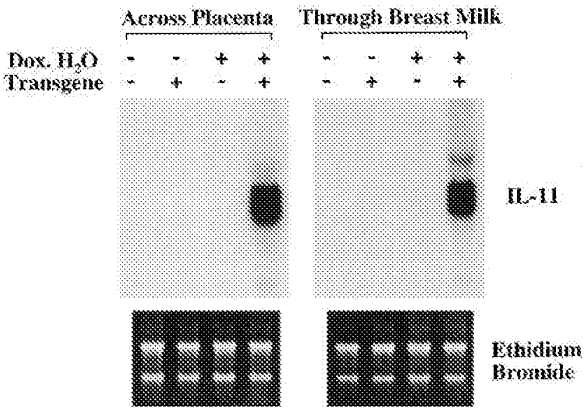

Figure 4. Activation of the IL-11 transgene in utero and in neonatal animals. Dual transgene positive male mice were crossed with transgene negative female mice. In the left panel (*Across Placenta*) the gravid female mice received normal water (−) or dox water (+) and the transgene status and levels of pulmonary IL-11 mRNA of the pups were assessed at birth. In the right panel (*Through Breast Milk*) dual transgene positive male mice were similarly mated with wild-type female mice and allowed to carry to term. The suckling mothers were then given either normal water (−) or dox water (+) and the lungs of their offspring were assessed at 2 wk of age. Comparisons were made of the levels of IL-11 mRNA in the lungs of transgene negative (−) and dual transgene positive (+) animals. The ethidium bromide loading controls are seen below each panel.

To determine if IL-11 gene expression was able to be activated in neonates, similar matings of dual transgene positive males and transgene negative females were undertaken and gravid female mice receiving normal water were allowed to carry to term. After their pups were born, some mothers were continued on normal water while others received dox water. 2 wk later, the IL-11 gene expression in the lungs of the pups was assessed. IL-11 mRNA was unable to be detected in the lungs of transgene negative pups whose mothers received normal water or dox water. IL-11 gene expression was also undetectable, or barely detectable, in the lungs of dual transgene positive pups whose mothers received normal water. In contrast, IL-11 gene expression was readily detected in the lungs of dual transgene positive pups whose mothers received dox water (Fig. 4). Thus, sufficient amounts of dox are transferred from lactating mothers to infants to activate rtTA-regulated genes in dual transgene positive offspring. When viewed in combination, these studies demonstrate that the CC10-rtTA-based system can be used to activate transgene expression in utero, in neonates, or in adult animals.

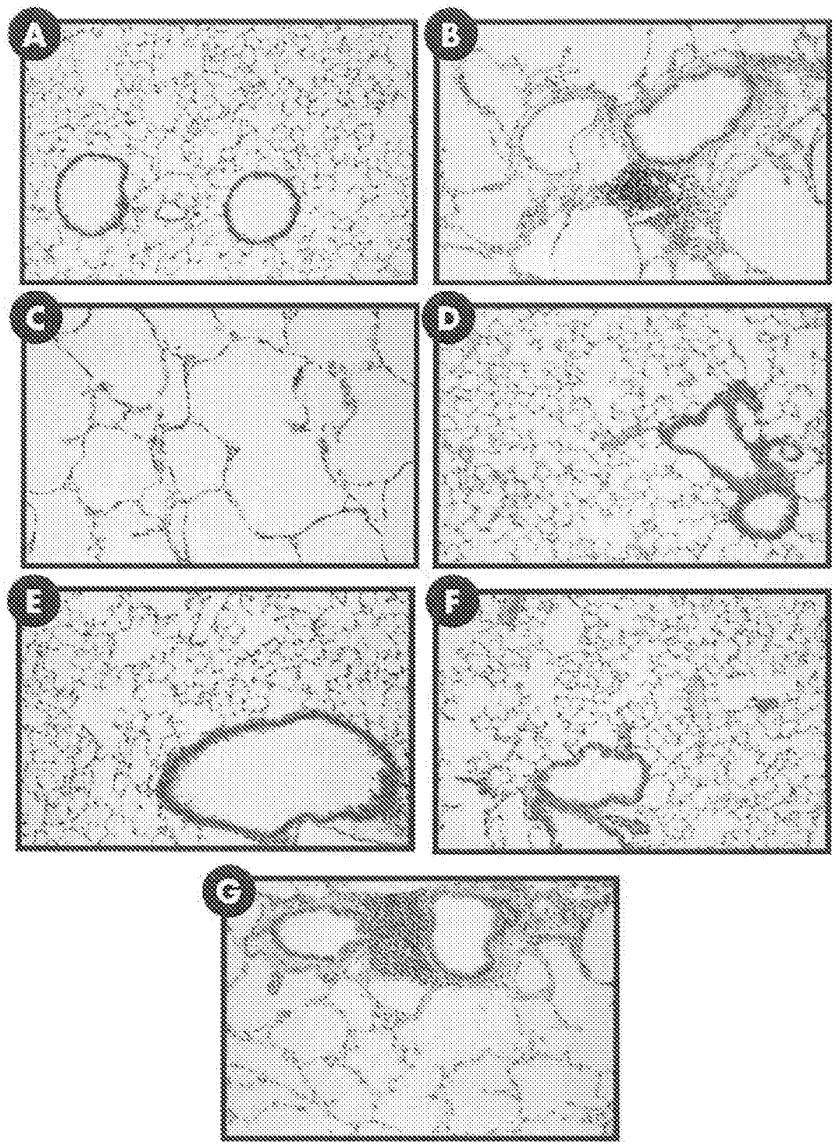

Figure 5. Comparison of the airway and alveolar phenotype of CC10-IL-11 and CC10-rtTA-hIL-11 animals when transgene activation was initiated in utero and maintained for 2 mo. *A* illustrates the normal pulmonary anatomy of transgene negative control mice. *B* illustrates the peribronchial nodules and subepithelial fibrosis seen in the airways of the CC10-IL-11 mice. *C* illustrates the large peripheral alveoli seen in CC10-IL-11 mice. *D* and *E* illustrate the normal pulmonary anatomy of transgene negative mice on normal water and dox water, respectively. *F* illustrates the normal pulmonary anatomy of dual transgene positive CC10-rtTA-hIL-11 mice on normal water. *G* illustrates the airway remodeling, peribronchiolar nodules, and enlarged air spaces seen in the CC10-rtTA-hIL-11 mice when the IL-11 transgene was activated in utero and expressed chronically thereafter. *H* illustrates the morphometric features (chord length) of the alveolar portions of the lungs from transgene positive and transgene negative animals from both lines. $^*P < 0.02$ comparing CC10-IL-11 transgene positive and negative littermates, and dual transgene positive CC10-rtTA-hIL-11 mice on dox water to transgene negative littermates on normal or dox water or dual transgene positive littermate mice on normal water. Original magnification for all photomicrographs, ×39.2.

Characterization of kinetics of CC10 activation. To be able to accurately compare the traditional CC10-IL-11 and inducible CC10-rtTA-hIL-11 mice, studies were undertaken to accurately define the kinetics of IL-11 production in the CC10-IL-11 animals. As described previously (16), IL-11 mRNA and/or protein were easily appreciated in the lungs and/or BAL fluid of 2-d-old to 6-mo-old transgene positive mice, but not their transgene negative littermates (data not shown). To determine if CC10 was activated in utero, lung organ cultures were prepared from transgene positive mice 14–19 d postcoitus (pc) and the IL-11 content of the supernatants of these cultures was assessed by ELISA. In keeping with prior reports (20, 21), IL-11 could not be detected in supernatants from cultures of day 15 or 16 pc lungs, but was readily detected in supernatants from days 17–18 pc lungs (data not shown). Thus, in traditional CC10-IL-11 transgenic mice, CC10 promoter activation can be detected by days 17–18 of gestation and continues for at least 6 mo thereafter.

Comparison of phenotypes of CC10-rtTA-hIL-11 and CC10-IL-11 mice. Knowledge of the kinetics of IL-11 expression in the traditional transgenic animals was then used to allow us to compare the phenotype of adult (2–3-mo-old) CC10-IL-11 mice and CC10-rtTA-hIL-11 mice in which IL-11 was expressed for similar periods of time. The CC10-IL-11 transgene positive animals had three major pathologic alterations. As previously noted (16), their airway alterations included peribronchiolar mononuclear cell predominant nodules and subepithelial fibrosis (Fig. 5 *B*). In addition, their pulmonary parenchyma contained impressively enlarged alveoli. These enlarged alveoli could be appreciated histologically (Fig. 5 *C*) and in the morphometric evaluations as significantly increased chord lengths (Fig. 5 *H*). Respiratory abnormalities were not

seen in the lungs of transgene negative animals receiving normal water or dox water or dual transgene positive animals receiving normal water (Fig. 5, *D*, *E*, and *F*, respectively). In contrast, dual transgene positive animals that received dox water in utero and chronically for 2 mo thereafter manifest peribronchiolar mononuclear cell predominant nodules, subepithelial fibrosis, and large alveoli documented histologically and via morphometric analysis (Fig. 5, *G* and *H*). Thus, the histologic abnormalities seen in the CC10-IL-11 transgenic mice can be reproduced in the CC10-rtTA-hIL-11 transgenic mice when the timing of gene activation in the traditional transgenic mice is reproduced with the externally regulatable system.

Importance of timing and duration of gene expression in determining pulmonary phenotype. To further define the importance of the timing and duration of gene expression in the generation of these pulmonary phenotypes, we compared the lungs of CC10-rtTA-hIL-11 mice in which IL-11 gene expression was activated at different times and for brief periods or extended intervals. When the IL-11 transgene was activated in normal mature (> 1-mo-old) lungs, interesting results were noted. Short periods of dox administration (2–5 d) did not consistently alter pulmonary phenotype. Occasional mononuclear cell predominant nodular changes were noted, but this was not a consistent finding (data not shown). However, extended periods of dox administration caused peribronchiolar nodules and subepithelial fibrosis (Fig. 6, *D* and *E*, respectively). In spite of this extended period of IL-11 production, significant alveolar enlargement could not be appreciated histologically (Fig. 6 *F*) or with morphometric techniques (Fig. 6 *G*). In contrast, IL-11 gene activation that was initiated in utero consistently led to murine lungs with large alveoli. Activation of IL-11 in utero and for 10–14 d after birth resulted in very large alveolar air spaces and impressive alterations in lung morphometry (Fig. 7, *D* and *E*, respectively). These animals had only a small number of true alveoli and instead had lungs that were arrested in the early alveolarization phase of lung development (33). However, these animals did not manifest peribronchiolar nodules or significant subepithelial fibrosis (Fig. 7 *D*). Thus,

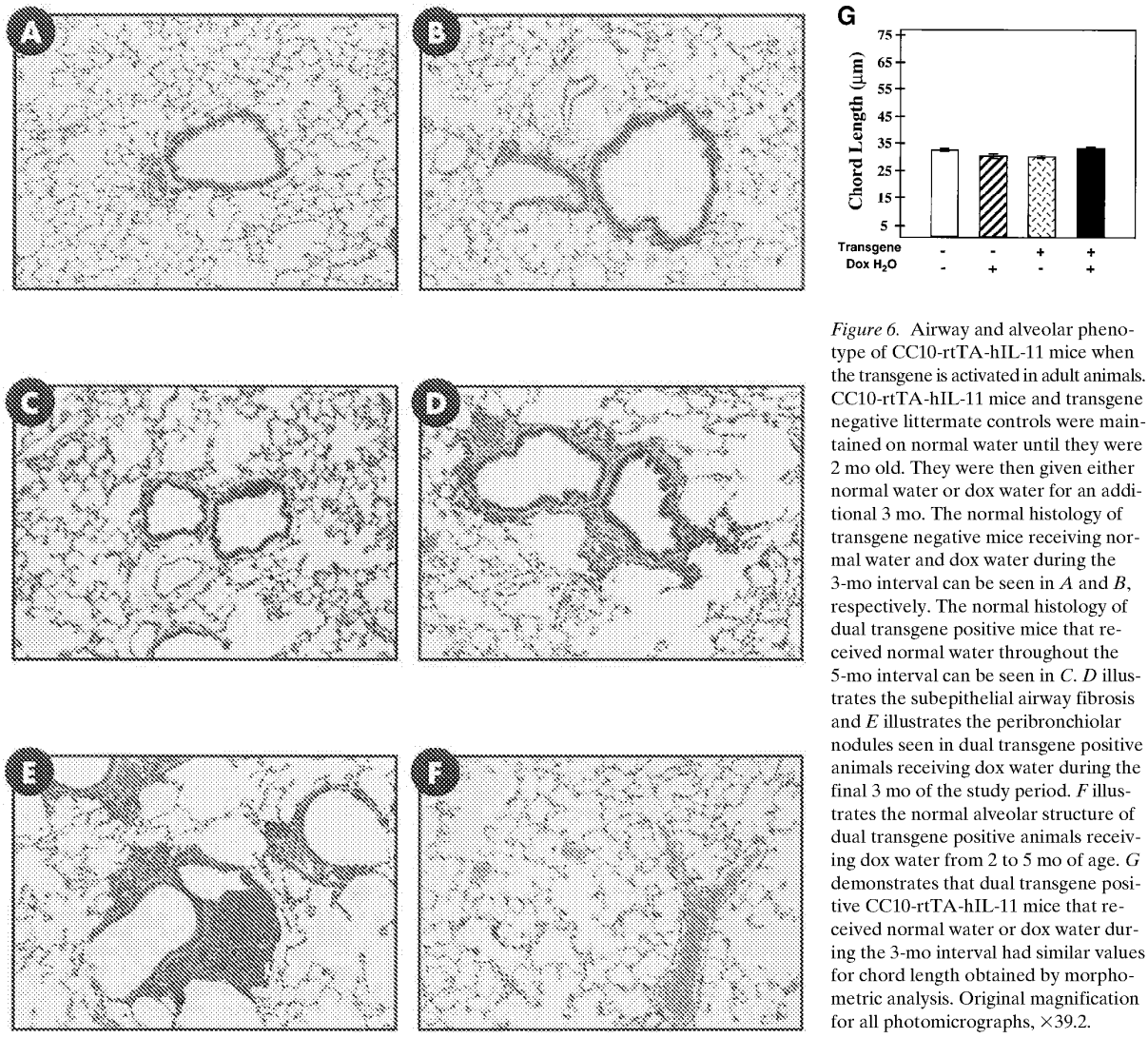

Figure 6. Airway and alveolar phenotype of CC10-rtTA-hIL-11 mice when the transgene is activated in adult animals. CC10-rtTA-hIL-11 mice and transgene negative littermate controls were maintained on normal water until they were 2 mo old. They were then given either normal water or dox water for an additional 3 mo. The normal histology of transgene negative mice receiving normal water and dox water during the 3-mo interval can be seen in *A* and *B*, respectively. The normal histology of dual transgene positive mice that received normal water throughout the 5-mo interval can be seen in *C*. *D* illustrates the subepithelial airway fibrosis and *E* illustrates the peribronchiolar nodules seen in dual transgene positive animals receiving dox water during the final 3 mo of the study period. *F* illustrates the normal alveolar structure of dual transgene positive animals receiving dox water from 2 to 5 mo of age. *G* demonstrates that dual transgene positive CC10-rtTA-hIL-11 mice that received normal water or dox water during the 3-mo interval had similar values for chord length obtained by morphometric analysis. Original magnification for all photomicrographs, ×39.2.

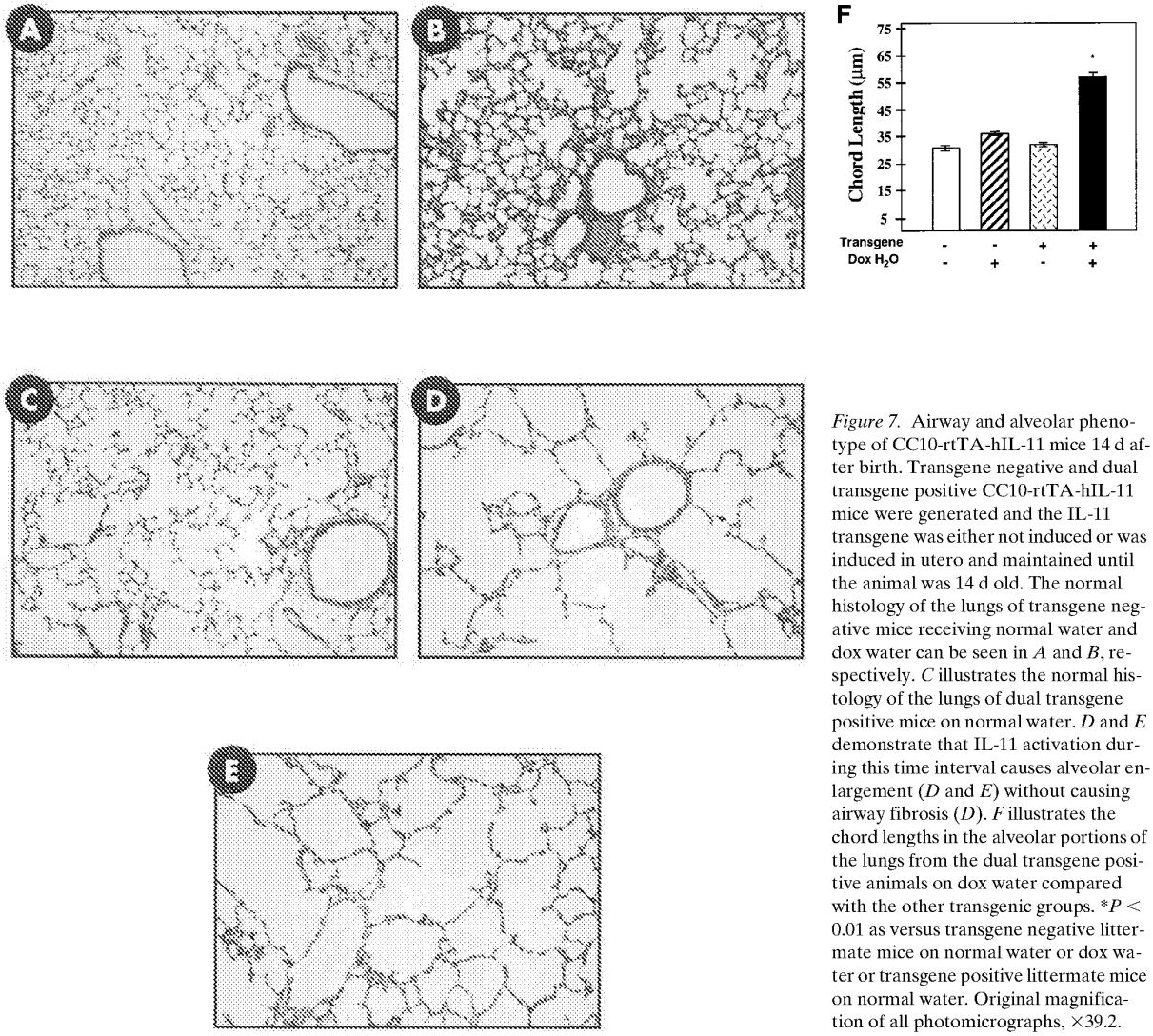

Figure 7. Airway and alveolar phenotype of CC10-rtTA-hIL-11 mice 14 d after birth. Transgene negative and dual transgene positive CC10-rtTA-hIL-11 mice were generated and the IL-11 transgene was either not induced or was induced in utero and maintained until the animal was 14 d old. The normal histology of the lungs of transgene negative mice receiving normal water and dox water can be seen in *A* and *B*, respectively. *C* illustrates the normal histology of the lungs of dual transgene positive mice on normal water. *D* and *E* demonstrate that IL-11 activation during this time interval causes alveolar enlargement (*D* and *E*) without causing airway fibrosis (*D*). *F* illustrates the chord lengths in the alveolar portions of the lungs from the dual transgene positive animals on dox water compared with the other transgenic groups. $*P <$ 0.01 as versus transgene negative littermate mice on normal water or dox water or transgene positive littermate mice on normal water. Original magnification of all photomicrographs, ×39.2.

the peribronchiolar nodules and subepithelial fibrosis seen in CC10-driven IL-11 overexpression transgenic mice occur when gene activation is initiated in utero or in adult animals and maintained for an extended period of time. In contrast, the alveolar enlargement was the result of alveolar hypoplasia and was only noted when IL-11 was activated in utero and/or in the early neonatal period. These studies demonstrate that the pulmonary phenotype of CC10-IL-11 overexpression animals contains abnormalities that are dependent on (large alveoli) and independent of (airway remodeling, peribronchiolar nodules) pulmonary growth and development and highlight the ability of the CC10-rtTA system to differentiate among these features.

Discussion

Mouse lung development begins 9.5 d pc with an outgrowth of paired lung buds from the foregut endoderm. This is followed by a defined series of developmental steps that form conducting airways and terminal acinar buds and dilatation of the terminal lung buds to form the sac-like primary saccules that are the gas exchanging structures present at birth (21, 33). During the first 2–3 d of postnatal life the primary saccules enlarge and the previously smooth saccule wall is modified by the development of low "secondary crests" (33, 34). The primary saccules then become subdivided into alveoli by the rapid elongation of the secondary crests, a process that occurs, in great extent, between days 4 and 14 after birth (the alveolarization phase of lung development) (33, 34). To determine if transgene-induced alterations in this developmental format contribute to the phenotype of overexpression transgenic animals, we compared the phenotype of animals in which IL-11 was expressed under the influence of the CC10 promoter in the presence and absence of a genetic regulatory feature that allowed gene expression to be induced in utero or delayed until adulthood. These studies demonstrate that animals in which IL-11 was expressed in utero, and for a significant period of

time thereafter, manifest airway remodeling, peribronchiolar nodules, and alveolar air space enlargement (emphysema). They also demonstrate that animals in which IL-11 gene expression is limited to the adult lung manifest airway remodeling and nodules without emphysema and that emphysema alone was seen when gene expression was activated in utero and stopped within 14 d of birth. Thus, the ability of IL-11 to cause airway remodeling and peribronchiolar inflammatory nodules appears to be independent of pulmonary growth and development. In contrast, the alveolar enlargement that is seen in IL-11 overexpression transgenic animals represents alveolar hypoplasia due to a defect in alveolarization of the developing lung. These studies are the first to demonstrate that IL-11 can alter pulmonary alveolar development. Importantly, they are also the first to demonstrate that conventional overexpression transgenic animals can have complex phenotypes that include features that are dependent and independent of lung growth and development and that inducible transgenic systems, such as the one described in this report, can be used to differentiate among these manifestations.

Numerous reports have demonstrated that the stage of alveolarization is a very critical period of lung development that is highly sensitive to a variety of influences. Glucocorticoids, hypoxia, hyperoxia, and inhibitors of thyroid function all impede normal alveolar development (33, 35). The present studies further support this contention by demonstrating that the overexpression of IL-11 during this developmental stage also inhibits the formation of alveoli. These observations have important implications for a number of other transgenic systems that have been reported to date. Large alveoli (emphysema) were noted in overexpression transgenic mice in which the surfactant apoprotein-C promoter was used to drive the expression of TNF-α (19)and TGF-α (18). In the TNF-α overexpression mice, it was assumed that the alveolar enlargement was the result of the rupture of alveolar septa. However, a cytokine-induced defect in alveolar development, analogous to that described in this report is an attractive alternative explanation. Transgenic modeling with an inducible system might be useful in addressing the mechanism of alveolar enlargement in these animals.

The mechanism by which IL-11 causes alveolar hypoplasia is unknown. However, there are a number of clues that can be derived from the biology of IL-11 and the known mechanisms of alveolus formation. First, α-smooth muscle actin–containing cells (presumably myocytes and myofibroblasts) have been shown to play an important role in lung morphogenesis, possibly by providing a mesenchymal influence that stabilizes the lung's branching points allowing the expansion of the distal leading edges of epithelial tubules and terminal buds (21, 36). The homozygous knockout of the platelet-derived growth factor-α gene (36) and the overexpression of TGF-β_1 (21), which eliminate and increase the number of α-smooth muscle actin positive cells, respectively, both lead to defects in alveolar development. Previous studies from our laboratory demonstrated that IL-11 induces the development of α-smooth muscle actin-containing cells in airway structures (16). Thus, it is tempting to hypothesize that IL-11 might be mediating its effects on alveolar development via stimulating α-smooth muscle actin cell accumulation. However, if abnormalities in α-smooth muscle actin–containing cells are noted, it is also possible that they are the result of, and not the cause of, the IL-11–induced developmental abnormalities. In addition, since TGF-β_1 is an important stimulator of IL-11 production by a variety of stromal tissues (23, 24) it is reasonable to hypothesize that the effects of TGF-β_1 may be mediated, in part, by IL-11 in these overexpression modeling systems. An additional interesting property of IL-11 is its ability to inhibit epithelial cell proliferation (37). Since epithelial proliferation is required for the formation and elongation of structures like alveolar septa (35), it is easy to see how an inhibitor of epithelial proliferation might alter the development of alveolar structures. Additional investigations will be needed to differentiate among these and other possible mechanisms of this intriguing biologic event.

Inducible transgenic systems such as the one described in this report are most useful when the basal levels of transgene expression are below the levels at which biologic effects of the transgene can be seen and the induced levels of the transgene are well within the physiologic range of the expressed protein. An analysis of the CC10-rtTA-hIL-11 mice suggests that this has been accomplished in our system. In the absence of dox, BAL levels of IL-11 $\leq$ 50 pg/ml were noted and histologic alterations in pulmonary structure were not appreciated. This observation is in accord with a number of studies that demonstrate that IL-11 concentrations $>$ 50 pg/ml are required to induce important IL-11 biologic effects in vitro (38–40). In contrast, dual transgene positive animals receiving dox water had levels of BAL IL-11 $\geq$ 0.3 ng/ml and major alterations in their airway and alveolar structures. This is in keeping with studies in the literature demonstrating that nanogram per milliliter concentrations of IL-11 are found in supernatants from appropriately stimulated stromal cells in vitro (23, 24, 26) and that picogram per milliliter to nanogram per milliliter concentrations of IL-11 are present in the nasal washings of children experiencing upper respiratory tract infections (26). However, it is important to view these conclusions with caution for a number of reasons. First, it is impossible to know what the levels of IL-11 are at local tissue sites in dual transgene positive animals receiving normal water since dilution occurs during BAL. Second, IL-11 may mediate its effects, in selected circumstances, at very low concentrations. This is seen in the bioassays that are used to detect IL-11 that are based on the proliferation of specially selected plasmacytoma cells (41). Thus, although the present system appears to meet the requirements one would wish to have for an inducible transgenic model, the potential limitations of the system must always be kept in mind.

Although the timing of developmental stages and their relationship to birth can differ from one species to another, in general, the major steps and mechanisms of lung development are well preserved from species to species. Thus, insights obtained in experimental animals may be extrapolated with caution to other species (33). In keeping with these similarities, alveolar development in humans begins at week 36 of gestation and lasts into early childhood with 85% of human alveoli formed after birth (33). Not surprisingly, abnormalities of alveolar development have been reported in a number of pediatric respiratory disorders. Among the most common is bronchopulmonary dysplasia in which large alveoli can be readily appreciated (42). The mechanisms responsible for these abnormalities have not been defined. However, modeling systems such as the one described in this report offer, for the first time, an approach that can be used to characterize the processes that generate these important pathologic abnormalities.

Early events in childhood are felt to play a key role in the pathogenesis of a variety of pulmonary disorders. This is par-

ticularly true in asthma where associations between severe viral respiratory tract infections in early life, atopy, and the development of chronic asthma have been noted (12–14). Experimental modeling of viral effects in the airway have demonstrated that temporal windows exist in which viral infections have different manifestations. For example, parainfluenza type 1 virus caused a necrotizing bronchiolitis and interstitial pneumonia in neonatal and weaning rats. However, the virus also caused airway remodeling, peribronchiolar mononuclear nodules, and alveolar hypoplasia only in neonatal rats (43). Studies of this sort demonstrate that timing is a crucial variable that influences the phenotype that arises from interactions between environmental and inflammatory stimuli and endogenous developmental programs. The regulatable overexpression transgenic system described in this report provides, for the first time, a system in which these crucial interactions can be investigated.

In summary, these studies describe the first externally regulatable organ-specific overexpression transgenic system and the utilization of this system to differentiate the development-dependent and -independent phenotypic features caused by the overexpression of IL-11 in the murine lung. Organ-specific externally regulatable transgenic systems of this sort can provide impressive insights into the biology of protein effector functions, the biology of organ growth and development, and the timing of crucial interactions between environmental stimuli and endogenous programs of growth and development. This approach will allow us to model developmental, early life, and waxing and waning biologic processes with a level of fidelity not previously available with standard overexpression transgenic approaches.

Acknowledgments

The authors thank the investigators and institutions that provided the reagents that were used, Dr. Jeffrey A. Whitsett and Dr. Barry Stripp for the gift of the CC10 promoter, and Ms. Kathleen Bertier for her excellent secretarial assistance.

This work was supported by National Institutes of Health grants HL-36708, AI-34953, HL-54989 (to J.A. Elias), HL-56389 (to J.A. Elias, R. Homer, and R.A. Flavell), and HL-52014 (to P. Ray). R.A. Flavell is an Investigator of the Howard Hughes Medical Institute.

References

1. Mader, S., and J.H. White. 1993. A steroid-inducible promoter for the controlled overexpression of cloned genes in eukaryotic cells. *Biochemistry.* 90: 5603–5607.

2. Palmiter, R.D., H.Y. Chen, and R.L. Brinster. 1982. Differential regulation of metallothionein-thymidine kinase fusion genes in transgenic mice and their offspring. *Cell.* 29:701–710.

3. Gossen, M., and H. Bujard. 1992. Tight control of gene expression in mammalian cells by tetracycline-responsive promoters. *Proc. Natl. Acad. Sci. USA.* 89:5547–5551.

4. Gossen, M., A.L. Bonin, and H. Bujard. 1993. Control of gene activity in higher eukaryotic cells by prokaryotic regulatory elements. *Trends Biochem. Sci.* 18:471–475.

5. Gossen, M., S. Freundlieb, G. Bender, G. Muller, W. Hillen, and H. Bujard. 1995. Transcriptional activation by tetracyclines in mammalian cells. *Science.* 268:1766–1769.

6. Fishman, G.I., M.L. Kaplan, and P.M. Buttrick. 1994. Tetracycline-regulated cardiac gene expression in vivo. *J. Clin. Invest.* 93:1864–1868.

7. Kitamura, M. 1996. Creation of a reversible on/off system for site-specific in vivo control of exogenous gene activity in the renal glomerulus. *Proc. Natl. Acad. Sci. USA.* 98:7387–7391.

8. Kistner, A., M. Gossen, F. Zimmermann, J. Jerecic, C. Ullmer, H. Lubbert, and H. Bujard. 1996. Doxycycline-mediated quantitative and tissue-specific control of gene expression in transgenic mice. *Proc. Natl. Acad. Sci. USA.* 93:10933–10938.

9. Efrat, S., D. Fusco-DeMane, H. Lemberg, O.A. Emran, and X. Wang. 1995. Conditional transformation of a pancreatic β-cell line derived from transgenic mice expressing a tetracycline-regulated oncogene. *Proc. Natl. Acad. Sci. USA.* 92:3576–3580.

10. Furth, P.A., L. St. Onge, H. Boger, P. Gruss, M. Gossen, A. Kistner, H. Bujard, and L. Hennighausen. 1994. Temporal control of gene expression in transgenic mice by a tetracycline-responsive promoter. *Proc. Natl. Acad. Sci. USA.* 91:9302–9306.

11. Mayford, M., M.E. Bach, Y.-Y. Huang, L. Wang, R.D. Hawkins, and E.R. Kandel. 1996. Control of memory formation through regulated expression of a CaMKII transgene. *Science.* 274:1678–1683.

12. Sigurs, N., R. Bjarnason, F. Sigurbergsson, B. Kjellman, and B. Bjorksten. 1995. Asthma and immunoglobulin E antibodies after respiratory syncytial virus bronchiolitis: a prospective cohort study with matched controls. *Pediatrics.* 95:500–505.

13. Geppert, E.F., L.A. Lester, and C. Ober. 1995. Prioritizing asthma research: the need to investigate childhood asthma. *Am. J. Respir. Crit. Care Med.* 151:1294–1295.

14. Busse, W., S.P. Banks-Schlegel, and G.L. Larsen. 1995. NHLBI Workshop Summary: Childhood- versus adult-onset asthma. *Am. J. Respir. Crit. Care Med.* 151:1635–1639.

15. Rankin, J.A., D.E. Picarella, G.P. Geba, U.-A. Temann, B. Prasad, B. DiCosmo, A. Tarallo, B. Stripp, J. Whitsett, and R.A. Flavell. 1996. Phenotypic and physiologic characterization of transgenic mice expressing interleukin 4 in the lung: lymphocytic and eosinophilic inflammation without airway hyperreactivity. *Proc. Natl. Acad. Sci. USA.* 93:7821–7825.

16. Tang, W., G.P. Geba, T. Zheng, P. Ray, R. Homer, C.I. Kuhn, R.A. Favell, and J.A. Elias. 1996. Targeted expression of IL-11 in the murine airway causes airways obstruction, bronchial remodeling and lymphocytic inflammation. *J. Clin. Invest.* 98:2845–2853.

17. DiCosmo, B.F., G.P. Geba, D. Picarella, J.A. Elias, J.A. Rankin, B.R. Stripp, J.A. Whitsett, and R.A. Flavell. 1994. Airway targeted interleukin 6 in transgenic mice. Uncoupling of airway inflammation and bronchial hyperreactivity. *J. Clin. Invest.* 94:2028–2035.

18. Korfhagen, T.R., R.J. Swantz, S.E. Wert, J.M. McCarty, C.B. Kerlakian, S.W. Glasser, and J.A. Whitsett. 1994. Respiratory epithelial cell expression of human transforming growth factor-α induces lung fibrosis in transgenic mice. *J. Clin. Invest.* 93:1691–1694.

19. Miyazaki, Y., K. Araki, C. Vesin, I. Garcia, Y. Kapanci, J.A. Whitsett, P.-F. Piguet, and P. Vassalli. 1995. Expression of a tumor necrosis factor-α transgene in murine lung causes lymphocytic and fibrosing alveolitis. *J. Clin. Invest.* 96:250–259.

20. Ho, Y.-S. 1994. Transgenic models for the study of lung biology and disease. *Am. J. Physiol. (Lung Cell. Mol. Physiol. 10).* 266:L319–L353.

21. Zhou, L., C.R. Dey, S.E. Wert, and J.A. Whitsett. 1996. Arrested lung morphogenesis in transgenic mice bearing an SP-C-TGF-β1 chimeric gene. *Dev. Biol.* 175:227–238.

22. Zheng, T., M. Nathanson, and J.A. Elias. 1994. Histamine augments cytokine-stimulated interleukin-11 production by human lung fibroblasts. *J. Immunol.* 153:4742–4752.

23. Elias, J.A., T. Zheng, N.L. Whiting, T.K. Trow, W.W. Merrill, R. Zitnik, P. Ray, and E.M. Alderman. 1994. Interleukin-1 and transforming growth factor β regulation of fibroblast-derived interleukin-11. *J. Immunol.* 152:2421–2429.

24. Elias, J.A., T. Zheng, O. Einarsson, M. Landry, T.K. Trow, N. Rebert, and J. Panuska. 1994. Epithelial interleukin-11: regulation by cytokines, respiratory syncytial virus and retinoic acid. *J. Biol. Chem.* 169:22261–22268.

25. Rochester, C.L., S.J. Ackerman, T. Zheng, and J.A. Elias. 1996. Eosinophil-fibroblast interactions: granule major basic protein stimulation of fibroblast interleukin-6, interleukin-11 and leukemia inhibitory factor expression. *J. Immunol.* 156:4449–4456.

26. Einarsson, O., G.P. Geba, Z. Zhu, M. Landry, and J.A. Elias. 1996. Interleukin 11: stimulation in vivo and in vitro by respiratory viruses and induction of airways hyperresponsiveness. *J. Clin. Invest.* 97:915–924.

27. Pack, R.J., L.H. Al-Ugaily, and G. Morris. 1981. The cells of the tracheo-bronchial epithelium of the mouse: a quantitative light and electron microscope study. *J. Anat.* 132:71–84.

28. Stripp, B.R., P.L. Sawaya, D.S. Luse, K.A. Wikenheiser, S.E. Wert, J.A. Huffman, D.L. Lattier, G. Singh, S.L. Katyal, and J.A. Whitsett. 1992. *Cis*-acting elements that confer lung epithelial cell expression of the CC10 gene. *J. Biol. Chem.* 267:14703–14712.

29. Gross, I., and C.M. Wilson. 1983. Fetal rat lung maturation: initiation and modulation. *J. Appl. Physiol. (Respirat. Environ. Exercise Physiol.)* 55: 1725–1732.

30. Escolar, J.D.D., B. Gallego, C. Tejero, and M.A. Escolar. 1994. Changes occurring with increasing age in the rat lung: morphometrical study. *Anat. Rec.* 239:287–296.

31. Weibel, E.R. 1979. Stereological methods. *In* Practical Methods for Biological Morphometry. Vol. 1. Academic Press, Inc., London. 30.

32. Gundersen, H.J.G., and R. Osterby. 1981. Optimizing sampling effi-

ciency of stereological studies in biology: or "Do more less well!". *J. Microsc.* 121:65–73.

33. Burri, P.H. 1997. Structural aspects of prenatal and postnatal development and growth of the lung. *In* Lung Growth and Development. Vol. 100. J.A. McDonald, editor. Marcel Dekker, Inc., New York. 1–35.

34. Amy, R.W., D. Bowes, P.H. Burri, J. Haines, and W.M. Thurlbeck. 1977. Postnatal growth of the mouse lung. *J. Anat.* 124:131–151.

35. Massaro, D., N. Teich, S. Maxwell, G.D. Massaro, and P. Whitney. 1985. Postnatal development of alveoli. *J. Clin. Invest.* 76:1297–1305.

36. Bostrom, H., K. Willetts, M. Pekny, P. Leveen, P. Lindahl, H. Hedstrand, M. Pekna, M. Hellstrom, S. Gebre-Medhin, M. Schalling, et al. 1996. PDGF-A signaling is a critical event in lung alveolar myofibroblast development and alveogenesis. *Cell.* 85:863–873.

37. Peterson, R.L., M.M. Bozza, and A.J. Dorner. 1996. Interleukin-11 induces intestinal epithelial cell growth arrest through effects on retinoblastoma protein phosphorylation. *Am. J. Pathol.* 149:895–902.

38. Leng, S.X., and J.A. Elias. 1997. Interleukin-11 inhibits macrophage interleukin-12 production. *J. Immunol.* 159:2161–2168.

39. Redlich, A.A., X. Gao, S. Rockwell, M. Kelley, and J.A. Elias. 1996. IL-11 enhances survival and decreases TNF production after radiation-induced thoracic injury. *J. Immunol.* 157:1705–1710.

40. Trepicchio, W.L., M. Bozza, G. Pedneault, and A.J. Dorner. 1996. Recombinant human IL-11 attenuates the inflammatory response through down-regulation of proinflammatory cytokine release and nitric oxide production. *J. Immunol.* 157:3627–3634.

41. Gu, Z.-J., J. Wijdenes, X.-G. Zhang, M.-M. Hallet, C. Clement, and B. Klein. 1996. Anti-gp 130 transducer monoclonal antibodies specifically inhibiting ciliary neurotrophic factor, interleukin-6, interleukin-11, leukemia inhibitory factor or oncostatin M. *J. Immunol. Methods.* 190:21–27.

42. Margraf, L.R., J.F.J. Tomashefski, M.C. Bruce, and B.B. Dahms. 1991. Morphometric analysis of the lung in bronchopulmonary dysplasia. *Am. Rev. Respir. Dis.* 143:391–400.

43. Castleman, W.L., R.L. Sorkness, R.F. Lemanske, G. Grasee, and M.M. Suyemoto. 1988. Neonatal viral bronchiolitis and pneumonia induces bronchiolar hypoplasia and alveolar dysplasia in rats. *Lab. Invest.* 59:387–396.

The Journal of Infectious Diseases Advance Access published May 31, 2016

The Journal of Infectious Diseases

MAJOR ARTICLE

Therapeutic Effect of Recombinant Mutated Interleukin 11 in the Mouse Model of Tuberculosis

Galina Shepelkova, Vladimir Evstifeev, Konstantin Majorov, Irina Bocharova, and Alexander Apt

Laboratory for Immunogenetics, Central Institute for Tuberculosis, Moscow, Russia

Earlier we demonstrated that blocking of interleukin 11 (IL-11) by systemic administration of anti–IL-11 antibodies attenuates severity of *Mycobacterium tuberculosis* infection in mice. The substitution W147A in the IL-11 molecule creates the form of cytokine capable to disrupt gp130/IL11R signaling complex formation, thus serving as a high-affinity specific antagonist of IL-11–mediated signaling. We hypothesized that this mutant form of IL-11 may serve as an effective tool for inhibition of native IL-11 activity in vivo. We established the recombinant W147A mutant form of IL-11 in an optimized *Escherichia coli* expression system and administered it as the aerosol in the lungs of *M. tuberculosis*–susceptible I/St mice infected with *M. tuberculosis*. Our results show that this therapeutic approach markedly inhibits tuberculous inflammation in lungs, increases the survival time of infected animals, and decreases expression of key inflammatory factors at the RNA and protein levels. These findings are a step toward clinical evaluation of the anti–IL-11 therapy for tuberculosis.

Keywords. tuberculosis; mouse model; IL-11; inflammation.

Immune response to *Mycobacterium tuberculosis* infection in the lung involves a multitude of interacting cells possessing activating/effector and inhibitory/regulatory functions [1, 2]. The balance between upregulation and downregulation of immune response pathways is critical for host protection against tuberculosis. Control of bacterial population by activated cells of the immune system is beneficial for the host if only it does not lead to excessive lung tissue damage, failure of breathing function, and, at the population level, the spread of mycobacteria to new hosts [3]. Thus, the lack of balance in tuberculous inflammation is a central element of the disease pathogenesis.

Despite the complexity of innate and adaptive mechanisms of tuberculosis control, cell populations, soluble mediators, and signaling pathways balancing immune responses and inflammatory reactions are relatively well characterized [2, 4–6]. However, some potentially important players participating in tuberculosis-related regulatory cascades received less attention. Among those are cytokines from the interleukin 6 (IL-6) family (except IL-6 itself), whose general feature is signaling via receptor complexes containing gp130 molecule [7]. In particular, the physiological role of interleukin 11 (IL-11) in *M. tuberculosis* infection was discovered and is being studied only in our laboratory, although the role of this cytokine and its therapeutic applications/blocking in other experimental and clinical settings were explored much more intensively [8–12].

Earlier we demonstrated that the important producers of IL-11 are interstitial lung macrophages and that the level of IL-11 messenger RNA (mRNA) in these cells substantially differs between mouse strains, being higher in *M. tuberculosis*–susceptible I/St mice than in *M. tuberculosis*–resistant A/Sn mice [13]. More recently, we showed that in vivo blocking of IL-11 with antibodies attenuates the severity of the tuberculosis course in genetically susceptible mice [14]. Antibody treatment decreased the content of IL-11 and other proinflammatory cytokines in the lung and downregulated *Il11* mRNA expression, indicating the existence of a positive feedback loop at the transcriptional level. These results suggest that anti–IL-11 therapy could be a useful immune modulatory treatment of tuberculosis. However, systemic administration of antibodies on multiple occasions is hardly suitable for therapeutic applications. Apart from safety concerns, interventions of this kind often induce an anti–idiotypic-like response against administered antibodies, which may abrogate the effect [15, 16].

Previously it was shown that the substitution W147A in the IL-11 molecule creates an IL-11 variant capable of competitively disrupting formation of the gp130/IL11R signaling complex, thus serving as a high-affinity specific antagonist of IL-11–mediated signaling [17]. In this study, we established the recombinant W147A mutant form of murine IL-11 in an optimized *Escherichia coli* expression system and administered it in the aerosol form to the lungs of mice infected with a low dose of *M. tuberculosis* via the respiratory tract. This therapeutic approach markedly inhibited tuberculous inflammation in the lungs, increased the survival time of infected animals, and decreased expression of genes encoding key inflammatory factors. These findings are a step toward clinical evaluation of anti–IL-11 therapy for tuberculosis.

Received 4 February 2016; accepted 25 April 2016.

Correspondence: A. Apt, Laboratory for Immunogenetics, Central Institute for Tuberculosis, Yauza Alley, 2, Moscow107564, Russia (asapt@aha.ru).

The Journal of Infectious Diseases®

DOI: 10.1093/infdis/jiw176

MATERIALS AND METHODS

Mice

Mice of the inbred strain I/StSnEgYCit (I/St) were bred and maintained at the Animal Facilities of the Central Institute for Tuberculosis (Moscow, Russia) in accordance with guidelines from the Russian Ministry of Health (no. 755) and under the National Institutes of Health Office of Laboratory Animal Welfare (assurance no. A5502-11). Female mice aged 2.5 months at the beginning of experiments were used. All experimental procedures were approved by the Central Institute for Tuberculosis Animal Care and Use Committee (protocols 2, 6, 8, 11, and 16; approved on 18 March 2014).

Il11 Artificial Genes and Their Expression

The gene sequence was deduced from the amino acid sequence provided by GeneBank (available at: http://www.ncbi.nlm.nih.gov) and reversely translated into frequently used *E. coli* codons, using the Vector NTI Advance program (Supplementary Figure 1). Sequences for restriction endonucleases required for cloning into the pQE13 vector (Qiagen, Valencia, California) were inserted into the *Il11* nucleotide sequence, and the whole DNA molecule was split in 5 fragments of about 90 base pairs each. Complementary oligonucleotide fragments were annealed and cloned in the coding vector pQE13 for the expression in *E. coli* strain M15, using 2 intermediate plasmids (Supplementary Figure 2). To obtain the mutant form of *Il11* (m-*Il11*), the wild-type form (wt-*Il11*) was mutated in vitro, using the quick–change polymerase chain reaction (PCR) method and reagents recommended by the manufacturer (Stratogene, San Diego, California). *E. coli* strain M15 was transformed by electroporation. Proteins from lysed *E. coli* cells were isolated using a WB 40Ni column and reagents from Pharmacia, and they were detected by sodium dodecyl sulfate polyacrylamide gel electrophoresis. Identical procedures were used to develop wild-type IL-11 (wtIL-11) and mutant IL-11 (mIL-11).

Infection, IL-11 Treatment, Colony-Forming Unit (CFU) Counts, and Survival Curves

At day 0, mice were infected with 10^2 CFU of *M. tuberculosis* H37Rv (Pasteur) using an Inhalation Exposure System (Glas-Col, Terre Haute, Indiana) exactly as described previously [27]. The size of the challenge dose was confirmed in preliminary experiments by plating serial 2-fold dilutions of 2-mL homogenates of whole lungs obtained 2 hours after exposure onto Dubos agar and counting colonies after incubation for 3 weeks at 37°C.

After infection in the lungs was established [28], at days +15, +17, +19, +21, +25, +27, and +29 mice were treated with 2 μg/mouse of either mIL-11 or wtIL-11 or with saline (control) administered via the trachea as aerosols obtained from 25 μL of solution (Supplementary Figure 3), using the MicroSprayer aerosolizer and a high-pressure syringe [29]. At indicated time points, mice were euthanized, and apical right lung lobes from individual mice were homogenized in 2 mL of sterile saline. A total of 0.1 mL of serial 10-fold dilutions of homogenates was plated onto Dubos agar, and colonies were counted after incubation for 18–20 days. Two independent experiments involving groups of 9 animals each provided similar results combined for the statistical analysis of major phenotypes. Survival time was monitored daily starting 1 month after infection.

Histological Analysis

Lung tissue specimens (from the middle-right lobe) were frozen across a temperature gradient of −60°C to −20°C in the electronic CryotomeH system (ThermoShandon, Runcorn, United Kingdom), and serial 6–8-mm-thick sections were made across the widest area of the lobe. Lung cryosections were fixed with acetone and stained with hematoxylin-eosin. All slides were examined by an experienced pathologist and photographed using an Axioskop40 microscope and AxioCamMRc 5 camera (Carl Zeiss, Berlin, Germany).

Gene Expression Evaluation

Total RNA from the lower right lobes of individual mice was isolated at day 32 after challenge, using the SV Total RNA Isolation System, and reverse transcription of mRNA was performed using reagents and protocols from Promega (Madison, Wisconsin). The mRNA levels for a number of inflammation-related genes were assessed by quantitative real-time reverse-transcription PCR on the iCycler iQ Multicolor Real-Time PCR Detection System (BioRad, Hercules, California), using specific primers, TaqMan probes, and reagents from Applied Biosystems (Foster City, California). Gene expression levels in individual mice were normalized to those of *GAPDH*. To quantify the results obtained by real-time PCR, the comparative threshold method was used exactly as described elsewhere [30], with the expression that the results were reported as mean fold increase ± standard of the mean (SEM) for groups of 4 mice each in 2 independent experiments (total number, 8 mice).

Flow Cytometry

Left lungs were individually isolated and enzymatically disrupted as described previously [18], and single-cell suspensions were analyzed by flow cytometry using fluorescein isothiocyanate– or phycoerythrin-labeled mAbs to the surface markers CD4, CD8, CD19, F4/80, and Ly6G (Supplementary Figure 4). Results are presented as summarized mean ± SEM for all animals.

Cytokine Enzyme-Linked Immunosorbent Assay (ELISA)

To measure cytokine contents, lung tissue homogenates were centrifuged, and the pellets were frozen at −70°C until assessed. The samples were diluted in 2 mL of phosphate-buffered saline, debris was removed by centrifugation at 500 *g*, and the cytokine content was assessed in the ELISA format, using the kits for IL-6, tumor necrosis factor α (TNF-α), interferon γ (IFN-γ;

BioLegend, San Diego, CA), and IL-11 (R&D Systems, Minneapolis, Minnesota), according to the manufacturers' instructions.

Statistical Analyses

All analyses were performed using GraphPad Prism, version 4. Mortality was assessed using Kaplan–Meier survival analysis and log-rank tests. One-tailed analysis of variance (ANOVA) and Student *t* tests were used as indicated in figure legends. A *P* value of $< .05$ was considered statistically significant.

RESULTS AND DISCUSSION

Administration of Mutated IL-11 Provides Beneficial Effects Onto Major Tuberculosis Phenotypes

We first evaluated how administration of wtIL-11 and mIL-11 influences the expression of major tuberculosis phenotypes: survival time after challenge, mycobacterial burden in the lungs, and lung pathology. Lung pathology and CFU counts were assessed after 4 IL-11 inhalations (on day 24) and after 3 additional inhalations (on day 32); survival curves were obtained after 7 inhalations in 3 experimental groups: mIL-11, wtIL-11, and saline (control) recipients.

As shown in Figure 1*A*, inhalations with mIL-11 resulted in a moderate increase of survival time as compared to control and wtIL-11 groups ($P < .01$, by Kaplan–Meier survival analysis). These results are in agreement with those obtained with polyclonal anti–IL-11 antibodies [14] and suggest that the W147A form of IL-11 diminishes the detrimental effect of native IL-11. This conclusion was supported by the results of CFU assessment (Figure 1*B* and 1*C*): recipients of wtIL-11 controlled mycobacterial multiplication in the lungs less effectively than animals from other groups (approximately 3-fold difference; $P < .05$, by ANOVA). In contrast to the data obtained with polyclonal antibodies [14], inhalation of mIL-11 did not affect CFU counts as compared to findings for the control group. Whether systemic versus local blocking of IL-11 has a generally different impact on mycobacterial control in lung tissue or whether antibody neutralization of IL-11 is more effective with respect to the mycobacterial growth control remains to be determined.

Evaluation of lung pathology provided additional evidence of the therapeutic effects of mIL-11 and the deleterious effects of wtIL-11. Mice from 2 control groups developed massive diffuse infiltration of the lung tissue at day 24 after challenge (Figure 1*D*). The pathology rapidly progressed, and by day 32 reached the stage of severe systemic inflammation, with affected zones poorly delimited from the remaining breathing tissue and necrotic granulomas in the lungs of wtIL-11 recipients (Figure 1*D*). The recipients of mIL-11 developed much milder

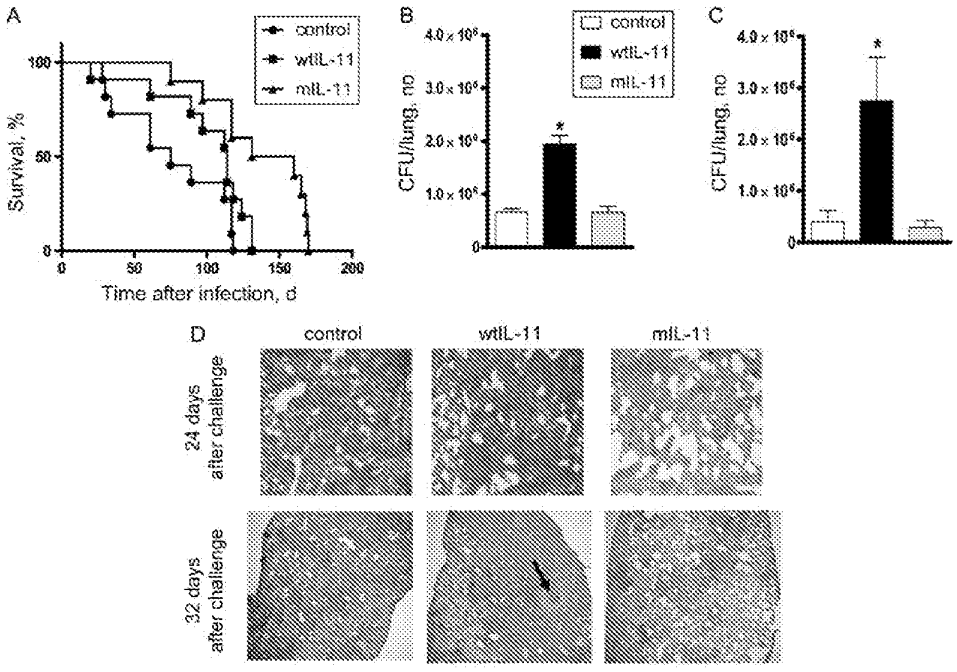

Figure 1. Administration of mutant interleukin 11 (mIL-11) has a therapeutic effect. *A*, Kaplan–Meier survival analysis revealed that mice treated with mIL-11 had a longer survival time than control groups treated with saline or wild-type IL-11 (wtIL-11; saline vs mIL-11, $P = .001$; wtIL-11 vs mIL-11, $P = .01$; saline vs wtIL-11 $P = .074$ [nonsignificant]; all *P* values were calculated by the log-rank test). Lung colony-forming unit (CFU) counts were significantly ($P < .05$, by analysis of variance) higher in the recipients of wtIL-11 as compared to those in mIL-11–treated and saline-treated groups, at day 24 (*B*) and day 32 (*C*) of infection. *D*, Lung pathological findings by hematoxylin-eosin staining on day 24 (upper panels; original magnification ×150) and day 32 (bottom panels; original magnification ×37). Low-magnification photographs taken at day 32 display about two-thirds of the whole-lung section, allowing quantification of pathological findings. The arrow indicates a necrotic focus in the lung of wtIL-11–treated mouse.

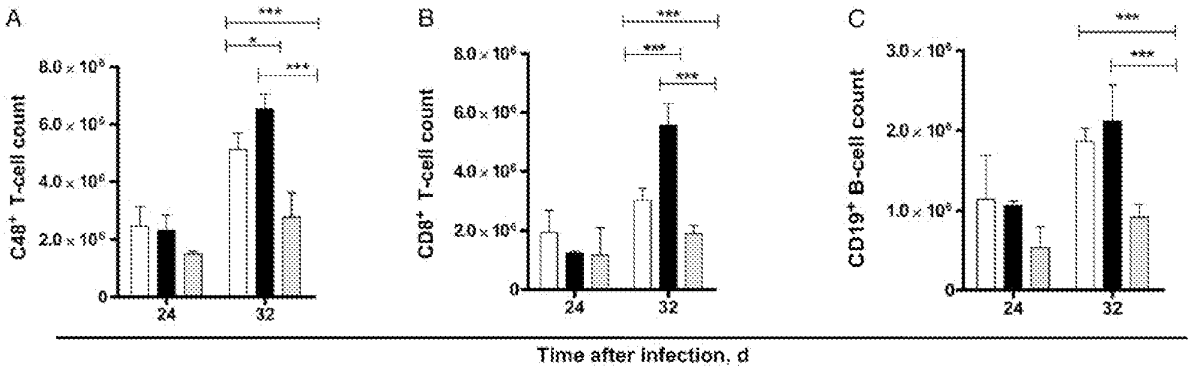

Figure 2. Opposite effect of mutant interleukin 11 (mIL-11) and wild-type IL-11 (wtIL-11) administration on the level of lung tissue infiltration with lymphocytes. After 4 inhalations (day 24), groups of mice did not differ by the lung $CD4^+$ T-cell (*A*), $CD8^+$ T-cell (*B*), and $CD19^+$ B-cell (*C*) content. After 7 inhalations (day 32), treatment with mIL-11 (gray) decreased and wtIL-11 (black) increased the content of all major lymphocyte populations in the lungs of infected mice as compared to levels in the saline-treated (white) group. $^*P < .05$, $^{**}P < .01$, and $^{***}P < .001$, by the Student *t* test.

pathology, expressed as an increase in the thickness of alveolar walls at day 24 and as compact inflammatory foci, mostly surrounding bronchi, at day 32. These results are also in line with our data demonstrating attenuation of lung pathology after systemic administration of anti–IL-11 antibodies [14].

Cellular and Molecular Features of Inflammatory Response

To obtain a more detailed picture of the antiinflammatory effect of mIL-11, we assessed the content of leukocytes and the expression of a few genes encoding inflammatory factors in the lungs of mice from 3 groups. As shown in Figure 2, at day 24 after challenge, there were no significant differences between groups regarding the size of major lymphocyte populations in the lungs: mice differed neither by the numbers of $CD4^+$ and $CD8^+$ T cells nor by the numbers of $CD19^+$ B cells. This result was expected, since 2–3 weeks are required for initiation of an adaptive lymphocyte-mediated anti–*M. tuberculosis* response in the lungs of mice [18]. On the other hand, there were differences in the content of cells responsible for natural immunity, $F4/80^+$ macrophages and Ly-$6G^+$ neutrophils, the numbers of which were significantly lower in mIL-11 recipients (Figure 3).

By day 32, the sizes of all 3 lymphocyte populations substantially increased in groups of control mice, especially in wtIL-11 recipients, but there was only a moderate increase in mIL-11 recipients (Figure 2). This resulted in highly significant ($P < .001$) differences in numbers of lung-infiltrating lymphocytes between experimental and control groups. The sizes of neutrophil and macrophage populations were more stable but continued to stay significantly smaller in mIL-11 recipients. Thus, the results of flow cytometry analysis were in agreement with histological observations: compared with mock-treated mice, the total number of immune cells infiltrating infected lungs was significantly lower in mIL-11 recipients (Figure 3*C*). Taken together, these results suggest that local administration of the IL-11 antagonist has a more pronounced inhibitory effect on lung tissue cell

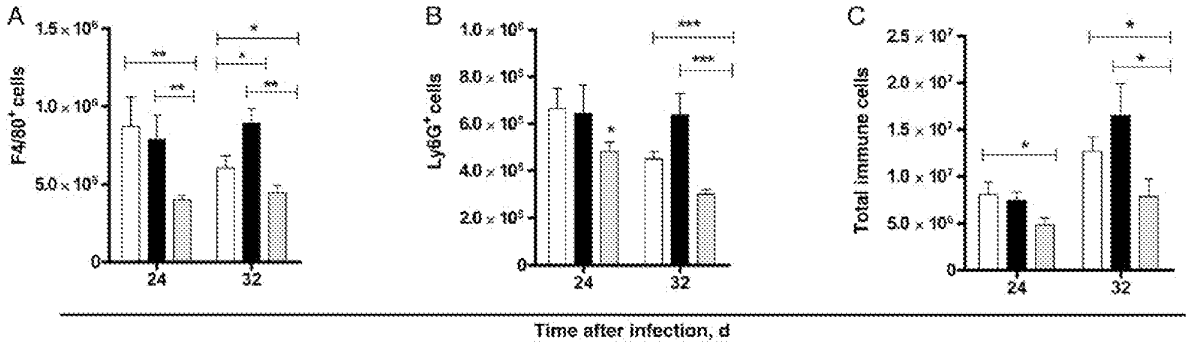

Figure 3. Recipients of mutant interleukin 11 (mIL-11; gray) displayed diminished lung infiltration with macrophages (*A*) and neutrophils (*B*), as well as general cellularity (*C*), 24 and 32 days after challenge. Data for the wild-type IL-11 group are in black, and data for the saline group are in white. $^*P < .05$, $^{**}P < .01$, and $^{***}P < .001$, by the Student *t* test.

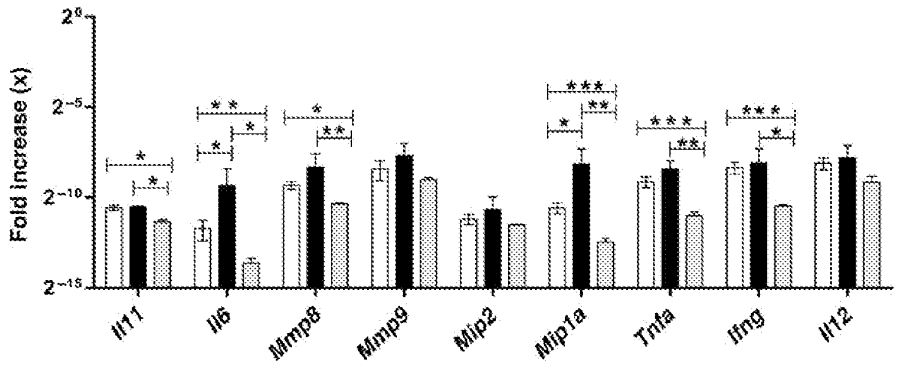

Figure 4. Expression of several genes involved in inflammation is downregulated in vivo following treatment with mutant interleukin 11 (mIL-11; gray). Gene expression levels were normalized to those of *GAPDH*. Results of real-time polymerase chain reaction evaluation were quantified using the comparative threshold method and expressed as mean fold increase ± standard error of the mean for groups of 4 mice each in 2 independent experiments (total number, 8 mice). Data for the wild-type IL-11 group are in black, and data for the saline group are in white. See also the legend for Figure 2. $*P < .05$, $**P < .01$, and $***P < .001$, by the Student *t* test.

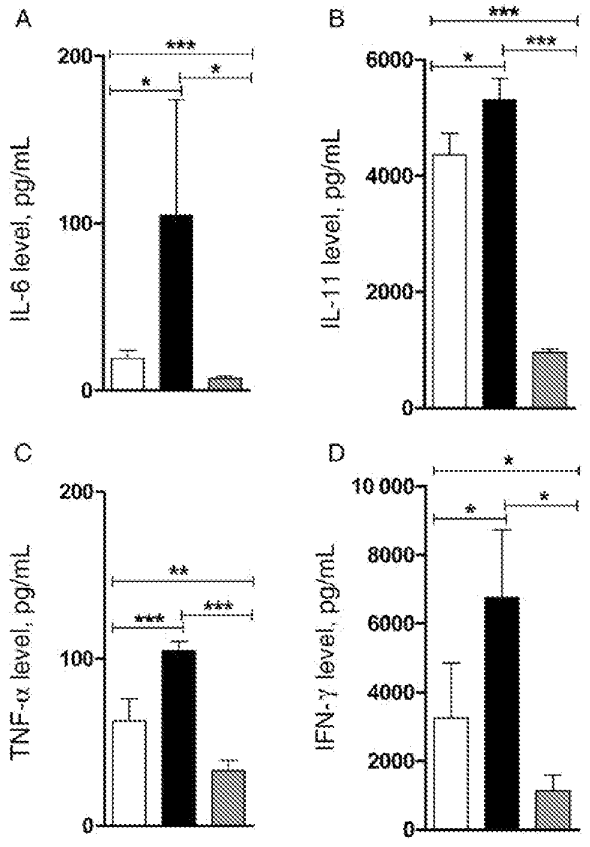

Figure 5. Therapy with mutant interleukin 11 (mIL-11; gray) decreases the levels of IL-11 and proinflammatory cytokines. Levels of interleukin (IL-6; *A*), IL-11 (*B*), tumor necrosis factor α (TNF-α; *C*), and interferon γ (IFN-γ; *D*) in lung homogenates were assessed at day 32 after challenge by enzyme-linked immunosorbent assay for 4 mice in each group. The results of 1 of 2 similar experiments are displayed as means ± standard errors of the mean. Data for the wild-type IL-11 group are in black, and data for the saline group are in white. See also the legend for Figure 2. $*P < .05$, $**P < .01$, and $***P < .001$, by the Student *t* test.

infiltration as compared to systemic administration of anti–IL-11 antibodies; in the latter case, a decrease in cell numbers was observed only in the neutrophil population [14].

Evaluation of the expression of genes involved in inflammation provided results that were in line with physiological observations. Administration of mIL-11 resulted in downregulation of the expression of inflammation-promoting *Il11*, *Il6*, *Mmp8*, *Mip1a*, *Tnfa*, *Ifng*, and *Il12*, whereas wtIL-11 administration upregulated *Il6* and *Mip1a* (Figure 4).

We also assessed how administration of mIL-11 and wtIL-11 affects production of key inflammatory cytokines in the lung tissue of infected mice at the protein level. Treatment with mIL-11 significantly decreased the level of IL-11 itself, as well as the levels of the proinflammatory and immune regulatory molecules IL-6, TNF-α, and IFN-γ, whereas administration of wtIL-11 increased production of these factors (Figure 5).

Overall, the therapeutic effect of the nonsignaling form of IL-11 was similar to that of polyclonal anti–IL-11 antibodies [14]. To our knowledge, this is the first demonstration of an antiinflammatory therapeutic effect provided in vivo by a mutated antagonistic form of a cytokine. Importantly, the effect was achieved by using a low-invasive inhalation system. Since IL-11 plays important roles in several physiological pathways [19], its systemic blocking may have serious adverse effects; thus, local administration of the antagonist to the respiratory tract has obvious advantages regarding possible clinical applications.

The IL-6 family of cytokines, especially IL-6 and IL-11, is upregulated in many cancers and considered one of the important cytokine families during tumorigenesis and metastasis, whose activity is released via STAT3-signaling and inflammation [9, 12, 20]. The role of IL-11 in infectious diseases is less well defined. A recent pilot proteome study in patients with tuberculosis demonstrated elevated levels of IL-11 and IL-11Ra/gp130 in fast responders to chemotherapy, compared with

slow responders [21], but parallel information on lung inflammatory status was not provided, which prevents physiological interpretation and comparison to the results obtained in mice. Our results indicate that, during *M. tuberculosis* infection, IL-11 plays a proinflammatory role in affected lungs, exacerbates lung pathology, and provides deleterious, pathogenic effects, as reported here and elsewhere [14, 22]. On the other hand, a few studies reported protective activity of IL-11 during infection [23, 24]. Remarkably, this protective activity concerned acute infections, in which a rapid neutrophil response against the parasite is essential for protection [23]. Contrary, in chronic *M. tuberculosis* infection, in which excessive neutrophil accumulation in affected lungs is pathogenic rather than protective [25, 26], selective blocking of IL-11 provides protective effects, perhaps by diminishing the neutrophil influx in the first instance [14].

Supplementary Data

Supplementary materials are available at http://jid.oxfordjournals.org. Consisting of data provided by the author to benefit the reader, the posted materials are not copyedited and are the sole responsibility of the author, so questions or comments should be addressed to the author.

Notes

Acknowledgments. G. S. designed and performed experiments, analyzed data, and wrote the manuscript. V. E. performed experiments and analyzed data. K. M. and I. B. performed experiments. A. A. analyzed data and wrote the manuscript.

Financial support. This work was supported by the Russian Scientific Foundation (grants 14-15-00029 and 15-15-30020 for ELISA experiments).

Potential conflicts of interest. All authors: No reported conflicts. All authors have submitted the ICMJE Form for Disclosure of Potential Conflicts of Interest. Conflicts that the editors consider relevant to the content of the manuscript have been disclosed.

References

1. Ottenhoff TH, Kaufmann SH. Vaccines against tuberculosis: where are we and where do we need to go? PLoS Pathog **2012**; 8:e1002607.
2. Orme IM, Robinson RT, Cooper AM. The balance between protective and pathogenic immune responses in the TB-infected lung. Nat Immunol **2015**; 16:57–63.
3. Dorhoi A, Reece ST, Kaufmann SHE. For better or for worse: the immune response against *Mycobacterium tuberculosis* balances pathology and protection. Immunol Rev **2011**; 240:235–51.
4. Russell D. Who puts the tubercle in tuberculosis? Nat Rev Microbiol **2007**; 5:39–47.
5. Cooper AM, Torrado E. Protection versus pathology in tuberculosis: recent insights. Curr Opin Immunol **2012**; 24:431–7.
6. Boer MC, Joosten SA, Ottenhoff TH. Regulatory T-Cells at the interface between human host and pathogens in infectious diseases and vaccination. Front Immunol **2015**; 6:217.
7. Bravo J, Heath JK. Receptor recognition by gp130 cytokines. EMBO J **2000**; 19:2399–411.
8. Hauer-Jensen M. Toward development of interleukin-11 as a medical countermeasure for use in radiological/nuclear emergencies. Dig Dis Sci **2014**; 59:1349–51.
9. Taniguchi K, Karin M. IL-6 and related cytokines as the critical lynchpins between inflammation and cancer. Semin Immunol **2014**; 26:54–74.
10. Herrlinger K, Witthoeft T, Raedler A, et al. Randomized, double-blind, controlled trial of subcutaneous recombinant human interleukin-11 versus prednisolone in active Crohn's disease. Am J Gastroenterol **2006**; 101:793–7.
11. Feinglass S, Deodhar A. Treatment of lupus-induced thrombocytopenia with recombinant human interleukin-11. Arthritis Rheum **2001**; 44:170–5.
12. Putoczki TL, Thiem S, Loving A, et al. Interleukin-11 is the dominant IL-6 family cytokine during gastrointestinal tumorigenesis and can be targeted therapeutically. Cancer Cell **2013**; 24:257–71.
13. Orlova MO, Majorov KB, Lyadova IV, et al. Constitutive differences in gene expression profiles parallel genetic patterns of susceptibility to tuberculosis in mice. Infect Immun **2006**; 74:3668–72.
14. Kapina MA, Shepelkova GS, Avdeenko VG, et al. Interleukin-11 drives early lung inflammation during *Mycobacterium tuberculosis* infection in genetically susceptible mice. PLoS One **2011**; 6:e21878.
15. Seiler P, Aichele P, Raupach B, Odermatt B, Steihoff U, Kaufmann SHE. Rapid neutrophil response controls fast-replicating intracellular bacteria but not slow-replicating *Mycobacterium tuberculosis*. J Infect Dis **2000**; 181:671–80.
16. Fulton SA, Reba SM, Martin TD, Boom WH. Neutrophil-mediated mycobactericidal immunity in the lung during *Mycobacterium bovis* BCG infection in C57BL/6 mice. Infect Immun **2002**; 70:5322–7.
17. Underhill-Day N, McGovern LA, Karpovich N, Mardon HJ, Barton VA, Heath JK. Functional characterization of W147A: a high-affinity interleukin-11 antagonist. Endocrinology **2003**; 144:3406–14.
18. Eruslanov EB, Majorov RB, Orlova MO, et al. Lung cell responses to *M. tuberculosis* in genetically susceptible and resistant mice following intratracheal challenge. Clin Exp Immunol **2004**; 135:19–28.
19. Ernst M, Thiem S, Nguyen PM, Eissmann M, Putoczki TL. Epithelial gp130/Stat3 functions: an intestinal signaling node in health and disease. Semin Immunol **2014**; 26:29–37.
20. Merchant JL. What lurks beneath: IL-11, via Stat3, promotes inflammation-associated gastric tumorigenesis. J Clin Inves **2008**; 118:1628–31.
21. Nahid P, Bliven-Sizemore E, Jarlsberg LG, et al. Aptamer-based proteomic signature of intensive phase treatment response in pulmonary tuberculosis. Tuberculosis (Edinb) **2014**; 94:187–96.
22. Lyadova IV, Tsiganov EN, Kapina MA, et al. In mice, tuberculosis progression is associated with intensive inflammatory response and the accumulation of Gr-1 cells in the lungs. PLoS One **2010**; 5:e10469.
23. Quinton LJ, Jones MR, Robson BE, Simms BT, Whitsett JA, Mizgerd JP. Alveolar epithelial STAT3, IL-6 family cytokines, and host defense during Escherichia coli pneumonia. Am J Respir Cell Mol Biol **2008**; 38:699–706.
24. Wan B, Zhang H, Fu H, et al. Recombinant human interleukin-11 (IL-11) is a protective factor in severe sepsis with thrombocytopenia: A case-control study. Cytokine **2015**; 76:138–43.
25. Eruslanov EB, Lyadova IV, Kondratieva TK, et al. Neutrophil responses to Mycobacterium tuberculosis infection in genetically susceptible and resistant mice. Infect Immun **2005**; 73:1744–53.
26. Yeremeev V, Linge I, Kondratieva T, Apt A. Neutrophils exacerbate tuberculosis infection in genetically susceptible mice. Tuberculosis (Edinb) **2015**; 95:447–51.
27. Radaeva TV, Kondratieva EV, Sosunov VV, Majorov KB, Apt A. A human-like TB in genetically susceptible mice followed by the true dormancy in a Cornell-like model. Tuberculosis (Edinb) **2008**; 88:576–85.
28. Mischenko VV, Kapina MA, Eruslanov EB, et al. Mycobacterial dissemination and cellular responses after 1-lobe restricted tuberculosis infection of genetically susceptible and resistant mice. J Infect Dis **2004**; 190:2137–45.
29. Bivas-Benita M, Zwier R, Junginger YE, Borchard G. Non-invasive pulmonary aerosol delivery in mice by the endotracheal route. Eur J Pharmac Biopharm **2005**; 61:214–8.
30. Livak KJ, Schmittgen TD. Analysis of relative gene expression data using real-time quantitative PCR and the 2(-Delta DeltaC(T)) method. Methods **2001**; 25:402–8.

JNEPHROL 2011; 24(01): 106-111
DOI:10.5301/JN.2010.5094

Effect of IL-11 on glomerular expression of TGF-beta and extracellular matrix in nephrotoxic nephritis in Wistar Kyoto rats

Maria Stangou [1], Gurjeet Bhangal [1], Ping-Chin Lai [1,2], Jennifer Smith [1], James C. Keith Jr [3], Joseph J. Boyle [4], Charles D. Pusey [1], Terence Cook [1,4], Frederick W.K. Tam [1]

[1] Imperial College Kidney and Transplant Institute, Division of Medicine, Imperial College London, London - UK
[2] Kidney Institute, Department of Nephrology, Chang Gung Memorial Hospital, School of Medicine, Chang Gung University, Taoyuan - Taiwan
[3] Wyeth Research, Cambridge, Massachusetts - USA
[4] Department of Histopathology, Hammersmith Hospital, London - UK

Abstract

Background: **The effect of interleukin-11 (IL-11) on transforming growth factor-β (TGF-β) is controversial and has not been examined in renal diseases. In this study, we (i) characterised the up-regulation of TGF-β1, phospho-p38 MAPK (p-p38 MAPK) and extracellular matrix during pathogenesis of glomerulonephritis and (ii) examined the effect of rhIL-11 on these processes in vivo.**

Methods: **Following induction of nephrotoxic nephritis, expression of TGF-β1, α-smooth muscle actin (α-SMA), fibronectin and p-p38 MAPK was detected in the kidney. Rats were treated either with vehicle or rhIL-11 at a high or low dose and culled on day 6.**

Results: **A high dose of rhIL-11 resulted in a significant reduction in the glomerular expression of TGF-β1 (0.4 ± 0.1 vs. 2.04 ± 0.4 semiquantitative score, $p<0.005$), α-SMA (0.6 ± 0.2 vs. 1.5 ± 0.3, $p<0.01$) and fibronectin (0.6 ± 0.1 vs. 1.5 ± 0.1, $p<0.02$). The periglomerular expression of α-SMA and fibronectin was significantly reduced in rats treated with the high dose of rhIL-11 (9.6% ± 2% vs. 92% ± 2.5% of glomeruli, $p<0.01$; and 26% ± 4.9% vs. 94% ± 1.9% of glomeruli, $p<0.005$, respectively). There was a slight but insignificant reduction of p-p38 MAPK in IL-11 treated rats. Treatment with low-dose rhIL-11 did not reduce expression of these molecules.**

Conclusion: **IL-11 suppresses glomerular expression of TGF-β1 and extracellular matrix deposition in experimental glomerulonephritis.**

Key words: *Extracellular matrix, Glomerulonephritis, IL-11, Myofibroblasts, TGF- β1*

Introduction

Interleukin-11 (IL-11) is a pleiotropic cytokine which exerts different actions in various cell types (1-3). Recombinant human IL-11 (rhIL-11) is clinically indicated in the treatment of chemotherapy-induced thrombocytopenia (4, 5) and in von Willebrand disease (6). The effect of IL-11 on fibrosis is controversial. It inhibits fibroblast proliferation in vitro (7) and ameliorates fibrosis in the HLA-B27 rat model of inflammatory bowel disease (8), but its overexpression in transgenic mice leads to lung fibrosis and airway obstruction (9). In previous studies, we have demonstrated that treatment with rhIL-11 reduces acute inflammation in nephrotoxic nephritis (NTN) in rats and mice (10, 11). NTN resembles human necrotizing and crescentic glomerulonephritis. Its pathogenesis and natural history have been characterised previously (12).

In this study, we report the effect of IL-11 on the expression of transforming growth factor-β1 (TGF-β1), a key profibrotic growth factor; α-smooth muscle actin (α-SMA), a myofibroblast marker; fibronectin, a component of extracellular matrix; and phospho-p38 MAPK (p-p38MAPK), a signal transduction pathway, in NTN in rats. TGF-β, as a positive regulator of myofibroblast differentiation, has a central role in the development and progression of fibrosis. The MAPK signalling pathway has been shown to exhibit cross-talk with the TGF-β signalling pathway; TGF-β-induced α-SMA expression and myofibroblast differentiation require the activation of MAPKs (13, 14).

To our knowledge, this is the first evidence that IL-11 treatment may retard glomerular expression of TGF-β1 and extracellular matrix deposition in glomerulonephritis.

Subjects and methods

For this study, we used renal tissue from previously reported experiments (10, 12).

Experiment 1: natural history of NTN in Wistar Kyoto rats

NTN was induced in male Wistar Kyoto (WKY) rats weighing 200-250 g by intravenous administration of 0.1 mL rabbit anti-rat glomerular basement membrane (GBM) nephrotoxic serum (12). Rats were sacrificed at different time points between 2.5 hours and 44 days. Three to 4 rats were studied at each time point.

Experiment 2: effect of IL-11 treatment on NTN in WKY rats

RhIL-11 supplied by Wyeth/Genetics Institute (Cambridge, MA, USA) was administered intraperitoneally to 16 NTN rats, in either 800 µg (n=6) or 1,360 µg (n=10) daily. The first treatment was given 2 hours before induction of NTN, and then once daily for 6 days. Vehicle-treated rats (n=8) received 0.2 mL of vehicle, intraperitoneally, on the same schedule. Rats were culled on day 6 (10).

Immunohistochemistry

TGF-β1, α-SMA and fibronectin

Immunohistochemistry on cryostat sections was performed for TGF-β1 (polyclonal goat anti-mouse, sc-146-G; Santa-Cruz Biotechnology, Santa Cruz, CA, USA), α-SMA (mouse anti-human mAb, clone 1A4, M0851; DAKO, Ely, UK) and fibronectin (mouse anti-human mAb, OBT0082; Oxford Biotechnology, Oxford, UK). The polyclonal anti-TGF-β1 antibody was diluted in 0.1% bovine serum albumin (BSA) / phosphate-buffered saline (PBS) + 0.1% polyoxyethylene sorbitan monolaurate (Tween 20) + 10% normal rabbit serum, and slides were incubated overnight at 4°C. The other antibodies were diluted in 0.1% BSA/PBS. The intensity of glomerular staining was assessed by semiquantitative score, on a scale of 0 to 3, with the observer unaware of the details of the groups. Periglomerular staining was expressed as percentage of glomeruli affected. In 6 rats of each group, there was enough tissue for immunostaining on cryostat sections.

Phospho-p38 MAPK

Immunostaining for p-p38 MAPK was performed on formalin-fixed, paraffin-embedded tissue. The slides were incubated overnight with 1:100 of the p-p38 MAPK mouse mAb (M 8177, clone p38-TY; Sigma-Aldrich, Poole, UK) and then with a peroxidase-conjugated goat anti-mouse antibody, for 45 minutes at 4°C. In each rat, the number of positive cells was counted in 25 glomerular sections.

Statistical analysis

All parameters are expressed as mean ± standard error. Mann-Whitney *U*-test was used to compare the different groups; $p<0.05$ was considered to be significant.

Results

Experiment 1: TGF-β1, α-SMA, fibronectin and p-p38 MAPK expression during the natural history of NTN

TGF-β1 was first detected in the glomerular mesangium on day 6 and in the tubulointerstitium on day 11, both increasing during disease progression. α-SMA, a marker for myofibroblasts, was detected on day 4 in the periglomerular area, and on day 6 in both periglomerular and mesangial regions, which increased further at the later stages of the disease. Fibronectin was first detected in the glomerular mesangium on day 4 and in the periglomerular area on day 6. The intensity of p-p38 MAPK expression was increased initially only 5 hours after nephrotoxic serum (NTS) administration, reduced subsequently during days 2-4, but increased again on day 6. At these time points, staining was nuclear in the mesangial and parietal epithelial cells and cytoplasmic in tubular epithelial cells. Representative results are shown in Figure 1.

Experiment 2: effect of rhIL-11 treatment

The intensity of TGF-β1 glomerular expression was reduced from 2.04 ± 0.1 semi-quantitative score in the vehicle group to 0.4 ± 0.1 ($p<0.005$) in rats treated with high-dose rhIL-11.

Both glomerular and periglomerular expression of α-SMA and fibronectin were reduced by high-dose IL-11 treatment (α-SMA from 1.5 ± 0.1 to 0.4 ± 0.1 semiquantitative score, $p<0.01$, and from 92% ± 2.5% to 9.6% ± 2% of

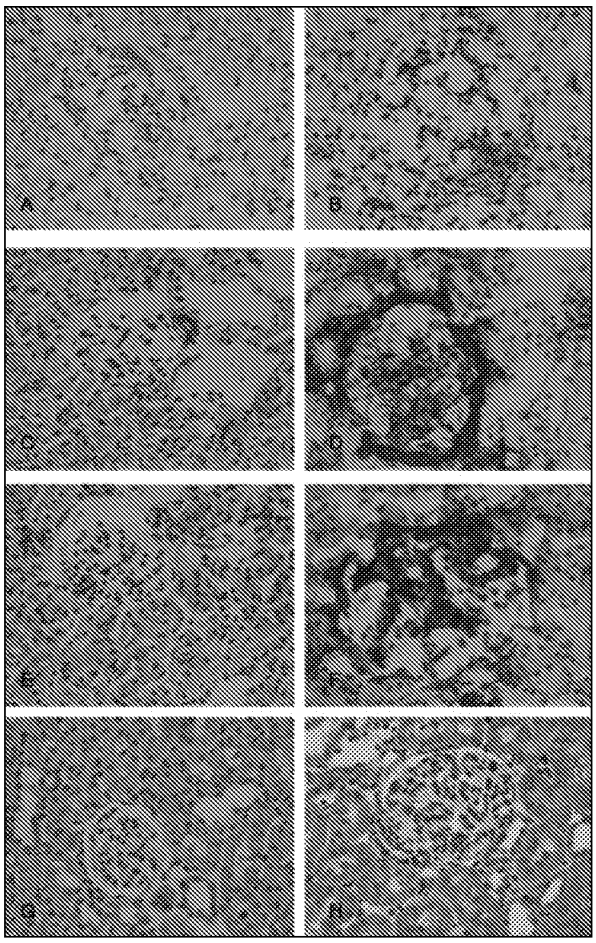

Fig. 1 - Fibrotic processes in nephrotoxic nephritis (NTN). A) TGF-β1 was not detected in the normal rat tissue. B) Increased glomerular TGF-β1 expression was detected after induction of NTN. C) In normal control kidneys, α-SMA was detected only in vascular smooth muscle cells. D) Increase in glomerular and periglomerular α-SMA staining was detected after induction of NTN. E) Fibronectin was not detected in normal control kidneys. F) Glomerular and periglomerular expression of fibronectin was increased after induction of NTN. G) Only very low levels of phospho-p38 MAPK (p-p38 MAPK) were detected in normal control rats. H) Increased expression of p-p38 MAPK after induction of NTN.

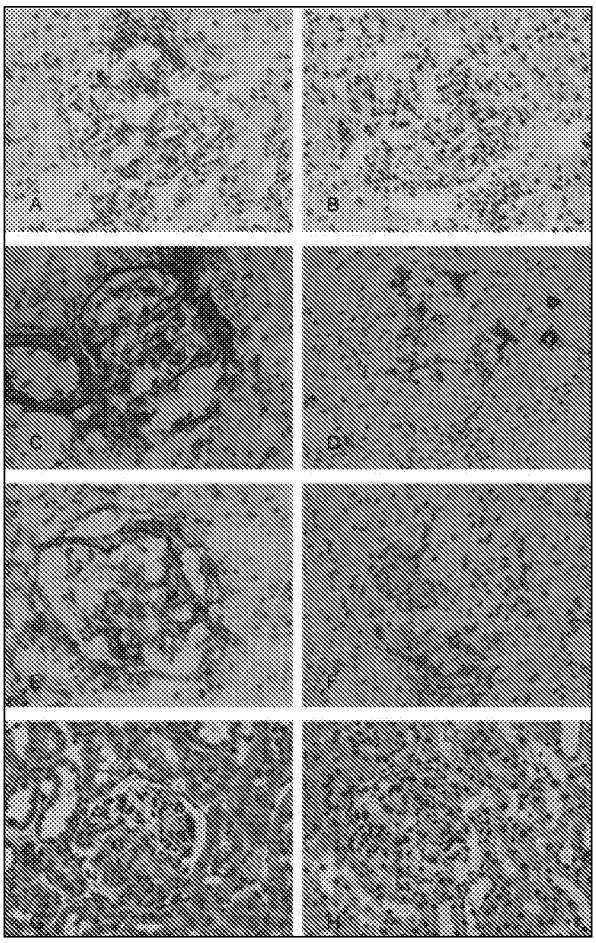

Fig. 2 - Treatment with rhIL-11 in nephrotoxic nephritis (NTN). Increased renal expression of TGF-β1 (A), α-SMA (C), fibronectin (E) and p-p38 MAPK (G) was detected in vehicle-treated rats 6 days after induction of NTN. Treatment with high-dose rhIL-11 (1,360 μg daily) reduced expression of TGF-β1 (B), α-SMA (D) and fibronectin (F). There was also a slight reduction of p-p38 MAPK (H) in the glomeruli of IL-11–treated rats.

glomeruli, $p<0.01$, respectively, and fibronectin from 1.5 ± 0.1 to 0.6 ± 0.1 semiquantitative score, $p<0.02$, and from 94% ± 1.9% to 26% ± 4.9% of glomeruli, $p<0.005$, respectively) (Figs. 2 and 3). Treatment with low-dose IL-11 did not affect significantly the expression of TGF-β1, α-SMA and fibronectin (data not shown).

In rats receiving IL-11 there was a slight reduction in the number of glomerular and tubular cells expressing p-p38 MAPK, and in the intensity of the staining, compared to vehicle group, but this reduction did not reach statistical significance (Figs. 2 and 3). The effect of low-dose IL-11 on renal p-p38 MAPK was not studied.